Bridge Engineering Handbook
SECOND EDITION

SUBSTRUCTURE DESIGN

EDITED BY
Wai-Fah Chen and Lian Duan

CRC Press
Taylor & Francis Group

Bridge Engineering Handbook

SECOND EDITION

SUBSTRUCTURE DESIGN

Bridge Engineering Handbook, Second Edition

Bridge Engineering Handbook, Second Edition: Fundamentals

Bridge Engineering Handbook, Second Edition: Superstructure Design

Bridge Engineering Handbook, Second Edition: Substructure Design

Bridge Engineering Handbook, Second Edition: Seismic Design

Bridge Engineering Handbook, Second Edition: Construction and Maintenance

Bridge Engineering Handbook

SECOND EDITION

SUBSTRUCTURE DESIGN

EDITED BY
Wai-Fah Chen and Lian Duan

CRC Press
Taylor & Francis Group
Boca Raton London New York

CRC Press is an imprint of the
Taylor & Francis Group, an **informa** business

CRC Press
Taylor & Francis Group
6000 Broken Sound Parkway NW, Suite 300
Boca Raton, FL 33487-2742

Version Date: 20130923

International Standard Book Number-13: 978-1-4398-5230-9 (eBook - PDF)

Contents

Foreword

Throughout the history of civilization bridges have been the icons of cities, regions, and countries. All bridges are useful for transportation, commerce, and war. Bridges are necessary for civilization to exist, and many bridges are beautiful. A few have become the symbols of the best, noblest, and most beautiful that mankind has achieved. The secrets of the design and construction of the ancient bridges have been lost, but how could one not marvel at the magnificence, for example, of the Roman viaducts?

The second edition of the *Bridge Engineering Handbook* expands and updates the previous edition by including the new developments of the first decade of the twenty-first century. Modern bridge engineering has its roots in the nineteenth century, when wrought iron, steel, and reinforced concrete began to compete with timber, stone, and brick bridges. By the beginning of World War II, the transportation infrastructure of Europe and North America was essentially complete, and it served to sustain civilization as we know it. The iconic bridge symbols of modern cities were in place: Golden Gate Bridge of San Francisco, Brooklyn Bridge, London Bridge, Eads Bridge of St. Louis, and the bridges of Paris, Lisbon, and the bridges on the Rhine and the Danube. Budapest, my birthplace, had seven beautiful bridges across the Danube. Bridge engineering had reached its golden age, and what more and better could be attained than that which was already achieved?

Then came World War II, and most bridges on the European continent were destroyed. All seven bridges of Budapest were blown apart by January 1945. Bridge engineers after the war were suddenly forced to start to rebuild with scant resources and with open minds. A renaissance of bridge engineering started in Europe, then spreading to America, Japan, China, and advancing to who knows where in the world, maybe Siberia, Africa? It just keeps going! The past 60 years of bridge engineering have brought us many new forms of bridge architecture (plate girder bridges, cable stayed bridges, segmental prestressed concrete bridges, composite bridges), and longer spans. Meanwhile enormous knowledge and experience have been amassed by the profession, and progress has benefitted greatly by the availability of the digital computer. The purpose of the *Bridge Engineering Handbook* is to bring much of this knowledge and experience to the bridge engineering community of the world. The contents encompass the whole spectrum of the life cycle of the bridge, from conception to demolition.

The editors have convinced 146 experts from many parts of the world to contribute their knowledge and to share the secrets of their successful and unsuccessful experiences. Despite all that is known, there are still failures: engineers are human, they make errors; nature is capricious, it brings unexpected surprises! But bridge engineers learn from failures, and even errors help to foster progress.

The *Bridge Engineering Handbook*, second edition consists of five books:

Fundamentals
Superstructure Design
Substructure Design
Seismic Design
Construction and Maintenance

Fundamentals, Superstructure Design, and *Substructure Design* present the many topics necessary for planning and designing modern bridges of all types, made of many kinds of materials and systems, and subject to the typical loads and environmental effects. *Seismic Design* and *Construction and Maintenance* recognize the importance that bridges in parts of the world where there is a chance of earthquake occurrences must survive such an event, and that they need inspection, maintenance, and possible repair throughout their intended life span. Seismic events require that a bridge sustain repeated dynamic load cycles without functional failure because it must be part of the postearthquake lifeline for the affected area. *Construction and Maintenance* touches on the many very important aspects of bridge management that become more and more important as the world's bridge inventory ages.

The editors of the *Bridge Engineering Handbook*, Second Edition are to be highly commended for undertaking this effort for the benefit of the world's bridge engineers. The enduring result will be a safer and more cost effective family of bridges and bridge systems. I thank them for their effort, and I also thank the 146 contributors.

Theodore V. Galambos, PE
Emeritus professor of structural engineering
University of Minnesota

Preface to the Second Edition

In the approximately 13 years since the original edition of the *Bridge Engineering Handbook* was published in 2000, we have received numerous letters, e-mails, and reviews from readers including educators and practitioners commenting on the handbook and suggesting how it could be improved. We have also built up a large file of ideas based on our own experiences. With the aid of all this information, we have completely revised and updated the handbook. In writing this Preface to the Second Edition, we assume readers have read the original Preface. Following its tradition, the second edition handbook stresses professional applications and practical solutions; describes the basic concepts and assumptions omitting the derivations of formulas and theories; emphasizes seismic design, rehabilitation, retrofit and maintenance; covers traditional and new, innovative practices; provides over 2500 tables, charts, and illustrations in ready-to-use format and an abundance of worked-out examples giving readers step-by-step design procedures. The most significant changes in this second edition are as follows:

- The handbook of 89 chapters is published in five books: *Fundamentals, Superstructure Design, Substructure Design, Seismic Design,* and *Construction and Maintenance*.
- *Fundamentals,* with 22 chapters, combines Section I, Fundamentals, and Section VI, Special Topics, of the original edition and covers the basic concepts, theory and special topics of bridge engineering. Seven new chapters are Finite Element Method, High-Speed Railway Bridges, Structural Performance Indicators for Bridges, Concrete Design, Steel Design, High Performance Steel, and Design and Damage Evaluation Methods for Reinforced Concrete Beams under Impact Loading. Three chapters including Conceptual Design, Bridge Aesthetics: Achieving Structural Art in Bridge Design, and Application of Fiber Reinforced Polymers in Bridges, are completely rewritten. Three special topic chapters, Weigh-In-Motion Measurement of Trucks on Bridges, Impact Effect of Moving Vehicles, and Active Control on Bridge Engineering, were deleted.
- *Superstructure Design,* with 19 chapters, provides information on how to design all types of bridges. Two new chapters are Extradosed Bridges and Stress Ribbon Pedestrian Bridges. The Prestressed Concrete Girder Bridges chapter is completely rewritten into two chapters: Precast–Pretensioned Concrete Girder Bridges and Cast-In-Place Posttensioned Prestressed Concrete Girder Bridges. The Bridge Decks and Approach Slabs chapter is completely rewritten into two chapters: Concrete Decks and Approach Slabs. Seven chapters, including Segmental Concrete Bridges, Composite Steel I-Girder Bridges, Composite Steel Box Girder Bridges, Arch Bridges, Cable-Stayed Bridges, Orthotropic Steel Decks, and Railings, are completely rewritten. The chapter Reinforced Concrete Girder Bridges was deleted because it is rarely used in modern time.
- *Substructure Design* has 11 chapters and addresses the various substructure components. A new chapter, Landslide Risk Assessment and Mitigation, is added. The Geotechnical Consideration chapter is completely rewritten and retitled as Ground Investigation. The Abutments and

Retaining Structures chapter is divided in two and updated as two chapters: Abutments and Earth Retaining Structures.

- *Seismic Design,* with 18 chapters, presents the latest in seismic bridge analysis and design. New chapters include Seismic Random Response Analysis, Displacement-Based Seismic Design of Bridges, Seismic Design of Thin-Walled Steel and CFT Piers, Seismic Design of Cable-Supported Bridges, and three chapters covering Seismic Design Practice in California, China, and Italy. Two chapters of Earthquake Damage to Bridges and Seismic Design of Concrete Bridges have been rewritten. Two chapters of Seismic Design Philosophies and Performance-Based Design Criteria, and Seismic Isolation and Supplemental Energy Dissipation, have also been completely rewritten and retitled as Seismic Bridge Design Specifications for the United States, and Seismic Isolation Design for Bridges, respectively. Two chapters covering Seismic Retrofit Practice and Seismic Retrofit Technology are combined into one chapter called Seismic Retrofit Technology.
- *Construction and Maintenance* has 19 chapters and focuses on the practical issues of bridge structures. Nine new chapters are Steel Bridge Fabrication, Cable-Supported Bridge Construction, Accelerated Bridge Construction, Bridge Management Using Pontis and Improved Concepts, Bridge Maintenance, Bridge Health Monitoring, Nondestructive Evaluation Methods for Bridge Elements, Life-Cycle Performance Analysis and Optimization, and Bridge Construction Methods. The Strengthening and Rehabilitation chapter is completely rewritten as two chapters: Rehabilitation and Strengthening of Highway Bridge Superstructures, and Rehabilitation and Strengthening of Orthotropic Steel Bridge Decks. The Maintenance Inspection and Rating chapter is completely rewritten as three chapters: Bridge Inspection, Steel Bridge Evaluation and Rating, and Concrete Bridge Evaluation and Rating.
- The section on Worldwide Practice in the original edition has been deleted, including the chapters on Design Practice in China, Europe, Japan, Russia, and the United States. An international team of bridge experts from 26 countries and areas in Africa, Asia, Europe, North America, and South America, has joined forces to produce the *Handbook of International Bridge Engineering, Second Edition*, the first comprehensive, and up-to-date resource book covering the state-of-the-practice in bridge engineering around the world. Each of the 26 country chapters presents that country's historical sketch; design specifications; and various types of bridges including girder, truss, arch, cable-stayed, suspension, and so on, in various types of materials—stone, timber, concrete, steel, advanced composite, and of varying purposes—highway, railway, and pedestrian. Ten benchmark highway composite girder designs, the highest bridges, the top 100 longest bridges, and the top 20 longest bridge spans for various bridge types are presented. More than 1650 beautiful bridge photos are provided to illustrate great achievements of engineering professions.

The 146 bridge experts contributing to these books have written chapters to cover the latest bridge engineering practices, as well as research and development from North America, Europe, and Pacific Rim countries. More than 80% of the contributors are practicing bridge engineers. In general, the handbook is aimed toward the needs of practicing engineers, but materials may be re-organized to accommodate several bridge courses at the undergraduate and graduate levels.

The authors acknowledge with thanks the comments, suggestions, and recommendations made during the development of the second edition of the handbook by Dr. Erik Yding Andersen, COWI A/S, Denmark; Michael J. Abrahams, Parsons Brinckerhoff, Inc.; Dr. Xiaohua Cheng, New Jersey Department of Transportation; Joyce E. Copelan, California Department of Transportation; Prof. Dan M. Frangopol, Lehigh University; Dr. John M. Kulicki, Modjeski and Masters; Dr. Amir M. Malek, California Department of Transportation; Teddy S. Theryo, Parsons Brinckerhoff, Inc.; Prof. Shouji Toma, Horrai-Gakuen University, Japan; Dr. Larry Wu, California Department of Transportation; Prof. Eiki Yamaguchi, Kyushu Institute of Technology, Japan; and Dr. Yi Edward Zhou, URS Corp.

We thank all the contributors for their contributions and also acknowledge Joseph Clements, acquiring editor; Jennifer Ahringer, project coordinator; and Joette Lynch, project editor, at Taylor & Francis/CRC Press.

Preface to the First Edition

The *Bridge Engineering Handbook* is a unique, comprehensive, and state-of-the-art reference work and resource book covering the major areas of bridge engineering with the theme "bridge to the twenty-first century." It has been written with practicing bridge and structural engineers in mind. The ideal readers will be MS-level structural and bridge engineers with a need for a single reference source to keep abreast of new developments and the state-of-the-practice, as well as to review standard practices.

The areas of bridge engineering include planning, analysis and design, construction, maintenance, and rehabilitation. To provide engineers a well-organized, user-friendly, and easy-to-follow resource, the handbook is divided into seven sections. Section I, Fundamentals, presents conceptual design, aesthetics, planning, design philosophies, bridge loads, structural analysis, and modeling. Section II, Superstructure Design, reviews how to design various bridges made of concrete, steel, steel-concrete composites, and timbers; horizontally curved, truss, arch, cable-stayed, suspension, floating, movable, and railroad bridges; and expansion joints, deck systems, and approach slabs. Section III, Substructure Design, addresses the various substructure components: bearings, piers and columns, towers, abutments and retaining structures, geotechnical considerations, footings, and foundations. Section IV, Seismic Design, provides earthquake geotechnical and damage considerations, seismic analysis and design, seismic isolation and energy dissipation, soil–structure–foundation interactions, and seismic retrofit technology and practice. Section V, Construction and Maintenance, includes construction of steel and concrete bridges, substructures of major overwater bridges, construction inspections, maintenance inspection and rating, strengthening, and rehabilitation. Section VI, Special Topics, addresses in-depth treatments of some important topics and their recent developments in bridge engineering. Section VII, Worldwide Practice, provides the global picture of bridge engineering history and practice from China, Europe, Japan, and Russia to the U.S.

The handbook stresses professional applications and practical solutions. Emphasis has been placed on ready-to-use materials, and special attention is given to rehabilitation, retrofit, and maintenance. The handbook contains many formulas and tables that give immediate answers to questions arising from practical works. It describes the basic concepts and assumptions, omitting the derivations of formulas and theories, and covers both traditional and new, innovative practices. An overview of the structure, organization, and contents of the book can be seen by examining the table of contents presented at the beginning, while the individual table of contents preceding each chapter provides an in-depth view of a particular subject. References at the end of each chapter can be consulted for more detailed studies.

Many internationally known authors have written the chapters from different countries covering bridge engineering practices, research, and development in North America, Europe, and the Pacific Rim. This handbook may provide a glimpse of a rapidly growing trend in global economy in recent years toward international outsourcing of practice and competition in all dimensions of engineering.

In general, the handbook is aimed toward the needs of practicing engineers, but materials may be reorganized to accommodate undergraduate and graduate level bridge courses. The book may also be used as a survey of the practice of bridge engineering around the world.

The authors acknowledge with thanks the comments, suggestions, and recommendations during the development of the handbook by Fritz Leonhardt, Professor Emeritus, Stuttgart University, Germany; Shouji Toma, Professor, Horrai-Gakuen University, Japan; Gerard F. Fox, Consulting Engineer; Jackson L. Durkee, Consulting Engineer; Michael J. Abrahams, Senior Vice President, Parsons, Brinckerhoff, Quade & Douglas, Inc.; Ben C. Gerwick, Jr., Professor Emeritus, University of California at Berkeley; Gregory F. Fenves, Professor, University of California at Berkeley; John M. Kulicki, President and Chief Engineer, Modjeski and Masters; James Chai, Senior Materials and Research Engineer, California Department of Transportation; Jinrong Wang, Senior Bridge Engineer, URS Greiner; and David W. Liu, Principal, Imbsen & Associates, Inc.

We thank all the authors for their contributions and also acknowledge at CRC Press Nora Konopka, acquiring editor, and Carol Whitehead and Sylvia Wood, project editors.

Editors

Dr. Wai-Fah Chen is a research professor of civil engineering at the University of Hawaii. He was dean of the College of Engineering at the University of Hawaii from 1999 to 2007, and a George E. Goodwin Distinguished Professor of Civil Engineering and head of the Department of Structural Engineering at Purdue University from 1976 to 1999.

He earned his BS in civil engineering from the National Cheng-Kung University, Taiwan, in 1959, MS in structural engineering from Lehigh University in 1963, and PhD in solid mechanics from Brown University in 1966. He received the Distinguished Alumnus Award from the National Cheng-Kung University in 1988 and the Distinguished Engineering Alumnus Medal from Brown University in 1999.

Dr. Chen's research interests cover several areas, including constitutive modeling of engineering materials, soil and concrete plasticity, structural connections, and structural stability. He is the recipient of several national engineering awards, including the Raymond Reese Research Prize and the Shortridge Hardesty Award, both from the American Society of Civil Engineers, and the T. R. Higgins Lectureship Award in 1985 and the Lifetime Achievement Award, both from the American Institute of Steel Construction. In 1995, he was elected to the U.S. National Academy of Engineering. In 1997, he was awarded Honorary Membership by the American Society of Civil Engineers, and in 1998, he was elected to the Academia Sinica (National Academy of Science) in Taiwan.

A widely respected author, Dr. Chen has authored and coauthored more than 20 engineering books and 500 technical papers. His books include several classical works such as *Limit Analysis and Soil Plasticity* (Elsevier, 1975), the two-volume *Theory of Beam-Columns* (McGraw-Hill, 1976 and 1977), *Plasticity in Reinforced Concrete* (McGraw-Hill, 1982), and the two-volume *Constitutive Equations for Engineering Materials* (Elsevier, 1994). He currently serves on the editorial boards of more than 15 technical journals.

Dr. Chen is the editor-in-chief for the popular *Civil Engineering Handbook* (CRC Press, 1995 and 2003), the *Handbook of Structural Engineering* (CRC Press, 1997 and 2005), the *Earthquake Engineering Handbook* (CRC Press, 2003), the *Semi-Rigid Connections Handbook* (J. Ross Publishing, 2011), and the *Handbook of International Bridge Engineering* (CRC Press, 2014). He currently serves as the consulting editor for the *McGraw-Hill Yearbook of Science & Technology* for the field of civil and architectural engineering.

He was a longtime member of the executive committee of the Structural Stability Research Council and the specification committee of the American Institute of Steel Construction. He was a consultant for Exxon Production Research on offshore structures, for Skidmore, Owings, and Merrill in Chicago on tall steel buildings, and for the World Bank on the Chinese University Development Projects, among many others. Dr. Chen has taught at Lehigh University, Purdue University, and the University of Hawaii.

Dr. Lian Duan is a senior bridge engineer and structural steel committee chair with the California Department of Transportation (Caltrans). He worked at the North China Power Design Institute from 1975 to 1978 and taught at Taiyuan University of Technology, China, from 1981 to 1985.

He earned his diploma in civil engineering in 1975, MS in structural engineering in 1981 from Taiyuan University of Technology, China, and PhD in structural engineering from Purdue University in 1990.

Dr. Duan's research interests cover areas including inelastic behavior of reinforced concrete and steel structures, structural stability, seismic bridge analysis, and design. With more than 70 authored and coauthored papers, chapters, and reports, his research focuses on the development of unified interaction equations for steel beam-columns, flexural stiffness of reinforced concrete members, effective length factors of compression members, and design of bridge structures.

Dr. Duan has over 35 years experience in structural and bridge engineering. He was lead engineer for the development of Caltrans *Guide Specifications for Seismic Design of Steel Bridges*. He is a registered professional engineer in California. He served as a member for several National Highway Cooperative Research Program panels and was a Transportation Research Board Steel Committee member from 2000 to 2006.

He is the coeditor of the *Handbook of International Bridge Engineering,* (CRC Press, 2014). He received the prestigious 2001 Arthur M. Wellington Prize from the American Society of Civil Engineers for the paper, "Section Properties for Latticed Members of San Francisco-Oakland Bay Bridge," in the *Journal of Bridge Engineering,* May 2000. He received the Professional Achievement Award from Professional Engineers in California Government in 2007 and the Distinguished Engineering Achievement Award from the Engineers' Council in 2010.

Contributors

Nan Deng
Bechtel Corporation
San Francisco, California

Ralph J. Dornsife
Washington State Department of Transportation
Olympia, Washington

Jason Fan
California Department of Transportation
Sacramento, California

Chao Gong
URS Corporation
Oakland, California

Junke Guo
University of Nebraska–Lincoln
Lincoln, Nebraska

Mohammed S. Islam
California Department of Transportation
Sacramento, California

Michael Knott
Moffatt & Nichol
Richmond, Virginia

Youzhi Ma
AMEC Environmental and Infrastructure Inc.
Oakland, California

Amir M. Malek
California Department of Transportation
Sacramento, California

Thomas W. McNeilan
Fugro Atlantic
Norfolk, Virginia

Mihail E. Popescu
Illinois Institute of Technology
Chicago, Illinois

Zolan Prucz
Modjeski and Masters Inc.
New Orleans, Louisiana

Charles Seim
Consulting Engineer
El Cerrito, California

Kevin R. Smith
Fugro Atlantic
Norfolk, Virginia

Aurelian C. Trandafir
Fugro GeoConsulting Inc.
Houston, Texas

Jinrong Wang
California Department of Transportation
Sacramento, California

Linan Wang
California Department of Transportation
Sacramento, California

1

Bearings

Ralph J. Dornsife
Washington State Department of Transportation

1.1 Introduction

Bridge bearings facilitate the transfer of vehicular and other environmentally imposed loads from the superstructure down to the substructure, and ultimately, to the ground. In fulfilling this function, bearings must accommodate anticipated service movements while also restraining extraordinary movements induced by extreme load cases. Because the movements allowed by an adjacent expansion joint must be compatible with the movement restrictions imposed by a bearing, bearings and expansion joints must be designed interdependently and in conjunction with the anticipated behavior of the overall structure.

1.2 Bearing Types

Historically, many types of bearings have been used for bridges. Contemporary bearing types include steel reinforced elastomeric bearings, fabric pad sliding bearings, steel pin bearings, rocker bearings, roller bearings, steel pin bearings, pot bearings, disc bearings, spherical bearings, and seismic isolation bearings. Each of these bearings possesses different characteristics in regard to vertical and horizontal load carrying capacity, vertical stiffness, horizontal stiffness, and rotational flexibility. A thorough understanding of these characteristics is essential for economical bearing selection and design. Pot bearings, disc bearings, and spherical bearings are sometimes collectively referred to as high-load multi-rotational (HLMR) bearings.

1.2.1 Steel Reinforced Elastomeric Bearings

Elastomeric bearings are perhaps the simplest and most economical of all modern bridge bearings. They are broadly classified into four types: plain elastomeric pads, fiberglass reinforced elastomeric pads, steel reinforced elastomeric pads, and cotton duck reinforced elastomeric pads. Of these four types, steel reinforced elastomeric pads are used most extensively for bridge construction applications. Plain elastomeric pads are used occasionally for lightly loaded applications. Cotton duck reinforced elastomeric pads, generally referred to as fabric pad bearings, are used occasionally. This subsection will address steel reinforced elastomeric bearings. A subsequent section will address fabric pad bearings.

A steel reinforced elastomeric bearing consists of discrete steel shims vulcanized between adjacent discrete layers of elastomer. This vulcanization process occurs under conditions of high temperature and pressure. The constituent elastomer is either natural rubber or synthetic rubber (neoprene). Steel reinforced elastomeric bearings are commonly used with prestressed concrete girder bridges and may be used with other bridge types. Because of their relative simplicity and fabrication ease, steel reinforced elastomeric bearings offer significant economy relative to HLMR bearings.

Prestressed concrete girder bridges use steel reinforced elastomeric bearings almost exclusively. A concrete bridge application is shown in Figure 1.1. Steel reinforced elastomeric bearings have also been used in steel plate girder bridge applications. Figure 1.2 depicts one such application in which service load transverse movements are accommodated by the shear flexibility of the elastomer while larger seismically induced transverse force effects are resisted by concrete girder stops.

Steel reinforced elastomeric bearings rely upon the inherent shear flexibility of the elastomeric layers to accommodate bridge movements in any horizontal direction. The steel shims limit the tendency for the elastomeric layers to bulge laterally under compressive load, thus limiting vertical deformation of the bearing. The shear flexibility of the elastomeric layers also allows them to accommodate rotational demands induced by loading.

1.2.2 Fabric Pad Bearings

Cotton duck, or fabric, pads are preformed elastomeric pads reinforced with very closely spaced layers of cotton or polyester fabric. Fabric pads are typically manufactured in large sheets under military specifications and with limited guidance from American Association of State Highway and Transportation Officials (AASHTO) Specifications (Lehman 2003). The close spacing of the reinforcing fibers, while allowing fabric pads to support large compressive loads, imposes stringent limits upon their shear

FIGURE 1.1 Steel reinforced elastomeric bearing (concrete bridge) application.

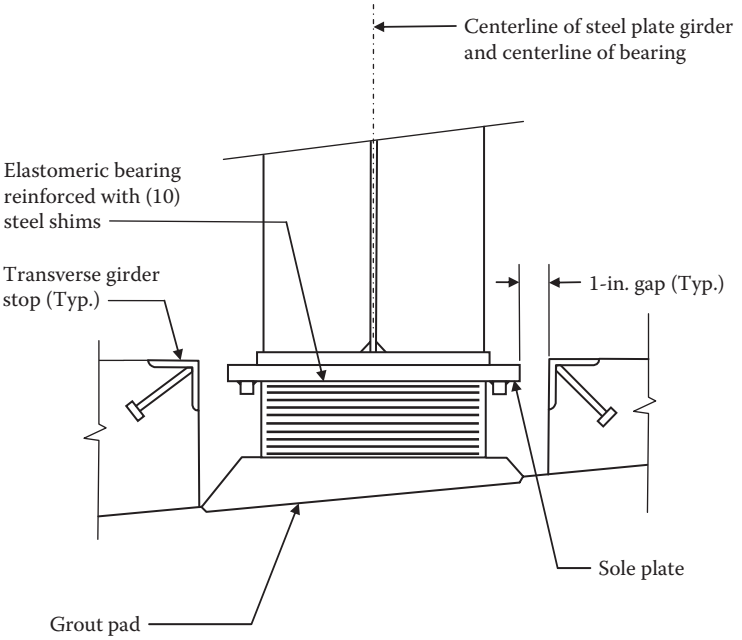

FIGURE 1.2 Steel reinforced elastomeric bearing (steel bridge).

displacement and rotational capacities. Unlike a steel reinforced elastomeric bearing having substantial shear flexibility, the fabric pad alone cannot accommodate translational movement. Fabric pads can accommodate very small amounts of rotational movement; substantially less than can be accommodated by more flexible steel reinforced elastomeric bearings.

1.2.3 Elastomeric Sliding Bearings

Both steel reinforced elastomeric bearings and fabric pad bearings can be modified to incorporate a PTFE (PolyTetraFluoroEthylene, more commonly known by the DuPont trade name Teflon)-stainless steel sliding interface to accommodate large translational movements. Such modifications extend the range of use of steel reinforced elastomeric bearings and make fabric pad bearings a viable and economical solution for applications with minimal rotational demand. A schematic representation of a fabric pad sliding bearing is depicted in Figure 1.3. A typical fabric pad sliding bearing is shown in Figure 1.4.

PTFE material is available in several forms: unfilled, filled, dimpled lubricated, and woven. These various forms of PTFE differ substantially in their frictional properties and ability to resist creep (cold flow) under sustained load. Creep resistance is most effectively enhanced by confining the PTFE material in a recess. Filled PTFE contains glass, carbon, or other chemically inert fibers that enhance its resistance to creep and wear. Woven PTFE is created by interweaving high strength fibers through PTFE material. Dimpled PTFE contains dimples machined into its surface. These dimples act as reservoirs for silicone grease lubricant. The use of silicone grease in dimpled PTFE reduces the friction coefficient in the early life of the bearing. However, silicone grease will squeeze out under high pressure and attract dust and other debris, which may accelerate wear and detrimentally impact a bearing's durability.

The low-friction characteristics of a PTFE-stainless steel interface are actually facilitated by fragmentary PTFE sliding against solid PTFE after the fragmentary PTFE particles are absorbed into the asperities of the stainless steel surface. The optimum surface finish is thus associated with an optimum asperity size and distribution. In order to minimize frictional resistance, a Number 8 (Mirror) finish is generally specified for all flat stainless steel surfaces in contact with PTFE. However, recent research

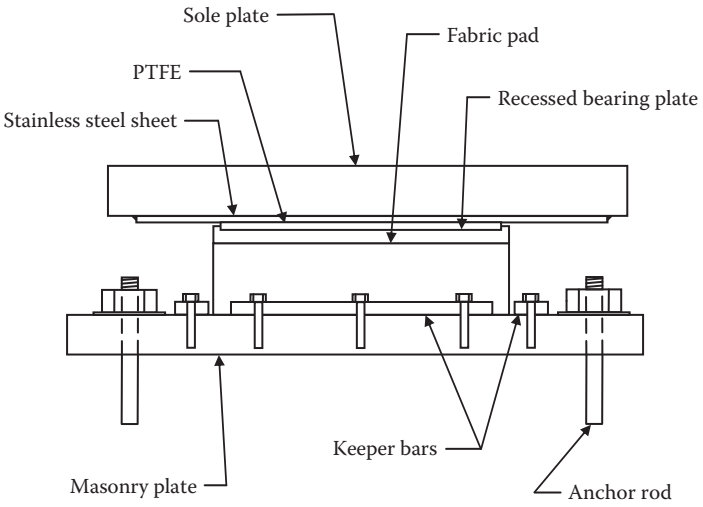

FIGURE 1.3 Fabric pad sliding bearing.

FIGURE 1.4 Fabric pad sliding bearing application.

has concluded that stainless steel having a 2B surface finish achieves similarly low-friction properties with no measurable increase in wear (Stanton 2010). Unlike a Number 8 (Mirror) finish, a 2B finish is achieved by cold rolling without further polishing. Thus it is easier to obtain and more economical. The research did not investigate the performance characteristics of the 2B finish at very low temperatures.

For a given steel surface finish, friction coefficients for PTFE-stainless steel sliding interfaces vary significantly as a function of PTFE type, magnitude of contact pressure, and ambient temperature. The AASHTO Load and Resistance Factor Design (LRFD) specifications provide friction coefficients associated with a Number 8 (Mirror) finish as a function of these variables. Dimpled lubricated PTFE at high temperature and high contact pressures typically exhibits the lowest friction coefficients, as low as 0.020 (AASHTO 2012). Filled PTFE at very low temperatures and low contact pressures exhibits the highest friction coefficients, as high as 0.65 (AASHTO 2012).

Resistance against creep of PTFE material is achieved by limiting both average and edge contact stresses under both permanent and total loads. The AASHTO LRFD specifications limit unconfined unfilled PTFE average contact stress to 1500 psi under permanent service load and 2500 psi under total

service load. These specifications also limit unconfined filled PTFE, confined unfilled PTFE, and woven PTFE fiber average contact stress to 3000 psi under permanent service load and 4500 psi under total service load (AASHTO 2012). The AASHTO LRFD specifications permit slightly higher edge contact stresses under both permanent and total service load.

In fabric pad sliding bearings, the unfilled PTFE material is generally recessed half its thickness into a steel backing plate. The backing plate is generally bonded to the top of a fabric pad. A stainless steel sheet is typically seal welded to a steel sole plate attached to the superstructure to provide the low-friction sliding interface.

1.2.4 Pin Bearings

Steel pin bearings are generally used to support high loads with moderate to high levels of rotation about a single predetermined axis. This situation generally occurs with long straight steel plate girder superstructures. Rotational capacity is afforded by rotation of a smoothly machined steel pin against upper and lower smoothly machined steel bearing blocks. Steel keeper rings are typically designed and detailed to provide uplift resistance. A schematic representation of the elements constituting a pin bearing is depicted in Figure 1.5. A typical pin bearing of a bridge under construction prior to grout pad placement is shown in Figure 1.6.

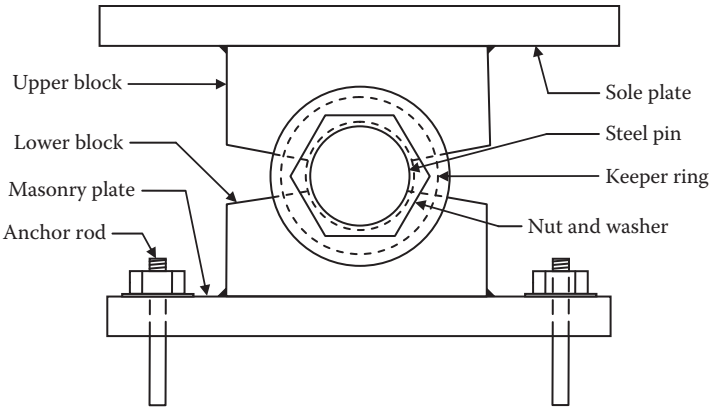

FIGURE 1.5 Steel pin bearing.

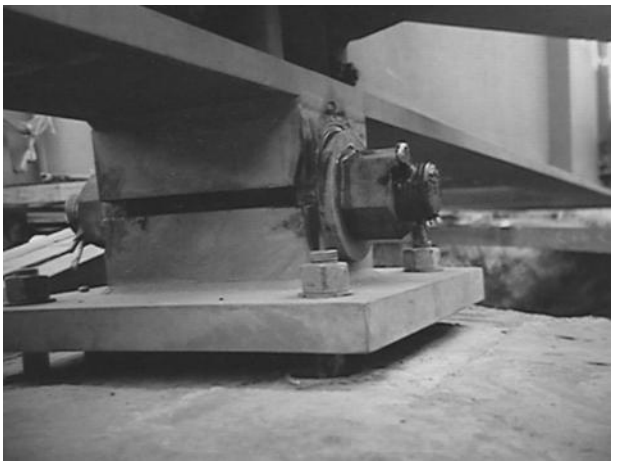

FIGURE 1.6 Steel pin bearing application.

1.2.5 Rocker/Roller Bearings

Steel rocker bearings have been used extensively in the past to allow both rotation and longitudinal movement while supporting moderately high loads. Because of their seismic vulnerability and the more extensive use of steel reinforced elastomeric bearings, rocker bearings are now rarely specified for new bridges. A typical rocker bearing adjacent to a pin (fixed) bearing of an older reinforced concrete bridge is shown in Figure 1.7.

Steel roller bearings have also been used extensively in the past. Roller bearings permit both rotational and longitudinal movement. Pintles are often used to effect transverse force transfer by connecting the roller bearing to the superstructure above and to the bearing plate below. Two views of a steel roller bearing are shown in Figure 1.8. This roller bearing has displaced up against its stop bar and cannot accommodate any further movement.

Nested roller bearings have also been used in the past. They are composed of a series of rollers. Without adequate preventative maintenance, these bearings can experience corrosion and lockup. Figure 1.9 is a photograph of a nested roller bearing application. Having been supplanted by more economical steel reinforced elastomeric bearings, roller bearings are infrequently used for new bridges today.

FIGURE 1.7 Steel rocker bearing application.

FIGURE 1.8 Steel roller bearing application.

FIGURE 1.9 Nested roller bearing application.

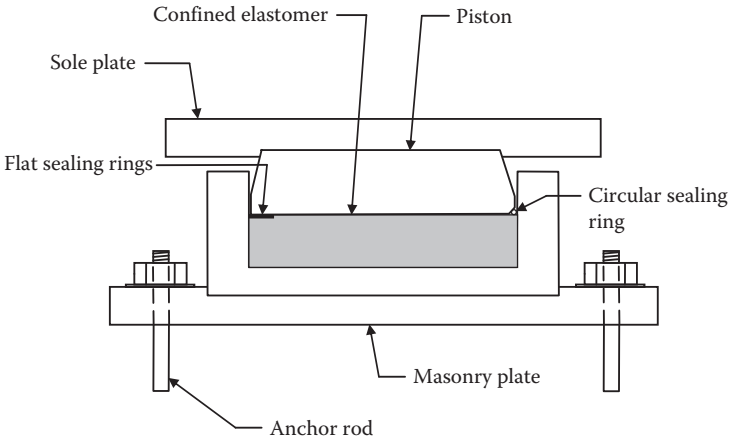

FIGURE 1.10 Pot bearing.

1.2.6 Pot Bearings

A pot bearing is composed of a plain elastomeric disc that is confined in a vertically oriented steel cylinder, or pot, as depicted schematically in Figure 1.10. Vertical loads are transmitted through a steel piston that sits atop the elastomeric disc within the pot. The pot walls confine the elastomeric disc, enabling it to sustain much higher compressive loads than could be sustained by more conventional unconfined elastomeric material. Rotational demands are accommodated by the ability of the elastomeric disc to deform under compressive load and induced rotation. The rotational capacity of pot bearings is generally limited by the clearances between elements of the pot, piston, sliding surface, guides, and restraints (Stanton 1999). A pot bearing application detailed to provide uplift resistance is shown in Figure 1.11.

Flat or circular sealing rings prevent the pinching and escape of elastomeric material through the gap between the piston and pot wall. In spite of these sealing elements, some pot bearings have demonstrated susceptibility to elastomer leakage. These problems have occurred predominantly on steel bridges, which tend to be more lightly loaded. Unanticipated rotations during steel erection may contribute to and exacerbate these problems. Excessive elastomeric leakage could result in the bearing experiencing hard metal-to-metal contact between components. Despite these occasional problems, most pot bearings have performed well in serving as economical alternatives to more expensive HLMR bearings.

FIGURE 1.11 Pot bearing application.

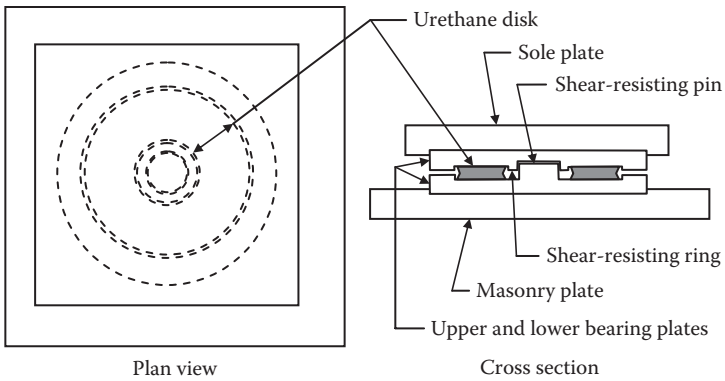

FIGURE 1.12 Disc bearing.

A flat PTFE-stainless steel interface can be built into a pot bearing assembly to additionally provide translation movement capability, either guided or nonguided.

1.2.7 Disc Bearings

A disc bearing relies upon the compressive flexibility of an annular shaped polyether urethane disc to provide moderate levels of rotational movement capacity while supporting high loads. A steel shear-resisting pin in the center provides resistance against lateral force. A flat PTFE-stainless steel sliding interface can be incorporated into a disc bearing to additionally provide translational movement capability, either guided or nonguided. The primary constituent elements of a disc bearing are identified in the schematic representation of a disc bearing in Figure 1.12. Two views of a typical disc bearing application are shown in Figure 1.13.

1.2.8 Spherical Bearings

A spherical bearing, sometimes referred to as a curved sliding bearing, relies upon the low-friction characteristics of a curved PTFE-stainless steel sliding interface to provide a high level of rotational flexibility in multiple directions while supporting high loads. Unlike pot bearings and disc bearings, spherical bearing rotational capacities are not limited by strains, dimensions, and clearances of deformable

FIGURE 1.13 Disc bearing application.

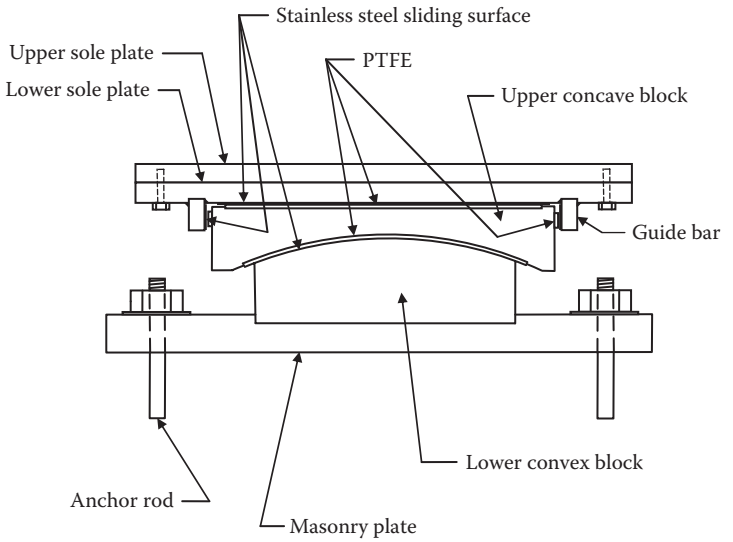

FIGURE 1.14 Spherical bearing.

elements. Spherical bearings are capable of sustaining very large rotations provided that adequate clearances are provided to avoid hard contact between steel components.

A flat PTFE-stainless steel sliding interface can be incorporated into a spherical bearing to additionally provide either guided or nonguided translational movement capability. The constituent elements of a guided spherical bearing are depicted in Figure 1.14. This depiction includes a flat PTFE-stainless steel sliding interface to provide translational movement capability. The steel guide bars limit translational movement to one direction only. A typical spherical bearing application is shown in Figure 1.15.

Woven PTFE material is generally used on the curved surfaces of spherical bearings. As noted earlier, woven PTFE exhibits enhanced creep (cold flow) resistance and durability relative to unwoven PTFE. When spherical bearings are detailed to accommodate translational movement, woven PTFE is generally specified at the flat sliding interface also.

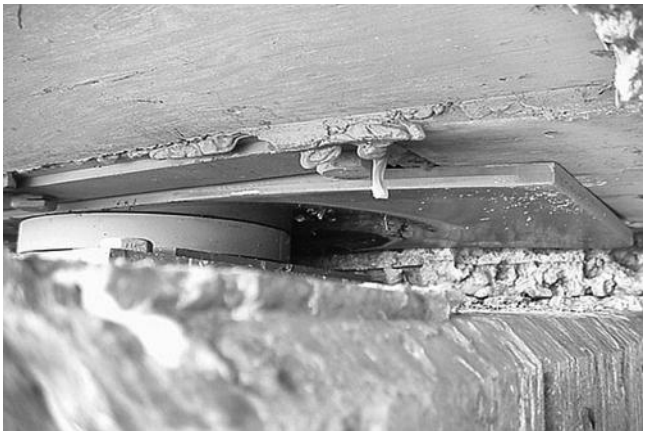

FIGURE 1.15 Spherical bearing application.

Both stainless steel sheet and solid stainless steel have been used for the convex sliding surface of spherical bearings. According to one manufacturer, curved sheet is generally acceptable for contact surface radii greater than 14 in. to 18 in. For smaller radii, a solid stainless steel convex plate or stainless steel inlay is typically used. The inlay is welded to solid standard steel. For taller convex plates, a stainless steel inlay would likely be more economical.

Most spherical bearings are fabricated with the concave surface oriented downward to minimize dirt infiltration between the PTFE material and the stainless steel surface. Calculation of translational and rotational movement demands on the bearing must recognize that the center of rotation of the bearing is generally not coincident with the neutral axis of the girder being supported.

1.2.9 Seismic Isolation Bearings

Seismic isolation bearings mitigate the potential for seismic damage by utilizing two related phenomena: dynamic isolation and energy dissipation. Dynamic isolation allows the superstructure to essentially float, to some degree, while substructure elements below move with the ground during an earthquake. The ability of some bearing materials and elements to deform in certain predictable ways allows them to dissipate seismic energy that might otherwise damage critical structural elements.

Numerous seismic isolation bearings exist, each relying upon varying combinations of dynamic isolation and energy dissipation. These devices include lead core elastomeric bearings, high damping rubber bearings, friction pendulum bearings, hydraulic dampers, and various hybrid variations.

Effective seismic isolation bearing design requires a thorough understanding of the dynamic characteristics of the overall structure as well as the candidate isolation devices. Isolation devices are differentiated by maximum compressive load capacity, lateral stiffness, lateral displacement range, maximum lateral load capacity, energy dissipation capacity per cycle, functionality in extreme environments, resistance to aging, fatigue and wear properties, and effects of size.

1.3 Design Considerations

Bearings must be designed both to transfer forces between the superstructure and the substructure and to accommodate anticipated service movements. Bearings must additionally restrain undesired movements and transmit extraordinary forces associated with extreme loads. This section discusses force and movement considerations as well as some of the design aspects associated with steel reinforced elastomeric and HLMR bearings.

1.3.1 Force Considerations

Bridge bearings must be explicitly designed to transfer all anticipated loads from the superstructure to the substructure. Sources of these loads include dead load, vehicular live load, wind loads, seismic loads, and restraint against posttensioning elastic shortening, creep, and shrinkage. These forces may be directed vertically, longitudinally, or transversely with respect to the global orientation of the bridge. In some instances, bearings must be designed to resist uplift. In accordance with the AASHTO LRFD specifications, most bearing design calculations are based upon service limit state stresses. Impact need not be applied to live load forces in the design of bearings.

1.3.2 Movement Considerations

Bridge bearings can be detailed to provide translational fixity, to permit free translation in any horizontal direction, or to permit guided translation. The movement restriction thus imposed by a bearing must be compatible with the movements allowed by any adjacent expansion joint. Additionally, both bearings and expansion joints must be designed consistent with the anticipated load and displacement behavior of the overall structure. Sources of anticipated movement include concrete shrinkage and creep, posttensioning shortening, thermal fluctuations, dead and live loads, and wind or seismic loads. Design rotations can be calculated as follows:

1. *Elastomeric and Fabric Pad Bearings:* The AASHTO LRFD specifications stipulate that the maximum service limit state rotation for bearings that do not have the potential to achieve hard contact between metal components shall be taken as the sum of unfactored dead and live load rotations plus an allowance for uncertainties of 0.005 radians. If a bearing is subject to rotation in opposing directions due to different effects, then this allowance applies in each direction.
2. *HLMR Bearings:* The AASHTO LRFD specifications stipulate that the maximum strength limit state rotation for bearings that are subject to potential hard contact between metal components shall be taken as the sum of all applicable factored load rotations plus an allowance of 0.005 radians for fabrication and installation tolerances and an additional allowance of 0.005 radians for uncertainties. The rationale for this more stringent requirement is that metal or concrete elements are susceptible to damage under a single rotation that causes contact between hard elements. Such bearings include spherical, pot, steel pin, and some types of seismic isolation bearings.

   Disc bearings are less likely to experience metal-to-metal contact because they use an unconfined load element. Accordingly, they are designed for a maximum strength limit state rotation equal to the sum of the applicable strength load rotation plus an allowance of 0.005 radians for uncertainties. If a bearing is subject to rotation in opposing directions due to different effects, then this allowance applies in each direction.

1.3.3 Elastomeric Bearing Design

Steel reinforced elastomeric bearings and fabric pad sliding bearings are generally designed by the bridge design engineer. These relatively simple bearings are easy to depict and fabrication procedures are relatively uniform and straightforward.

Steel reinforced elastomeric bearings can be designed by either the Method A or Method B procedure delineated in the AASHTO LRFD specifications. The Method B provisions provide more relief in meeting rotational demands than Method A. The Method A design procedure is a carryover based upon more conservative interpretation of past theoretical analyses and empirical observations prior to research leading up to the publication of *NCHRP Report 596 Rotation Limits for Elastomeric Bearings* (Stanton 2008).

Both Method A and Method B design procedures require determination of the optimal geometric parameters to achieve an appropriate balance of compressive, shear, and rotational stiffnesses and capacities.

Fatigue susceptibility is controlled by limiting live load compressive stress. Susceptibility of steel shims to delamination from adjacent elastomer is controlled by limiting total compressive stress. Assuring adequate shim thickness precludes yield and rupture of the steel shims. Excessive shear deformation is controlled and rotational flexibility is assured by providing adequate total elastomer height. Generally, total elastomer thickness shall be no less than twice the maximum anticipated lateral deformation. Overall bearing stability is controlled by limiting total bearing height relative to its plan dimensions.

The most important design parameter for reinforced elastomeric bearings is the shape factor. The shape factor is defined as the plan area of the bearing divided by the area of the perimeter free to bulge (plan perimeter multiplied by elastomeric layer thickness). Figure 1.16 illustrates the shape factor concept for a typical steel reinforced elastomeric bearing and for a fabric pad bearing.

Axial, rotational, and shear loading generate shear strain in the constituent layers of a typical elastomeric bearing as shown in Figure 1.17. Computationally, Method B imposes a limit on the sum of these shear strains. It distinguishes between static and cyclic components of shear strain by applying an amplification factor of 1.75 to cyclic effects to reflect cumulative degradation caused by repetitive loading.

Both the Method A and Method B design procedures limit translational movement to one-half the total height of the constituent elastomeric material composing the bearing. Translational capacity can be increased by incorporating an additional low-friction sliding interface. In this case, a portion of the translational movement is accommodated by shear deformation in the elastomeric layers. Movement exceeding the slip load displacement of the low-friction interface is accommodated by sliding.

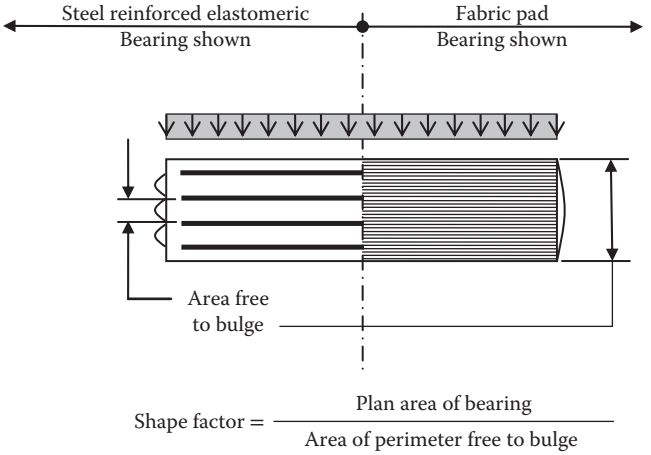

FIGURE 1.16 Shape factor for elastomeric bearings.

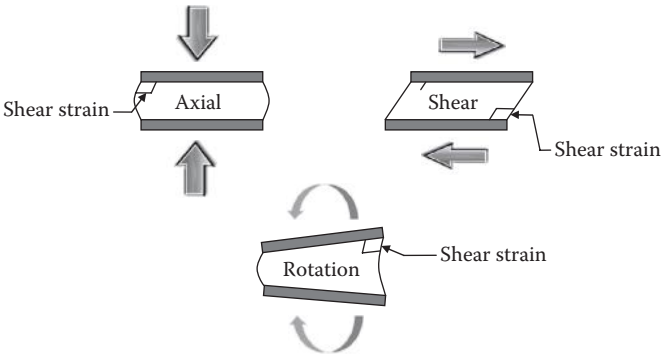

FIGURE 1.17 Shear strains in elastomeric bearings.

In essence, elastomeric bearing design reduces to checking several mathematical equations while varying bearing plan dimensions, number of elastomeric layers and their corresponding thicknesses, and steel shim thicknesses. Mathematical spreadsheets have been developed to evaluate these tedious calculations.

Although constituent elastomer has historically been specified by durometer hardness, shear modulus is the most important physical property of the elastomer for purposes of bearing design. Research has concluded that shear modulus may vary significantly among compounds of the same hardness. Accordingly, shear modulus shall preferably be specified without reference to durometer hardness.

Elastomeric bearings shall conform to the requirements contained in AASHTO Specification M 251 *Plain and Laminated Elastomeric Bridge Bearings*. Constituent elastomeric layers and steel shims shall be fabricated in standard thicknesses. For overall bearing heights less than about 5 in., a minimum of ¼ in. of horizontal cover is recommended over steel shim edges. For overall bearing heights greater than 5 in., a minimum of ½ in. of horizontal cover is recommended (WSDOT 2011). AASHTO Specifications M 251 requires elastomeric bearings to be subjected to a series of tests, including a compression test at 150% of total service load. For this reason, compressive service dead and live loads should be specified in the project plans or specifications.

As mentioned earlier, the AASHTO LRFD specifications stipulate that a 0.005 radian allowance for uncertainties be included in the design of steel reinforced elastomeric bearings. This allowance applies to rotation in each opposing direction. Commentary within the AASHTO LRFD specifications states that an owner may reduce this allowance if justified by "a suitable quality control plan." In the absence of a very specific implementable plan, this is inadvisable given that 0.005 radians corresponds to a slope of only about 1/16 in. in 12 in.

Unlike many HLMR bearing types, elastomeric bearings cannot be easily installed with an imposed offset to accommodate actual temperature at installation in addition to any anticipated long-term movements such as creep and shrinkage. For practical reasons, girders are rarely set atop elastomeric bearings at the mean of the expected overall temperature range. Rarely are girders subsequently lifted to relieve imposed vertical load to allow the bearings to replumb themselves at the mean temperature. The AASHTO LRFD specifications statistically reconcile this reality by stipulating a design thermal movement, applicable in either direction, of 65% of the total thermal movement range. This percentage may be reduced in instances in which girders are originally set or reset at the average of the design temperature range. For precast prestressed concrete girder bridges, the maximum design thermal movement shall be added to shrinkage, long-term creep, and posttensioning movements to determine the total bearing height required.

The material properties of most elastomers vary with temperature. Both natural rubber and neoprene stiffen and become brittle at colder temperatures. Therefore, it is important that the type of elastomer be considered explicitly in specifying the bearing and determining the resulting lateral forces that will be transferred to substructure elements. The AASHTO LRFD specifications categorize elastomers as being of Grade 0, 2, 3, 4, or 5. A higher grade number corresponds to greater resistance against stiffening under sustained cold conditions. Special compounding and curing are needed to provide this resistance and thus increase the cost of the constituent bearing. Determination of the minimum grade required depends upon the more critical of (1) the 50-year low temperature and (2) the maximum number of consecutive days in which the temperature does not rise above 32°F (0°C). The intent of specifying a minimum grade is to limit the forces transferred to the substructure to 1.5 times the service limit state design. The AASHTO LRFD specifications allow using lower grade elastomers if a low-friction sliding interface is incorporated and/or if the substructure is designed to resist a multiple of the calculated lateral force.

1.3.4 HLMR Bearing Design

Although design procedures have historically been largely proprietary, the AASHTO LRFD specifications do provide some guidance for the design of all three primary HLMR bearing types: pot bearings, disc bearings, and spherical bearings. Thus, all three HLMR bearing types may be allowed on most projects.

Because of their inherent complexity and sensitivity to fabrication methods, HLMR and seismic isolation bearings should generally be designed by their manufacturers (AASHTO/NSBA 2004). Each bearing manufacturer has unique fabricating methods, personnel, and procedures that allow it to fabricate a bearing most economically. For these reasons, these bearing types are generally depicted schematically in contract drawings. Depicting the bearings schematically with specified loads, movements, and rotations provides each manufacturer the flexibility to innovatively achieve optimal economy subject to the limitations imposed by the contract drawings and specifications.

Contract drawings must show the approximate diameter and height of the HLMR bearing in addition to all dead, live, and lateral wind/seismic loadings. This generally requires a preliminary design to be performed by the bridge designer or bearing manufacturer. Diameter of a HLMR bearing is governed primarily by load magnitude and material properties of the flexible load bearing element. The height of a pot bearing or disc bearing is governed primarily by the rotational demand and flexibility of the deformable bearing element. The height of a spherical bearing depends upon the radius of the curved surface, the diameter of the bearing, and the total rotational capacity required.

Accessory elements of the bearing, such as masonry plates, sole plates, anchor rods, and any appurtenance for horizontal force transfer should be designed and detailed on the contract drawings by the bridge designer. Notes should be included on the plans allowing the bearing manufacturer to make minor adjustments to the dimensions of sole plates, masonry plates, and anchor rods. The HLMR bearing manufacturer is generally required to submit shop drawings and detailed structural design calculations for review and approval by the bridge design engineer.

HLMR bearings incorporating sliding interfaces require inspection and long-term maintenance. It is important that these bearings be designed and detailed to allow future removal and replacement of sliding interface elements. Such provisions should allow these elements to be removed and replaced with a maximum vertical jacking height of ¼ in. (6 mm) after the vertical load is removed from the bearing assembly. By limiting the jacking height, this work can be performed under live load and without damaging expansion joint components.

HLMR bearings must be designed, detailed, fabricated, and installed to provide a continuous load path through the bearing from the superstructure to the substructure. The load path must account for all vertical and horizontal service, strength, and extreme limit state loads. The importance of providing positive connections as part of a continuous load path cannot be overemphasized. The spherical bearing shown in Figure 1.15 shows both an upper and lower sole plate, with the lower sole plate displaced longitudinally relative to the upper sole plate. The upper sole plate was embedded in the concrete superstructure. Because uplift had not been anticipated in the design of this Seattle bridge, the lower sole plate was designed to fit loosely in a recess in the bottom of the upper sole plate. During the 2001 Nisqually Earthquake, the upper and lower sole plates of this bearing separated, causing the lower sole plate to dislodge and displace.

1.4 Ancillary Details

HLMR bearings should be detailed and installed in such a way as to allow the bearings to be serviced and/or replaced during the lifetime of the bridge. A masonry plate connects the bottom of the bearing to the top of the supporting structural elements below. A sole plate connects the top of the bearing to the superstructure above.

1.4.1 Masonry Plates

Masonry plates help to more uniformly distribute loads from a bearing to supporting concrete substructure elements below. Additionally, they provide platforms to facilitate maintenance and repairs of bearings. Analysis shows that a steel masonry plate will deform under concentrated bearing loads (Stanton 1999). This potential deformation, which tends to cause a dishing effect because of the relatively flexible

nature of the concrete below, must be recognized in the design of the masonry plate. The masonry plate supporting a HLMR bearing is generally supported either on a thin preformed elastomeric pad or directly atop a grout pad that is poured after the superstructure girders have been erected. Each of these two methods has associated advantages and disadvantages.

A ⅛-in. thick preformed plain elastomeric pad or fabric pad placed atop the concrete bearing surface or grout pad most economically compensates for any minor surface irregularities. Fully threaded anchor rods can be either cast into the concrete or drilled and grouted into place. An anchor plate can be either bolted or welded to the bottom of the anchor rod to augment uplift capacity in the concrete. If no uplift capacity is required, a swedged rod may be substituted for a threaded one. The swedged rod may be terminated just below the top of the masonry plate and the void filled with a flexible sealant.

A grout pad poured underneath the masonry plate after girder erection can provide the contractor more flexibility in leveling and adjusting the horizontal position of the bearing. A variation of this method incorporating postgrouted hollow steel pipes can be used to substantially increase uplift capacity of the anchor rods and provide some additional anchor rod adjustability. Several methods have been used successfully to temporarily support the masonry plate until the grout is poured. The two most commonly used methods are

1. *Shim Packs*—Multiple stacks of steel shim plates are placed atop the concrete supporting surface to temporarily support the load on the masonry plate before grouting. Engineering judgment must be used in selecting the number and plan size of the shims, taking grout flowability, load distribution, and shim pack height adjustability into consideration. To enhance uplift resistance, steel anchor rods are sometimes installed in hollow steel pipes embedded into the concrete. The steel pipes have plates welded to their bottoms through which the anchor rods are bolted. Grouting is accomplished using grout tubes that extend to the bottom of the pipes. Once all pipes are fully grouted around the anchor rods, the space between the top of the concrete support surface and the underside of the masonry plate is grouted.
2. *Two-step Grouting with Voided Cores/Studs*—A two-step grouting procedure with cast-in-place voided cores can be used for smaller HLMR bearings not generally subjected to significant uplift. Steel studs are welded to the underside of the masonry plate to coincide with voided core locations. With the girders erected and temporary shims installed between the top of the concrete surface and the underside of the masonry plate, the voided cores are fully grouted. Once the first stage grout has attained strength, the steel shims are removed, the masonry plate is dammed, and grout is placed between the top of the concrete support surface and the underside of the masonry plate.

The use of anchor rod leveling nuts, without shim packs, to level a masonry plate prior to grout placement is not recommended. The absence of shim packs results in the application of point loads at anchor rod locations. This phenomenon is a consequence of the high stiffness of the anchor rods relative to the grout material and can result in warping of the masonry plate (AASHTO/NSBA 2004). Similar consideration must be given to the sizing and number of shim plates as it relates to potential dishing of the masonry plate under load.

1.4.2 Sole Plates

For concrete bridge superstructures, headed steel studs are typically welded to the top of the sole plate and embedded into the superstructure. In steel bridge superstructures, sole plates may be bolted or welded to I-shaped plate girder bottom flanges. Sole plate assemblies should be bolted to the bottom flange of steel box girder bridges because welded connections would require overhead welding, which may be difficult to perform because of limited access.

Welding of sole plates to steel I-shaped girders allows for greater adjustment during installation and is generally more economical. Damage associated with removal of the weld as required for future

maintenance and replacement operations can be reasonably repaired. For these welded connections, it is recommended that the sole plate extend transversely beyond the edge of the bottom flange by at least 1 in. in order to allow ½ in. of field adjustment. Welds for sole plate connections should be longitudinal to the girder axis. The transverse joints should be sealed with an approved caulking material. The longitudinal welds are made in the horizontal position, which is the position most likely to achieve a quality fillet weld. Transverse welds would require overhead welding, which may be difficult to perform because of limited clearance. Caulking is installed along the transverse seams following longitudinal welding to prevent corrosion between the sole plate and the bottom flange. The minimum thickness of the welded sole plate should be ¾ in. to minimize plate distortion during welding (AASHTO/NSBA 2004).

Bolting of sole plates to steel I-shaped girders is also used. Bolting typically requires minimal paint repair, as opposed to welding, and simplifies removal of a bearing for future maintenance and replacement needs. Oversized holes allow for minor field adjustments of the bearing during installation.

In some instances, an upper and lower sole plate may be used to simplify the bolted connection to a steel girder or to account for grade effects. The upper uniform thickness sole plate is bolted to the bottom flange while the lower tapered sole plate is welded to the upper sole plate. For a concrete bridge, the lower sole plate may be drilled and the embedded upper sole plate tapped for bolting together. The spherical bearing depicted in Figure 1.14 includes an upper and lower sole plate to facilitate removal and replacement of bearing elements.

Flatness of the steel mating surfaces may be a concern when bolting a sole plate to a steel girder bottom flange. In lieu of specifying a tighter flatness tolerance on the girder bottom flange, epoxy bedding can be used between the sole plate and the girder bottom flange. Silicone grease is used as a bond breaker on one of the surfaces in order to allow removal of the sole plate for servicing the bearing during the life of the bridge.

1.5 Shop Drawings, Calculations, Review, and Approval

As part of the overall process of HLMR and isolation bearing design, the manufacturer generates design calculations and produces shop drawings for review and approval by the bridge design engineer. The bridge design engineer is typically responsible for checking and approving these design calculations and shop drawings. This review shall assure that the calculations confirm the structural adequacy of all components of the bearing, a continuous load path is provided for all vertically and horizontally imposed loads, and each bearing is detailed to permit the inspection and replacement of components subject to wear.

The approved shop drawings should note that all HLMR bearings shall be marked prior to shipping. These marks shall be permanent and in a readily visible location on the bearing. They shall note the position of the bearing and the direction ahead on station. Numerous field problems have occurred when bearings were not so marked. This is particularly true for minimally beveled sole plates. It is not always apparent which orientation a bearing must take prior to imposition of the dead load rotation.

1.6 Bearing Replacement Considerations

In some situations, existing bearings or elements thereof must be replaced as a result of excessive wear, damage, or seismic rehabilitation needs. Bearing replacement operations generally require lifting of superstructure elements using hydraulic jacks. Anticipated lifting loads should be stipulated on the contract drawings. Limitations on lift height should also be specified. Considerations should be given to lift height as it relates to adjacent expansion joint components and adjoining sections of safety railing. As mentioned earlier, new bearings should be detailed to allow replaceable elements to be removed and replaced with a maximum vertical jacking height of ¼ in. (6 mm). Superstructure stresses induced by nonuniform lifting are limited by imposing restrictions on differential lift height between adjacent jacks.

Experience concludes that actual lifting loads nearly always exceed calculated lifting loads. Many factors may contribute to this phenomenon, including friction in the hydraulic jack system and underestimation of superstructure dead loads. A typical contract provision is to require that all hydraulic jacks be sized for 200% of the calculated lifting load. In planning a bearing replacement project, the designer should verify from manufacturers' literature that appropriate hydraulic jacks are available to operate within the space limitations imposed by a particular design situation.

1.7 Design Examples

Two design examples are provided to illustrate the bearing design procedure: a steel reinforced elastomeric bearing and a longitudinally guided disc bearing.

1.7.1 Design Example 1—Steel Reinforced Elastomeric Bearing

Design of steel reinforced elastomeric bearings, as mentioned earlier, is an iterative process of checking several design requirements while varying bearing plan dimensions, number of elastomeric layers and corresponding thickness, and steel shim thicknesses. For precast prestressed concrete girders, this process is somewhat complicated by the need to track camber rotations at various stages under different loading conditions. In general, two times are most likely to be critical: (1) after girders are set but immediately before the slab is cast, at which time some of the prestressing has been lost and (2) after the bridge is constructed and live load is applied, at which time all prestressing losses have occurred. Both cases should be checked. For each instance, the 0.005 radian tolerance needs to be applied in the most critical direction, positive or negative.

Excellent examples of elastomeric bearing design for a precast prestressed concrete girders are included in Chapter 10 *Bearings* of the *Precast Prestressed Concrete Bridge Design Manual* (PCI 2011). A condensed version of one of these examples has been adapted to the following example.

1.7.1.1 Given

A single span precast prestressed concrete girder bridge near Minneapolis, Minnesota, has a total length of 120 ft. (36.6 m) with six equally loaded girders. The abutments are not skewed. Each girder end is supported on a 22-in. (559 mm) wide by 8-in. (203 mm) long steel reinforced elastomeric bearing. These bearings contain four interior elastomeric layers of ½-in. (12.7 mm) thickness and two exterior elastomeric layers of ¼-in. (6 mm) thickness. These layers are reinforced with five steel plates having a yield stress of 36 ksi (248 MPa). Assume that one end of the bridge is fixed against movement. The contract documents specify the shear modulus of the elastomer at 73°F (22.8°C) to be 165 psi (1.138 MPa). Current acceptance criteria allow the actual shear modulus, G, to vary by +/− 15% from the specified value. With the exception of checking the bearing against slippage, the critical extreme range value of 140 psi (0.965 MPa) is used in this example.

For the purpose of determining resulting displacements imposed upon each bearing, a sequence of nine movement phenomena are considered and included in this problem. These movements are: transfer of prestressing following girder casting, girder self-weight, creep and shrinkage occurring before each girder is erected on bearings, creep and shrinkage occurring after each girder is erected on the bearings, weight of slab on each girder, differential shrinkage of the slab after it is placed, uniform thermal expansion and contraction, lane live load, and truck live load. Because they occur prior to the girders being set onto the elastomeric bearings, the uniform shortening movements associated with the first three phenomena do not induce corresponding shear deformations in the bearings. However, because the bottom of the girder does not have a sloped recess to accommodate anticipated end rotations, all phenomena, with the exception of uniform thermal expansion and contraction, induce rotation in the bearings.

Nonthermal related longitudinal movements at the top of the bearing at the free end of the bridge have been calculated as follows, with negative numbers denoting movement toward midspan:

$\Delta_{\text{creep+shrinkage after girder erection}} = -0.418$ in.
$\Delta_{\text{DL slab}} = 0.333$ in.
$\Delta\text{differential}_{\text{shrinkage of slab}} = -0.071$ in.
$\Delta_{\text{LL lane}} = 0.109$ in.
$\Delta_{\text{LL truck}} = 0.208$ in.

It should be noted that the horizontal displacements reported earlier result from a combination of two effects: (1) change in the length of the concrete girder at its centroid and (2) end rotation of the girder about its centroid. For instance, creep and shrinkage of the girder following erection causes it to uniformly shorten and to deflect upward and rotate about its ends. The end rotation causes the bottom of the girder at the bearing to shift inward (toward midspan), augmenting the shortening effect. Similarly, differential shrinkage of the slab causes the girder to uniformly shorten and to deflect downward and rotate about its ends. In this case, the end rotation causes the bottom of the girder at the bearing to shift outward (away from midspan), reducing the uniform shortening effect. The longitudinal bearing movements listed earlier include both of these effects. For numerical derivation of the individual effects, see the *Precast Prestressed Concrete Bridge Design Manual* (PCI 2011).

Rotations imposed upon the bearings have been calculated as follows:

$\theta_{\text{initial prestress}} = -9.260 \times 10^{-3}$ rads
$\theta_{\text{DL girder}} = 3.597 \times 10^{-3}$ rads
$\theta_{\text{creep + shrinkage before girder erection}} = -2.900 \times 10^{-3}$ rads
$\theta_{\text{creep + shrinkage after girder erection}} = -1.450 \times 10^{-3}$ rads
$\theta_{\text{DL slab}} = 4.545 \times 10^{-3}$ rads
$\theta_{\text{differential shrinkage of slab}} = 2.370 \times 10^{-3}$ rads
$\theta_{\text{uniform thermal}} = 0.000$ rads
$\theta_{\text{LL lane}} = 0.997 \times 10^{-3}$ rads
$\theta_{\text{LL truck}} = 1.896 \times 10^{-3}$ rads

Vertical load effects on each bearing are as follows:

$P_{\text{DL girder}} = 47.9$ kips
$P_{\text{DL slab}} = 73.3$ kips
$P_{\text{LL lane}} = 33.9$ kips
$P_{\text{LL truck}} = 78.1$ kips

1.7.1.2 Requirements

Perform the following design calculations for a steel reinforced elastomeric beating in accordance with the *AASHTO LRFD Bridge Design Specifications*, 6th edition. (AASHTO 2012.)

- Determine the design thermal movement
- Check the adequacy of the bearing to accommodate maximum horizontal displacement, using the AASHTO LRFD Method B design procedure
- Calculate shape factor of the bearing
- Check service load combination
- Check condition immediately before deck placement
- Evaluate stability of the bearing
- Determine required thickness of steel reinforcement
- Determine low temperature requirements for the constituent elastomer
- Calculate approximate instantaneous dead load, the long-term dead load, and the live load compressive deformation of the bearings
- Consider hydrostatic stress

- Evaluate the need for providing anchorage against slippage

1.7.1.3 Solution

Step 1: Determine the design thermal movement

AASHTO LRFD Article 3.12.2 includes thermal contour maps for determining uniform temperature effects using the Method B procedure defined therein. These maps show $T_{MaxDesign}$ as 110°F (43.3°C) and $T_{MinDesign}$ as −20°F (−6.7°C) for concrete girder bridges with concrete decks near Minneapolis, Minnesota. These values are used to calculate the design thermal movement range, Δ_T.

$$\Delta_T = \alpha L(T_{MaxDesign} - T_{MinDesign}) \quad \text{[LRFD Eqn. 3.12.2.3–1]}$$

where L is expansion length (in.); α is coefficient of thermal expansion (in./in./°F).

$$\Delta_T = (0.000006)(120)(12)[110-(-20)] = 1.123\,\text{in.}$$

AASHTO LRFD Article 14.7.5.3.2 states that the maximum horizontal displacement of the bridge superstructure, Δ_0, shall be taken as 65% of the design thermal movement range, Δ_T, computed in accordance with Article 3.12.2 combined with the movement caused by creep, shrinkage, and posttensioning. Note that movement associated with superimposed dead load is not specified in this provision.

$$\text{Design thermal movement} = 0.65\Delta_T = 0.65(1.123) = 0.730\,\text{in.}$$

This movement can be either expansion or contraction. Uniform temperature change does not produce girder end rotation augmenting this movement.

Step 2: Check adequacy of the bearing to accommodate maximum horizontal displacement

As noted earlier, for the purpose of calculating the shear deformation in each bearing, the design thermal movement is added to all creep, shrinkage, and posttensioning effects that occur after the girders are set on the bearings.

$$\begin{aligned}\Delta_o &= 0.65\Delta_T + \Delta_{\text{creep + shrinkage after girder erection}} + \Delta_{\text{differential shrinkage of slab}} \\ &= -0.730 - 0.418 - 0.071 = -1.219\,\text{in.}\end{aligned}$$

AASHTO LRFD Article 14.7.5.3.2 requires that the total elastomer thickness, h_{rt}, should exceed twice the maximum total shear deformation, Δ_S. In this example, we take maximum total shear deformation as Δ_0.

$$h_{rt} = 4(0.5) + 2(0.25) = 2.5\ \text{in.} > 2(\Delta_S) = 2(\Delta_0) = 2(1.219) = 2.44\ \text{in.}\quad \text{O.K.}$$

Step 3: Calculate shape factor of the bearing

Shape factor is calculated by the following equation:

$$S_i = \frac{LW}{2h_{ri}(L+W)} \quad \text{[LRFD 14.7.5.1-1]}$$

where h_{ri} is thickness of the ith interior elastomeric layer of the bearing (in.); L is plan dimension of the bearing generally parallel to the global longitudinal bridge axis (in.); and W is plan dimension of the bearing generally parallel to the global transverse bridge axis (in.).

$$S_i = \frac{LW}{2h_{ri}(L+W)} = \frac{(8)(22)}{2(0.5)(8+22)} = 5.867$$

Step 4: Check service load combination

In this example, dead loading constitutes static loads while vehicular live loading constitutes cyclic loads. Vertical bearing force from static loads, P_{st} and vertical bearing force from cyclic loads, P_{cy} are calculated as follows:

$$P_{st} = P_{DL\,girder} + P_{DL\,slab} = 47.9 + 73.3 = 121.2 \text{ kip}$$

$$P_{cy} = P_{LL\,lane} + P_{LL\,truck} = 33.9 + 78.1 = 112.0 \text{ kip}$$

Vertical bearing stresses are calculated as follows:

$$\sigma_{a,st} = \frac{P_{st}}{LW} = \frac{121.2}{(8)(22)} = 0.689 \text{ ksi}$$

$$\sigma_{a,cy} = \frac{P_{cy}}{LW} = \frac{112.0}{(8)(22)} = 0.636 \text{ ksi}$$

$$\sigma_s = \sigma_{a,st} + \sigma_{a,cy} = 0.689 + 0.636 = 1.325 \text{ ksi}$$

Shear strain due to axial static load is taken as

$$\gamma_{a,st} = \frac{D_a \sigma_{a,st}}{GS_i} \quad \text{[LRFD 14.7.5.3.3-3]}$$

where D_a is a dimensionless coefficient taken as 1.4 for a rectangular bearing and 1.0 for a circular bearing. Shear strain due to axial cyclic load is taken similarly.
Shear strain due to axial static and cyclic loads are calculated as

$$\gamma_{a,st} = \frac{D_a \sigma_{a,st}}{GS_i} = \frac{(1.4)(0.689)}{(0.140)(5.867)} = 1.174$$

$$\gamma_{a,cy} = \frac{D_a \sigma_{a,cy}}{GS_i} = \frac{(1.4)(0.636)}{(0.140)(5.867)} = 1.084$$

Rotation due to static load is calculated as

$$\begin{aligned}\theta_{st} &= \theta_{\text{initial prestress}} + \theta_{DL\ girder} + \theta_{\text{creep+shrinkage before girder erection}} \\ &\quad + \theta_{\text{creep+shrinkage after girder erection}} + \theta_{DL\ slab} + \theta_{\text{differential shrinkage of slab}} \\ &= (-9.260 + 3.597 - 2.900 - 1.450 + 4.545 + 2.370)10^{-3} \\ &= -3.098(10^{-3}) \text{ rads}\end{aligned}$$

Rotation due to cyclic load is calculated as

$$\theta_{cy} = \theta_{LL\,lane} + \theta_{LL\,truck}$$
$$= (-0.997 + 1.896)10^{-3} = 2.893(10^{-3}) \text{ rads}$$

Apply the 0.005 rads tolerance for static rotation as both positive and negative:

$$\theta_{st-} = (-3.098)10^{-3} - 0.005 = -8.098(10^{-3}) \text{ rads}$$

$$\theta_{st+} = (-3.098)10^{-3} + 0.005 = 1.902(10^{-3}) \text{ rads}$$

Shear strain due to rotation is calculated as

$$\gamma_r = D_r\left(\frac{L}{h_{ri}}\right)^2\left(\frac{\theta_s}{n}\right) \quad \text{[LRFD 14.7.5.3.3-6]}$$

where D_r is a dimensionless coefficient taken as 0.5 for a rectangular bearing and 0.375 for a circular bearing; n is the number of internal elastomeric layers, allowing n to be augmented by ½ for each exterior layer having a thickness that is equal to or greater than half the thickness of an interior layer. θ_s is maximum static or cyclic rotation angle. Shear strains due to static and cyclic rotations are calculated as

$$\gamma_{r,st} = D_r\left(\frac{L}{h_{ri}}\right)^2\left(\frac{\theta_{st}}{n}\right) = (0.5)\left(\frac{8}{0.5}\right)^2\left(\frac{1.902\times10^{-3}}{5}\right) = 0.0487$$

$$\gamma_{r,cy} = D_r\left(\frac{L}{h_{ri}}\right)^2\left(\frac{\theta_{cy}}{n}\right) = (0.5)\left(\frac{8}{0.5}\right)^2\left(\frac{2.893\times10^{-3}}{5}\right) = 0.0741$$

Longitudinal deformations due to static and cyclic loads are calculated as

$$\Delta_{st} = 0.65(\Delta_T) + \Delta_{creep\,+\,shrinkage\,after\,girder\,erection} + \Delta_{DL\,slab} + \Delta_{differential\,shrinkage\,of\,slab}$$
$$= 0.730 - 0.418 + 0.333 - 0.071 = 0.574 \text{ in.}$$

$$\Delta_{cy} = \Delta_{LL\,lane} + \Delta_{LL\,truck} = 0.109 + 0.208 = 0.317 \text{ in.}$$

Shear strains due to shear deformation are calculated as

$$\gamma_s = \frac{\Delta_s}{h_{rt}} \quad \text{[LRFD 14.7.5.3.3-10]}$$

Shear strains due to static and cyclic longitudinal deformations are calculated as

$$\gamma_{s,st} = \frac{\Delta_{st}}{h_{rt}} = \frac{0.574}{2.5} = 0.230$$

$$\gamma_{s,cy} = \frac{\Delta_{cy}}{h_{rt}} = \frac{0.317}{2.5} = 0.127$$

Check service limit state requirements (LRFD Article 14.7.5.3.3) for the longitudinal direction:

$$\gamma_{a,st} = 1.174 < 3.0 \quad \text{O.K.}$$

$$\left(\gamma_{a,st}+\gamma_{r,st}+\gamma_{s,st}\right)+1.75\left(\gamma_{a,cy}+\gamma_{r,cy}+\gamma_{s,cy}\right)$$
$$=(1.174+0.0487+0.230)+(1.75)(1.084+0.0741+0.127)$$
$$=3.702<5.0 \quad \text{O.K.}$$

Check service limit state requirements (LRFD Article 14.7.5.3.3) for the transverse direction:

$\gamma_{a,st} = 1.174$ (same as longitudinal direction) < 3.00 O.K.
$\gamma_{a,cy} = 1.084$ (same as longitudinal direction)
$\theta_{st} = \theta_{cy} = 0.000$
$\theta_{st+} = 0.005$ rads

$$\gamma_{r,st} = D_r\left(\frac{W}{h_{ri}}\right)^2\left(\frac{\theta_{st}}{n}\right)=(0.5)\left(\frac{22}{0.5}\right)^2\left(\frac{0.005}{5}\right)=0.968$$

$$\gamma_{r,cy} = D_r\left(\frac{W}{h_{ri}}\right)^2\left(\frac{\theta_{cy}}{n}\right)=(0.5)\left(\frac{22}{0.5}\right)^2\left(\frac{0.000}{5}\right)=0$$

$$\left(\gamma_{a,st}+\gamma_{r,st}+\gamma_{s,st}\right)+1.75\left(\gamma_{a,cy}+\gamma_{r,cy}+\gamma_{s,cy}\right)$$
$$=(1.174+0.968+0)+(1.75)(1.084+0+0)$$
$$=4.039<5.0 \quad \text{O.K.}$$

Step 5: Check condition immediately before deck placement

$$P_{st} = 47.9 \text{ kip}$$

$$P_{cy} = 0.0 \text{ kip}$$

$$\sigma_{a,st} = \frac{P_{st}}{LW} = \frac{47.9}{(8)(22)} = 0.272 \text{ ksi}$$

$$\sigma_{a,cy} = \frac{P_{cy}}{LW} = \frac{0}{(8)(22)} = 0 \text{ ksi}$$

Check the longitudinal direction:

$$\gamma_{a,st} = \frac{D_a\sigma_{a,st}}{GS_i} = \frac{(1.4)(0.272)}{(0.140)(5.867)} = 0.464 < 3.0 \quad \text{O.K.}$$

$$\gamma_{a,cy} = \frac{D_a\sigma_{a,cy}}{GS_i} = \frac{(1.4)(0)}{(0.140)(5.867)} = 0$$

Rotation due to static load is calculated as

$$\theta_{st} = \theta_{\text{initial prestress}} + \theta_{\text{DL girder}} + \theta_{\text{creep+shrinkage before girder erection}} + \theta_{\text{creep+shrinkage after girder erection}}$$
$$=(-9.260+3.597-2.900-1.450)10^{-3}$$
$$=-10.013\left(10^{-3}\right) \text{ rads}$$

$$\theta_{cy} = \theta_{\text{LL lane}} + \theta_{\text{LL truck}} = 0 \text{ rads}$$

Apply the 0.005 rads tolerance as negative:

$$\theta_{st} = (-10.103)(10^{-3}) - 0.005 = -15.103(10^{-3}) \text{ rads}$$

$$\gamma_{r,st} = D_r\left(\frac{L}{h_{ri}}\right)^2\left(\frac{\theta_{st}}{n}\right) = (0.5)\left(\frac{8}{0.5}\right)^2\left(\frac{15.013\times10^{-3}}{5}\right) = 0.384$$

$$\gamma_{r,cy} = D_r\left(\frac{L}{h_{ri}}\right)^2\left(\frac{\theta_{cy}}{n}\right) = (0.5)\left(\frac{8}{0.5}\right)^2\left(\frac{0.000}{5}\right) = 0$$

The only significant horizontal displacement imposed upon the bearings immediately prior to slab placement is creep and shrinkage that occurs after the girder are erected upon the bearings. The thermal displacement range during the short interval between when the girders are erected and the slab is poured is deemed to be negligible.

$$\Delta_{st} = -0.418 \text{ in.}$$

$$\Delta_{cy} = 0 \text{ in.}$$

$$\gamma_{s,st} = \frac{\Delta_{st}}{h_{rt}} = \frac{0.418}{2.5} = 0.167$$

$$\gamma_{s,cy} = \frac{\Delta_{cy}}{h_{rt}} = \frac{0}{2.5} = 0$$

$$\begin{aligned}&(\gamma_{a,st} + \gamma_{r,st} + \gamma_{s,st}) + 1.75(\gamma_{a,cy} + \gamma_{r,cy} + \gamma_{s,cy})\\ &= (0.464 + 0.384 + 0.167) + (1.75)(0 + 0 + 0)\\ &= 1.015 < 5.0 \quad \text{O.K.}\end{aligned}$$

Check the transverse direction:

$\gamma_{a,st} = 0.464$ (same as longitudinal direction) < 3.00 O.K.
$\gamma_{a,cy} = 0.000$ (same as longitudinal direction)
$\theta_{st} = \theta_{cy} = 0.000$
$\theta_{st+} = 0.005$ rads

$$\gamma_{r,st} = D_r\left(\frac{W}{h_{ri}}\right)^2\left(\frac{\theta_{st}}{n}\right) = (0.5)\left(\frac{22}{0.5}\right)^2\left(\frac{0.005}{5}\right) = 0.968$$

$$\gamma_{r,cy} = D_r\left(\frac{W}{h_{ri}}\right)^2\left(\frac{\theta_{cy}}{n}\right) = (0.5)\left(\frac{22}{0.5}\right)^2\left(\frac{0.000}{5}\right) = 0$$

$$\gamma_{s,st} = \gamma_{s,cy} = 0.000$$

$$\begin{aligned}&\left(\gamma_{a,st}+\gamma_{r,st}+\gamma_{s,st}\right)+1.75\left(\gamma_{a,cy}+\gamma_{r,cy}+\gamma_{s,cy}\right)\\&=(0.464+0.968+0.000)+(1.75)(0+0+0)\\&=1.432<5.0\quad\text{O.K.}\end{aligned}$$

Step 6: Evaluate stability of the bearing

Per LRFD Article 14.7.5.3.4, bearings shall be investigated for instability at the service limit state load combination. First, consider stability in the longitudinal direction.

$$A=\frac{1.92\frac{h_{rt}}{L}}{\sqrt{1+\frac{2L}{W}}}=\frac{(1.92)\frac{2.5}{8.0}}{\sqrt{1+\frac{(2)(8)}{22}}}=0.457\qquad\text{[LRFD 14.7.5.3.4-2]}$$

$$B=\frac{2.67}{(S_i+2.0)\left(1+\frac{L}{4W}\right)}=\frac{2.67}{(5.867+2)\left(1+\frac{8}{(4)(22)}\right)}=0.311\qquad\text{[LRFD 14.7.5.3.4-3]}$$

Because $2A = 2(0.457) = 0.914 > B = 0.311$, further investigation is required.

The bridge is fixed against horizontal translation in the longitudinal direction, requiring that

$$\sigma_s=\sigma_{a,st}+\sigma_{a,cy}=0.689+0.636=1.325\text{ ksi}$$

$$\sigma_s=1.325\text{ ksi}<\frac{GS_i}{A-B}=\frac{(0.140)(5.867)}{0.457-0.311}=5.626\text{ ksi}\qquad\text{[LRFD 14.7.5.3.4-5]}\quad\text{O.K.}$$

Next, consider stability in the transverse direction.

$$A=\frac{1.92\frac{h_{rt}}{W}}{\sqrt{1+\frac{2W}{L}}}=\frac{(1.92)\frac{2.5}{22}}{\sqrt{1+\frac{(2)(22)}{8}}}=0.0856\qquad\text{[LRFD 14.7.5.3.4-2]}$$

$$B=\frac{2.67}{(S_i+2.0)\left(1+\frac{W}{4L}\right)}=\frac{2.67}{(5.867+2)\left(1+\frac{22}{(4)(8)}\right)}=0.201\qquad\text{[LRFD 14.7.5.3.4-3]}$$

Because $2A = 2(0.0856) = 0.171 < B = 0.201$, no further investigation is required.

Step 7: Determine required thickness of steel reinforcement

At the service limit state:

$$h_s\ge\frac{3h_{ri}\sigma_s}{F_y}\qquad\text{[LRFD 14.7.5.3.5-1]}$$

where F_y is the yield strength of steel reinforcement = 36 ksi; and σ_s is average compressive stress due to total load at the service limit state.

$$h_s \geq \frac{3h_{ri}\sigma_s}{F_y} = \frac{(3)(0.5)(1.325)}{36} = 0.055 \text{ in.}$$

At the fatigue limit state:

$$h_s \geq \frac{2h_{ri}\sigma_L}{\Delta F_{TH}} \quad \text{[LRFD 14.7.5.3.5-2]}$$

where σ_L is average compressive stress due to live load; ΔF_{TH} is constant amplitude fatigue threshold for Category A, as specified in LRFD Article 6.6.

$$h_s \geq \frac{2h_{ri}\sigma_L}{\Delta F_{TH}} = \frac{(2)(0.5)(0.636)}{20} = 0.032 \text{ in.}$$

Since the minimum thickness of steel reinforcement $h_{s,min} = 0.0625$ in. is specified in the current AASHTO M251 specification, the steel shims shall be at least 1/16 in. thick.

Step 8: Determine low temperature requirements for the constituent elastomer

For the purpose of bearing design, the AASHTO LRFD classifies all bridges in the United States as being in either Zone A, B, C, D, or E. LRFD Figure 14.7.5.2-1 shows Minneapolis as being within Zone D. Zone D is associated with a 50-year low temperature of −45°F (−42.8°C). LRFD Table 14.7.5.2-1 requires a Grade 4 elastomer for bridges located in Zone D unless special force provisions are incorporated into the design. When special force provisions are incorporated into the design, a Grade 3 elastomer is permissible. In summary, LRFD Article 14.7.5.2 allows three options:

Option 1: Specify a Grade 4 elastomer and determine the shear force transmitted by the bearing in accordance with LRFD Article 14.6.3.1.

Option 2: Specify a Grade 3 elastomer and provide a low-friction sliding surface, in which case the shear force transmitted by the bearing shall be assumed as twice that computed in accordance with LRFD Article 14.6.3.1.

Option 3: Specify a Grade 3 elastomer without providing a low-friction sliding surface, in which case the shear force transmitted by the bearing shall be assumed as four times that computed in accordance with LRFD Article 14.6.3.1.

Step 9: Calculate approximate instantaneous dead, long-term dead, and live load compressive deformation of the bearing

Limiting instantaneous live load deflections is important to ensure that deck expansion joints are not damaged. Steel reinforced elastomeric bearings exhibit nonlinear compressive load-deflection behavior. Compressive stiffness of an elastomeric layer substantially increases with increasing shape factor. The total compressive deformation of an elastomeric bearing is equal to the sum of the compressive deformation of all its constituent elastomeric layers.

LRFD commentary allows an assumed linear relationship between compressive stress and compressive strain. Specifically, compressive strain can be estimated as

$$\varepsilon = \frac{\sigma}{6GS_i^2} \quad \text{[LRFD C14.7.5.3.6-1]}$$

Thus, initial dead load deformation can be estimated as follows:

$$\varepsilon_{di} = \frac{\sigma_{a,st}}{6GS_i^2} = \frac{0.689}{(6)(0.140)(5.867)^2} = 0.0238$$

Note that the smallest acceptable value of shear modulus has been used. This will result in the largest compressive deformation. Because the bearing is composed of four interior layers and two exterior layers all having essentially the same shape factor, the total initial dead load deflection can be estimated as

$$\delta_d = \sum \varepsilon_{di} h_{ri} = (0.0238)(5)(0.5) = 0.06 \text{ in.}$$

Long-term dead load deflection includes the effects of creep as follows:

$$\delta_{lt} = \delta_d + a_{cr}\delta_d \quad \text{[LRFD 14.7.5.3.6-3]}$$

where a_{cr} is a factor representing approximate creep deformation divided by initial dead load deformation.
For an elastomer having a Shore A Hardness of 60 (assumed shear modulus at 73°F between 0.130 ksi and 0.200 ksi), LRFD Table 14.7.6.2-1 estimates a_{cr} as being 0.35. Hence,

$$\delta_{lt} = \delta_d + a_{cr}\delta_d = 0.06 + (0.35)(0.06) = 0.081 \text{ in.}$$

Similarly, the instantaneous live load deformation can be estimated as follows:

$$\varepsilon_{Li} = \frac{\sigma_{a,cy}}{6GS_i^2} = \frac{0.636}{(6)(0.140)(5.867)^2} = 0.022$$

$$\delta_L = \sum \varepsilon_{Li} h_{ri} = (0.022)(5)(0.5) = 0.055 \text{ in.}$$

Step 10: Consider hydrostatic stress
The bearing has no externally bonded steel plates. Therefore, hydrostatic stress is not a consideration.

Step 11: Evaluate the need for providing anchorage against slippage
The traditional anchorage check contained in previous editions of AASHTO design codes has been to compare the maximum horizontal force induced in the elastomeric bearing versus the incipient force required to cause the bearing to slip. This check was generally performed using service loads and assumed a friction coefficient of 0.20 between the elastomer and the concrete surface.
The maximum shear displacement of the bearings occurs at the extreme low temperature in the absence of live loading.

$$\Delta = -0.418 - 0.071 + 0.333 - 0.730 = -0.886 \text{ in.}$$

The maximum longitudinal force induced in the elastomeric bearing, assuming a Grade 4 elastomer, as a result of this shear displacement is

$$H_s = \frac{GA_{br}\Delta_s}{h_{rt}} = \frac{(0.190)(22)(8)(0.886)}{2.5} = 11.85 \text{ kip} \quad \text{O.K.}$$

$$H_{sliding} = \mu P_{DL} = \mu P_{st} = (0.2)(121.2) = 24.24 \text{ kip} > H_s = 11.85 \text{ kip}$$

The upper range shear modulus of 0.190 ksi (1.31 MPa) is the critical value in this calculation. It represents 115% of the nominal specified value. LRFD Article 14.6.3.1 further requires that the superstructure and substructure be designed to transmit, at the strength and extreme limit states, the horizontal forces induced by sliding friction or shear deformation of flexible bearing elements.

Article 14.7.5.4 of the current LRFD specifications requires a check of rotation versus axial strain for bearings without externally bonded steel plates. A restraint system is required whenever

$$\frac{\theta_s}{n} \geq \frac{3\varepsilon_a}{S_i} \quad \text{[LRFD 14.7.5.4-1]}$$

where ε_a is total of static and cyclic average axial strain taken as positive for compression in which the cyclic component if multiplied by 1.75 from the applicable service load combination in AASHTO LRFD Table 3.4.1-1; θ_s is total of static and cyclic maximum service limit state design rotations of the elastomer specified in which the cyclic component is multiplied by 1.75.

$$\theta_s = \theta_{st} + 1.75\theta_{cy} = (1.902)(10^{-3}) + (1.75)(2.893)(10^{-3}) = 6.965 \times 10^{-3} \text{ rads}$$

$$\varepsilon_a = \frac{\sigma_{st} + 1.75\sigma_{cy}}{6GS_i^2} = \frac{0.689 + (1.75)(0.636)}{(6)(0.140)(5.867)^2} = 0.0623$$

$$\frac{\theta_s}{n} = \frac{6.965 \times 10^{-3}}{5} = 0.00139 > \frac{3\varepsilon_a}{S} = \frac{(3)(0.0623)}{5.867} = 0.0319$$

Therefore, no restraint system is required.

1.7.2 Design Example 2—Longitudinally Guided Disc Bearing

1.7.2.1 Given

For a steel box girder bridge, the service dead load is 680 kips (3,025 kN). The service live load without impact is 320 kips (1423 kN). The horizontal strength limit state load is 640 kips (2847 kN). The allowable compressive stress for the polyether urethane material constituting the disc is 5.00 ksi (34.5 MPa). The compressive stress–strain relationship for the disc may be estimated as $\sigma = E(1+S^2)\varepsilon$, where E is Young's modulus. For the polyether urethane used in this bearing, E may be taken as 10 ksi (68.9 MPa). Long-term creep is taken as 20% of dead load compressive deformation. The disc element is sandwiched by upper and lower bearing plates having a yield strength of 50 ksi (345 MPa). The 95 ksi (655 MPa) yield strength shear resisting pin is threaded (12 threads per inch) into the lower bearing plate and bears against a hole in the upper bearing plate.

A longitudinally guided disc bearing differs from the fixed disc bearing depicted in Figure 1.12 in that it incorporates a horizontal PTFE/stainless steel sliding interface and guide bars similar to those depicted in the spherical bearing shown in Figure 1.14. The top of the upper bearing plate is recessed 3/32 in. (2.4 mm) for 3/16 in. (4.8 mm) thick unfilled PTFE having a diameter of 18½ in. (470 mm).

The maximum service limit state rotation for the bearing is 0.020 rads. The maximum strength limit state rotation for the bearing is 0.029 rads. Both these rotations include a 0.005 rads allowance for uncertainties.

1.7.2.2 Requirements

Perform the following design calculations for a longitudinally guided disc bearing in accordance with the *AASHTO LRFD Bridge Design Specifications*, 6th edition (2012).

- Determine the required diameter of the steel shear-resisting pin
- Determine the required diameter of the polyether urethane disc
- Verify the adequacy of a 1–7/8 in. (48 mm) thick disc
- Determine the minimum length of engagement and check the adequacy of the shear-resisting pin for combined flexure and shear
- Check PTFE average contact stresses and edge contact stress

1.7.2.3 Solution

The design of the disc is governed by AASHTO LRFD Article 14.7.8. The design of the PTFE is governed by AASHTO LRFD Article 14.7.2. The design of the shear-resisting pin is governed by AASHTO LRFD Article 6.7.6. Strength limit state resistance factors for shear, bearing, and flexure are taken from AASHTO LRFD Article 6.5.4.2.

Step 1: Determine required diameter of the shear-resisting pin

The shear force associated with the horizontal strength limit state load determines the minimum diameter of the steel shear-resisting pin.

$$H_{\text{strength}} \le \varphi_v (0.58)(F_{\text{y,pin}})(\pi) D_{\text{pin,eff}}^2 / 4$$

$$D_{\text{pin,eff}} = D_{\text{pin}} - \frac{0.9743}{n_{\text{tpi}}}$$

where H_{strength} is the horizontal strength limit state load (kips); φ_v is the shear resistance factor = 1.0; $F_{\text{y, pin}}$ is the yield stress of the steel shear-resisting pin = 95 (ksi); D_{pin} is the nominal diameter of the steel shear-resisting pin (in.); $D_{\text{pin,eff}}$ is the minimum effective diameter of the threaded portion of the steel shear-resisting pin calculated in accordance with ASME B1.1-1989 (in.); and n_{tpi} is the number of threads per inch.

$$D_{\text{pin,eff}} \ge \sqrt{\frac{4(H_{\text{strength}})}{\varphi_v (0.58)(F_{\text{y,pin}})\pi}}$$

$$= \sqrt{\frac{4(640)}{(1.00)(0.58)(95)(3.14)}}$$

$$= 3.85 \text{ in.}$$

$$D_{\text{pin}} \ge D_{\text{pin,eff}} + \frac{0.9743}{n_{\text{tpi}}} = 3.85 + \frac{0.9743}{12} = 3.93 \text{ in.}$$

To optimize machining operations, D_{pin} is selected as 5.25 in.

Step 2: Determine the required diameter of the polyether urethane disc

$$A_{\text{reqd}} \geq \frac{P_{\text{service}}}{\sigma_{\text{disc}}} = \frac{(320+680)}{5.000} = 200 \text{ in.}^2$$

where P_{service} is the vertical service load (kips); σ_{disc} is the allowable compressive stress in the disc (ksi); and A_{reqd} is the required net area of the disc (in.^{2}).
The polyether urethane disc is essentially an annular ring with a steel shear-resisting pin in the center. A 1/16 in. gap separates the pin from the inside vertical edge of the annular disc. The outer edge of the disc is V-shaped as depicted in Figure 1.12. The V-shape accommodates bulging under load. Each leg of the "V" forms a 30° angle with the vertical.

$$D_{\text{inside}} = 5.25 + 2(0.0625) = 5.375 \text{ in.}$$

$$\begin{aligned} A_{\text{lost}} &= \pi(D_{\text{inside}})^2/4 \\ &= (3.1416)(5.375)^2/4 \\ &= 22.69 \text{ in.}^2 \end{aligned}$$

where D_{inside} is the inside diameter of the disc; and A_{lost} is the voided central area of the disc (in.^{2}).

$$A_{\text{reqd}} \leq \frac{\pi D_{\text{disc}}^2}{4} - A_{\text{lost}}$$

where D_{disc} is the outside diameter of the disk at its mid-depth.

$$\begin{aligned} D_{\text{disc}} &\leq \sqrt{\frac{4(A_{\text{reqd}} + A_{\text{lost}})}{\pi}} \\ &= \sqrt{\frac{4(200+22.69)}{3.1416}} \\ &= 16.84 \text{ in.} \end{aligned}$$

Establish a practical manufacturing diameter of the top and bottom bearing surfaces of the disk, accounting for the "V"-shaped notch.

$$D_{\text{base}} \geq 16.84 + (1.875)(\tan 30°) = 17.92 \text{ in.} \rightarrow \text{Use } 18 \text{ in.}$$

Step 3: Verify adequacy of the 1–7/8 in. thickness of the polyether urethane disc

$$D_{\text{disc}} = D_{\text{base}} - (t_{\text{disc}})(\tan\theta_v) = 18 - (1.875)(\tan 30°) = 16.92 \text{ in.}$$

where t_{disc} is thickness of the disc (in.); θ_v is the angle of the "V"-shaped edge relative to vertical.

$$A_{\text{disc}} = \pi(D_{\text{disc}}^2 - D_{\text{inside}}^2)/4$$

$$A_{\text{disc}} = \frac{(3.1416)[(16.92)^2 - (5.375)^2]}{4} = 202.16 \text{ in.}^2$$

$$\sigma_s = \frac{P_{\text{service}}}{A_{\text{disc}}} = \frac{(320+680)}{202.16} = 4.947 \text{ ksi} < 5.000 \text{ ksi} \quad \rightarrow \quad \text{O.K.}$$

Calculate the shape factor of the disc.

$$S = \text{Shape factor} = \frac{\text{Plan area of bearing}}{\text{Bearing area free to bulge}}$$

$$S = \frac{A_{\text{disc}}}{(\pi)(D_{\text{disc}})(t_{\text{disc}})} = \frac{202.16}{(3.1416)(16.92)(1.875)} = 2.028$$

AASHTO LRFD Article 14.7.8.3 limits instantaneous compressive deformation under total service load to not more than 10% of the thickness of the unstressed disc. It additionally limits additional deformation due to creep to no more than 8% of the unstressed disc thickness. This article further proscribes lift off of component elements of the disc bearing, effectively imposing limits on allowable service limit state rotation.
Calculate the instantaneous compressive deformation of the disk under total service load and compare with the allowable deformation.

$$\varepsilon_{si} = \frac{1}{E(1+S^2)}\sigma_s = \frac{1}{(10)(1+2.028^2)}\sigma_s = 0.0196\sigma_s$$

$$\varepsilon_{si} = (0.0196)(4.947) = 0.0970 \text{ in./in.}$$

$$\delta_{si} = \varepsilon_{si} t_{\text{disc}}$$

$$\delta_{si} = (0.0970)(1.875) = 0.182 \text{ in.}$$

where ε_{si} is the instantaneous compressive strain in the disk under full service load (in./in.); and δ_{si} is the instantaneous compressive deformation of the disk under full service load (in.).

$$\delta_{si,\text{allowable}} = (0.10)(1.875) = 0.188 \text{ in.} > 0.182 \text{ in.} = \delta_{si} \quad \text{O.K.}$$

Calculate the additional creep deformation of the disc under dead load and compare with the allowable deformation.

$$\sigma_d = \frac{P_d}{A_{\text{disc}}} = \frac{320}{202.16} = 1.583 \text{ ksi}$$

$$\varepsilon_{di} = 0.0196\,\sigma_d = (0.0196)(1.583) = 0.0310 \text{ in./in.}$$

$$\delta_{di} = \varepsilon_{di} t_{\text{disc}} = (0.0310)(1.875) = 0.058 \text{ in.}$$

$$\delta_{\text{creep}} = 0.20\,\delta_{di} = (0.20)(0.058) = 0.012 \text{ in.}$$

where P_d is the dead load (kips); σ_d is the average dead load compressive stress on the disc (ksi); ε_{di} is the instantaneous compressive strain in the disk under dead load (in./in.); and δ_{di} is the instantaneous compressive deformation of the disk under dead load (in.).

$$\delta_{\text{creep,allowable}} = (0.08)(1.875) = 0.150 \text{ in.} > 0.012 \text{ in.} = \delta_{\text{creep}} \qquad \text{O.K.}$$

Compare rotation at liftoff to maximum service limit state rotation.

$$\theta_{s,liftoff} = \frac{2(\delta_{si})}{D_{disc}} = \frac{2(0.182)}{16.92} = 0.022 \text{ rads} \geq 0.020 \text{ rads} = \theta_s \qquad \text{O.K.}$$

Step 4: Determine minimum engagement length and check combined flexure and shear on the shear-resisting pin

The required diameter of the steel shear-resisting pin has already been determined in *Step 1*. AASHTO LRFD Article 6.7.6 further stipulates the design of the steel shear-resisting pin as it relates to bearing and combined flexure and shear. The pin is threaded into the lower bearing plate and bears against a hole in the upper bearing plate. The minimum engagement length of the pin against each bearing plate is determined by checking against the allowable bearing force. The maximum bending moment in the pin is calculated from the required engagement length and the compressed height of the disc under dead load.

$$H_{strength} \leq \varphi_b(1.5)(L_{engage})(D_{pin,eff})(F_y) \quad \text{[LRFD 6.7.6.2.2-1 and 2]}$$

where L_{engage} is the engagement length of the pin with each bearing plate (in.); F_y is the lesser of the yield strengths of the pin and bearing plates (ksi); and φ_b is the bearing resistance factor = 1.0.

$$D_{pin,eff} = D_{pin} - \frac{0.9743}{n_{tpi}} = 5.25 - \frac{0.9743}{12} = 5.169 \text{ in.}$$

$$L_{engage} \geq \frac{H_{strength}}{(\varphi_b)(1.5)(D_{pin,eff})(F_y)} = \frac{640}{(1.0)(1.5)(5.169)(50)} = 1.651 \text{ in.}$$

$$d = t_{disc} - \delta_{di} + \frac{L_{engage}}{2}$$
$$= 1.875 - 0.058 + \frac{1.651}{2} = 2.642 \text{ in.}$$

where d is the distance from the point of maximum bending moment in the pin (top of lower bearing plate) to the resultant of the bearing force in the upper bearing plate (in.).

$$M_u = H_{strength}(d) = (640)(2.642) = 1691 \text{ in. kips}$$

$$Z = \frac{D_{pin,eff}^3}{6} = \frac{5.169^3}{6} = 23.018 \text{ in.}^3$$

where M_u is the strength limit state maximum moment in the pin; and Z is the plastic section modulus of the pin (in.^{3}).

$$\varphi_f M_n = Z(F_{y,pin}) = (1.00)(23.018)(95) = 2187 \text{ in. kips} > 1690 \text{ in. kips}$$

where φ_f is the flexure resistance factor = 1.0; and M_n is the nominal plastic moment capacity of the pin.
Check combined flexure and shear.

$$\frac{6(M_u)}{\varphi_f\left(D_{pin,eff}^3\right)\left(F_{y,pin}\right)}+\left(\frac{2.2(V_u)}{\varphi_v\left(D_{pin,eff}^2\right)\left(F_{y,pin}\right)}\right)^3 \le 0.95 \quad \text{[LRFD 6.7.6.2.1-1]}$$

$$\frac{6(1691)}{1.00(5.169)^3(95)}+\left(\frac{2.2(640)}{1.00(5.169)^2(95)}\right)^3 = 0.944 \le 0.95 \quad \text{O.K.}$$

Step 5: Check PTFE contact stresses
For confined sheet PTFE, AASHTO LRFD Article 14.7.2.4 limits average contact stress for permanent loads to 3.0 ksi and average contact stress for all loads to 4.5 ksi at the service limit state. Edge contact stress for all loads at the service limit state is further limited to 5.5 ksi.

$$A_{ptfe} = \frac{\pi}{4}D_{ptfe}^2 = \frac{3.1416}{4}(18.5)^2 = 268.8 \text{ in.}^2$$

where D_{ptfe} is the diameter of the confined PTFE sheet (in.); and A_{ptfe} is the plan area of the confined PTFE sheet (in.^{2}).

$$\sigma_{d,ptfe} = \frac{P_d}{A_{ptfe}} = \frac{320}{268.8} = 1.190 \text{ ksi} < 3.0 \text{ ksi} \quad \text{O.K.}$$

where $\sigma_{d,ptfe}$ is the average dead load contact stress on the PTFE.

$$\sigma_{s,ptfe} = \frac{P_{service}}{A_{ptfe}} = \frac{(320+680)}{268.8} = 3.720 \text{ ksi} < 4.5 \text{ ksi} \quad \text{O.K.}$$

where $\sigma_{s,ptfe}$ is the average service load contact stress on the PTFE.
Edge contact stress is evaluated by calculating the moment induced in the polyether urethane disc element due to the maximum service limit state rotation. This moment is transferred through the PTFE by contact stresses.

$$I_{disc} = \frac{\pi}{64}(D_{disc}^4 - D_{inside}^4) = \frac{\pi}{64}(16.92^4 - 5.375^4) = 3982 \text{ in.}^4$$

$$M_s = 0.5(E_c)(I)\frac{\theta_s}{t} = 0.5(E)(1+S^2)\frac{\theta_s}{t}$$

$$M_s = 0.5(10)(1+2.028^2)(3982)\frac{0.020}{1.875} = 1086 \text{ in. kips}$$

$$S_{ptfe} = \frac{\pi}{32}D_{ptfe}^3 = \frac{3.1416}{32}(18.5)^3 = 621.6 \text{ in.}^3$$

where M_s is the moment induced in the polyether urethane disc element due to the maximum service limit state rotation; and S_{ptfe} is the section modulus of the PTFE surface.

$$\sigma_{ptfe,edge} = \frac{P_{service}}{A_{ptfe}} + \frac{M_s}{S_{ptfe}} = \frac{(320+680)}{268.8} + \frac{1086}{621.6} = 5.467 \text{ ksi} < 5.500 \text{ ksi} \quad \text{O.K.}$$

where $\sigma_{ptfe,edge}$ is the maximum compressive stress on a PTFE edge.

The upper and lower bearing plates, sole plate, masonry plate, and bolted connections need to be designed to transfer all loads between the superstructure and the substructure. As part of a continuous load path, the bearing plates need to be designed of sufficient thickness to transfer to the sole and masonry plates the same horizontal loads imposed upon the steel shear-resisting pins. Stainless steel sliding surfaces need to be detailed to provide sufficient travel distance to accommodate all anticipated movements. Clearances must be adequate to accommodate unrestrained service limit state movements. Additionally, guide bars need to be designed and detailed to accommodate the transfer of transverse loads between the sole plate and the upper bearing block. As noted earlier, it is important that bearings be designed and detailed to allow for the inspection, maintenance, and future removal and replacement of all sliding interface elements.

References

AASHTO. 2012. *AASHTO LRFD Bridge Design Specifications, 6th Edition*. American Association of State Highway and Transportation Officials, Washington, DC.

AASHTO/NSBA. 2004. *Steel Bridge Bearing Design and Detailing Guidelines, G 9.1* – 2004. American Association of State Highway and Transportation Official/National Steel Bridge Alliance Steel Bridge Collaboration, Chicago, IL.

Lehman, D.E., C.W. Roeder, R. Larson, K. Curtin. 2003. Cotton duck Bearing Pads: Engineering Evaluation and Design Recommendations. Prepared for the Washington State Transportation Commission. Available at: http://www.wsdot.wa.gov/research/reports/fullreports/569.1.pdf

PCI. 2011. *Precast Prestressed Concrete Bridge Design Manual*. Precast/Prestressed Concrete Institute, Chicago, IL.

Stanton, J.F., C.W. Roeder, P. Mackenzie-Helnwein, C. White, C. Kuester, B. Craig. 2008. Rotation Limits for Elastomeric Bearings, NCHRP Report 596, Transportation Research Board, National Research Council, Washington, DC.

Stanton, J.F., C.W. Roeder, T.I. Campbell. 1999. High Load Multi-Rotational Bridge Bearings, National Cooperative Highway Research Program Report 432, Transportation Research Board, National Research Council, Washington, DC.

Stanton, J.F., J.C. Taylor. 2010. Friction Coefficients for Stainless Steel (PTFE) Bearings, Report No. WHRP 10-01, Wisconsin Highway Research Program, Madison, WI.

Washington State Department of Transportation. 2011. *Bridge Design Manual*, Chapter 9. Washington State Department of Transportation, Olympia, WA.

2

Piers and Columns

Jinrong Wang
California Department of Transportation

2.1 Introduction

Piers provide vertical supports for bridge spans at intermediate points and perform two main functions: transferring superstructure vertical loads to the foundations and resisting horizontal forces acting on the bridge. Although piers are traditionally designed to carry vertical loads, these days it is common for designers to take into account the high lateral loads caused by seismic events. Even in some low-seismic areas, designers are paying more attention to the ductility aspect of the design.

Piers are predominately constructed with reinforced concrete. Steel, to a lesser degree, is also used for piers. Steel tubes filled with concrete, known as composite columns, have been used in some recent projects in China and other countries.

This chapter deals only with piers or columns for conventional highway bridges, such as grade separations, overcrossings, overheads, underpasses, and simple river crossings. Reinforced concrete columns will be discussed in detail, whereas steel and composite columns will be discussed briefly. Substructures for arch, suspension, segmental, cable-stayed, and movable bridges are excluded from this chapter. Chapter 3 discusses the substructures for some of these special types of bridges.

2.2 Structural Types

2.2.1 General

"Pier" is usually used as a general term for any type of intermediate substructures located between horizontal spans and foundations. However, from time to time, it is also used particularly for a solid wall in order to distinguish it from columns or bents. From a structural point of view, a column is a member that resists the lateral force mainly by flexure action, whereas a pier is a member that resists the lateral force mainly by a shear mechanism. A pier consisting of multiple columns is often called the "bent."

There are several ways of defining pier types. One is by its structural connectivity to the superstructure: monolithic or cantilevered. Another is by its sectional shape: solid or hollow; round, octagonal, hexagonal, or rectangular. It can also be distinguished by its framing configuration: single- or multiple-column bent; hammerhead or pier wall. Figure 2.1 shows a series of columns in a typical urban

FIGURE 2.1 Columns in a typical urban interchange.

FIGURE 2.2 Columns in Skyway structure of San Francisco–Oakland Bay Bridge.

interchange. The smooth monolithic construction not only creates an esthetically appealing structure but also provides an integral system to resist the seismic forces. Figure 2.2 shows one example of water crossings, the newly constructed Skyway of San Francisco–Oakland Bay Bridge.

2.2.2 Selection Criteria

Selection of the type of piers for a bridge should be based on functional, structural, and geometric requirements. Esthetics is also a very important factor of selection because modern highway bridges are

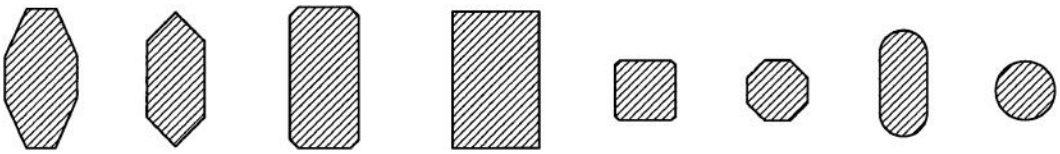

FIGURE 2.3 Typical cross-section shapes of piers for overcrossings or viaducts on land.

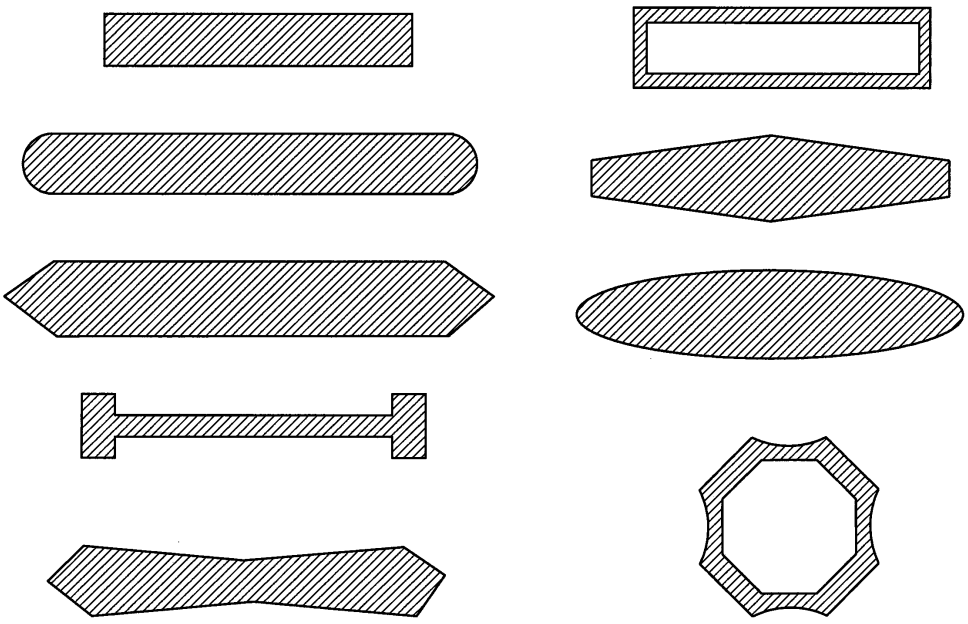

FIGURE 2.4 Typical cross-section shapes of piers for river and waterway crossings.

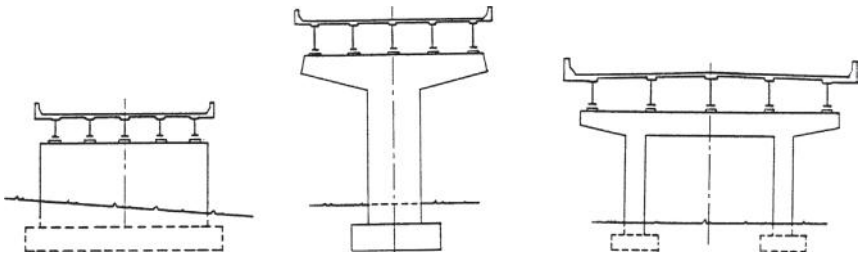

FIGURE 2.5 Typical pier types for steel bridges: (a) Solid wall pier (b) Hammerhead pier (c) Rigid frame pier.

often a part of the landscape of a city. Figure 2.3 shows a collection of typical cross-section shapes for overcrossings and viaducts on land, and Figure 2.4 shows some typical cross-section shapes for piers of river and waterway crossings. Often times, pier types are mandated by government agencies or owners. Many state Departments of Transportation in the United States have their own standard column shapes.

Solid wall piers, as shown in Figures 2.5a and 2.6, are often used at water crossings because they can be constructed to proportions that both are slender and streamlined. These features lend themselves well for providing minimal resistance to water flows.

Hammerhead piers, as shown in Figure 2.5b, are often found in urban areas where space limitation is a concern. They are used to support steel girder or precast prestressed concrete girder superstructures. They are esthetically appealing and generally occupy less space, thereby providing more room for the traffic underneath. Standards for the use of hammerhead piers are often maintained by individual transportation department.

A bent consists of a cap beam and supporting columns forming a frame. Bents, as shown in Figure 2.5c and Figure 2.7, can be used either to support a steel girder superstructure or as an integral bent where the cast-in-place construction technique is used. The columns can be either circular or polygonal in cross section. They are by far the most popular forms of piers in the modern highway systems.

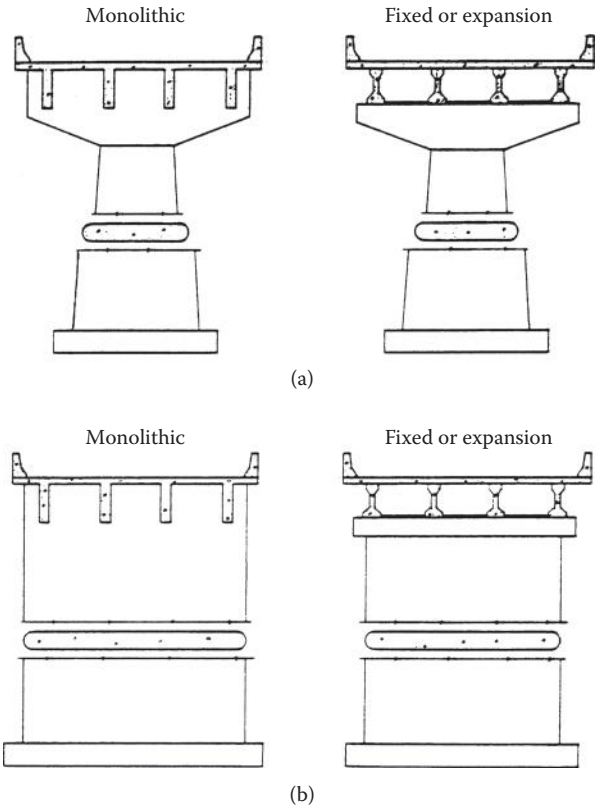

FIGURE 2.6 Typical pier types and configurations for river and waterway crossings: (a) Hammerhead (b) Solid wall.

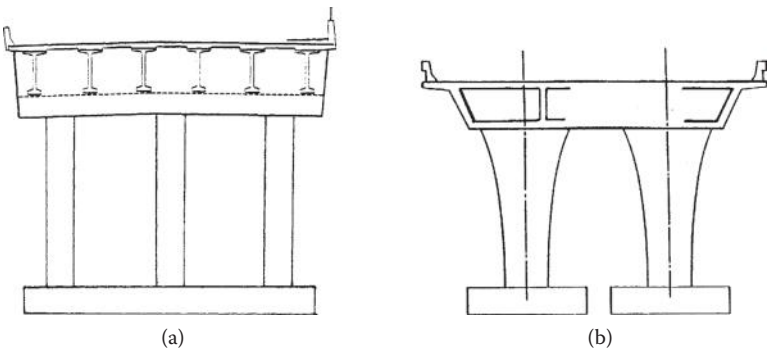

FIGURE 2.7 Typical pier types for concrete bridges: (a) Bent for precast girders (b) Bent for cast-in place griders.

A pile extension pier consists of a drilled shaft as the foundation and the circular column extended above the shaft to form the substructure. An obvious advantage of this type of pier is that they occupy a minimal amount of space. Widening an existing bridge in some instances may require pile extensions because space limitation precludes the use of other types of foundations.

Selection of proper pier type depends on many factors. First, it depends on the type of superstructure. For example, steel girder superstructures are normally supported by cantilevered piers, whereas the cast-in-place concrete superstructures are normally supported by monolithic bents. Second, it depends on the locations of bridges. Pier walls are preferred on river crossings, where debris is a concern and hydraulics dictates. Column bents are typically used in street crossings and highway separations. Multiple pile extension bents are commonly used on slab bridges. Last, the height of piers also dictates the type of selection of piers. The taller piers often require hollow cross sections in order to reduce the weight of the substructure. This then reduces the load demands on the costly foundations. Table 2.1 summarizes the general type selection guidelines for different types of bridges.

TABLE 2.1 General Guidelines for Selecting Pier Types

Location	Tall or Short Piers	Applicable Pier Types
	Steel Superstructure	
Over water	Tall piers	Pier walls or hammerheads (T-piers) (Figure 2.5a and b), hollow cross sections for most cases, cantilevered, could use combined hammerheads with pier wall base and step tapered shaft
	Short piers	Pier walls or hammerheads (T-piers) (Figure 2.5b and c), solid cross sections, cantilevered
On land	Tall piers	Hammerheads (T-piers) and possibly rigid frames (multiple column bents) (Figure 2.5b and c), hollow cross sections for single shaft and solid cross sections for rigid frames, cantilevered
	Short piers	Hammerheads and rigid frames (Figure 2.5b and c), solid cross sections, cantilevered
	Precast prestressed concrete superstructure	
Over water	Tall piers	Pier walls or hammerheads (Figure 2.6), hollow cross sections for most cases, cantilevered, could use combined hammerheads with pier wall base and step tapered shaft
	Short piers	Pier walls or hammerheads, solid cross sections, cantilevered
On land	Tall piers	Hammerheads and possibly rigid frames (multiple column bents), hollow cross sections for single shafts and solid cross sections for rigid frames, cantilevered
	Short piers	Hammerheads and rigid frames (multiple column bents) (Figure 2.7a), solid cross sections, cantilevered
	Cast-in-place concrete superstructure	
Over water	Tall piers	Single shaft pier (Figure 2.6), superstructure will likely cast by traveled forms with balanced cantilevered construction method, hollow cross sections, monolithic, fixed at bottom
	Short piers	Pier walls (Figure 2.6), solid cross sections, monolithic, fixed at bottom
On land	Tall piers	Single or multiple column bents, solid cross sections for most cases, monolithic, fixed at bottom
	Short piers	Single or multiple column bents (Figure 2.7b), solid cross sections, monolithic, pinned at bottom

2.3 Design Loads

Piers are commonly subjected to forces and loads transmitted from the superstructure and forces acting directly on the substructure. Some of the loads and forces to be resisted by piers include the following:

- Dead loads
- Live loads and impact from the superstructure
- Wind loads on the structure and the live loads
- Centrifugal force from the live loads
- Longitudinal force from live loads
- Drag forces due to the friction at bearings
- Stream flow pressure
- Ice pressure
- Earthquake forces
- Thermal and shrinkage forces
- Ship impact forces
- Force due to prestressing of superstructure
- Forces due to differential settlement of foundations

The effect of temperature changes and shrinkage of the superstructure needs to be considered when the superstructure is rigidly connected with the supports. Where expansion bearings are used, forces caused by temperature changes are limited to the frictional resistance of the bearings.

The readers should refer to Chapter 6 of *Bridge Engineering Handbook, Second Edition: Fundamentals* for more details about various loads and load combinations and Chapter 7 of *Bridge Engineering Handbook, Second Edition: Seismic Design* about earthquake loads. In the following, however, two load cases, live loads and thermal forces, are discussed in detail because they are two of the most common loads on the piers but are often applied incorrectly in the design.

2.3.1 Live Loads

Bridge live loads are the loads specified or approved by the contracting agencies and owners. They are usually specified in the design codes such as AASHTO LRFD Bridge Design Specifications (AASHTO 2012). There are other special loading conditions peculiar to the type or location of the bridge structure, which should be specified in the contracting documents.

Live load reactions obtained from the design of individual member of the superstructure should not be used directly for substructure design. These reactions are based on maximum conditions for one beam and make no allowance for the distribution of live loads across the roadway. Using these maximum loadings would result in a pier design with an unrealistically severe loading condition and uneconomical sections.

For substructure design, the maximum reaction of design traffic lane using either the standard truck load or standard lane load or a combination of both should be used. In AASHTO LRFD (AASHTO 2012), Section 3.6 specifies the width of design traffic lane as 3.6 m (12 ft) and three load combinations:

1. A design tandem combined with the design lane load.
2. A design truck with variable axial spacing combined with the design lane load.
3. Ninety percent of two design trucks spaced a minimum 15.2 m (50 ft) between the lead axle of one truck and the rear axle of the other truck, combined with 90% of the design lane load. The distance between the 142.3 kN (32 kip) axle should be fixed at 4.3 m (14 ft) (Figure 2.8).

Each state transportation agency may add one more load condition that considers its own permit loads and their combination.

For the calculation of the actual beam reactions on the piers, the maximum lane reaction can be applied within the design traffic lanes as wheel loads and then distributed to the beams, assuming the

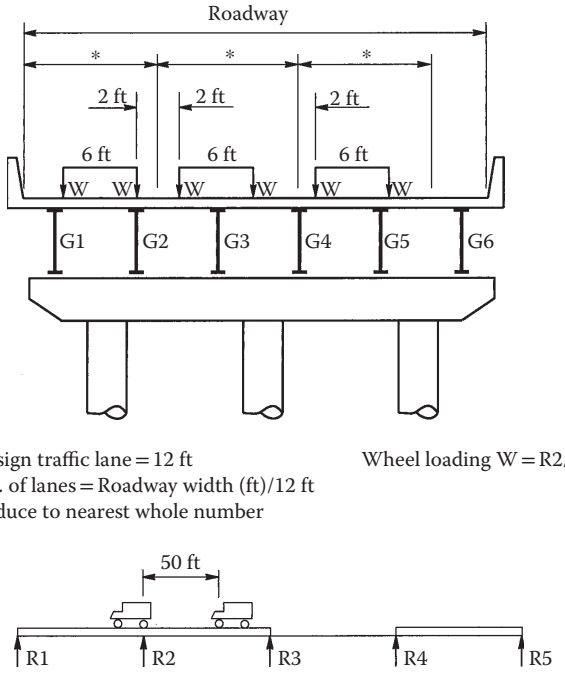

FIGURE 2.8 Wheel load arrangement to produce maximum reaction at R2.

TABLE 2.2 Dynamic Load Allowance, IM

Component	IM (%)
Deck joints—all limit states	75
All other components	
• Fatigue and fracture limit state	15
• All other limit states	33

slab between the beams to be simply supported (Figure 2.8) if the bent is cantilevered. Wheel loads can be positioned anywhere within the design traffic lane with a minimum distance between lane boundary and wheel load of 0.61 m (2 ft). For integral bent cap, the bent should be modeled as a frame. The calculated reactions due to the wheel load should be applied to the beam element of this frame. The design traffic lanes and the live load within the lanes should be arranged to produce beam reactions that result in maximum loads on the piers. These reactions should be multiplied by a multiple presence factor, *m*, as specified in Section 3.6.1.1.2 of AASHTO LRFD (AASHTO 2012).

Live load reactions shall be increased due to impact effect. AASHTO LRFD (AASHTO 2012) refers to this as the *Dynamic load allowance, IM*, and is listed here in Table 2.2.

2.3.2 Thermal Forces

Forces on piers due to thermal movements, shrinkage and prestressing of superstructures can become significant on short, stiff bents of prestressed concrete bridges with monolithic bents. Pier design should be checked against these forces. Design codes or specifications normally specify the design temperature range. Some codes even specify temperature distribution along the depth of the superstructure member.

The first step in determining the thermal forces on the substructures for a bridge with monolithic bents is to determine the point of no movement. After this point is determined, one can calculate the relative displacement of any point along the superstructure to this point by the distance to this point times the temperature range and times the coefficient of expansion. With known displacement at the top and known boundary conditions at the top and bottom, the forces on the pier due to the temperature change can be calculated by using the displacement times the stiffness of the pier.

The determination of point of no movement is best demonstrated by the following example, which is adapted from Memo to Designers issued by California Department of Transportation (Caltrans 1994).

Example 2.1

A 225.55-m (740-ft) long and 23.77-m (78-ft) wide concrete box girder superstructure is supported by 5 two-column bents. The size of the column is 1.52 m (5 ft) in diameter, and the heights vary between 10.67 m (35 ft) and 12.80 m (42 ft). Other assumptions are listed in the calculations. The calculation is done through a table. Figure 2.9 demonstrates the calculation for determining the point of no movement.

2.4 Design Considerations

2.4.1 Overview

Like the design of any structural component, the design of piers or columns is performed to fulfill strength and serviceability requirements. A pier as a structure component is subjected to combined forces of axial, bending, and shear. For a reinforced concrete pier, the bending strength is axial force dependent. The shear strength is also affected by bending and axial loads. To consider the actual behavior of a longer column, the bending moment will be magnified by the axial force due to the P-Δ effect.

In current design practice, the bridge designers are paying increasing attention to the adverse effects of earthquake. Therefore, ductility consideration has become a very important factor for bridge design. Failure due to scouring is also a common cause of failure of bridges. In order to prevent this type of failure, the bridge designers need to work closely with the hydraulic engineers to determine adequate depths of cover for the foundations and provide proper protection measures.

2.4.2 Slenderness and Second-Order Effect

The design of compression members must be based on forces and moments determined from an analysis of the structure. Small deflection theory is usually adequate for the analysis of beam-type members. For compression members, however, the second-order effects must be considered. According to AASHTO LRFD (AASHTO 2012), the second-order effect is defined as follows: "The presence of compressive axial forces amplify both out-of-straightness of a component and the deformation due to nontangential loads acting thereon, therefore increasing the eccentricity of the axial force with respect to the centerline of the component. The synergistic effect of this interaction is the apparent softening of the component, i.e., a loss of stiffness." To accurately assess this effect, a properly formulated large deflection nonlinear analysis can be performed. Discussions on this subject can be found in White and Hajjar (1994), Galambos (1998), and Chapter 5 of *Bridge Engineering Handbook, Second Edition: Seismic Design*. However, it is impractical to expect the practicing engineers to perform this type of sophisticated analysis on regular bases. The moment magnification procedure given in AASHTO LRFD (AASHTO 2012) is an approximate process that was selected as a compromise between accuracy and ease of use. Therefore, the AASHTO LRFD (AASHTO 2012) moment magnification procedure is outlined in the following.

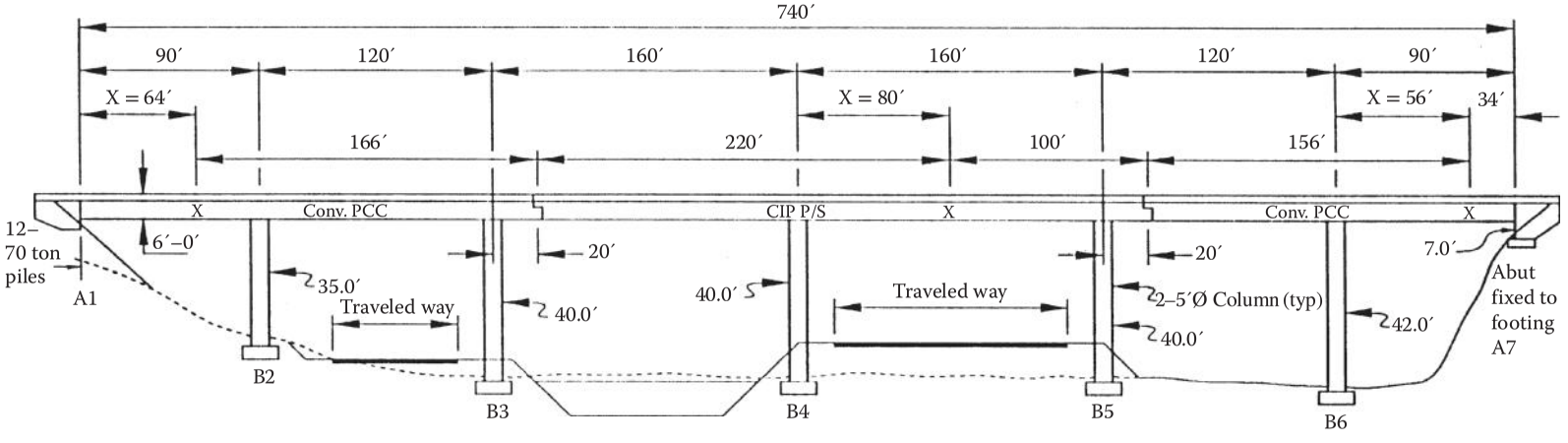

	A1		B2		B3			B4		B5			B6		A7		
I (Ft)^4	1.38		61.36		61.36			61.36		61.36			61.36		102		
L (Ft)	5.50		35.0		40.0		Sum	40.0		40.0		Sum	42.0		7.0		Sum
P (kips) @ 1" side sway	1200	+	618	+	415	=	2233	415	+	415	=	830	359 Will slide	+	600	=	959
D (distance from 1st member of frame)	0		90		210			0		160			0		90		
P × D / 100	0	+	556	+	872	=	1428	0	+	664	=	664	0	+	540	=	540
$X = \frac{\Sigma(P \times D)/100}{\Sigma P}(100) = \frac{1428}{2233}(100) = \underline{64'}$								$\frac{664}{830}(100) = \underline{80'}$					$\frac{540}{959}(100) = \underline{56'}$				

Notes:

Width of structure = 78′
Diameter of column = 5′–0′
K/Pile @ 1" deflection = 100 kips
Point of no movement = X
Refer to properties/piles table

Assumptions:

1. Super str. inf. rigid
2. Columns fixed top and bottom
3. Abutment footing will slide @ a force equal to D.W.
4. E (piles) = 4×10^8 psi
   E (columns) = 3×10^6 psi

Fixed/fixed condition

$$P\,(\text{Col.}) = 12EI\,\frac{A}{L^3}$$

$$@\ 1\text{" defl.} = \frac{4321}{\left(\frac{L}{10}\right)^3}$$

Pinned/fixed condition

$$P\,(\text{Col.}) = 3EI\,\frac{A}{L^3}$$

$$@\ 1\text{" defl.} = \frac{1081}{\left(\frac{L}{10}\right)^3}$$

D.W. Abut 7 = 600 k (assume linear up to 1" deflection)

$$I\,(\text{abut}) = \frac{78}{12}\,(2.5)^3$$

$$= 102$$

FIGURE 2.9 Calculation of points of no movement.

When a compression member's cross-sectional dimensions are small in comparison with its length, the member is said to be slender. Whether a member can be considered slender is dependent on the magnitude of the member's slenderness ratio. The slenderness ratio of a compression member is defined as, KL_u/r, where K is the effective length factor for compression members; L_u is the unsupported length of compression member; r radius of gyration $= \sqrt{I/A}$; I the moment of inertia; A the cross-sectional area.

When a compression member is braced against sidesway, the effective length factor, $K = 1.0$ can be used. However, a lower value of K may be used if further analysis demonstrated that a lower value is warranted. L_u is defined as the clear distance between slabs, girders, or other members that is capable of providing lateral support for the compression member. If haunches are present, then, the unsupported length is taken from the lower extremity of the haunch in the considered plane (AASHTO LRFD 5.7.4.3). For a detailed discussion of the K-factor, refer to Chapter 18 of *Bridge Engineering Handbook, Second Edition: Fundamentals*.

For a concrete column braced against sidesway, the effect of slenderness may be ignored as long as the following condition is met (AASHTO LRFD 5.7.4.3):

$$\frac{KL_u}{r} < 34 - \left(\frac{12M_1}{M_2}\right) \tag{2.1}$$

where M_1 and M_2 are smaller and larger end moments on a compression member, respectively, the term (M_1/M_2) is positive for single-curvature flexure.

For an unbraced concrete column, the effect of slenderness may be ignored as long as the following condition is met (AASHTO LRFD 5.7.4.3):

$$\frac{KL_u}{r} < 22 \tag{2.2}$$

If the slenderness ratio exceeds the above specified limits, the effects can be approximated by the use of moment magnification factor. If the slenderness ratio KL_u/r exceeds 100, however, a more detailed second-order nonlinear analysis will be required. Any detailed analysis should consider the influence of axial loads and variable moment of inertia on member stiffness and forces and the effects of the duration of the loads.

$$M_c = \delta_b M_{2b} + \delta_s M_{2s} \tag{2.3}$$

The factored moments may be increased to reflect effects of deformations as follows:

where M_{2b} = moment on compression member due to factored gravity loads that result in no appreciable sidesway calculated by conventional first-order elastic frame analysis, always positive.

M_{2s} = moment on compression member due to lateral or gravity loads that result in sidesway, Δ, greater than $L_u/1500$, calculated by conventional first-order elastic frame analysis, always positive. L_u is in same unit as Δ.

The moment magnification factors are defined as follows:

$$\delta_b = \frac{C_m}{1 - \dfrac{P_u}{\phi_K P_e}} \geq 1.0 \tag{2.4}$$

$$\delta_s = \frac{1}{1 - \dfrac{\sum P_u}{\phi_K \sum P_e}} \tag{2.5}$$

(Please note that the above two equations are revised in AASHTO 2012 edition.)

where ϕ_K is stiffness reduction factor; 0.75 for concrete, 1.0 for steel and aluminum members; P_u is factored axial load; and P_e is Euler buckling load that is determined as follows:

$$P_e = \frac{\pi^2 EI}{(KL_u)^2} \tag{2.6}$$

C_m, a factor that relates the actual moment diagram to an equivalent uniform moment diagram, is typically taken as 1.0. However, in the case where the member is braced against sidesway and without transverse loads between supports, it may be taken by the following expression:

$$C_m = 0.6 + 0.4\left(\frac{M_{1b}}{M_{2b}}\right) \tag{2.7}$$

where M_{1b} and M_{2b} are smaller and larger end moments on a compression member, respectively, the ratio (M_{1b}/M_{2b}) is positive for single-curvature flexure and negative for double-curvature flexure.

To compute the flexural rigidity EI for concrete columns, AASHTO LRFD (AASHTO 2012) offers two possible solutions taken as the greater of

$$EI = \frac{\frac{E_c I_g}{5} + E_s I_s}{1 + \beta_d} \tag{2.8}$$

$$EI = \frac{\frac{E_c I_g}{2.5}}{1 + \beta_d} \tag{2.9}$$

where E_c is the elastic modulus of concrete, I_g the gross moment inertia, E_s the elastic modules of reinforcement, I_s the moment inertia of reinforcement about centroidal axis, and β_d is the ratio of maximum factored permanent load moment to maximum factored total load moment and is always positive. It is an approximation of the effects of creep, so that when larger moments are induced by loads sustained over a long period of time, the creep deformation and associated curvature will also be increased.

2.4.3 Concrete Piers and Columns

2.4.3.1 Combined Axial and Flexural Strength

A critical aspect of the design of bridge piers is the design of compression members. We use AASHTO LRFD Bridge Design Specifications (AASHTO 2012) as the reference code. The following discussion provides an overview of some of the major criteria governing the design of compression members.

Under the Strength Limit State Design, the factored resistance is determined by the product of nominal resistance, P_n, and the resistance factor, ϕ. For nonprestressed members, a lower ϕ factor of 0.75 is used for compression-controlled sections, whereas a higher ϕ factor of 0.9 is used for tension-controlled sections. The value ϕ is linearly varied from 0.75 to 0.9 depending on the net tensile strain as follows:

$$0.75 \le 0.65 + 0.15\left(\frac{d_t}{c} - 1\right) \le 0.9 \tag{2.10}$$

where c is distance from the extreme compression fiber to the neutral axis, and d_t is distance from the extreme compression fiber to the centroid of the extreme tension steel element.

2.4.3.1.1 Interaction Diagrams

Flexural resistance of a concrete member is dependent on the axial force acting on the member. Interaction diagrams are usually used as aids for the design of the compression members. Interaction diagrams for columns are usually created assuming a series of strain distributions and computing the corresponding values of P and M. Once enough points have been computed, the results are plotted to produce an interaction diagram.

Figure 2.10 shows a series of strain distributions and the resulting points on the interaction diagram. In an actual design, though, a few points on the diagrams can be easily obtained and can define the diagram rather closely.

Pure Compression The factored axial resistance for pure compression, ϕP_n, may be computed by

For nonprestressed members with spiral reinforcement

$$P_r = \phi P_n = \phi 0.85 P_o = \phi 0.85\left[0.85 f_c'(A_g - A_{st}) + A_{st} f_y\right] \tag{2.11}$$

For nonprestressed members with tie reinforcement:

$$P_r = \phi P_n = \phi 0.80 P_o = \phi 0.80\left[0.85 f_c'(A_g - A_{st}) + A_{st} f_y\right] \tag{2.12}$$

For design, pure compression strength is a hypothetical condition since almost always there will be moments present due to various reasons. For this reason, AASHTO LRFD 5.7.4.4 limits the nominal axial load resistance of compression members to 85% and 80% of the axial resistance at zero eccentricity, P_o, for spiral and tied columns, respectively.

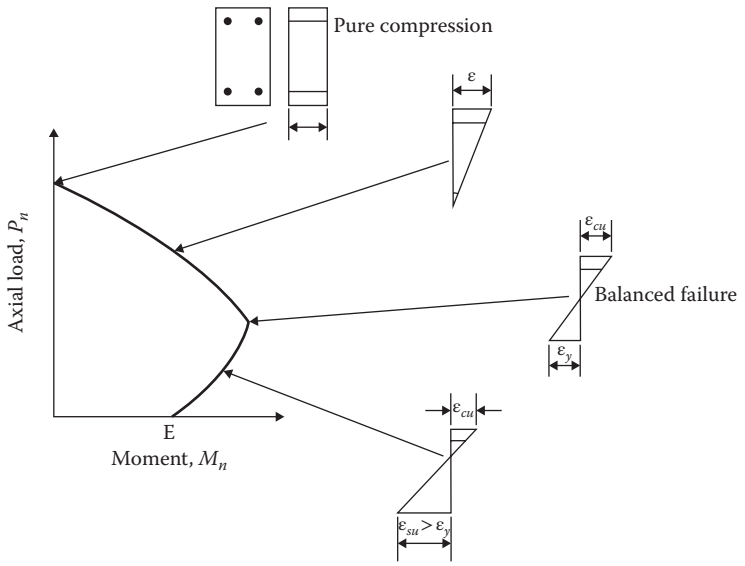

FIGURE 2.10 Strain distributions corresponding to points on interaction diagram.

Pure Flexure The rectangular section in this case is only subjected to bending moment and without any axial force. The factored flexural resistance, M_r, may be computed by

$$\begin{aligned} M_r &= \phi M_n = \phi\left[A_s f_y d\left(1 - 0.6\rho\frac{f_y}{f_c'}\right)\right] \\ &= \phi\left[A_s f_y\left(d - \frac{a}{2}\right)\right] \end{aligned} \tag{2.13}$$

where

$$a = \frac{A_s f_y}{0.85 b f_c'} \tag{2.14}$$

Balanced Strain Condition Balanced strain condition corresponds to the strain distribution where the extreme concrete strain reaches 0.003 and the strain in reinforcement reaches yield at the same time. At this condition, the section has the highest moment capacity. For a rectangular section with reinforcement in one face or located in two faces at approximately the same distance from the axis of bending, the balanced factored axial resistance, P_r, and balanced factored flexural resistance, M_r, may be computed by

$$P_r = \phi P_b = \phi\left[0.85 f_c' b a_b + A_s' f_s' - A_s f_y\right] \tag{2.15}$$

and

$$M_r = \phi M_b = \phi\left[0.85 f_c' b a_b\left(d - d'' - \frac{a_b}{2}\right) + A_s' f_s'(d - d' - d'') + A_s f_y d''\right] \tag{2.16}$$

where

$$a_b = \left(\frac{600}{600 + f_y}\right)\beta_1 d \qquad \left(f_y \text{ in MPa}; a_b \text{ and } d \text{ in mm}\right) \tag{2.17}$$

$$a_b = \left(\frac{87{,}000}{87{,}000 + f_y}\right)\beta_1 d \qquad \left(f_y \text{ in psi}; a_b \text{ and } d \text{ in inch}\right) \text{ and}$$

$$f_s' = 0.003\left[\frac{a - \beta_1 d'}{a}\right]E_s \le f_y \qquad \left(f_y \text{ in the same unit as } E_s\right) \tag{2.18}$$

2.4.3.1.2 Biaxial Bending

AASHTO LRFD 5.7.4.5 stipulates that the design strength of noncircular members subjected to biaxial bending may be computed, in lieu of a general section analysis based on stress and strain compatibility, by one of the following approximate expressions:

When the factored axial load, $P_u \ge 0.10\phi f_c' A_g$

$$\frac{1}{P_{rxy}} = \frac{1}{P_{rx}} + \frac{1}{P_{ry}} - \frac{1}{P_o} \tag{2.19}$$

when the factored axial load, $P_u < 0.10\phi f_c' A_g$

$$\frac{M_{ux}}{M_{rx}}+\frac{M_{uy}}{M_{ry}}\le 1 \tag{2.20}$$

where P_{rxy} is factored axial resistance in biaxial flexure; P_{rx}, P_{ry} are factored axial resistance corresponding to M_{rx} and M_{ry}, respectively; M_{ux}, M_{uy} are factored applied moment about the x-axis and y-axis, respectively; M_{rx}, M_{ry} are uniaxial factored flexural resistance of a section about the x-axis and y-axis, respectively, corresponding to the eccentricity produced by the applied factored axial load and moment and

$$P_o = 0.85 f_c'\left(A_g - A_s\right) + A_s f_y \tag{2.21}$$

The above procedure is only used in special circumstances. Generally, designers rely on computer programs based on equilibrium and strain compatibility to generate a moment–axial interaction diagram. For cases like noncircular members with biaxial flexure, an interaction surface is required to describe the behavior. Figure 2.11 shows a typical moment–axial load interaction surface for a concrete section. In a day-to-day practice, such a surface has little value to designers. Rather, the design program normally gives out a series of lines, basically slices of the surface, at fixed interval, such as 15°. Figure 2.12 is an example of such plot.

From these lines, one can see that below the balanced condition the moment capacity increases with the increase of axial load. So, when designing a column, it is not enough to simply take a set of maximum axial load with maximum bending moments. The following combinations should to be evaluated:

1. $M_{ux\,max}$, corresponding M_{uy} and P_u
2. $M_{uy\,max}$, corresponding M_{ux} and P_u
3. A set of M_{ux} and M_{uy} that gives largest M_u combined and corresponding P_u
4. $P_{u\,max}$ and corresponding M_{ux} and M_{uy}

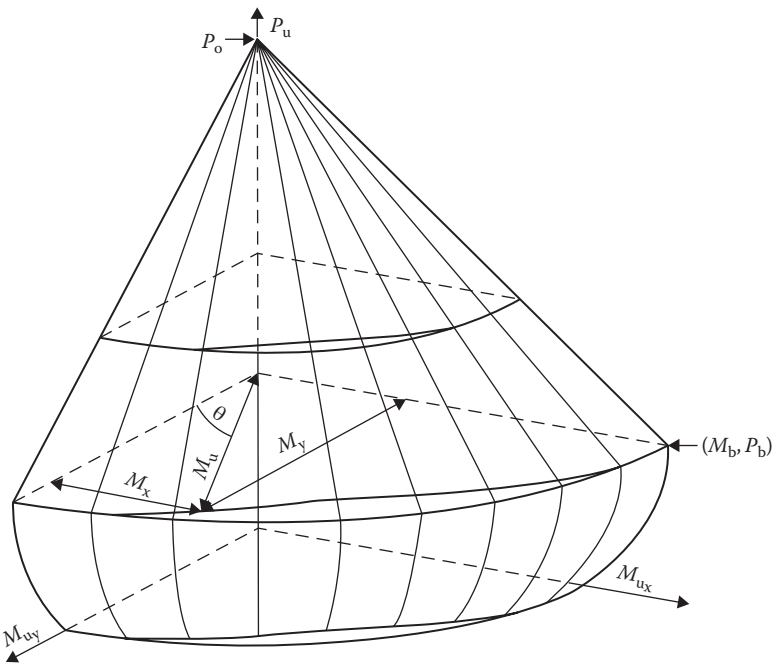

FIGURE 2.11 The moment–axial load interaction surface for a noncircular section.

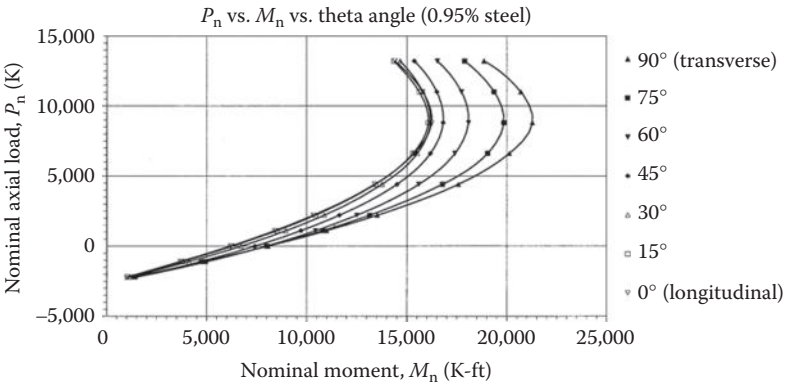

FIGURE 2.12 Interaction diagrams generated by a column design program.

2.4.3.2 Shear Strength

Under the normal load conditions, the shear seldom governs the design of the column for conventional bridges because the lateral loads are usually small compared to the vertical loads. However, in a seismic design, the shear is very important. In recent years, great effort has been put forth on the evaluation of shear strength of columns, especially on the interaction between shear and flexure in the plastic hinge zone. AASHTO LRFD (2012) provides a general shear strength calculation procedure that applies for both beams and columns. The concrete shear capacity component and the angle of inclination of diagonal compressive stresses are functions of the shear stress on the concrete and the strain in the reinforcement on the flexural tension side of the member. It is rather involved and hard to use. ACI Code (2011) has a set of simpler equations, but they do not address the shear strength in the plastic hinge zones. The procedure presented by Paulay and Priestley (1992) overcomes both of those shortcomings but does not include the effect of displacement ductility demand on the shear strength. The procedure adapted by California Department of Transportation (Caltrans) in its *Seismic Design Criteria* (Caltrans 2013) addresses all these factors and is presented here.

The shear strength at a section is given as follows:

$$V_n = V_c + V_s \tag{2.22}$$

where V_c is the contribution of the concrete to shear strength and V_s the contribution of shear reinforcement.

$$V_c = v_c A_e \tag{2.23}$$

$$A_e = 0.8 \times A_g \tag{2.24}$$

- Inside the plastic hinge zone

$$v_c = \text{Factor}\,1 \times \text{Factor}\,2 \times \sqrt{f_c'} \le 0.33\sqrt{f_c'}\ (\text{MPa}) \tag{2.25}$$

$$v_c = \text{Factor}\,1 \times \text{Factor}\,2 \times \sqrt{f_c'} \le 4\sqrt{f_c'}\ (\text{psi})$$

- Outside the plastic hinge zone

$$v_c = 0.25 \times \text{Factor 2} \times \sqrt{f'_c} \le 0.33\sqrt{f'_c}\ (\text{MPa}) \tag{2.26}$$

$$v_c = 3 \times \text{Factor 2} \times \sqrt{f'_c} \le 4\sqrt{f'_c}(\text{psi})$$

where

$$0.025 \le \text{Factor 1} = \frac{\rho_s f_{yh}}{12.5} + 0.305 - 0.083\mu_d \le 0.25 \left(f_{yh} \text{ in MPa}\right) \tag{2.27}$$

$$0.3 \le \text{Factor 1} = \frac{\rho_s f_{yh}}{0.150\ ksi} + 3.67 - \mu_d \le 3 \left(f_{yh} \text{ in ksi}\right)$$

In Equation 2.27, the value of "$\rho_s f_{yh}$" shall be limited to 0.35 ksi. Figure 2.13 shows value of Factor 1 that varies over the range of displacement ductility demand ratios, μ_d.

$$\text{Factor 2} = 1 + \frac{P_c}{13.8 \times A_g} \le 1.5 \quad (\text{metric units}) \tag{2.28}$$

$$\text{Factor 2} = 1 + \frac{P_c}{2000 \times A_g} \le 1.5 \left(\text{English units}\right)$$

In Equation 2.28, P_c is in N (lb), and A_g is in mm^2 (in^2).

For members whose net axial load is in tension, *Seismic Design Criteria* does not count the concrete in resisting shear, $v_c = 0$.

For members subjected to minor tension, totally ignoring the shear strength of concrete may be unnecessarily conservative. ACI Code (2011) uses the following multiplier to account for the reduction of the strength due to tension, which is equivalent to Factor 2 of above equation:

$$\text{Factor 2} = \left(1 + \frac{P_c}{3.45 A_g}\right) \qquad (\text{metric units}) \tag{2.29}$$

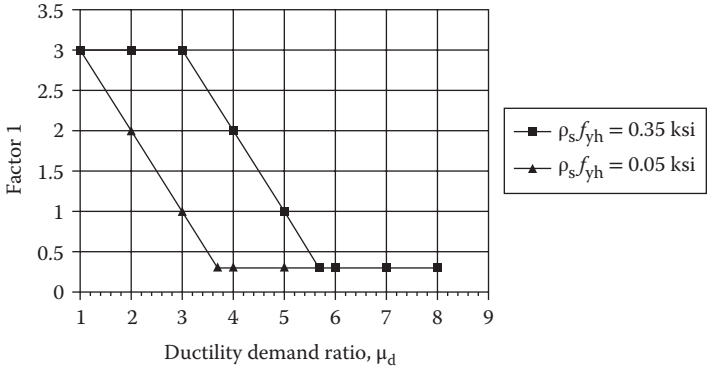

FIGURE 2.13 Factor 1 versus displacement ductility demand ratio, μ_d.

$$\text{Factor } 2 = \left(1 + \frac{P_c}{500\ A_g}\right) \qquad (\text{English units})$$

In Equation 2.29, P_c is in N (lb), and A_g is in mm^2 (in^2).

This multiplier should not be less than zero, where P_c is negative for tension,

where A_g is gross section area of the column; A_e is effective section area, can be taken as $0.8A_g$; P_c is axial force applied to the column; and f_c' is compressive strength of concrete.

The nominal shear contribution from reinforcement is given by

$$V_s = \frac{A_v f_{yh} d}{s} \tag{2.30}$$

for tied rectangular sections and

$$V_s = \frac{\pi}{2}\frac{A_h f_{yh} D'}{s} \tag{2.31}$$

for spirally reinforced circular sections. In these equations, A_v is the total area of shear reinforcement parallel to the applied shear force, A_h the area of a single hoop, f_{yh} the yield stress of horizontal reinforcement, D' the diameter of a circular hoop, and s the spacing of horizontal reinforcement.

2.4.3.3 Ductility of Columns

The AASHTO LRFD (2012) introduces the term of ductility and requires that a structural system of bridge shall be designed to ensure the development of significant and visible inelastic deformations before failure.

The term *ductility* defines the ability of a structure and selected structural components to deform beyond elastic limits without excessive strength or stiffness degradation. In mathematic terms, the ductility μ is defined by the ratio of the total imposed displacement Δ at any instant to that at the onset of yield Δ_y. This is a measure of the ability for a structure, or a component of a structure, to absorb energy. The goal of seismic design is to limit the estimated maximum ductility demand to the ductility capacity of the structure during a seismic event. For concrete columns, the confinement of concrete must be provided, and a good detailing practice must be followed to ensure a ductile column.

According to AASHTO LRFD (2012), for a circular column, the transverse reinforcement for confinement inside the plastic hinge zones, ratio of spiral reinforcement to total volume of concrete core, measured out-to-out of spirals, shall be determined as follows:

$$\rho_s = 0.12\frac{f_c'}{f_y} \tag{2.32}$$

It is recommended that the confinement reinforcement outside the zones should be at least more than half of that inside the zones but not less than

$$\rho_s = 0.45\left(\frac{A_g}{A_c} - 1\right)\frac{f_c'}{f_{yh}} \tag{2.33}$$

For a rectangular column, the total cross-sectional area (A_{sh}) of rectangular hoop (stirrup) reinforcement shall be either

$$A_{sh} = 0.30ah_c \frac{f'_c}{f_{yh}}\left(\frac{A_g}{A_c} - 1\right) \tag{2.34}$$

or

$$A_{sh} \geq 0.12sh_c \frac{f'_c}{f_y} \tag{2.35}$$

where a is vertical spacing of hoops (stirrups) (in) with a maximum of 4 in, A_c is the area of column core measured to the outside of the transverse spiral reinforcement (in^2), A_g the gross area of column (in^2), A_{sh} the total cross-sectional area (in^2) of hoop (stirrup) reinforcement, f'_c the specified compressive strength of concrete (ksi), f_{yh} the yield strength of hoop or spiral reinforcement (ksi), h_c the core dimension of tied column in mm in the direction under consideration (in), ρ_s the ratio of volume of spiral reinforcement to total volume of concrete core (out-to-out of spiral), and P_u the factored axial load (kip).

Example 2.2: Design of a Two-Column Bent

Problem: Design the columns of a two span overcrossing. The typical section of the structure is shown in Figure 2.14. The concrete box girder is supported by a two-column bent and is subjected to HL-93 loading. The columns are pinned at the bottom. Therefore, only the loads at the top of columns are given here. Table 2.3 lists all the forces due to HL-93 live load plus impact. Table 2.4 lists the forces due to seismic loads.

Material data:

f'_c = 4.0 ksi (27.6 MPa) E_c = 3,605 ksi (24,855 MPa) E_s = 29,000 ksi (199,946 MPa) f_y = 60 ksi (414 MPa)

Try a column size of 4′ (1.22 m) in diameter. Provide 32-#9 (32-#30) longitudinal reinforcement. The reinforcement ratio is 1.78%.

Section properties:

A_g = 12.51 ft^2 (1.16 m^2) A_{st} = 26.0 in^2 (16,774 mm^2)

$I_{xc} = I_{yc}$ = 12.46 ft^4 (0.1075 m^4) $I_{xs} = I_{ys}$ = 0.3338 ft^4 (0.0029 m^4)

The analysis follows the procedure discussed in Section 2.4.3.1. The moment and axial force interaction diagram is generated and is shown in Figure 2.15.

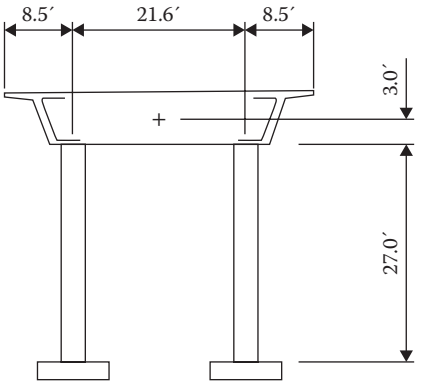

FIGURE 2.14 Example 2.2—typical section.

TABLE 2.3 Column Group Loads—Service

		Live Load + Impact										
		Case 1		Case 2		Case 3						
	Dead Load	Trans $M_{y\,max}$		Long $M_{x\,max}$		Axial N_{max}		Wind	Wind on LL	Brake Force	Centrifugal Force (M_y)	Temperature (°C)
		HS + IM	Lane	HS + IM	Lane	HS + IM	Lane					
M_y (k-ft)	220	75	35	15	8	32	16	532	153	208	127	180
M_x (k-ft)	148	67	26	545	289	50	25	192	86	295	2	0
P (kip)	1108	173	120	131	113	280	212	44	17	12	23	0

IM, dynamic load allowance.

TABLE 2.4 Unreduced Seismic Loads

	Unreduced Seismic Forces (ARS)	
	Case 1 Max Transverse	Case 2 Max Longitudinal
M_y—transverse (k-ft)	4855	3286
M_x—longitudinal (k-ft)	3126	3334
P—axial (kip)	−282	−220

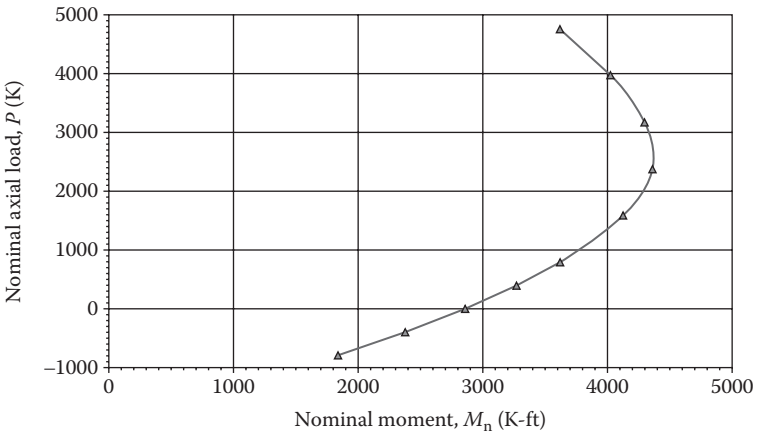

FIGURE 2.15 Example 2.2—interaction diagram.

Following the procedure outlined in Section 2.4.2, the moment magnification factors for each load group can be calculated, and the results are summarized in Table 2.5.

In which

$$K_y = K_x = 2.00$$

$$K_y \times L/R = K_x \times L/R = 2.00 \times 27.0/(0.998) = 54.11$$

$$r = \text{radio of gyration} = \sqrt{\frac{I}{A}} = \sqrt{\frac{12.46}{12.51}} = 0.998 \text{ ft}$$

TABLE 2.5 Moment Magnification and Buckling Calculations

		Moment Magnification			Approximate EI for Cracked Section		Critical Buckling		Axial
Limit State	Case	Trans M_{agy}	Long M_{agx}	Comb M_{ag}	EI_y (K-ft^2)	EI_x (K-ft^2)	P_{cy} (kip)	P_{cx} (kip)	Load P_u (kip)
Str-I	1	1.557	1.578	1.541	2,113,465	2,213,999	7,153	7,494	1,919
Str-I	2	1.549	1.412	1.431	2,036,337	2,476,065	6,892	8,381	1,833
Str-I	3	1.765	1.684	1.728	2,060,541	2,199,323	6,974	7,444	2,267
Str-I	la	1.373	1.353	1.365	2,210,094	2,309,333	7,507	7,816	1,531
Str-I	2a	1.361	1.391	1.299	2,145,100	2,528,371	7,260	8,558	1,445
Str-I	3a	1.518	1.476	1.498	2,168,298	2,296,280	7,339	7,772	1,879
Str-II	1	1.483	1.683	1.513	1,675,434	1,344,031	5,671	4,549	1,385
Str-II	2	1.483	1.683	1.513	1,675,434	1,344,031	5,671	4,549	1,365
Str-II	3	1.483	1.683	1.513	1,675,434	1,344,031	5,671	4,549	1,365
Str-II	1a	1.286	1.413	1.301	1,764,039	1,344,031	5,971	4,549	997
Str-II	2a	1.286	1.413	1.301	1,764,039	1,344,031	5,971	4,549	997
Str-II	3a	1.286	1.413	1.301	1,764,039	1,344,031	5,971	4,549	997
Str-III	1	1.352	1.425	1.362	2,186,828	1,909,584	7,402	6,463	1,447
Str-III	2	1.483	1.683	1.513	1,675,434	1,344,031	5,671	4,549	1,365
Str-III	3	1.352	1.425	1.362	2,186,828	1,909,584	7,402	6,463	1,447
Str-III	la	1.223	1.260	1.228	2,285,095	2,019,060	7,734	6,834	1,059
Str-III	2a	1.286	1.413	1.301	1,764,039	1,344,031	5,971	4,549	997
Str-III	3a	1.223	1.260	1.228	2,285,095	2,019,060	7,734	6,834	1,059
Stx-IV	1	1.670	1.950	1.718	1,632,036	1,344,031	5,524	4,549	1,662
Stx-IV	2	1.670	1.950	1.718	1,632,036	1,344,031	5,524	4,549	1,662
Str-IV	3	1.670	1.950	1.718	1,632,036	1,344,031	5,524	4,549	1,662
Str-IV	la	1.286	1.413	1.301	1,764,039	1,344,031	5,971	4,549	997
Str-IV	2a	1.286	1.413	1.301	1,764,039	1,344,031	5,971	4,549	997
Str-IV	3a	1.286	1.413	1.301	1,764,039	1,344,031	5,971	4,549	997
Str-V	1	1.487	1.482	1.485	2,203,359	2217,409	7,458	7,505	1,831
Str-V	2	1.526	1.391	1.414	1,978,537	2,425,521	6,697	8,210	1,731
Str-V	3	1.614	1.600	1.609	2,175,213	2,206,330	7,362	7,463	2,100

Str-V	la	1.328	1.326	1.328	2,299,878	2,312,354	7,784	7,826	1,444
Str-V	2a	1.339	1.270	1.280	2,088,594	2,488,095	7,069	3,421	1,343
Str-V	3a	1.422	1.414	1.419	2,274,640	2,302,523	7,699	7,793	1,712
Ext-I	1	1.000	1.000	1.000	2,268,943	2,256,198	7,680	7,636	1,052
Ext-I	2	1.000	1.000	1.000	2,149,076	2,274,357	7,274	7,700	1,064
Ext-I	3	1.000	1.000	1.000	2,149,076	2,274,857	7,274	7,700	1,064
Ext-I	la	1.000	1.000	1.000	2,268,943	2,256,198	7,630	7,636	1,052
Ext-I	2a	1.000	1.000	1.000	2,149,076	2,274,857	7,274	7,700	1,064
Ext-I	3a	1.000	1.000	1.000	2,149,076	2,274,857	7,274	7,700	1,064
EKI-II	1	1.412	1.360	1.389	1,700,792	1,376,157	5,757	6,350	1,261
Ext-II	2	1.428	1.280	1.308	1,623,432	2,225,734	5,495	7,533	1,236
Ext-II	3	1.482	1.404	1.445	1,646,910	1,360,966	5,574	6,299	1,360
Ext-II	la	1.412	1.360	1.389	1,700,792	1,676,157	5,757	6,350	1,261
Ext-II	2a	1.428	1.280	1.308	1,623,482	2,225,734	5,495	7,533	1,236
Ext-II	3a	1.482	1.404	1.445	1,646,910	1,860,966	5,574	6,299	1,360

Note: Axial load, P_u, is calculated at column top for buckling calculations.

$$\frac{K_y l_{uy}}{r_y} = \frac{K_x l_{ux}}{r_x} = \frac{(2.0)(27.0)}{(0.998)} = 54.11$$

$$22 < \frac{K_y l_{uy}}{r_y} = \frac{K_x l_{ux}}{r_x} = 54.11 < 100 \qquad \therefore \textit{Second-order effect should be considered.}$$

The calculations for limit state, strength I, and case 2 (maximum longitudinal moment) are demonstrated in the following:

Bending in the longitudinal direction: M_{ux}

$$\text{Factored load } M_{ux} = 1.0\left[1.25\text{DC} + 1.5\text{DW} + 1.75(\text{LL} + \text{IM} + \text{BF} + \text{CF}) + 1.2\ \text{TU} + \text{W} + \text{WL}\right]$$

β_d in Equation 2.8 = max factored dead load moment, M_{DL}/max factored total moment, M_{ux}

$$M_{DL} = 1.25 \times 148 = 185\ \text{k-ft}(252\text{KN-m})$$

$$M_{ux} = 1.25 \times 148 + 1.75(545 + 289 + 295) = 2{,}160\ \text{k-ft}(2{,}929\text{KN-m})$$

$$\beta_d = 185/2160 = 0.09$$

$$\text{EI}_x = \frac{\frac{E_c I_g}{5} + E_s I_s}{1 + \beta_d} = \frac{\frac{3{,}640 \times 144 \times 12.46}{5} + 29{,}000 \times 144 \times 0.3338}{1 + 0.09} = 2{,}476{,}065\ \text{K/ft}^2$$

$$P_c = \frac{\pi^2 \times \text{EI}_x}{(KL)^2} = \frac{3.1416^2 \times 2{,}476{,}065}{(2.0 \times 27)^2} = 8{,}381k\ \ (37{,}292\ \text{KN})$$

$C_m = 1.0$ for frame not braced against sidesway

$$\delta_s = \frac{1}{1 - \frac{\sum P_u}{\varphi \sum P_c}} = \frac{1}{1 - \frac{1{,}833}{0.75 \times 8381}} = 1.412$$

The magnified factored moment $\delta_s \times M_{ux} = 1.412 \times 2{,}160 = 3{,}050$ k-ft (4,135 KN-m)

Go through the same procedure, the magnified factored moment in transverse direction = 1,331 k-ft. The combined moment is $M_u = 3{,}328$ k-ft. The nominal moment capacity of the section corresponding to the axial force of 1,833 Kip is 4,357 k-ft. The factored moment capacity $\phi M_n = M_r = 3{,}428$ k-ft ($\phi = 0.789$).

Therefore, $\frac{M_r}{M_u} = \frac{3{,}328}{3{,}428} \approx 1.0$ $\qquad \therefore \textit{Design is OK.}$

The analysis results with the comparison of applied moments to capacities are summarized in Table 2.6.

Column lateral reinforcement is calculated for two cases: (1) for applied shear and (2) for confinement. Typically, the confinement requirement governs. Apply Equation 2.32 or Equation 2.33 to calculate the confinement reinforcement. For seismic analysis, the unreduced seismic shear forces shall be compared with the shear forces due to plastic hinging of columns. The smaller shall be used. The plastic hinging analysis procedure is discussed elsewhere in this handbook and will not be repeated here.

First, determine the lateral reinforcement by confinement.

TABLE 2.6 Comparison of Factored Loads to Factored Capacity of the Column

		Applied LRFD Factored				Capacity (P_hM_n)		Maximum		
Limit State	Case	Tran M_{uy}	Long M_{ux}	Comb M_u	Axial $P_u = P_r$	M_r	Phi	Rebar Strain	Ratio M_r/M_u	
Str-I	1	1575	1312	2050	1919	3412	0.780	0.00262	1.66	OK
Str-I	2	1331	3050	3328	1833	3438	0.789	0.00279	1.03	OK
Str-I	3	1594	1402	2122	2267	3270	0.753	0.00206	1.54	OK
Str-I	la	1283	1099	1650	1531	3480	0.821	0.00342	2.06	OK
Str-I	2a	1065	2722	2923	1445	3484	0.831	0.00363	1.19	OK
Str-I	3a	1254	1152	1703	1373	3422	0.784	0.00269	2.01	OK
Str-II	1	675	311	743	1385	3482	0.838	0.00377	4.69	
Str-II	2	675	311	743	1385	3482	0.838	0.00377	4.69	
Str-II	3	675	311	743	1385	3482	0.838	0.00377	4.69	
Str-II	1a	486	188	521	997	3446	0.893	0.00487	6.61	
Str-II	2a	466	188	521	997	3446	0.893	0.00487	6.61	
Str-II	3a	486	188	521	997	3446	0.893	0.00487	6.61	
Str-III	1	1623	647	1747	1447	3484	0.831	0.00363	1.99	OK
Str--III	2	675	311	743	1385	3482	0.838	0.00377	4.69	OK
Str-III	3	1623	647	1747	1447	3484	0.831	0.00363	1.99	OK
Str-III	1a	1374	507	1464	1059	3453	0.883	0.00466	2.36	OK
Str-III	2a	486	188	521	997	3446	0.893	0.00487	6.61	OK
Str-III	3a	1374	507	1464	1059	3453	0.883	0.00466	2.36	OK
Str-IV	1	852	433	955	1662	3464	0.805	0.00311	3.63	OK
Str-IV	2	852	433	955	1662	3464	0.805	0.00311	3.63	OK
Str-IV	3	852	433	955	1662	3464	0.805	0.00311	3.63	OK
Str-IV	la	486	188	521	997	3446	0.893	0.00487	6.61	OK
Str-IV	2a	486	188	521	997	3446	0.893	0.00487	6.61	OK
Str-IV	3a	486	188	521	997	3446	0.893	0.00487	6.61	OK
Str-V	1	1859	1292	2264	1831	3438	0.789	0.00279	1.52	OK
Str-V	2	1170	2377	2650	1731	3455	0.799	0.00298	1.30	OK
Str-V	3	1882	1356	2320	2100	3350	0.765	0.00231	1.44	OK
Str-V	la	1558	1087	1900	1444	3481	0.831	0.00362	1.83	OK
Str-V	2a	924	2105	2299	1343	3482	0.844	0.00388	1.51	OK
Str-V	3a	1549	1125	1914	1712	3459	0.801	0.00302	1.81	OK
Ext-I	1	1191	773	1420	1052	3818	1.000	0.00502	2.69	OK
Ext-I	2	877	815	1197	1064	3824	1.000	0.00499	3.19	OK
Ext-1	3	877	815	1197	1064	3824	1.000	0.00499	3.19	OK
Ext-I	la	1191	773	1420	1052	3818	1.000	0.00502	2.69	OK
Ext-I	2a	877	815	1197	1064	3824	1.000	0.00499	3.19	OK
Ext-I	3a	877	815	1197	1064	3824	1.000	0.00499	3.19	OK
Ext-II	1	535	465	709	1261	3478	0.854	0.00409	4.90	OK
Ext-II	2	479	912	1030	1236	3472	0.857	0.00414	3.37	OK
Ext-II	3	516	468	696	1360	3482	0.841	0.00383	5.00	OK
Ext-II	la	535	465	709	1261	3478	0.854	0.00409	4.90	OK
Ext-II	2a	479	912	1030	1236	3472	0.857	0.00414	3.37	OK
Ext-II	3a	516	468	696	1360	3482	0.841	0.00.83	5.00	OK

Note: Permit load was not input; hence, calculation for Str-II limit state is incomplete.

Inside the plastic hinge zones

$$\rho_s = 0.12\frac{f'_c}{f_y} = 0.12\frac{4.0}{60.0} = 0.008$$

Outside the plastic hinge zones

$$\rho_s = 0.45\left(\frac{A_g}{A_c} - 1\right)\frac{f'_c}{f_{yh}} = 0.45\left(\frac{12.56}{10.56} - 1\right)\frac{4.0}{60.0} = 0.0057$$

$$\text{Reinforcement for confinement} = \rho_s = \frac{4A_b}{D's}$$

If use #5 bar,
Inside plastic hinge zones: $s = 3.4$ in say $s = 3$ in
Outside plastic hinge zones: $s = 4.8$ in say $s = 4.5$ in
Then, check the lateral reinforcement for shear.
For left column:
$V_u = 167$ kip (743 KN) (shear due to plastic hinging governs)
Inside the plastic hinge zones (assume displacement ductility $\mu_d = 5$):

$$\text{Factor}\,1 = \frac{0.008 \times 60}{0.15} + 3.67 - 5 = 1.87$$

$$\text{Factor}\,2 = 1 + \frac{(1108 - 508) \times 1000}{2000 \times 12.56 \times 144} = 1.17$$

$$v_c = 1.87 \times 1.17 \times \sqrt{4000} = 138.4 \text{ psi } (0.95 \text{ Mpa})$$

$$V_c = 10.56 \times 144 \times 138.4 = 210.4 \text{ kip}$$

$$\phi V_c = 0.85 \times 210.4 = 179 > V_u = 167 \text{ kip}$$

∴ No lateral reinforcement is required for shear.
For right column:
The shear force due to plastic hinging is $V_u = 199$ kip.
However, the axial force in right column is larger than that of the left column, the shear capacity will be larger. By observation, the shear will not govern.
Final design:
4 ft (1.22 m) diameter of column with 32-#9 (32-#30) for main reinforcement and #5@3" (#16 @ 76.2 mm) for spiral confinement in the top 6 ft of column and #5@4.5" (#16 @114.2 mm) in the rest of the column.

2.4.4 Steel and Composite Columns

Steel columns are not as commonly used as concrete columns. Nevertheless, they are viable solutions for some special occasions, for example, in space-restricted area. Steel pipes or tubes filled with concrete known as composite columns (Figure 2.16) offer the most efficient use of the two basic materials. Steel at the perimeter of the cross section provides stiffness and triaxial confinement, and

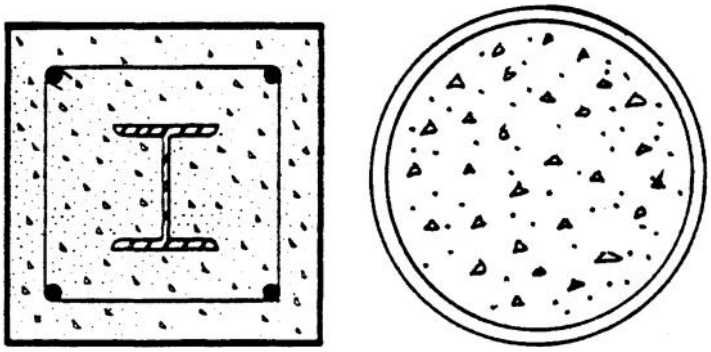

FIGURE 2.16 Typical cross sections of composite columns.

the concrete core resists compression and prohibits local elastic buckling of the steel encasement. The toughness and ductility of composite columns makes them the preferred column type for earthquake-resistant structures in Japan. In China, the composite columns were first used in Beijing subway stations as early as 1963. Over the years, the composite columns have been used extensively in building structures and bridges (Cai 1987 and 1992; Zhong 1996). The design specifications of steel and composite columns are given in various codes. (CECS 1990; Galambos and Chapuis 1990; AISC 2010). In this section, the design provisions of AASHTO LRFD (2012) for steel and composite columns are summarized as follows.

2.4.4.1 Compressive Resistance

For prismatic members with at least one plane of symmetry and subjected to either axial compression or combined axial compression and flexure about an axis of symmetry, the factored resistance of components in compression, P_r, shall be calculated as

$$P_r = \phi_c P_n \tag{2.36}$$

where

P_n = nominal compressive resistance
ϕ_c = resistance factor for compression = 0.90
The nominal compressive resistance of a steel or composite column shall be determined as

$$P_n = P_n = \begin{cases} 0.66^{\lambda} F_e A_s & \text{if } \lambda \le 2.25 \\ \dfrac{0.88 F_e A_s}{\lambda} & \text{if } \lambda > 2.25 \end{cases} \tag{2.37}$$

in which
For steel columns

$$\lambda = \left(\frac{KL}{r_s}\pi\right)^2 \frac{F_y}{E_e} \tag{2.38}$$

For composite column

$$\lambda = \left(\frac{KL}{r_s}\pi\right)^2 \frac{F_e}{E_e} \tag{2.39}$$

$$F_e = F_y + C_1 F_{yr}\left(\frac{A_r}{A_s}\right) + C_2 f_c\left(\frac{A_c}{A_s}\right) \tag{2.40}$$

$$E_c = E\left[1 + \left(\frac{C_3}{n}\right)\left(\frac{A_c}{A_s}\right)\right] \tag{2.41}$$

where A_s is the cross-sectional area of the steel section (in^2), A_c the cross-sectional area of the concrete (in^2), A_r the total cross-sectional area of the longitudinal reinforcement (in^2), F_y the specified minimum yield strength of steel section (ksi), F_{yr} the specified minimum yield strength of the longitudinal reinforcement (ksi), f_c' the specified minimum 28-day compressive strength of the concrete (ksi), E *is* the modules of elasticity of the steel (ksi), L the unbraced length of the column (in), K the effective length factor, n the modular ratio of the steel to concrete, r_s the radius of gyration of the steel section in the plane of bending, but not less than 0.3 times the width of the composite member in the plane of bending for composite columns (in), and for concrete filled in steel tube, $C_1 = 1.0$, $C_2 = 0.85$, and $C_3 = 0.40$.

In order to use the above equation, the following limiting width/thickness ratios for axial compression of steel members of any shape shall be satisfied:

$$\frac{b}{t} \le k\sqrt{\frac{E}{F_y}} \tag{2.42}$$

where k is the plate buckling coefficient as specified in Table 2.7, b the width of plate (in) as specified in Table 2.7, and t the plate thickness (in).

Wall thickness of steel or composite tubes shall satisfy the following:

For circular tubes

$$\frac{D}{t} \le 2.8\sqrt{\frac{E}{F_y}} \tag{2.43}$$

TABLE 2.7 Limiting Width–Thickness Ratios

	k	*b*
		Plates supported along one edge
Flanges and projecting leg or plates	0.56	Half-flange width of I-section
		Full-flange width of channels
		Distance between free edge and first line of bolts or welds in plates
		Full-width of an outstanding leg for pairs of angles on continuous contact
Stems of rolled tees	0.75	Full-depth of tee
Other projecting elements	0.45	Full-width of outstanding leg for single angle strut or double angle strut with separator
		Full projecting width for others
		Plates supported along two edges
Box flanges and cover plates	1.40	Clear distance between webs minus inside corner radius on each side for box flanges
		Distance between lines of welds or bolts for flange cover plates
Webs and other plates elements	1.49	Clear distance between flanges minus fillet radii for webs of rolled beams
		Clear distance between edge supports for all others
Perforated cover plates	1.86	Clear distance between edge supports

For rectangular tubes

$$\frac{b}{t} \le 1.7\sqrt{\frac{E}{F_y}} \tag{2.44}$$

where D is the diameter of tube (in), b the width of face (in), and t the thickness of tube (in).

2.4.4.2 Flexural Resistance

The factored flexural resistance, M_r, shall be determined as

$$M_r = \phi_f M_n \tag{2.45}$$

where

M_n = nominal flexural resistance
ϕ_f = resistance factor for flexure, $\phi_f = 1.0$
The nominal flexural resistance of concrete-filled steel tubes that satisfy the limitation

$$\frac{D}{t} \le 2.8\sqrt{\frac{E}{F_y}} \tag{2.46}$$

may be determined

$$\text{If} \quad \frac{D}{t} < 2.0\sqrt{\frac{E}{F_y}}, \quad \text{then} \quad M_n = M_{ps} \tag{2.47}$$

$$\text{If} \quad 2.0\sqrt{\frac{E}{F_y}} < \frac{D}{t} \le 8.8\sqrt{\frac{E}{F_y}}, \quad M_n = M_{yc} \tag{2.48}$$

where

M_{ps} = plastic moment of the steel section
M_{yc} = yield moment of the composite section

2.4.4.3 Combined Axial Compression and Flexure

The axial compressive load, P_u, and concurrent moments, M_{ux} and M_{uy}, calculated for the factored loadings for both steel and composite columns shall satisfy the following relationship:

$$\text{If} \quad \frac{P_u}{P_r} < 0.2, \quad \text{then} \quad \frac{P_u}{2.0P_r} + \left(\frac{M_{ux}}{M_{rx}} + \frac{M_{uy}}{M_{ry}}\right) \le 1.0 \tag{2.49}$$

$$\text{If} \quad \frac{P_u}{P_r} \ge 0.2, \quad \text{then} \quad \frac{P_u}{P_r} + \frac{8.0}{9.0}\left(\frac{M_{ux}}{M_{rx}} + \frac{M_{uy}}{M_{ry}}\right) \le 1.0 \tag{2.50}$$

where P_r is factored compressive resistance (kip); M_{rx}, M_{ry} are factored flexural resistances about x and y axis, respectively (kip-ft); M_{ux}, M_{uy} factored flexural moments about the x and y axis, respectively (kip-ft).

References

AASHTO. 2012. *AASHTO LRFD Bridge Design Specifications*, Customary U.S. Unit, 2012, American Association of State Highway and Transportation Officials, Washington, DC.

ACI. 2011. *318–11: Building Code Requirements for Structural Concrete and Commentary, (ACI 318–11)*, American Concrete Institute, Farmington Hills, MI.

AISC. 2010. *Specification for Structural Steel Buildings*, ANSI/AISC 360–10, American Institute of Steel Construction, Chicago, IL.

Cai, S. H. 1987. "Ultimate Strength of Concrete-Filled Tube Columns," in *Composite construction in Steel and Concrete*, Proc. of an Engineering Foundation Conference, Dale Buckner, C., and Viest, Ivan M., Eds, Henniker, NH. 703.

Cai, S. H. 1992. "Chinese Standard for Concrete-Filled Tube Columns," in *Composite Construction in Steel and Concrete II*, Proc. of an Engineering Foundation Conference, Samuel Easterling, W., and Kim Roddis, W. M., Eds, Potosi, MO. 143.

Caltrans. 1994. *Bridge Memo to Designers (7–10)* - Bridge Deck Joints and Deck Joint Seals, California Department of Transportation, Sacramento, CA.

Caltrans. 2013. *Seismic Design Criteria, Version 1.6*, California Department of Transportation, Sacramento, CA.

CECS 28:90. 1990. *Specifications for the Design and Construction of Concrete-Filled Steel Tubular Structures*, China Planning Press, Beijing, China. (in Chinese)

Galambos, T. V. and Chapuis, J. 1990. *LRFD Criteria for Composite Columns and Beam Columns*, Revised Draft, Washington University, Department of Civil Engineering, St. Louis, MO. December.

Galambos, T. V. 1998. *Guide to Stability Design for Metal Structures*, 5th Ed., the Structural Stability Research Council, John Wiley & Sons, New York, NY.

Paulay, T. and Priestley, M. J. N. 1992. *Seismic Design of Reinforced Concrete and Masonry Building*, John Wiley & Sons, New York, NY.

White, D. W. and Hajjar, J. F. 1994. "Application of Second-Order Elastic Analysis in LRFD: Research to Practice," *Engineering Journal*, American Institute of Steel Construction, 28(4), 133–148.

Zhong, S. T. 1996. "New Concept and Development of Research on Concrete-Filled Steel Tube (CFST) Members", *Proc. of The 2nd Int'l Symp. On Civil Infrastructure Systems*, December 9-12, 1996, Hong Kong, China

3

Towers

Charles Seim
Consulting Engineer

Jason Fan
California Department of Transportation

3.1 Introduction

Towers are the most visible structural elements of long-span bridges, because they project above the superstructure and can be seen from all directions by both viewers and bridge users. Towers give to a bridge a characteristic identity, a unifying theme, a motif from which people can identify that particular bridge. Towers project a mnemonic bridge image that people can recall as their lasting impression of that bridge itself, making towers an important part of the overall esthetics.

As examples of the powerful imagery of towers, contrast the elegant art deco towers of the 1937 Golden Gate Bridge (Figure 3.1) with the utilitarian, but timeless, architecture of the towers of the 1936 San Francisco–Oakland Bay Bridge (Figure 3.2).

Then compare these robust towers to those of the 1964 delicate towers of the Firth of Forth Suspension Bridge (Figure 3.3); ponder the disproportions between the massive, rugged stone towers of the 1883 Brooklyn Bridge (Figure 3.4) with the awkward and confusing steel towers of the 1903 Williamsburg Bridge in New York (Figure 3.5).

Alternatively, one may contrast those older, Iconic Bridges, with the new and distinctive San Francisco–Oakland Bay Bridge East Span with its single-tower suspension bridge (Figure 3.19d, later in the chapter) and with the quasi-diamond-shaped towers of the 2000 Yeongjong Grand Bridge, Incheon, South Korea (Figure 3.6). Both of these are self-anchored suspension bridges and have no heavy and bulky concrete anchorages visible at each end.

Then compare the concrete quasi-diamond-shaped towers of the 1995 Glebe Island Bridge (Figure 3.7) to the concrete full-diamond-shaped towers of the 2005 Cooper River Bridge (Figure 3.8); the heights of the roadways dictated the differences between these tower shapes and not the whims of the designers!

One can easily see that there is great diversity in bridge tower designs; the only requirement that these towers have in common is that they must resist the loads and forces of nature and be in equilibrium according to the three equations of statics. Towers surely do impact the appearance of bridges, for good or for bad.

FIGURE 3.1 Golden Gate Bridge, San Francisco. (Courtesy of Charles Seim.)

FIGURE 3.2 San Francisco–Oakland Bay Bridge. (Courtesy of Charles Seim.)

FIGURE 3.3 Firth of Forth Suspension Bridge. (Courtesy of Charles Seim.)

FIGURE 3.4 Brooklyn Bridge, New York. (Courtesy of Charles Seim.)

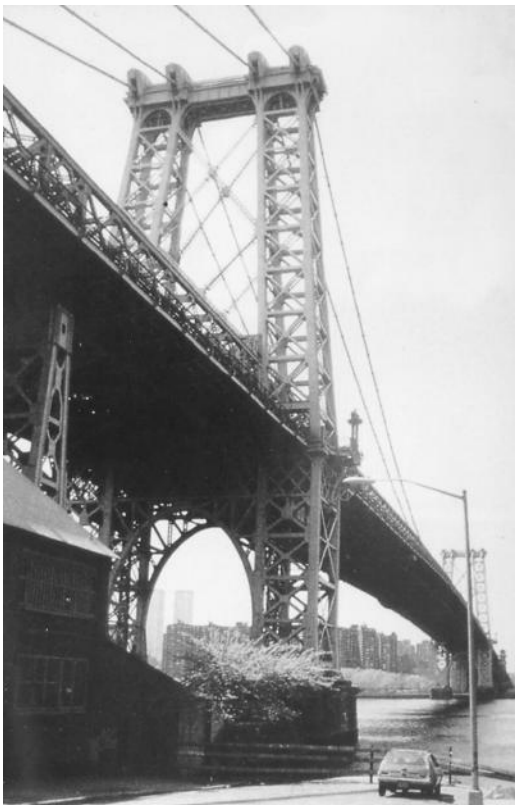

FIGURE 3.5 Williamsburg Bridge, New York. (Courtesy of Charles Seim.)

FIGURE 3.6 Yeongjong Grand Bridge, Incheon, South Korea.

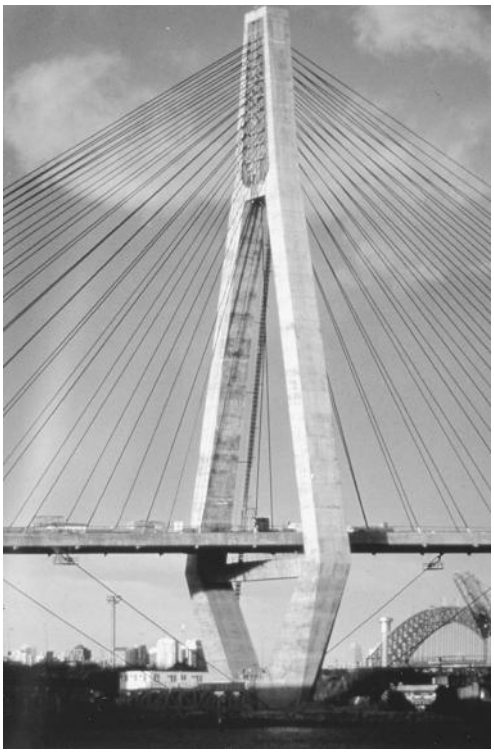

FIGURE 3.7 Glebe Island Bridge, Sydney, Australia. (Courtesy of T. Y. Lin International.)

FIGURE 3.8 Cooper River Bridge, Charleston, South Carolina, under construction. (Courtesy of Charles Seim.)

The famous bridges noted above are all older than three-quarters of a century. If they are well maintained, all these bridges could continue to serve for another 100 years.

The service lives of the new self-anchored suspension span of the San Francisco–Oakland Bay Bridge and the Yeongjong Grand Bridge could be 150 years. These bridges are excellent examples of enduring structures; they serve as a reminder to bridge engineers that well-designed and well-maintained structures can last for 100–150 years, or perhaps longer. Robust designs, durable materials, provisions for inspection and maintenance access, and a well-executed maintenance program will help to ensure long service lives.

Both suspension and cable-stayed bridges are supported by abutments or piers at the point at which these structures transition to an approach roadway or to an approach structure. Abutments are discussed in Chapter 6. Piers and columns that support the superstructure for other types of bridge structures, such as girders, trusses, or arches, usually do not project above the deck. Piers and columns are discussed in Chapter 2.

3.2 Functions

"Towers" are usually defined as the vertical steel or concrete structures that project above the bridge deck to support both themselves and the bridge cables and function to carry the loads and the forces to which the bridge is subjected to the ground.

Thus, by this definition, towers are used only for suspension bridges, cable-stayed bridges, or hybrid suspension-cable-stayed structures. The word "pylon" is sometimes used to designate the single-shaft tower of a cable-stayed bridge. In this chapter, the word "tower" is used for structures that are self-supporting; "pylons" is not used, to avoid confusion.

Recently a new term "spar" has been introduced to describe vertical or near-vertical members that are not self-supporting and must depend on cables for its support; however, the spar does function as a tower carrying some bridge loads and forces to the ground. In this chapter, the word "spar" is used to describe a member that cannot support itself but functions as a tower.

Towers must perform its functions economically, be esthetically pleasing and constructible. Towers must also be reliable and serviceable for the entire life of the bridge, as unlike other bridge components, towers cannot be replaced without tearing down the bridge.

Structural serviceability is an important component of good bridge design. This requires that the bridge and towers be designed to allow for ease of carrying out both inspection and maintenance functions to provide continuous good service to its users. The public demands that bridges and towers be attractive, esthetic statements having long service lives, so as not to be wasteful of public funds.

3.3 Esthetics

Although the main function of the towers is structural, an important secondary function is visual—beyond mere esthetics, the towers reveal the true character, or motif, of a bridge. The bridges used as examples in Section 3.1 are good illustrations of the image of the structure, as revealed by the towers. Indeed, most are famous because of their towers!

Many people visualize the character of the Brooklyn Bridge by its gothic, arched-masonry towers, the Golden Gate Bridge by its tall, tapered, red steel towers, and across the Bay, the San Francisco–Oakland Bay Bridge by its robust-looking cross bracing and shiny aluminum paint. The elegant white, single tower of the new San Francisco–Oakland Bay Bridge East Span self-anchored suspension bridge will perhaps leave an even more distinctive impression after the bridge is opened in 2013.

Seim (1996) measured the aspect ratios of the length, divided by the thickness of the visible components of the towers of both the Golden Gate and the San Francisco–Oakland Bay Bridges. He found important, but subtle, reduction of these ratios with increasing heights above the tower base; the higher the member, the smaller the aspect ratio. It is these subtle changes in the ratios within the heights of the towers that produce the much-admired proportions of these world-renowned bridges. The towers for a

long span bridge should be carefully shaped and proportioned so as to give that entire bridge a strong and sturdy, but graceful, soaring visual image to the eyes of the viewing public.

The two main cable suspension bridges drape in a parabolic curve between towers that many people instinctively enjoy viewing. The large diameter of the cables makes them stand out as the important contributors to the overall visual impression of the supporting elements of the roadway. The towers of these common types of suspension bridges are as wide as the bridge and extend full height, making them the visual supporting elements, and they project the motif of the bridge design. Just a few suspension bridges employ a single cable, in which case the towers are usually tapered.

The cables of most cable-stayed bridges are small in diameter and usually do not visually stand out as do the large cables of a suspension bridge. The cables can be arrayed in a single plane along the centerline of the bridge, a double plane at the sides of the roadway girder, or a single plane on one side of the tower and a double plane on the other side. A single plane array is usually used with a single-shaft tower and a double plane array usually used with a two-shaft tower. See Chapter 10, *Bridge Engineering Handbook, Second Edition: Superstructure Design*, Cable-Stayed Bridges.

However, arrays of the cable stays, such as a fan, radiating fan, or the little-used harp, should be considered in the context of the form of the tower. The parallel cables of a harp array, for example, usually will not be as obtrusive to the bridge towers as are other cable arrangements, such as a radiating fan array that dominates visually over the tower. Thus, the cables and the towers together should be considered as both visual systems and structural systems.

Billington (1983) presents an overview of the importance of the role of esthetics in the history of the development of modern bridge design. Prof. Billington coined the words "Structural Art" to honor bridges that are efficient, economical, and elegant structures. Leonhardt (1984) presents many examples of completed bridges with many tower shapes and cable arrangements for both suspension and for cable-stayed bridges. Esthetics of bridges is discussed in more detail in Chapters 2 and 3 of *Bridge Engineering Handbook, Second Edition: Fundamentals*.

3.4 Towers and Spectacular Bridges

Although efficiency, economy, and elegance are usually the major elements in bridge design, occasionally, since the 1990s, efficiency and economy have often not been the prime objectives of bridge designers. This trend started as bridge owners, the public, or both, began demanding "spectacular," "picturesque," or "distinctive" bridges, because bridge engineers could design and construct them!

Such a trend often calls for configuring the stay cables in unusual arrays that may dominate the towers, thus allowing the stay cables to become the principle esthetic statements of these bridges. This trend also featured curved, inclined, or kinked towers to add "visual impact" to bridges.

These new spectacular bridge types are designed to attract attention, because efficiency is not an objective and cost is not restricted. One could also argue that although they may be spectacular, these bridge types are not elegant. Regardless, such bridges are not considered "Structural art," as defined by Billington (1983), because they do not conduct the forces of the bridge to its foundation in the most efficient manner, and they are not economical, because they cost more than a conventional bridge. Instead, such bridges may be considered "extravagant structural art," and a form of art, nonetheless.

This extravaganza started in the early 1990s, when proven structural engineering programs became accessible to most engineers, and high-performance steel and concrete were readily available; thus, it was inevitable that engineers and architects would begin to exploit these relatively new developments by designing and constructing spectacular bridges that featured distinctive towers.

One of the first of these "spectacular" bridges was the Alamillo Bridge (Figure 3.9), constructed for the 1992 Expo in Seville, Spain. It was designed by Santiago Calatrava, who acted as both architect and engineer. The bridge features a 142-m (466-ft) tall, concrete-filled, steel box tower, angled at 68 degrees; painted white, it is a visible landmark from the old town of Seville. The concrete box girder roadway is a 200-m (656-ft) single span and anchors the single plane, harp-arrayed cables.

FIGURE 3.9 Alamillo Bridge, Seville, Spain.

FIGURE 3.10 Erasmus Bridge in Rotterdam, the Netherlands. (Courtesy of Charles Seim.)

The very tall tower and the parallel cables create a beautiful, dramatic structure that immediately attracts the attention of people viewing the bridge. However, this structure is not a genuine cable-stayed bridge, because the tower is not anchored to the ground with backstay cables (Petroski 1996). The traffic crossing the bridge deflects the girder and loads the cables, but the cable loads at the tower are not in horizontal equilibrium, and the tower simply tilts a little.

The bridge was very costly. However, the people who view the structure see it as a very attractive bridge and consider it to be well worth the cost. This motif has been successfully used several times since, most notably on Sun Dial Bridge in California, where the single, pointed tower casts a shadow that tells the time of day. More importantly, the Alamillo Bridge cleared the way for engineers and architects to design and construct outstanding bridges, whenever cost is not an important factor to the bridge owners or to the cities desiring a spectacularly designed bridge as a city icon.

The Erasmus Bridge of Rotterdam, the Netherlands (Figure 3.10), opened in 1996, is another example of a spectacular bridge that is admired by all who view it. This bridge, designed by architect Ben van Berkel, features a tapered-steel tower with a "kink" near the midpoint that instantly attracts attention,

because a kink in a tower is highly unusual! Towers are not usually kinked, because they are compression members; a kink in a compression member introduces a large bending moment, which requires the engineer to add extra steel to resist that moment, substantially increasing the tower cost.

The modified, fan-arrayed stay cables in the main span load the upper portion of the tower in compression and bending; they also produce a reaction force at the top of the tower that is resisted by the two backstay cables that are attached at the top of the tower. The vertical component from the backstay cables adds large compression forces in the tower. Thus, the tower carries the bending moments and the compression from the main span stay cables, compression forces from the backstays, and the bending moments from the kink. The sum total of these cable arrangements and the kink added considerable costs to reinforce the tower to resist the huge bending and compression loads. However, this bridge is a great success because Rotterdam now has a city icon, and the people can marvel at the bridge's unique architecture!

In 2009, the city of Dublin opened the Samuel Beckett Bridge, named after the famous Irish writer, and designed by Calavatra. This bridge is certainly a picturesque structure, having a thin, curved tower described as a forward-leaning, tubular curved spar (Figure 3.11).

The Samuel Beckett Bridge is a short, 120-m long cable-stayed bridge that is balanced as a swing bridge that pivots on a pier located directly under the base of its 48-m high spar. Each of the two backstay cables connects both to the tip of the spar and to the two backstay edge-girders, forming a "V." The backstay cables and the forward stay cables combine to create a self-anchored structure that allows the structure to swing open to provide ship passage. The curved spar acts as a tilted-up arch as it is loaded transversely with the forward stay cables that support the main span.

This very picturesque bridge is an ingenious assemblage of girders, cables, and a curved spar. Although costly, it is a true bridge, compared to the Alamillo Bridge, and was supposedly designed to mimic an Irish Harp laid on its side.

China has built many distinctive bridges, and the Nanjing Third Yangtze Bridge is a good example of this type (Figure 3.12). This cable-stayed bridge was the longest of this type in China, when it was opened in 2005 with a central span of 628 m and 215 m tall steel towers. The city fathers wanted each of the two towers of the bridge to look similar to the curved Eiffel Tower in Paris, because one of them had visited Paris and was impressed with the beauty of Eiffel's masterpiece.

The upper portions of the two steel shafts of each tower are straight and braced by three cross-struts; the lower portions of the two shafts do not have cross-struts but are curved to simulate the curvature of

FIGURE 3.11 Samuel Beckett Bridge by Calavatra. (Courtesy of Charles Seim.)

FIGURE 3.12 Third Nanjing Yangtze River Bridge Towers under construction. (Courtesy of Charles Seim.)

the Eiffel Tower. The curvature produced extremely large bending moment in each of the curved lower portions of the shaft, and that required additional steel to reduce the stress from the large bending moment to an acceptable value. The Eiffel Tower has cross-struts spaced along the tower height to reduce the bending moments in the four corner shafts of that Paris icon.

Each tower shaft was fabricated in segment approximately 10–12 m high; thus each segment in the tower shafts was fabricated to different dimensions and angles. Every segment required geometric control, which required very accurate field surveying to ensure that each segment was accurately placed on the proper curvature. The contractor believed that the dimensions and angles in each segments could not be controlled accurately enough to use welded connections between the segments and therefore used bolted connections. These bolted connections required very thick splice plates and a large number of high-strength bolts to carry both bending and compression forces. All these items added cost to the construction of the towers.

In addition, the caisson concrete cap required a massive amount of prestressing steel to contain the outwardly directed thrust distributed to the caisson cap from each inclined shaft at the base of the tower.

The Eiffel Tower emulation added cost to the bridge and tower construction. However, it is a very successful bridge, because the curved shafts add a dynamic effect to what otherwise could be dull-looking towers. The City Fathers are delighted, and the bridge users admire the curved appearance of the towers.

Another example of a distinctive bridge is the Sanhao Bridge in Shenyang City, China (Figure 3.13), designed by Man-Chung Tang, who also acted as the architect of this bridge. The bridge features two concrete struts springing from a common support and inclined away from each other and each supporting a curved concrete arch spanning across the bridge roadway.

From each inclined tower, cable stays, arrayed in a harp arrangement, support the 100-m roadway on each side of the piers supporting the towers. Horizontal cables, parallel arrayed, tie the twin towers together.

FIGURE 3.13 Sanhao Bridge, Shenyang, China. (Courtesy of Man-Chung Tang.)

FIGURE 3.14 Jiayue Bridge, in Chongqing City, China. (Courtesy of Man-Chung Tang.)

The towers and cables added a small cost to this very distinctive bridge. The bridge is a success, because Shenyang City now has a distinctive icon, and the people who use and view the bridge from city streets are delighted.

Another distinctive bridge by Man-Chung Tang is the Jiayue Bridge, in Chongqing City, China (Figure 3.14), which is a conventional cable-stayed bridge with unconventional towers projecting 33 m above the roadway and with a total height of 126 m. The main span is 250 m, but the attraction of the bridge is not the main span but the portion of the towers that project above the roadway, acting as out-stretching arms holding up the cable stays. The arms leaning outwardly open up the bridge to the horizon for drivers compared to the conventional tower types that lean inward, enclosing the bridge.

The outward-leaning arms added little cost to the bridge, but they do create a distinctive bridge for all to enjoy, which is the principle feature of a successful bridge.

From these few examples, one can see that these types of bridges can range from the truly spectacular to picturesque, to distinctive bridges; all can be considered art, artistic, or even elegant structures; however, they cannot be considered "Structural Art" according to Prof. Billington's definition of efficiency, economy, and elegance.

These "bridge" types will continue to be constructed wherever people desire bridge extravaganzas and have the money to back up such desires. Thus, such bridge types as these have entered the repertoire of the bridges that bridge engineers are required to design, construct, and maintain.

Any future discussion of towers for these spectacular bridges is beyond the scope of this chapter.

3.5 Conceptual Design

The most important step in the design of a new bridge is the structural design concept that will ultimately be developed into a final design and then be constructed. The cost, the appearance, the reliability and serviceability of the facility will all be determined, for good or for bad, by the conceptual design of the structure. Towers act as the bridge framework because the superstructure will hang from the towers; thus, towers play a significant role in the conceptual design process. Once it is constructed, the bridge will always be there for users to admire or to criticize. The user ultimately pays for the cost of a structure and also pays for the cost of maintaining that structure.

Gimsing and Georgakis (2012) treat the conceptual design issues of both cable-stayed and suspension bridges very extensively and present examples to help guide bridge designers. Chapter 1 of *Bridge Engineering Handbook, Second Edition: Fundamentals* presents typical practice and general principles of bridge conceptual design.

A recent trend is to employ an architect to be part of the design team. An architect if employed should start during the conceptual design phase, as the esthetics of the bridge is set during that phase of the work.

Generally the role of the engineer is to develop the structure adequacy and ensure the structural function of the bridge according to the codes of practice. The role of the architect will generally involve only the esthetics function; however, there are no codes of practice for that.

Their two roles do overlap in achieving an esthetic and functional structural design that is within budget. As the common objective of both the engineer and the architect is to build an elegant and economical bridge, cooperation and respect between them is vital to the success of their joint effort.

However, differences may occur when the esthetic desires of the architect and the structural calculations of the engineer conflict. Towers, the most visible components of the bridge, are often the focal point for this type of conflict. Each professional should understand if these differences in viewpoint occur; they must be resolved so that a successful and fruitful union between their two disciplines will produce a strong and beautiful bridge.

3.5.1 Materials

Until the 1970s, steel was the predominant material used for towers for both cable-stayed and suspension bridges. Such towers were often rectangular in elevation, having cross sections shaped as rectangles, cruciforms, tees, or other similar shapes that could be easily fabricated in steel.

Two examples of such suspension-bridge steel-tower designs are the typical, rectangular steel towers of the two Delaware Memorial Bridges: the first bridge was built in 1951, and the parallel bridge was built in 1968 (Figure 3.15).

An example of a cable-stayed bridge that is an exception to the rectangular tower form, is the modified A frame, weathering steel towers of the Luling Bridge near New Orleans, 1983 (Figure 3.16).

FIGURE 3.15 Delaware Memorial Bridges. (Courtesy of D. Sailors.)

FIGURE 3.16 Luling Bridge, New Orleans, Louisiana. (Courtesy of Charles Seim.)

The cross section of a steel tower is usually designed as a series of adjoining cells, formed by shop-welding steel plates together in units from 20 to 40 ft (6–12 m) long. The steel cellular towers for a cable-stayed bridge with cables framing into the towers must be designed for the local forces from the numerous anchorages of the cables. The steel towers for a suspension bridge, and for cable-stayed bridges with stays passing over the top of the tower in saddles, must be designed for the local, concentrated load from the saddles.

An excellent example of such a steel tower is the new 525 ft (160 m) tower for the Suspension Span of the San Francisco–Oakland Bay Bridge East Span. This tower is composed of four separated pentagonal, cross-sectional shaped shafts, connected by shear-link beams. The tower shafts are separated about 2 m, allowing light to permeate between the shafts that are tapered toward the top to enhance their appearance. The shear-link beams are both attractive esthetic elements, and the structural steel beams yield in shear and absorb energy when activated by strong earthquakes (Figure 3.17).

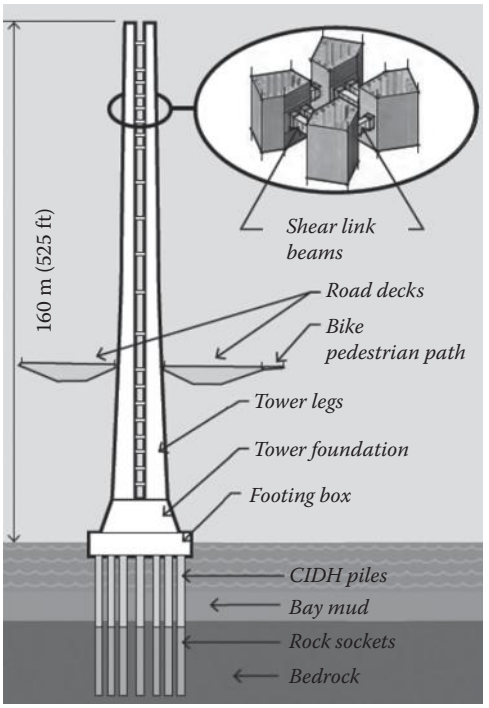

FIGURE 3.17 Tower of new San Francisco–Oakland Bay Bridge self-anchored suspension span.

For suspension bridges and cable-stayed structures, starting about the 1970s, reinforced concrete began to be extensively used in towers. Concrete towers are usually designed as hollow shafts to save weight and reduce the amount of concrete and reinforcing bars required. As with steel towers, concrete towers must be designed for the concentrated load from the saddles at the top, if used, or for the local forces from the numerous anchorages of the cables framing into the tower shafts.

Towers designed in steel will be lighter than towers designed in concrete, thus giving potential for savings in foundation costs. Steel towers will generally be more flexible, more ductile, and can be erected in less time than concrete towers. Steel towers will require periodic maintenance—painting—although weathering steel can be used for nonmarine environments as for the Luling Bridge, as noted above.

Costs of steel or concrete towers can vary with a number of factors; hence, market conditions, contractor's experience, equipment availability, design details, and site-specific influences will likely determine whether steel or concrete is the most economic material.

During the conceptual design phase of the bridge, approximate construction costs of all the materials need to be developed and compared. If life-cycle cost is important, then maintenance operations and the frequencies of those operations need to be evaluated and compared, usually by present worth evaluation.

3.5.2 Forms and Shapes

3.5.2.1 Cable-Stayed Bridge Towers

Towers of cable-stayed bridges can have a wide variety of shapes and forms (Figure 3.18). For conceptual design, the heights of cable-stayed towers, tower height (TH), above the deck can be assumed to be approximately 20% of the main-span length, span length (SL). Figure 3.18 lists the ratios of typical bridges. To this value must be added the structural depth of the girder and the clearance to the foundation to determine the approximate total tower height. The final height of the towers will be determined during the final design phase. Figure 3.19 lists distinctive towers for cable-stayed and suspension bridges.

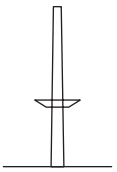

(a) Single Tower, I

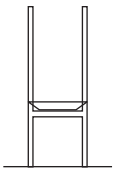

(b) Double vertical shafts, H

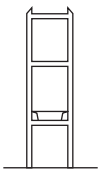

(c) Double vertical shafts with cross struts above the roadway

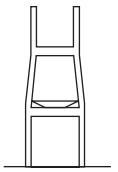

(d) Double cranked shafts with cross strut above the roadway

Stonecutters Bridge (Morgenthal et al. 2010), carries dual three-lane highway, crosses Rambler Channel, Hong Kong. Pylon height: 298 m (978 ft), with reinforced concrete from base up to 175 m level and composite top 120 m consisting of inner concrete ring with a stainless steel skin, longest span: 1018 m (3340 ft), clearance below: 73.5 m (241 ft), opened: December 2009, TH/SL: 0.22

Øresund Bridge (Gimsing 2009; Oresund Bridge 2012), carries four lanes of European route E20 and Oresund railway line, crosses Oresund Strait between Copenhagen (Denmark) and Malmö (Sweden). Pylon height: 204 m (669 ft), reinforced concrete, longest span: 490 m (1608 ft), clearance below: 57 m (187 ft), opened: July 1, 2000, TH/SL: 0.3

John James Audubon Bridge (Fossier and Duggar 2007), carries four lanes of LA 10, crosses Mississippi River, Louisiana, USA. Pylon height: 152.4 m (500 ft), longest span: 482 m (1583 ft), clearance below: 40 m (130 ft), reinforced concrete, opened: May 5, 2011, TH/SL: 0.23

Talmadge Memorial Bridge (Tang 1995), carries four lanes of US 17 to I-16, crosses Savannah River, Georgia, USA. Pylon height: 127 m (418 ft), longest span 335 m (1100 ft), clearance below: 56 m (185 ft), reinforced concrete, opened: November 1990, TH/SL: 0.2

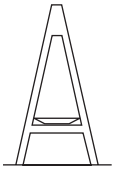

(e) Inclined shafts, A

(f) Inclined shafts, diamond

(g) Inverted Y

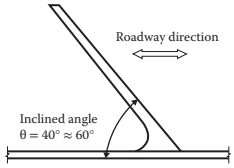

(h) Single inclined tower

Bridge to Russky Island (SK-MOST 2011), carries four lanes of roadway, crosses Eastern Bosphorus Strait, Vladivostok (Nazimov peninsula) and Russian Island (Novosiltseva cape). Pylon height: 320.9 m (1052 ft), longest span: 1104 m (3621 ft), clearance: 70 m (230 ft), opened: July 2012 (plans), TH/SL: 0.23

ANZAC Bridge (Moore 1996), carries, freeway, pedestrians and bicycles, crosses Johnstons Bay, Sydney, Australia. Pylon height: 120 m (390 ft), longest span: 345 m (1132 ft), clearance below: 27 m (88 ft), reinforced concrete, opened: December 2, 1995, TH/SL: 0.27

Yangpu Bridge (Ma and Fan 1993), carries six-lane motorway, crosses Huangpu River, China. Pylon height: 223 m (731 ft), longest span: 602 m (1975 ft), clearance below: 48 m (257 ft) reinforced concrete, opened: October 1993, TH/SL: 0.24

Sundial Bridge (Sundial Bridge 2013), cantilever spar cable-stayed bridge, carries bicycles and pedestrians, crosses Sacramento River, Redding, California, USA, pylon height: 66 m (217 ft), clearance below: 8 m (26 ft), opened: July 4, 2004

FIGURE 3.18 Generic forms and typical examples of towers for cable-stayed bridges.




FIGURE 3.18 (*Continued*) Generic forms and typical examples of towers for cable-stayed bridges.

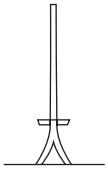
(a)

Special Pylon with a very long neck inverted Y-shape, instead of straddling the roadway, located in between.
Shanghai Yangtze River Bridge (Zhang and Lu 2008), cable stayed bridge, carries six-lane freeway, crosses Yangtze River, China. Pylon height: 212 m (695 ft), longest span: 730 m (2395 ft), clearance below: 54 m (177 ft), opened: October 31, 2009. TH/SL: 0.22

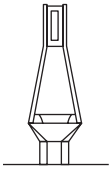
(b)

Unique Pylon with four legs
Rio–Antirrio bridge (Combault et al. 2005), five-span four-pylon cable-stayed bridge, carries six-lane roadway and one pedestrian and bicycle lane, crosses Gulf of Corinth, Greece. Pylon height: 164 m (538 ft), longest span: 560 m (1837 ft), clearance below: 52 m (170 ft), opened: August 7, 2004. TH/SL: 0.2

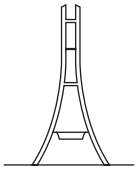
(c)

Third Nanjing Yangtze River Bridge (Cun et al. 2009), cable-stayed bridge with two curve ladder-shaped steel towers, carries six-lane freeway, crosses Yangtze River, China. Pylon height: 215 m (705 ft), longest span: 648 m (2125 ft), clearance below: 24 m (79 ft), opened: October 7, 2005. TH/SL: 0.3


(d)

Single tower self-anchored suspension bridge, San Francisco-Oakland Bay Bridge East Span (Nader and Maroney 2007), carries 10-lane I-80, bike and pedestrian way, crosses San Francisco Bay, California, USA. Tower height: 160 m (525 ft), longest span: 385 m (1263 ft), clearance below: 30 m (100 ft), single steel tower with four legs connected with shear link beams, opened: September 2013. TH/SL: 0.34.


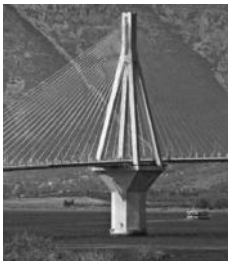

FIGURE 3.19 Distinctive towers for cable-stayed and suspension bridges.

People driving over a bridge view the towers projecting above the roadway, making this portion of the towers visually the most important feature of the bridge; thus, the towers should be carefully considered by the designers of the bridge.

The simplest tower form is a single shaft, usually vertical (Figure 3.18a). Stay cables from a single tower can be arranged in a single plane to align with a longitudinal center girder or can be splayed outwardly to connect with the longitudinal edge girders. Occasionally, the single shaft may be inclined longitudinally, usually away from the main span; rarely toward the main span. Even more infrequently, on short,

curved spans, a single tower is inclined transversely, which adds a dynamic factor to the esthetics of the bridge. The cables are usually arranged in a star array, radiating from the top of the tower.

Two vertical shafts straddling the roadway, with or without cross struts above the roadway, form a simple tower, which can be used with two planes of cables (Figure 3.18b and 3.18c). The stay cables incline inward to connect to the edge girders or to the edges of a box girder, introducing a tension component across the deck support system. The tower shafts can also be "cranked" or offset above the roadway (Figure 3.18d). This allows the cables to be aligned in a vertical plane and attached to the girder that can pass continuously through the towers. This method was used for the Talmadge Bridge, Georgia (Figure 3.20). A horizontal strut is always used between the tower shafts at the offset to stabilize the towers.

The two shafts of cable-stayed bridges can be inclined inward toward each other to form a modified "A" frame, similar to that of the Luling Bridge towers (Figure 3.16) or the two shafts inclined to bring the shafts tops together to form a full "A" frame (Figure 3.18e). The two planes of stay cables are inclined outward, producing a desirable compression component across the deck support system.

Most of the two shafts of the H-shaped, A-shaped, and the quasi-diamond- and full-diamond-shaped towers for cable-stayed bridges are designed as straight members, for ease of construction. A few of the recently built bridges have curved shafts. The Third Nanjing Yangtze Bridge is an excellent example (Figure 3.19d). As noted in Section 3.5, the form of these towers was copied from the Eiffel Tower in Paris and was the first cable-stayed bridge in China with curved steel towers.

The form of the towers of a cable-stayed bridge below the roadway is also important for reasons of both esthetics and costs. People viewing a bridge from a distance will see the towers as part of a complete structural unit. This total view is important because it displays the motif of the bridge, and it should be carefully considered by the designers of the bridge.

The shafts of the towers for a modified "A" frame bridge can be carried down to their foundations at the same slope as was used above the roadway and particularly on sites with low clearances.

However, at high-clearance locations, if the shafts of the towers for a full "A" frame or for an inverted "Y" frame are carried down to the foundations at the same slope as above the roadway, the foundations may become very wide and costly.

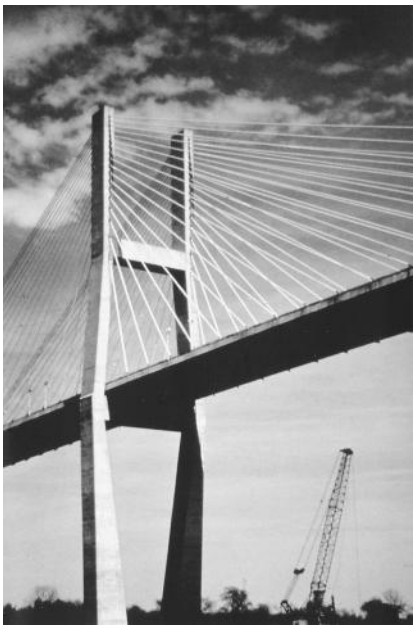

FIGURE 3.20 Talmadge Bridge, Georgia. (Courtesy of T. Y. Lin International.)

Sometimes the lower shafts are inclined inward under the roadway, producing a modified or "squat" diamond (Figure 3.18f), similar to the towers of the Glebe Island Bridge, Sydney, Australia (Figure 3.7). For very high roadways, the inward inclination can form a full diamond, as in the Cooper River Bridge, Charleston, South Carolina (Figure 3.8), or a double diamond as in the Baytown Bridge, Texas (Figure 3.21). For very long spans requiring tall towers, the "A" frame can be extended by using a single vertical shaft forming an inverted "Y" shape (Figure 3.18g) as in the Yang Pu Bridge (Figure 3.19b) and as in the Shanghai Yangtze River Bridge, China. This form is very effective for very long spans for which additional tower height is required, and the inclined legs add stiffness and frame action for wind resistance.

The numbers of shafts within the towers of cable-stayed bridges can vary from one to four; the Rio-Antirrio Bridge, Greece, has four shafts (Figure 3.19c). Three-shaft towers generally are not used for cable-stayed bridges, except for those with very wide decks. Four-shaft towers are best used to support two separate structures, rather than to support one wide deck. The four shafts of a tower may share a common foundation, or two pairs of shafts may have their own foundations, depending on costs.

3.5.2.2 Suspension Bridge Towers

Suspension bridges are designed to be used on much longer spans than are cable-stayed bridges. Thus, the towers of a suspension bridge must be far more robust than are those of a cable-stayed bridge, to support adequately the large loads and great wind forces a suspension bridge will encounter during its life span.

Usually the towers of suspension bridges follow a traditional design, using two vertical shafts and two planes of cables, as is illustrated by the steel towers for the Delaware Memorial Bridges (Figure 3.15). However, concrete towers have recently proven to be economical for some bridges. The very long span of the 4626 ft (1410 m) Humber Bridge, England, 1983, used uniformly spaced multistruts and concrete towers (Figure 3.22). The crossing of the Great Belt sea way in Denmark (Figure 3.23), opened in 1999, has concrete towers 833 ft (254 m) high with two struts—one near the mid-height and one at the top.

The shafts of suspension bridge towers are usually designed for the full height of the towers, from the foundation to the cable saddles. The tower must accommodate the large aspect ratio for good esthetics. Only a few single-cable suspension bridges have been designed with an "A" or an inverted "Y" form of towers. Typical shapes and forms of suspension bridges are shown in Figure 3.24.

For conceptual designs, the heights of suspension bridges towers, above the deck, depend on the sag-to-span ratio, which can vary from about 1:8 to 1:12. A good preliminary value is approximately 1:10. To this value, one must add the structural depth of the deck and the clearance to the foundations to

FIGURE 3.21 Baytown Bridge, Texas. (Courtesy of T. Y. Lin International.)

FIGURE 3.22 Humber Bridge, England. (Courtesy of Charles Seim.)

FIGURE 3.23 Great Belt Bridge, Denmark. (Courtesy of Ben C. Gerwick, Inc.)

obtain the approximate total tower height. The shafts are usually connected together with several struts, or cross bracing along the height of the tower, or the shafts are connected at the top with a large single strut. Some form of strut between the towers is usually required for suspension bridges because the large cables carry lateral wind and seismic loads to the tops of the tower shafts, which then need to be braced against each other with struts or "X" cross bracing to form a tower-frame action.

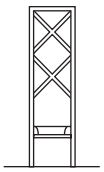

(a)

Akashi Kaikyō Bridge (HSBA 1998), longest suspension bridge in the world with two steel X-braced moment frame towers, carries six lanes of roadway, crosses Akashi Strait, Japan. Tower height: 282.8 m (928 ft), longest span: 1991 m (6532 ft), clearance below: 65.7 m (216 ft), opened: April 5, 1998, TH/SL: 0.11

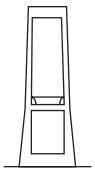

(b)

Höga Kusten Bridge, suspension bridge with two reinforced concrete towers, carries four lanes of European route E4, crosses the mouth of the Ångermanälven river, Sweden. Tower height: 180 m (591 ft), longest span: 1210 m (3970 ft), clearance below: 40 m (131 ft), opened: December 1, 1997, TH/SP: 0.12

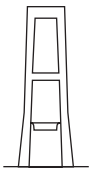

(c)

Østbroen (East Bridge 2012), suspension bridge, two reinforced concrete towers with moment frame of two vertical shafts straddling the roadway with two cross struts above the roadway, carries motor vehicles, crosses Great Belt, Denmark. Tower height: 254 m (833 ft), longest span: 1624 m (5328 ft), clearance below: 65 m (213 ft), opened: June 14, 1998, TH/SL: 0.12

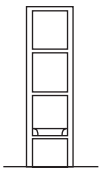

(d)

Golden Gate Bridge, suspension bridge, two steel towers with moment frame, carries six lanes of US 101, pedestrians and bicycles, crosses Golden Gate, San Francisco, USA. Tower height: 227.4 m (746 ft), longest span: 1280 m (4200 ft), clearance below: 67 m (220 ft), opened: April 19, 1937, TH/SL: 0.13

FIGURE 3.24 Generic forms and typical examples of towers for suspension bridges.

3.5.3 Erection

The most crucial stage in the life of a bridge is the erection time of that structure because the risk of adverse happenings is highest during this phase. Adverse happenings can occur from the high cost of opening the bridge to service late, to locked-in unanticipated stresses because of faulty erection procedures, to partial or full collapse. Bridge designers have little control of the first risks; however, unanticipated stresses or partial or full collapse are very troubling because they can be prevented by having a detailed erection scheme. Ordinary towers can usually be erected without much difficulty; however, thin, curved, or inclined towers or towers temporarily supporting or resisting erection forces or loads require a detailed erection plan.

Some bridge designers say that erection is the responsibility of the contractors; however, if something listed above does happen, everyone will become involved, including the designer, and someone will end up paying money.

A better solution is to design a detailed erection scheme that will construct the structure to the proper camber, position, and alignment and with acceptable stresses in all the members. The best person to design this erection scheme is the bridge designer, because the designer knows the structure intimately, works on the design for a year, and develops a bridge model for the design of the bridge; that model can

also be used to develop all erection stages for the structure. If this is done, the specifications should allow the contractor full freedom to modify that scheme or to develop a separate erection scheme. If the specifications require the contractor to develop the erection scheme, the bridge designer should check and approve the scheme before erection begins.

During the concept-design phase, many different tower forms and cable arrangements may be considered; each should be evaluated for esthetics, constructability, and cost. Each alternative considered should have at least one method of erection developed during the concept-design phase to ensure that the scheme under consideration is constructible. The costs of erecting unusual tower designs such as inclined towers, or curved spars, can be difficult to estimate and may add significant costs to the project.

3.6 Final Design

The *AASHTO Standard Specifications for Highway Bridges* (AASHTO 2002) and the *AASHTO LRFD Bridge Design Specifications* (AASHTO 2012) apply to bridges 150 m (500 ft) or less in span. For important bridges, and for long-span cable-supported bridge projects, special design criteria may need to be developed by the owner and/or the designer. The special-design criteria may also need to be developed in cooperation with the owners of the facility, so as to include their operations, maintenance requirements, and bridge performance expectations after large natural events such as earthquakes. See Chapter 9 for suspension bridge design and Chapter 10 for cable-stayed bridge design in *Bridge Engineering Handbook, Second Edition: Superstructure Design*. Troitsky (1988), Podolny and Scalzi (1986), and Walther et al., (1999) also present detailed design theory for cable-stayed bridges.

Design methodology for the towers should follow the same practices as does the design methodology for the entire bridge. The towers should be part of a global analysis in which the entire structure is treated as a whole. From the global analysis, the towers may be modeled as substructural units with their forces and deformations imposed as boundary conditions.

Detailed structural analyses form the basis for the final designs of the tower, its components, and its connections. Both cable-stayed and suspension bridges are highly indeterminate and both require careful analyses by at least one geometric nonlinear program if erections are to be determined. Prudent design should also include analysis of at least one erection scheme to demonstrate that an experienced contractor may erect the structure.

3.6.1 Design Loads

The towers are subject to many different load cases. The towers, as well as the entire structure, must be analyzed, designed, and checked for the controlling load case. Chapter 6 of *Bridge Engineering Handbook, Second Edition: Fundamentals* presents a detailed discussion of highway bridge loading.

The weight of the superstructure, including the self-weight of the towers, is obtained in the design process by utilizing the unit weights of the materials used for both the tower and the superstructure. The forces that are distributed to the tower can be calculated by a structural analysis of the completed structure. The forces distributed to the tower may be analyzed for a staged erection of the superstructure, to determine whether the towers will be over-stressed during construction of the superstructure.

Design loads from traffic using the bridge, such as trains, transit, trucks, or pedestrians, are usually prescribed in design codes and specifications or by the owners of the facility. These loads move across the bridge, and the forces imparted to the towers from such moving loads must be obtained from a structural analysis. These are all gravity effects, acting downward on the superstructure, but can induce both vertical and horizontal forces on the towers.

A current trend for spanning wide widths of waterways is to design multispan cable-stayed and suspension bridges, linked together to form a long, continuous structure with the towers evenly spaced for uniform appearance, and having a short span at each end. These multispan bridge roadways will deflect

excessively unless the towers are specially designed for added stiffness. This is because ordinary towers are not sufficiently stiff to resist the pull from cables that are supporting the flexible, multispan roadway.

Several methods have been proposed to stiffen these towers, such as adding four shafts to the towers as was done to the Rio Antirrio Bridge crossing of the Gulf of Corinth, Greece (Figure 3.19). A second method would be to use cables arranged in various ways to stiffen the towers externally; but this is beyond the scope of this chapter.

Towers are also subjected to temperature-induced displacements, from the superstructure and the cables framing into the towers, and the temperature-induced movement of the tower itself. Towers may expand and contract differentially along their tower height because of heat from the sun that shines on them from morning until sunset. Such temperature effects may cause deflection and torsional twisting along the height of the tower.

Wind blowing on the towers as a bluff shape will induce both forces and displacements in the tower. Force will be induced into the cables by the wind pressure on the superstructure and from the wind forces on the cables themselves. These additional forces will be carried to the towers, which must be designed for them.

For long-span bridges and locations with known high-wind speeds, the wind factor should be treated as a dynamic loading. This will usually require a wind-tunnel test on a sectional model of a proposed superstructure in a wind tunnel and for important bridges, a full aeroelastic model test in a large wind tunnel. See Chapter 22 of *Bridge Engineering Handbook, Second Edition: Fundamentals*. Under certain wind flows, the wind may excite the tower itself. In the rare instances where wind-induced excitation of the tower does occur, appropriate changes in the cross section of the tower may be made, or a faring added, to change the dynamic characteristics of the towers. If these methods are not effective in changing the response, installing tuned-mass dampers at various locations within the towers will dampen out excessive vibrations. These types of dampers need periodic maintenance, which requires ladders and elevators for access by maintenance personnel.

Seismic excitations should be treated as dynamic inertia loadings, inducing responses within the structure by exciting the vibrational modes of the towers. Tuned mass dampers can also be installed to dampen seismic excitations. Seismic forces and displacement may control tower design in locations with high seismic activity. For locations with lower seismic activity, the tower design should be checked at least for code-prescribed seismic loadings. The dynamic analysis of bridges is discussed in Chapter 3 of *Bridge Engineering Handbook, Second Edition: Seismic Design*.

A full analysis of the final design will reveal all the forces, displacements, and other design requirements for all loading cases for the final design of the towers.

3.6.2 Other Design Considerations

Suspension bridge cables pass over cable saddles that are usually anchored to the top of the tower. A cable produces a large vertical force, as well as smaller, but important, transverse and longitudinal forces from temperature, wind, earthquake, or any unbalanced cable forces between the main and the side spans. These forces are transmitted through the cable-saddle anchorage at each cable location, to the top of the tower. The towers and the permanent saddle anchorages must be designed to resist these cable forces.

The erection of a suspension bridge must be analyzed and the chosen sequence shown on the construction plans. To induce the correct loading into the cables of the side span, the erection sequence usually requires that the saddles be displaced toward the side spans. This is usually accomplished for short spans by displacing the tops of the towers by pulling them with heavy cables. For long spans, the saddles can be displaced temporarily, on rollers. As the stiffening girders or trusses are being erected into position and the cable begins to take loads, the towers or saddles are gradually rolled into final alignment on the tower. After erection of the stiffening girders or trusses is completed, the saddles are permanently fastened into position to take the unbalanced cable loads from the center and the side spans.

At the deck level, other forces may be imposed on the tower, from the box girder or the stiffening truss carrying the roadway. Such forces depend on the structural framing of the connections of the deck and the tower. Traditional suspension bridge designs usually terminate the stiffening truss, or the box girder, at the towers; that produces transverse and longitudinal forces on the tower at this point. More recent suspension bridge designs usually provide for the passing of a box girder continuously through the tower opening; this may produce transverse forces, but not longitudinal forces. For this arrangement, the longitudinal forces must be carried by the stiffing girder or trusses to the abutments.

The most critical area of the tower design is the tower-to-foundation connection. Both shear forces and moments are at a maximum at this point. Anchor bolts are generally used at the base of steel towers. Such bolts must be proportioned to transfer overturning loads from the tower to the bolts. The bolts must be deeply embedded in the concrete footing block in order to transfer their loads to the footing reinforcement.

Providing good drainage for rainwater running down the tower shafts will increase the life of the steel paint system at the tower base and will provide some protection to the anchor bolts.

Concrete towers must be joined to the foundations with full shear and moment connections. Lapped reinforcing bar splices are usually avoided as the lapping tends to congest the connections; the strength of the bars cannot then be developed, and lapped splices cannot be used for high-seismic areas. Using compact mechanical or welded splices will result in less congestion, with easier placement of concrete around the reinforcement, and a more robust tower-to-footing connection. The design of the joint of the tower shafts to the foundation should produce a constructible, efficient, and reliable connection.

The cable arrangements for cable-stayed bridges are many and varied. Some arrangements terminate the cables in the tower, whereas other arrangements pass the cable through the tower on cable saddles. Cables terminating in the tower may pass completely through the tower cross section and then be anchored on the far side of the tower. This method of anchoring produces compression in the tower cross section at the anchorage points. Cables can also be terminated at anchors within the walls of the tower, producing tension in the tower cross section at the anchorage points. These tension forces require special designing to provide reliable, long-life support for the cables.

As for suspension bridges, the erection of cable-stayed bridges must be analyzed, and the sequence be shown on the construction plans. The girders, as they are cantilevered outward from the towers, are very vulnerable. The most critical erection sequence is just before the closing of the two arms of the girders, at the center of the span. High winds can displace the arms and torque the towers, and heavy construction equipment can load the arms that are yet without benefit of the girder continuity to distribute the loads to towers.

3.7 Construction

The towers and superstructure should be constructed according to an erection plan as noted in Section 3.5.3.

Towers constructed of structural steel are usually fabricated in a shop by welding together steel plates and rolled shapes to form cells. Cells must be large enough to allow welders and welding equipment, and if the steel is to be painted, painters and cleaning and painting equipment inside each cell.

The steel tower components are transported to the bridge site and are erected by cranes and are either welded or bolted together with high-strength bolts. For bolting, the contractor should use a method of tensioning the high strength bolts to give consistent results needed to achieve the required tension such as turn-of-the-nut method. Field welding presents difficulties in holding the component rigidly in position while the weld is completed. Field welding may be difficult to control when exposed to windy weather, making ductile welds difficult, particularly the vertical and overhead welds. Field welding should be made within a protective covering that keeps out water and wind. Full-penetration welds require backup bars that must be removed carefully if the weld is subject to fatigue loading.

Towers constructed of reinforced concrete are usually cast in forms that can be removed and reused, or "jumped," to the next level. Placing height for concrete is usually restricted to approximately 20–40 ft (6–12 m), to limit pressure from the freshly placed concrete. Reinforcing bar cages are usually preassembled on the ground, or on a work barge, and are lifted into position by crane. This requires the reinforcing bars to be spliced with each lift. Lapped splices are the easiest to make, but these are not allowed in seismic areas.

Slip forming is an alternative method that uses forms that are pulled slowly upward, reinforcing bars positioned and the concrete placed in one continuous operation around the clock until the tower is completed. Slip forming can be economical, particularly for constant cross-section towers. Some changes in cross-section geometry can be accommodated. For shorter spans, precast concrete segments can be stacked together and steel tendons tensioned to form the towers.

Tower designers should consider the method of erection that contractors may use in constructing the towers. Often the design can reduce construction costs by incorporating more easily fabricated and assembled steel components or easily assembled reinforcing bar cages and tower shapes that are easily formed. Of course, the tower design cannot be compromised just to lower erection costs.

Some engineers and many architects design towers that are angled longitudinally toward or away from the main span or are curved or kinked. This can be done if such a design can be justified structurally and esthetically, and the extra cost can be covered within the project budget. These types of towers require special erection methods.

Many towers of cable-stayed bridges have legs sloped toward each other to form an "A," an inverted "Y," a diamond, or similar shapes. These are not as difficult to construct as the longitudinally inclined tower design. The sloping concrete forms can be supported by vertical temporary supports and cross struts that tie the concrete forms together for each shaft. This arrangement braces the partly cast concrete tower legs against each other for support. Some of the concrete form supports for the double-diamond towers of the Baytown Bridge are visible in Figure 3.19.

As the sloped legs are erected, the inclination may induce bending moments and lateral deflection in the plane of the slope of the legs. Both of these secondary effects must be adjusted by jacking the legs apart by a calculated amount of force or displacement to release the locked-in bending stresses. If the amount of secondary stress is small, then cambering the leg to compensate for the deflection and adding material to lower the induced stress can be used. The jacking procedure adds cost but is an essential step in the tower erection. Neglecting this important construction detail can "lock-in" stresses and deflections that will lower the factor of safety of the tower and, in an extreme case, could cause a failure.

Tower construction usually requires special equipment to erect steel components or concrete forms to the full height of the tower. Suspension bridges and some cable-stayed bridges require cable saddles to be erected on the tower tops. Floating cranes rarely have the capacity to reach to the heights of towers designed for long spans. Tower cranes, connected to the tower as it is erected, can be employed for most tower designs and are a good choice for handling steel forms for the erection of concrete towers. A tower crane used to jump the forms and raise materials can be seen in Figure 3.8. Occasionally, vertical traveling cranes are used to erect steel towers by pulling themselves up the face of the tower following the erection of each new tower component.

Because the tower erection must be done in stages, each stage must be checked for stability and for stresses and deflections. The tower construction specifications should require the tower erection be checked by an engineer, employed by the contractor, for stability and safety at each erection stage. The construction specifications should also require the tower erection stages to be submitted to the design engineer for an evaluation and approval. This evaluation should be full enough to determine whether the proposed tower erection staging will meet the intent of the original design or needs to be modified to bring the completed tower into compliance. Chapters 1 and 4 of *Bridge Engineering Handbook, Second Edition: Construction and Maintenance* present more detailed construction procedure and techniques for long-span bridges.

3.8 Summary

Towers provide the structural and visible means of support of the bridge superstructure. Towers project above the roadway and are the most visible structural elements in a bridge. Towers usually form visible portals through which people pass as they travel from one point to another. They give the bridge, for good or for bad, its character, its motif, and its identifying esthetic statement and form the enduring impression of the bridge in people's minds.

Towers are the most critical structural element in the bridge as their function is to carry the weight of the bridge and the forces imposed on the bridge to the foundations. Unlike most other bridge components, they cannot be replaced during the life of the bridge. Towers must fulfill their function in a reliable, serviceable, economical, and esthete manner for the entire life of the bridge. Towers must also be practicable to erect without extraordinary expense; the exception to this economical requirement is the owners or the public want a spectacular bridge and are willing to pay for the extra cost.

Practicable tower shapes for cable-stayed bridges are many and varied. These towers can have one or several shafts arrayed from vertical to inclined, forming various shapes. Practicable tower shapes for a suspension bridge are usually restricted to two vertical shafts connected with one or several cross struts, although single shafts have been used on a few suspension bridges.

In the early 1990s, a trend began where efficiency and low cost were not always an objective because the owner or the public, or both, desires spectacular, picturesque, or distinctive bridges. This resulted in configuring stay cables and a few suspension bridge cables in unusual arrays that can dominate the towers and act as the principle esthetic statement of the bridge or the opposite of featuring towers that have unusual shapes, kinks, or inclination to add visual impact. This trend will continue into the foreseeable future.

The conceptual design phase is the most important phase in the design of towers for long span bridges. This phase sets, among other items, the span length, type of deck system, and the materials and shape of the towers. It also determines the esthetic, economics, and constructability of the bridge. A conceptual erection scheme should be developed during this phase to ensure the bridge can be economically constructed.

The final design phase sets the specific shape, dimensions, and materials for the bridge. If a usual tower design is used, the tower erection should also be shown. It is preferred that the design engineer follow the project into the construction stages. The design engineer must understand each erection step that is submitted by the contractor to ensure the construction complies with the design documents. The owner assured only by this means that the serviceable and reliability that he is paying for is actually achieved in construction.

The successful design of towers for cable-stayed and suspension bridges involves many factors and decision that must be made during the conceptual and design phases and the construction phase of the project. The final judge of a successful project is always made by the people who use the facility, pay for its construction and maintenance, and view the results of all the effort to provide a long-life bridge to service society (Cerver 1992).

References

AASHTO. 2002. *Standard Specifications for Highway Bridges*, 17th Edition, American Association of State Highway and Transportation Officials, Washington, DC.

AASHTO. 2012. *AASHTO LRFD Bridge Design Specifications*, *Customary U.S. Unit*, 2012, American Association of State Highway and Transportation Officials, Washington, DC.

Billington, D. P. 1983. *The Tower and the Bridge, The New Art of Structural Engineering*, Basic Books, New York, NY.

Combault, J., Pecker, A., Teyssandier, J. P. and Tourtois, J. M. 2005. "Rion-Antirion Bridge, Greece-Concept, Design, and Construction," *Structural Engineering International*, 15(1): 22–27.

Cun, B., Zhao, C. H., Dong, M. and Tang, L. 2009. "Design of Steel-Concrete Segment of Main Tower of the Thrid Naijing Yangtze River Bridge," *Highway*, No. 5, Beijing, China. (In Chinese)

Fossier, P. and Duggar, C. 2007. "John James Audubon Bridge Design-Build Project Update," *2007 Louisiana Transportation Engineering Conference*, February 12, Baton Rouge, LA.

Gimsing, N. J. 2009. "From Bridges across Great Belt and Øresund towards a Femern Belt Bridge," *IABSE Workshop – Recent Major Bridges*, May 11–20, Shanghai, China.

Gimsing, N. J. and Georgakis, C. T. 2012. *Cable Supported Bridges - Concept and Design*, 3rd Edition, John Wiley & Sons, New York, NY.

HSBA. 1998. *The Akashi-Kaikyo Bridge – Design and Construction of the World's Longest Bridge*, Honshu-Shikoku Bridge Authority, Japan.

Leonhardt, F. 1984. *Bridges, Aesthetics and Design*, MIT Press, Cambridge, MA.

Ma, X. B. and Fan, Q. G. 1993. "Construction Planning and Management of Yangpu Bridge Main Tower," *Construction Technology*, No. 3. Beijing, China. (In Chinese).

Moore, D. 1996. *To build a Bridge, Glebe Island, Sydney, Australia*, Chapter & Verse, Sydney, Australia.

Morgenthal, G., Sham, R. and West, B. 2010. "Engineering the Tower and Main Span Construction of Stonecutters Bridge," *Journal of Bridge Engineering*, ASCE, 15(2): 144–152.

Nader, M. and Maroney, B. 2007. "One-of-a-Kind Design, The New San Francisco-Oakland Bay Bridge Eastern Span", *STRUCTURE magazine*, October.

Øresund Bridge. 2013. http://en.wikipedia.org/wiki/Great_Belt_Fixed_Link.

Petroski, H. 1996. *Engineers of Dreams*, Vintage Books, New York, NY.

Podolny, W. and Scalzi, J. B. 1986. *Construction and Design of Cable Stayed Bridges*, Second Edition, John Wiley & Sons, New York, USA.

Seim, C. 1996, "San Francisco Bay's Jeweled Necklace," *ASCE Civil Engineering*, 66(1): 14A, January.

Sundial Bridge. 2013. http://www.turtlebay.org/sundialbridge.

Tang, M. C. 1995. "Talmadge Memorial Bridge, Savannah, Georgia," *Structural Engineering International*, 5(1): 15–16.

SK-MOST. 2011. *Construction of acable-stayed bridge to the Russky Island across the Eastern Bosphorus StraitinV ladivostok*, http://rusbridge.net/2011/01/.

Troitsky, M. S. 1988. *Cable Stayed Bridges*, Van Nostand Reinhold Co, New York, NY.

Walther, R., Houriet, B., Isler, W., Moia, P. and Klein, J.F. 1999. *Cable Stayed Bridges*, 2nd Edition, Thomas Telford Ltd. London, UK.

Zhang, C. L. and Lu, Y. C. 2008. "Design of Main Tower of Shanghai Yangtze River Bridge Main Span," *Shanghai Highway*, No. 4, Shanghai, China. (In Chinese).

4

Vessel Collision Design of Bridges

Michael Knott
Moffatt & Nichol

Zolan Prucz
Modjeski and Masters Inc.

Notations

The following symbols are used in this chapter. The section number in parentheses after definition of a symbol refers to the section or figure number where the symbol first appears or is identified.

AF = annual frequency of bridge element collapse (Section 4.5.2)
B_M = beam (width) of vessel (Figure 4.7)
B_P = width of bridge pier (Figure 4.7)
DWT = size of vessel based on deadweight tonnage (1 ton = 2205 lb. = 9.80 kN) (Section 4.4.1)
H = ultimate bridge element strength (Section 4.5.2)
N = number of one-way vessel passages through the bridge (Section 4.5.2)

P = vessel collision impact force (Section 4.5.2)
P_{BH} = ship collision impact force for head-on collision between ship bow and a rigid object (Section 4.6.1)
P_{DH} = ship collision impact force between ship deckhouse and a rigid superstructure (Section 4.6.1)
P_{MT} = ship collision impact force between ship mast and a rigid superstructure (Section 4.6.1)
P_S = ship collision impact force for head-on collision between ship bow and a rigid object (Section 4.6.1)
PA = probability of vessel aberrancy (Section 4.5.2)
PC = probability of bridge collapse (Section 4.5.2)
PG = geometric probability of vessel collision with bridge element (Section 4.5.2)
PF = protection factor for bridge location (Section 4.5.2)
R_{BH} = ratio of exposed superstructure depth to the total ship bow depth (Section 4.6.1)
R_{DH} = reduction factor for ship deckhouse collision force (Section 4.6.1)
V = design impact speed of vessel (Section 4.6.1)
x = distance to bridge element from the centerline of vessel-transit path (Figure 4.7)
φ = angle between channel and bridge centerlines (Figure 4.7)

4.1 Introduction

4.1.1 Background

Vulnerability of critical infrastructures to extreme events have made headlines worldwide in the past decades due to structural failures, loss of life, and financial damages due to earthquakes, hurricanes, storm surge and waves, tsunamis, flooding and scour, vessel collisions, and terrorist attacks. For major bridge structures, the risk and magnitude of such extreme events is often the controlling load case for the structure design.

It was only after a marked increase in the frequency and severity of vessel collisions with bridges that studies of the vessel collision problem were initiated in the 1980s. In the period from 1960 to 2011, there have been 36 major bridge collapses worldwide due to ship or barge collision, with a total loss of life of 342 people. The greatest loss of life occurred in 1983 when a passenger ship collided with a railroad bridge on the Volga River, Russia. One hundred and seventy six people were killed when the aberrant vessel attempted to transit through a side span of the massive bridge. Most of the deaths occurred when a packed movie theatre on the top deck of the passenger ship was sheared off by the low vertical clearance of the bridge superstructure.

Seventeen of the bridge catastrophes mentioned above occurred in the United States, including the 1980 collapse of the Sunshine Skyway Bridge crossing Tampa Bay, Florida, in which 396 m of the main span collapsed and 35 lives were lost as a result of the collision by an empty 35,000 DWT (deadweight tonnage) bulk carrier (Figure 4.1). Recent collapse of bridges due to barge collision include the Queen Isabella Causeway Bridge, Texas, in 2001 that resulted in 8 fatalities, the I-40 Bridge, Oklahoma, in 2002 that resulted in 13 fatalities (Figure 4.2) and the Popps Ferry Bridge, Mississippi in 2009 (Figure 4.3). A recent collapse due to ship collision was the Eggner's Ferry Bridge in Kentucky, where a 322-foot approach span collapsed when hit by 8400 DWT cargo ship on January 26, 2012.

One of the more publicized tragedies in the United States involved the 1993 collapse of a CSX Railroad Bridge across Bayou Canot near Mobile, Alabama. During dense fog, a barge tow became lost and entered a side channel of the Mobile River where it struck a railroad bridge causing a large shifting of the superstructure. The bridge collapsed a few minutes later when a fully loaded Amtrak passenger train attempted to cross the damaged structure. Forty-seven fatalities occurred as a result of the collapse and train derailment.

It should be noted that there are numerous vessel collision accidents with bridges, which cause damage that varies from minor to significant damage but do not necessarily result in collapse of the structure or loss of life. A U.S. Coast Guard Study (U.S. Coast Guard 2003) of towing vessels and barge collisions

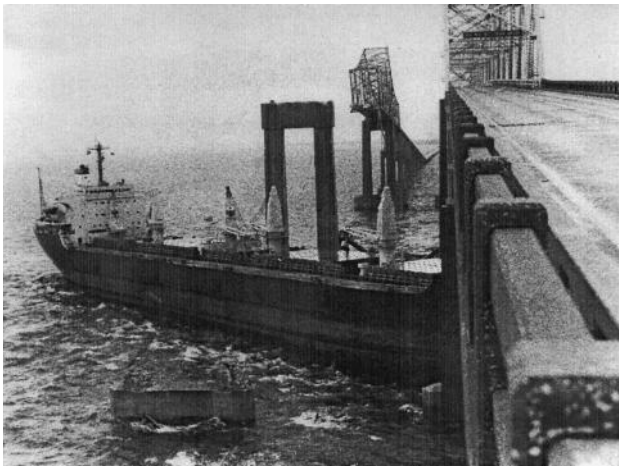

FIGURE 4.1 Sunshine Skyway Bridge after being struck by the M/V Summit Venture, FL (1980).

FIGURE 4.2 I-40 Bridge over Arkansas River, OK (2002).

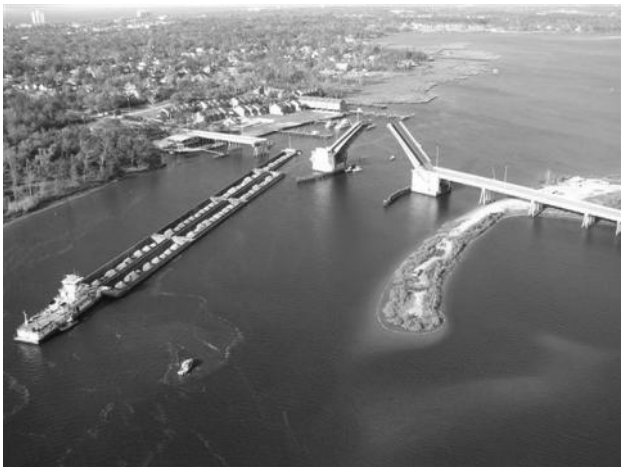

FIGURE 4.3 Popps Ferry Bridge, MS (2009).

with bridges located on the U.S. inland waterway system during the 10-year period from 1992 to 2001 revealed that there were 2692 accidents with bridges. Only 61 of these caused bridge damage in excess of $500,000, and there were no fatalities during the study period. The study concluded that 90% of the barge tow accidents were related to human performance (78% to pilot error and 12% to other operational factors). Only 5% were related to mechanical problems, and for the remaining 5% there was insufficient information to assign a cause.

In addition to motorist disruption, structural damage and potential loss of life, significant environmental damage can also occur in a waterway due to oil and chemical spills as a result of vessel collision. Examples include the spillage of 170,000 gallons of fuel oil in the Fore River, Maine in 1996 when a collision occurred with a bascule bridge pier of the Million Dollar Bridge that ripped a 9-m hole in a loaded tanker ship (caused by an underwater protrusion of the concrete support pier footing); and the spillage of 53,600 gallons of fuel oil into San Francisco Bay in 2007 when a container ship hit one of the main pier fender systems of the San Francisco–Oakland Bay Bridge during dense fog.

The 1980 collapse of the Sunshine Skyway Bridge was a major turning point in awareness and increased concern for the safety of bridges crossing navigable waterways in the United States. Investigations and research subsequent to the Skyway and other major bridge accidents worldwide (National Research Council 1983; IABSE 1983; Modjeski and Masters 1984; Prucz and Conway 1987) ultimately lead to the development of the *AASHTO Guide Specification for Vessel Collision Design of Highway Bridges* in 1991 (AASHTO 1991). This landmark publication provided the bridge design community (for the first time) the ability to evaluate the risk of vessel collision and estimate the magnitudes of impact forces associated with ship and barge collisions. A second edition of the *Guide Specification* was developed by AASHTO in 2009 (AASHTO 2009) to update and incorporate lessons learned from the use of the original 1991 Vessel Collision Guide Specification; incorporate current LRFD Bridge Design methodologies; and incorporate results from barge and ship collision research conducted since the original vessel collision publication.

Current highway bridge design practices in the United States follow the AASHTO specifications (AASHTO 2009, 2012). The design of railroad bridge protection systems against vessel collision is addressed in the American Railway Engineering and Maintenance of Way Association (AREMA) Manual for Railway Engineering (AREMA 2013).

Research and development work in the area of vessel collision with bridges is ongoing, though compared to more mature and established fields such as wind and earthquake engineering, vessel collision analysis and design is in its infancy stages. Important research needs within the discipline include ship impact forces, barge impact forces, risk acceptance criteria, physical protection systems, and aids-to-navigation improvements. As further research results become available, appropriate code changes and updates could be expected.

4.1.2 Basic Concepts

The vulnerability of a bridge to vessel collision is affected by various factors, including

- Waterway geometry, water stage fluctuations, current speeds, and weather conditions.
- Vessel characteristics and navigation conditions, including vessel types and size distributions, speed and loading conditions, navigation procedures, and hazards to navigation.
- Bridge size, location, horizontal and vertical geometry, resistance to vessel impact, structural redundancy, and effectiveness of existing bridge protection systems.
- Serious vessel collisions with bridges are extreme events associated with a great amount of uncertainty, especially with respect to the impact loads involved. As designing for the worst case scenario could be overly conservative and economically undesirable, a certain amount of risk must be considered as acceptable. The commonly accepted design objective is to minimize (in a cost-effective manner) the risk of catastrophic failure of a bridge component, and at the same time reduce the risk of vessel damage and environmental pollution.

The intent of vessel collision provisions is to provide bridge components with a "reasonable" resistance capacity against ship and barge collisions. In navigable waterway areas where collision by merchant vessels may be anticipated, bridge structures should be designed to prevent collapse of the superstructure by considering the size and type of vessel, available water depth, vessel speed, structure response, the risk of collision, and the importance classification of the bridge. It should be noted that damage to the bridge (even failure of secondary structural members) is usually permitted as long as the bridge deck carrying motorist traffic does not collapse (i.e., sufficient redundancy and alternate load paths exist in the remaining structure to prevent collapse of the superstructure).

4.1.3 Application

The vessel collision design recommendations provided in this chapter are consistent with the AASHTO specifications (AASHTO 2009, 2012), and they apply to all bridge components in navigable waterways with water depths over 2.0 ft (0.6 m). The vessels considered include merchant ships larger than 1000 DWT and typical inland barges.

4.2 Initial Planning

It is very important to consider vessel collision aspects as early as possible in the planning process for a new bridge, because they can have a significant effect on the total cost of the bridge. Decisions related to the bridge type, location, and layout should take into account the waterway geometry, the navigation channel layout and the vessel traffic characteristics.

4.2.1 Selection of Bridge Site

The location of a bridge structure over a waterway is usually predetermined based on various other considerations, such as environmental impacts, right-of-way, costs, roadway geometry, and political considerations. However, to the possible extent, the following vessel collision guidelines should be followed:

- Bridges should be located away from turns in the channel. The distance to the bridge should be such that vessels can line-up before passing the bridge, usually at least eight times the length of the vessel. An even larger distance is preferable when high currents and winds are likely to occur at the site.
- Bridges should be designed to cross the navigation channel at right angles and should be symmetrical with respect to the channel.
- An adequate distance should exist between bridge locations and areas with congested navigation, port facilities, vessel berthing maneuvers, or other navigation problems.
- Locations where the waterway is shallow or narrow so that bridge piers could be located out of vessel reach are preferable.

4.2.2 Selection of Bridge Type, Configuration, and Layout

The selection of the type and configuration of a bridge crossing should consider the characteristics of the waterway and the vessel traffic, so that the bridge would not be an unnecessary hazard to navigation. The layout of the bridge should maximize the horizontal and vertical clearances for navigation, and the bridge piers should be placed away from the reach of vessels. Finding the optimum bridge configuration and layout for different bridge types and degrees of protection is an iterative process that weighs the costs involved in risk reduction, including political and social aspects.

4.2.3 Horizontal and Vertical Clearance

The horizontal clearance of the navigation span can have a significant impact on the risk of vessel collision with the main piers. Analysis of past collision accidents has shown that bridges with a main span less than two to three times the design vessel length or less than two times the channel width are particularly vulnerable to vessel collision.

The vertical clearance provided in the navigation span is usually based on the highest vessel that uses the waterway in a ballasted condition and during periods of high water level. The vertical clearance requirements need to consider site-specific data on actual and projected vessels and must be coordinated with the Coast Guard in the United States. General data on vessel height characteristics are included in AASHTO (2009) and Larsen (1993).

4.2.4 Approach Spans

The initial planning of the bridge layout should also consider the vulnerability of the approach spans to vessel collision. Historical vessel collisions have shown that bridge approach spans were damaged in more than 60% of the total number of accidents. Therefore, the number of approach piers exposed to vessel collision should be minimized, and horizontal and vertical clearance considerations should also be applied to the approach spans.

4.2.5 Protection Systems

Bridge protection alternatives should be considered during the initial planning phase, because the cost of bridge protection systems can be a significant portion of the total bridge cost. Bridge protection systems include fender systems, dolphins, protective islands, or other structures designed to redirect, withstand, or absorb the impact force and energy, as described in Section 4.8.

4.3 Waterway Characteristics

The characteristics of the waterway in the vicinity of the bridge site such as the width and depth of the navigation channel, the current speed and direction, the channel alignment and cross section, the water elevation, and the hydraulic conditions have a great influence on the risk of vessel collision and must be taken into account.

4.3.1 Channel Layout and Geometry

The channel layout and geometry can affect the navigation conditions, the largest vessel size that can use the waterway, and the loading condition and speed of vessels.

The presence of bends and intersections with other waterways near the bridge increase the probability of vessels losing control and become aberrant. The navigation of downstream barge tows through bends is especially difficult.

The vessel-transit paths in the waterway in relation to the navigation channel and the bridge piers can affect the risk of aberrant vessels hitting the substructure.

4.3.2 Water Depth and Fluctuations

The design water depth for the channel limits the size and draft of vessels using the waterway. In addition, the water depth plays a critical role in the accessibility of vessels to piers outside the navigation channel. The vessel collision analysis must include the possibility of ships and barges transiting ballasted or empty in the waterway, as well as the possibility that upstream and downstream

water depths may be different. For example, a loaded ocean-going barge with a 6-m draft would run aground before it could strike a pier in 4 m of water, but the same barge empty with a 1-m draft could potentially strike the pier.

The water level along with the loading condition of vessels influences the location on the pier where vessel impact loads are applied, and the susceptibility of the superstructure to vessel hits. The annual mean high water elevation is usually the minimum water level used in design. In waterways with large water stage fluctuations, the water level used can have a significant effect on the structural requirements for the pier and/or pier protection design. In these cases, a closer review of the water stage statistics at the bridge site is necessary in order to select an appropriate design water level.

4.3.3 Current Speed and Direction

Water currents at the location of the bridge can have a significant effect on navigation and the probability of vessel aberrancy. The design water currents commonly used represent annual average values rather than the occasional extreme values that occur only a few times per year and during which vessel traffic restrictions may also apply.

4.4 Vessel Traffic Characteristics

4.4.1 Physical and Operating Characteristics

General knowledge on the operation of vessels and their characteristics is essential for safe bridge design. The types of commercial vessels encountered in navigable waterways may be divided into ships and barge tows.

4.4.1.1 Ships

Ships are self-propelled vessels using deep draft waterways. Their size may be determined based on the DWT. The DWT is the weight in metric tons (1 ton = 2205 lb. = 9.80 kN) of cargo, stores, fuel, passenger, and crew carried by the ship when fully loaded. There are three main classes of merchant ships: bulk carriers, product carriers/tankers, and freighter/containers. General information on ship profiles, dimensions, and sizes as a function of the class of ship and its DWT is provided in AASHTO (2009) and Larsen (1993). The dimensions given in AASHTO (2009) and Larsen (1993) are typical values, and due to the large variety of existing vessels, they should be regarded as general approximations.

The steering of ships in coastal waterways is a difficult process. It involves constant communications among the shipmaster, the helmsman, and the engine room. There is a time delay before a ship starts responding to an order to change speed or course, and the response of the ship itself is relatively slow. Therefore, the shipmaster has to be familiar with the waterway and be aware of obstructions, navigation, and weather conditions in advance. Very often local pilots are used to navigate the ships through a given portion of a coastal waterway. When the navigation conditions are difficult, tugboats are used to assist ships in making turns. Ships need speed to be able to steer and maintain rudder control. A minimum vessel speed of approximately 5 knots (8 km/h) is usually needed to maintain steering. Fully loaded ships are more maneuverable, and in deep water they are directionally stable and can make turns with a radius equal to one to two times the length of the ship. However, as the underkeel clearance decreases to less than half the draft of the ship, many ships tend to become directionally unstable, which means that they require constant steering to keep them traveling in a straight line. In the coastal waterways of the United States, the underkeel clearance of many laden ships may be far less than this limit, in some cases as small as 5% of the draft of the ship. Ships riding in ballast with shallow draft are less maneuverable than loaded ships, and, in addition, they can be greatly affected by winds and currents. Historical accident data indicate that most bridge accidents involve empty or ballasted vessels.

4.4.1.2 Barge Tows

Barge tows use both deep draft and shallow draft waterways. The majority of the existing bridges cross shallow draft waterways where the vessel fleet is comprised of barge tows only. The size of barges in the United States are usually defined in terms of the cargo carrying capacity in short tons (1 ton = 2000 lb. = 8.90 kN). The types of inland barges include open and covered hoppers, tank barges, and deck barges. They are rectangular in shape, and their dimensions are quite standard so that they can travel in tows. The number of barges per tow can vary from 1 to over 20, and their configuration is affected by the conditions of the waterway. A statistical analysis of barge tow types, configurations and dimensions, which utilizes barge traffic data from the Ohio River, is reported in Whitney, Harik, Griffin, and Allen (1996). In most cases barges are pushed by a towboat. Information on barge dimensions and capacity as well as on barge tow configurations is included in AASHTO (2009) and Larsen (1993).

The size of the individual barges affects the collision energy and the shape, size, and strength characteristics of the bow rake affects the location, extent, and magnitude of the impact loads. The most common barge type is the hopper barge, which is 10.7 m wide, 59.5 m long, and approximately 4 m deep at its bow and with a bow rake head log height of 0.6–0.9 m. Because the collision load formulation and the recent barge tests and studies are all based on a typical hopper barge construction with a 0.6–0.9 m bow rake head log height (Figure 4.4), it is important for the bridge designer to become knowledgeable of the barge types transiting the waterway and their orientation in a tow. For example, the use of the hopper barge collision load formulation would have not been appropriate for the much deeper head log of the tanker barge (Figure 4.5) that hit one of the piers of the I-40 Bridge over the Arkansas River in Oklahoma causing the collapse of several spans (Figure 4.2). At times, as in this particular case, barges that are usually at the rear of a tow are turned around with their stronger end, that is normally in contact and pushed by the towboat, becoming the front of the tow (Figure 4.6) further increasing the likelihood of higher collision loads.

It is very difficult to control and steer barge tows, especially in waterways with high stream velocities and cross currents. Taking a turn in a fast waterway with high current is a serious undertaking. In maneuvering a bend, tows experience a sliding effect in a direction opposite to the direction of the turn, due to inertial forces, which are often coupled with the current flow. Sometimes bridge piers and fenders are used to line up the tow before the turn. Bridges located in a high velocity waterway near a bend in the channel will probably be hit by barges numerous times during their lifetime. In general, there is a high likelihood that any bridge element that can be reached by a barge will be hit during the life of the bridge.

4.4.2 Vessel Fleet Characteristics

The vessel data required for bridge design includes types of vessels and size distributions, transit frequencies, typical vessel speeds, and loading conditions. In order to determine the vessel size distribution at the bridge site, detailed information on both present and projected future vessel traffic is needed. Collecting data on the vessel fleet characteristics for the waterway is an important and often

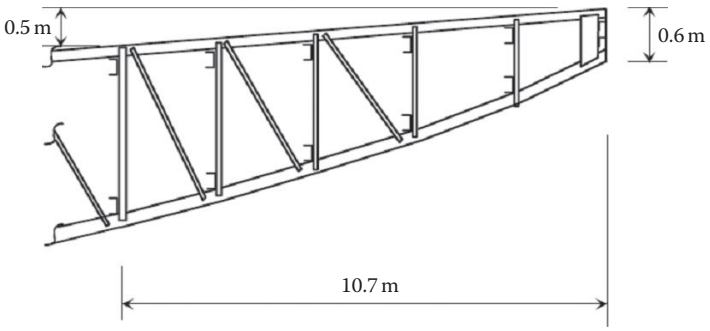

FIGURE 4.4 Common hopper barge bow rake dimensions.

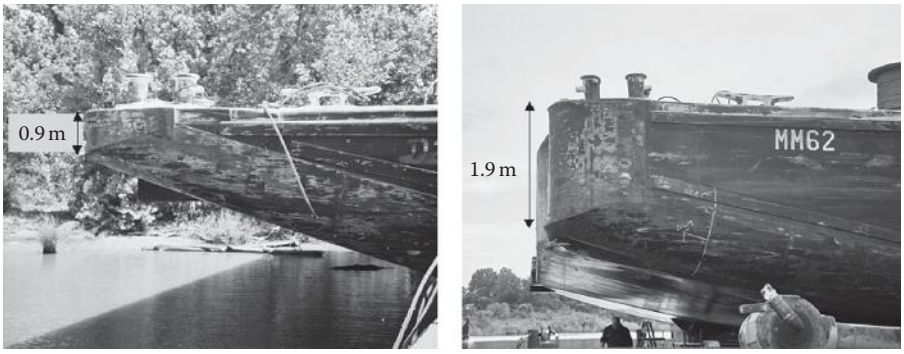

FIGURE 4.5 Bow rake head log height comparison. Typical hopper barge (left) and typical tanker barge (right). (*Note*: Barge MM62 was involved in the I-40 Bridge Collapse.)

FIGURE 4.6 Tanker barge approaching a bridge. Note the bow depth of at least 1.8 m and the four push knees.

time-consuming process. The Internet is an important source of navigation data and most U.S. government agencies maintain online resources.

Some of the sources in the United States for collecting vessel traffic data are as follows:

- U.S. Army Corps of Engineers, District Offices
- Port Authorities and Industries along the Waterway
- Local Pilot Associations and Merchant Marine Organizations
- U.S. Coast Guard, Marine Safety and Bridge Administration Offices
- U.S. Army Corps of Engineers, "Products and Services Available to the Public," Water Resources Support Center (WRSC), Navigation Data Center, Fort Belvoir, Virginia, NDC Reports
- U.S. Army Corps of Engineers, "Waterborne Commerce of the United States (WCUS), Parts 1 through 5," WRSC, Fort Belvoir, Virginia
- U.S. Army Corps of Engineers, "Lock Performance Monitoring (LPM) Reports," WRSC, Fort Belvoir, Virginia
- Shipping Registers (American Bureau of Shipping Register, New York; and Lloyd's Register of Shipping, London)
- Bridge Tender Reports for movable bridges

Projections for anticipated vessel traffic during the service life of the bridge should address both changes in the volume of traffic and in the size of vessels. The following factors need to be considered:

- Changes in region economics
- Plans for deepening or widening the navigation channel

- Planned changes in alternate waterway routes and in navigation patterns
- Plans for increasing the size and capacity of locks leading to the bridge
- Port development plans

Vessel traffic projections that are made by the Maritime Administration of the U.S. Department of Transportation, Port Authorities, and U.S. Army Corps of Engineers in conjunction with planned channel deepening projects or lock replacements are also a good source of information for bridge design. As a very large number of factors can affect the vessel traffic in the future, it is important to review and update the projected traffic during the life of the bridge.

4.5 Collision Risk Analysis

4.5.1 Risk Acceptance Criteria

Bridge components exposed to vessel collision could be subjected to a very wide range of impact loads. Owing to economic and structural constraints bridge design for vessel collision is not based on the worst case scenario, and a certain amount of risk is considered acceptable.

The risk acceptance criteria consider both the probability of occurrence of a vessel collision and the consequences of the collision. The probability of occurrence of a vessel collision is affected by factors related to the waterway, vessel traffic, and bridge characteristics. The consequences of a collision depend on the magnitude of the collision loads and the bridge strength, ductility, and redundancy characteristics. In addition to the potential for loss of life, the consequences of a collision can include damage to the bridge, disruption of motorist and marine traffic, damage to the vessel and cargo, regional economic losses, and environmental pollution.

Acceptable risk levels have been established by various codes and for individual bridge projects. The acceptable annual frequencies of bridge collapse values used generally range from 0.001 to 0.0001. These values were usually determined in conjunction with the risk analysis procedure recommended and should be used accordingly.

The AASHTO provisions (AASHTO 2009, 2012) specify an annual frequency of bridge collapse of 0.0001 for critical bridges and an annual frequency of bridge collapse of 0.001 for regular bridges. These annual frequencies correspond to return periods of bridge collapse equal to 1 in 10,000 years, and 1 in 1,000 years, respectively. Critical bridges are defined as those bridges that are expected to continue to function after a major impact, because of social/survival or security/defense requirements.

4.5.2 Collision Risk Models

4.5.2.1 General Approach

Various collision risk models have been developed to achieve design acceptance criteria. In general, the occurrence of a collision is separated into four events: (1) a vessel approaching the bridge becomes aberrant, (2) the aberrant vessel hits a bridge element, (3) the bridge element that is hit fails, and (4) a protection factor based on bridge location. Collision risk models consider the effects of the vessel traffic, the navigation conditions, the bridge geometry with respect to the waterway, and the bridge element strength with respect to the impact loads. They are commonly expressed in the following form (AASHTO 2009, 2012):

$$\mathrm{AF} = (N)(\mathrm{PA})(\mathrm{PG})(\mathrm{PC})(\mathrm{PF}) \tag{4.1}$$

where AF is the annual frequency of collapse of a bridge element; N is the annual number of vessel transits (classified by type, size, and loading condition) that can strike a bridge element; PA is the probability

of vessel aberrancy; PG is the geometric probability of a collision between an aberrant vessel and a bridge pier or span; PC is the probability of bridge collapse due to a collision with an aberrant vessel; and PF is an adjustment factor to account for potential protection of the piers.

4.5.2.2 Vessel Traffic Distribution, *N*

The number of vessels, *N*, passing the bridge based on size, type, and loading condition and available water depth has to be developed for each pier and span component to be evaluated. All vessels of a given type and loading condition have to be divided into discrete groupings of vessel size by DWT to determine the contribution of each group to the annual frequency of bridge element collapse. Once the vessels are grouped and their frequency distribution is established, information on typical vessel characteristics may be obtained from site specific data or from published general data such as AASHTO (2009) and Larsen (1993).

4.5.2.3 Probability of Aberrancy, PA

The probability of vessel aberrancy reflects the likelihood that a vessel is out of control in the vicinity of a bridge. Loss of control may occur as a result of pilot error, mechanical failure, or adverse environmental conditions. The PA is mainly related to the navigation conditions at the bridge site. Vessel traffic regulations, vessel traffic management systems, and aids to navigation can improve the navigation conditions and reduce the PA.

The probability of vessel aberrancy may be evaluated based on site-specific information that includes historical data on vessel collisions, rammings and groundings in the waterway, vessel traffic, navigation conditions and bridge/waterway geometry. This has been done for various bridge design provisions and specific bridge projects worldwide (IABSE 1983; AASHTO 2009; Larsen 1993). The PA values determined range from 0.5×10^{-4} to over 7.0×10^{-4}.

As an alternative, the AASHTO provisions (AASHTO 2009, 2012) recommend base rates for the probability of vessel aberrancy that are multiplied by correction factors for bridge location relative to bends in the waterway, currents acting parallel to vessel-transit path, crosscurrents acting perpendicular to vessel-transit path, and the traffic density of vessels using the waterway. The recommended base rates are 0.6×10^{-4} for ships and 1.2×10^{-4} for barges.

4.5.2.4 Geometric Probability, PG

The geometric probability is the probability that a vessel will hit a particular bridge pier given that it has lost control (i.e., is aberrant) in the vicinity of the bridge. It is mainly a function of the geometry of the bridge in relation to the waterway. Other factors that can affect the likelihood that an aberrant vessel will strike a bridge element include the original vessel-transit path, course, rudder position, velocity at the time of failure, vessel type, size, draft and maneuvering characteristics, and the hydraulic and environmental conditions at the bridge site. Various geometric probability models, some based on simulation studies, have been recommended and used on different bridge projects (IABSE 1983; Modjeski and Masters 1984; Larsen 1993). The AASHTO provisions (AASHTO 2009, 2012) use a normal probability density function about the centerline of the vessel-transit path for estimating the likelihood of an aberrant vessel being within a certain impact zone along the bridge axis. Using a normal distribution accounts for the fact that aberrant vessels are more likely to pass under the bridge closer to the navigation channel than further away from it. The standard deviation of the distribution equals the length of vessel associated with each vessel category or grouping. The probability that an aberrant vessel is located within a certain zone is the area under the normal probability density function within that zone (see Figure 4.7).

Bridge elements beyond three times the standard deviation from the centerline of vessel-transit path are designed for specified minimum impact load requirements, which are usually associated with an empty vessel drifting with the current.

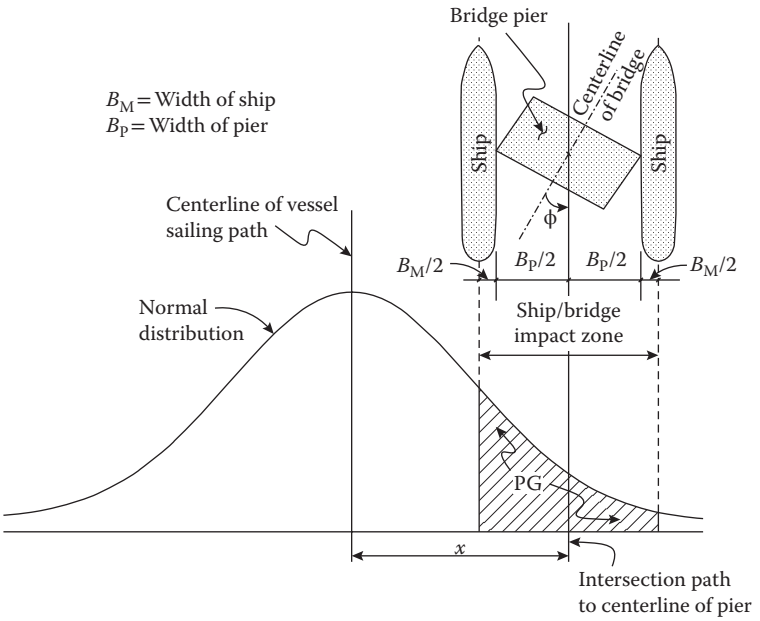

FIGURE 4.7 Geometric probability of pier collision.

4.5.2.5 Probability of Collapse, PC

The probability of collapse, PC, is a function of many variables, including vessel size, type, forepeak ballast and shape, speed, direction of impact, and mass. It is also dependent on the ultimate lateral load strength of the bridge pier (particularly the local portion of the pier impacted by the bow of the vessel). Based on collision damages observed from numerous ship–ship collision accidents that have been correlated to the bridge–ship collision situation (IABSE 1983), an empirical relationship has been developed based on the ratio of the ultimate pier strength, *H*, to the vessel impact force, *P*. As shown in Figure 4.8, for *H*/*P* ratios less than 0.1, PC varies linearly from 0.1 at $H/P = 0.1$, to 1.0 at $H/P = 0.0$. For *H*/*P* ratios greater than 0.1, PC varies linearly from 0.1 at $H/P = 0.1$, to 0.0 at $H/P = 1.0$.

4.5.2.6 Protection Factor, PF

The protection factor is an adjustment to AF to account for full or partial protection of selected bridge piers against vessel collisions due to protection measures (dolphins, islands, etc.), or due to existing site conditions such as a parallel bridge protecting a bridge from impacts in one direction, or a feature of the waterway (such as a peninsula extending out on one side of the bridge) that may block vessels from hitting bridge piers, or a wharf structure near the bridge that may block vessels from a certain direction. PF is computed as

$$\text{PF} = 1 - (\%\ \text{Protection Provided} / 100) \tag{4.2}$$

If no protection of the pier exists, then PF = 1.0. If the pier is 100% protected, then PF = 0.0. As an example, if dolphin pier protection system provided 70% protection, then PF would be equal to 0.3. Values for PF may vary from pier to pier and may vary depending on the direction of the vessel traffic (i.e., vessel traffic moving inbound versus traffic moving outbound) (AASHTO 2009).

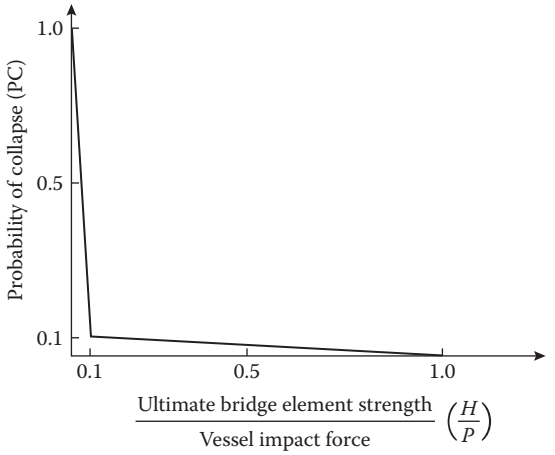

FIGURE 4.8 Probability of collapse distribution.

4.6 Vessel Impact Loads

4.6.1 Ship Impact

The estimation of the load on a bridge pier during a ship collision is a very complex problem. The actual force is time dependent and varies depending on the type, size, and construction of the vessel; its velocity; the degree of water ballast in the forepeak of the bow; the geometry of the collision; and the geometry and strength characteristics of the bridge. There is a very large scatter among the collision force values recommended in various vessel collision guidelines or used in various bridge projects.

Ship collision forces are commonly applied as equivalent static loads. Procedures for evaluating dynamic effects when the vessel force indentation behavior is known are included in IABSE (1983), Modjeski and Masters (1984), Larsen (1998), Prucz and Conway (1987, 1989), Grob and Hajdin (1996). The AASHTO provisions (AASHTO 2009, 2012) use the following formula for estimating the static head-on ship collision force, P_S, on a rigid pier:

$$P_s = 0.98(\mathrm{DWT})^{1/2}(V/16) \tag{4.3}$$

where P_S is the equivalent static vessel impact force (MN); DWT is the ship deadweight tonnage in tons; and V is the vessel impact velocity in knots (see Figure 4.9). This formulation was primarily developed from research conducted by Woisin in West Germany during 1967–1976 on physical ship models to generate data for protecting the reactors of nuclear power ships from collisions with other ships. A schematic representation of a typical impact force time history is shown in Figure 4.10 based on Woisin's test data. The scatter in the results of these tests is of the order of ±50%. The formula recommended (Equation 4.3) uses a 70% fractile of an assumed triangular distribution with zero values at 0% and 100% and a maximum value at the 50% level (see Figure 4.11).

Formulas for computing design ship collision loads on a bridge superstructure are given in the AASHTO provisions (AASHTO 2009, 2012) as a function of the design ship impact force, P_S, as follows:

- Ship bow impact force, P_{BH}:

$$P_{BH} = (R_{BH})(P_S) \tag{4.4}$$

  where R_{BH} is a reduction coefficient equal to the ratio of exposed superstructure depth to the total bow depth.

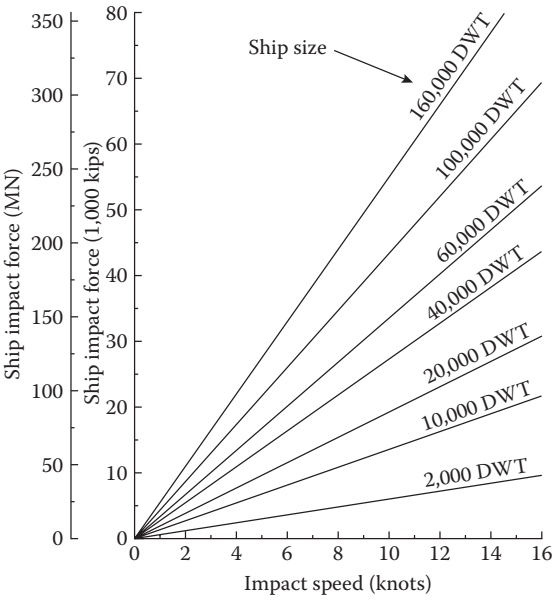

FIGURE 4.9 Ship impact force.

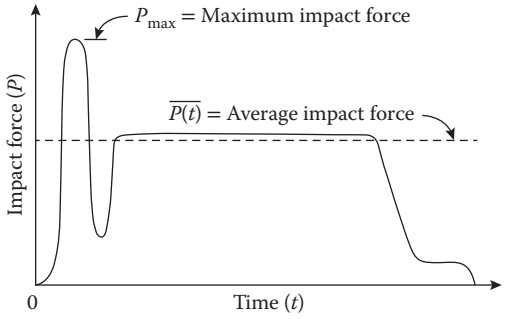

FIGURE 4.10 Typical ship impact force time history by Woisin.

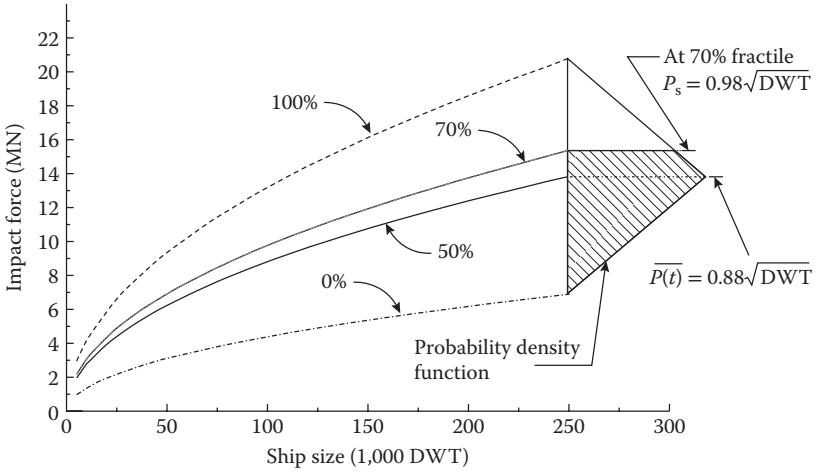

FIGURE 4.11 Probability density function of ship impact force.

- Ship deck house impact force, P_{DH}:

$$P_{DH} = (R_{DH})(P_S) \tag{4.5}$$

where R_{DH} is a reduction coefficient equal to 0.10 for ship larger than 100,000 DWT, and, $0.2 - \frac{DWT}{100{,}000}(0.10)$ for ships under 100,000 DWT.

- Ship mast impact force, P_{MT}:

$$P_{MT} = 0.10 P_{DH} \tag{4.6}$$

where P_{DH} is the ship deck house impact force.

The magnitude of the impact loads computed for ship bow and deck house collisions are quite high relative to the strength of most bridge superstructure designs. Also, there is great uncertainty associated with predicting ship collision loads on superstructures because of the limited data available and the ship/superstructure load interaction effects. It is therefore suggested that superstructures, and also weak or slender parts of the substructure, be located out of the reach of a ship's hull or bow.

4.6.2 Barge Impact

The barge collision loads recommended by AASHTO for the design of piers are shown in Figure 4.12 as a function of the tow length and the impact speed. Numerical formulations for deriving these relationships may be found in AASHTO (2009, 2012).

The loads in Figure 4.12 were computed using a standard 59.5 × 10.7 m hopper barge. In previous AASHTO Guide Specification (AASHTO 2009) and AASHTO LRFD Bridge Design Specifications (AASHTO 2012), the impact force recommended for barges larger than the standard hopper barge was determined by increasing the standard barge impact force by a factor related to the ratio of the width of the wider barge to the width of the standard hopper barge. This approach, although not directly related

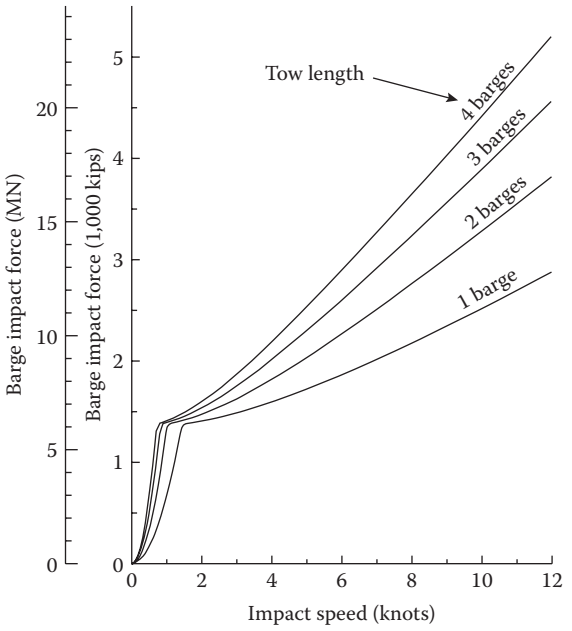

FIGURE 4.12 Barge impact force.

to the strength of the barge at the point of impact, accounted for the increased likelihood of higher collision loads being associated with larger barges due to other reasons such as deeper bow rake head logs and stronger structures at push knees and corner locations (Figures 4.5 and 4.6). It is recommended that the bridge designer evaluate the vessel traffic characteristics at the bridge, determine the likelihood of barges with deeper bows, and use the ratio between the height of the deeper head log and the head log of the standard hopper barge to increase the standard barge impact force where needed.

4.6.3 Application of Impact Forces

Collision forces on bridge substructures are commonly applied as follows:

- One hundred percent of the design impact force in a direction parallel to the navigation channel (i.e., head-on).
- Fifty percent of the design impact force in the direction normal to the channel (but not simultaneous with the head-on force).
- For overall stability, the design impact force is applied as a concentrated force at the mean high water level.
- For local collision forces, the design impact force is applied as a vertical line load equally distributed along the ship's bow depth for ships and along head block depth for barges.
- For superstructure design, the impact forces are applied transversely to the superstructure component in a direction parallel to the navigation channel.

When determining the bridge components exposed to physical contact by any portion of the hull or bow of the vessel considered, the bow overhang, rake, or flair distance of vessels have to be taken into account. The bow overhang of ships and barges is particularly dangerous for bridge columns and for movable bridges with relatively small navigation clearances.

4.6.4 Minimum Impact Requirements

AASHTO specifications (AASHTO 2009, 2012) require that all bridge piers located in design water depths of more than 0.6 m be designed for a minimum impact force associated with an empty hopper barge drifting at a speed equal to the mean yearly current in the waterway. Owing to the high frequency of occurrence of barge breakaways resulting in bridge hits during high river stage periods and the involvement of loaded barges in these incidents, it is recommended that loaded barge scenario also be considered. Barges can break away from docks and mooring facilities, and they can also break away from a barge tow in transit that grounded or hit another bridge. A recent study initiated by the Oklahoma Department of Transportation (Modjeski and Masters 2009) confirmed the need to properly assess the risks at a given bridge site and account for the likelihood of barge breakaways by type, loading condition, and current conditions.

4.6.5 Recent U.S. Barge Research

Since the AASHTO Guide Specification's adoption in 1991 and its use in analysis and design of bridges for vessel collision, the specification has spurred various research projects to better understand the magnitude of the barge collision loads involved and the bridge response. Of particular importance are the extensive research efforts conducted by the University of Florida (Whitney, Harik, Griffin, and Allen 1996; Brown and Bollmann 1992; Hoit, McVay and Hayes 1996; Florida Bridge Software Institute 2002, 2007; Consolazio, Hendrix et al. 2004a; Consolazio, Lehr et al. 2004b; Consolazio and Cowan 2005; Consolazio, Cook, and McVay 2006) and the University of Kentucky (Yuan, Harik, and Davidson 2008; Yuan and Harik 2008, 2009,2010). The research by these institutions reflect the importance of using dynamic analysis to estimate barge impact forces.

A key portion of the research program conducted by the University of Florida involved the use of a full-scale barge impact testing on several bridge piers of the St. George Island Bridge across Florida's Apalachicola Bay (Consolazio, Cook, and McVay 2006). The existing bridge was being replaced by a new bridge; hence, two of the abandoned bridge piers (a channel pier with a relatively massive mudline foundation and an approach pier with two waterline footings) were studied in three different structural configurations in a full-scale test program, which included ramming a small 600-ton barge against the piers at various speeds (some with the superstructure in place and others with the superstructure removed) and measuring a wide variety of responses in the structure and soil using extensive measurement and recording systems.

Based on the University of Florida test data from the St. George Bridge program, several general observations can be made in comparing the measured barge impact forces with those predicted by the AASHTO equations. For relatively stiff piers with below mudline pile supported footings, the measures impact forces ranged from 50% to 100% of the AASHTO force (with most measurements near the 50% level). For relatively flexible pile-supported piers with the footings at or above the waterline, the measured impact forces ranged from 100% to 130% of the AASHTO forces (with most measurements near the 130% level). The test results indicate that the dynamic response of the structure and the stiffness of the underlying soil are key components in the development of the barge impact force transmitted to the pier. The University of Florida barge test data also indicated that there are differences in load effects (e.g., displacements, shears, moments) between the application of the AASHTO static loads versus the dynamic loads of the test data. Nevertheless, the study indicated that even though there were differences in the measured forces versus AASHTO, the static analysis performed using the AASHTO loads appear to yield foundation design forces that are consistent with results obtained by more refined analysis techniques (e.g., dynamic analysis combined with experimentally measured dynamic loads).

The University of Kentucky conducted analytical studies on multibarge tow impact forces (Yuan, Harik, and Davidson 2008) and concluded that counting the barges in the length of the tow may yield conservative impact forces using the AASHTO equations, particularly in those cases where the width of the pier is smaller (approximately 10%) than the width of the barge. Where the width of the pier is about 50% of the width of the barge, the barge impact forces are close to the AASHTO values, and where the width of the pier is about the same or greater than the width of the barge, the AASHTO forces are less than those computed using finite element models and dynamic analysis. Their research indicates that an "accordion"-type effect occurs where the barges in the tow length buckle upward/downward, which reduces the impact energy being transferred to the pier. The study also indicated that the barges in the width of the tow do not simply break away on impact, but stay connected sufficiently to affect the collision energy. Interestingly, dynamic finite element analysis applied to the entire tow resulted in overall impact forces very similar to the forces derived using the AASHTO method (i.e., the reduction of the forces by buckling in the length of the tow is offset by an increase in force due to the influence of adjacent barges in the width of the tow).

4.7 Bridge Analysis and Design

Vessel collisions are extreme events with a very low probability of occurrence; therefore, the limit state considered is usually structural survival. Depending on the importance of the bridge various degrees of damage are allowed—provided that the structure maintains its integrity, hazards to traffic are minimized, and repairs could be made in a relatively short period of time. When the design is based on more frequent but less severe collisions, structural damage and traffic interruptions are not allowed.

Designing for vessel collision is commonly based on equivalent static loads that include global forces for checking overall capacity of piers and local forces for checking local strength of bridge components. The contribution of the superstructure to transfer loads to adjacent piers may also be considered. A clear load path from the location of the vessel impact to the bridge foundation needs to be established, and the components and connections within the load path must be adequately designed and detailed. The design of individual bridge components is based on strength and stability criteria. Overall stability, redundancy, and ductility are important criteria for structural survival.

4.7.1 Global Pier Capacity

The global pier capacity is determined in terms of a concentrated collision load applied at the design water elevation, which is commonly the mean high water elevation. It is determined based on the ultimate strength and stability of the pier and its foundation in the Extreme Event II Limit State load combination as defined in AASHTO LRFD (AASHTO 2012). Strength or service limit states may need to be considered as well, depending on the performance criteria requirements.

The modeling of pile foundations could vary from the simple assumption of a point of fixity to nonlinear soil–structure interaction models, depending on the limit state considered and the sensitivity of the response to the soil conditions. Lateral load capacity analysis methods for pile groups that include nonlinear behavior can be found in Kuzmanovic and Sanchez (1992) and Brown and Bollmann (1992) and the basic features of a finite element analysis computer program developed for bridge piers composed of pier columns and cap supported on a pile cap and nonlinear piles and soil are described in Hoit, McVay, and Hays (1996). The most recent version of the program, FB-PIER, is commercially available from the Florida Bridge Software Institute. If analysis indicates that piles will be loaded in tension by vessel impact forces, the design engineer must determine that the piles and their connection to the footing or cap have adequate pullout resistance.

Transient foundation uplift or rocking involving separation from the subsoil of an end-bearing foundation pile group or the contact area of a foundation footing could be allowed under impact loading provided sufficient consideration is given to the structural stability of the substructure.

Guidelines for the design, detailing, and construction of concrete and steel elements and connections are included in AASHTO LRFD (AASHTO 2012). Adequate transverse reinforcement, spacing, and splices must be provided if plastic hinging is allowed to form.

4.7.2 Local Pier Capacity

The local pier capacity is assessed in relation to distributed collision loads in the zone of impact to prevent premature localized failures of the more slender bridge components that can still be reached by vessels hull. Local moment, shear, and shear friction capacity must be checked, and special attention must be given to detailing in the zone of impact. Concrete will tend to spall upon impact, and it is therefore important to provide increase concrete cover, closely spaced transverse reinforcement, and to avoid lap splicing of longitudinal and transverse bars in the zone of impact.

4.7.3 Contribution of the Superstructure

The contribution of the superstructure to the transfer of loads to adjacent substructure units depends on the capacity of the connection of the superstructure to substructure and the relative stiffness of the substructure at the location of the impact. However, in order to consider partial transfer of lateral forces to the superstructure, positive steel or concrete connections of superstructure to substructure such as shear keys must be provided. Similarly, for partial transfer to the superstructure of the longitudinal component of the impact force, the shear capacity of the bearings must be adequate. When elastomeric bearings are used their longitudinal flexibility may be added to the longitudinal flexibility of the piers. If the ultimate capacity of the bearings is exceeded, then the pier must take the total longitudinal force and be treated as a cantilever.

Simplified guidelines for determining the distribution of collision loads to adjacent piers are included in Kuzmanovic and Sanchez (1992). To find out how much of the transverse impact force is taken by the pier and how much is transferred to the superstructure, two analytical models may be used. One is a two-dimensional or a three-dimensional model of the complete pier, and the other is a two-dimensional model of the superstructure projected on a horizontal plane. The projected superstructure may be modeled as a beam with the moment of inertia referred to a vertical axis through the center of the

roadway and with hinges at expansion joint locations. The beam is supported at pier locations by elastic horizontal springs representing the flexibility of each pier. The flexibility of the piers is obtained from pier models using virtual forces. The superstructure model is loaded with a transverse virtual force acting at the place where the pier under consideration is located. The spring in the model at that place is omitted to obtain a flexibility coefficient of the superstructure at the location of the top of pier under consideration. Thus, the horizontal displacement of the top of pier due to the impact force on the pier (usually applied at mean high water level) is equal to the true displacement of the superstructure due to the transmitted part of the impact force. The magnitude of the force transmitted to the superstructure is obtained by equating the total true displacement of the top of pier from the pier model to the displacement of the superstructure.

The superstructure contribution analysis can also be done modeling the entire bridge within a general purpose structural analysis program or more efficiently using a special purpose program such as FB-MULTIPIER available from the Florida Bridge Software Institute that can include soil–structure interaction and superstructure participation in one model and was developed by the University of Florida specifically for vessel collision analysis. This program can also perform dynamic analysis of barge impact.

4.7.4 Movable Bridges

Movable bridges are particularly susceptible to interrupted service as a result of vessel collision because even minor impact can cause mechanical equipment to jam or fail. Guidelines for the design and protection of movable bridges are included in the AASHTO Guide Specification (AASHTO 2009) and the AASHTO LRFD Movable Highway Bridge Design Specifications (AASHTO 2000).

In addition to the design vessels determined based on the AASHTO LRFD and Guide Specification criteria, the AASHTO LRFD Movable Highway Bridge Design Specifications also include an operating vessel used to minimized damage from routine marine traffic and ensure that the bridge remains operational and to help proportion the fender system so that it is not severely damaged after minor collisions. The AASHTO LRFD Movable Highway Bridge Design Specifications also include movable bridge specific analysis considerations and design and detailing guidelines.

4.8 Bridge Protection Measures

The cost associated with protecting a bridge from catastrophic vessel collision can be a significant portion of the total bridge cost, and must be included as one of the key planning elements in establishing a bridge's type, location, and geometry. The following alternatives are usually evaluated in order to develop a cost-effective solution for a new bridge project:

- Design the bridge piers, foundations, and superstructure to directly withstand the vessel collision forces and impact energies.
- Design a pier fender system to reduce the impact loads to a level below the capacity of the pier and foundation.
- Increase span lengths and locate piers in shallow water out-of-reach from large vessels in order to reduce the impact design loads.
- Protect piers from vessel collision by means of physical protection systems.

4.8.1 Physical Protection Systems

Piers exposed to vessel collision can be protected by special structures designed to absorb the impact loads (forces or energies) or redirect the aberrant vessel away from the pier. Because of the large forces and energies involved in a vessel collision, protection structures are usually designed for plastic

deformation under impact (i.e., they are essentially destroyed during the head-on design collision and must be replaced). General types of physical protection systems include the following:

Fender systems. These usually consist of timber, rubber, steel, or concrete elements attached to a pier to fully, or partially, absorb vessel impact loads. The load and energy absorbing characteristics of such fenders is relatively low compared to typical vessel impact design loads.

Pile-supported systems. These usually consist of pile groups connected by either flexible or rigid caps to absorb vessel impact forces. The piles may be vertical (plumb) or battered depending on the design approach followed and may incorporate relatively large diameter steel pipe or concrete pile sizes. The pile supported protection structure may be either free standing away from the pier or attached to the pier itself. Fender systems may be attached to the pile structure to help resist a portion of the impact loads.

Dolphin protection systems. These usually consist of large diameter circular cells constructed of driven steel sheet piles, filled with rock or sand, and topped by a thick concrete cap. Vessel collision loads are absorbed by rotation and lateral deformation of the cell during impact.

Island protection systems. These usually consist of protective islands built of a sand or quarry-run rock core and protected by outer layers of heavy rock rip-rap for wave, current, and ice protection. The island geometry is developed to stop an aberrant vessel from hitting a pier by forcing it to run aground. Although extremely effective as protection systems, islands are often difficult to use due to adverse environmental impacts on river bottoms (dredge and fill permits) and river currents (increase due to blockage), as well as impacts due to settlement and downdrag forces on the bridge piers.

Floating protection systems. These usually consist of cable net systems suspended across the waterway to engage and capture the bow of an aberrant vessel, or floating pontoons anchored in front of the piers. Floating protection systems have a number of serious drawbacks (environmental, effectiveness, maintenance, cost, etc.) and are usually only considered for extremely deep water situations where other protection options are not practicable.

The AASHTO Guide Specification (AASHTO 2009) provides examples and contains a relatively extensive discussion of various types of physical protection systems such as fenders, pile supported structures, dolphins, protective islands, and floating structures. However, the guide does not include specific procedures and recommendations on the actual design of such protection structures. Further research is needed to establish consistent analysis and design methodologies for protection structures, particularly because these structures undergo large plastic deformations during the collision.

4.8.2 Aids to Navigation Alternatives

As 60%–85% of all vessel collisions are caused by pilot error, it is important that all aspects of the bridge design, siting, and aids to navigation with respect to the navigation channel be carefully evaluated with the purpose of improving or maintaining safe navigation in the waterway near the bridge. Traditional aids include buoys, range markers, navigation lighting, and radar reflectors as well as standard operating procedures and regulations specifically developed for the waterway by government agencies and pilot associations. Modern aids include advanced vessel traffic control systems (VTS) using shore-based radar surveillance and radio-telephone communication systems; special electronic transmitters known as Racon devices mounted to bridge spans for improved radar images indicating the centerline of channel; and advanced navigation positioning systems based on ship-board global positioning satellite (GPS) systems and electronic charts. It should be noted that bridge designers are very limited in their ability to require any modifications that affect operations on a navigable waterway since the responsibility and authority for implementing such navigation improvements within U.S. waterways belongs to the U.S. Coast Guard and is protected under Federal Regulations.

Following the terrorist attacks upon the United States on September 11, 2001, the Coast Guard has required that all foreign ships entering the U.S. waterway system to be equipped with various advanced electronic navigation aids and tracking systems. These requirements however do not extend to domestic barge tows on the inland waterway system. It is believed that the use of such advanced electronic navigation systems should also reduce the risk of vessel collision with bridges by providing pilots and vessel operators with accurate location information. At present, no studies have been performed to analyze and document the potential reduction in PA due to such electronic aids-to-navigation. If a case can be made at a particular waterway and bridge site that improved electronic navigation aids would reduce the PA, then such a factor could be used in the risk analysis—provided it is approved by the owner (AASHTO 2009).

It should be noted that the traditional isolation of the maritime community must come to an end. In addition to the bridge costs, motorist inconvenience, and loss of life associated with a catastrophic vessel collision, significant environmental damage can also occur due to spilled hazardous or noxious cargoes in the waterway. The days when the primary losses associated with an accident rested with the vessel and her crew are over. The $13 million value of the *M/V Summit Venture* was far below the $250 million replacement cost of the Sunshine Skyway Bridge that the vessel destroyed. The losses associated with the 11 million gallons of crude oil spilled from the *M/V Exxon Valdez* accident off the coast of Alaska in 1989 are over $3.5 billion. Both of these accidents could probably have been prevented using advanced electronic navigation systems.

4.8.3 Motorist and Vessel Operator Warning Systems

Motorist warning systems may be used on bridges to minimize the loss of life, which may occur in the event of a bridge span collapse due to a vessel collision. These include the following:

- Hazard detection systems, such as ship impact vibration detectors, continuity circuits, and VHF radio link
- Verification devices, such as closed circuit television (CCTV), visual delineation devices, and motorist call boxes
- Traffic control and information devices, such as variable message sign, flashing beacons, and movable gates

Vessel operator warning systems include nonmovement detectors in the vessel operator's house to warn if the vessel operator fell asleep or became incapacitated.

4.9 Summary

Experience to date has shown that the use of the vessel impact and bridge protection requirements such as the AASHTO specifications (AASHTO 2009, 2012) for planning and design of new bridges has resulted in a significant change in proposed structure types over navigable waterways. Incorporation of the risk of vessel collision and cost of protection in the total bridge cost has almost always resulted in longer span bridges being more economical than traditional shorter span structures, because the design goal for developing the bridge pier and span layout is the least cost of the total structure (including the protection costs). Typical costs for incorporating vessel collision and protection issues in the planning stages of a new bridge have ranged from 5% to 50% of the basic structure cost without protection.

Experience has also shown that it is less expensive to include the cost of protection in the planning stages of a proposed bridge than to add it after the basic span configuration has been established without considering vessel collision concerns. Typical costs for adding protection, or for retrofitting an existing bridge for vessel collision, have ranged from 25% to more than 100% of the existing bridge costs.

It is recognized that vessel collision is but one of a multitude of factors involved in the planning process for a new bridge. The designer must balance various needs including political, social, and economic

in arriving at an optimal bridge solution for a proposed highway crossing. Because of the relatively high bridge costs associated with vessel collision design for most waterway crossings, it is important that additional research be conducted to improve our understanding of vessel impact mechanics, the response of the structure, and the development of cost-effective protection systems.

References

AASHTO. 1991. *Guide Specification and Commentary for Vessel Collision Design of Highway Bridges*, American Association of State Highway and Transportation Officials, Washington, D.C.

AASHTO. 2000. *LRFD Movable Highway Bridge Design Specifications*, 1st ed., American Association of State Highway and Transportation Officials, Washington, D.C.

AASHTO. 2009. *Guide Specification and Commentary for Vessel Collision Design of Highway Bridges*, 2nd ed., American Association of State Highway and Transportation Officials, Washington, D.C.

AASHTO. 2012. *AASHTO LRFD Bridge Design Specification, Customary U.S. Units*, 6th ed., American Association of State Highway and Transportation Officials, Washington, D.C.

AREMA. 2013. *Manual for Railway Engineering*, Part 23, American Railway Engineering and Maintenance-of-Way Association, Lanham, MD.

Brown, D. A. and Bollmann, H. T. 1992. "Pile Supported Bridge Foundations Designed for Impact Loading", *Transportation Research Record 1331*, TRB, National Research Council, Washington, D.C., pp. 87–91.

Consolazio, G. R. and Cowan, D. R. 2005. "Numerically Efficient Dynamic Analysis of Barge Collisions with Bridge Piers", *ASCE Journal of Structural Engineering*, ASCE, Vol. 131, No. 8, New York, NY, pp. 1256–1266.

Consolazio, G. R., Cook, R. A., and McVay, M. C. 2006. "Barge Impact Testing of the St. George Island Causeway Bridge-Phase III; Physical Testing and Data Interpretation", *Structures Research Report No. 2006/26868*, Engineering and Industrial Experiment Station, University of Florida, Gainesville, FL.

Consolazio, G. R., Hendix, J. L., McVay, M. C., Williams, M. E., and Bollman, H. T. 2004a. "Prediction of Pier Response to Barge Impacts Using Design-Oriented Dynamic Finite Element Analysis", *Transportation Research Record 1868*, Transportation Research Board, Washington, D.C., pp. 177–189.

Consolazio, G. R., Lehr, G. B., and McVay, M. C. 2004b. "Dynamic Finite Element Analysis of Vessel-Pier-Soil Interaction During Barge Impact Events", *Transportation Research Record 1849*, Transportation Research Board, Washington, D.C., pp. 81–90.

Florida Bridge Software Institute. 2002. *FB-PIER Users' Manual*, University of Florida, Gainesville, FL.

Florida Bridge Software Institute. 2007. *FB-MULTIPIER Users' Manual*, University of Florida, Gainesville, FL.

Grob, B. and Hajdin, N. 1996. "Ship Impact on Inland Waterways", *Structural Engineering International*, Vol. 4, IABSE, Zürich, Switzerland, pp. 230–235.

Hoit, M., McVay, M., and Hays, C. 1996. "Florida Pier Computer Program for Bridge Substructure Analysis: Models and Methods", *Conference Proceedings, Design of Bridges for Extreme Events*, FHWA, Washington, D.C.

IABSE. 1983. *Ship Collision with Bridges and Offshore Structures*, International Association for Bridge and Structural Engineering, Colloquium Proceedings, Copenhagen, Denmark, 3 Volumes (Introductory, Preliminary, and Final Reports).

Kuzmanovic, B. O., and Sanchez, M. R. 1992. "Design of Bridge Pier Pile Foundations for Ship Impact", *Journal of Structural Engineering*, ASCE, Vol. 118, No. 8, pp. 2151–2167.

Larsen, A. and Esdahl, S., eds. 1998. *Proceedings of International Symposium on Advances in Bridge Aerodynamics, Ship Collision Analysis, and Operation & Maintenance*, Copenhagen, Denmark, May 10–13, 1998, Balkema Publishers, Rotterdam, Netherlands.

Larsen, O. D. 1993. *Ship Collision with Bridges: The Interaction between Vessel Traffic and Bridge Structures*, IABSE Structural Engineering Document 4, IABSE-AIPC-IVBH, Zürich, Switzerland.

Modjeski and Masters. 1984. "Criteria for: The Design of Bridge Piers with Respect to Vessel Collision in Louisiana Waterways", *Report prepared for Louisiana Department of Transportation and Development and the Federal Highway Administration*, Mechanicsburg, PA.

Modjeski and Masters. 2009. "Vessel Collision Risk Assessment of Bridges Over The McClellan-Kerr Arkansas River Navigation System With Respect to Loaded Runaway Barges", *Report prepared for Oklahoma Department of Transportation*, Mechanicsburg, PA.

National Research Council. 1983. *Ship Collisions with Bridges - The Nature of the Accidents, their Prevention and Mitigation*, National Academy Press, Washington, D.C.

Prucz, Z. and Conway, W. B. 1987. "Design of Bridge Piers Against Ship Collision", *Bridges and Transmission Line Structures*, (Edited by L. Tall), ASCE, New York, NY, pp. 209–223.

Prucz, Z. and Conway, W. B. 1989. "Ship Collision with Bridge Piers-Dynamic Effects", *Transportation Research Board Paper 890712*, Transportation Research Board, Washington, D.C.

U.S. Coast Guard. 2003. *American Waterways Operators Bridge Allision Work Group*. Report of the U.S. Coast Guard-American Waterways Operators, Inc. Safety Partnership, Washington, D.C.

Whitney, M. W., Harik, I. E., Griffin, J. J., and Allen, D. L. 1996. "Barge Collision Design of Highway Bridges", *Journal of Bridge Engineering*, ASCE, Vol. 1, No. 2, pp. 47–58.

Yuan, P. and Harik, I. E. 2008, "One-Dimensional Model for Multi-Barge Flotillas Impacting Bridge Piers", *Computer-Aided Civil and Infrastructure Engineering*, Vol. 23, pp. 437–447.

Yuan, P., and Harik, I. E. 2008. "Equivalent Barge and Flotilla Impact Forces on Bridge Piers", *Kentucky Transportation Center research report No. KTC-08-12/SPR261-03-1F*, University of Kentucky, Lexington, KY.

Yuan, P., and Harik, I. E. 2010. "Equivalent Barge and Flotilla Impact Forces on Bridge Piers", *ASCE Journal of Bridge Engineering*, ASCE, Vol. 15, No. 5, New York, NY, pp. 523–532.

Yuan, P., Harik, I. E., and Davidson, M. T. 2008. "Multi-Barge Flotilla Impact Forces on Bridges", *Kentucky Transportation Center research report No. KTC-08-13/SPR261-03-2F*, University of Kentucky, Lexington, KY.

5

Bridge Scour Design and Protection*

Junke Guo
University of Nebraska–Lincoln

5.1 Introduction

This chapter presents basic concepts, methods, and procedures in bridge scour design and protection, including hydrology study, hydraulic analysis, scour evaluation, and scour protection.

Hydrology study is to determine design discharge, either the peak discharge or the flood hydrograph (in some cases both) at the highway stream crossings. Hydraulic analysis is to convert design discharge to hydraulic variables such as velocity, flow depth, and bed shear stress eroding bed materials around bridge piers and abutments. Scour design is to evaluate the maximum possible scour depth corresponding to design discharge. Scour protection provides counter measurements resisting scour process. Below the state-of-the-practice in bridge design and protection is outlined.

5.2 Hydrology and Hydraulics

5.2.1 Hydrology

5.2.1.1 Data Collection

Hydrology data are fundamental in bridge design, obtained from the following sources: as built plans, site investigations and field studies, bridge maintenance books, hydraulic files from experienced report writers, files of government agencies such as U.S. Corps of Engineers, USGS, Soil Conservation Service (SCS) and FEMA, rainfall data from local water agencies, stream gage data, USGS & State water agency reservoir regulation, aerial photos, and floodways.

Site investigations are conducted except in simple cases. Field studies are important because they reveal conditions that are not readily apparent from maps, aerial photographs, and previous studies. The typical data collection during a field study includes high water (HW) marks, scour potential and stream

* This chapter was updated based on Chapter 61 "Bridge Hydraulics" in the first edition by Jim Springer and Ke Zhou.

stability nearby drainage structures, changes in land use not indicated on the maps, and debris potential nearby physical features. See FHWA (1984) for a typical Survey Data Report Form.

5.2.1.2 Drainage Basin

The area of drainage basin above a given point along a stream is a major contributing factor to the quantity of flow past that point. For the given conditions, the peak flow at the proposed site is approximately proportional to the drainage area.

The basin shape affects the peak discharge; long narrow basins give lower peak discharges than pear-shaped basins. The basin slope affects the concentration time; steep slope decreases but flatter slope increases the concentration time. The mean elevation of a drainage basin affects runoff; higher elevation basins receive a significant amount of precipitation as snow. A basin orientation with respect to the direction of storm movement affects peak discharge; storms moving upstream produce lower peaks than those moving downstream.

5.2.1.3 Discharge

Several methods are used for determining discharge. Most of them are based on statistical analyses of rainfall and runoff records, involving preliminary or trial selections of alternative plans that are judged to fit the site conditions and to accommodate the flood flows selected for analysis.

Flood flow frequencies are usually calculated, through the overtopping flood, for discharges of 2.33 years that is considered the "Mean Annual Discharge." The base flood is the 100-year discharge (1% frequency). The design discharge is the 50-year discharge (2% frequency) or the greatest of record, if practical. Many times, the historical flood is so large that a structure to manage the flow becomes uneconomical. In such a case, engineering judgment is needed. The overtopping discharge is calculated on the site, but may overtop the roadway some distance away from the site.

Changes in land use alter the surface runoff so that future land use changes during the bridge life should be considered in the field. The surface soil type affects the peak discharge calculation. Rock formations underlying the surface and other geophysical characteristics such as volcanic, glacial, and river deposits have a significant effect on runoff. In the United States, the major source of soil information is the SCS. Detention storage reduces the basin peak discharge by its size and location.

The most commonly used methods to determine discharges are (1) rational method, (2) statistical gage analysis method, (3) discharge comparison of adjacent basins from gage analysis, (4) regional flood-frequency equations, and (5) design hydrograph. The results from these methods should be compared, not averaged.

5.2.1.3.1 Rational Method

The rational method was first employed in Ireland in 1847. This method assumes: (1) drainage area is smaller than 300 acres; (2) peak flow occurs when all of the watershed is contributing; (3) the rainfall intensity is uniform over a duration equal to or greater than the time of concentration, T_c; and (4) the frequency of the peak flow is equal to the frequency of the rainfall intensity. These assumptions imply steady flow conditions and the mass conservation law gives

$$Q = CiA \tag{5.1}$$

where Q = discharge (ft³/s), i = rainfall intensity (in/h) determined from either regional IDF (Intensity Duration Frequency) maps or individual IDF curves, A = basin area (acres) determined from topographic map (note: 1 mile² = 640 acres = 0.386 km²), and C = runoff coefficient (%) determined in the field and from Tables 5.1 and 5.2 (FHWA 2002) or estimated below for a weighted value if basin is covered with different materials, namely

$$C = \frac{\sum C_j A_j}{\sum A_j} \tag{5.2}$$

with subscript j for the value in a subarea.

TABLE 5.1 Runoff Coefficients for Developed Areas

Business	
Downtown areas	0.70–0.95
Neighborhood areas	0.50–0.70
Residential areas	
Single–family areas	0.30–0.50
Multiunits, detached	0.40–0.60
Multiunits, attached	0.60–0.75
Suburban	0.25–0.40
Apartment dwelling areas	0.50–0.70
Industrial	
Light areas	0.50–0.80
Heavy areas	0.60–0.90
Parks, cemeteries	0.10–0.25
Playgrounds	0.20–0.40
Railroad yard areas	0.20–0.40
Unimproved areas	0.10–0.30

TABLE 5.2 Runoff Coefficients for Undeveloped Area Watershed Types

Soil	0.12–0.16 No effective soil cover, either rock or thin soil mantle of negligible infiltration capacity	0.08–0.12 Slow to take up water, clay or shallow loam soils of low infiltration capacity, imperfectly or poorly drained	0.06–0.08 Normal, well-drained light or medium-textured soils, sandy loams, silt and silt loams	0.04–0.06 High, deep sand or other soil that takes up water readily, very light well-drained soils
Vegetal Cover	0.12–0.16 No effective plant cover, bare or very sparse cover	0.08–0.12 Poor to fair; clean cultivation crops, or poor natural cover, less than 20% of drainage area over good cover	0.06–0.08 Fair to good; about 50% of area in good grassland or woodland, not more than 50% of area in cultivated crops	0.04–0.06 Good to excellent; about 90% of drainage area in good grassland, woodland, or equivalent cover
Surface Storage	0.10–0.12 Negligible surface depression few and shallow, drainage ways steep and small, no marshes	0.08–0.10 Low, well-defined system of small drainage ways; no ponds or marshes	0.06–0.08 Normal; considerable surface depression storage; lakes and pond marshes	0.04–0.06 High; surface storage, high; drainage system not sharply defined; large floodplain storage or large number of ponds or marshes

The concentration time for a pear-shaped drainage basin is determined by the Kirpich equation:

$$T_C = 0.0195\left(\frac{L}{S^{0.5}}\right)^{0.77} \tag{5.3}$$

where T_c = concentration time (min), L = horizontally projected length (m) of the watershed, and $S = H/L$ with H = difference (m) in elevations between the most remote point in the basin and the outlet. Equation 5.3 combines overland and channel flows.

5.2.1.3.2 Statistical Gage Analysis Methods

The following two methods are the major statistical analysis methods used with Stream Gage Records: (1) Log Pearson Type III Method and (2) Gumbel Extreme Value Method.

The use of stream gage records is preferred for estimating discharge/frequencies since they reflect actual climatology and runoff. Discharge records are obtained from a state Department of Water Resources in the United States. A good data set should contain at least 25 years of continuous data.

It is important to review each individual stream gage record carefully to guarantee that the database is consistent with good statistical analysis practice. For example, a drainage basin with a large storage facility results in a skewed or inconsistent database since smaller basin discharges are influenced to a much greater extent than larger discharges.

The most current published stream gage description page should be reviewed to obtain a complete idea of the data record. A note should be given to changes in the basin area over time, diversions, revisions, and so on. All reliable historical data outside of the recording period should be included. The adjacent gage records for supplemental information should be controlled and utilized to extend the record if possible. Natural runoff data should be separated from later controlled data. It is known that high-altitude basin snow melt discharges are not compatible with rain flood discharges. The zero years must also be accounted for by adjusting the final plot positions, not by inclusion as minor flows. The generalized skew number can be obtained from the chart in USGS (1981).

Quite often the database requires modification for use in the Log Pearson III analysis. Occasionally, a high outlier but most often low outliers need to be removed from the database to avoid skewing results. This need is determined for high outliers by using $Q_H = \overline{Q}_H + K.S_H$, and low outliers by using $Q_L = \overline{Q}_L + KS_L$ where K is a factor determined by the sample size, $\overline{Q}_H$ and $\overline{Q}_L$ are the high and low mean logarithm of systematic peaks, Q_H and Q_L are the high and low outlier thresholds in log units, S_H and S_L are the high and low standard deviation of the log-distribution. Refer to FHWA (2002) or USGS (1981) for this method and to find the values of "K."

The data plotted are: "PEAK DISCHARGE, Q (CFS)" vs. "PROBABILITY, Pr" as shown in Figure 5.1 that results in a very flat curve with a reasonably straight center portion. An extension of this center portion gives a line for interpolation of the various needed discharges and frequencies.

The engineer should use an Adjusted Skew, which is calculated from the generalized and station skews. Generalized skews should be developed from at least 40 stations with each station having at least 25 years of record. The equation for the adjusted skew is

$$G_w = \frac{MSE_{G_S}(G_L) + MSE_{G_L}(G_S)}{MSE_{G_S} + MSE_{G_L}} \tag{5.4}$$

where G_w = weighted skew coefficient, G_S = station skew, G_L = generalized skew, MSE_{G_S} = mean square error of station skew, and MSE_{G_L} = mean square error of generalized skew.

The entire Log Pearson Type III procedure is found in USGS (1981). The Gumbel Extreme Value Method is also used to describe the distribution of hydrological variables. For peak discharges, it is written as

$$f(Q) = e^{-e^{a(Q-b)}} \tag{5.5}$$

with $a = 1.281/S$, $b = \overline{Q} - 0.450S$, S = standard deviation, and $\overline{Q}$ = mean annual flow.

The characteristics of the Gumbel extreme value distribution are from Equation 5.5. The mean discharge, $\overline{Q}$, corresponds to the return period of $T_r = 2.33$ years and skews toward the high flows or extreme values as shown in Figure 5.2. Even though it does not account directly for the computed skew

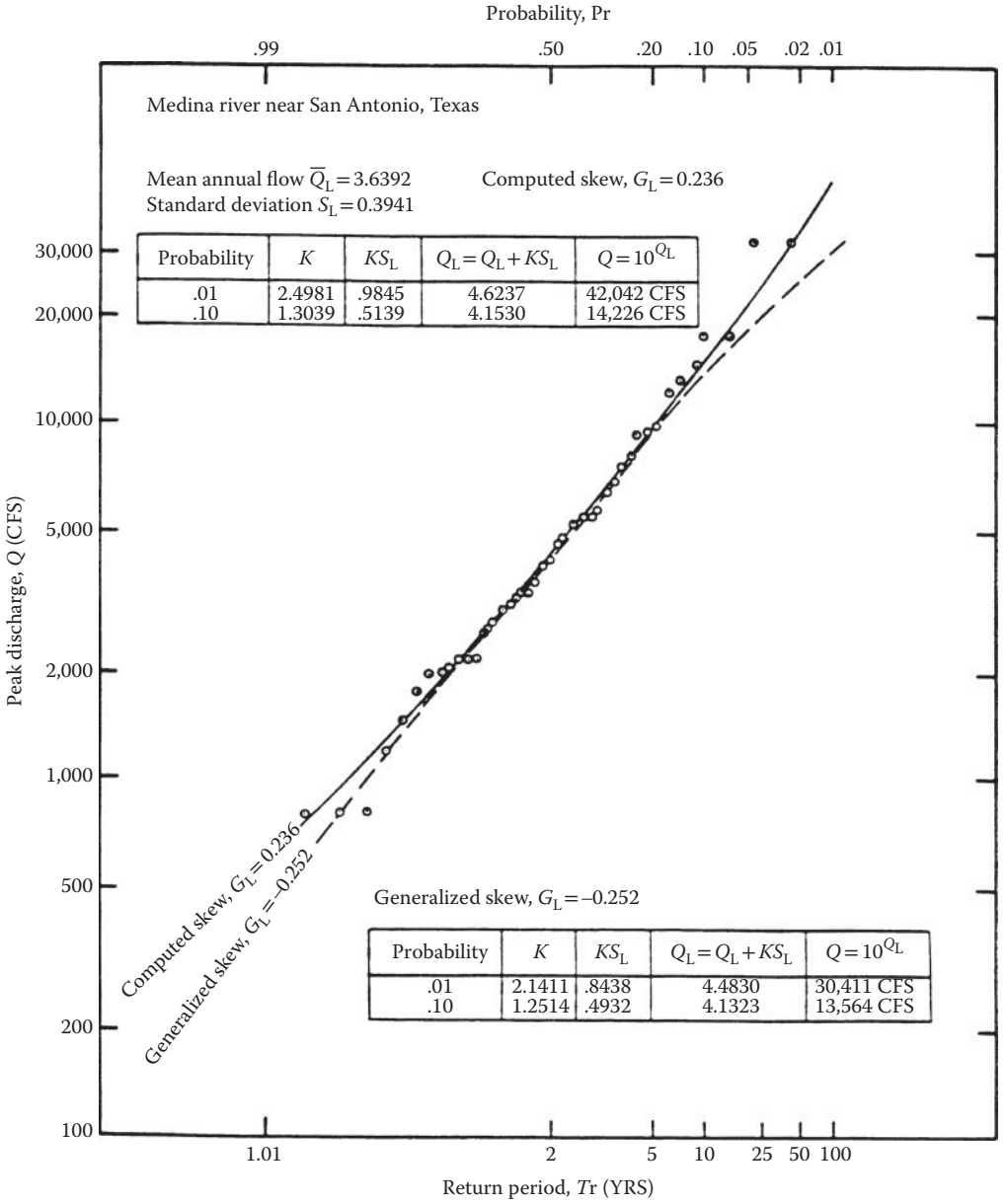

FIGURE 5.1 Log pearson type III distribution analysis, Medina River, Texas, USA.

of the data, it does predict the high flows reasonably well. Further information about this method is in FHWA (2002) or USGS (1981). Results from this method should be plotted on a special Gumbel paper, as shown in Figure 5.2.

5.2.1.3.3 Discharge Comparison of Adjacent Basins

FHWA (1984) contains a list of reports for various states in the United States with discharges at gages determined for frequencies from 2- to 100-year frequencies. The discharges were determined by the Log Pearson III method. The discharge–frequency at the gages should be updated by the engineer using Log Pearson III and the Gumbel Extreme Value method.

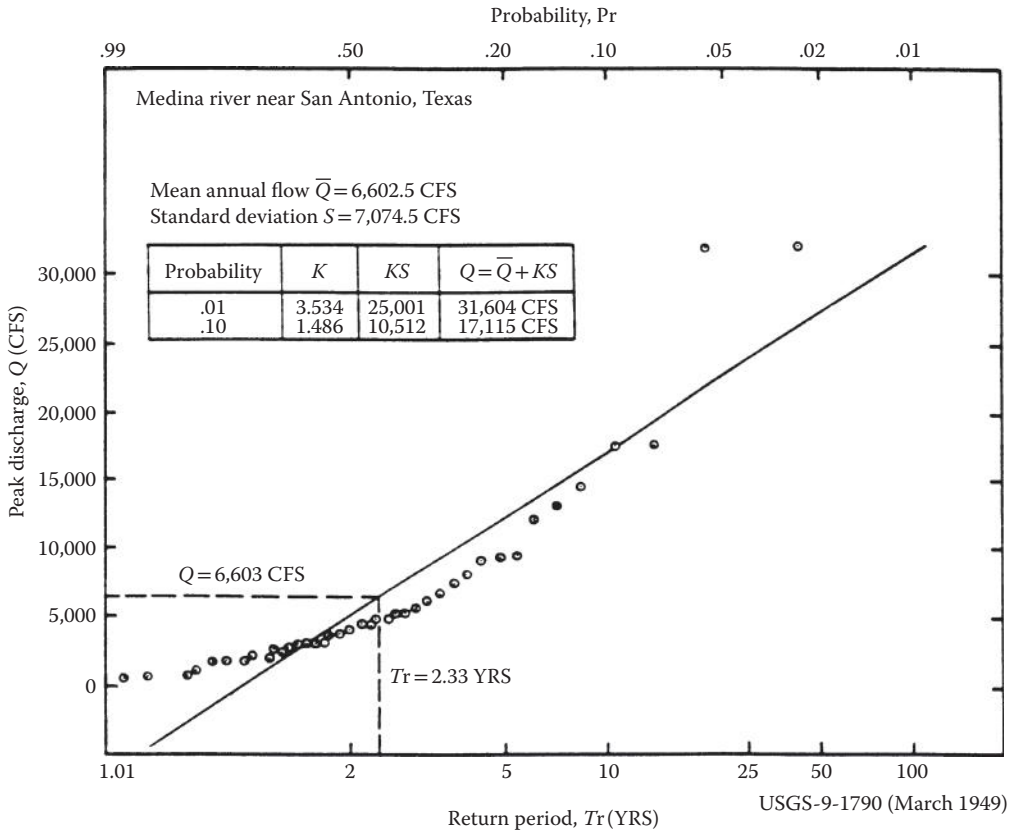

FIGURE 5.2 Gumbel extreme value frequency distribution analysis, Medina River, Texas, USA.

The gage data are used directly as equivalent if the drainage areas are about the same (within less than 5%). Otherwise, the discharge is determined by

$$Q_u = Q_g (A_u / A_g)^b \tag{5.6}$$

where Q_u = discharge at ungaged site, Q_g = discharge at gaged site, A_u = area of ungaged site, A_g = area of gaged site, and b = exponent of drainage area.

5.2.1.3.4 Regional Flood-Frequency Equations

If no gaged site is nearby or the record for the gage is short, then the discharge is computed using the applicable regional flood-frequency equations. Statewide regional regression equations have been established in the United States. These equations permit peak flows to be estimated for return periods varying between 2 and 100 years, based on the Log Pearson III method (FHWA 2002).

5.2.1.3.5 Design Hydrographs

Design hydrographs (FHWA 2005) give a complete time history of the passage of a flood at a particular site, including the peak flow. A runoff hydrograph is a plot of the response of a watershed to a particular rainfall event. A unit hydrograph is defined as the direct runoff hydrograph resulting from a rainfall event lasting for the unit duration of time. The ordinates of the unit hydrograph are such that the volume of direct runoff represented by the area under the hydrograph is equal to one inch of runoff from the drainage area. Data on low water discharges and dates should be given as it controls methods and

procedures of pier excavation and construction. The low water discharges and dates are found in the USGS Water Resources Data Reports published each year, which are determined by reviewing the past 5 or 6 years of records.

5.2.1.4 Remarks

Before arriving at a final discharge, the existing channel capacity should be checked by the calculated velocity times the channel waterway area. Note that a portion of the discharge may overflow the banks and never reaches the site.

The proposed design discharge should also be checked to see if it is reasonable and practicable. As a rule of thumb, the unit runoff should be 300 to 600 $ft^2/mile^2$ for small basins (<20 $mile^2$), 100 to 300 $ft^2/mile^2$ for median areas (<50 $mile^2$) and 25 to 150 $ft^2/mile^2$ for large basins (>50 $mile^2$). The best results depend on intelligent engineering judgment.

5.2.2 Bridge Deck Drainage Design

5.2.2.1 Runoff and Capacity Analysis

The preferred on-site hydrology method is the rational method, requiring a minimum concentration time of 10 minutes. Often the concentration time for the contributing on-site pavement runoff is less than 10 minutes. The initial concentration time is determined by an overland flow method until the runoff is concentrated in a curbed section. Channel flow using the roadway-curb cross-section should be used to determine velocity and flow time to the first inlet. The channel flow velocity and flooded width are calculated by Manning's formula:

$$V = \frac{1.486}{n} A R^{2/3} S_f^{1/2} \tag{5.7}$$

where V = velocity, A = cross-sectional area of flow, R = hydraulic radius, S_f = slope of channel, and n = Manning's roughness coefficient (FHWA 2012a).

The intercepted flow is subtracted from the initial flow, and the bypass is combined with runoff from the subsequent drainage area to determine the location of the next inlet. The placement of inlets is determined by the allowable flooded width on the roadway.

Often, bridges are in sump areas, or the lowest spot on the roadway profile. This necessitates the interception of most of the flow before reaching the bridge deck. Two overland flow equations are the kinematic wave equation

$$t_o = \frac{6.92(nL)^{0.6}}{i^{0.4} S^{0.3}} \tag{5.8}$$

and the overland equation

$$t_o = \frac{3.3(1.1-C)L^{1/2}}{(100S)^{1/3}} \tag{5.9}$$

where t_o = overland flow travel time (min), L = length (m) of overland flow path, S = slope of overland flow, n = Manning's roughness coefficient (FHWA 1984), i = design storm rainfall intensity (in/h), and C = runoff coefficient (Tables 5.1 and 5.2).

5.2.2.2 Select and Size Drainage Facilities

The selection of inlets is based on the allowable flooded width that is usually outside the traveled way. The type of inlet leading up to the bridge deck can vary, depending on the flooded width and velocity. Grate inlets are very common, and curb opening inlets are another alternative in areas with curbs; further information is in Brater et al. (1996).

5.2.3 Stage Hydraulics

HW stage is important in bridge design. All available information should be obtained from the field and the Bridge Hydrology Report regarding HW marks, HW on upstream and downstream sides of the existing bridges, high drift profiles, and possible backwater due to existing or proposed construction.

Note that observed high drift and HW marks are not always what they seem. Drift in trees and brush that could have been bent down by the flow of the water is extremely higher than the actual conditions. Besides, drift may be pushed up on objects or slopes above actual HW elevation by the water velocity or wave action. Painted HW marks on the bridge should be searched carefully. Some Flood Insurance Rate Maps and Flood Insurance Study Reports may show stages for various discharges. Backwater stages caused by other structures in streams should be included.

Duration of high stages should be given, along with the Base Flood Stage and HW for the design discharge. It should be calculated for existing and proposed conditions that may restrict the channel producing a higher level. Elevation and season of low water should be given, as this may control design of tremie seals for foundations and other possible methods of construction. Elevation of overtopping flow and its location should be given. Normally, overtopping occurs at the bridge site but at a low sag in the roadway away from the bridge site.

5.2.3.1 Waterway Analysis

When specifying the required waterway at the proposed bridge, engineers must consider all adjacent bridges if these bridges are reasonably close. The waterway section of these bridges should be tied into the stream profile of the proposed structure. Structures that are upstream or downstream of the proposed bridge may have an impact on the water surface profile. When calculating the effective waterway area, adjustments must be made for the skew and piers and bents. The required waterway should be below the 50-year design HW stage.

If stream velocities, scour and erosive forces are high, abutments with wingwall construction may be necessary. Drift will affect the horizontal clearance and the minimum vertical clearance line of the proposed structure. Field surveys should note the size and type of drift found in the canal. Design based on the 50-year flow requires drift clearance. On major streams and rivers, drift clearance of 2 to 5 m above the 50-year discharge is needed. On smaller streams, 0.3 to 1 m may be adequate. A formula for calculating freeboard is

$$\text{Freeboard} = 0.1Q^{0.3} + 0.008V^2 \tag{5.10}$$

with Q = discharge and V = velocity.

5.2.3.2 Water Surface Profile Calculation

There are three prominent water surface profile calculation programs available (AASHTO 2005, 2007). FHWA recommends HEC-RAS (Hydrologic Engineering Centers River Analysis System) that can use GIS (Geographic Information System) data for input for water surface profile calculations. Besides, WSPRO (Water Surface Profile) and SMS (Surface-water Modeling System) are two alternatives in practice.

5.2.3.3 Flow Velocity and Distribution

Mean channel, overflow velocities at peak level, and localized velocity at obstructions such as piers should be estimated for anticipated high levels. Mean velocities may be calculated from known stream discharges at known channel section areas or known waterway areas of the bridge, using the correct HW stage.

Surface water velocities are measured roughly by floats during field surveys. Flow velocities are computed on a uniform channel reach by Manning's formula (Equation 5.7) if the slope, channel section (area and wetted perimeter), and roughness coefficient (n) are known.

At least three profiles should be obtained for the channel slope: the channel bottom, the existing water surface, and the HW surface based on the drift or HW marks. The top of low bank, if overflow is allowed, should also be obtained. These profiles are plotted, with existing and proposed bridges or other obstructions in the channel. The changes of HW slope due to these obstructions and possible backwater slopes should be estimated.

The channel section used in calculating stream velocities should be more or less uniform. This condition is usually not always available so that the nearest to uniform conditions should be used with any necessary modifications made for irregularities.

Velocities may be calculated from PC programs, or calculator programs, if the hydraulic radius, roughness coefficient, and channel slope are given. The hydraulic radius is the waterway area divided by the wetted perimeter of an average section of the uniform channel. A section under a bridge whose piers, abutments, or approach fills obstruct the uniformity of the channel cannot be used because there will not be uniform flow with the structure. If no part of the bridge structure seriously obstructs or restricts the channel, however, the section at the bridge could be used in the earlier uniform flow calculations.

The roughness coefficient "n" for various locations and conditions is found in AASHTO (2005), Brater et al. (1996), FHWA (1984), and Yen and Chow (1997). At the time of a field survey, the party chief should estimate the value of "n" used for the channel section under consideration. Experience is required for field determination of a relatively close to actual "n" value. In general, values for natural streams will vary between 0.03 and 0.07. Consider both low and HW "n" value. The water surface slope should be used in this plot and the slope should be adjusted for obstructions such as bridges, check dams, falls, turbulence, and so on.

The results obtained from this plot may be inaccurate unless considerable thought is given to the various values of slope, hydraulic radius, and "n." High velocities between 15 and 20 ft/s (4.57–6.10 m/s) through a bridge opening may be undesirable and require special design considerations. Velocities over 20 ft/s (6.10 m/s) should not be used unless special design features are incorporated or if the stream is mostly confined in rock or an artificial channel.

5.3 Scour Design and Protection

5.3.1 Scour Analysis

5.3.1.1 Basic Scour Concepts

Scour results from the erosive action of flowing water, excavating and carrying away material from the bed and banks of streams. Determining the magnitude of scour is complicated by the cyclic nature of scour process. Designers and inspectors need to carefully study site-specific subsurface information in evaluating scour potential at bridges. In this section, the basic bridge scour design procedures and methods are briefly introduced.

Scour should be investigated closely in the field when designing a bridge. The designer usually places the top of the footings at or below the total potential scour depth; therefore determining the scour depth is very important. The total potential scour at a highway crossing is usually comprised of the following components (FHWA 2012a): aggradation and degradation, stream contraction scour, local scour, and sometimes with lateral stream migration.

5.3.1.1.1 Long-Term Aggradation and Degradation

When natural or human activities cause streambed elevation changes over a long period of time, aggradation or degradation occurs. Aggradation involves the deposition of material eroded from the channel or watershed upstream of the bridge, whereas degradation involves the lowering or scouring of the streambed due to a deficit in sediment supply from upstream.

Long-term streambed elevation changes result from the changing natural trend of the stream or the man-made modification to the stream or river basin. Factors that affect long-term bed elevation changes are dams and reservoirs up- or downstream of the bridge, changes in watershed land use, channelization, cutoffs of meander river bends, changes in the downstream channel base level, gravel mining from the streambed, diversion of water into or out of the stream, natural lowering of the fluvial system, movement of a bend, bridge location with respect to stream planform, and stream movement in relation to the crossing. Tidal ebb and flood may degrade a coastal stream; whereas, littoral drift may cause aggradation. The problem for the bridge engineer is to estimate the long-term bed elevation changes that will occur during the life time of the bridge.

5.3.1.1.2 Stream Contraction Scour

Contraction scour usually occurs when the flow area of a stream at flood stage is reduced, either by a natural contraction or a man-made contraction (like a bridge). It can also be caused by the overbank flow that is forced back by structural embankments at the approaches to a bridge. There are some other causes to lead to a contraction scour at a bridge crossing (FHWA 2012a). The decreased flow area causes an increase in average velocity in the stream and bed shear stress through the contraction reach. This in turn triggers an increase in erosive forces in the contraction. Hence, more bed material is removed from the contracted reach than from the upstream reach. The natural streambed elevation is lowered by this contraction phenomenon until relative equilibrium is achieved in the contracted stream reach.

There are two kinds of contraction scour: live-bed and clear-water scours. Live-bed scour occurs when there is sediment being transported into the contracted reach from upstream. In this case, the equilibrium state is reached when the transported bed material out of the scour hole is equal to that transported into the scour hole from upstream. Clear-water scour occurs when the bed sediment transport in the uncontracted approach flow is negligible or the material being transported in the upstream reach is transported through the downstream at less than the capacity of the flow. The equilibrium state of scour is reached when the average bed shear stress is less than that required for the incipient movement of the bed material in this case (Figure 5.3).

5.3.1.1.3 Local Scour

When upstream flow is obstructed by obstruction such as piers, abutments, spurs, and embankments, flow vortices are formed at their base, as shown in Figure 5.4 (known as horseshoe vortex). This vortex removes bed material from around the base of the obstruction. A scour hole eventually develops around the base. Local scour is either clear-water or live-bed scour. In considering local scour, a bridge engineer needs to look into the following factors: flow velocity, flow depth, flow attack angle to the obstruction, obstruction width and shape, projected length of the obstruction, bed material characteristics, bed configuration of the stream channel, and also potential ice and debris effects (FHWA 2001, 2012a).

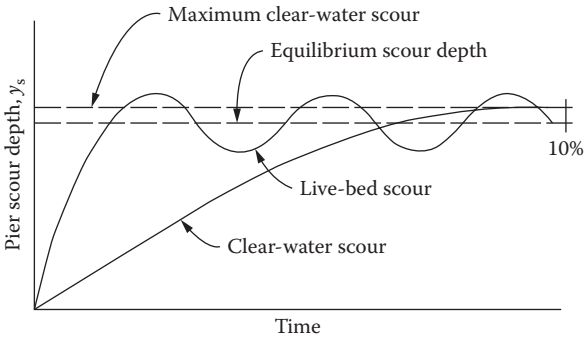

FIGURE 5.3 Illustrative pier scour depth in a sand-bed stream as a function of time.

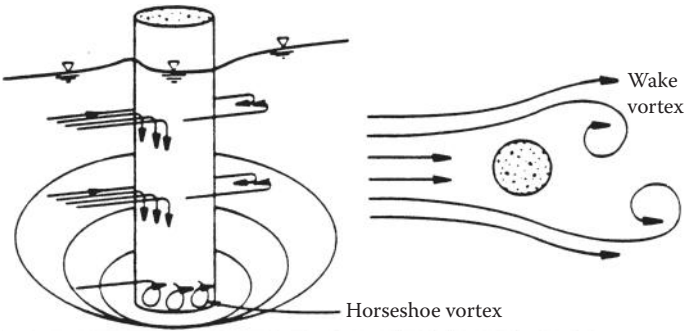

FIGURE 5.4 Schematic representation of local scour at a cylindrical pier.

5.3.1.1.4 Lateral Stream Migration

Streams are dynamic. The lateral migration of the main channel within a floodplain may increase pier scour, embankment or approach road erosion, or change the total scour depth by altering the flow angle of attach at piers. Lateral stream movements are affected mainly by the geomorphology of the stream, location of the crossing on the stream, flood characteristics, and the characteristics of the bed and bank materials (FHWA 2001, 2012a).

5.3.1.2 Designing Bridges to Resist Scour

It is obvious that all scour problems cannot be covered in this special topic section of bridge scour. A more detailed study is found in FHWA (2012a, b). As described earlier, the three most important components of bridge scour are: long-term aggradation or degradation, contraction scour, and local scour. The total potential scour is a combination of the three components. To design a bridge to resist scour, a bridge engineer needs to follow the following observation and investigation steps in the design process.

1. Field observation—The purposes of the filed observation are to: (1) observe conditions around piers, columns, and abutments (Is the hydraulic skew correct), (2) observe scour holes at bends in the stream, (3) determine streambed material, (4) estimate depth of scour, and (5) complete Geomorphic Factor Analysis. There is usually no fail-safe method to protect bridges from scour except possibly keeping piers and abutments out of the HW area; however, proper hydraulic bridge design can minimize bridge scour and its potential negative impacts.
2. Historic scour investigation—Structures experienced scour in the past are likely to continue displaying scour problems in the future. The bridges that are most concerned with include those currently experiencing scour problems and exhibiting a history of local scour problems.
3. Problem location investigation—Problem locations include "unsteady stream" locations such as: near the confluence of two streams, at the crossing of stream bends, and alluvial fan deposits.
4. Problem stream investigation—Problem streams are those that have the following characteristics of aggressive tendencies: indication of active degradation or aggradation, migration of the stream or lateral channel movement, streams with a steep lateral slope and/or high velocity, current, past, or potential in-stream aggregate mining operations, and loss of bank protection in the areas adjacent to the structure.
5. Design feature considerations—The following features, which increase the susceptibility to local scour, should be considered: (1) inadequate waterway opening leads to inadequate clearance to pass large drift during heavy runoff, (2) debris/drift problem: light drift or debris may cause significant scour problems, moderate drift or debris may cause significant scour but will not create severe lateral forces on the structure, and heavy drift can cause strong lateral forces or impact damage as well as severe scour, (3) lack of overtopping relief: water may rise above deck level.

This may not cause scour problems but does increase vulnerability to severe damage from impact by heavy drift, and (4) incorrect pier skew: when the bridge pier does not match the channel alignment, it may cause scour at bridge piers and abutments.

6. Traffic considerations—The amount of traffic such as average daily traffic (ADT), type of traffic, the length of the detour, the importance of the crossings, and availability of the other crossings should be taken into consideration.
7. Potential for unacceptable damage—Potential for collapse during flood, safety of traveling public and neighbors, effect on regional transportation system, and safety of other facilities (other bridges, properties) need to be evaluated.
8. Susceptibility of the combined hazard of scour and seismic—The earthquake prioritization list and the scour critical list are usually combined for bridge design use.

5.3.1.3 Scour Rating

According to California Department of Transportation, structure rating is based upon the following:

1. Letter grading—The letter grade is related to the potential for scour-related problems at this location.
2. Numerical grading—The numerical rating associated with each structure is a determination of the severity for the potential scour:

   A-1 No problem anticipated
   A-2 No problem anticipated/New bridge—No history
   A-3 Very remote possibility of problems
   B-1 Slight possibility of problems
   B-2 Moderate possibility of problems
   B-3 Strong possibility of problems
   C-1 Some probability of problems
   C-2 Moderate probability of problems
   C-3 Very strong probability of problems

Scour due to storms is usually greater than from design frequency, say 500-year frequency. FHWA specifies 500-year frequency is 1.7 times 100-year frequency. Most calculations indicate 500-year frequency is 1.25 to 1.33 times greater than the 100-year frequency (USGS 1981), the 1.7 multiplier should be a maximum. Consider the amount of scour that would occur at overtopping stages and also pressure flows. Be aware that storms of lesser frequency may cause larger scour stress on the bridge.

5.3.2 Scour Calculation

All the equations for estimating contraction and local scour are based on laboratory experiments with limited field verification (FHWA 2012a). However, the equations recommended in this section are considered to be the most applicable for estimating scour depths. Designers also need to give different considerations to clear-water scour and live-bed scour at highway crossings and encroachments.

Prior to applying the bridge scour estimating methods, it is necessary to (1) obtain the fixed-bed channel hydraulics, (2) determine the long-term impact of degradation or aggradation on the bed profile, (3) adjust the fixed-bed hydraulics to reflect either degradation or aggradation impact, and (4) compute the bridge hydraulics accordingly.

5.3.2.1 Specific Design Approach

The following steps are recommended for determining scour depth at bridges:

Step 1: Analyze long-term bed elevation change
Step 2: Compute the magnitude of contraction scour

Step 3: Compute the magnitude of local scour at abutments
Step 4: Compute the magnitude of local scour at piers
Step 5: Estimate and evaluate the total potential scour depths

The bridge engineers should evaluate if the individual estimates of contraction and local scour depths from Step 2 to 4 are reasonable and evaluate the total scour derived from Step 5.

5.3.2.2 Detailed Procedures

Step 1: Analyze long-term Bed Elevation Change
Face of bridge sections showing bed elevation is available in the Maintenance Bridge Books, old Preliminary Reports, and sometimes in FEMA Studies and USA Corps of Engineers Studies. Use this information to estimate aggradation or degradation.

Step 2: Compute the magnitude of contraction scour
It is best to keep the bridge out of the normal channel width. However, if any of the following conditions are present, calculate contraction scour:
Structure over channel in floodplain where the flows are forced through the structure due to bridge approaches.
Structure over channel where river width becomes narrow.
Relief structure in overbank area with little or no bed material transport.
Relief structure in overbank area with bed material transport.
The general equation for determining contraction scour is:

$$y_s = y_2 - y_1 \tag{5.11a}$$

where y_s = depth of scour, y_1 = average water depth in the main channel, and y_2= average water depth in the contracted section.

FHWA (2012a) provides two methods estimating y_2. For live-bed scour, y_2 is estimated by

$$\frac{y_2}{y_1} = \left(\frac{Q_2}{Q_1}\right)^{6/7} \left(\frac{W_1}{W_2}\right)^{k_1} \tag{5.11b}$$

where Q and W are the discharge and channel width, respectively, and subscript "1" is for upstream and "2" for contraction channel. The exponent k_1 is determined as follows:

V^*/T	K_1	Mode of Bed Material Transport
<0.5	0.59	Mostly contacted material discharge
0.5 to 2.0	0.64	Some suspended material discharge
>2.0	0.69	Mostly suspended bed material discharge

Herein, V^* is the shear velocity and T the fall velocity of D_{50}. For clear-water scour, FHWA (2012a) suggests

$$y_2 = \left[\frac{K_u Q^2}{D_m^{2/3} W^2}\right]^{3/7} \tag{5.11c}$$

where $K_u = 0.0077$ for English units or 0.025 for SI units, Q, $D_{m,}$ and W are the discharge, median sediment diameter, and channel width in the contraction reach. Clear-water scour occurs if the average approach velocity is less than critical velocity V_c for sediment inception described by

$$V_c = K_u y^{1/6} D_{50}^{1/3} \tag{5.11d}$$

where $K_u = 6.19$ for SI units or 11.17 for English units. In general, clear-water scour is about 10% bigger than corresponding live-bed scour.

Step 3: Compute the magnitude of local scour at the abutments

FHWA (2012a) recommends three methods calculating abutment scour: Froehlich's equation, HIRE equation, and NCHRP 24-20 approach. For example, HIRE equation reads as

$$\frac{y_s}{y_1} = 4F_r^{0.33}\frac{K_1}{0.55}K_2 \tag{5.11e}$$

where y_s = scour depth, y_1 = flow depth at the abutment on the overbank or in the main channel, F_r = Froude number based on the velocity and depth adjacent to and upstream of the abutment, K_1 = abutment shape coefficient below, and K_2 = coefficient for skew angle of abutment to flow.

Description	K_1
Vertical-wall abutment	1.00
Vertical-wall abutment with wing walls	0.82
Spill-through abutment	0.55

Step 4: Compute the magnitude of local scour at the piers

The pier alignment is the most critical factor in determining scour depth. Piers should align with stream flow. When flow direction changes with the stages, cylindrical piers or some variation may be the best alternative. Be cautious, since large diameter cylindrical piers can cause considerable scour. Pier width and pier nose are also critical elements in causing excessive scour depth.

FHWA (2012a) provides several methods estimating pier scour depth. For a sand bed channel, an acceptable method to specify the maximum possible scour depth for both live-bed and clear-water channel proposed by the Colorado State University (FHWA 2012a) is as follows:

$$\frac{y_s}{y_1} = 2.0K_1K_2K_3\left(\frac{a}{y_1}\right)^{0.65}F_{r1}^{0.43} \tag{5.12}$$

where y_s = scour depth, y_1 = flow depth just upstream of the pier, K_1 = correction for pier shape from Figure 5.5 and Table 5.3, K_2 = correction for angle of attack of flow from Table 5.4, K_3 = correction for Bed Condition from Table 5.5, a = pier width, l = pier length, and F_{rl} = Froude number = $V/(gy)^{0.5}$ (Just upstream from bridge).

Note that Equation 5.12 does not include the effect of sediment mixture. For nonuniform sediment, Guo's (2012) equation is recommended as

$$\frac{y_s}{\sqrt{ay_1}} = \tanh\left(\frac{H^2/\sigma^{3/2} - H_{cp}^2}{3.75}\right) \tag{5.13a}$$

where H_{cp} is the critical Hager number for uniform sediment (= 1), determined by

$$H_{cp} = \left[1 - \frac{2}{3}\left(\frac{b}{B}\right)^{1/4}\right]H_c \tag{5.13b}$$

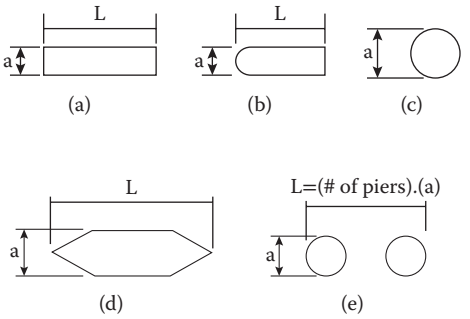

FIGURE 5.5 Common pier shapes: (a) Square nose (b) Round nose (c) Cylinder (d) Sharp nose (e) Group of cylinders (See multiple coloumns).

TABLE 5.3 Correction Factor, K_1, for Pier Nose Shape

Shape of Pier Nose	K_1
Square nose	1.1
Round nose	1.0
Circular cylinder	1.0
Sharp nose	0.9
Group of cylinders	1.0

TABLE 5.4 Correction Factor, K_2, for Flow Angle of Attack

Angle	$L/a = 4$	$L/a = 8$	$L/a = 12$
0	1.0	1.0	1.0
15	1.5	2.0	2.5
30	2.0	2.75	3.5
45	2.3	3.3	4.3
90	2.5	3.9	5

TABLE 5.5 Increase in Equilibrium Pier Scour Depths K_3 for Bed Conditions

Bed Conditions	Dune Height H, ft	K_3
Clear-water scour	N/A	1.1
Plane bed and antidune flow	N/A	1.1
Small dunes	$10 > H > 2$	1.1
Medium dunes	$30 > H > 10$	1.1–1.2
Large dunes	$H > 30$	1.3

where B = channel width and H_c is the critical Hager number corresponding to

$$H_c = \begin{cases} 2.33 D_*^{-0.25} (R_h / D_{50})^{1/6} & \text{for } D_* \le 10 \\ 1.08 D_*^{1/12} (R_h / D_{50})^{1/6} & \text{for } 10 < D_* < 150 \\ 1.65 (R_h / D_{50})^{1/6} & \text{for } D_* \ge 150 \end{cases} \tag{5.13c}$$

where $D_* = [(\rho_s/\rho - 1)g/\nu^2]^{1/3} D_{50}$ is dimensionless sediment size, and R_h = hydraulic radius. In practice, the effect of critical Hager number can be neglected and Equation 5.13a is reduced to

$$\frac{y_s}{\sqrt{ay_1}} = \tanh\left(\frac{H^2/\sigma^{3/2}}{3.75}\right) \tag{5.14}$$

which gives the potential maximum scour depth as $y_s = (ay_1)^{0.5}$. Finally, HEC-18 (FHWA 2012a) recommends a revised version of Equation 5.14 as

$$\frac{y_s}{\sqrt{ay_1}} = 1.1K_1K_2K_3 \tanh\left(\frac{H^2/\sigma^{3/2}}{1.97}\right) \tag{5.15}$$

which is based on both laboratory and field data and detailed in Guo et al. (2012).

5.3.2.3 Estimate and Evaluate Total Potential Scour Depths

Total potential scour depths is usually the sum of long-term bed elevation change (only degradation is usually considered in scour computation), contraction scour, and local scour. Historical scour depths and depths of scourable material are determined by geology. When estimated depths from the above methods are in conflict with geology, the conflict shall be resolved by the hydraulic engineer and the geotechnical engineer, based on economics and experience, it is best to provide for maximum anticipated problems.

5.3.3 Pressure Flow Scour from Model Tests

Model tests use a small-scale bridge structure to simulate and predict the performance of a full-scale bridge. The equilibrium scour depth y_s is an important parameter, yet requiring a long period to be attained. In such cases, the following procedures are recommended (Guo 2011).

Suppose a laboratory bridge is scaled by Froude similitude. If the model scour starts with a flat bed and its depth is η_1 at time t_1, then the equilibrium scour depth y_{sm} is calculated by

$$y_{sm} = \eta_1 (1 - e^{-T_1/T_{90}})^{-n} \tag{5.16}$$

where η_1 is measured scour depth (m) at time t_1 (s), $T_1 = t_1 V/h_b$ the dimensionless time with V (m/s) as approach velocity and h_b the bridge opening height before scour, $T_{90} = 1.56 \times 10^5$ corresponding to the dimensionless time at 90% of y_s, and $n = 0.239$. The prototype scour depth is then scaled back according to Froude similitude as

$$\frac{y_{sp}}{y_{sm}} = \left(\frac{V_m}{V_p}\right)^2 \tag{5.17}$$

where y_{sp} and V_p are the scour depth and approach velocity, respectively, for prototype flow.

5.3.4 Bridge Scour Investigation and Prevention

5.3.4.1 Steps to Evaluate Bridge Scour

It is recommended that an interdisciplinary team of hydraulic, geotechnical, and bridge engineers should conduct the evaluation of bridge scour. The following approach is recommended for assessing the vulnerability of existing bridges to scour (FHWA 2012a):

Step 1: Screen all bridges over waterways into five categories: (1) low risk, (2) scour-susceptible, (3) scour-critical, (4) unknown foundations, or (5) tidal. Bridges that are particularly vulnerable to scour failure should be identified immediately and the associated scour problem addressed. These particularly vulnerable bridges are:
Bridges currently experiencing scour or that have a history of scour problems during past floods as identified from maintenance records and experience, bridge inspection records.
Bridges over erodible streambeds with design features that make them vulnerable to scour.
Bridges on aggressive streams and waterways.
Bridges located on stream reaches with adverse flow characteristics.

Step 2: Prioritize the scour-susceptible bridges and bridges with unknown foundations by conducting a preliminary office and field examination of the list of structure compiled in Step 1 using the following factors as a guide: (1) the potential for bridge collapse or for damage to the bridge in the event of a major flood; and (2) the functional classification of the highway on which the bridge is located, and the effect of a bridge collapse on the safety of the traveling public and on the operation of the overall transportation system for the area or region.

Step 3: Conduct office and field scour evaluations of the bridges on the prioritized list in Step 2 using an interdisciplinary team of hydraulic, geotechnical, and bridge engineers:
In the United States, FHWA recommends using 500-year flood or a flow 1.7 times the 100-year flood where the 500-year flood is unknown to estimate scour (Waananen and Crippen 1977), and then analyze the foundations for vertical and lateral stability for this condition of scour. The maximum scour depths that the existing foundation can withstand are compared with the total scour depth estimated. An engineering assessment must be then made as to whether the bridge should be classified as a scour-critical bridge.
Enter the results of the evaluation study in the inventory in accordance with the instructions in the FHWA (1995).

Step 4: For bridges identified as scour critical from the office and field review in Steps 2 and 3, determine a plan of action for correcting the scour problem.

5.3.5 Introduction to Bridge Scour Inspection

The bridge scour inspection is one of the most important parts of preventing bridge scour from endangering bridges. Two main objectives to be accomplished in inspecting bridges for scour are: (1) To accurately record the present condition of the bridge and the stream and (2) to identify conditions that are indicative of potential problems with scour and stream stability for further review and evaluation by other experts.

In this section, the bridge inspection practice recommended by USFHWA (Waananen and Crippen 1977, FHWA 1989) is presented for engineers to follow as guidance.

1. **Office Review**

   It is highly recommended to make an office review of bridge plans and previous inspection reports prior to making the bridge inspection. Information obtained from the office review provides a better foundation for inspecting the bridge and the stream. The following questions should be answered in the office review:

   a. Has an engineering scour evaluation been conducted? If so, is the bridge scour critical?
   b. If the bridge is scour critical, has a plan of action been made for monitoring the bridge and/or installing scour prevention measures?
   c. What do comparisons of streambed cross sections taken during successive inspections reveal about the streambed? Is it stable? Degrading? Aggrading? Moving laterally? Are there scour holes around piers and abutments?
   d. What equipment is needed to obtain streambed cross sections?
   e. Are there sketches and aerial photographs to indicate the planform locations of the stream and whether the main channel is changing direction at the bridge?

f. What type of bridge foundation was constructed? Do the foundations appear to be vulnerable to scour?
g. Do special conditions exist requiring particular methods and equipment for underwater inspections?
h. Are there special items that should be looked at including damaged riprap, stream channel at adverse angle of flow, problems with debris, and so on?

2. **Bridge Scour Inspection Guidance**

The condition of bridge waterway opening, substructure, channel protection, and scour prevention measures should be evaluated along with the condition of the stream during the bridge inspection. The following approaches are presented for inspecting and evaluating the present condition of the bridge foundation for scour and the overall scour potential at the bridge.

Substructure is the key item for rating the bridge foundations for vulnerability to scour damage. Both existing and potential problems with scour should be reported so that an interdisciplinary team can make a scour evaluation when a bridge inspection finds that a scour problem has already occurred. If the bridge is determined to be scour critical, the rating of the substructures should be evaluated to ensure that existing scour problems have been considered. The following items should be considered in inspecting the present condition of bridge foundations:

a. Evidence of movement of piers and abutments such as rotational movement and settlement
b. Damage to scour countermeasures protecting the foundations such as riprap, guide banks, sheet piling, sills, etc.
c. Changes in streambed elevation at foundations such as undermining of footings, exposure of piles
d. Changes in streambed cross section at the bridge, including location and depth of scour holes

In order to evaluate the conditions of the foundations, the inspectors should take cross sections of the stream and measure scour holes at piers and abutments. If equipment or conditions do not permit measurement of the stream bottom, it should be noted for further investigation.

To take and plot measurement of stream bottom elevations in relation to the bridge foundations is considered the single most important aspect of inspecting the bridge for actual or potential damage from scour. When the stream bottom cannot be accurately measured by conventional means, there other special measures need to be taken to determine the condition of the substructures or foundations such as using divers and using electronic scour detection equipment. For the purposes of evaluating resistance to scour of the substructures, the questions remain essentially the same for foundations in deep water as for foundations in shallow water (FHWA 1995) as follows:

a. How does the stream cross section look at the bridge?
b. Have there been any changes as compared to previous cross section measurements? If so, does this indicate that (1) the stream is aggrading or degrading; or (2) local or contraction scour is occurring around piers and abutments?
c. What are the shapes and depths of scour holes?
d. Is the foundation footing, pile cap, or the piling exposed to the stream flow; and if so, what is the extent and probable consequences of this condition?
e. Has riprap around a pier been moved and removed?

Any condition that a bridge inspector considers to be an emergency or potentially hazardous nature should be reported immediately. This information as well as other conditions, which do not pose an immediate hazard, but still warrant further investigation, should be conveyed to the interdisciplinary team for further review.

5.3.6 Real-Time Monitoring

Real-time bridge-scour monitoring details the scour developments using technology and communications systems. It provides timely and quality data of scour developments to bridge managers for decision making. Since scour is the most common cause of bridge failures and the most expensive kind of damage to repair bridges, the FHWA actively promotes real-time scour monitoring research and practice. With two consecutive data (t_0,η_0) and (t_1,η_1), the scour y_s at the next time step t is found as follows (Guo 2011).

Assume a quasi-steady state flow for time period $t_0 < t_1 < t$. The equilibrium scour depth y_s is calculated by

$$y_s = \left[\frac{\eta_1^{1/n} - \eta_0^{1/n}\exp[-(T_1 - T_0)/T_{90}]}{1 - \exp[-(T_1 - T_0)/T_{90}]}\right]^n \tag{5.18}$$

where $T_0 = t_0V/h_b$ and $T_1 = t_1V/h_b$ with V and h_b the approach velocity and bridge opening height before scour, respectively, $T_0 = 1.56 \times 10^5$ and $n = 0.239$. With Equation 5.18, the scour depth $\eta(t)$ is estimated by solving the following equation:

$$\frac{y_s^{1/n} - \eta^{1/n}}{y_s^{1/n} - \eta_0^{1/n}} = \exp\left(-\frac{T - T_0}{T_{90}}\right) \tag{5.19}$$

with $T = tV/h_b$. According to the value $\eta(t)$ from Equation 5.19, bridge managers can predict scour conditions at critical moments and formulate timely corrective strategies. Once a bridge scour is found critical during floods, the bridge should be closed for public safety and the damages should be immediately repaired after floods. Note that the above monitoring scheme was developed for pressure bridge scour, but it can be extended for pier scour by replacing h_b with pier diameter.

5.3.7 Scour Protection

Scour prevention measures are generally incorporated after the initial construction of a bridge to make it less vulnerable to damage or failure from scour. A plan of preventive action usually has three major components (FHWA 2012a): (1) timely installation of temporary scour prevention measures; (2) development and implementation of a monitoring program; and (3) schedule for timely design and construction of permanent scour prevention measures.

For new bridges (FHWA 2012a), the following summarizes the best solutions for minimizing scour damage: (1) locating the bridge to avoid adverse flood flow patterns; (2) streamlining bridge elements to minimize obstructions to the flow; (3) designing foundations safe from scour; (4) founding bridge pier foundations sufficiently deep to not require riprap or other prevention measures; and (5) founding abutment foundations above the estimated local scour depth when the abutment is protected by well-designed riprap or other suitable measures.

For existing bridges, the following alternatives are used: (1) monitoring scour depths and closing bridge if excessive bridge scour exists; (2) providing riprap at piers and/or abutments and monitoring the scour conditions; (3) constructing guide banks or spur dikes; (4) constructing channel improvements; (5) strengthening the bridge foundations; (6) constructing sills or drop structures; and (7) constructing relief bridges or lengthening existing bridges. Further scour prevention measures are found in FHWA (2012a, b).

References

AASHTO. 2005. *Model Drainage Manual*, 3rd Edition, American Association of State Highway and Transportation Officials, Washington, DC.

AASHTO. 2007. *Highway Drainage Guidelines*, 4th Edition, American Association of State Highway and Transportation Officials, Washington, DC.

Brater, E., King, H., Lindell, J., and Wei, C. 1996. *Handbook of Hydraulics*, 7th Edition, McGraw-Hill, New York, NY.

FHWA. 1984. *Hydrology*, FHWA-TS-84-204, Federal Highway Administration, Washington, DC.

FHWA. 1989. *Design of Riprap Revetments*, Hydraulic Engineering Circular No 11, FHWA- IP-89-016, Federal Highway Administration, Washington, DC.

FHWA. 1995. *Recording and Coding Guide for the Structure Inventory and Appraisal of the Nation's Bridges*, FHWA-PD-96-001, Federal Highway Administration, Washington, DC.

FHWA. 2001. *River Engineering For Highway Encroachments: Highways In The River Environment*, FHWA NHI 01-004, Federal Highway Administration, Washington, DC.

FHWA. 2002. *Highway Hydrology*, 2nd Edition, NHI-02-001, Federal Highway Administration, Washington, DC.

FHWA. 2005. *Debris Control Structures Evaluation and Countermeasures*, Hydraulic Engineering Circular No. 9, FHWA-IF-04-016, Federal Highway Administration, Washington, DC.

FHWA. 2012a. *Evaluating Scour at Bridges*, 5th Edition, HIF-12-003, Federal Highway Administration, Washington, DC.

FHWA. 2012b. *Stream Stability at Highway Structures*, 4th Edition, HIF-12-004, Federal Highway Administration, Washington, DC.

Guo, J. 2011. Time-dependent clear-water scour for submerged bridge flows. *J Hydraulic Research*, 49(6), 744–749.

Guo, J. 2012. Pier scour in clear water for sediment mixtures. *J Hydraulic Research*, 50(1), 18–27.

Guo, J., Suaznabar, O., Shan, H., and Shen, J. 2012. *Pier Scour in Clear-Water Conditions with Non-Uniform Bed Materials*, FHWA-HRT-12-022, Federal Highway Administration, Washington, DC.

USGS. 1981. *Guidelines for Determining Flood Flow Frequency*, United States Geological Survey, Reston, VA.

Waananen, A. O., and Crippen, J. R. 1977. *Magnitude and Frequency of Floods in California*, Water Resources Investigation 77-21, United States Geological Survey, Menlo Park, CA.

Yen, B. C., and Chow, V. T. 1997. *Feasibility on Research on Local Design Storms*, FHWA-RD-78-65, Federal Highway Administration, Washington, DC.

6

Abutments

Linan Wang
California Department of Transportation

6.1 Introduction

As a component of a bridge, the abutment provides the vertical support to the bridge superstructure at bridge ends, connects the bridge with the approach roadway, and retains the roadway base materials from the bridge spans. Although there are numerous types of abutments and the abutments for the important bridges may be extremely complicated, the analysis principles and design methods are very similar. In this chapter, the topics related to the design of conventional highway bridge abutment are discussed and a design example is illustrated.

6.2 Abutment Types

6.2.1 Open-End and Closed-End Abutments

From the view of the relation between the bridge abutment and roadway or channel that the bridge overcrosses, the bridge abutments can be divided into two categories: open-end abutment and closed-end abutment, as shown in Figure 6.1.

For open-end abutment, there are slopes between the bridge abutment face and the edge of the roadway or the channel. Those slopes provide a widely opened area to the traffic flows or water flows under the bridge. It imposes much less impact on the environment and the traffic flows under the bridge than closed-end abutment. Also it is easier to make future widening on roadway or the channel under the bridge by adjusting the slope ratios. However, the existing of slopes usually requires longer bridge spans and some extra earthwork. This may result in the raise of bridge construction cost.

The closed-end abutment is usually constructed close to the edge of the roadways or channels. In the case of limited right of way, a high abutment wall is usually constructed without front slope to meet

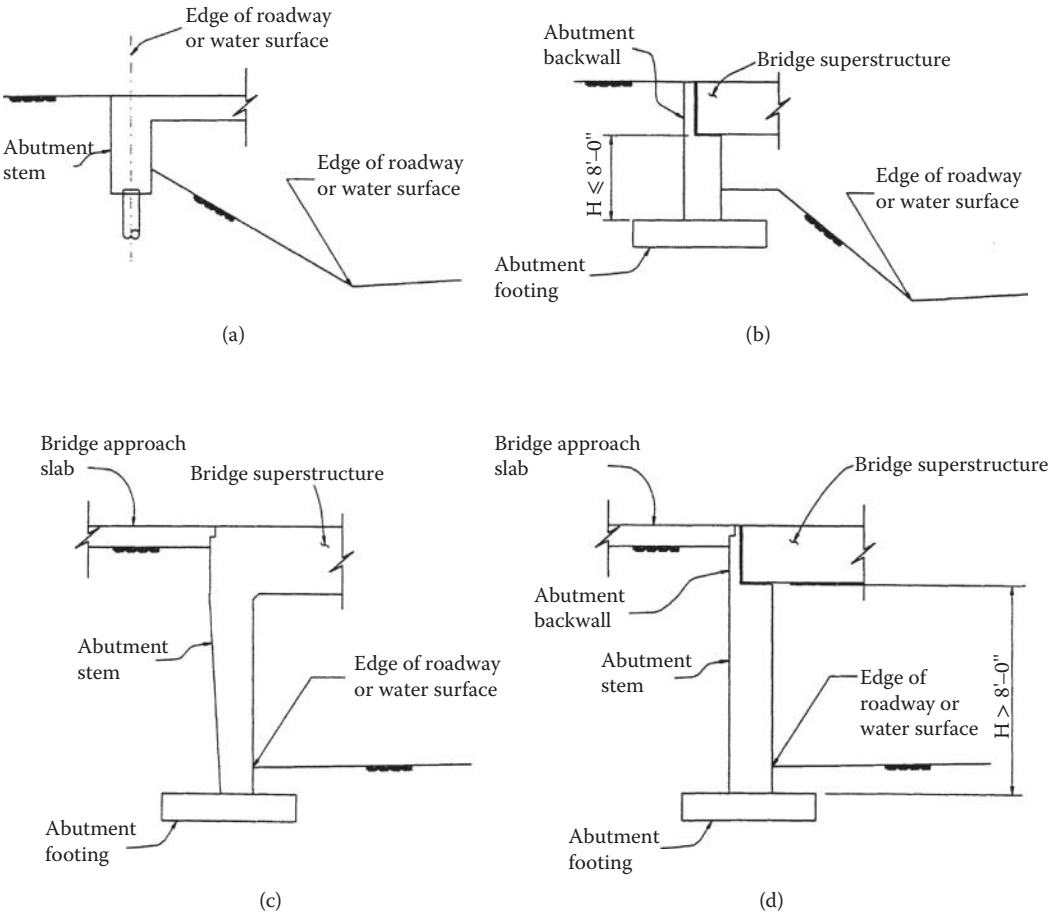

FIGURE 6.1 Typical abutment types. (a) Open end, monolithic type, (b) Open end short stem type, (c) Closed end, monolithic type, (d) Closed end, short stem type.

the vertical clearance requirements of the traffic or the water flows. Since there is no room or only little room exists between the abutment and the edge of traffic or water flow, it is very difficult to do the future widening on the roadways or channels under the bridge. Also the high abutment walls and larger volume of backfill material often result in higher abutment construction costs and more settlement of road approaches than for open-end abutment.

Generally the open-end abutments are more economical, adaptable, and attractive than the closed-end abutments. However, the bridges with closed-end abutments have been widely constructed in the urban area and for rail transportation system because of the right of way restriction and the large scale of the live load for trains, which usually results in short bridge spans.

6.2.2 Monolithic and Seat-Type Abutments

Based on the connection type between the abutment stem and bridge superstructure, the abutments also can be grouped as two categories: the monolithic or end diaphragm abutment and the seat-type abutment as shown in Figure 6.1.

For monolithic abutment, the abutment stem is monolithically constructed with the bridge superstructure. There is no relative displacement allowed between the bridge superstructure and abutment.

All superstructure forces at bridge ends are transferred to the abutment stem and then to the abutment backfill soil and footings. The advantages of this type of abutment are its initial lower construction cost and its immediate engagement of backfill soil that absorbs the energy when the bridge is subjected to transitional movement. However, the passive soil pressure induced by bridge lateral movement could result in the difficulty of designing the abutment stem. Also a higher maintenance cost on bridge approach might be expected for this type of abutment. In the practice, this type of abutment is mainly constructed for short bridges.

For seat-type abutment, the abutment stem is constructed separately with the bridge superstructure. The bridge superstructure seats on the abutment stem through bearing pads, rock bearings, or other devices. This type of abutment allows the bridge designer to control the superstructure forces that are to be transferred to the abutment stem and its backfill soil. By adjusting the devices between the bridge superstructure and abutment, the bridge displacement could be controlled. This type of abutment may have short stem or high stem as shown in Figure 6.1. For short-stem abutment, the abutment stiffness usually is much larger than the connection devices between the superstructure and the abutment. Therefore, those devices can be treated as boundary conditions in the bridge analysis. Comparatively, the high-stem abutment may subject significant displacement under the relative less forces. The stiffness of high-stem abutment and the response of surrounding soil may have to be considered in the bridge analysis. The availability of the displacement of connection devices, the allowance of the superstructure shrinkage, and concrete shortening make this type abutment be widely selected for the long bridge constructions, especially for prestressed concrete bridges and steel bridges. However, the bridge design practice shows that the relative weak connection devices between the superstructure and the abutment usually cause the adjacent columns to be specially designed. Although the seat-type abutment has relatively higher initial construction cost than monolithic abutment, its maintenance cost is relatively low.

6.2.3 Abutment Type Selection

The selection of an abutment type needs to consider all available information and bridge design requirements. Those may include bridge geometry, roadway and riverbank requirements, geotechnical condition, right-of-way restrictions, architect requirements, economical considerations, and so on. The knowledge of advantages and disadvantages for the different types of abutments will greatly benefit the bridge designer to choose a right type of abutment for the bridge structure from the beginning stage of the bridge design.

6.3 General Design Considerations

Abutment design loads usually include vertical and horizontal loads from bridge superstructure, vertical and lateral soil pressures, abutment gravity load, and the live load surcharge on the abutment backfill materials. An abutment shall be designed as no damage to withstand the earth pressure, the gravity loads of bridge superstructure and abutment, live load on superstructure or approach fill, wind loads and the transitional loads transferred through the connections between the superstructure and the abutment. Any possible combination of those loads, which produce the most severe condition of loading, shall be investigated in abutment design. Meanwhile, for the integral abutment or monolithic type abutment, the effects of bridge superstructure deformations, including bridge thermal movements, to the bridge approach structures must be considered in the abutment design. Nonseismic design loads at service level and their combinations are shown in Table 6.1 and Figure 6.2. For Load Factor Design (LFD) (AASHTO 2002) or Load and Resistant Factor Design (LRFD) (AASHTO 2012), the abutment design loads could be obtained by multiplying the load factors to the loads at service levels. Under the seismic loading, the abutment may be designed as no support lost to the bridge superstructure while the abutment may suffer some repairable damages during a major earthquake.

TABLE 6.1 Abutment Design Loads (Service Load Design)

	Case				
Abutment Design Loads	I	II	III	IV	V
Dead load of superstructure	X	X	—	X	X
Dead load of wall and footing	X	X	X	X	X
Dead load of earth on heel of wall including surcharge	X	X	X	X	—
Dead load of earth on toe of wall	X	X	X	X	—
Earth pressure on rear of wall including surcharge	X	X	X	X	—
Live load on superstructure	X	—	—	X	—
Temperature and shrinkage	—	—	—	X	—
Allowable pile capacity of allowable soil pressure in % or basic	100	100	150	125	150

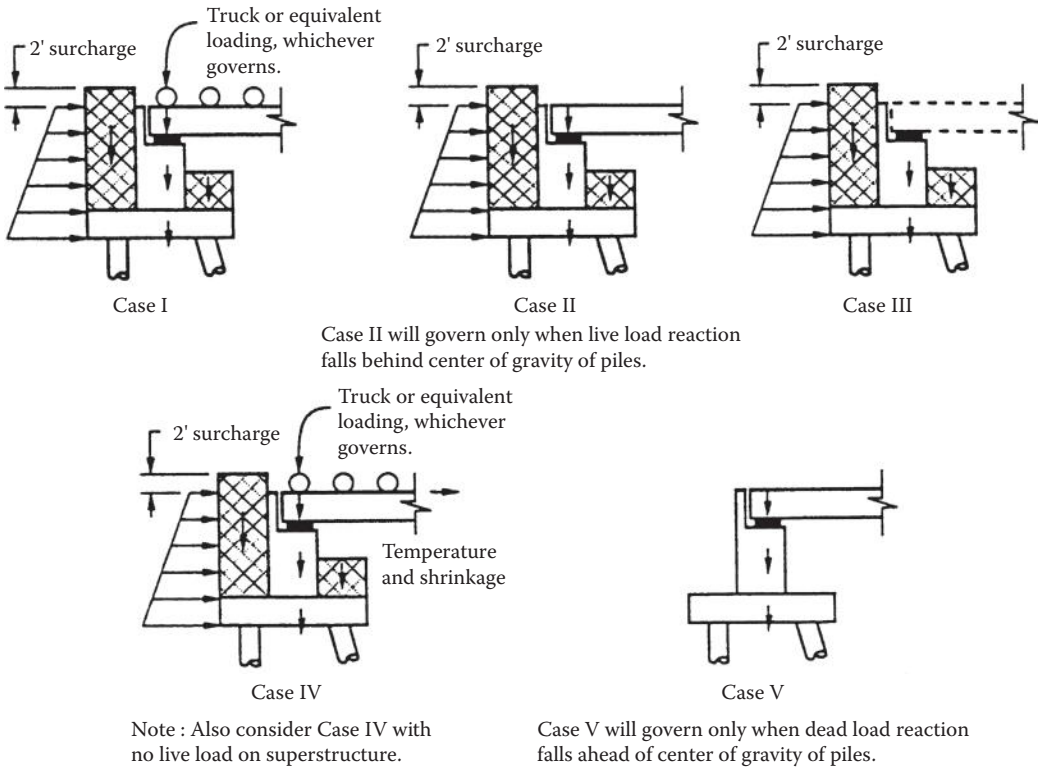

FIGURE 6.2 Configuration of abutment design load and load combinations.

The load and load combinations listed in Table 6.1 may cause abutment sliding, overturning, and soil bearing failures. Those stability characteristics of abutment must be checked to satisfy certain restrictions. For the abutment with spread footings in service load design, the factor of safety to resist sliding should be greater than 1.5; the factor of safety to resist overturning should be greater than 2.0; the factor of safety against the soil bearing failure should be greater than 3.0. For the abutment with pile support, the piles have to be designed to resist the forces that cause the abutment sliding, overturning, and bearing failure.

The abutment deep shear failure also needs to be studied in the abutment design. Usually, the potential of this kind of failure is pointed out in the geotechnical report to the bridge designers. Deep pilings or relocating the abutment may be used to avoid this kind of failure.

6.4 Seismic Design Considerations

The investigations of past earthquake damage to bridges reveal that there are commonly two types of abutment earthquake damage—the stability damage and the component damage.

The abutment stability damage during an earthquake is mainly caused by the foundation failure due to the excessive ground deformation or the loss of bearing capacities of the foundation soil. Those foundation failures result in the abutment suffering tilting, sliding, settling, and overturning. The foundation soil failure usually occurs at the poor soil conditions such as soft soil and the existence of high water table. In order to avoid these kinds of soil failures during an earthquake, borrowing backfill soil, pile foundations, high-degree soil compaction, previous materials, and drainage system may be considered in the design.

The abutment component damage is generally caused by the excessive soil pressure, which is mobilized by the large relative displacement between the abutment and its backfilled soil. Those excessive pressures may cause severe damage to abutment components such as abutment back walls and abutment wingwalls. However, the abutment component damages usually do not cause the bridge superstructure lost support at abutment and they are easy to be repaired. This may allow the bridge designer to use the deformation of abutment backfill soil under the seismic forces to dissipate the seismic energy to avoid the bridge losing support at columns under a major earthquake strike.

The behavior of abutment backfill soil deformed under seismic load is very efficient to dissipate the seismic energy especially for the bridges with total length of less than 300 ft (91.5 m) with no hinge, no skew, or slightly skewed (i.e., <15°). The tests and analysis revealed that if the abutments of a short bridge are capable to mobilize the backfill soil and are well tied into the backfill soil, a damping ratio in the range of 10%–15% is justified. This will elongate the bridge period and may reduce the ductility demand on the bridge columns. For short bridges, a damping reduction factor, D, may be applied to the forces and displacement obtained from the bridge elastic analysis. This factor D is given in Equation 6.1.

$$D = \frac{1.5}{40C + 1} + 0.5 \tag{6.1}$$

where C = damping ratio.

Based on Equation 6.1, for 10% damping ratio, a factor of $D = 0.8$ may be applied to the elastic forces and displacements resulted from the elastic structure analysis; for 15% damping ratio, a factor of $D = 0.7$ may be applied to such elastic forces and displacements. Generally, the reduction factor D should be applied to the forces corresponding to the bridge shake mode that shows the abutment being excited.

The earthquake forces that backfill soil applied to abutment are very difficult to predict (Goel 1997; Sorensen 1997). The Mononobe-Okabe method is usually used to quantify the active earth pressure induced by earthquake for earth-retaining structures with non-top-restrains. For the passive earth pressure induced by bridge movement at abutment under seismic loading, the study and tests revealed that the soil resistances mainly depend on the abutment movement direction and magnitude. The "near-full-scale" abutment tests performed at University of California at Davis (Maroney et al. 1993 and 1994) shows a nonlinear relationship between the abutment displacement and the backfill soil reactions under certain seismic loading when the abutments move toward its backfill soil. This relation was plotted as shown in Figure 6.3. It is difficult to simulate this nonlinear relationship between the abutment displacement and backfill soil reactions while performing the bridge dynamic analysis. However, the tests concluded an upper limit for the backfill soil reaction on the abutment. In design practice, a peak soil pressure acting on the abutment may be predicted corresponding to certain abutment displacement. Based on the tests and the investigations to the past earthquake damages, California Transportation Department guided for the bridge analysis considering abutment damping behavior as follows.

Using the peak abutment force and the effective area of the mobilized soil wedge, the peak soil pressure is compared to a maximum capacity of 7.7 ksf (369 kPa). If the peak soil pressure exceeds the soil

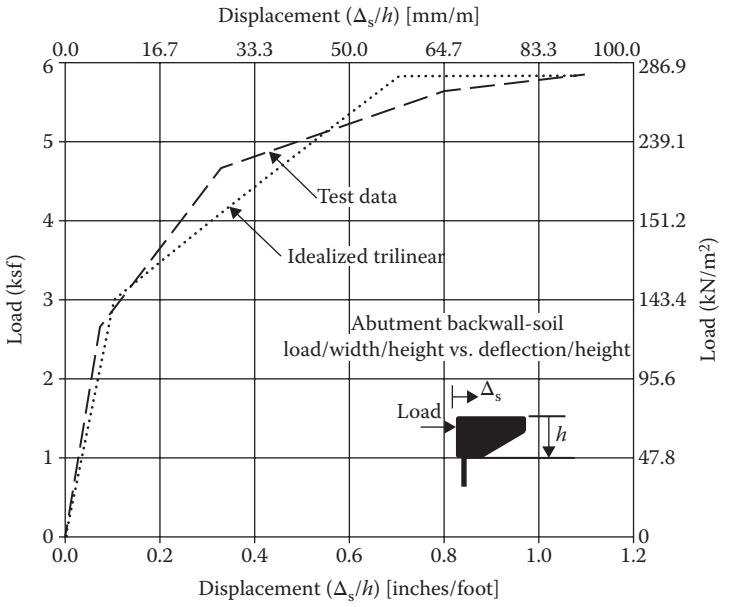

FIGURE 6.3 Proposed characteristics and experimental envelope for abutment backfill load deformation.

capacity, the analysis should be repeated with reduced abutment stiffness. It is important to note that the 7.7 ksf (369 kPa) soil pressure is based on a reliable minimum wall height of 8 ft (2.438 m). If the wall height is less than 8 ft (2.438 m), or if the wall is expected to shear off at a depth below the roadway less than 8 ft (2.438 m), the allowable passive soil pressure must be reduced by multiplying 7.7 ksf (369 kPa) with the ratio of $(h/8)^2$, where "h" is the effective height of abutment wall in feet. Furthermore, the shear capacity of the abutment wall diaphragm (structural member mobilizing soil wedge) should be compared to the demand shear forces to ensure the soil mobilizations. Abutment spring displacement is then evaluated against the acceptable level of displacement 0.2 ft (61 mm). For monolithic type abutment, this displacement is equal to the bridge superstructure displacement. For seat-type abutment, this displacement is usually not equal to the bridge superstructure displacement that may include the gap between the bridge superstructure and abutment backwall. However, a net displacement of about 0.2 ft (61 mm) at abutment should not be exceeded. Field investigations after the 1971 San Fernando Earthquake revealed that the abutment, which moved up to 0.2 ft (61 mm) in the longitudinal direction into the backfill soil, appeared to survive with little need for repair. The abutments in which the backwall breaks off before other abutment damage may also be satisfactory if a reasonable load path can be provided to adjacent bents and no collapse potential is indicated (Caltrans 1996).

The current seismic design criteria of California Transportation Department (Caltrans 2010) suggests an effective initial abutment stiffness of $K_i = 50$ ft/in/ft to be used in seismic analysis. This K_i could generate a larger backfill soil capacity with 0.2 ft abutment movement. However, an abutment displacement coefficient R_A is assigned to justify the contribution of the abutment stiffness in the analysis.

$$R_A = \Delta_D / \Delta_{eff} \tag{6.2}$$

where:

Δ_D = The longitudinal displacement demand at the abutment from elastic analysis
Δ_{eff} = The effective longitudinal abutment displacement at idealized yield

If $R_A \leq 2$: It indicates that the bridge stiffness is dominated by abutment stiffness and K_i used in the analysis should be realistic.

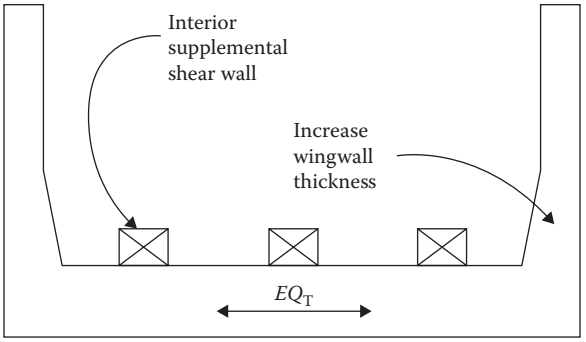

FIGURE 6.4 Abutment transverse enhancement.

If $R_A \geq 4$: It indicates that the contribution of abutment stiffness is not significant. The K_i could be reduced in value or even neglected in the analysis.

If $2 < R_A < 4$: The abutment stiffness may have to be set by try-and-error method following the 7.7 ksf and 0.2 ft rule (Caltrans 2010).

For seismic analysis in bridge transverse direction, since the backfill soil is usually slopping away from abutment wingwall and there is a relatively weak connection between the abutment wingwall and the stem, the displacement coefficient R_A shall not be applied directly in the analysis. Reduced R_A or fully released abutment cases shall be studied. In order to increase the transverse stiffness of the abutment, interior supplemental shear walls may be attached to the abutment or the wingwall thickness may be increased, as shown in Figure 6.4.

Based on the above guidelines, the abutment analysis can be carried out more realistically by try-and-error method on abutment soil springs. The criterion for abutment seismic resistance design may be set as follows:

Monolithic abutment or diaphragm abutment (Figure 6.5)

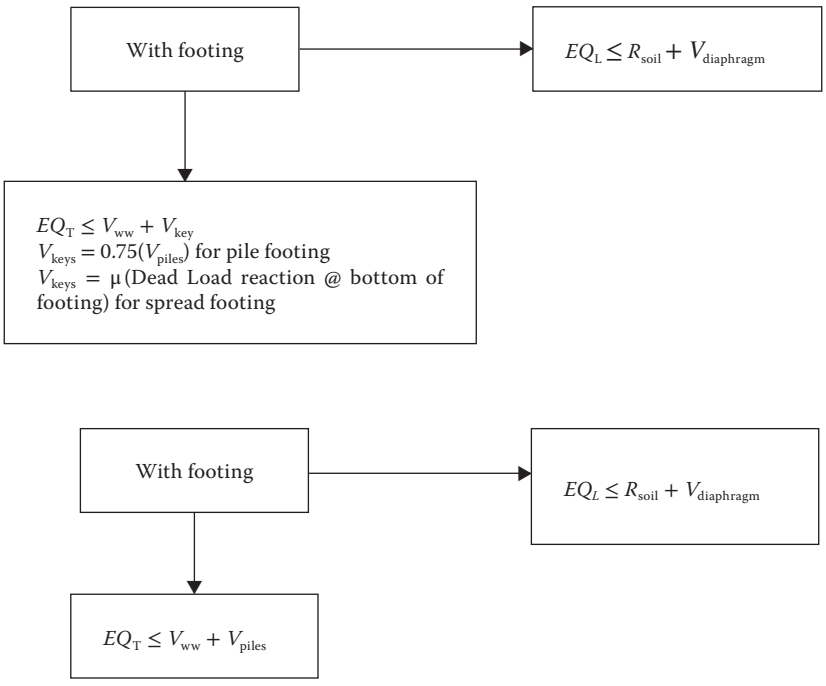

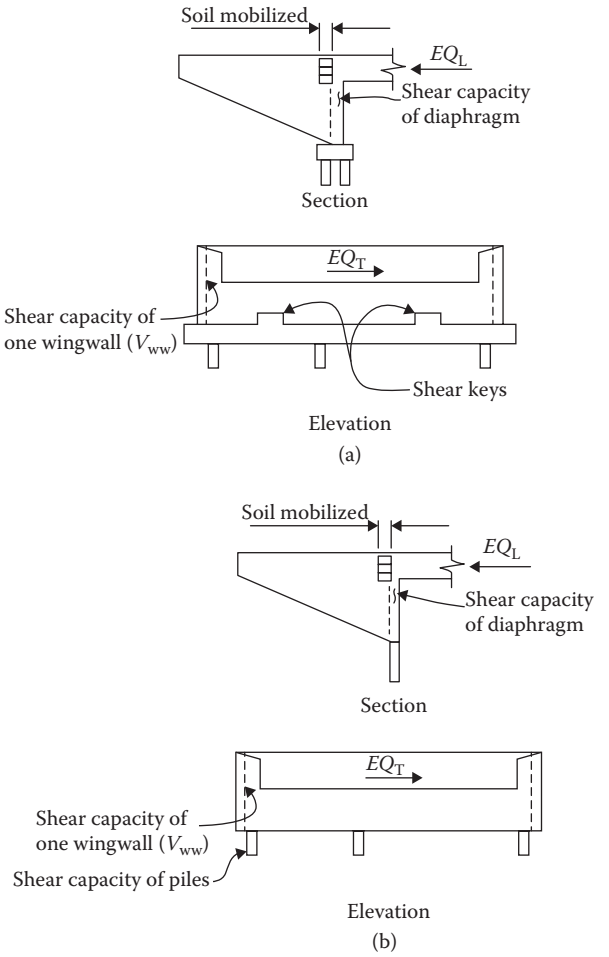

FIGURE 6.5 Seismic resistance elements for monolithic abutment (a) with footing, (b) without footing.

Seat-Type Abutment (Figure 6.6)

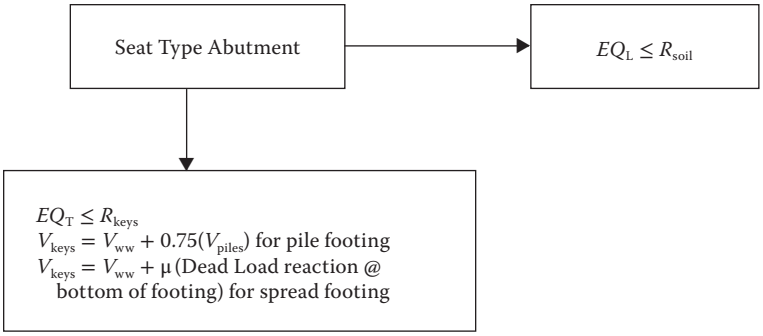

where

EQ_L = Longitudinal earthquake force from an elastic analysis
EQ_T = Transverse earthquake force from an elastic analysis

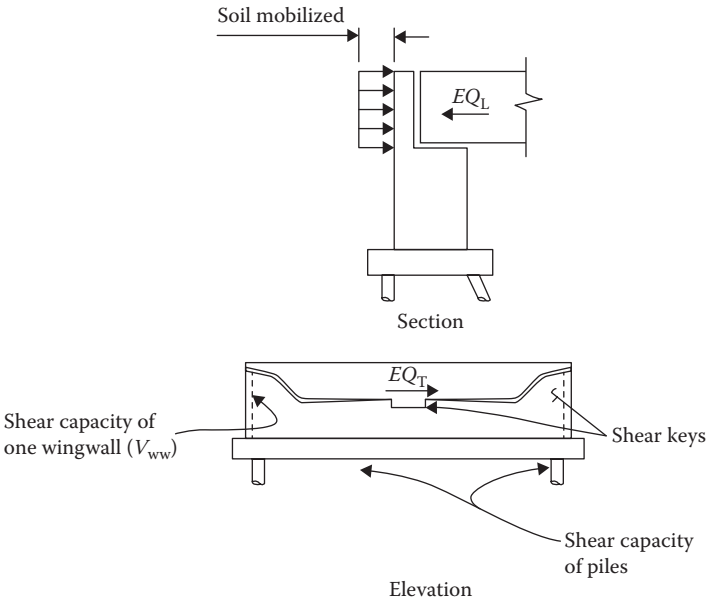

FIGURE 6.6 Seismic resistance elements for seat-type abutment.

R_{soil} = Resistance of soil mobilized behind abutment
$R_{diaphragm}$ = ϕ times the nominal shear strength of the diaphragm
R_{ww} = ϕ times the nominal shear strength of the wingwall
R_{piles} = ϕ times the nominal shear strength of the piles
R_{keys} = ϕ times the nominal shear strength of the keys in the direction of consideration
ϕ = Strength factor for seismic loading
μ = Coefficient factor between soil and concrete face at abutment bottom

The purpose of applying a factor of 0.75 to the design of abutment shear keys is to reduce the possible damage to the abutment piles. For all transverse cases, if the design transverse earthquake force exceeds the sum of the capacities of the wingwalls and piles, the transverse stiffness for the analysis should equal to zero ($EQ_T = 0$). Therefore, a released condition that usually results in a larger lateral displacement at adjacent bents should be studied.

Responding to seismic load, bridge usually accompanies a large displacement. In order to provide support at abutments for the bridge with large displacement under seismic loading, enough seat width at abutment must be designed. Theoretically, the abutment seat width, as shown in Figure 6.7, has to meet the requirement in the formula:

$$N_A \geq \Delta_{p/s} + \Delta_{cr+sh} + \Delta_{temp} + \Delta_{eq} + 4 \tag{6.3}$$

where

N_A = Abutment seat width normal to the center line of bearing (in)
$\Delta_{p/s}$ = Displacement attributed to prestress shoring
Δ_{cr+sh} = Displacement attributed to creep and shrinkage
Δ_{temp} = Displacement attributed to thermal expansion and contraction
Δ_{eq} = The maximum relative displacement between superstructure and abutment results in seismic global or local analysis

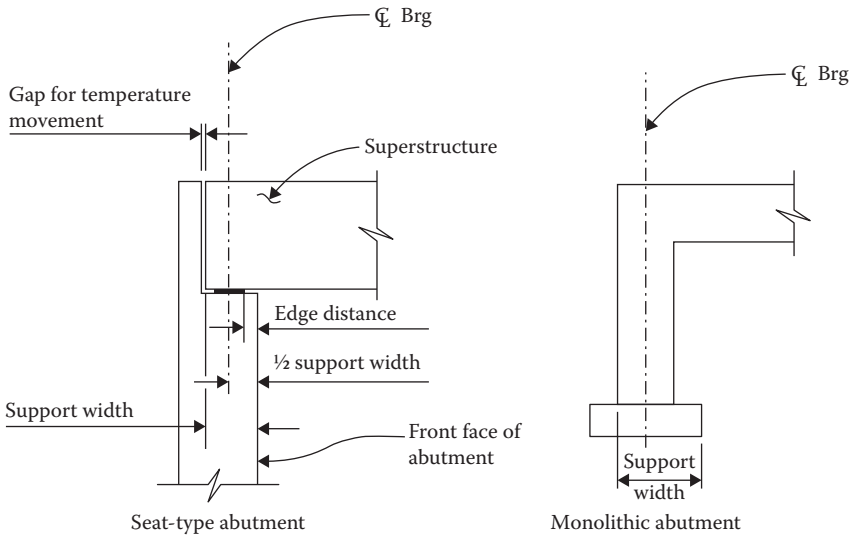

FIGURE 6.7 Abutment support width (seismic).

In practice, the minimum abutment support width may be calculated as shown in Equation 6.4:

$$N_{A\text{¢}} = (12 + 0.03L + 0.12H)(1 + 0.002S^2) \tag{6.4}$$

where

$N_{A'}$ = Abutment support width, (in)
L = Length, (ft), of the bridge deck to the adjacent expansion joint, or to the end of bridge deck. For single-span bridges L equals the length of the bridge deck.
S = Angle of skew at abutment in degrees
H = Average height, (ft), of columns or piers supporting the bridge deck from the abutment to the adjacent expansion joint, or to the end of the bridge deck
$H = 0$ for simple span bridges

6.5 Miscellaneous Design Considerations

6.5.1 Abutment Wingwall

Abutment wingwalls act as a retaining structure to retain the abutment backfill soil and roadway soil to slide transversely. Several types of wingwall for highway bridges are shown in Figure 6.8. The wingwall design is similar to the retaining wall design as presented in Chapter 10. However, the live load surcharge needs to be considered in the wingwall design. Table 6.2 lists the live load surcharge for different loading cases. Figure 6.9 shows the design loads for a conventional cantilever wingwall. For seismic design, the criteria in transverse direction discussed in Section 6.2.3 should be followed. The bridge wingwalls may be designed to sustain some damages in a major earthquake as long as the bridge collapse is not predicted.

6.5.2 Abutment Drainage

A drainage system is usually provided for the abutment construction. The drainage system embedded in the abutment backfill soil is designed to reduce the possible buildup of the hydrostatic pressure, to control the erosion of the roadway embankment, and to reduce the possibility of soil liquefaction during

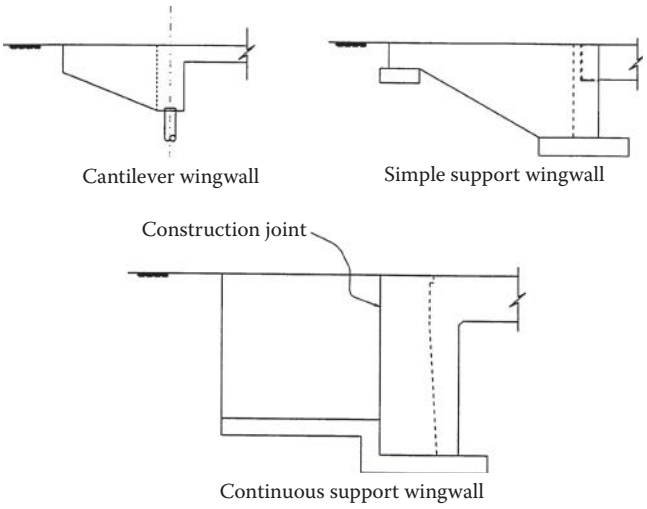

FIGURE 6.8 Typical wingwalls.

TABLE 6.2 Live Load Surcharges for Wingwall Design

Load Case	Equivalent Soil—Height
Highway truck loading	2.0 ft (610 mm)
Rail loading E-60	7.5 ft (2290 mm)
Rail loading E-70	8.75 ft (2670 mm)
Rail loading E-80	10.0 ft (3050 mm)

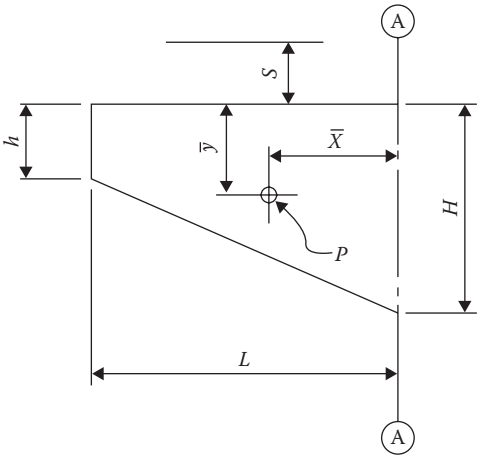

S = Surcharge, Ft.
h = End height, Ft.
H = Section height, Ft.
L = Length, Ft.
W =
= Equivalent fluid earth pressure

$$M_{AA} = \frac{WL^2}{24}[3h^2 + (H + 4S)(H + 2h)]$$

$$P = \frac{WL}{6}[H^2 + (h + H)(h + 3S)]$$

$$\bar{X} = \frac{M_{AA}}{P}$$

FIGURE 6.9 Design loading for cantilever wingwall.

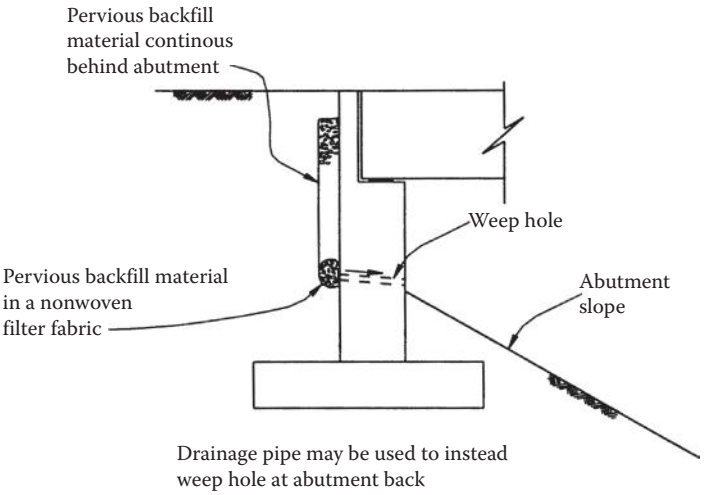

FIGURE 6.10 Typical abutment drainage system.

an earthquake. For the concrete-paved abutment slope, the drainage system also needs to be provided under the pavement. The drainage system may include the pervious materials, the PSP or PVC pipes, the wipe holes, and so on. Figure 6.10 shows a typical drainage system for highway bridge construction.

6.5.3 Abutment Slope Protection

The flow water scoring may severely damage the bridge structures by washing out the bridge abutment support soil. To reduce the water scoring damage to the bridge abutment, the pile support, rock slope protection, concrete slope paving, and gunnit cement slope paving may be used. Figure 6.11 shows the rock slope protection and the concrete slope paving protection for bridge abutment. The stability of the rock and concrete slope protection should be considered in the design. An enlarged block is usually designed at the toe of the protections.

6.5.4 Miscellaneous Details

Some details related to the abutment design are given in Figure 6.12. Although they are only for the regular bridge construction situations, those details presented valuable references to bridge designers.

6.6 Design Example

6.6.1 Design Data

A prestressed concrete box girder bridge with 5° skew is proposed overcrossing a busy freeway as shown in Figure 6.13. Based on the roadway requirement, geotechnical information, and the details mentioned earlier, an open-end, seat-type abutment is selected. The abutment in transverse direction is 89 ft (27.13 m) wide. Other abutment design information is listed as follows:

Abutment design loads (with load factors)

Factored superstructure dead load = 23.0 kips/ft width ($\gamma_p = 1.25$)
Factored normal vehicular load = 8.1 kips/ft width ($\gamma_{LL} = 1.75$)
Special truck vertical load = 11.2 kips/ft width ($\gamma_{LL} = 1.35$)
Maximum bearing pad capacity = 4.6 kips/ft width ($\gamma_{TU,CR,SH} = 1.25$)

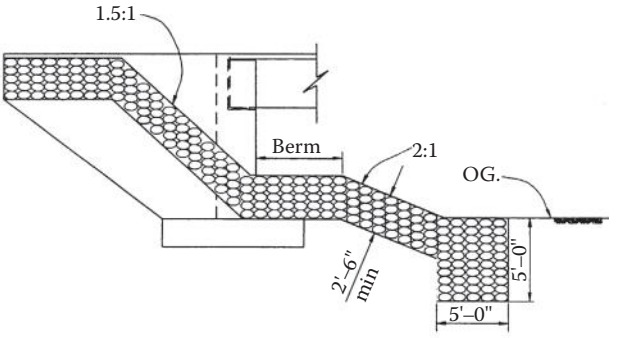

Rock slope protection

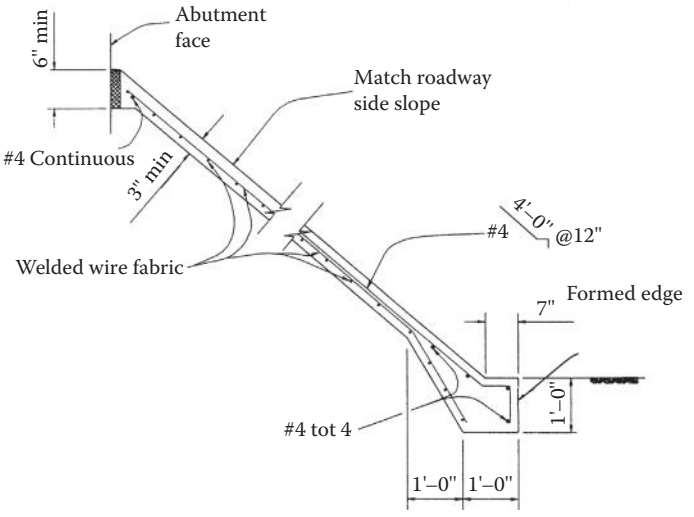

Concrete slope protection

FIGURE 6.11 Typical abutment slope protections.

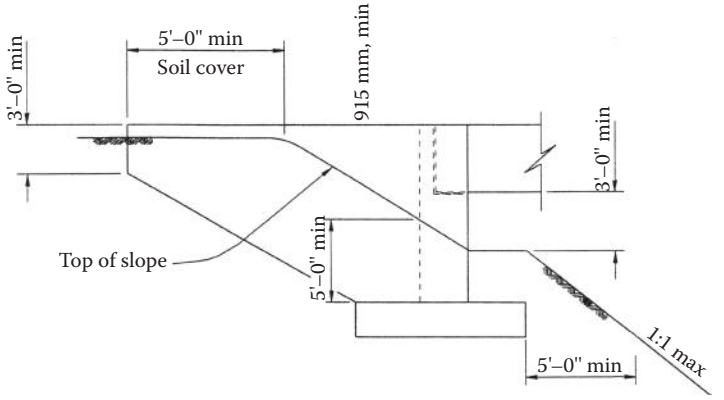

FIGURE 6.12 Abutment design miscellaneous details.

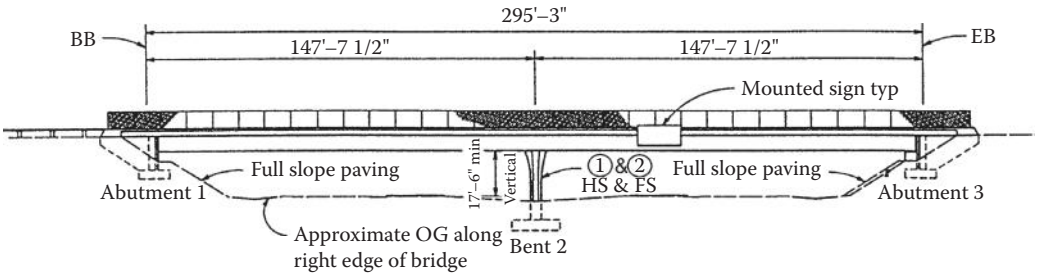

FIGURE 6.13 Bridge elevation (example).

Longitudinal seismic load
Transverse seismic load = 1241 kips
Bridge temperature displacement = 2.0 in
Maximum bridge seismic displacement = 6.5 in (with abutment releases)
Geotechnical information
Live load surcharge = 2 ft
Unit weight of backfill soil = 120 pcf
Nominal bearing resistance = 6.0 ksf (with resistant factor of 0.5)
Soil lateral pressure coefficient (K_a) = 0.3
Friction coefficient = tan 33°
Soil liquefaction potential = very low
Ground acceleration = 0.3 g
Design criteria
AASHTO LRFD bridge design specifications, customary U.S. units, 2012.
Design assumptions

- The soil passive pressure at abutment toe is neglected
- One feet width of abutment is used in the design
- Reinforcement yield stress, f_y = 60,000 psi
- Concrete strength, f'_c = 4000 psi
- Abutment backwall allowed damages in design earthquake

6.6.2 Abutment Support Width Design

Applying Equation 6.4 with L = 295.25 ft, H = 21.3 ft, and S = 5°.

The support width will be $N_{A'}$ = 23.6 in. Add 3 in required temperature movement, the total required support width equals to 26.5 in. The required minimum support width for seismic case equals to the sum of bridge seismic displacement, bridge temperature displacement, and the reserved edge displacement (usually 4 in). In this example, this requirement equals to 14 in, not in control. Based on the 26.5 in minimum requirement, the design uses 30 in, OK. A preliminary abutment configuration is shown in Figure 6.14 based on the given information and calculated support width.

6.6.3 Abutment Stability Check

Figure 6.15 shows the abutment force diagram.
where

q_{sc} = Soil lateral pressure by live load surcharge (γ_{LS} = 1.75)
q_e = Soil lateral pressure (γ_{EH} = 1.5)
q_{eq} = Soil lateral pressure by seismic load (γ_{EQ} = 1.0)

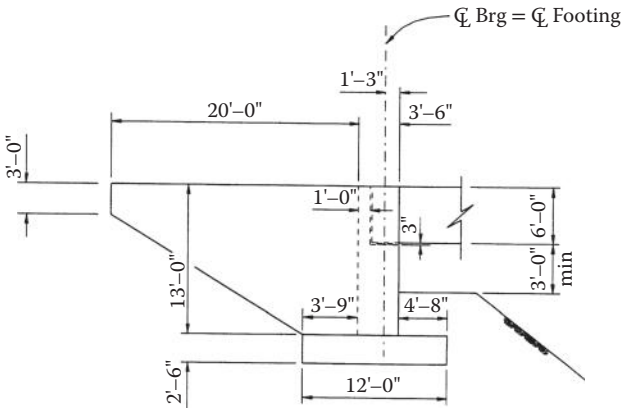

FIGURE 6.14 Abutment configuration (example).

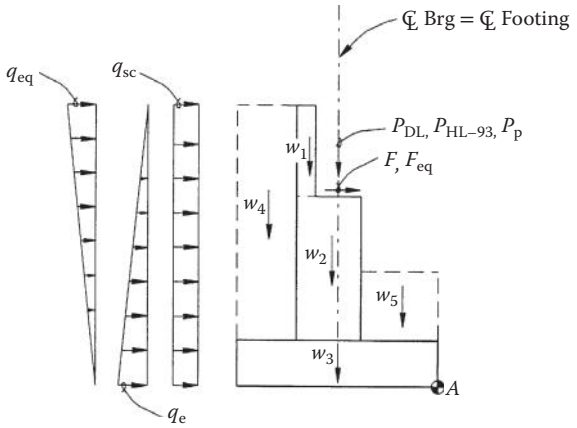

FIGURE 6.15 Abutment applied forces diagram (example).

P_{DL} = Superstructure dead load
P_{HL-93} = Normal vehicular truck load
P_p = Special truck load
F = Maximum bearing pad load with factor of 1.25
F_{eq} = Maximum bearing pad load with factor of 1.0
P_{ac} = Resultant of active seismic soil lateral pressure
h_{sc} = Height of live load surcharge = 2′–0″
ω = Unit weight of soil
W_i = Weight of abutment component and soil block
$q_{sc} = k_a \times \omega \times h_{sc} = 0.3 \times 0.12 \times 2 \times 1.75 = 0.126$ ksf/ft width
$q_e = k_a \times \omega \times H = 0.3 \times 0.12 \times 15.5 \times 1.5 = 0.84$ ksf/ft width
$q_{eq} = k_{ae} \times \omega \times H = 0.032 \times 0.12 \times 15.5 \times 1.0 = 0.06$ ksf/ft width

The calculated vertical loads, lateral loads, and moment about point *A* are listed in Table 6.3. The maximum and minimum soil pressure at abutment footing are calculated by

$$p = \frac{\sum V_i}{B}\left(1 \pm \frac{6e}{B}\right) \tag{6.5}$$

TABLE 6.3 Vertical Forces, Lateral Forces, and Moment about Point *A* (Example)

Load Description	Vertical Load (kip)	Lateral Load (kip)	Arm to *A* (ft)	Moment to *A* (kip-ft)
Backwall W_1	0.94	—	7.75	7.28
Stem W_2	3.54	—	6.00	23.01
Footing W_3	4.50	—	6.00	27.00
Backfill soil	5.85	—	10.13	59.23
Backfill soil	—	4.33	5.17	–22.34
Soil surcharge	—	1.16	7.75	–8.65
Front soil W_4	1.71	—	2.38	4.06
Keys	0.85	—	16.12	13.70
P_{DL}	0.17	—	6.00	1.04
P_{HS}	18.13	—	6.00	27.64
P_P	3.15	—	6.00	18.90
F	—	2.79	9.25	–25.80
F_{eq}	—	3.66	9.25	–33.90
Soil seismic load	—	0.47	9.30	–4.37

where p = Soil bearing pressure

V_i = Vertical force
B = Abutment footing width
e = Eccentricity of resultant of forces to center of footing
M_i = Moment to center of base

$$e = \frac{\sum M_i}{V_i} \tag{6.6}$$

Referring to Table 6.3 and Equations 6.5 and 6.6, the maximum and minimum soil pressures under footing corresponding to different load cases are calculated as follows:

Load case	p_{max} (ksi)	p_{min} (ksi)	Nominal Bearing Resistance (ksi)	Evaluate
Strength I	5.72	3.46	6.00	OK
Strength II	5.98	2.10	6.00	OK
Extreme Event	4.97	1.35	6.00	OK

Check for the stability resisting the overturning (load case Strength I, III, and Extreme Event):

Load Case	Eccentricity of resultant from center (ft)	¼ of the base width from center (ft)	Evaluation
Strength I	1.02	3.0	OK
Strength III	0.96	3.0	OK
Extreme Event	1.13	3.0	OK

Check for the stability resisting the sliding (load case Strength I, III and Extreme Event):

Load Case	Factored Driving Force (kips)	Factored Nominal Resistance (kips)	Evaluation
Strength I	12.77	20.98	OK
Strength III	12.77	22.41	OK
Extreme Event	12.30	21.55	OK

Resistance Factor of 0.8 applied for Strength I and III cases. Resistance Factor of 1.0 for Extreme Event limit state.

6.6.4 Abutment Backwall and Stem Design

Referring to AASHTO load combinations (AASHTO 2012), the maximum factored loads for abutment backwall and stem design are as follows:

Location	Load Cases	Factored V_u (kips)	Factored M_u (k-ft)
Backwall level	Strength I	1.95	4.87
	Strength III	1.95	4.87
	Extreme Event	2.25	5.89
Bottom of stem	Strength I	11.26	63.47
	Strength III	11.26	63.47
	Extreme Event	11.70	67.09
Footing Bot	All cases	19.40	61.16
Footing Top	All cases	10.07	22.40

- Footing was modeled as a cantilever supported at stem.
- Maximum bearing combination was applied to design footing bottom reinforcing.

6.6.5 Abutment Backwall Design

Try #5 @ 12 with 2 in clearance on both faces

$$d = 9.7 \text{ in}; \beta_1 = 0.85$$

$$A_s f_y = (0.31)(60) = 18.6 \text{ kips}; A_s' f_y' = 0$$

$$\beta_1 = 0.85; b_w = 12.0 \text{ in}$$

$$c = \frac{A_s f_s - A_s' f_s'}{0.85 f_c' \beta_1 b_w} = \frac{18.6}{(0.85)(4.0)(0.85)(12)} = 0.54 \text{ in}$$

$$a = \beta_1 c = (0.85)(0.54) = 0.46 \text{ in}$$

$$M_r = \phi M_n = \phi\left[A_s f_y\left(d_s - \frac{a}{2}\right) - A_s' f_s\left(d_s' - \frac{a}{2}\right)\right]$$

$$0.9\left[(18.6)\left(9.7 - \frac{0.46}{2}\right)\right]/12 = 13.2 \text{ kip-ft}$$

Check for shear, simplified procedure was utilized with $\beta = 2.0$, hence

$$V_r = \phi V_n = (0.9)\left(V_c + V_s + V_p\right)$$

$$V_c = 0.0316\beta\sqrt{f_c'} b_v d_c = (0.0316)(2.0)\sqrt{4}(12)(9.7 - 2.4) = 11.07 \text{ kip}$$

$$0.5\phi V_c = (0.5)(0.9)(11.07) = 4.98 \text{ kips}$$

Since

$$1.33M_u = (1.33)(5.98) = 7.89 \text{ kips-ft} < M_r = 11.07 \text{ kips-ft}, M_{cr} \text{ does not control.}$$

and

$$0.5\phi V_c = 4.98 \text{ kips} > 2.25 \text{ kips}, \text{ no shear reinforcement needed.}$$

6.6.6 Abutment Stem Design

Abutment stem could be design based on the applying moment variations along the abutment wall height. Here only the section at the bottom of stem is designed. Try using #7 @ 12 in at the back face of the stem and applying the same procedure as for abutment backwall, the results are as follows:

Max. Factored Load		Resistance Capacity		Evaluation	
M_u (*k*-ft)	V_u (kips)	M_r (*k*-ft)	V_r (kips)	Moment	Shear
67.09	11.7	104	55.0	OK	OK

At the front face of stem, using # 5 @ 12 in. in both longitudinal and horizontal direction, it meets the crack control requirements of the AASHTO specifications.

6.6.7 Abutment Footing Design

Footing will be modeled as a cantilever structure component supported at abutment stem. For the design of footing bottom reinforcing, the controlling factored maximum and minimum soil bearing pressures under the abutment footing are shown in Figure 6.16.

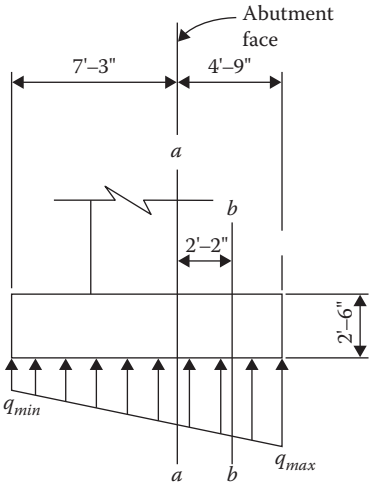

FIGURE 6.16 Bearing pressure under abutment footing (example).

The maximum factored demand moment, in all load cases, at Section a-a (design for top flexural reinforcement):

$$q_{a-a} = 4.825 \text{ ksf/ft wide}$$

$$M_{a-a} = 61.163 \text{ k} - \text{ft/ft wide}$$

The maximum factored demand shear, in all load cases, at Section b-b (d = 30 – 3-1 = 26 in from Section a-a, design for shear reinforcement):

$$q_{b-b} = 5.23 \text{ ksf/ft wide}$$

$$V_{b-b} = 14.9 \text{ kips/ft wide}$$

For the design of footing top reinforcing, the design model is shown in Figure 6.17.

The maximum factored demand moment, in all load cases, at Section c-c (design for bottom flexural reinforcement):

$$q_{c-c} = 7.05 \text{ ksf/ft wide}$$

$$M_{c-c} = 49.57 \text{ k} - \text{ft/ft wide}$$

The maximum factored demand shear, in all load cases, at Section d-d (d = 30 – 3-1 = 26 in from Section a-a, design for shear reinforcement):

$$q_{d-d} = 7.05 \text{ ksf/ft wide}$$

$$V_{d-d} = 11.14 \text{ kips/ft wide}$$

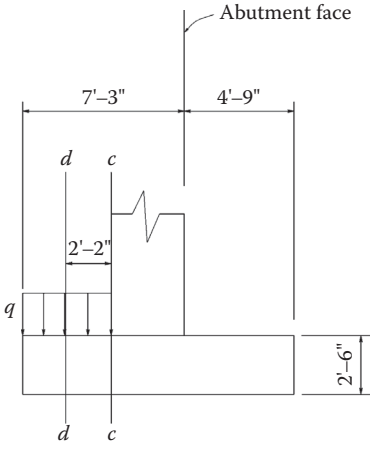

FIGURE 6.17 Footing top analysis model (example).

Try using #8 @ 12, with 3 in clearance at footing bottom, and # 6 @ 12, with 3 in clearance at footing top. Following the same procedure as for abutment back wall, the factored footing resistance and evaluation results are shown as follows:

Location	Max. Factored Load		Resistance Capacity		Evaluation	
	M_u (k-ft)	V_u (kips)	M_r (k-ft)	V_r (kips)	Moment	Shear
Footing Top	61.16	14.90	90.00	15.97	OK	OK
Footing Bot	49.57	11.14	70.52	15.97	OK	OK

Here

$$V_c = 0.0316\beta\sqrt{f_c'}b_v d_v = (0.0316)(2.0)\sqrt{4}(12)(30-6.5) = 35.64 \text{ kips}$$

Since

$$0.5\phi V_c = 15.97 \text{ kips} > 14.9 \text{ kips} \quad \text{No shear reinforcing needed.}$$

and $1.33M_u = 1.33 \times 61.16 = 81.34$ k-ft $< M_r = 90.0$ k-ft
$1.33M_u = 1.33 \times 49.57 = 65.92$ k-ft $< M_r = 7.052$ k-ft—M_{cr} does not control

6.6.8 Abutment Wingwall Design

The geometry of wingwall is
$h = 3.0$ ft; $S = 2.0$ ft;
$H = 13.0$ ft; $L = 18.25$ ft
Referring to Figure 6.15, the factored design load effects at the cantilever support are

$$V_u = \lambda_{EH}\left\{\frac{wL}{6}\left[H^2 + (h+H)(h+3S)\right]\right\}$$
$$= 1.35 \times \frac{0.36 \times 18.25}{6}\left[13^2 + (3+13)(3+3\times 2)\right] = 46.0 \text{ kips}$$

$$M_u = \lambda_{EH}\frac{wL^2}{24}\left[3h^2 + (H+4S)(H+2h)\right]$$
$$= 1.35 \times \frac{0.036 \times 18.25^2}{24}\left[3(3)^2 + (13+4+2)(12+2\times 3)\right] = 255.0 \text{ k}\cdot\text{ft}$$

Design flexural reinforcing. Try use # 8 @ 12 in at the inside face of the wingwall
Assume $f_s = f_y$

$$A_s f_s = A_s f_y = 13(0.79)(60) = 616.2 \text{ kips}$$

$$c = \frac{A_s f_y}{0.85\beta_1 f_c' b} = \frac{616.2}{(0.85)^2(4.0)(13)(12)} = 1.37 \text{ in} < 2.0 \text{ in (clearance)}$$

then in the section, using $\varepsilon_c = 0.003$, the strain in extreme tension steel $\varepsilon_t = 0.0178 > 0.005$. The section is tension-controlled, the assumption applied. Also there is no reinforcing in the compression zone. Then with $d = 12–2.0–0.5 = 9.5$ in and

$$a = \beta_1 c = (0.85)(1.37) = 1.165 \text{ in}$$

$$M_r = \phi M_n = \phi\left[A_s f_y\left(d_s - \frac{a}{2}\right)\right] = 0.9\left[(616.2)\left(9.5 - \frac{1.165}{2}\right)\right]/12 = 412.12 \text{ kip-ft}$$

Since $1.33 \times M_u = 1.33 \times 255 = 339.15$ k-ft $< M_r$ OK. No need to check M_{cr}.
Check for shear. Since

$$V_c = 0.0316\beta_1\sqrt{f'_c}b_v d_v = 0.0316(2)\sqrt{4}(12)\left(9.5 - \frac{1.165}{2}\right) = 175 \text{ kips}$$

and

$$0.5\phi V_c = 0.5(0.9)(175) = 78.75 \text{ kips} > V_u = 46.0 \text{ kips, no shear reinforcing needed.}$$

Since the wingwall allows to be broken off in a major earthquake, the adjacent columns of the bridge have to be designed to sustain the seismic loading with no wingwall resistant exist.

The abutment section, footing and wingwall reinforcing details are shown in Figure 6.18.

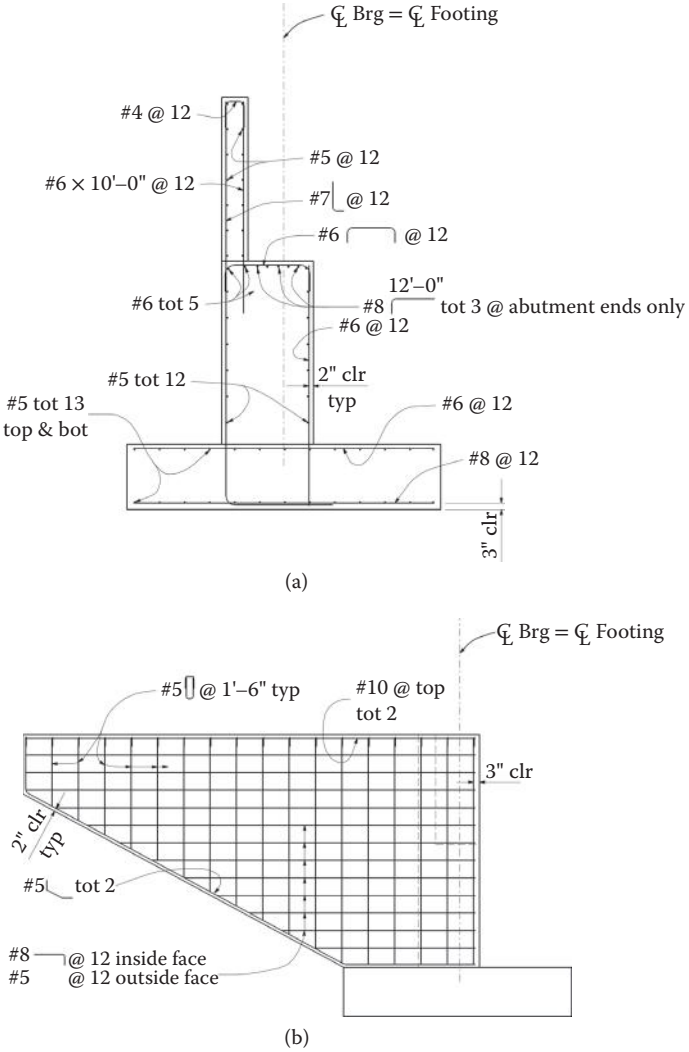

FIGURE 6.18 Abutment reinforcement details (example). (a) Abutment-typica section, (b) Wingwall reinforcement.

References

AASHTO. 2002. *Standard Specifications for Highway Bridges*, 17th ed., American Association of State Highway and Transportation Officials, Washington, DC.

AASHTO. 2012. *AASHTO LRFD Bridge Design Specifications,* Customary US Units, 2012, American Association of State Highway and Transportation Officials, Washington, DC.

Caltrans. 1996. *Bridge Memo to Designers 5-1 Abutments*, California Department of California Transportation, Sacramento, CA.

Caltrans. 2010. *Seismic Design Criteria*, Version 1.6, California Department of Transportation, Sacramento, CA.

Goel, R. K. 1997. Earthquake behavior of bridge with integral abutment, in *Proceeding of the National Seismic Conference on Bridges and Highway*s, July, Sacramento, CA.

Maroney, B. H. and Chai, Y. H. 1994. Bridge abutment stiffness and strength under earthquake loadings, in *Proceedings of the Second International Workshop of Seismic Design and Retrofitting of Reinforced Concrete Bridge*s, August, Queenstown, New Zealand.

Maroney, B. H., Griggs, M., Vanderbilt, E., et al. 1993. Experimental measurements of bridge abutment behavior, in *Proceeding of Second Annual Seismic Research Workshop, Division of Structures*, March, California Department of Transportation, Sacramento, CA.

Sorensen, E. C. 1997. Nonlinear soil-structure interaction analysis of a 2-span bridge on soft clay foundation, in *Proceeding of the National Seismic Conference on Bridges and Highways*, July, Sacramento, CA.

7

Ground Investigation

Thomas W. McNeilan
Fugro Atlantic

Kevin R. Smith
Fugro Atlantic

7.1 Introduction

The definition and understanding of the surface and subsurface "ground" conditions are among the most critical components of planning and developing cost models for and designs of bridges. Ground conditions affect the management of risk and uncertainty in three distinct ways, namely the following:

- Site and subsurface conditions and site variability
- Applicability of assumptions in design methods
- Quality of the constructed in ground foundations

Thus, the execution of a quality ground investigation is the fundamental "foundation" for the appropriate design and cost-effective construction of the bridge structures' foundations.

A complete geotechnical study of a site therefore should (1) determine the subsurface stratigraphy and stratigraphic relationships (and their variability), (2) define the physical properties of the earth materials, and (3) evaluate the data generated and formulate solutions to the project-specific and site-specific geotechnical issues. Geotechnical issues that can affect a project can be broadly grouped as follows:

- *Foundation issues*—Including the determination of the strength, stability, and deformations of the subsurface materials under the loads imposed by the structure foundations, in and beneath slopes and cuts, or surrounding the subsurface elements of the structure.
- *Earth pressure issues*—Including the loads and pressures imposed by the earth materials on foundations and against supporting structures, or loads and pressures created by seismic (or other) external forces.

- *Construction and constructability considerations*—Including the extent and characteristics of materials to be excavated, and the conditions that affect deep foundation installation or ground improvement.
- *Groundwater issues*—Including occurrence, hydrostatic pressures, seepage and flow, and erosion.

Site and subsurface characteristics directly affect the choice of foundation type, capacity of the foundation, foundation construction methods, and bridge cost. Subsurface and foundation conditions also frequently directly or indirectly affect the route alignment, bridge type selection, and/or foundation span lengths. Therefore, an appropriately scoped and executed foundation investigation and site characterization should include the following:

1. Provide the required data for the design of safe, reliable, and economic foundations.
2. Provide data for contractors to use to develop appropriate construction cost estimates.
3. Reduce the potential for a "changed condition" claim during construction.

In addition, the site investigation objectives frequently may be to provide the following:

1. Data for route selection and bridge type evaluation during planning and preliminary phase studies.
2. Data for as-built evaluation of foundation capacity, ground improvement, or other similar requirements.

For many projects, it is appropriate to conduct the geotechnical investigation in phases. For the first preliminary (or reconnaissance) phase, either a desktop study using only historical information or a desktop study and a limited field exploration program may be adequate. The results of the first phase study can then be used to develop a preliminary geologic model of the site, which is used to determine the key foundation design issues and plan the design-phase site investigation.

Bridge projects may require site investigations to be conducted on land, over water, and/or on marginal land at the water's edge. Similarly, site investigations for bridge projects can range from conventional, limited-scope investigations for simple overpasses and grade separations to major state-of-the-practice investigations for large bridges over major bodies of water.

This chapter includes discussions of the following:

- Field exploration techniques
- Definition of the requirements for and extent of the site investigation program
- Evaluation of the site investigation results and development/scoping of the laboratory testing program
- Data presentation and site characterization

The use of the site characterization results for foundation design is included in Chapters 8 through 10.

7.2 Field Exploration Techniques

For the purpose of the following discussion, we have divided field exploration techniques into the following groupings:

- Borings (including drilling, soil sampling, and rock-coring techniques)
- Downhole geophysical logging
- In situ testing including cone penetration test (CPT), T-bar and ball penetrometer soundings and vane shear, pressuremeter and dilatometer tests
- Test pits and trenches
- Geophysical survey techniques

7.2.1 Borings and Drilling Methods

Drilled soil (or rock) borings are the most commonly used subsurface exploration techniques. The drilled hole provides the opportunity to collect samples of the subsurface through the use of a variety of techniques and samplers. In addition to sample collection, drilling observations during the advancement of the borehole provide an important insight to the subsurface conditions. Unfortunately, this important opportunity for obtaining insight relative to the ground conditions is often underappreciated and underreported. Drilling methods can be used for land, over-water, and marginal land sites (Figure 7.1). It should be noted that the complexity introduced when working over water or on marginal land may require more sophisticated and specialized equipment and techniques and will significantly increase costs.

7.2.1.1 Wet (Mud) Rotary Borings

Wet rotary drilling is the most commonly used drilling method for the exploration of soil and rock, and also is used extensively for oil exploration and water well installation. It is generally the preferred method for (1) over-water borings; (2) where groundwater is shallow; and (3) where the subsurface includes soft, squeezing, or flowing soils.

With this technique, the borehole is advanced by rapid rotation of the drill bit that cuts, chips, and grinds the material at the bottom of the borehole. The cuttings are removed from the borehole by circulating water or drilling fluid down through the drill string to flush the cuttings up through the annular space of the drill hole. The fluids then flow into a settling pit or solids separator. Drilling fluid is typically bentonite (a highly refined clay) and water, or one of a number of synthetic products. The drilling fluids are used to flush the cuttings from the hole, compensate the fluid pressure, and stabilize borehole sidewalls. In broken or fractured rock, coarse gravel and cobbles, or other formations with voids, it may be necessary to case the borehole to prevent loss of circulation. Wet rotary drilling is conducive to

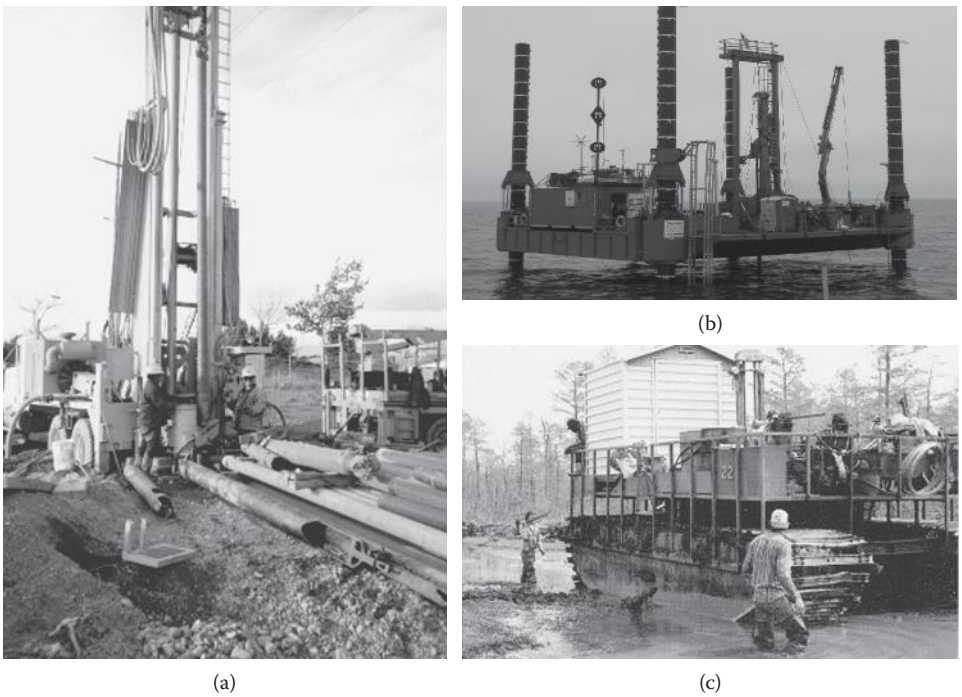

(a) (b) (c)

FIGURE 7.1 Drilling methods. (a) On land. (b) Over water. (c) On marginal land.

downhole geophysical testing, although the borehole must be thoroughly flushed before conducting some types of logging.

7.2.1.2 Air Rotary Borings

The air rotary drilling technology is similar to wet rotary except that the cuttings are removed with the circulation of high-pressure air rather than a fluid. Air rotary drilling techniques are typically used in hard bedrock or other conditions where drill hole stability is not an overriding issue. In very hard bedrock, a percussion hammer is often substituted for the bit. Air rotary drilling is conducive to downhole geophysical testing methods.

7.2.1.3 Bucket-Auger Borings

The rotary bucket is similar to a large (typically 18- to 24-in.) diameter posthole digger with a hinged bottom. The hole is advanced by rotating the bucket at the end of a kelly bar while pressing it into the soil. The bucket is removed from the hole to be emptied. Rotary-bucket-auger borings are used in alluvial soils and soft bedrock. This method is not always suitable in cobbly or rocky soils, but penetration of hard layers is sometimes possible with special coring buckets. Bucket-auger borings also may be unsuitable below the water table, although drilling fluids can be used to stabilize the borehole.

The rotary-bucket-auger drilling method allows an opportunity for continuous inspection and logging of the stratigraphic column of materials, by lowering the engineer or geologist on a platform attached to a drill rig winch. It is common in slope stability and fault hazards studies to downhole log 24-in.-diameter, rotary-bucket-auger boreholes advanced with this method.

7.2.1.4 Hollow-Stem-Auger Borings

The hollow-stem-auger drilling technique is frequently used for borings less than 20–30 m deep. The proliferation of the hollow-stem-auger technology in the 1980s occurred as the result of its use for contaminated soils and groundwater studies. The hollow-stem-auger consists of sections of steel pipe with welded helical flights. The shoe end of the pipe has a hollow bit assembly that is plugged while rotating and advancing the auger. That plug is removed for advancement of the sampling device ahead of the bit.

Hollow-stem auger-borings are used in alluvial soils and soft bedrock. This method is not always suitable where groundwater is shallow or in cobbly and rocky soils. When attempting to sample loose, saturated sands, the sands may flow into the hollow auger and produce misleading data. The hollow-stem-auger drill hole is not conducive to downhole geophysical testing methods.

7.2.1.5 Continuous-Flight-Auger Borings

Continuous-flight-auger borings are similar to the hollow-stem-auger drilling method except that the auger must be removed for sampling. With the auger removed, the borehole is unconfined and hole instability often results. Continuous flight auger drill holes are used for shallow exploration above the groundwater level.

7.2.1.6 Sonic Borings

Sonic drilling involves oscillation (vibration) of the drill casing into the subsurface without the use of water or air, although small quantities of water can be used to counter hydrostatic pressure. As the outer casing is advanced, an inner casing is used to recover a continuous sample of the subsurface materials. When the inner casing is recovered, the sample is typically transferred to a plastic sleeve. The sampling is repeated in increments as the outer casing

is advanced. The sampling process is generally faster than other drilling methods, and it can be possible to recover samples of difficult to sample materials such as layers with cobbles. This drilling technique recovers continuous, but disturbed samples, which are generally unsuitable for tests to determine engineering properties. Sonic drilling is a useful supplemental drilling and sampling technique for larger ground exploration programs. The continuous cores are helpful for visually defining and understanding the sequence of geologic layers, which otherwise must rely on drilling observations between sampling intervals or interpretations from in situ soundings.

7.2.2 Soil Sampling Methods

There are several widely used methods for recovering samples for visual classification and laboratory testing.

7.2.2.1 Driven Sampling

Driven sampling using Standard Penetration Test (SPT) or other size samplers is the most widely used sampling method. Although this sampling method recovers a disturbed sample, the "blow count" measured with this type of procedure provides a useful index of soil density or strength.

The most commonly used blow count is the SPT blow count (also referred to as *N*-value). Although the *N*-value is an approximate and imprecise measurement (its value is affected by many operating factors that are part of the sampling process, as well as the presence of gravel or cementation), various empirical relationships have been developed to relate *N*-value to engineering and performance properties of the soils. Caution is advised when applying empirical relationships based on *N*-values developed from land conditions to *N*-values obtained over water, since *N*-value measurements over water include variables not present on land (such as movement of the drilling platform or air gap) and the relationship between rod length and in situ stresses that are quite different between borings advanced over water than borings advanced on land.

7.2.2.2 Pushed Samples

A thin-wall tube (or in some cases, other types of samplers) can be pushed into the soil using hydraulic pressure from the drill rig, the weight of the drill rod, or a fixed piston. Pushed sampling generally recovers samples that are less disturbed than those recovered using driven sampling techniques. Thus, laboratory tests to determine strength and volume change characteristics preferably should be conducted on pushed samples rather than driven samples. Pushed sampling is the preferred sampling method in clay soils. Thin-wall samples recovered using push sampling techniques can either be extruded in the field or sealed in the tubes.

7.2.2.3 Drilled or Cored Samplers

Drilled-in samplers also have application in some types of subsurface conditions, such as hard soil and soft rock. With these types of samplers (e.g., Denison barrel and pitcher barrel), the sample barrel is either cored into the sediment or rock or is advanced inside the drill rod while the rod is advanced.

7.2.2.4 Geobor Coring

The Geobor-S system is an underused coring system that can provide good quality samples of various types of stratigraphic deposits. The core barrel is wire-line deployed and recovered. Penetration rate, pull down pressure, rotation, and bit weight are monitored and recorded to allow the driller to adjust coring for optimal recovery of the sediment or weak rock being cored. This soil (and rock) coring system can provide surprisingly high quality cores of glacial tills and other hard soils, and also provides quality samples of dense sands (Figure 7.2).

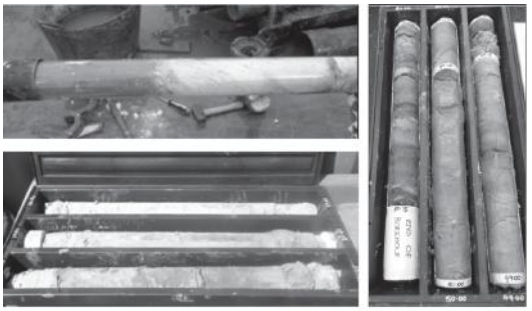

102-mm-diameter Geobore cores recovered in glacial till and soft rock.
Photo at top left shows contact between glacial till and chalk. Photo at right shows cores in soft sandstone

(a)

102-mm-diameter Geobor-S Cores recovered in dense sands in ~20 m water depth.
Top Photo shows 100% recovery (1.5 m of 1.5 m core run)
Bottom Photo shows 60% recovery (1.4 m of 2.3 m core run)

(b)

FIGURE 7.2 Soil cores collected using Geobor system. (a) Glacial till and soft rock. (b) Dense marine sands.

7.2.3 Rock Coring

The two rock coring systems most commonly used for engineering applications are the conventional core barrel and wireline (retrievable) system. At shallow depths above the water table, coring also sometimes can be performed with an air or a mist system.

Conventional core barrels consist of an inner and outer barrel with a bit assembly. To obtain a core at a discrete interval: (1) the borehole is advanced to the top of the desired interval, (2) the drill pipe is removed, (3) the core barrel/bit is placed on the bottom of the pipe, and (4) the assembly is run back to the desired depth. The selected interval is cored and the core barrel is removed to retrieve the core. Conventional systems typically are most effective at shallow depths or in cases where only discrete samples are required.

In contrast, wireline coring systems allow for continuous core retrieval without removal of the drill pipe/bit assembly. The wireline system has a retrievable inner core barrel that can be pulled to the surface on a wireline after each core run.

Variables in the coring process include the core bit type, fluid system, and drilling parameters. Drilling parameters include the revolutions per minute (RPM) and weight on bit (WOB). Typically, low RPM and WOB are used to start the core run and then both values are increased.

There are numerous bit types and compositions that are applicable to specific types of rock; however, commercial diamond or diamond-impregnated bits are usually the preferred bit from a core recovery and quality standpoint. Tungsten carbide core bits can sometimes be used in weak rock or in high-clay-content rocks. A thin bentonite mud is the typical drilling fluid used for coring. Thick mud can clog the small bit ports and is typically avoided.

Rock engineering parameters include percent recovery, rock quality designation (RQD), coring rate, and rock strength. Percent recovery is a measure of the core recovery versus the cored length, whereas RQD is a measure of the intact core pieces longer than 4 in. versus the cored length. Both values typically increase as the rock mass becomes less weathered/fractured with depth; however, both values are highly dependent on the type of rock, amount of fracturing, and so on, as well as the experience of the driller.

Rock strength (which is typically measured using unconfined triaxial compression [TX] test per ASTM guidelines) is used to evaluate bearing capacity, excavatability, and so on.

7.2.4 In Situ Testing

There are a variety of techniques that use instrumented probes or testing devices to measure soil properties and conditions in the ground. In contrast to sampling that removes a sample from its in situ stress conditions, in situ testing is used to measure soil and rock properties in the ground at their existing state of stress. The various in situ tests can either be conducted in a borehole or as a continuous sounding from the ground surface. Except as noted, those techniques are not applicable to rock.

7.2.4.1 Cone Penetration Test Soundings

CPT soundings are one of the most versatile and widely used in situ tests. The standard CPT cone consists of a 1.4-in.-diameter cone with an apex angle of 60°, although other cone sizes are available for special applications (Figure 7.3a). The cone tip resistance beneath the 10 cm^2 cone tip and the friction along the 150 cm^2 friction sleeve are measured with strain gauges and recorded electronically at 1- or 2-cm intervals as the cone is advanced into the ground at a rate of about 2 cm/s. In addition to the tip and sleeve resistances, many cones also are instrumented to record pore water pressure or other parameters as the cone is advanced.

Because CPT soundings provide continuous records of tip and sleeve resistances (and frequently pore pressure) versus depth (Figure 7.4), they provide a continuous indicator of soil and subsurface conditions, which is useful in defining soil stratification. Numerous correlations between the CPT measurements have been developed to define soil type and soil classification. In addition, empirical correlations have been published to relate the cone tip and sleeve friction resistances to engineering behavior, including undrained shear strength of clay soils and relative density and friction of granular soils.

Most land CPTs are performed as continuous soundings using large 20-ton cone trucks (Figure 7.5a), although smaller, more portable track-mounted equipment is also available. CPT soundings are commonly extended down to more than 20–50 m. CPT soundings also can be performed over water from a vessel using specialized equipment (Figure 7.5b) deployed by a crane or from a stern A-frame. In addition, downhole systems have been developed to conduct CPTs in boreholes during offshore site investigations. With a downhole system, CPT tests are interspersed with soil sampling to obtain CPT data to more than 100 m in depth.

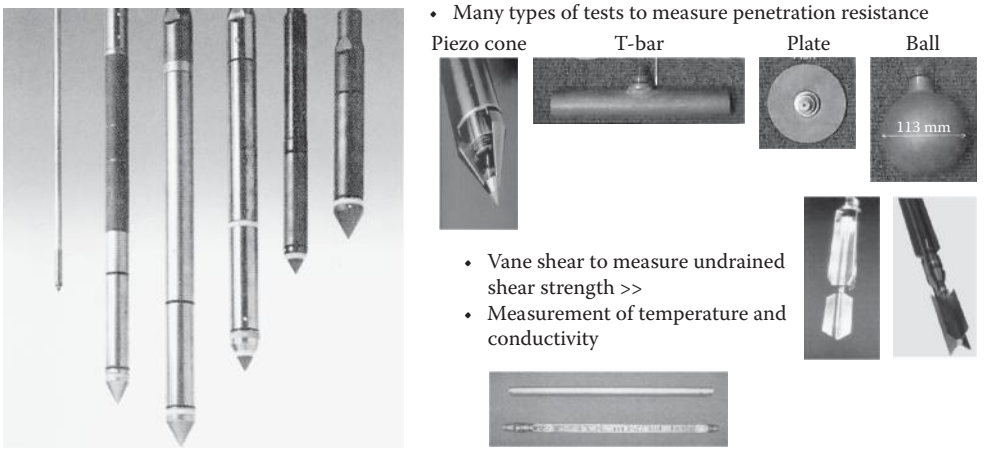

FIGURE 7.3 In situ test devices. (a) CPT cones. (b) Other penetrometers and test devices.

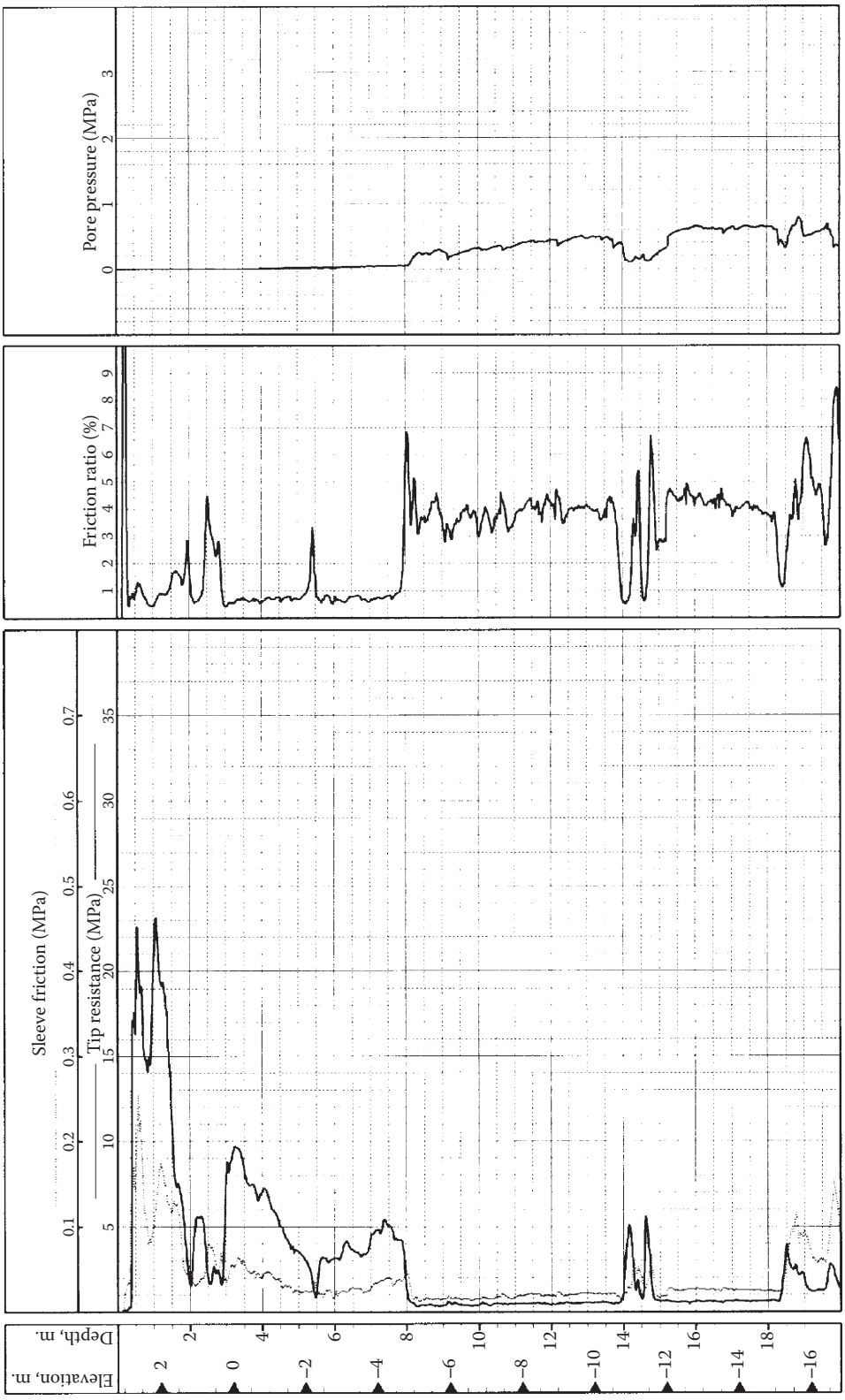

FIGURE 7.4 CPT data provides a continuous record of in situ conditions.

(a) (b)

FIGURE 7.5 CPT sounding methods. (a) On land. (b) Over water.

7.2.4.2 Full Flow Penetrometers (T-bar and Ball Soundings)

Full flow penetrometers include T-bars and ball penetrometers (Figure 7.3b). They were originally developed to conduct soundings in very soft marine sediments. Full flow penetrometers differ from a CPT in that (1) the soil being penetrated as a T-bar or ball penetrometer is advanced flows around the penetrometer; whereas the soil is pushed to the side as a CPT penetrates, (2) conversion from resistance to shear strength for full flow penetration does not require corrections for pore water pressure and overburden stresses, as are required for CPT; this reduces the theoretical range of bearing capacity factor used for that conversion, (3) T-bars and ball penetrometers are larger than a CPT, and therefore the precision of the measured resistances in soft materials is less susceptible to sensor calibration or zero drift of the sensor, (4) resistances can also be measured when withdrawing the T-bar or ball penetrometer, and (5) cyclic measurements to define strength degradation also can be obtained during penetrometer withdrawal (Figure 7.6). T-bars and ball soundings therefore are the preferred method to determine the undrained shear strength profile in very soft to soft cohesive deposits. T-bars (and to a lesser extent balls), however, cannot be advanced through layers or seams of granular sediments or more resistant materials.

7.2.4.3 In Situ Vane Shear Tests

The undrained shear strength of clay soils can be measured in situ using a vane shear test. This test is conducted by measuring the torque required to rotate a vane of known dimensions. The test can be conducted from the ground surface by attaching a vane blade onto a rod or downhole below the bottom of a borehole with a drop-in remote vane (Figure 7.7). The downhole vane is preferable, since the torque required to rotate the active rotating vane is not affected by the torque of the rod. The downhole vane is used both for land borings and over-water borings.

7.2.4.4 Pressuremeter and Dilatometer Tests

Pressuremeter testing is used to measure the in situ maximum and average shear modulus of the soil or rock by inflating the pressuremeter against the side walls of the borehole. The stresses, however, are measured in a horizontal direction, not in the vertical direction as would occur under most types of foundation loading. A test is performed by lowering the tool to the selected depth and expanding a flexible membrane through the use of hydraulic fluid. As the tool is inflated, the average displacement of the formation is measured with displacement sensors beneath the membrane, which is protected by stainless steel strips. A dilatometer is similar to a pressuremeter, except that the dilatometer consists of a flat plate that is pushed into the soil below the bottom of the borehole. A dilatometer is not applicable to hard soils or rock.

7.2.5 Downhole Geophysical Logging

Geophysical logs are run to acquire data about the formation or fluid penetrated by the borehole. Each log provides a continuous record of a measured value at a specific depth in the boring, and is therefore useful for interpolating stratigraphy between sample intervals. Most downhole geophysical logs are

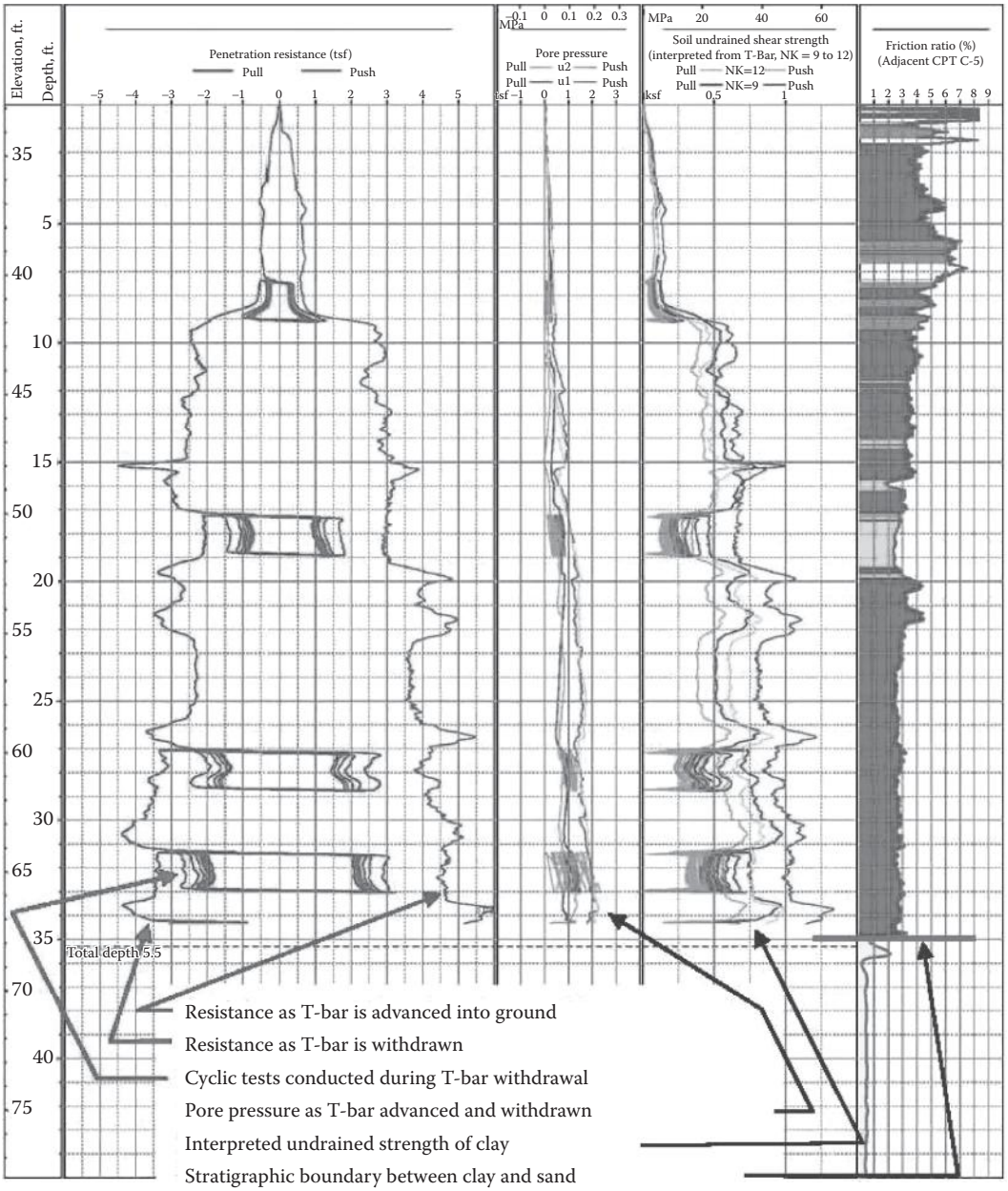

FIGURE 7.6 Full penetrometer T-bar data.

presented as curves on grid paper or as electronic files (Figure 7.8). Some of the more prevalent geophysical tools, used for geotechnical investigations, are described below.

- *Electrical logs (E-logs)* include resistivity, induction, and Spontaneous Potential (SP) logs. Resistivity and induction logs are used to determine lithology and fluid type. A resistivity log is used when the borehole is filled with a conductive fluid, while an induction log is used when the borehole is filled with a non- or low-conductivity fluid. Resistivity tools typically require an open, uncased, fluid-filled borehole. Clay formations and sands with higher salinity will have

FIGURE 7.7 In situ vane shear device.

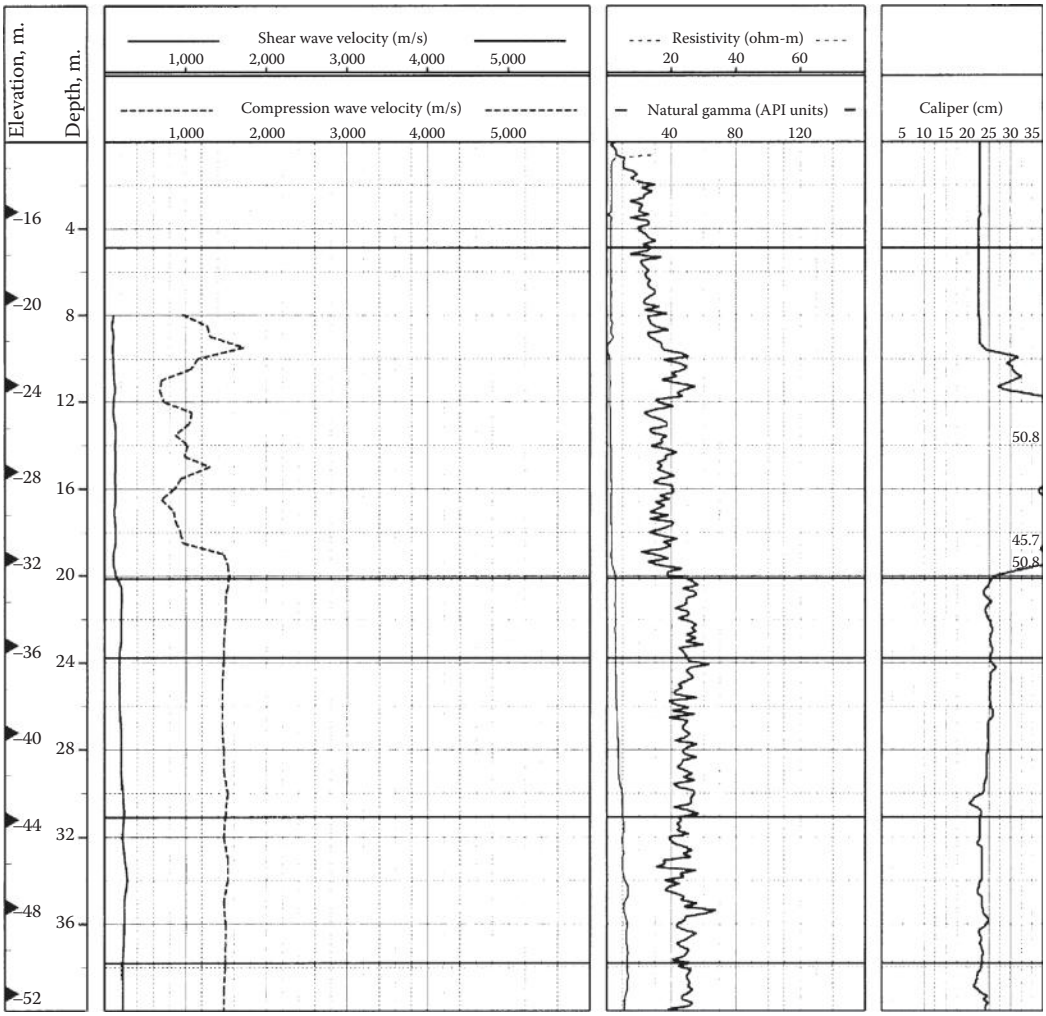

FIGURE 7.8 Example of downhole geophysical log.

low resistivity, while sands with freshwater will have higher resistivity values. Hard rock and dry formations have the highest resistivity values. An SP log is often used in suite with a resistivity or induction log to provide further information relative to formation permeability and lithology.

- *Suspension (velocity) logs* are used to measure the average primary, compression wave, and shear wave velocities of a 1-m-high segment of the soil and rock column surrounding the borehole. Those velocities are determined by measuring the elapsed time between arrivals of a wave propagating upward through the soil/rock column. The suspension probe includes both a shear wave source and compression wave source, and two biaxial receivers that detect the source waves. This technique requires an open, fluid-filled hole.
- *Natural gamma logs* measure the natural radioactive decay occurring in the formation to infer soil or rock lithology. In general, clay soils will exhibit higher gamma counts than granular soils, although decomposed granitic sands are an exception to that generality. Gamma logs can be run in any salinity fluid as well as air, and also can be run in cased boreholes.
- *Caliper logs* are used to measure the diameter of a borehole to provide insight relative to caving and swelling. An accurate determination of borehole diameter also is important for the interpretation of other downhole logs.
- *Acoustic televiewer and digital borehole logs* are conducted in rock to image the rock surface within the borehole (Figure 7.9). These logs use sound in an uncased borehole to create an oriented image of the borehole surface. These logs are useful for determining rock layering, bedding, and fracture identification and orientation.
- *Crosshole, downhole, and uphole shear wave velocity measurements* are used to determine the primary and shear wave velocities so as to either determine the elastic soil properties of soil and rock or calibrate seismic survey measurements. With the crosshole technique, the travel time is measured between a source in one borehole and a receiver in a second borehole. This technique can be used to directly measure the velocities of various strata. For downhole and uphole logs, the travel time is measured between the ground surface and a downhole source or receiver. Tests are conducted with the downhole source or receiver at different depths. These measurements should preferably be conducted in cased boreholes.

7.2.6 Test Pits and Trenches

Where near-surface conditions are variable or problematic, the results of borings and in situ testing can be supplemented by backhoe-excavated or hand-excavated test pits or trenches. These techniques are particularly suitable for purposes such as (1) collecting hand-cut, block samples of sensitive soils; (2) evaluating the variability of heterogeneous soils; (3) evaluating the extent of fill or rubble, (4) determining depth to groundwater, and (5) the investigation of faulting.

7.2.7 Geophysical Survey Techniques

Noninvasive geophysical survey techniques are available for remote sensing of the subsurface. In contrast to drilling and in situ testing methods, the geophysical survey methods explore large areas rapidly and economically. When integrated with boring data, these methods often are useful for extrapolating conditions between borings (Figure 7.10). When geophysical surveys are conducted in advance of the drilling program, it can help guide and optimize exploration locations and depths. Techniques are applicable either on land or below water. Some of the land techniques also are applicable for marginal land or in the shallow marine transition zone. Geophysical survey techniques can be used individually or as a group.

Advances in system design and increased data processing capabilities is continually improving data quality. Thus, the choice of systems should carefully consider the objectives of the data collection as well as opportunities of technological advances. Together those parameters should be the basis of program

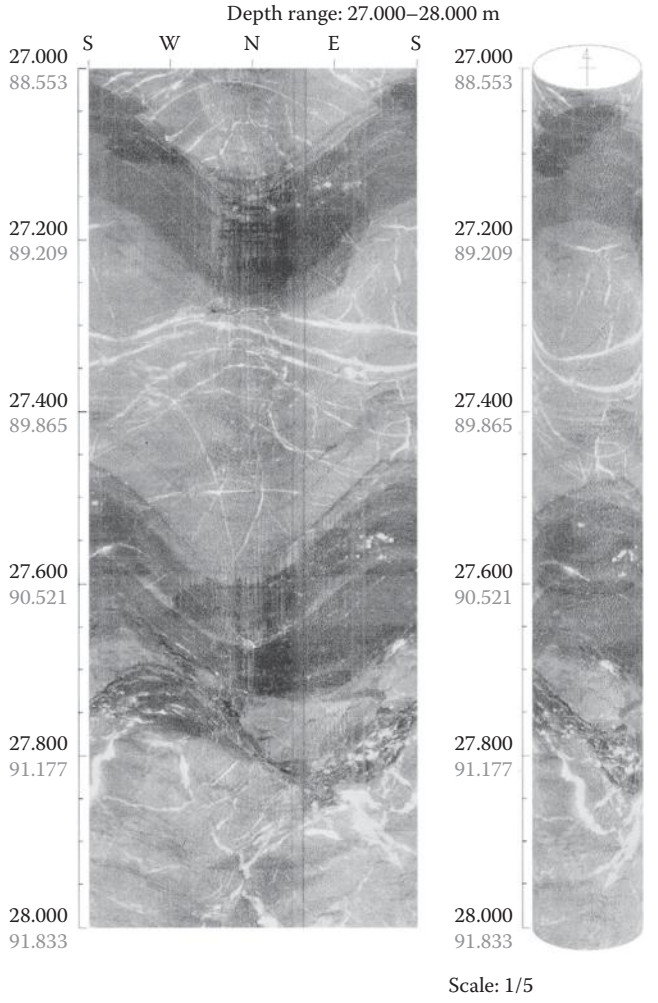

FIGURE 7.9 Example of digital borehole image in rock.

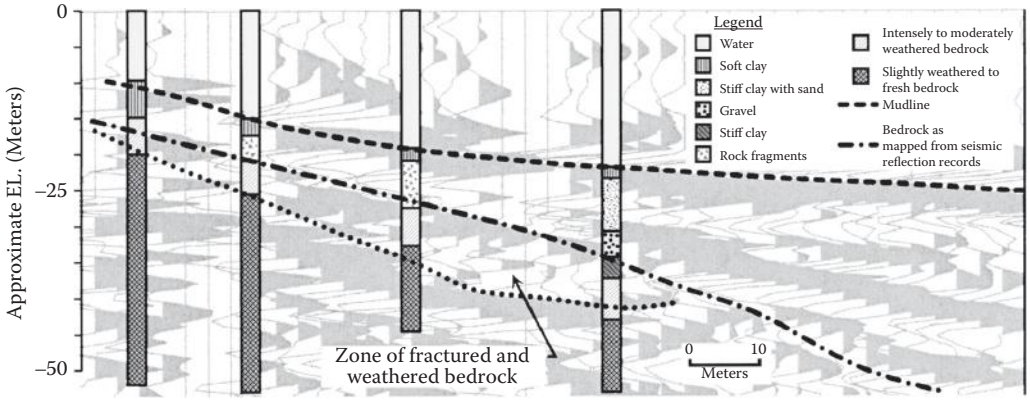

FIGURE 7.10 Example integration of seismic reflection and boring data.

definition and scope. Selection of methods and systems based on price alone often (usually) results in lost opportunity to enhance and improve the definition of ground conditions. Figure 7.11 shows an example of swath, hydrographic data collected in the mid-2000s with hydrographic data using a newer state of the practice multibeam system at the same location in 2012.

7.2.7.1 Hydrographic Surveys

Hydrographic surveys provide bathymetric contour maps and/or profiles of the seafloor, lake bed, or river bottom. Water depth measurements are usually made using a high-frequency sonic pulse from a depth sounder transducer mounted on a survey vessel. The choice of depth sounder system (single-beam, swath, and multibeam) is dependent upon water depths, survey site conditions, and project accuracy and coverage requirements.

The use and application of more sophisticated multibeam systems (Figure 7.12) has increased dramatically within the last few years. When using appropriate data collection, data quality assurance and control (QA/QC) and data processing techniques, it is now possible to identify and document river-bottom and seafloor debris as well as geomorphological features and changes in those features from survey to survey. Such imaging is particularly important in areas where bridge foundations may induce and must be design for river-bottom or seafloor scour.

7.2.7.2 Side Scan Sonar

Side scan sonar is used to locate and identify man-made objects (shipwrecks, pipelines, cables, debris, etc.) on the seafloor and determine sediment and rock characteristics of the seafloor. The side scan sonar provides a sonogram of the seafloor that appears similar to a continuous photographic strip (Figure 7.13). A mosaic of the seafloor can be provided by overlapping the coverage of adjacent survey lines.

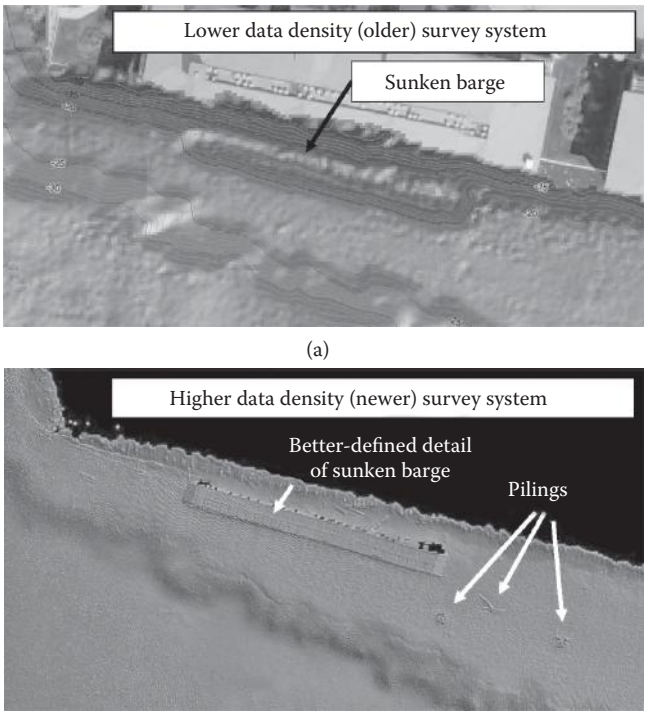

FIGURE 7.11 Comparison of multi-beam hydrographic data using (a) older (2005 vintage) swath system and (b) current, state-of-practice multibeam system.

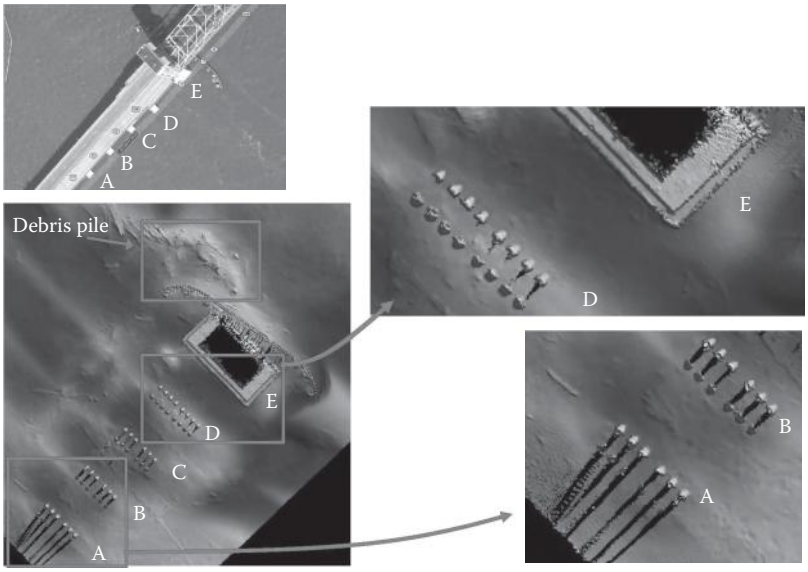

FIGURE 7.12 Multibeam image of river channel bathymetry.

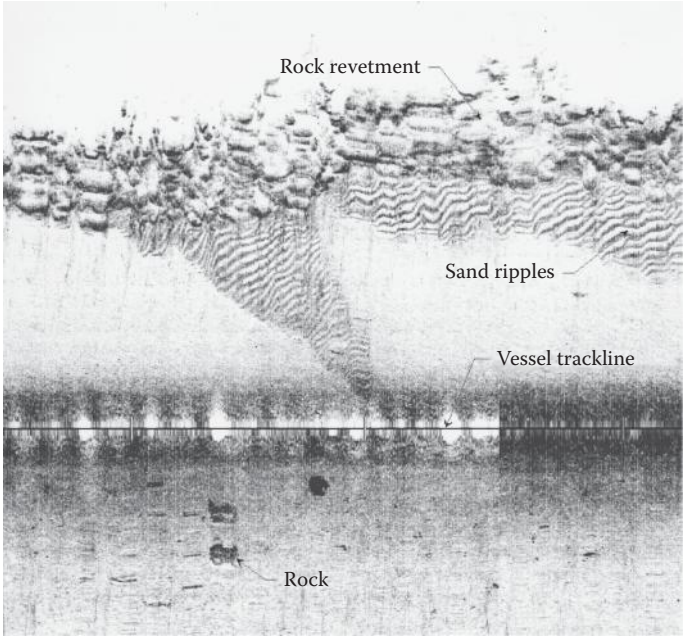

FIGURE 7.13 Side-scan sonar image of river bottom and rock-protected river side-slope.

7.2.7.3 Magnetometer

A magnetometer measures variations in the earth's magnetic field strength that result from metallic objects (surface or buried), variations in sediment and rock mineral content, and natural (diurnal) variations. Data are used to locate and identify buried objects for cultural, environmental, and archaeological site clearances.

7.2.7.4 High-Resolution Seismic Reflection and Subbottom Profilers

Seismic images of the subsurface beneath the seafloor can be developed by inducing sonic waves into the water column from a transducer, vibrating boomer plate, sparker, or small air or gas gun. Reflections of the sonic energy from the mudline and subsurface soils horizons are recorded to provide an image of the subsurface geologic structure and stratigraphy along the path of the survey vessel. The effective depth of a system and resolution of subsurface horizons depend on a number of variables, including the system energy, output frequency spectrum, the nature of the seafloor, and the subsea sediments and rocks. Seismic reflection data are commonly used to determine the geologic structure (stratigraphy, depth to bedrock, folds, faults, subsea landslides, gas in sediments, seafloor seeps, etc.) and evaluate the horizon continuity between borings (Figure 7.14).

There are fundamental differences between the frequency content and repeatability of energy induced by (1) mechanical, boomer systems; (2) electrical, sparker systems; and (3) air gun systems. Those differences

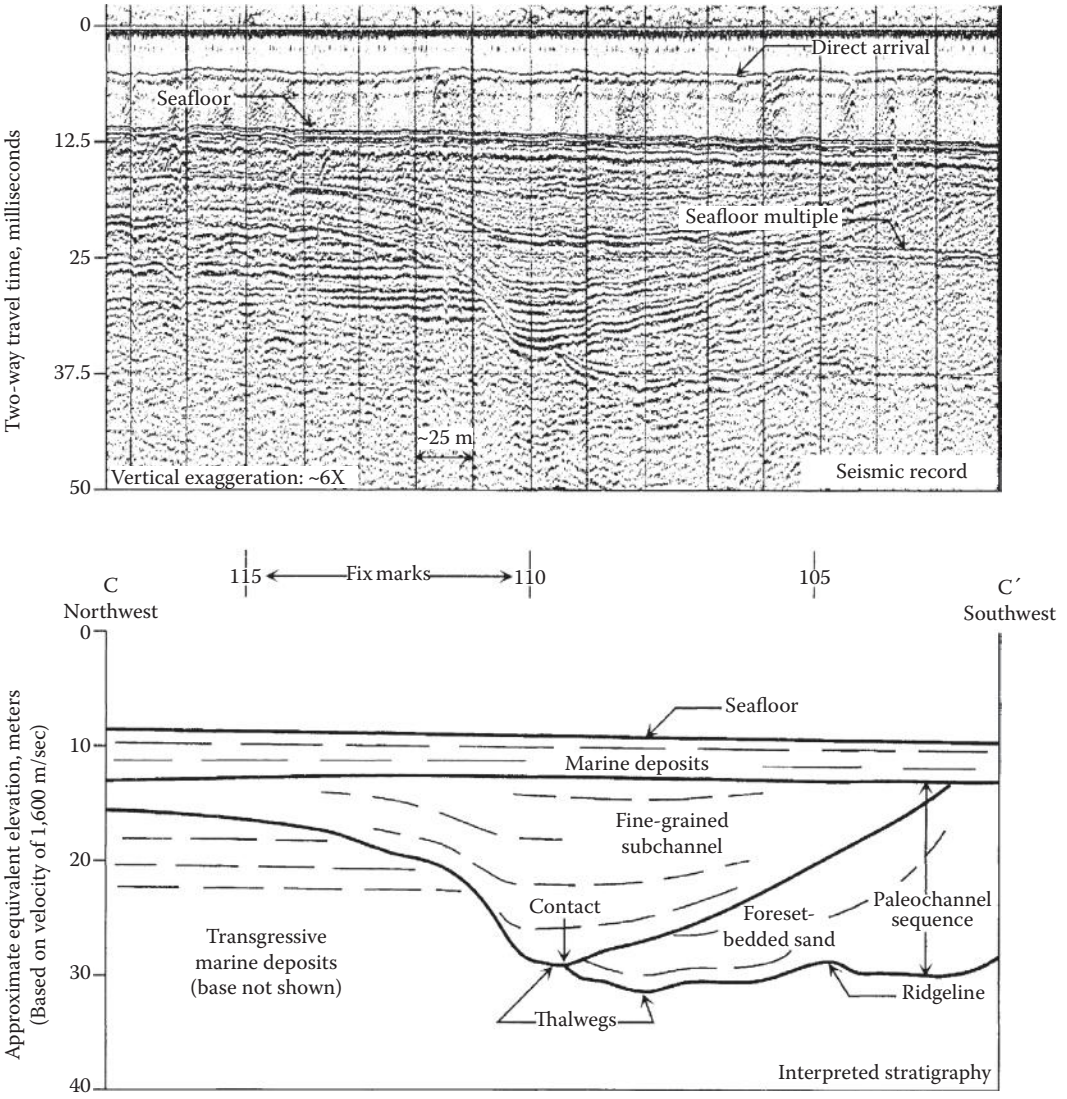

FIGURE 7.14 Interpreted stratigraphic relationships from seismic reflection data.

together with the source energy, firing rate, and recording systems provide opportunities to tailor data collection methods and systems for a specific project. Recent advances in the use of multichannel, hydrophone arrays enhance the opportunities to collect and process data to levels not possible a decade ago. When project objectives allow, it is important to engage professional staff, who have experience in collecting and processing data using modern systems, to review the project objectives (such as depth of imaging), expected subsurface conditions, water depth, and water column conditions (such as river flow, tides, currents) so as to advise and plan a meaningful scope of work using appropriate methods and equipment.

7.2.7.5 Seismic Refraction

Seismic refraction measurements are commonly used on land to estimate depth to bedrock and groundwater, and detect bedrock faulting. Measured velocities also are used for estimates of rippability and excavation characteristics. In the refraction technique, sonic energy is induced into the ground and energy refracted from subsurface soil and rock horizons is identified at a series of receivers laid out on the ground. The time–distance curves from a series of profiles are inverted to determine depths to various subsurface layers and the velocity of the layers. The data interpretation can be compromised where soft layers underlie hard layers and where the horizons are too thin to be detected by refraction arrivals at the surface. The technique also can be used in shallow water (surf zones, lakes, ponds, and river crossings) using bottom (bay) cables.

7.2.7.6 Ground Penetrating Radar Systems

Ground penetrating radar (GPR) systems measure the electromagnetic properties of the subsurface to locate buried utilities or rebar, estimate pavement thickness, interpret shallow subsurface stratigraphy, locate voids, and delineate bedrock and landslide surfaces. GPR also can be used in arctic conditions to estimate ice thickness and locate permafrost. Depths of investigation are usually limited to 50 ft or less. Where the surface soils are highly conductive, the effective depth of investigation may be limited to a few feet.

7.2.7.7 Resistivity Surveys

Resistivity surveys induce currents into the ground to locate buried objects and investigate shallow groundwater. As electrodes are moved in specific patterns of separation, the resistivity is measured and inverted to produce depth sections and contour maps of subsurface resistivity values. This method is used to identify and map subsurface fluids, including groundwater, surface and buried chemical plumes, and predict corrosion potential.

7.2.8 Groundwater Measurement

Groundwater conditions have a profound effect on foundation design, construction, and performance. Thus, the measurement of groundwater depth (or depth of water when drilling over water) is one of the most fundamentally important elements of the site investigation. In addition to the measurement of the water level, the site investigation should consider and define the potential for artesian or perched groundwater. It is also important to recognize that groundwater levels may change with season, rainfall, or other temporal reasons. All groundwater and water depth measurements should document the time of measurement and, where practical, should determine variations in depth over some period of elapsed time. To determine the long-term changes in water level, it is necessary to install and monitor piezometers or monitoring wells.

7.3 Defining Site Investigation Requirements

Many factors should be considered when defining the requirements (including types, numbers, locations, and depths of explorations) for the site investigation (Figure 7.15). These factors include the following:

- Importance, uncertainty, or risk associated with bridge design, construction, and performance
- Geologic conditions and their potential variability

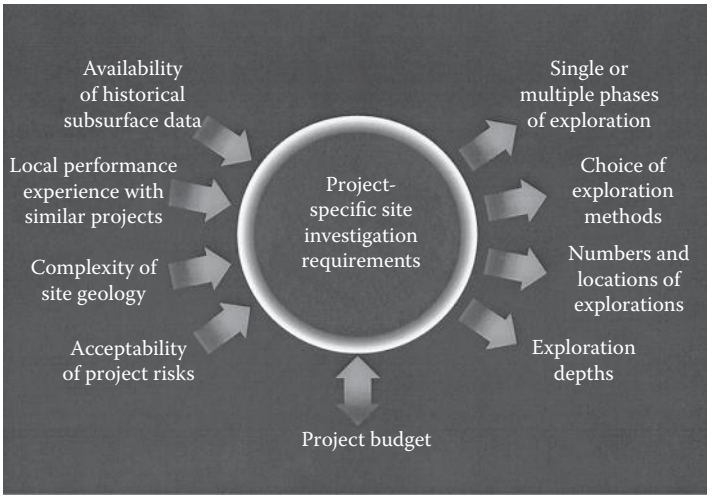

FIGURE 7.15 Key factors to consider when defining site investigation requirements.

- Availability (or unavailability) of historical subsurface data
- Availability (or unavailability) of performance observations from similar nearby projects
- Investigation budget

The following factors should be considered when evaluating the project risk: (1) What are the risks? (2) How likely are the risks to be realized? and (3) What are the consequences if the risks occur? Risks include the following:

- Certainty or uncertainty of subsurface conditions
- Design risks (e.g., possibility that inadequate subsurface data will compromise design decisions or schedule)
- Construction risks (e.g., potential for changed conditions claims and construction delays)
- Performance risks (e.g., seismic performance)

Two additional requirements that should be considered when planning a subsurface investigation are (1) reliability of the data collected and (2) timeliness of the data generated. Unfortunately, these factors are too often ignored or underappreciated during the site investigation planning process or geotechnical consultant selection process. Because poor quality or misleading subsurface data can lead to inappropriate selection of foundation locations, foundation types, and/or inadequate or inappropriate foundation capacities, selection of a project geotechnical consultant should be based on qualifications rather than cost. Similarly, the value of the data generated from the subsurface investigation is reduced if adequate data are not available when the design decisions, which are affected by subsurface conditions, are made. All too often, the execution of the subsurface exploration program is delayed and major decisions relative to the general structure design and foundation locations have been cast in stone prior to the availability of the subsurface exploration results.

Frequently, the execution of the subsurface investigation is an iterative process that should be conducted in phases (i.e., desktop study, reconnaissance site investigation, detailed design-phase investigation). During each phase of site exploration, it is appropriate for data to be reviewed as they are generated so that appropriate modifications can be made as the investigation is ongoing. Appropriate adjustments in the investigation work scope can save significant expense, increase the quality and value of the investigation results, and/or reduce the potential for a remobilization of equipment to fill in missing information.

7.3.1 Choice of Exploration Methods and Consideration of Local Practice

Because many exploration techniques are suitable in some subsurface conditions, but not as suitable or economical in other conditions, the local practice for the methods of exploration vary from region to region. Therefore, the approach to the field exploration program should consider and be tailored to the local practice. Conversely, there are occasions where the requirements for a project may justify using exploration techniques that are not common in the project area. The need to use special techniques will increase with the size and complexity of the project and uniqueness or complexity of the site conditions.

7.3.2 Exploration Depths

The depths to which subsurface exploration should be extended will depend on the structure, its size and loading, and the subsurface conditions at the project location. The subsurface exploration for any project should extend down through unsuitable layers into materials that are competent relative to the design loads to be applied by the bridge foundations. Some of the exploration should be deep enough to verify that unsuitable materials do not exist beneath the bearing strata on which the foundations will be embedded. When the base of the foundation is underlain by layers of compressible material, the exploration should extend down through the compressible strata and into deeper strata whose compressibility will not influence foundation performance. Noninvasive geophysical survey data and previous ground exploration at the project site or in the project area should be used to anticipate the required depth of ground investigation appropriate for the project requirements and anticipated subsurface conditions.

For lightly loaded structures, it may be adequate to terminate the exploration when rock is encountered, provided that the regional geology indicates that unsuitable strata do not underlie the rock surface. For heavily loaded foundations or foundations bearing on rock, it is appropriate to verify that the explorations indeed have encountered rock and not a boulder. It is similarly appropriate to extend at least some of the explorations through the weathered rock into sound or fresh rock.

7.3.3 Numbers of Explorations

The basic intent of the site investigation is to determine the subsurface stratigraphy and its variations, and to define the representative soil (or rock) properties of the strata together with their lateral and vertical variations. The locations and spacing of explorations should be adequate to provide a reasonably accurate definition of the subsurface conditions, and should disclose the presence of any important irregularities in the subsurface conditions. Thus, the numbers of explorations will depend on both the project size and the geologic and depositional variability of the site location. When subsurface conditions are complex and variable, a greater number of more closely spaced explorations are warranted. Conversely, when subsurface conditions are relatively uniform, fewer and more widely spaced explorations may be adequate. Noninvasive geophysical survey data and previous ground exploration at the project site or in the project area should be used to anticipate the subsurface conditions and their variability so as to define the appropriate exploration types, numbers, and locations required to meet the project requirements.

7.3.4 The Risk of Inadequate Site Characterization

When developing a site exploration program, it is often tempting to minimize the number of explorations or defer the use of specialized techniques due to their expense. The approach of minimizing the investment in ground investigation and site characterization is fraught with risk. Costs saved by the execution of an inadequate site investigation, whether in terms of the numbers of explorations or the exclusion of applicable site investigation techniques, rarely reduce the project cost. Conversely, the cost saved by an inadequate investigation frequently increases the cost of construction by many times the savings achieved during the site investigation.

Experience with large bridge, coastal infrastructure/industry, and offshore energy projects has repeatedly shown that adequate, high-quality, and timely ground investigation data directly (1) reduces risk of the unexpected, (2) enhances definition of uncertainties, (3) leads to design optimization, and (4) lowers the costs of the installed foundations. There is an adage in the marine construction industry that "*every project pays for a quality ground investigation, whether one is conducted or not*." This implies that when quality ground investigations are not executed, the project will undoubtedly (1) suffer from poor assumptions relative to ground conditions, thereby leading to less-efficient foundation designs, (2) potentially include (unrecognized) over- or unconservative foundation concepts and designs, (3) include unnecessarily large contingencies for uncertainties, and/or (4) experience construction surprises and claims of changed conditions.

The costs of improper, inadequate, or incomplete ground investigations inevitably will be far greater than the costs of conducting quality ground investigations. Relatively small expenditures for high-quality and comprehensive data can lead to 10%–25%, or greater, savings in the installed cost of the foundations. Thus, a small extra investment in the ground investigation program can, and often does, lead to a significantly greater savings in installed foundation costs.

7.4 Development of Laboratory Testing Program

7.4.1 Purpose of Testing Program

The following laboratory tests are performed on samples to

- Classify soil samples.
- Evaluate basic index soil properties that are useful in evaluating the engineering properties of the soil samples.
- Measure the strength, compressibility, and hydraulic properties of the soils
- Evaluate the suitability of onsite or borrow soils for use as fill.
- Define dynamic parameters for site response and soil-structure interaction analyses during earthquakes.
- Identify unusual subsurface conditions (e.g., presence of corrosive conditions, carbonate soils, expansive soils, or potentially liquefiable soils).

The extent of laboratory testing is generally defined by the risks associated with the project.

Soil classification, index property, and fill suitability tests generally can be performed on disturbed samples, while tests to determine engineering properties of the soils should preferably be performed on relatively undisturbed, intact specimen. The quality of the data obtained from the latter series of tests is significantly dependent on the magnitude of sample disturbance either during sampling or during subsequent processing and transportation.

7.4.2 Types and Uses of Tests

7.4.2.1 Soil Classification and Index Testing

Soil classification and index properties tests are generally performed for even low-risk projects. Engineering parameters often can be estimated from the available in situ data and basic index tests using published correlations. Site-specific correlations of these basic values may allow the results of a few relatively expensive advanced tests to be extrapolated. Index tests and their uses include the following:

- Unit weight and water content tests to evaluate the natural unit weight and water content.
- Atterberg (liquid and plastic) limit tests on cohesive soils for classification and correlation studies. Significant insight relative to strength and compressibility properties can be inferred from the natural water content and Atterberg limit test results.

- Sieve and hydrometer tests to define the grain size distribution of coarse- and fine-grained soils, respectively. Grain size data also are used for both classification and correlation studies.

Other index tests include tests for specific gravity, maximum and minimum density, expansion index, and sand equivalent.

7.4.2.2 Shear Strength Tests

Most bridge design projects require characterization of the undrained shear strength of cohesive soils and the drained strength of cohesionless soils. Strength determinations are necessary to evaluate the bearing capacity of foundations and to estimate the loads imposed on earth-retaining structures.

Undrained shear strength of cohesive soils can be estimated (often in the field) with calibrated tools such as a torvane, pocket penetrometer, fall cone, or miniature vane shear device. More definitive strength measurements are obtained in a laboratory by subjecting samples to TX, direct simple shear (DSS), or torsional shear (TS) tests. Triaxial shear tests (including unconsolidated-undrained [UU] tests and consolidated-undrained [CU] tests) are the most common type of strength test. In this type of test, the sample is subject to stresses that mimic in situ states of stress prior to being tested to failure in compression or shear. Large and more high-risk projects often warrant the performance of CU or DSS tests where samples are tested along stress paths that model the in situ conditions. In contrast, only less sophisticated UU tests may be warranted for less-important projects.

Drained strength parameters of cohesionless soils are generally measured in either relatively simple direct shear (DS) tests or in more sophisticated consolidated-drained (CD) triaxial tests. In general, few laboratory strength tests are performed on in situ specimens of cohesionless soil due to the relative difficulty in obtaining undisturbed specimens.

7.4.2.3 Compaction Tests

Compaction tests are performed to evaluate the moisture-density relationship of potential fill material. Once the relationship has been evaluated and the minimum level of compaction of fill material to be used has been determined, strength tests may be performed on compacted specimens to evaluate design parameters for the project.

7.4.2.4 Subgrade Modulus

R-value and California Bearing Ratio (CBR) tests are performed to determine subgrade modulus and evaluate the pavement support characteristics of the in situ or fill soils.

7.4.2.5 Consolidation Tests

Consolidation tests are commonly performed to (1) evaluate the compressibility of soil samples for the calculation of foundation settlement; (2) investigate the stress history of the soils at the boring locations to calculate settlement as well as to select stress paths to perform most advanced strength tests; (3) evaluate elastic properties from measured bulk modulus values; and (4) evaluate the time rate of settlement. Consolidation test procedures also can be modified to evaluate if foundation soils are susceptible to collapse or expansion, and to measure expansion pressures under various levels of confinement. Consolidation tests include incremental consolidation tests (which are performed at a number of discrete loads) and constant rate of strain (CRS) tests where load levels are constantly increased or decreased. CRS tests can generally be performed relatively quickly and provide a continuous stress–strain curve, but require more sophisticated equipment.

7.4.2.6 Permeability Tests

In general, constant-head permeability tests are performed on relatively permeable cohesionless soils, while falling-head permeability tests are performed on relatively impermeable cohesive soils. Estimates of the permeability of cohesive soils also can be obtained from consolidation test data.

7.4.2.7 Dynamic Tests

A number of tests are possible to evaluate the behavior of soils under dynamic loads such as wave or earthquake loads. Dynamic tests generally are strength tests with the sample subjected to some sort of cyclic loading. Tests can be performed to evaluate variations of strength, modulus, and damping, with variations in rate and magnitude of cyclic stresses or strains. Small strain parameters for earthquake loading cases can be evaluated from resonant column tests.

For earthquake-loading conditions, dynamic test data are often used to evaluate site response and soil-structure interaction. Cyclic testing also can provide insight into the behavior of potentially liquefiable soils, especially those which are not easily evaluated by empirical in situ test-based procedures.

7.4.2.8 Corrosion Tests

Corrosion tests are performed to evaluate potential impacts on steel or concrete structures due to chemical attack. Tests to evaluate corrosion potential include: resistivity, pH, sulfate content, and chloride content.

7.5 Data Presentation and Site Characterization

7.5.1 Site Characterization Report

The site characterization report should contain a presentation of the site data, and an interpretation and analysis of the foundation conditions at the project site. The site characterization report should include the following:

- Present the factual data generated during the site investigation.
- Describe the procedures and equipment used to obtain the factual data.
- Describe the subsurface stratigraphic relationships at the project site.
- Define the soil and rock properties that are relevant to the planning, design, construction, and performance of the project structures.
- Formulate the solutions to the design and construction of the project.

The site data presented in the site characterization report may be developed from the current and/or past field investigations at or near the project site, as-built documents, maintenance records, and construction notes. When historic data are included or summarized, the original sources of the data should be cited.

7.5.2 Factual Data Presentation

The project report should include the accurate and appropriate documentation of the factual data collected and generated during the site investigation and testing program(s). The presentation and organization of the factual data, by necessity, will depend upon the size and complexity of the project and the types and extent of the subsurface data. Regardless of the project size or extent of exploration, all reports should include an accurate plan of exploration that includes appropriate graphical portrayal of surface features and ground surface elevation in the project area.

The boring log (Figure 7.16) is one of the most fundamental components of the data documentation. Although many styles of presentation are used, there are several basic elements that generally should be included on a boring log. Those typical components include the following:

- Documentation of location and ground surface elevation
- Documentation of sampling and coring depths, types, and lengths (e.g., sample type, blow count [for driven samples], and sample length for soil samples; core run, recovery, and Rock Quality Designation (RQD) for rock cores) as well as in situ test depths and lengths
- Depths and elevations of groundwater and/or seepage encountered

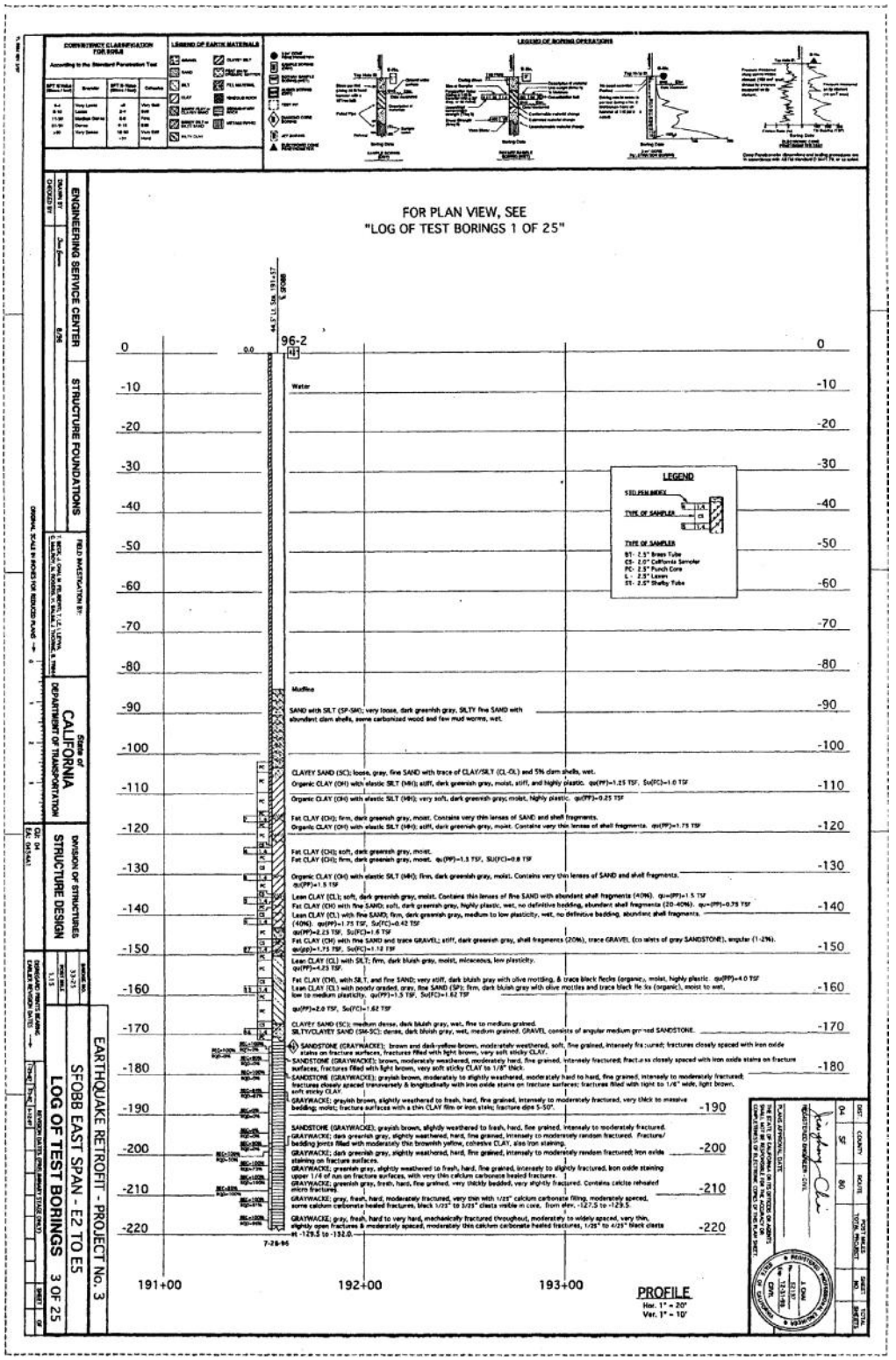

FIGURE 7.16 Typical log of test boring sheet for Caltrans project.

- Graphical representation of soil and rock lithology
- Description of soil and rock types, characteristics, consistency/density, or hardness
- Tabular or graphical representation of test data

In addition to the boring logs, the factual data should include tabulated summaries of test types, depths, and results together with the appropriate graphical output of the tests conducted.

7.5.3 Description of Subsurface Conditions and Stratigraphy

A sound geologic interpretation of the exploration and testing data are required for any project to assess the subsurface conditions. The description of the subsurface conditions should provide the users of the report with an understanding of the conditions, their possible variability, and the significance of the conditions relative to the project. The information should be presented in a useful format and terminology appropriate for the users, who usually will include design engineers and contractors who are not earth science professionals.

To achieve those objectives, the site characterization report should include descriptions of (1) site topography and/or bathymetry, (2) site geology, (3) subsurface stratigraphy and stratigraphic relationships, (4) continuity or lack of continuity of the various subsurface strata, (5) groundwater depths and conditions, and (6) assessment of the documented and possible undocumented variability of the subsurface conditions. Information relative to the subsurface conditions is usually provided in text, cross-sections, and maps.

Subsurface cross-sections, or profiles, are commonly used to illustrate the stratigraphic sequence, subsurface strata and their relationships, geologic structure, and other subsurface features across a site. The cross section can range from simple line drawings to complex illustrations that include boring logs and plotted test data (Figure 7.17).

Maps are commonly used to illustrate and define the subsurface conditions at a site. The maps can include topographic and bathymetric contour maps, maps of the structural contours of a stratigraphic

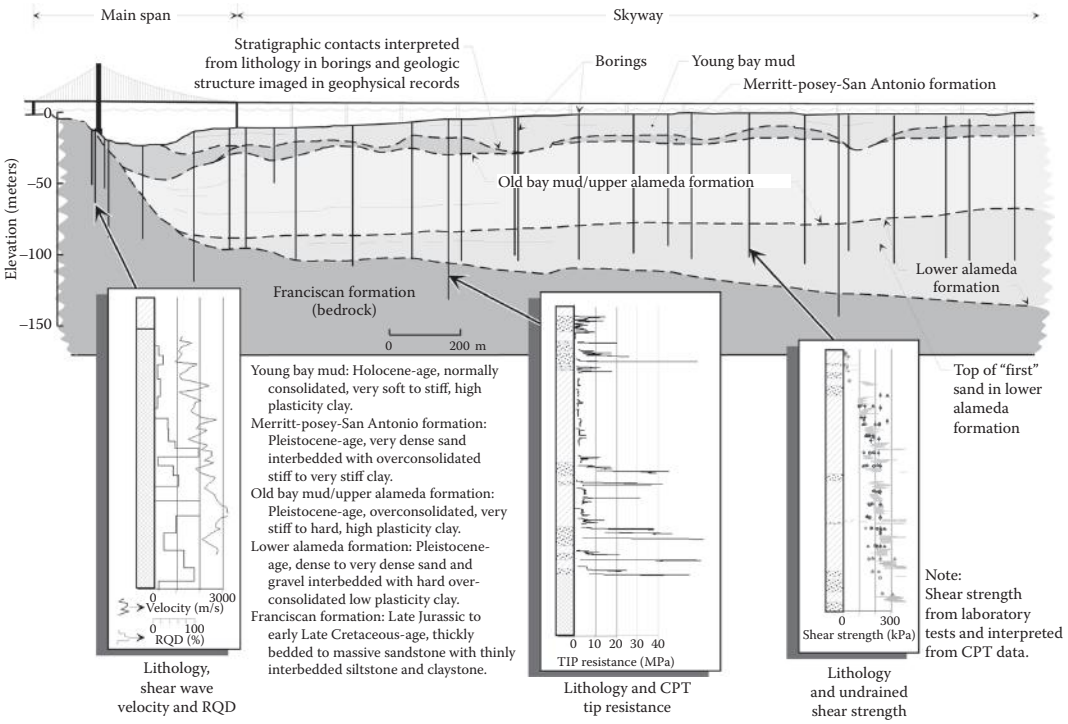

FIGURE 7.17 Subsurface cross-section for San Francisco-Oakland Bay Bridge East Span alignment.

surface, groundwater depth or elevation maps, isopach thickness maps of an individual stratum (or sequence of strata), and interpreted maps of geologic features (e.g., faulting, bedrock outcrops). The locations of explorations should generally be included on the interpretive maps.

The interpretive report also should describe data relative to the depths and elevations of groundwater and/or seepage encountered in the field. The potential types of groundwater surface(s) and possible seasonal fluctuation of groundwater should be described. The description of the subsurface conditions also should discuss how the groundwater conditions can affect construction.

7.5.4 Definition of Soil Properties

Soil properties generally should be interpreted in terms of stratigraphic units or geologic deposits. The interpretation of representative soil properties for design should consider lateral and vertical variability of the different soil deposits. Representative soil properties should consider the potential for possible in situ variations that have not been disclosed by the exploration program and laboratory testing. For large or variable sites, it should be recognized that global averages of a particular soil property may not appropriately represent the representative value at all locations. For that condition, use of average soil properties may lead to unconservative design.

Soil properties and design recommendations are usually presented with a combination of narrative text, graphs, and data presented in tabular and/or bulleted list format. It is often convenient and helpful to reference generalized subsurface profiles and boring logs in those discussions. The narrative descriptions should include such factors as depth range, general consistency or density, plasticity or grain size, occurrence of groundwater, occurrence of layers or seams, degree of weathering, and structure. For each stratigraphic unit, ranges of typical measured field and laboratory data (e.g., strength, index parameters, and blow counts) should be described.

7.5.5 Geotechnical Recommendations

The site characterization report should provide solutions to the geotechnical issues and contain geotechnical recommendations that are complete, concise, and definitive. The recommended foundation and geotechnical systems should be cost-effective, performance-proven, and constructible. Where appropriate, alternative foundation types should be discussed and evaluated. When construction problems are anticipated, solutions to these problems should be described.

In addition to the standard consideration of axial and lateral foundation capacity, load-deflection characteristics, settlement, slope stability, and earth pressures, there are a number of subsurface conditions that can affect foundation design and performance. Those conditions include the following:

- Liquefaction susceptibility of loose, granular soils
- Expansive or collapsible soils
- Mica-rich and carbonate soils
- Karst topography
- Corrosive soils
- Permafrost or frozen soils
- Perched or artesian groundwater

When any of those conditions are present, they should be described and evaluated.

7.5.6 Application of Computerized Databases

Computerized databases provide the opportunity to efficiently compile, organize, integrate, and analyze geotechnical data. All collected data are thereby stored, in a standard format, in a central accessible location. Use of a computerized database has a number of advantages. Use of automated interactive routines

allows the efficient production of boring logs, cross sections, maps, and parameter plots. Large volumes of data from multiple sources can be integrated and queried to evaluate or show trends and variability. New data from subsequent phases of study can be easily and rapidly incorporated into the existing database to update and revise the geologic model of the site.

Throughout the duration of a project, computerized database such as the geographic information system (GIS) can be used to efficiently synthesize and overlay new data onto the database. This expedites the QA/QC of the data as well as the synthesis and evaluation of new data. Additionally, this enables streamlined integration of new data into the database, which allows new data to be viewed in context of the prior data and information with ease. A multifaceted, inclusive framework can then be established—one that directly benefits the subsequent phases of the project by providing focus and knowledge as the phases of the project proceed—not solely after project completion.

GIS routines offer the unique ability to synthesize large amounts of raw data of multiple formats into visual end products that are readily communicated. This permits information to be readily communicated to other members of the client's organization and project team more expeditiously than is otherwise possible with less-integrated data management programs. Efficient application of such processes provide avenues of communication among all members of the project team through timely transmittal of information that allows a mutually beneficial cycle of feedback, which ultimately streamlines subsequent phases of the project. Figure 7.18 provides an example of such data output.

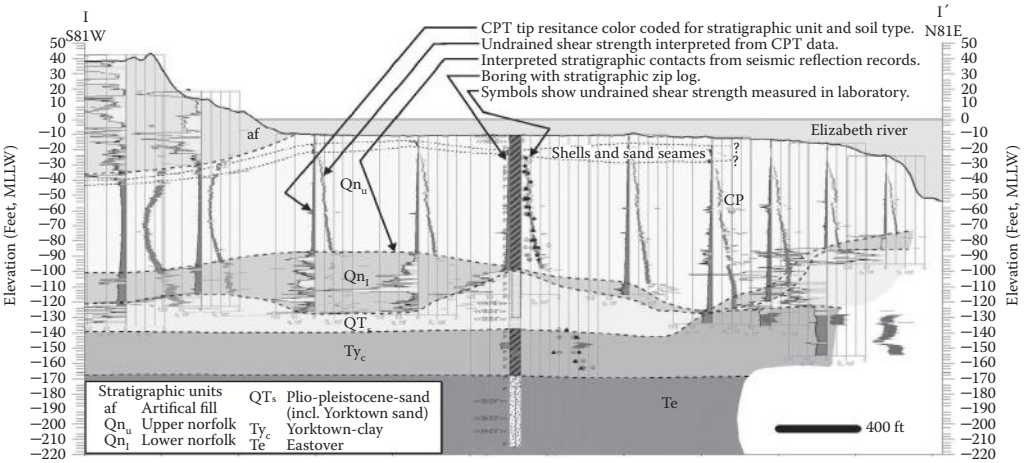

FIGURE 7.18 Subsurface cross-section interpreted from CPT soundings and seismic reflection data.

8

Shallow Foundations

Mohammed S. Islam
California Department of Transportation

Amir M. Malek
California Department of Transportation

8.1 Introduction

The term *foundation* is often used to refer to the part of the structure that transmits the weight of and other force effects on the structure on to the ground. This is a narrow definition of foundation that can lead to problems in designing foundations for structures. A complete definition of foundation should include the soil or rock, more generally the geomaterials that provide the necessary resistances so that the structure (1) will not experience unacceptable deformation that can render it unusable for the intended purposes and (2) will remain stable or not fail to protect life and the investment made by the owners at all times during the design life. A more representative definition refers to the structure and the geomaterial components of the foundation as "structure foundation" and "foundation geomaterial" or more commonly as "foundation soils," respectively.

The main purposes of the geotechnical design of foundations for civil engineering structures are to (1) limit any deformations or movements that the foundation may experience during the design life due to the expected day-to-day average or service loads so that the structure will maintain its intended functionality and (2) maintain its stability against all kinematically admissible failure or collapse mechanisms if, for some unexpected reason, subjected to a certain load that is significantly higher in magnitude or much less likely to occur during the design life, than the expected day-to-day average load.

Structure foundations are generally grouped into two primary categories: (1) *shallow foundations* and (2) *deep foundations*. This chapter is primarily devoted to the geotechnical design of *shallow foundations*.

Basic foundation design requirements, geotechnical considerations, and the current design methodologies are presented followed by the various methods available for the analysis and evaluation of the necessary geotechnical design parameters. Both the traditional Working Stress Design (WSD) and the more recent AASHTO (2012) Load and Resistance Factor Design (LRFD) methodologies are covered. Structural design aspects of shallow foundations are also briefly addressed. Deep foundations for bridges are covered in Chapter 10.

8.1.1 Basic Foundation Design Requirements

The primary objective of any foundation design is to transfer the structure loads to the foundation geomaterials in ways such that the specified performance requirements are met in a cost-effective manner. As such, foundation design needs to consider the following basic requirements:

- The type or nature, usage, design life, and performance requirements of the structures to be supported.
- The nature, magnitude, and the likelihood of the occurrence of the various types of loadings or demand on the foundation and those of the available resistances or capacities. The loading for design need to include the following:

  The average magnitude of the loads normally expected to occur during the day-to-day operation of the structure. In WSD this load is generally termed simply as the "design load." In LRFD it is often termed somewhat misleadingly as the "unfactored load," whereas the term "design service load" is more desirable and recommended for use.

  A certain significantly higher magnitude of the normally expected day-to-day loading that has some but much lower probability of being exceeded during the design life than the design service load. In LRFD this is termed the "design factored load."

  Other rare but significantly high magnitude loadings such as those due to ground motion generated by moderate to large magnitude earthquakes at the sites located near or within some moderate distances, most commonly on the order of 100 km or less, from the earthquake source, or the sites that may experience a rare but significant magnitude storm or hurricane. The design load(s) for these events, termed in LRFD as the "extreme events," depends on many factors. A more detailed description is outside the scope of this chapter, but noteworthy to state that the design loads for these events depend to a large extent on the cost of design and construction to reduce the associated risks and the acceptable level of risks. Most often it is not likely or even feasible to completely eliminate these rare risks, in particular against those due to significant deformations during large magnitude events. For seismic design these loads are often referred to as "design seismic loads," which could be for the functional-level or the safety-level design.
- Any potential effects on the soil stiffness and strength or resistances due to construction as well as the type or nature and the magnitude of the design loadings, such as the reduction in the strength of some soils during seismic events, need to be evaluated and considered in appropriate

combinations and in conjunction with the applicable loading types, magnitudes, and their combinations. Any uncertainties in the estimated soil ultimate strength or resistances need to be considered, most commonly by using reduced strength parameters or ultimate resistances. In addition to professional judgments, the magnitude of such reduction is generally achieved in the WSD by using the concept of a factor of safety (FS) and in LRFD by using a "resistance factor (ϕ)."

Structure foundation needs to be located and designed such that environmental and geologic factors or conditions, including frost, scour, erosion, corrosion, seepage, piping of foundation soils, or future planned and anticipated developments and other human actives will not jeopardize its stability as well as functionality during the design life.

The potential effects of construction on adjacent existing structures, if any, need to be considered, and when necessary, mitigation measures are implemented to eliminate or reduce any potential negative effects to within acceptable limits. The potential of effects of any nearby planned future development on the foundation also need considerations during design.

Foundation movements or deformations due to the design service loads need to be limited to small specified amount for the structure to be useful in an uninterrupted manner or serve its intended purpose throughout the design life without needing to spend excessive amount of additional resources for repair or maintenance. These maximum limiting foundation deformations are variably referred to in the literature as allowable, tolerable, or permissible limits. These specified maximum deformation limits, mostly based on past observed or measured performances of similar structures and professional judgments, often vary widely and is a matter of significant uncertainty and long-standing confusion among many professionals. For important structures projects, the permissible deformation limits should be set based on project-specific requirements.

Foundations need to be designed to remain stable against all possible types of failure or collapse mechanisms with an acceptable level of reliability when subjected to the design factored loads and, where applicable, the design loads due to extreme events. The acceptable degree of reliability against all potential instability mechanisms, including the magnitude of the design factored or seismic design loads discussed above, is represented by FS in the traditional WSD and by a unique combinations of load and resistance factors in the LRFD methodology, for each of the potential instability or failure mechanisms.

Additional discussion on the various aspects of geotechnical or soil deformations and stability aspects of foundation design is presented in the following sections for both the WSD and the LRFD methodologies. FHWA (2002) provides guidelines for the determination of soil and rock properties for use in the analysis and design of bridge foundations.

8.1.2 Basic Geotechnical Considerations

Foundation geomaterials are generally classified as soil or rock. Both soil and rock, even at a given site, can and often do vary, sometimes significantly, in composition and engineering characteristics. Yet, often for simplicity in foundation design, soils are restrictively classified into only two groups: *cohesive soils* and *cohesionless* soils. Often, it is difficult and requires careful considerations to make a distinction between these two types of soils in real applications. For many applications, an inaccurate distinction can lead to trouble. Furthermore, foundation soil profiles commonly consist of layers of significantly different soil types or characteristics, rather than the uniform and homogeneous assumed in many in the examples in the textbooks or by some practicing engineer for many projects. Some level of simplification is essential for most project sites; however, oversimplification or inaccurate representation of the foundation soil conditions can be problematic.

The rate of the load application and the permeability of the foundation geomaterials need to be considered in the foundation design, especially when classifying a certain soil as either cohesive or cohesionless. For the purpose of foundation design, it is more appropriate and useful to classify foundation soils as either *coarse-grained* or *fine-grained* compared to the often used "cohesionless" or "cohesive," respectively.

The later classification, if used without a sound understanding of how soils behave when loads are applied at different rates, can be problematic. Additionally, in many parts of the world, for example, the Western United States, often a clear distinction cannot be made between soils and what geologists classify as bedrock or formation material from the geotechnical engineering points of view. These later geomaterials, in many engineering aspects, fall between soil and what engineers normally understand as rock—the relatively strong earth materials with distinct geologic features. For geotechnical engineering purposes, these very dense or very hard soil-like geologically classified bedrock materials have been termed as "intermediate geomaterial" (O'Neill et al. 1996) or IGM. Similar to soils, IGM has been classified into two categories: cohesive IGM and cohesionless IGM.

Soil behavior under applied loads is significantly affected by the presence of water in the pores or voids, and how quickly relative to the rate of the load application the pore water can flow out of the stressed foundation soil zone. Soil, when subjected to loads, tends to change in volume. For this volume change to occur in saturated soils, the pore water that is considered relatively incompressible compared to the soil skeleton needs to flow out of the stressed soil zone.

The rate at which the pore water can flow out depends on the soil permeability, the length of the flow path, and other boundary conditions.

The generation of excess pore pressure and its potential effects on the soil strength also depends on the rate of loading. At the rates in which the static permanent loads are generally applied, little or no excess pore pressures are usually generated in clean coarse-grained soils. In these cases, drainage of the pore water and the resulting volume change occur instantaneously compared to the rates of loadings, including those generally expected of for the day-to-day or service live or transient and temporary loads. For this reason, such soils are often identified as "free-draining." However, this categorization, unless done carefully, could be misleading because even these so-called free-draining soils may experience significant excess pore water pressure when the rate of load application is very fast, such as that occurs during earthquake events.

On the other hand, most fine-grained soils experience initial excess pore on the same order of magnitude as the applied stress even when static permanent loads are applied at the rates normally expected of. Whereas, when the loads are applied at a faster rate such as those expected of for the day-to-day live loads and for the seismic loads, little or no excess pore pressure generates in most low-permeable fine-grained soils.

The change in the pore water pressure above that existed for the equilibrium conditions (u_o) before the application of the load is termed as the "excess pore pressure" (Δu). It can be positive (increase) or negative (decrease) depending on the initial "state" of the soils. The "state" of a soil element is expressed in terms of its initial void ratio and the average effective confining stress. The initial state of a soil element implicitly incorporates its past stress history—which is an important factor in this regard.

Shear strength of soils depends on the effective stress. Depending on the permeability the soil effective stress, and thus its shear strength, can vary over the period of time starting from the initial load application and ending with the complete dissipation of the generated excess pore water pressures. As stated above, the generated excess pore water pressure can be either positive or negative resulting in a short-term decrease or increase in the soil strength, respectively. For most projects the dissipation of the excess pore water pressure can be expected to complete well before the end of the design life. For soils experiencing positive excess pore pressure, the initial strength, that is when the excess pore pressure is the maximum, will govern the stability conditions. On the other hand, for soils experiencing negative excess pore pressure, the long-term strength, that is when the excess pore pressure is fully dissipated,

will govern the stability conditions. Often it is difficult to determine whether the generated excess pore pressure will be positive or negative at a given project site. For such cases, analyses should be performed to evaluate both the (1) short-term or initial stability conditions when the loads are applied and (2) long-term or the stability conditions that may exist once the dissipation of any generated excess is completed.

Additional and sometime more significant difficulties are associated with the determination of the magnitude of the excess pore water pressure that may be generated at a project site. For most projects, even for static design, these difficulties are avoided by using the total stress based or undrained strength for the fine-grained soil layers in the evaluation of the short-term or initial stability conditions that may exist during or for a short time after the application of the loads.

The long-term or the stability conditions that may exist once the dissipation of the excess pore water, if any were generated, is complete and is conveniently evaluated based on the effective stress-based strength for all types of soil layers.

For seismic design, stability conditions during or immediately following the design ground motion event is generally evaluated by the utilizing appropriate fully undrained strengths for the nonliquefiable fine-grained soils layers.

When complete liquefaction of a soil layer is predicted at any instant of time at which stability conditions are to be evaluated, the undrained residual or steady-state shear strength (S_r) for liquefied soils recommended by several researchers (Seed and Harder 1990; Stark and Mesri 1992; Olsen and Stark (2008); Idriss and Boulanger 2008; Robertson 2013) is generally used in lieu of the effective stress-based strengths.

For all other soil layers, the potential effects of the development of partial excess pore water pressures, if any is predicted to develop, at the instant of time during or immediately after the end of the design ground motion event at which stability conditions are evaluated should be considered in the seismic stability analyses.

The terms "cohesionless' and "cohesive" are sometime mistakenly used as representing soils whose shear strengths are characterized with friction and cohesion only, respectively. This could lead to a problem in the foundation design. In the long term following the application of all types of permanent loads, most soils are likely to behave as purely frictional materials, and inclusion of any cohesion in the long-term stability evaluation can lead to dangerous consequences.

8.1.3 Definitions

A shallow foundation, often referred to as a spread foundation or simply as footing, may be defined as the one with an embedment depth (D) below the lowest adjacent ground on the order of its effective width (B'), as illustrated in Figure 8.1. The D/B' ratio for shallow foundation commonly ranges from 0.25 to 1.0 but may be as high as 2.5 (Munfakh et al. 2001).

8.1.4 Types of Shallow Foundations

Commonly used types of shallow foundations include individual footings, strip or continuous footings, combined footings, and mat or raft. Shallow foundations or spread footings derive their vertical load–supporting capacity entirely from their base bearing resistance, whereas deep foundations derive their axial load–supporting capacity from both side and base resistances.

Shallow foundations are generally more economical to design and construct. Therefore, shallow foundations are often preferred over deep foundation if the geomaterials at shallow depths are firm and suitable for supporting the anticipated structure loads. Even in firm ground, use of shallow foundations may not be feasible due to other considerations such as the unusually high loads, vertical or lateral or both, difficult underwater construction conditions, and limited right-of-way.

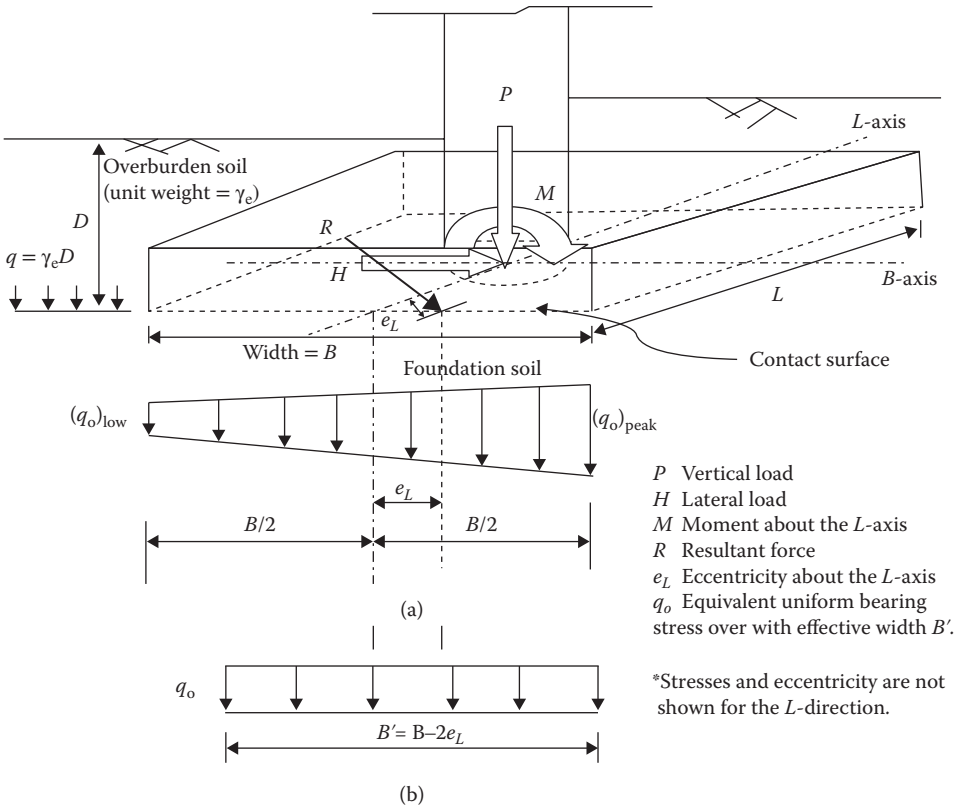

FIGURE 8.1 Definition sketch for shallow foundations. (a) Idealized contact stress distribution and (b) stress distribution for geotechnical analysis and design.

8.2 Design Methodologies

In the WSD, performance requirements for the design are specified based on past experiences and, to a great extent, on professional judgments. Stability requirements are generally specified in terms of an FS defined as the ratio of the available ultimate capacity to the expected day-to-day average destabilizing load or demand during the design life. However, both the parameters used to define the FS are subject to different degrees of uncertainties. The concept of the FS used in the stability design of a structure and, in some cases, components thereof against the various potential modes of failures has been used to incorporate these uncertainties in an empirical manner. This design concept, however, does not permit the evaluation of the uncertainties and the resulting reliability of the design in a systematic, uniform, or universal manner.

As a simple example, consider a case where spread footing foundations for two adjacent bridge structures are similar in all aspects, except they are located at two different nearby locations with different foundation soil types and conditions. One of the bridges also has a fewer number of supports than the other. Footings for both the bridge structures were designed for an FS of 3.0 against soil bearing capacity–type failures. Although the spread footings for each structure were designed for the same FS, the reliabilities associated against bearing capacity failures are not likely to be the same, because both the loads and the soil bearing capacities for each structure are likely to be subjected to different degrees of uncertainty. Furthermore, the estimated magnitude or the degree or even the likely range of the uncertainty or reliability associated with the bearing capacity failure for neither of these bridges is known.

In the aforementioned example, it would have been desirable and prudent to design such that the same degree of reliability against bearing failure is provided for each structure and also that the

magnitude of this reliability is known. These would have permitted to optimize these designs and meet the performance requirements with a known and the same level of reliability. Furthermore, if needed, the specified performance requirements could have been evaluated in terms of their effects on the cost and other aspects of the design and modified or adjusted within the limits of the overall project requirements and the acceptable level of reliability.

The object of the LRFD methodology is to address some of the limitations, including those discussed earlier, associated with the WSD methodology by systematic evaluation of the uncertainties involved in the determination of both the demand or load and resistance or capacity and incorporating those uncertainties in the design to achieve an acceptable and preselected level of reliability against a given mode of instability. It achieves these objectives by utilizing the concepts of the *load factors* (γ_i) and the *resistance factors* (ϕ_j).

LRFD also permits to specify for and design to achieve or provide the same degree of reliability for similar structures, in terms of use and/or importance irrespective of their locations and other differences. LRFD also provides for clear identification of the various performance and stability or failure conditions or mechanisms (states) and their limiting magnitudes (limits) for which to perform analysis and design a given structure for so that it will perform during the entire design life in the manners intended by the owners as well as the designers.

In summary, both WSD and LRFD involve analysis and design to limit foundation movements due to the service or day-to-day average load to maintain serviceability of the structure and to ensure adequate stability or safety against all applicable instability or failure mechanisms. Thus, the geotechnical deformation and soil strength parameters necessary for the evaluation of the various stability conditions are generally applicable to both WSD and LRFD except that, as noted where necessary, there are differences in some terminologies and techniques by which the stabilities are evaluated and minimum requirements are met by the design.

The mechanisms involved in the development of foundation deformations or movements, generally referred to as *soil–foundation interactions* (SFIs), are often complex. For practical purposes or design, most often it is adequate to decouple the foundation movements due to soil flexibility from those due to the structural flexibility of the footing and/or the supported structure or parts thereof. This permits the geotechnical and structural deformation analyzes to be performed separately and more easily by the respective designers.

For small deformations, that is, for serviceability design, this approach should be sufficiently accurate for most projects. Owing to soil nonlinearity and the complex interactions between the foundation soils and the structure foundation(s), additional considerations are required when soil movements or deformations are large, especially when structure foundations are subjected to kinematic forces. In such cases, application of the simple decoupling methods is not likely to provide sufficiently reliable results, in particular for important structures. For important structures or complex situations, a detailed SFI or a soil–foundation–structure interaction (SFSI) analyses are usually required to estimate and be able to evaluate foundation movements more accurately.

For the serviceability design of spread footing foundations, geotechnical consideration is limited to the movements of the footing due to the soil flexibility or deformations and/or rigid movements of the soil–foundation system. These types of footing movements are generally referred to as the *geotechnical deformation or movements*. Deformations of the footing and the supported structure, or the elements thereof, due to the structural flexibility of the footing due to applied loads, including those due to soil pressures and kinematic movements of the soils, if any, are generally referred to as *structural deformation*. Discussion in this chapter is limited only to the geotechnical movements of shallow foundations.

Similarly, in this chapter stability considerations of shallow foundations are limited to those associated with the soil strength. These types of foundation stabilities are referred to as *geotechnical stabilities*.

Structural deformations and structural stability conditions are not covered in this section. For design, however, geotechnical movements and structural deformations need to be combined to evaluate the estimated total deformations or movements of the foundation and the supported structure or its parts thereof.

All applicable geotechnical and structural stability conditions or failure mechanisms must be identified, evaluated, and the footing designed to ensure adequate stability or an acceptable level of reliability against failure or collapse of the foundation.

8.2.1 Working Stress Design

The WSD and the allowable stress design (ASD) methods are similar, and for shallow foundation design involves (1) evaluation of and designing to limit movements to meet serviceability needs and (2) evaluation of and designing to achieve adequate stability against all kinematically admissible collapse or failure mechanisms. In WSD, all stability conditions are evaluated, and their adequacy verified by utilizing the concept of FS. For any given instability or failure mechanism, FS is defined as the ratio of the available total ultimate resistance or capacity to the total destabilizing load or demand.

In some WSD analyses, such as those performed to evaluate soil mass or global slope stability including the spread footing foundations, the FS is sometimes defined as the ratio of the unit shear strength (τ_f) or the corresponding shear strength parameters, such as the cohesion (c_f) and the friction angle (φ_f) of the soils to the actually mobilized magnitude of the corresponding strength parameters. For example, when the short-term global stability of slope consisting of fine-grained soils and containing a shallow foundation is to be evaluated using the total stress strength, that is the undrained shear strength (S_u), the FS safety may be defined as equal to (S_u/S_d), where S_d is the fraction of the total available undrained shear strength that is estimated to have been mobilized to support the destabilizing loads.

8.2.1.1 Foundation Movements or Deformations

For the serviceability design of shallow foundations, geotechnical movement or deformation include the evaluation and design for the following soil–foundation response parameters when the footing is subjected to the design service load.

- Settlement or uplift movements
- Lateral movements or deformations
- Rotation

Lateral displacements of the supported structure may occur due to lateral loads or rotation of the shallow foundation or both and are likely to vary with the height of the structure. It is, therefore, often necessary to identify the elevation or location along the height of the structure at which lateral movement(s) is being considered.

Deformation evaluation can be difficult due to the complex SFSIs. Often it is sufficient to decouple the soil-related deformation from structure deformations and use simplified estimation methods. Discussion in this chapter is limited to the soil-related movements or deformations.

When shallow foundations are constructed on, within, or near slopes or recently placed fill embankments and adjacent to another structure, potential exists for additional settlement or deformation occurring beyond the directly stressed or foundation zones or due to loads other than those imposed by the foundation under consideration. For example, settlement of the soils below the foundation level due to the additional loads imposed by recently placed embankment fill at the abutments will add to the foundation settlement due to applied structure service loads. Furthermore, a certain type of foundations soils, known as collapsible soils, may experience significant compression due to the introduction of additional moisture.

Shallow foundation design for bridge structures is commonly concerned only with the settlement. Settlement refers to the downward movement of the foundation which occurs due to compression of the foundation soils and other reasons discussed in the preceding paragraph.

For a given structure, the maximum amount of total settlement that a footing may be permitted to experience under service load without adversely affecting the serviceability or function of the supported

structure(s) is commonly referred to as the *allowable, tolerable, or permissible settlement* (s_{perm}). The net uniform contact or bearing stress that is estimated to cause this amount of settlement is termed as the "allowable contact or bearing stress" $(q_a)_s$ in WSD and net permissible contact or bearing stress (q_{pn}) in LRFD.

The limiting settlement depends on many factors including the types and functions of the structure and the spacing between the two adjacent supports. Most often, however, the differential settlement (Δ) between the two adjacent supports is more critical than the total settlement of the foundations. Additionally, as pointed out by Skempton and MacDonald (1956) the aspect of foundation settlement that relates more directly to the potential bridge superstructure cracking is the angular distortion (β) defined as the ratio of the differential settlement (Δ) and the span length (L) between two adjacent supports.

However, large total settlement at abutment foundations with respect to the approach roadway embankment can severely impact the functionality of the bridge. Total foundation settlement at both abutments and interior support locations can also cause distress to utilities carried by the bridge structure. It should be noted that the differential settlement between two adjacent supports is of most concern when it is occurring after the supported structure is connected and achieved sufficient rigidity (i.e., postdeck construction) such that it will experience distortion if any additional differential movements of the supports occurs. In addition, the total settlement is of concern once the approach road grades and appurtenant facilities adjacent to, supported by, or connected to the bridge supports are constructed and can be affected by any additional foundation settlements.

Owing to significant variations in the types, geometry, structural details, serviceability, and other aspects of bridge structures, establishing limits for either the total support settlement or the differential settlement between adjacent supports that can be used for most, if not all, cases is challenging. Guidance in this regard is very limited, often incomplete, and mostly commonly not practical or applicable to specific bridge design project in hand. Moulton et al. (1985) and Gifford et al. (1987) provide information on the tolerable movements for highway bridges.

Based on the *AASHTO LRFD Bridge Design Specifications* (2012), angular distortion (Δ/L) between the two adjacent supports of a simply supported bridge span should be limited to 0.008 radians. The corresponding limiting angular distortion for continuous span is 0.004 radians or about half of that for the simply supported span. It should be noted that, for a given limiting angular distortion, the corresponding limiting differential settlement will depend on the span length. Therefore, project-specific evaluation and specifications for the limiting total as well as differential settlement are usually necessary. Most often professional judgment plays a necessary and important role in establishing the values of the settlement limits. More fundamentally, limiting strains that would cause unacceptable cracking in structural elements due to differential settlement of adjacent foundations can be evaluated to establish tolerable differential settlement limits.

If the estimated differential settlement between two adjacent supports founded on shallow foundation is excessive, the foundation type should be changed to deep foundation unless ground improvement to reduce foundation settlement is a viable option.

The above discussion on foundation settlement is equally applicable to upward movement of foundations. Upward movement of foundations can be due to heave of the foundation soil or uplift of the foundation. Heave of shallow foundations occurs due to increase in the volume of *expansive soils* when additional moisture is introduced into these soils. Heave usually is only a concern for lightly loaded foundations and not for most bridges, because their foundations are generally heavily loaded. Uplift movements of foundations occur due to the externally applied upward (or tensile) load on foundations. Bridge foundations, in particular shallow foundations, are not usually allowed to be subjected to service level or sustained uplift forces. Thus, uplift movement is generally not a design concern for shallow foundation used to support bridge structures.

Large differential settlement or upward movement between two adjacent supports can result in the significant redistribution of the support loads leading to additional differential settlement, which can

ultimately lead to foundation bearing failure. Excessive foundation differential settlement can also overstress or even cause failure of the supported structure or its elements. Therefore, limiting differential settlement is important not only to maintain serviceability but also to prevent collapse. Even though design requires limiting the foundation differential settlement to some relatively small magnitude, the potential effects of the estimated foundation settlement should be considered in the evaluation of loads for the stability analyses for both static and seismic design.

It should be noted that for the safety-level seismic design, foundation settlement or movements should not be a concern unless such settlement or movement is predicted to cause failure of the otherwise adequately stable structure. This can be evaluated by considering the effects of the estimated seismic settlement in the stability analysis of the structure and, when necessary, also its components.

As depicted in Figure 8.2, eccentrically loaded shallow foundation experiences rotation (α) about the central axes of the contact surface. This rotation occurs as a result of nonuniform settlement along the transverse direction due to nonuniform contact stress caused by unbalanced moment about the longitudinal central axis of the bottom surface of the foundation. This type of foundation rotation results in the titling of the supported structure. Tilt is defined as

$$\text{Tilt}(\%) = \frac{\rho}{H} \times 100 \tag{8.1}$$

where ρ is lateral displacement of the structure at height H due to the footing rotation (α). Both the foundation and the supported structure are generally assumed to be rigid, in which case tilt is constant, and the tilt angle, $i = \tan^{-1}(\rho/H)$, is equal to the angle of rotation of the footing (α).

Rotation of shallow foundation (α) due to service loads must be limited to some small value to maintain the serviceability of the supported structure. Guidance or specifications on the maximum amount of allowable or permissible rotation for spread footings or the supported structure are hard to find. It should be noted that Moulton et al. (1982) and Gifford et al. (1987) discussed earlier provide useful information on the maximum allowable limits of the longitudinal distortion or rotation that occurs due to differential settlement between two adjacent supports.

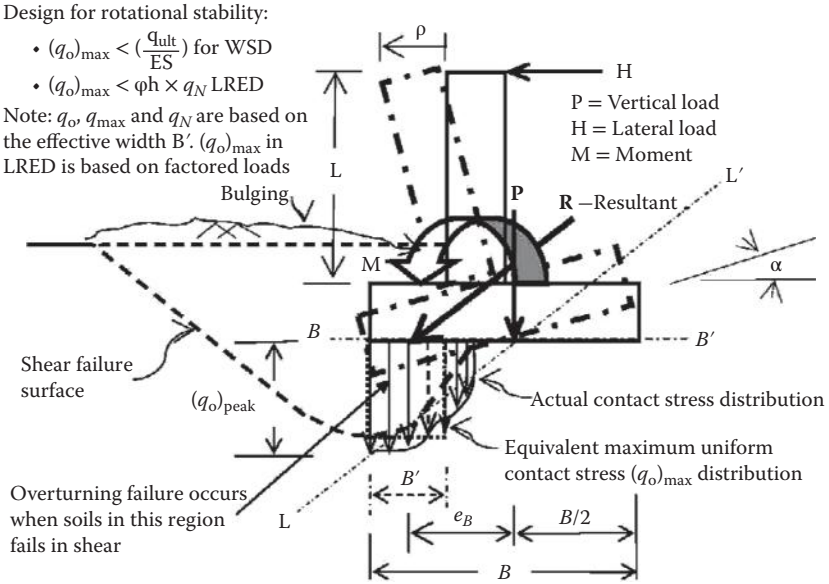

FIGURE 8.2 Rotation/tilting of shallow foundations.

The maximum amount of footing rotation that can be allowed due to service load depends on many factors, including the height and types of the supported structure, its use, esthetics, and the perception of the users. Scott and Schoustra (1968) states that as little as 1.0 in. of settlement in 20 ft. (0.5%) can be discovered, and any larger tilt is very objectionable from the esthetic and psychological perspective even if stability, both structural or geotechnical, is not an issue. TRCC (2009) specifies a limiting tilt of 1.0% for residential and other low rise buildings. This amount of allowable tilt is likely too high for most bridge structures in particular those that are relatively high. A 0.25% tilt corresponds to 0.5 and 1.5 in. of lateral displacement at the top of a 16- and 50–ft.-high column, respectively. Intermediate supports are not usually subjected to sustained lateral load. Therefore, tilting of the intermediate support columns is usually not a concern for the static design. On the other hand, abutments are commonly subjected to significant sustained lateral loads due to lateral earth pressures. A 0.25% tilt of a spread footing foundation will result in approximately 0.6 and 0.9 in. of lateral deflection at the top of a 20- and 30-ft.-high abutment walls, respectively. Therefore, depending on the height of the bridge, 0.25%–0.5% should be allowed for most bridge structures from the esthetic and perception point of view. *However, similar to differential settlement, both geotechnical and structural design must consider the potential effects of the estimated tilt due to service load in the stability analysis and design.*

It should be noted that excessive rotation of the footing due to the shear failure of the soils underneath the toe areas would result in the rotational or tilting failure, which has traditionally been termed as the "overturning," failure, of the supported structure. This aspect of footing behavior and the design requirements will be discussed in Section 8.4.

8.2.1.2 Foundation Stability or Failures

The stability conditions generally associated with shallow foundation design include the following:

- Soil bearing stability in compression
- Soil bearing stability in uplift or tension
- Lateral stability
- Rotational stability
- Hydraulic stability

Lateral stability is most often referred to as sliding stability and sometimes as lateral bearing stability. Generally, lateral stability of shallow foundations is achieved by a combination of sliding resistances at the footing base and the sides, and the soil lateral bearing, resistance, more specifically passive soil resistance, on the side of the footing toward which the resultant unbalanced lateral load is acting. Sliding resistances along the sides of the footing are not generally considered in the routine design but in some cases can be significant.

In addition to deformation, the overall or the global slopes supporting or adjacent to the spread footing foundations must be stable. The overall stability is generally analyzed utilizing the limit equilibrium methods. The spread footing foundation as well as all applicable external loads including those imposed by the structure on the foundation and the slope surfaces must be considered in the overall or global slope stability evaluation.

As discussed earlier, the WSD methodology utilized the concept of FS to ensure the stability of foundations. Design must ensure that the calculated factors of safety against all potential failure or collapse mechanisms are equal to or greater than certain specified minimum value of the FS. Typical values of the FS used in the static design of spread footing foundations are presented in Table 8.1.

For the design of spread footings for bridge structures, AASHTO (2002) specified safety factors are presented in Table 8.2.

Design requirements as well as the methods of analysis, for the so-called overturning failure of spread footing foundations have been somewhat ambiguous or inconsistent throughout the literature. As a result, this matter is given a special treatment later in this chapter.

TABLE 8.1 Typical Values of Safety Factors Used for the Static Design of Shallow Foundations

Stability or Failure Mode		Factor of Safety (FS)	Comments
Overall or slope stability		1.5–2.0	Lower values are used when uncertainties in the design are low and/or consequences of failure will not be significant. Higher values are used when uncertainties in the design are high and/or consequences of failure will be significant. Higher values are also recommended for some FS for footing founded in clay soils.
Bearing capacity		2.5–3.5	
Lateral (sliding) stability		1.5–2.0	
Overturning		1.5–2.5	
Hydraulic stability	Uplift/flotation	1.5–2.0	
	Heave	1.5–2.0	
	Piping	2.0–3.0	

Source: Data from Terzaghi, K. and Peck, R. B., *Soil Mechanics in Engineering Practice*, Second Edition, John Wiley & Sons, New York, 1967; NCHRP, Manual for the Design of Bridge Foundations, National Cooperative Highway Research Program Report No. 343, National Science Foundation, Washington, D.C., 1991; and Munfakh, G., Arman, A., Collin, J. G., Hung, J. C., and Brouillette, R. P. (2001), *Shallow Foundations*, Federal Highway Publication No. NHI-01-023, Washington, D.C., 2001.

TABLE 8.2 AASHTO (2002) Specified Factor of Safety (FS) for the Static Design of Bridge Shallow Foundations

Stability or Failure Mode		FS	Comments
Overall or slope stability		1.3–1.8	FS ≥ 1.3 when soil/rock parameters are based on in situ and/or laboratory testing. Otherwise, FS ≥ 1.5. When the footing is founded on a slope or above an earth retaining system, the corresponding FS are ≥1.5 and ≥1.8, respectively
Soil bearing stability		≥3.0	Bearing capacity based on effective footing width
Lateral stability		≥1.5	Based on effective footing area
Overturning		1.5–2.0	Based on summing moments about toe. FS ≥ 2.0 in soils and ≥1.5 in rocks
		$E \leq B/6$ or $B/4$	$e \leq B/6$ in soils and $e \leq B/4$ in rock
Hydraulic stability	Uplift	—	No FS values are specified. Investigation into uplift and prevention of piping are specified
	Heave	—	
	Piping	—	

8.2.2 Load and Resistance Factor Design

LRFD of shallow foundations involves identification of and analysis and design for three different groups of conditions or mechanisms called limit states, namely (1) service limit states, (2) strength limit states, and (3) extreme limit states, which include seismic design.

8.2.2.1 Service Limit States

The service limit states design pertains to the performance of the bridge with regard to serviceability during the design life of the bridge and is evaluated under expected day-to-day, operating, or service loading conditions. The various components of the expected service loads are estimated or calculated in a way similar to the traditions working stress method. Sometimes these loads are referred to as "unfactored loads." Although strictly speaking it is a misnomer, it does facilitate communication. Service ability or service limit state performance requirements are generally defined in terms of limiting or permissible deformation, primarily total and differential settlements for shallow foundations. Service limit states design also include analysis for and design to limited lateral movements and rotation, when applicable or significant.

Loads for the service limit state design of shallow foundations for bridge structures are evaluated based on the service limit state 1 load combination provided in the *AASHTO LRFD* (AASHTO 2012). As stated earlier, detailed guidance on the deformations to be used for service limit states design is not available, and the development of specifications on limit deformations for general use is complicated. Such limits among other factors depend on the owner's requirement, type of facilities or the required level of service, structure types, and distance between supports.

AASHTO LRFD Bridge Design Specifications (AASHTO 2012) provides additional information and guidance on this issue. For ordinary bridge structures, the California Department of Transportation (Caltrans 2008) limits total support settlement for simply supported bridge spans to 2.0 in. and for continuously supported bridge spans to 1.0 in. Differential settlement between two adjacent supports for continuously supported bridges is limited to 0.5 in. Additional total as well as differential settlement is allowed for ordinary bridges based on project-specific evaluation and consideration of the potential effects of larger settlements on the serviceability and stability of the structure.

Permissible deformation limits for important and unusual bridge structures should be evaluated and specified on a project-specific basis.

Furthermore, the capability of the profession at this time is limited on the evaluation of uncertainties involved with the available methods of movement or deformation analysis. As a result, reliability aspect of LRFD design cannot be implemented at this time. Thus, once the design load is available, the remainder of the LRFD service limit state design, including the types and components of deformations, and techniques and methods of analysis and design is similar to the serviceability aspects of WSD or ASD.

The other exception to the aforementioned similarities between the WSD serviceability design and LRFD service limit state design is the overall or global slope stability aspect of the shallow foundation design. Soils in slope stability analysis, similar to many other geotechnical engineering analyses in particular those related to the stability of earth and earth-supported or retaining structures, act both as load and resisting elements simultaneously. This makes the implementation of the concept of load and resistance factors, the main aspect of the LRFD, in the analysis and design. Thus, slope stability is currently evaluated using unfactored loads.

With the use of unfactored loads to determine the demand or destabilizing forces and soil capacities, reliability against sliding failure of the overall slope on the same order as that used in the WSD by utilizing an FS can be achieved in the LRFD strength and extreme limit state design by using a resistance equal to the inverse of the FS (i.e., $\phi = 1/FS$). This is possible because the loads involved with the overall stability analysis are mostly, if not all, permanent or dead loads. This is exactly what has been recommended in the current *AASHTO LRFD* (AASHTO 2012). However, currently *AASHTO LRFD Bridge Design Specifications* placed the slope stability aspect of the foundation design under the service limit state design. This has resulted in some confusion on the fundamental aspects of LRFD design methodology.

A somewhat lower resistance factor than that given should be used if the total live load relative to the total dead load involved with the overall stability analysis is significant.

Thus, it should be recognized that *AASHTO LRFD* (AASHTO 2012) includes overall or global stability under the service limit states design due to complexities involved in defining load and resistance factors when soil acts to exert both load and resistance simultaneously. Slope stability analysis for LRFD is performed in the same manner as for WSD, except that resistance factor, as stated above, is taken as the inverse of the FS determined based on the limit equilibrium methods.

8.2.2.2 Strength and Extreme Limit States

In LRFD design, both the strength and extreme event limit states pertain to the strength or stability aspects of shallow foundation. The stability and stability mechanisms considered are the same as those mentioned earlier for the WSD stability analyses.

With the respect to the design procedure, the primary difference with the WSD methodology is that in LRFD, instead of the FS and as discussed earlier, the adequate stability conditions are ensured by the combinations of load factors (γ) that generally increase the destabilizing load effects but currently

sometime, especially for earth structures and when combining different load components, also decrease the stabilizing effects of certain loads and always reduce the resistances or capacities by utilizing a co-dependent set of resistance factors (ϕ).

In LRFD, for both strength and extreme limit state designs, the factored resistance obtained by multiplying the nominal resistance by the specified resistance factor must be greater than or equal to the factored load for each mode of failure. That is,

$$\sum \varphi_i R_i \geq \sum \gamma_j Q_j \tag{8.2}$$

where ϕ = resistance factor, R = nominal resistance, γ = load factor, and Q = load.

Resistance factors specified by AASHTO (2012) for the strength limit state design are presented in Table 8.3.

AASHTO LRFD (AASHTO 2012) specifies a resistance factor (ϕ_g) of 0.67 for global stability of slopes supporting or containing a spread footing.

For LRFD extreme event limit states, the resistance factors are generally taken in the range of 0.9–1.0. For seismic design, AASHTO (2012) specifies a resistance of 0.9 for all stability or failure analysis. California Department of Transportation (Caltrans 2011a) specified a resistance factor of 1.0 for extreme event limit states design, including the safety-level seismic design of bridge structures.

It should be noted that for the safety-level seismic design, limiting deformation should not be a consideration unless the estimated deformation lead to collapse of the structure. Some agencies require a functional-level seismic design in which deformations are required to be limited so that a specified level of functionality of the bridge will be maintained after more frequent ground motion events. However, a significantly lower level of ground motion is specified for the functional-level design than that for the safety-level design.

In addition to applicable loads, changes in soil capacities or resistances and other potential effects such as ground movements inducing kinematic forces must be considered in the seismic design for safety-level design earthquake ground motion and also, when required, for functional level design earthquake ground motion. Neither the loads nor the resistances specified or applicable for one limit state should be considered in combination with a different limit states. For example, estimated effects of soil liquefaction downdrag or kinematic forces due to lateral spreading or deformation due the design seismic event must not be considered in conjunction with the service or strength limit state design.

TABLE 8.3 Resistance Factors for Strength Limit States Design of Shallow Foundations

Geotechnical Nominal Resistance	Notation	Method/Soil/Condition	Resistance Factor
Bearing resistance	ϕ_b	Theoretical method (Munfakh et al. 2001), in clay	0.50
		Theoretical method (Munfakh et al. 2001), in sand using *CPT*	0.50
		Theoretical method (Munfakh et al. 2001), in sand using *SPT*	0.45
		Semiempirical methods (Meyerhof 1956), in sand	0.45
		Footings on rock	0.45
		Plate load test	0.55
Sliding	ϕ_τ	Precast concrete placed on sand	0.90
		Cast-in-place concrete on sand	0.80
		Cast-in-place or precast concrete on clay	0.85
		Soil on soil	0.90
	ϕ_{ep}	Passive earth pressure component of sliding resistance	0.50

Source: Data from AASHTO, *AASHTO LRFD Bridge Design Specifications*, Customary U.S. Units, 2012, American Association of State Highway and Transportation Officials, Washington D.C., 2012.

Note: Modified by the authors to refer to the correct reference. Meyerhof (1957) provides theoretical methods, whereas Meyerhof (1956) provides semiempirical methods for sand using both SPT and CPT.

Resistance factors depend, among other factors, on the load factors and the methods of resistance evaluation. The "nominal resistance" for each type of stability evaluation is determined based on calibrated theoretical, semiempirical, or test methods. The definition of the ultimate capacity or the nominal resistance may vary from method to method. Thus, it is important to note that nominal resistance to be used in association with a specified resistance factor should not be modified based on arbitrarily defined deformation or settlement limits. In general, the nominal resistance should be the resistance at which the associated structure or the component thereof collapses or fails and should not be associated with any limiting deformation in the sense used in serviceability evaluation. Owing to certain inherent theoretical or testing limitations, as well as some practical considerations that prevent from defining a universally accepted definition of the failure or collapse, some nominal resistance determination methods uses certain magnitude of deformation as the limiting deformation to evaluate nominal resistance. However, such deformation limit is usually large to constitute a failure and need not be considered in design. This is because, by definition, the purpose of the stability evaluation is to prevent collapse with certain acceptable and generally degree of reliability not to limit deformation or settlement. Limiting deformation that, if any, used to define the nominal resistance in the original determination method, under the factored load that has a very low probability of occurrence, will necessitate an extremely conservative design beyond that necessary or required by the *AASHTO LRFD* specifications (AASHTO 2012).

It should be noted that load factors for a given load combination (as given in Chapters 5 and 6 of *Bridge Engineering Handbook, Second Edition: Fundamentals*) can be different for different stability or failure modes. Additionally, a load factor may have a specified single value or specified minimum and maximum depending on the type of effects (e.g., stabilizing/positive or destabilizing/negative) of the associated load component on the stability condition being evaluated.

8.3 Settlement and Bearing Stability Considerations

Figure 8.3 illustrates typical load–settlement relationships for spread footing of width B when subjected to a vertical load P resulting in a uniform contact or bearing stress of q_o. It may be noted the vertical load P is assumed to be applied concentrically. The concentric loading can be considered as a special case of eccentrically loaded footing where eccentricity $e = 0$, that is, the effective width $B' = B$. This permits the use of the effective footing width in all geotechnical analyses and designs.

Geotechnical correlations for footing settlement and bearing capacity depend on the size of the loaded width of the footing. These correlations are always developed, and presented in the literature and in the following sections, as a function of the width parameter B. For this width parameter B to be the same as the actual footing width, the load P must be applied concentrically so that the footing is uniformly loaded over the full width. For eccentrically loaded footing, the width parameters B must be replaced with the effective width $B' = B - 2e$. This presents a challenge when performing geotechnical analyses, evaluations, and design, because both the footing width and the eccentricity parameters are not known at this time. In order to obtain the most cost-effective or optimal design, an iterative design procedure involving significant interaction between the geotechnical and the structure designers would be needed

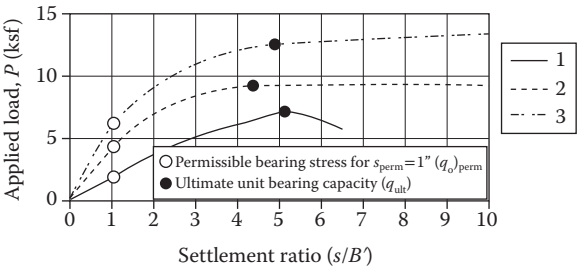

FIGURE 8.3 Load–settlement curves for spread footings.

to complete the design. In reality, this is often difficult and not executed resulting in less than optimum design. These difficulties can be easily avoided by following the procedure recommended below.

With the understanding that the concentrically loaded footing is a special case of eccentrically loaded footing with $e = 0.0$ or $B' = B$, it can be easily seen that it is appropriate, and at the same time more convenient, to simply consider the footing width parameter B in the geotechnical correlations, as presented in the current literature, and analyses and designs as the effective footing width. This can be accomplished in two different ways: (1) replace the symbol B with the symbol B' in all geotechnical correlations and analyses and (2) consider the parameter B in these correlations as representing the footing effective width (B') rather than the actual width when performing geotechnical analyses and design. For structure design, the actual footing width is used.

Based on the this, irrespective of the symbol used (i.e., B or B'), it is necessary to understand that the geotechnical correlations, and thus the design geotechnical parameters, are conveniently presented in terms of the effective footing width irrespective of the actual footing width and the load eccentricity. This permits the geotechnical designers to provide plots or tables of the recommended geotechnical design parameters for settlement and stability analyses as a function of the footing effective width. The range of the effective width for which these parameters are provided should be chosen, so that it well encompasses the effective width of the design footing. The structure designers can use these data in an iterative manner to size the design footing with the need to request updated geotechnical design parameters and recommendations every time either the footing size or the eccentricity changes during the analysis and design process until the most optimal design is obtained, which not only satisfies all applicable deformation and stability requirements, but also is the most cost-effective.

As indicated in Figure 8.3, the settlement ratio (S/B') increases as the applied load increases. If the applied vertical load is P, then the uniform unit contact or bearing stress (q_o) is obtained by

$$q_o = \frac{P}{A'} \tag{8.3}$$

where $A' = (B') \times L'$ is the effective area of the footing.

The maximum vertical load P_{max} that can be applied on the footing is the peak load (curves 1 and 2) or the load at which settlement continues to increase with little or no further increase in the load (curve 3). When these conditions are reached, the footing is considered to have failed. In other words, the applied load becomes equal to the ultimate bearing capacity of the footing (Q_{ult}). That is,

$$Q_{ult} = q_{ult} \times A' = P_{max} = (q_o)_{max} \times A' = Q_N = q_N \times A' \tag{8.4}$$

where q_{ult}, = uniform unit ultimate bearing capacity = Q_{ult}/A' for WSD; q_N = uniform unit nominal bearing resistance in compression = Q_N/A'; $(q_o)_{max}$ = equivalent uniform contact or bearing stress = P_{max}/A'; and A' = effective footing width = $B' \times L'$.

In this case as the load is applied concentrically, $A' = A = B \times L$.

As stated earlier, the "nominal resistance" in LRFD is synonymous with the "ultimate capacity" in WSD. Therefore, ultimate capacities and nominal resistances are used interchangeably in this section and applicable to both WSD and LRFD. Distinctions in other geotechnical parameters, when necessary, are clearly noted.

With reference to Figure 8.3, it should be noted that

- For a given footing size, the settlement at which the applied uniform contact stress (q_o) becomes equal to the ultimate unit bearing capacity (q_{ult}) of the footing, as defined earlier, depends on the types and conditions of the foundation soils and the rate of loading.
- The total settlement at which the applied uniform contact stress (q_o) becomes equal to the ultimate unit bearing capacity (q_{ult}) depends on the effective width (B'). The larger the footing the greater is the settlement at which a footing reaches one of its failure states, as shown in Figure 8.4. If one

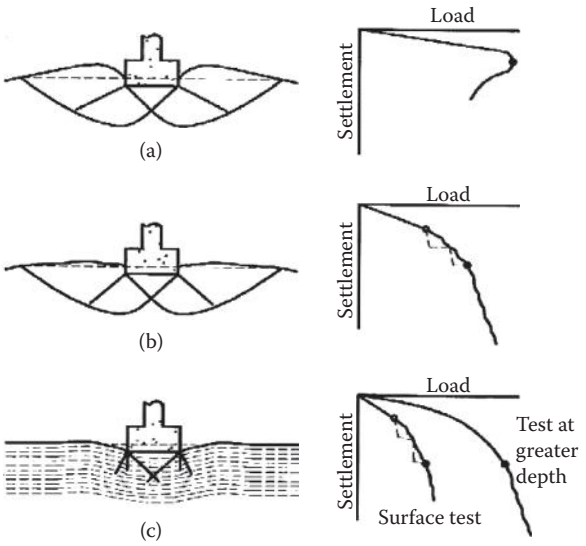

FIGURE 8.4 Bearing capacity failure modes for shallow foundations. (a) General shear; (b) local shear; and (c) punching shear. (Adapted from Vesic, A. S., *Foundation Engineering Handbook*, Edited by Winterkorn, H. F. and Fang, H. Y., Van Nostrand Reinhold Company, 1975.)

of these states is reached, the footing is said to have failed in bearing capacity. For all practical purposes, the corresponding settlement is very large and is not a consideration in that required safety against reaching such a state is provided by the FS in WSD and by the combination of load and resistance factors in LRFD strength and extreme limit states.

Model (Vesic 1963) and centrifuge (Kutter et al. 1988) testing has shown that settlement of spread footing foundation ranges from approximately 5% B' in dense soil to 20% B' in loose soils. In practice, an average settlement of approximately 10% B' is often considered at the failure settlement for spread footings as well as base failures of deep foundations (Randolph 2003). Therefore, it is clear that the total settlement at which spread footings, except those with very small width, fail is generally very large compared to the settlement that can be permitted to occur to maintain the serviceability of the supported structures, including bridges.

It should however be noted that the bearing capacity estimated based on the theoretical methods discussed later corresponds to this large displacement. The generally used FS in WSD and the load and resistance factors for stability analyses are based on the ultimate capacities. As such, the use of any other arbitrary definition of bearing capacity, such as that corresponding to a relatively small magnitude of the footing or support settlement (such as 0.5 or 1.0 in.), is inappropriate for use with the currently recommended factors of safety and/or the load and resistance factors for foundation design. This misleading concept is probably the result of misunderstanding on the use of such definitions in the past for recommending and use of the so-called presumptive bearing capacity that was developed based on limiting settlement to some small magnitude such as 0.5 or 1.0 in. (Scott and Schoustra 1968; Lambe and Whiteman 1979; Terzaghi et al. 1996). The "presumptive bearing capacity" is in fact a misnomer, which should be referred as the "presumptive allowable or permissible bearing stress" due to design load in WSD and the design service (or unfactored load) in LRFD to be accurate.

As discussed earlier, to achieve an acceptable degree of reliability or confidence in the design against shear failure, the bearing capacity of the footing that can be used in the WSD design reduces to some lower value by dividing by the FS. The corresponding reduced unit bearing capacity is termed as the "allowable unit bearing capacity" $(q_a)_c$ in WSD. The footing is sized so that the applied maximum

uniform contact or bearing stress $(q_o)_{max}$ due to service load is equal to or less than the $(q_a)_c$. That is, for WSD,

$$(q_o)_{max} \le (q_a)_c = \frac{q_{ult}}{FS} \tag{8.5}$$

In LRFD the nominal bearing resistance used in the design is reduced by multiplying by the resistance factor (ϕ_b). This reduced bearing capacity is termed as the "factored nominal unit bearing resistance" (q_R). This footing is designed such that the factored maximum uniform contact or bearing stress, which can be designed as $(q_o)_{max-f}$ for the strength as well as the extreme limit states, is equal to or less than the reduced or factored unit bearing capacity (q_R). That is, for LRFD,

$$(q_o)_{max-f}\left(\frac{P_f}{A'_f}\right) \le q_R = \varphi_b q_N \tag{8.6}$$

It should be noted that $(q_o)_{max}$ in Equation 8.5 is based on the working or design load used in WSD. In Equation 8.6, the applied maximum equivalent contact stress $(q_o)_{max\text{-}f}$ is based on the design factored load (P_f) and A'_f is the corresponding effective footing area for the LRFD strength limit state.

It is important to recognize that both the permissible total and the differential settlement for structures should not depend on the footing size, rather on some factors such as the span length, esthetics, and so on, discussed earlier that are related to the type and other characteristics, and use of the supported structure. Thus, for a given structure, the maximum amount of both total and differential settlement need to be defined in terms of some limiting values that should not depend on the size of the footing or even the foundation type.

It is also clear from above that if the footing sizes at the different supports of a given structure are different, $(q_a)_c$, and thus $(q_o)_{max}$, used on WSD will be different for different footings even for the same foundation soil conditions. In this case if the footings at each support are loaded up to the corresponding $(q_o)_{max}$, the corresponding settlement at each support is most likely to be different. Furthermore, contact or bearing stress–settlement curves are highly nonlinear and their shape depends on the types and conditions of the foundation soils. As a result it is not possible to design spread footings based only on $(q_a)_c$ in order to be able to limit the maximum total settlement under the service load to the specified permissible limit (s_{perm}), which should be the same for all the supports to reduce the risk of unacceptable different settlements between supports.

Therefore, in both WSD and LRFD service limit state design considerations must be given to limit the total settlement to the same predetermined value or the permissible settlement limit (s_{perm}) at each support irrespective of the footing size and the foundation soil conditions. This is achieved by first evaluating the maximum equivalent uniform contact stress $(q_a)_s$ or q_{perm} that can be applied on the footing without exceeding the specified permissible settlement limit (s_{perm}), as shown in Figure 8.5. Thus, for WSD,

$$(q_o)_{max} \le (q_a)_s \tag{8.7}$$

For LRFD service limit state,

$$(q_o)_{max} \le q_{perm} = \frac{P_s}{A'_s} \tag{8.8}$$

where P_s is the total net design vertical load on the footing and A'_s is the corresponding effective footing area for LRFD service limit state.

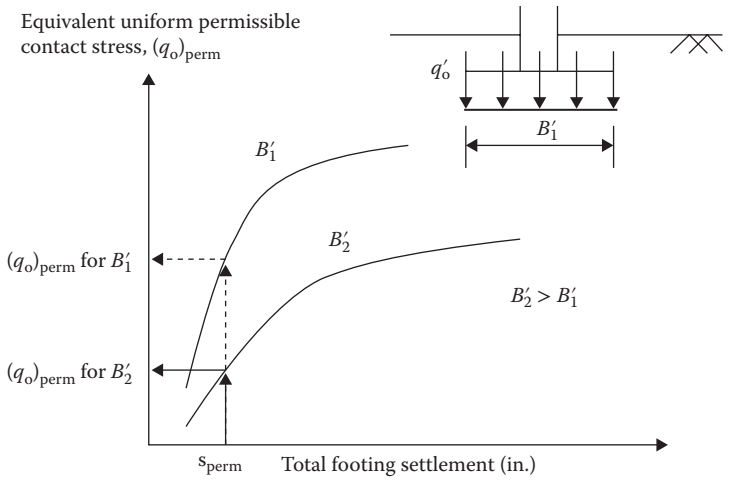

FIGURE 8.5 Plots of equivalent uniform permissible contact stress versus the footing effective width (B').

Note that unlike LRFD where the design loads for the standard static design (i.e., service and strength limit states) are different, there is only one value for the design load in WSD. Thus, the corresponding applied maximum equivalent uniform contact stress $(q_o)_{max}$ must be less than both $(q_a)_c$ and $(q_a)_s$. In other words, the footing must be designed such that $(q_o)_{max}$ is less than or equal to the lower of $(q_a)_c$ and $(q_a)_s$. Traditionally, the lower of the two parameters $(q_a)_c$ and $(q_a)_s$ has been misleadingly termed as the "footing allowable bearing capacity." This has often been the cause of confusion. Herein, the lower of these two parameters is termed as the "allowable contact or bearing stress" (q_a). That is

$$q_a = \text{lower of } \left(q_a\right)_c \text{ and } \left(q_a\right)_s \tag{8.9}$$

For WSD, the footing design requirements to meet both the safety by an FS (i.e., Equation 8.5) and the serviceability requirement as specified by a limiting settlement s_{perm} (i.e., Equation 8.7), can be replaced with the following requirement:

$$(q_o)_{max} \leq q_a \tag{8.10}$$

It should be noted that if the footing is designed by satisfying the above either WSD or LRFD bearing stability and the limiting settlement requirements, it is neither necessary nor appropriate to consider the amount of settlement, however high it may be, at which shear failure of the footing occurs. Only exception would be if the footing unit ultimate bearing capacity (q_{ult}) or the nominal unit bearing resistance (q_N) of the footing is defined based on the settlement criteria and the corresponding FS and resistance factor (ϕ_b) are specified by considering the associated definition of the footing capacity. At this time, this not a common practice for the design of spread footing foundations.

For the same reason, the deformations at which the ultimate capacity or nominal resistance against any of the other modes of failure or stability conditions are not a design consideration. Such deformations constitute failure, and the requited safeguard is provided by the FS in WSD and by the load and resistance factors in LRFD.

In determining the footing bearing capacity in this example, we can include in the ultimate uniform contact stress $(q_o)_{max}$ the loads due to the structure component of the footing and the soils above the footing area of the footing with the structure load. In this case, the term "gross" is used as an adjective to the bearing capacities discussed earlier. If the $(q_o)_{max}$ were due to the structure load only, the unit bearing capacity (q_{ult}) evaluated above would termed as the "net" ultimate unit bearing capacity. For ease of

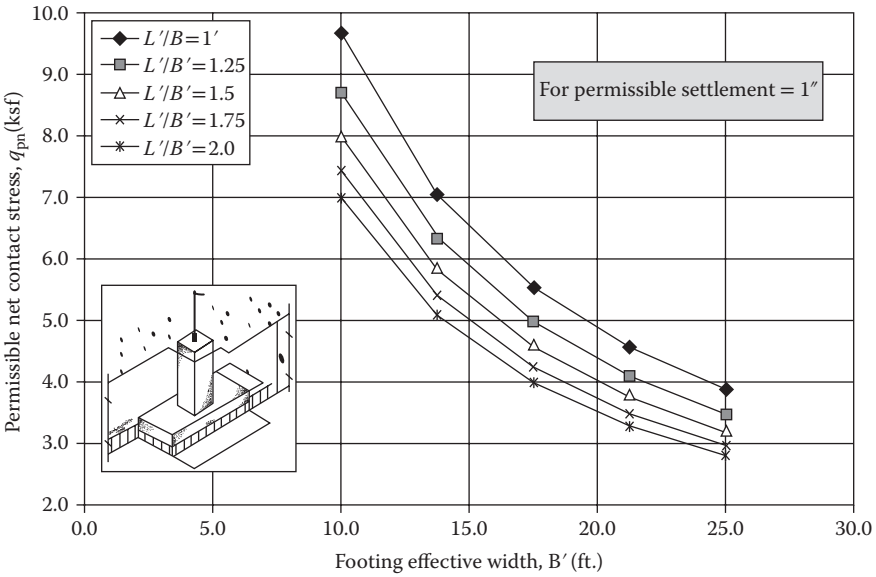

FIGURE 8.6 Schematic plots of permissible equivalent uniform contact stress versus footing effective width (B').

calculations and design, and sometimes due to small differences between the two conditions, the gross bearing capacities are generally in the analysis and design for spread foundations for bridge structures.

It should be noted that the soil settlement depends on the net stress increases. Thus, unlike bearing stability, net bearing stresses should be used in the settlement analysis. However, often when footings are founded on relatively shallow depth, differences settlement estimated by using net and gross applied bearing stresses may be small.

In general, shallow foundations design should start with establishing the appropriate embedment depth of the footing (D) and making a rough estimation of the likely range of the footing size or the width.

In LRFD, the next step is to develop plots of the the permissible equivalent uniform contact stress (qo) perm and equivalent uniform factored nominal bearing resistance (qR) as a function of the footing effective width (B), as shown in Figures 8.6 and 8.7, respectively. Similar plots can be developed for the WSD.

For rectangular footing, these plots should be generated for a range of the footing effective length to the effective width ratio L'/B'. In addition to the embedment depth D, information necessary to develop these plots include the permissible settlement limit (s_{perm}), the resistance factor (ϕ_b), and the foundation soil profile with appropriate design soil parameters.

The range of the effective with (B') can be selected based on preliminary site conditions and the loads. It should be noted that the footing width used in the geotechnical analysis and design calculations is the effective width (B'). Thus, unless noted otherwise, the footing width (B) throughout this chapter refers to the effective width (B'). However, in structural analysis and design of the footing, the actual width (B) is used. For concentrically loaded footings, the effective width is the same as the total width.

8.4 Rotational Stability

Over the years, the analysis methodologies and design requirements for rotational stability spread footings, resulting in the tilting failure of the supported structure have been inconsistent and major sources of confusion. Tschebotarioff (1970) presents several cases of bridge abutment failures due to rotational failure of spread footing foundations. Bowles (1982) reported that five different methods are available in the literature for evaluating rotations, none of them were in good agreement with one another. Earlier textbooks on foundation design (e.g., Tschebotarioff 1951; Karol 1960) analyzed such stabilities

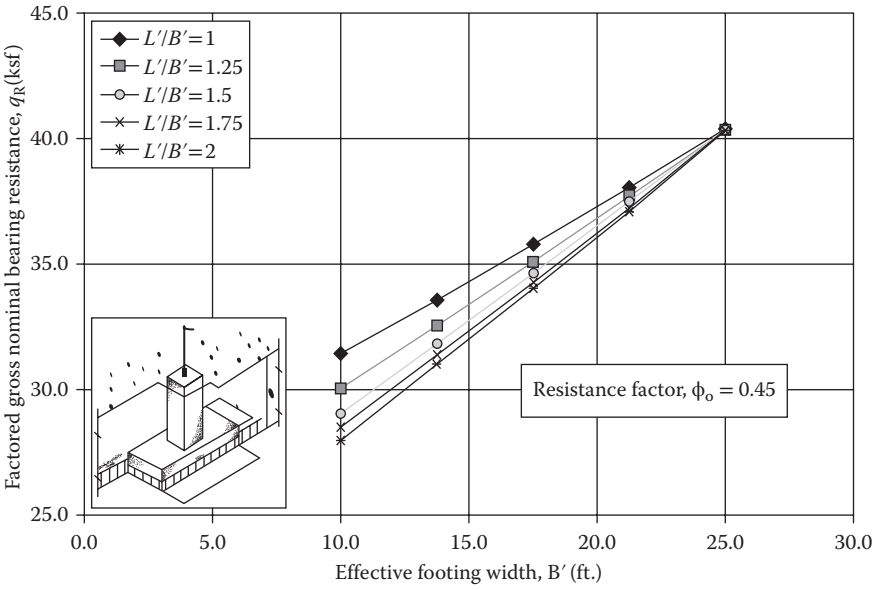

FIGURE 8.7 Schematic plots of equivalent uniform factored gross nominal bearing resistance versus footing effective width (B').

as overturning stability. Stability was achieved by using an FS against overturning defined as the ratio of moment due to the destabilizing forces to that due to the resisting forces about the toe of the footing.

Many later literatures (e.g., NAVFAC 1986, Bowles 1988, AASHTO 2002) included a limiting eccentricity requirement as an additional design requirement to ensure stability against overturning failure. Most recent literatures (AASHTO 2012; USACE 2005) require that the design meet only the minimum eccentricity requirements, whereas some recent texts still require meeting both the moment FS and the eccentricity requirements (AASHTO 2002). On the basis of Bowles (1989) designing footing by limiting the eccentricity to the commonly recommended value of $B/6$ is not sufficient to limit base rotation. Bowles (1989) recommends limiting the maximum contact stress such that the ratio of average contact stress for the entire footing to the maximum contact stress for the eccentrically loaded footing will be greater than 0.5. This lateral recommendation has been mostly ignored in practice resulting in unacceptable rotation of many constructed structures.

Before the current LRFD, AASHTO included ASD, which is the same as WSD, and the load factor design (LFD) for bridge foundations. For the LFD, to account for the *Effects of Load Eccentricity*, AASHTO (2002) specifies that footings under eccentric loading shall be designed to ensure that (1) the product of the (ultimate) bearing capacity (of the effective footing) and an appropriate performance factor exceeds the effects of vertical design loads and (2) eccentricity of loading, evaluated based on factored loads, is less than ¼ and ⅜ of the footing dimension in any direction for footings on soil and rock, respectively. *AASHTO LRFD* (AASHTO 2012) specifies the same eccentricity requirements as in the LFD but does not include the other traditionally used requirement, that is, the moment-based FS for overturning design. The first requirement above that states the product of the bearing capacity and an appropriate performance factor exceeds the effects of the maximum bearing pressure is a new requirement and of particular interest.

USACE (2005) states that referring to the analysis performed for the determination of the resultant location for concrete hydraulic structures as the *overturning stability analysis* is a misnomer. It states that a foundation bearing, crushing of the structure toe, and/or a sliding failure will occur before the structure overturns. USACE (2005) refers to the pertinent mode of failure as the rotational failures. However, it recommends using the location of the resultant to ensure rotational stability as presented in Table 8.4.

TABLE 8.4 Requirements for Location of the Resultant—All Structures

Load Conditions	Usual Events	Unusual Events	Extreme Events
Limiting eccentricity	100% of the base in compression (i.e., $e \leq B/6$)	75% of the base in compression (i.e., $e \leq B/4$)	Resultant within base (i.e., $e < B/2$)

Source: Modified after USACE, Stability Analyses of Hydraulic Structures, EM 1110-2-2100, U.S. Army Corps of Engineers, 2005.

Based on USACE (2005), full base contact (i.e., $e \leq B/6$ is specified for usual loading; return period, $T \leq 10$ years) so that there is no chance for uplift pressure to develop in the cracks. In addition, it is also stated that this requirement will help ensure linear behavior for common loading conditions. The limiting eccentricity specified for the unusual loading (10 years $< T \leq 300$ years) permits minor nonlinear behavior. For the extreme loading ($T > 300$ years), it is stated that a shear or bearing failure will occur before overturning (i.e., rotational) failure could occur. As a result, the resultant is permitted to be anywhere within the base. The stability of the structures is said to be ensured by the safety factor requirements for other stability modes, including the limits on the allowable bearing stresses. Although USACE (2005) recognized the correct mechanism involved in the so-called overturning failure of shallow foundation–supported structures, it added more confusion by the specified design requirements and the supporting reasoning.

It is interesting to note that USACE (2005) does not mention the need for limiting the allowable bearing stresses for the usual as well as the unusual loading cases. This, however, is clearly necessary because even if the specified limiting eccentricity conditions are met, the foundation may be subjected to excessive bearing stress, especially near the toe if the vertical load is high. This aspect of the design requirements seems to have been recognized in AASHTO (2002) although the specified requirement that the product of the bearing capacity and an appropriate performance factor exceeds the effects of the maximum bearing pressure is problematic as shown later in this section.

A review of the literature to trace back the original basis for the limiting eccentricity requirements for shallow foundations will assist in the understanding of this issue.

The concept of a limiting eccentricity in the design of shallow foundations originated from the recognition, based on numerous field and laboratory observations, that shallow foundations subjected to lateral loads are susceptible to titling or rotation due to differential settlements in the transverse direction of retaining structure. This differential settlement, and hence tilting, occurs due to nonuniform contact or bearing stress distribution (Lambe and Whitman 1979; Bowles 1982) induced by the load eccentricity.

Tomlinson and Boorman (2001) in discussing the need to calculate settlement for checking the serviceability limit state design pointed out that excessive tilting of the foundation will cause an increase in eccentricity and result in even higher edge pressures. This can lead to yielding or bearing failure of the soils underneath the edge causing the shallow foundation and any supported structure to fail what would appear to be a rotational (or overturning)-type failure. It is important to understand that although the footing or the structure fails in the form for excessive rotation, the soils underneath the footing edge fail in shear or bearing capacity due to excessive bearing stress in compression, as shown in Figure 8.7.

A large eccentricity is neither necessary nor a sufficient cause for soil yielding or bearing failure to occur underneath the footing toe. It is the combination of the eccentricity and the vertical load that exerts higher contact or bearing stress and cause the soil to yield underneath the toe and ultimately resulting in a rotational failure of the structure. More generally, excessive contact bearing stress solely due a concentrically load spread footing (i.e., $e = 0$) causes a bearing failure of the footing in the traditional sense. As the eccentricity increases above zero, bearing stresses becomes progressively more nonuniform leading, and finally depending on the magnitude of the vertical load, to yielding or bearing failure of the soil underneath the edge. A low vertical load is not likely to cause rotational failure even if the eccentricity is very high. In this case, it is more likely a sliding failure will occur. The other extreme is the traditional bearing failure when vertical load is very high, but the eccentricity is either zero or very low.

Note that in Figure 8.8, rotational failure of the footing occurs due to bearing capacity failure in local shear of the soils underneath the toe area due to excessive nonuniform contact stress resulting from eccentric loading. As the footing tilts, its base, at least some part of it, maintains in firm contact with the foundation soils at all times and does not "overturn" by rotating about a point at the toe. Thus, it is necessary to consider the so-called overturning failure of spread footing as a *soil bearing capacity failure in local shear* as discussed below.

The type of footing behavior discussed earlier is similar to the familiar and widely used axial load (P) and moment interaction (M) curve used in determining the capacities of structural elements. The main difference is that soils cannot support tension or flexural loading. Spread footing foundations resist any unbalanced moment by developing nonuniform distribution of the compressive contact or bearing stress. Foundation failures always occur due the failure of soils in shear. Thus, the moment equilibrium methodology, which does not consider the shear failure of soils, is not reliable in ensuring the stability of the footing against rotational failure.

Furthermore, as pointed out by Bowles (1995), for a footing designed to support a concentrically applied vertical service load (P_s) corresponding to a uniform permissible bearing stress (q_{perm}), if due to lateral load the eccentricity increases to $e = B/6$, the maximum bearing stress at toe q_{max} will be equal to $2q_{perm}$ and q_{min} at the will be equal to zero.

The recommendation that the eccentricity (e) for shallow foundations in soils be limited to $B/6$ was based on the postulation that the q_{max} will be limited to two times the q_{perm} and that for this nonuniform bearing stress conditions the resulting rotation or tilting of shallow foundations when founded on competent soils will be within tolerable or permissible limit. Furthermore, if the footing design was controlled by the allowable bearing capacity (q_a) with an FS $\geq$ 3.0, for eccentricity, $e = B/6$, q_{max} will be equal to two times q_a. That is, the FS against bearing capacity failure of the toe is $\geq$1.5, which was considered acceptable against overturning failure. The original and main purpose, however, was to simplify the design so that detailed analysis for evaluating tilting or rotation, which often can be complex, will not be necessary when footings are founded in competent soils. However, to evaluate the estimated or

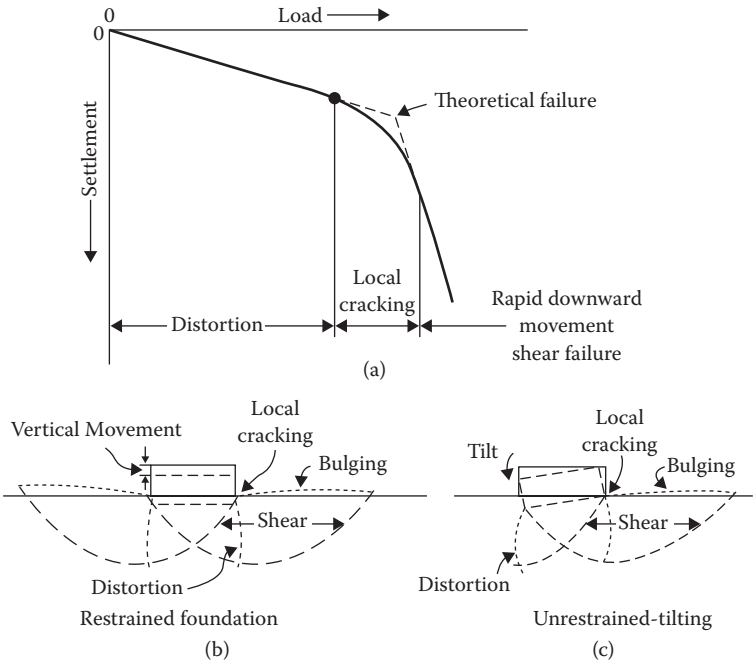

FIGURE 8.8 Bearing capacity failures. (a) Load–settlement curve; (b) shear failures; and (c) rotational ("overturning") failure. (Modified after Sowers, G. F., and Vesic, A. B., *Highway Research Board Bulletin*, No. 342, 1962.)

expected rotation or tilting due to eccentric loading, detailed differential settlement analysis should be performed when foundation soil conditions are highly variable, for critical structure, and footings founded on weak or more compressible soils.

The above limiting eccentricity requirement for footings founded on soils started as a simplified substitute analysis method for evaluating differential settlement or tilting of footing was soon specified as a check against overturning failure. The concept of limiting eccentricity was then extended for footings founded on rock and misleadingly for seismic design (NCHRP 1991; AASHTO 2002) and more recently for each of the three LRFD limit states (AASHTO 2012) for bridge foundation design.

The widely recommended practice of limiting load eccentricity although results in a design with adequate stability against rotation when footings are founded on competent soils, it cannot ensure rotational stability when footings are founded on more compressible soils. Most significantly, the limiting eccentricity requirement is based on limiting differential settlement, which is a service limit state design parameter, Therefore, in LRFD use of the limiting eccentricity requirements must be limited to service limit states design to limit differential settlement of the footing and thus rotation or tilting of the supported structure. Rotational stability under the factored load must be ensured by evaluating the shear failure of the soils due to excessive factored contact or bearing stress for both the strength and the extreme limit states design.

On the basis of the above discussion, stability against both traditional bearing capacity failure and rotational failure will be prevented provided shallow foundations are designed to achieve adequate FS against soil bearing failures evaluated by considering all possible combinations of the total vertical loads and the eccentricities of the resultant loads.

In summary, the requirements that the eccentricity (e) of $B/6$ and $B/4$ are appropriate for use in the WSD and LRFD service limit state design of shallow foundations in competent soils with low compressibility and rock, respectively. The rotational stability evaluation of shallow foundations for seismic and LRFD strength and extreme limit state design should be performed based on the evaluation of the soil bearing stability under the extreme eccentricity and total vertical load combinations. The design must ensure that the maximum factored uniform bearing stress $(q_o)_{max}$ is less than or equal to the factored uniform nominal bearing resistance for all possible combinations of the factored vertical loads and the eccentricities of the factored resultant load.

Finally, it should be noted that tilting failure of spread footing supported structures can also occur due to the global slope stability–type failures. However, the failure mechanism in this case is different than that involved in tilting failure discussed earlier, which occurs due to excessive rotation of the footing due to load eccentric loading. Eccentric loading is not necessary to cause tilting failure associated with the global slope failure and the titling in the case is generally inwards, that is toward the slope or the retained ground. Furthermore, spread footing rotation resulting in the inward tilting of earth retaining structures such as bridge abutments can also occur due to the settlement of the heel when compressible soil are present below the foundation (Bowles 1982).

8.5 Bearing Capacity for Shallow Foundations

8.5.1 Static Bearing Capacity—Theoretical Methods

This section deals with the ultimate bearing (q_{ult}) of shallow foundations under compression loading. The nominal bearing resistance in compression (q_n) in the LRFD is synonymous with q_{ult} in the WSD.

The foundation soils underneath a spread footing subjected to compression loading can be failure in three different shear mechanisms. The corresponding bearing capacity failures are referred to as (1) general shear failure, (2) local shear failure, and (3) punching shear failure as shown in Figure 8.4. The shear mechanism by which a given footing is likely to fail depends mainly on the density of the foundation soils and the footing depth to width ratio (D/B') as shown in Figure 8.9.

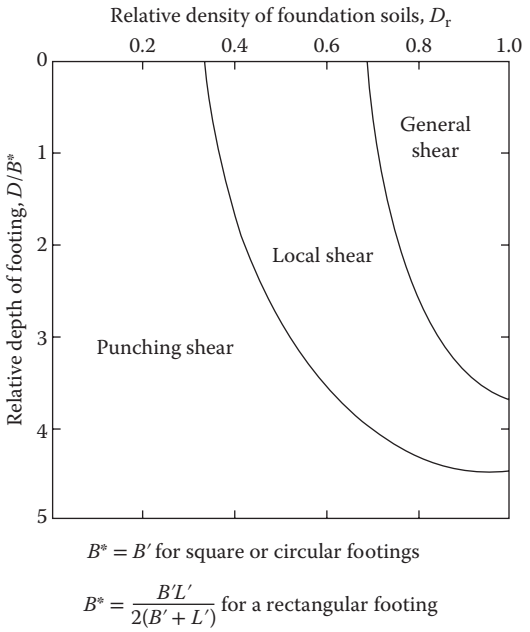

FIGURE 8.9 Modes of bearing capacity failure of spread footing in sand. (After Vesic, A. S., *Foundation Engineering Handbook*, Edited by Winterkorn, H. F. and Fang, H. Y., Van Nostrand Reinhold Company, 1975.)

8.5.1.1 Bearing Capacity Failure in General Shear

The computation of q_{ult} for shallow foundations on soil can be considered as an elastic–plastic kinematic equilibrium problem. However, what hinders us from finding closed form analytical solutions is the difficulty in the selection of a mathematical model of soil constitutive relationships. Bearing capacity theory is still limited to solutions established for the rigid plastic solid of the classic theory of plasticity. Consequently, only approximate methods are currently available for solving the problem. Prandtl (1924) and Reissner (1924) developed kinematic conditions and solutions to the bearing capacity problem by considering a uniform, rigid plastic, weightless soil. Terzaghi and Peck (1948) defined three different zones of plastic failures under a footing experiencing bearing capacity failure in general shear as shown in Figure 8.10.

A strip or continuous footings is a shallow footing with $L'/B' \geq 5$. Based on the work by Prandtl (1920), Reissner (1924), and others, the gross ultimate bearing capacity in compression (q_{ult}) of a centrically loaded strip footing is given by

$$q_{ult} = q_N = cN_c + qN_q + 0.5\gamma B'N_\gamma \tag{8.11}$$

where c is the soil cohesion, q the overburden stress at the level of the footing bottom ($\gamma_e D$), γ_e the unit weight of the soil above the footing bottom, and γ_g the unit weight of the soil below the footing, and B' is the effective width of the strip footing. The parameters N_c, N_q, and N_γ are bearing capacity factors defined as functions of the friction angle of the foundation soils (φ) as presented below.

$$N_q = \text{bearing capacity factor related to surcharge } (\overline{q})$$

$$= \left(e^{\pi \tan\varphi}\right) \tan^2\left(45^o + \frac{\varphi}{2}\right) \tag{8.12}$$

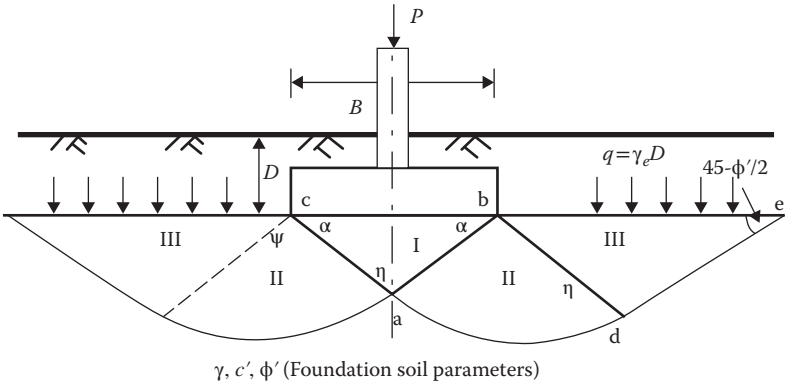

FIGURE 8.10 General shear failures.

$$N_c = \text{bearing capacity factor related to cohesion } (c)$$

$$= (N_q - 1)\cot\varphi, \quad \text{for } \varphi > 0$$

$$= (2 + \pi) = 5.14, \quad \text{for } \phi = 0.0, \text{ and}$$

$$N_\gamma = \text{bearing capacity factor related to soil unit weight } (\gamma)$$

$$= 2\,(N_q + 1)\tan\varphi$$

The three N factors are used to represent the influence of the cohesion (N_c), unit weight (N_γ), and overburden pressure (N_q) of the soil on bearing capacity. The above bearing capacity factor N_γ was developed by Caquot and Kerisel (1948). Values of the above bearing capacity factors are presented in Table 8.5 and Figure 8.11.

For long-term analyses, the friction of the above bearing capacity equations is the effective or drained friction angle (φ' and $c = c'$, where c' is the effective cohesion that in general should be taken as equal to 0.0 for soils. In this case, the term q in the second term of the Equation 8.11 is the effective overburden stress (q') at the bottom of the footing. Thus for long-term bearing capacity, the ultimate bearing capacity equation for strip footing founded on soil is given by

$$q_{ult} = q_N = q'N_q + 0.5\gamma B'N_\gamma \tag{8.13}$$

If the strip footing is founded on fine-grained or clay soils, the short-term ultimate bearing capacity may be obtained from Equation 8.11 by replacing cohesion (c) with the soil undrained shear strength (s_u), and $N_c = 5.14$, $N_\gamma = 0.0$ $N_q = 1.0$ from Figure 8.11 because in this case the friction angle, $\varphi = 0.0$. That is,

$$q_{ult} = q_N = s_u N_c + qN_q \tag{8.14a}$$

$$q_{ult} = q_N = 5.14\ S_u + q \tag{8.14b}$$

In the Equation 8.14, q is the total overburden stress at the bottom of the footing.

Once the ultimate gross bearing capacity or the nominal bearing resistance in compression is known, the unit gross allowable bearing capacity (q_a) as well as the unit factored nominal resistance (q_R) can be determined as follows:

$$q_a = \frac{q_{ult}}{FS} \tag{8.15}$$

and

$$q_R = \phi_b q_N \tag{8.16}$$

TABLE 8.5 Values of the Bearing Capacity Factors in Equation 8.13

φ	N_c	N_q	N_γ	φ	N_c	N_q	N_γ
0	5.14	1.00	0.00	26	22.25	11.85	12.54
1	5.38	1.09	0.07	27	23.94	13.20	14.47
2	5.63	1.20	0.15	28	25.80	14.72	16.72
3	5.90	1.31	0.24	29	27.86	16.44	19.34
4	6.19	1.43	0.34	30	30.14	18.40	22.40
5	6.49	1.57	0.45	31	32.67		25.99
6	6.81	1.72	0.57	32	35.49	23.18	30.22
7	7.16	1.88	0.71	33	38.64	26.09	35.19
8	7.53	2.06	0.86	34	42.16	29.44	41.06
9	7.92	2.25	1.03	35	46.12	33.30	48.03
10	8.35	2.47	1.22	36	50.59	37.75	56.31
11	8.80	2.71	1.44	37	55.63	42.92	66.19
12	9.28	2.97	1.69	38	61.35	48.93	78.03
13	9.81	3.26	1.97	39	67.87	55.96	92.25
14	10.37	3.59	2.29	40	75.31	64.20	109.41
15	10.98	3.94	2.65	41	83.86	73.90	130.22
16	11.63	4.34	3.06	42	93.71	85.38	155.55
17	12.34	4.77	3.53	43	105.11	99.02	186.54
18	13.10	5.26	4.07	44	118.37	115.31	224.64
19	13.93	5.80	4.68	45	133.88	134.88	271.76
20	14.83	6.40	5.39	46	152.10	158.51	330.35
21	15.82	7.07	6.20	47	173.64	187.21	403.67
22	16.88	7.82	7.13	48	199.26	222.31	496.01
23	18.05	8.66	8.20	49	229.93	265.51	613.16
24	19.32	9.60	9.44	50	266.89	319.07	762.89
25	20.72	10.66	10.88	—	—	—	—

Source: Data from AASHTO, *AASHTO LRFD Bridge Design Specifications*, Customary U.S. Units, 2012, American Association of State Highway and Transportation Officials, Washington D.C., 2012.

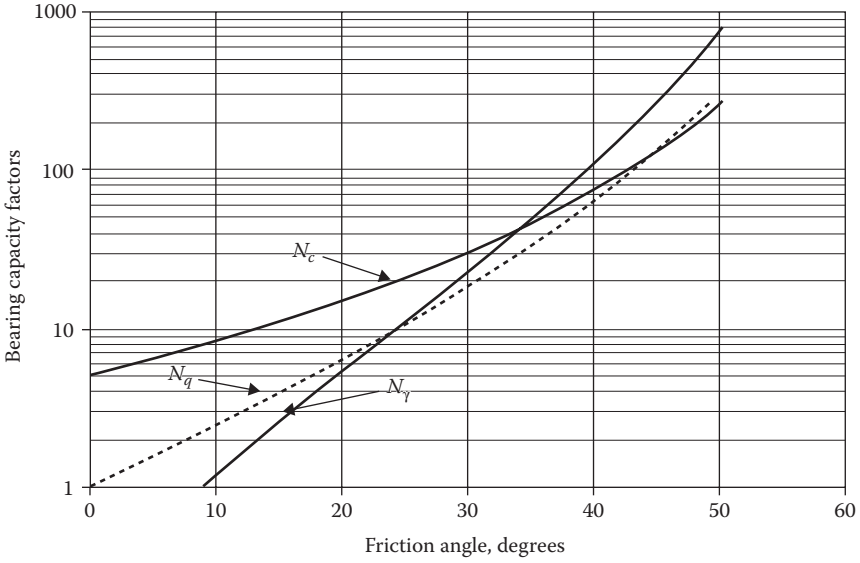

FIGURE 8.11 Bearing capacity factors N_c, N_q, and N_γ as functions of the friction angle.

For simplicity, the q_{ult} will be used in the rest of this chapter to represent both the ultimate bearing capacity for use in WSD and the nominal bearing resistance in compression (q_N) for use in LRFD.

One of the well-known more generalized bearing capacity equations applicable to strip, round as well as rectangular footings, is the well-known Terzaghi's equation (Terzaghi 1943), which can be written as

$$q_{ult} = cN_c s_c + \bar{q}N_q s_q + 0.5\gamma B' N_\gamma s_\gamma \tag{8.17}$$

The values of the N parameters for use in Equation 8.17 are provided in Table 8.6.

The factors, s_c, s_q, and s_γ are shape correction factors as defined below.

- For free draining coarse-grained soils and long-term or drained bearing capacity in saturated fine-grained soils (i.e., when $c' = 0.0$),

$$s_c = 1 + \left(\frac{B'}{L'}\right)\left(\frac{N_q}{N_c}\right), \quad \frac{s_q = 1 + (B'/L')\tan\phi}{s_\gamma = 1 - 0.4(B'/L')} \tag{8.18}$$

- For short-term or undrained bearing capacity in saturated fine-grained soils (i.e., $\phi = 0$),

$$s_c = 1 + \left(\frac{B'}{5L'}\right), \quad s_q = 1, \quad \text{and } s_\gamma = 1 \tag{8.19}$$

The values of the shape correction parameters s_c and s_r for strip, round, and square footings are presented in Table 8.7.

The bearing capacity equations presented earlier are valid only for the general shear failure case shown in Figures 8.3 and 8.10. The assumptions used in the development of these equations include the following:

- The footing base is rough and the soil beneath the base is incompressible, which implies that the wedge abc (zone I) in Figure 8.10 is no longer an active Rankine zone but is in an elastic state. Consequently, zone I must move together with the footing base.

TABLE 8.6 Bearing Capacity Factors for the Terzaghi Equation 8.17

φ (degree)	N_c	N_q	N_γ	$K_{p\gamma}$
0	5.7[a]	1.0	0	10.8
5	7.3	1.6	0.5	12.2
10	9.6	2.7	1.2	14.7
15	12.9	4.4	2.5	18.6
20	17.7	7.4	5.0	25.0
25	25.1	12.7	9.7	35.0
30	37.2	22.5	19.7	52.0
34	52.6	36.5	36.0	—
35	57.8	41.4	42.4	82.0
40	95.7	81.3	100.4	141.0
45	172.3	173.3	297.5	298.0
48	258.3	287.9	780.1	—
50	347.5	415.1	1153.2	800.0

Source: After Bowles, J. E., *Foundation Analysis and Design*, Fifth Edition, McGraw-Hill Companies, Inc., 1996.

Note: Values of N_γ for φ of 0°, 34°, and 48° are original Terzaghi values and used to back-compute $K_{p\gamma}$.

[a] $N_c = 1.5\pi + 1$ (Terzaghi 1943, p. 127).

TABLE 8.7 Shape Factors for the Terzaghi Equation 8.17

	Footing Shape		
Shape Factor	Strip	Round	Square
s_c	1.0	1.3	1.3
s_γ	1.0	0.6	0.8

Source: After Terzaghi, K., *Theoretical Soil Mechanics*, John Wiley & Sons, New York, 1943.

- Zone II in Figure 8.10 is an immediate state lying on a log spiral arc ad.
- Zone III is a passive Rankine zone and is in a plastic state bounded by a straight line ed.
- The shear resistance along bd is neglected because the equation was intended for footings where $D < B'$.

Meyerhof (1951, 1963), Hansen (1970), and Vesic (1973, 1975) further extended Terzaghi's bearing capacity equation by including footing shape factor (s_i), footing embedment depth factor (d_i), load inclination factor (i_i), sloping ground factor (g_i), and tilted base factor (b_i). Chen (1975) reevaluated N factors in Terzaghi's equation using limit analysis method. These efforts resulted in significant extensions of Terzaghi's bearing capacity equation. The general form of the bearing capacity equation (Hansen 1970; Vesic 1973, 1975) can be expressed as

$$q_{\text{ult}} = cN_c s_c d_c i_c g_c b_c + \bar{q} N_q s_q d_q b_q + 0.5\gamma B' N_\gamma s_\gamma d_\gamma i_\gamma g_\gamma b_\gamma \tag{8.20}$$

Values of bearing capacity factors N_c, N_q, and N_γ can be found in Table 8.8. Values of the other factors are summarized in Table 8.9.

For saturated cohesive soils under short-term conditions, $c = s_u$ and $\varphi = 0$. For the ultimate short-term bearing capacity of spread footing founded in this type of soil, Equation 8.20 reduces to

$$q_{\text{ult}} = 5.14 s_{\text{u}} (1 + s'_c + d'_c - i'_c - b'_c - g'_c) + \bar{q} \tag{8.21}$$

where s_{u} is the undrained shear strength of cohesive soils.

As shown in Table 8.8, N_c and N_q are the same as proposed by Meyerhof (1963), Hansen (1970), Vesic (1973), or Chen (1975). Nevertheless, there is a wide range of values for N_γ as suggested by different authors. Meyerhof (1963) and Hansen (1970) use the plain-strain value of φ, which may be up to 10% higher than those obtained from the conventional triaxial tests. Vesic (1975) argued that a shear failure in soil under the footing is a process of progressive rupture at variable stress levels, and an average mean normal stress should be used for bearing capacity computations. Another reason causing the differences in the N_γ value is how to evaluate the impact of the soil compressibility on bearing capacity computations. The value of N_γ still remains controversial because rigorous theoretical solutions are not available. In addition, comparisons of predicted solutions against model footing test results are inconclusive.

8.5.1.2 Local and Punching Shear Failures

The bearing capacity equations presented above are applicable to the footings when the failure mode is one of the general shear failure types. On the basis of Terzaghi (1943), the above bearing capacity equation may be used to evaluate the bearing capacity footings that is predicted to fail in one of the other two modes of shear failures shown in Figure 8.3 provided the shear strength parameters c and φ of the foundation soil are reduced as follows:

$$c^* = 0.67c \tag{8.22}$$

$$\varphi^* = \tan^{-1}(0.67 \tan \varphi) \tag{8.23}$$

TABLE 8.8 Bearing Capacity Factors for Equation 8.20

φ	N_c	N_q	$N_{\gamma(M)}$	$N_{\gamma(H)}$	$N_{\gamma(V)}$	$N_{\gamma(C)}$	N_q/N_c	tan φ
0	5.14	1.00	0.00	0.00	0.00	0.00	0.19	0.00
1	5.38	1.09	0.00	0.00	0.07	0.07	0.20	0.02
2	5.63	1.20	0.01	0.01	0.15	0.16	0.21	0.03
3	5.90	1.31	0.02	0.02	0.24	0.25	0.22	0.05
4	6.18	1.43	0.04	0.05	0.34	0.35	0.23	0.07
5	6.49	1.57	0.07	0.07	0.45	0.47	0.24	0.09
6	6.81	1.72	0.11	0.11	0.57	0.60	0.25	0.11
7	7.16	1.88	0.15	0.16	0.71	0.74	0.26	0.12
8	7.53	2.06	0.21	0.22	0.86	0.91	0.27	0.14
9	7.92	2.25	0.28	0.30	1.03	1.10	0.28	0.16
10	8.34	2.47	0.37	0.39	1.22	1.31	0.30	0.18
11	8.80	2.71	0.47	0.50	1.44	1.56	0.31	0.19
12	9.28	2.97	0.60	0.63	1.69	1.84	0.32	0.21
13	9.81	3.26	0.74	0.78	1.97	2.16	0.33	0.23
14	10.37	3.59	0.92	0.97	2.29	2.52	0.35	0.25
15	10.98	3.94	1.13	1.18	2.65	2.94	0.36	0.27
16	11.63	4.34	1.37	1.43	3.06	3.42	0.37	0.29
17	12.34	4.77	1.66	1.73	3.53	3.98	0.39	0.31
18	13.10	5.26	2.00	2.08	4.07	4.61	0.40	0.32
19	13.93	5.80	2.40	2.48	4.68	5.35	0.42	0.34
20	14.83	6.40	2.87	2.95	5.39	6.20	0.43	0.36
21	15.81	7.07	3.42	3.50	6.20	7.18	0.45	0.38
22	16.88	7.82	4.07	4.13	7.13	8.32	0.46	0.40
23	18.05	8.66	4.82	4.88	8.20	9.64	0.48	0.42
24	19.32	9.60	5.72	5.75	9.44	11.17	0.50	0.45
25	20.72	10.66	6.77	6.76	10.88	12.96	0.51	0.47
26	22.25	11.85	8.00	7.94	12.54	15.05	0.53	0.49
27	23.94	13.20	9.46	9.32	14.47	17.49	0.55	0.51
28	25.80	14.72	11.19	10.94	16.72	20.35	0.57	0.53
29	27.86	16.44	13.24	12.84	19.34	23.71	0.59	0.55
30	30.14	18.40	15.67	15.07	22.40	27.66	0.61	0.58
31	32.67	20.63	18.56	17.69	25.99	32.33	0.63	0.60
32	35.49	23.18	22.02	20.79	30.21	37.85	0.65	0.62
33	38.64	26.09	26.17	24.44	35.19	44.40	0.68	0.65
34	42.16	29.44	31.15	28.77	41.06	52.18	0.70	0.67
35	46.12	33.30	37.15	33.92	48.03	61.47	0.72	0.70
36	50.59	37.75	44.43	40.05	56.31	72.59	0.75	0.73
37	55.63	42.92	53.27	47.38	66.19	85.95	0.77	0.75
38	61.35	48.93	64.07	56.17	78.02	102.05	0.80	0.78
39	67.87	55.96	77.33	66.75	92.25	121.53	0.82	0.81
40	75.31	64.19	93.69	79.54	109.41	145.19	0.85	0.84
41	83.86	73.90	113.98	95.05	130.21	174.06	0.88	0.87
42	93.71	85.37	139.32	113.95	155.54	209.43	0.91	0.90
43	105.11	99.01	171.14	137.10	186.53	253.00	0.94	0.93
44	118.37	115.31	211.41	165.58	224.63	306.92	0.97	0.97
45	133.87	134.87	262.74	200.81	271.74	374.02	1.01	1.00
46	152.10	158.50	328.73	244.64	330.33	458.02	1.04	1.04
47	173.64	187.20	414.32	299.52	403.65	563.81	1.08	1.07
48	199.26	222.30	526.44	368.66	495.99	697.93	1.12	1.11
49	229.92	265.49	674.91	456.40	613.13	869.17	1.15	1.15
50	266.88	319.05	873.84	568.56	762.85	1089.46	1.20	1.19

Source: Data from Meyerhof, G. G., *Canadian Geotechnical Journal*, **I**, No. 1, pp.16–26, 1963; Hansen, B. J., *A Revised and Extended Formula for Bearing Capacity*, Bulletin No. 28, Danish Geotechnical Institute, Copenhagen, pp. 5–11, 1970; Vesic, A. S., *Foundation Engineering Handbook*, Edited by Winterkorn, H. F. and Fang, H. Y., Van Nostrand Reinhold Company, 1975; and Chen, W. F., *Limit Analysis and Soil Plasticity*, Elsevier, Amsterdam, the Netherlands, 1975.

Note: N_c and N_q are the same for all four methods; subscripts identify author for N_γ.

TABLE 8.9 Footing Shape, Footing Depth, Load Inclination, Foundation Ground (Slope) Inclination (Slope), and Footing Base Inclination Factors for Equations 8.20 and 8.21

Shape Factors	Depth Factors
$s_c = 1.0 + \frac{N_q}{N_c}\frac{B'}{L'}$ $s_c = 1.0$ (for strip footing)	$d_c = 1.0 + 0.4k$ $\begin{cases} k = \frac{D}{B'} & \text{for } \frac{D}{B'} \le 1 \\ k = \tan^{-1}\left(\frac{D}{B'}\right) & \text{for } \frac{D}{B'} > 1 \end{cases}$
$s_q = 1.0 + \frac{B'}{L'}\tan\phi$ (for all ϕ)	$d_q = 1 + 2\tan\phi(1-\sin\phi)^2 k$ (k defined above)
$s_\gamma = 1.0 - 0.4\frac{B'}{L'} \ge 0.6$	$d_\gamma = 1.00$ (for all ϕ)
Inclination Factors	**Ground Factors (Base on Slope)**
$i'_c = 1 - \frac{mHi}{A'c_a N_c}(\phi = 0)$	$g'_c = \frac{\beta}{5.14}$ β in radians $(\phi = 0)$
$i_c = i_q - \frac{1-i_q}{N_q - 1}(\phi > 0)$	$g_c = i_q - \frac{1-i_q}{5.14\tan\phi}$ $(\phi > 0)$
$i_q = \left[1.0 - \frac{H}{P + A'c_a\cot\phi}\right]^m$	$g_q = g_\gamma = (1.0 - \tan\beta)^2$ (for all ϕ)
$i_\gamma = \left[1.0 - \frac{H}{P + A'c_a\cot\phi}\right]^{m+1}$	**Base Factors (Tilted Base)**
$m = m_B = \frac{2 + B'/L'}{1 + B'/L'}$ or	$b'_c = g'_c$ $(\phi = 0)$
$m = m_L = \frac{2 + L'/B'}{1 + L'/B'}$	$b_c = 1 - \frac{2\beta}{5.14\tan\phi}$ $(\phi > 0)$
	$b_q = b_\gamma = (1.0 - \eta\tan\phi)^2$ (for all ϕ)

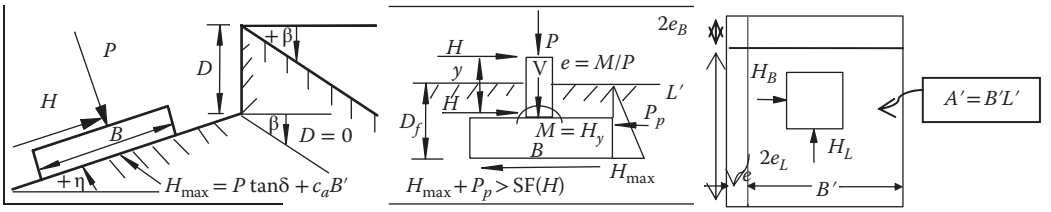

Source: After Vesic, A. S., *ASCE Journal of the Soil Mechanics and Foundation Engineering Division*, **99**, No. SM1, pp. 45–73, 1973; and Vesic, A. S., *Foundation Engineering Handbook*, Edited by Winterkorn, H. F. and Fang, H. Y., Van Nostrand Reinhold Company, 1975.

Notes:

1. When $\varphi = 0$ (and $\beta \neq 0$) use $N_\gamma = -2\sin(\pm\beta)$ in N_γ term.
2. Compute $m = m_B$ when $H_i = H_B$ (H parallel to B) and $m = m_L$ when $H_i = H_L$ (H parallel to L). For both H_B and H_L use $m = \sqrt{m_B^2 + m_L^2}$.
3. $0 \le i_q,\ i_\gamma \le 1$
4. $\beta + \eta \le 90°;\ \beta \le \phi$

where

A' = effective footing dimension as shown in Figure 8.12
D = depth from ground surface to base of footing
P = vertical load on footing
H = horizontal component of load on footing with $H_{max} \le P\tan\delta + c_a A'$
c_a = adhesion to base $(0.6c \le c_a \le 1.0c)$
δ = friction angle between base and soil $(0.5\varphi \le \delta \le \varphi)$
β = slope of ground away from base with (+) downward
η = tilt angle of base from horizontal with (+) upward $2e_B$

Vesic (1975) suggested that the above reduction of φ is too conservative. He proposed the following equation for a reduction factor for cohesionless soils that varies with the relative density D_r:

$$\phi^* = \tan^{-1}[(0.67 + D_r - 0.75D_r^2)\tan\phi] \quad (\text{for } 0 < D_r < 0.67) \tag{8.24}$$

8.5.1.3 Effects of Ground Water Table

Ultimate bearing capacity should be estimated considering the highest anticipated ground water table. When groundwater is present with the equivalent effective unit weight γ_e, as defined below, it should be used in evaluating the overburden stress $\bar{q}$ used with N_q and also to replace γ used with N_γ. As illustrated in Figure 8.12, the weighted average unit weight for the *0.5γB* term can be determined as follows:

$$\gamma = \begin{cases} \gamma_{avg} & \text{for } d_w \geq B' \\ \gamma' + (d_w/B')(\gamma_{avg} - \gamma') & \text{for } 0 < d_w < B' \\ \gamma' & \text{for } d \leq 0 \end{cases} \tag{8.25}$$

8.5.1.4 Effects of Eccentric Load

As stated earlier, for footings with eccentricity, effective footing size is determined as follows:

$$A' = B' \times L' \tag{8.26}$$

where, $B' = B - 2e_L$, and $L' = L - 2e_B$. Refer to Figures 8.1, 8.13, and 8.14 for loading definitions and footing dimensions. For example, the actual distribution of contact pressure along the *L*-direction for a rigid footing with eccentricity e_B about the *B*-axis may be obtained as follows:

$$q_{\substack{\max \\ \min}} = P(1 \pm 6e_B/L)/BL \quad (\text{for } e_B < L/6) \tag{8.27}$$

$$q_{\substack{\max \\ \min}} = \begin{cases} \dfrac{2P}{3B(L/2 - e_B)} & (\text{for } L/6 < e_B < L/2) \\ 0 \end{cases} \tag{8.28}$$

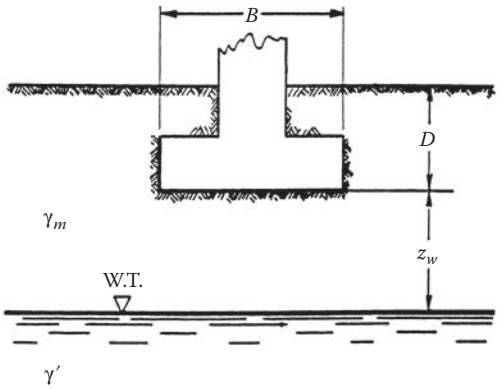

FIGURE 8.12 Influence of ground water table on bearing capacity. (After AASHTO, *Standard Specifications for Highway Bridges,* Seventeenth Edition, American Association of State Highway and Transportation Officials, Washington, DC, 2002.)

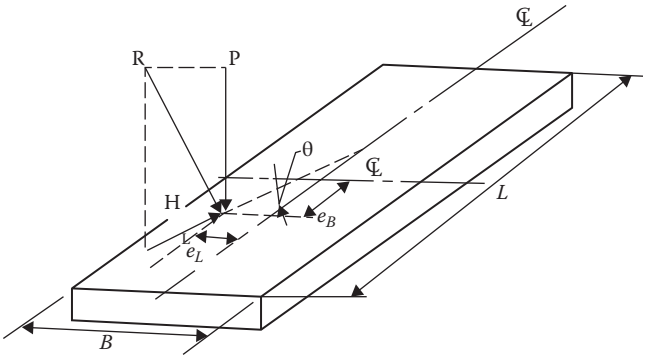

FIGURE 8.13 Method of computing effective footing dimensions for eccentrically loaded footing. (After AASHTO, *Standard Specifications for Highway Bridges,* Seventeenth Edition, American Association of State Highway and Transportation Officials, Washington, DC, 2002.)

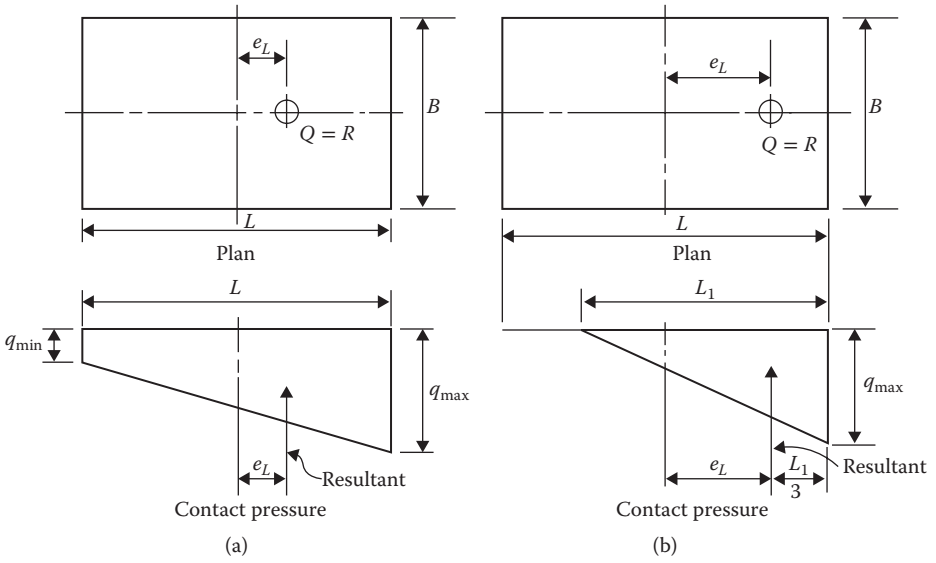

FIGURE 8.14 Contact pressure for footing loaded eccentrically about one axis. (a) For $e_L \le \frac{L}{6}$; and (b) For $\frac{L}{6} < e_L < \frac{L}{2}$. (After AASHTO, *Standard Specifications for Highway Bridges*, Seventeenth Edition, American Association of State Highway and Transportation Officials, Washington, DC, 2002.)

Contact pressure for footings with eccentric loading in the *B* direction may be determined using the above equations by replacing terms *L* with *B* and terms *B* with *L*, respectively. For an eccentricity in both the directions, reference is available in AASHTO (2002 and 2012).

8.6 Static Bearing Capacity—Empirical Methods

8.6.1 Based on Standard Penetration Tests (SPT)

Terzaghi and Peck (1948, 1967) proposed a method using SPT blow counts to estimate ultimate bearing capacity for footings on sand. Modified by Peck et al. (1974), this method is presented in the form of the chart shown in Figure 8.15. For a given combination of footing width and SPT blow counts, the chart can be used to determine the ultimate bearing pressure associated with 25.4 mm (1.0 in.) settlement.

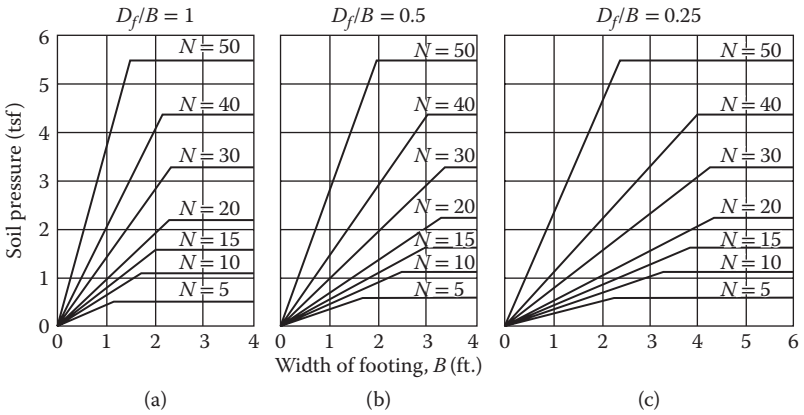

FIGURE 8.15 Design chart for proportioning shallow footings on sand. (After Peck, R. B. et al., *Foundation Engineering*, Second Edition, John Wiley & Sons, Inc., 1974.)

The design chart applies to shallow footings ($D_f \leq B'$ sitting on sand with water table at great depth. The N values used in this figure should be $(N_1)_{60}$, that is, the energy corrected to correspond to 60% of the theoretical hammer energy and normalized to an effective overburden stress of 1.0 tsf (see Skempton 1986).

Similarly, Meyerhof (1956) published the following formula for estimating ultimate bearing capacity using SPT blow counts:

$$q_{\text{ult}} = \left(N'_{\text{avg}}\right)_{60} \frac{B'}{10}\left(C_{w1} + C_{w2}\frac{D_f}{B'}\right)R_I \tag{8.29}$$

where, R_I is load inclination factor shown in Table 8.10 ($R_I = 1.0$ for vertical loads). C_{w1} and C_{w2} are correction factors whose values depend on the position of the water table:

$$\begin{cases} C_{w1} = C_{w2} = 0.5 & \text{for } D_w = 0 \\ C_{w1} = C_{w2} = 1.0 & \text{for } D_w \geq D_f + 1.5B' \\ C_{w1} = 0.5 \text{ and } C_{w2} = 1.0 & \text{for } D_w = D_f \end{cases} \tag{8.30}$$

where $\left(N'_{\text{avg}}\right)_{60}$ is the energy corrected average value of the measured corrected SPT blow counts, which is determined within the range of depths from footing base to $1.5B'$ below the footing. In very fine or silty saturated sand, the measured SPT blow count (N) is corrected for submergence effect as follows:

$$N' = 15 + 0.5(N - 15) \quad \text{for } N > 15 \tag{8.31}$$

8.6.2 Based on Cone Penetration Tests (CPT)

Meyerhof (1956) proposed a relationship between ultimate bearing capacity and cone penetration resistance in sands.

$$q_{\text{ult}} = q_c \frac{B'}{40}\left(C_{w1} + C_{w2}\frac{D_f}{B'}\right)R_I \tag{8.32}$$

where q_c is average value of cone penetration resistance measured at depths from footing base to $1.5B'$ below the footing base. C_{w1}, C_{w2}, and R_I are the same as those defined in Equation 8.29.

Schertmann (1978) recommended correlated values of ultimate bearing capacity to cone penetration resistance in clays as shown in Table 8.11.

TABLE 8.10 Load Inclination Factor (R_I)

For Square Footings

$\frac{H}{P}$	Load Inclination Factor (R_I)		
	$D/B' = 0$	$D/B' = 1$	$D/B' = 3$
0.10	0.75	0.80	0.85
0.15	0.65	0.75	0.80
0.20	0.55	0.65	0.70
0.25	0.50	0.55	0.65
0.30	0.40	0.50	0.55
0.35	0.35	0.45	0.50
0.40	0.30	0.35	0.45
0.45	0.25	0.30	0.40
0.50	0.20	0.25	0.30
0.55	0.15	0.20	0.25
0.60	0.10	0.15	0.20

For Rectangular Footings

$\frac{H}{P}$	Load Inclination Factor (R_I)					
	$D/B' = 0$	$D/B' = 1$	$D/B' = 5$	$D/B' = 0$	$D/B' = 1$	$D/B' = 5$
0.10	0.70	0.75	0.80	0.80	0.85	0.90
0.15	0.60	0.65	0.70	0.70	0.80	0.85
0.20	0.50	0.60	0.65	0.65	0.70	0.75
0.25	0.40	0.50	0.55	0.55	0.65	0.70
0.30	0.35	0.40	0.50	0.50	0.60	0.65
0.35	0.30	0.35	0.40	0.40	0.55	0.60
0.40	0.25	0.30	0.35	0.35	0.50	0.55
0.45	0.20	0.25	0.30	0.30	0.45	0.50
0.50	0.15	0.20	0.25	0.25	0.35	0.45
0.55	0.10	0.15	0.20	0.20	0.30	0.40
0.60	0.05	0.10	0.15	0.15	0.25	0.35

Source: After Barker, R. M. et al., *Manuals for the Design of Bridge Foundations*, National Cooperative Highway Research Program Report 343, Transportation Research Board, National Research Council, Washington, D.C., 1991.

TABLE 8.11 Correlation between Uniform Ultimate Bearing Capacity (q_{ult}) or Nominal Bearing Resistance in Compression (q_N) and Cone Penetration Resistance (q_c)

	q_{ult} or q_N (ton/ft.^{2})	
q_c (kg/cm^2 or ton/ft.^{2})	Strip Footings	Square Footings
10	5	9
20	8	12
30	11	16
40	13	19
50	15	22

Source: After Schertmann, J. H., *Federal Highway Administration*, Report FHWA-TS-78-209, 1978; and Awkati (1970) Unpublished work as cited in Schmertmann (1978).

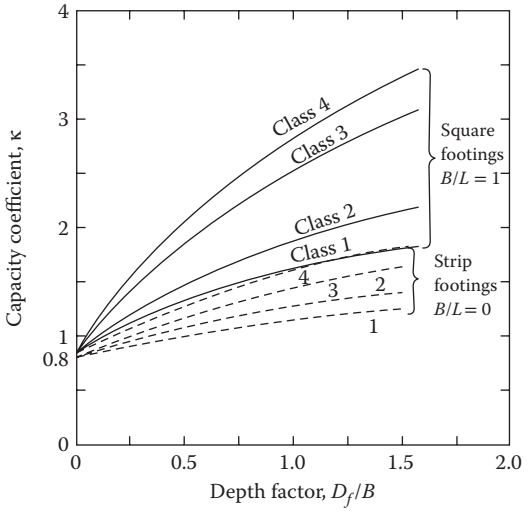

Soil Type	Consistency or Density	$(P–P_0)$ (tsf)	Class
Clay	Soft to very firm	<12	1
	Stiff	8–40	2
Sand and gravel	Loose	4–8	2
	Medium to dense	10–20	3
	Very dense	30–60	4
Silt	Loose to medium	<7	1
	Dense	12–30	2
Rock	Very low strength	10–30	2
	Low strength	30–60	3
	Medium to high Strength	$60–100^+$	4

FIGURE 8.16 Values of empirical capacity coefficient, κ. (After Canadian Geotechnical Society 1985.)

8.6.3 Based on Pressuremeter Tests (PMT)

Menard (1965), Baguelin et al. (1978), and Briaud (1986, 1992) proposed using the limit pressure measured in PMT to estimate ultimate bearing capacity.

$$q_{\text{ult}} = r_0 + \kappa(p_l - p_0) \tag{8.33}$$

where r_0 is initial total vertical pressure at foundation level, κ dimensionless bearing capacity coefficient from Figure 8.16, p_l limit pressure measured in PMT at depths from $1.5B'$ above to $1.5B'$ below foundation level, and p_0 total horizontal pressure at the depth where the PMT is performed.

8.7 Presumptive Static Allowable Bearing Pressures

Recommendations for allowable bearing stress $(q_a)_s$ of shallow foundations are available in most of building codes, as presented in Table 8.12. Presumptive value of allowable bearing stress for spread footings are intended for preliminary design when site-specific investigation is not justified. Presumptive allowable bearing stresses usually do not reflect the size, shape, and depth of footing and local water table. Therefore, footing design using such a procedure could be either overly conservative in some cases or unsafe in other cases (Barker et al. 1991). Recommended practice is to use presumptive allowable bearing stresses for preliminary footing sizing and finalize the design using one of the more reliable methods discussed in the preceding sections.

8.8 Seismic Bearing Capacity

Theoretical works by many researchers including Richards et al. (1993), Budhu and Al-Karni (1993), Dormieux and Pecker (1995), Paolucci and Pecker (1997), Kumar and Rao (2003), and Choudhury and Rao (2006) show significant reduction in bearing capacity of spread footings when subjected to seismic loading. This reduction was due to the inertial forces in the foundation soil due to a horizontal seismic acceleration of $k_h g$, where k_h is the coefficient of horizontal seismic acceleration and g is the acceleration due to gravity, and a horizontal load (T) on the foundation due to the inertial forces in the supported structure. In general, any reduction in the seismic bearing capacity due to the inertial forces in the foundation soils is relatively minor and may be neglected. The majority of the reduction occurs due to

TABLE 8.12 Presumptive Allowable Bearing Pressures for Spread Foundations

Type of Bearing Earth Material	In-Place Conditions	q_{all} (ton/ft.^{2}) Range	q_{all} (ton/ft.^{2}) Recommended Value for Use
Massive crystalline igneous and metamorphic rock: granite, diorite, basalt, gneiss, thoroughly cemented conglomerate (sound condition allows minor cracks)	Hard, sound rock	60–100	80
Foliated metamorphic rock: slate, schist (sound condition allows minor cracks)	Medium hard sound rock	30–40	35
Sedimentary rock: hard cemented shales, siltstone, sandstone, limestone without cavities	Medium hard sound rock	15–25	20
Weathered or broken bed rock of any kind except highly argillaceous rock (shale); rock quality designation <25	Soft rock	8–12	10
Compaction shale or other highly argillaceous rock in sound condition	Soft rock	8–12	10
Well graded mixture of fine and coarse-grained soil: glacial till, hardpan, boulder clay (GW-GC, GC, SC)	Very compact	8–12	10
Gravel, gravel–sand mixtures, boulder–gravel mixtures (SW, SP)	Very compact	6–10	7
	Medium to compact	4–7	5
	Loose	2–6	3
Coarse to medium sand, sand with little gravel (SW, SP)	Very compact	4–6	4
	Medium to compact	2–4	3
	Loose	1–3	1.5
Fine to medium sand, silty or clayey medium to coarse sand (SW, SM, SC)	Very compact	3–5	3
	Medium to compact	2–4	2.5
	Loose	1–2	1.5

Source: Modified from NAVFAC, Foundations and Earth Structures, DM 7.02, Naval Facilities Engineering Command, Alexandria, VA, 1986.

Notes:

1. Presumptive allowable bearing pressures are based on allowable footing settlement. For working stress design, limiting net uniform contact stress (q_0') to these presumptive allowable pressures may provide a reasonable, but known, factor of safety against bearing capacity failure.
2. If fine-grained soils, organic soils, collapsible or swelling soils, very loose cohesionless soils, or uncompacted fill soils are present within the depth of influence of the footing, which can vary from $3B'$ to $5B'$ below the bottom of the footing, site- and project-specific investigation is required to determine q_{all}.
3. If tabulated recommended values for q_{all} for rock exceed measured unconfined compressive strength of intact rock specimen, limit q_{all} to the measured unconfined compressive strength.
4. The tabulated values were developed and recommended for building structures and should only be used for preliminary design of spread footings for bridge structures.
5. Variations of q_{all} for size, depth, and arrangement of footings are given in Table 2 of NAVFAC (1986).

the inclination of the resultant applied load induced by the horizontal load H. In this case, the seismic bearing capacity $(q_{ult})_{seismic}$ or the nominal resistance in compression $(q_N)_{seismic}$ may be taken as that for the static loading, that is, q_{ult} or q_N of the same footing effective width (B′) provided the theoretical equation are used and potential effects of the load inclination is considered in the evaluation of q_{ult} or q_N.

It should be noted that the above methods do not consider the effects of seismic loading on the dynamic properties of the foundation soils. Saturated loose to medium dense cohesionless soils are prone to significant reduction in shear strength commensurate with the increase in the pore pressure due to seismic loading. Reduction in the bearing capacity of spread footing due to such reduction in the soil shear strengths, in particular in case of complete liquefaction, can be more significant than any reduction due to the above inertial effects and thus should be carefully considered. The theoretical static bearing capacity equations may be used with the reduced soil shear strength parameters to estimate seismic bearing capacity. Effects of the load inclination should be considered as above.

8.9 Stress Distributions Beneath Shallow Foundations

Elastic theory is often used to estimate the distribution of stress and settlement as well. Although soils are generally treated as elastic-plastic materials, the use of elastic theory for solving the problems is mainly due to the reasonable match between the boundary conditions for most footings and those of elastic solutions (Holtz 1990). Another reason is due to the lack of availability of acceptable alternatives. Observation and experience have shown that this practice provides satisfactory solutions (Scott 1981; Perloff 1975; Holtz 1990; Bowles 1996).

8.9.1 Semiinfinite, Elastic Foundations

Bossinesq equations based on elastic theory are the most commonly used methods for obtaining subsurface stresses produced by surface loads on semiinfinite, elastic, isotropic, homogeneous, weightless

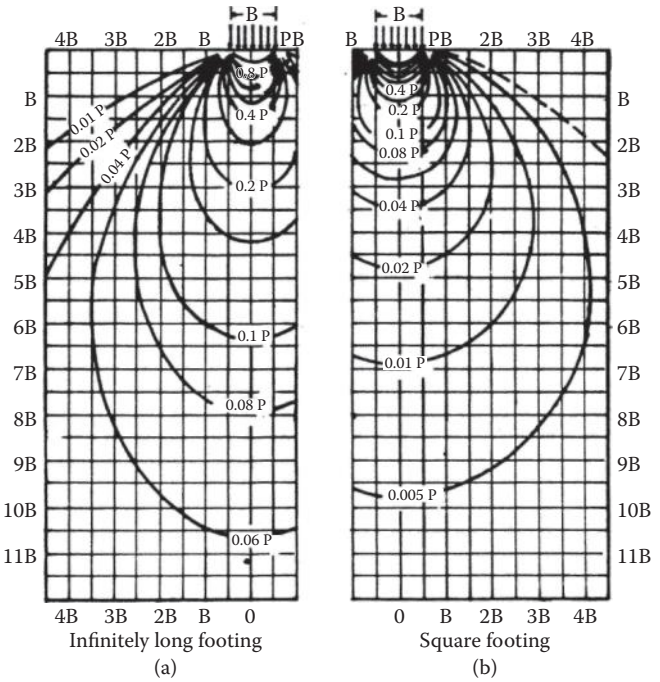

Square footing

Given

Footing size = 20′ × 20′

Unit pressure P = 2 tsf

Find

Profile of stress increase beneath center of footing due to applied load

B = 20′ P = 2 tsf

Z (ft.)	$\frac{Z}{B}$	σ_z (tsf)
10	0.5	0.70 × 2 = 1.4
20	1	0.38 × 2 = 0.76
30	1.5	0.19 × 2 = 0.38
40	2.0	0.12 × 2 = 0.24
50	2.5	0.07 × 2 = 0.14
60	3.0	0.05 × 2 = 0.10

FIGURE 8.17 Pressure bulbs based on the Bossinesq equation for (a) Long; and (b) square footings. (After Bowles, J. E., *Foundation Analysis and Design*, Fifth Edition, McGraw-Hill Companies, Inc., 1996.)

foundations. Formulas and plots of Bossinesq equations for common design problems are available in NAVFAC (1986). Figure 8.17 shows the isobars of pressure bulbs for square and continuous footings. For other geometry, refer to Poulos and Davis (1974).

8.9.2 Layered Soils

Westergaard (1938), Burmister (1943, 1958, 1967), Sowers and Vesic (1962), Poulos and Davis (1974), and Perloff (1975) discussed the solutions to stress distributions for layered soil strata. The reality of interlayer shear is very complicated due to in situ nonlinearity and material inhomogeneity (Perloff 1975; Holtz 1990). Either zero (frictionless) or with perfect fixity is assumed for the interlayer shear to obtain possible solutions. The Westergaard method assumed that the soil being loaded is constrained by closed spaced horizontal layers that prevent horizontal displacement (NAVFAC, 1986). Figures 8.18 and 8.19 by the Westergaard method can be used for calculating vertical stresses in soils consisting of alternative layers of soft (loose) and stiff (dense) materials.

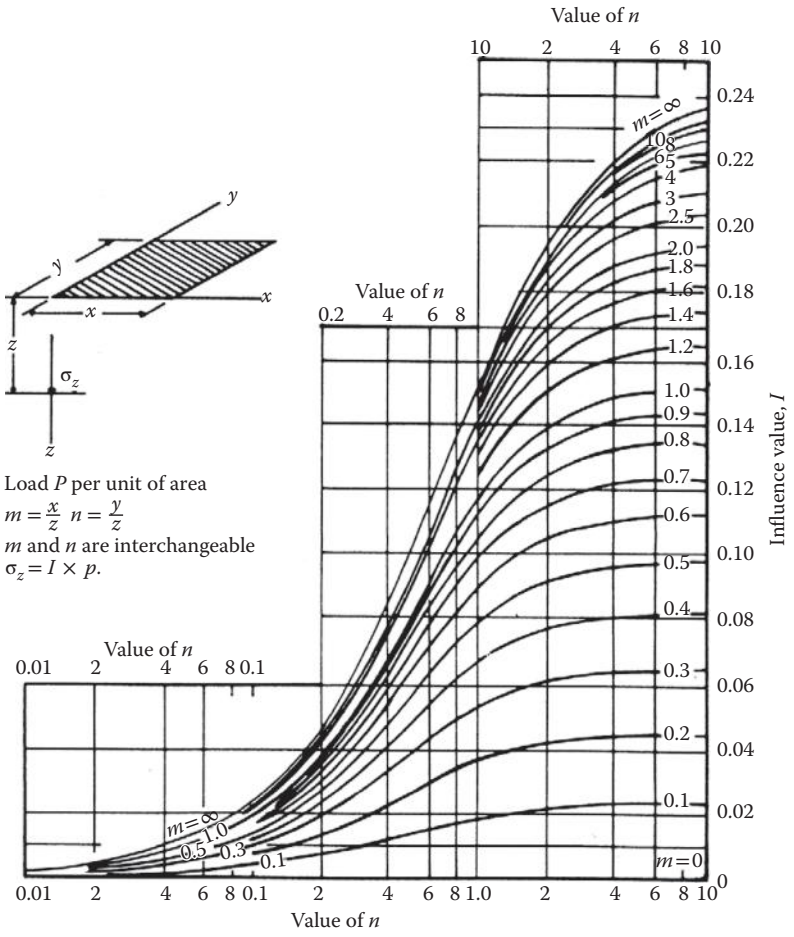

FIGURE 8.18 Influence value for vertical stress beneath a corner of a uniformly loaded rectangular area (Westerqaard case). (After NAVFAC, Design Manual 7.0, Naval Facilities Engineering Command, Department of the Navy, Washington, D.C., 1986.)

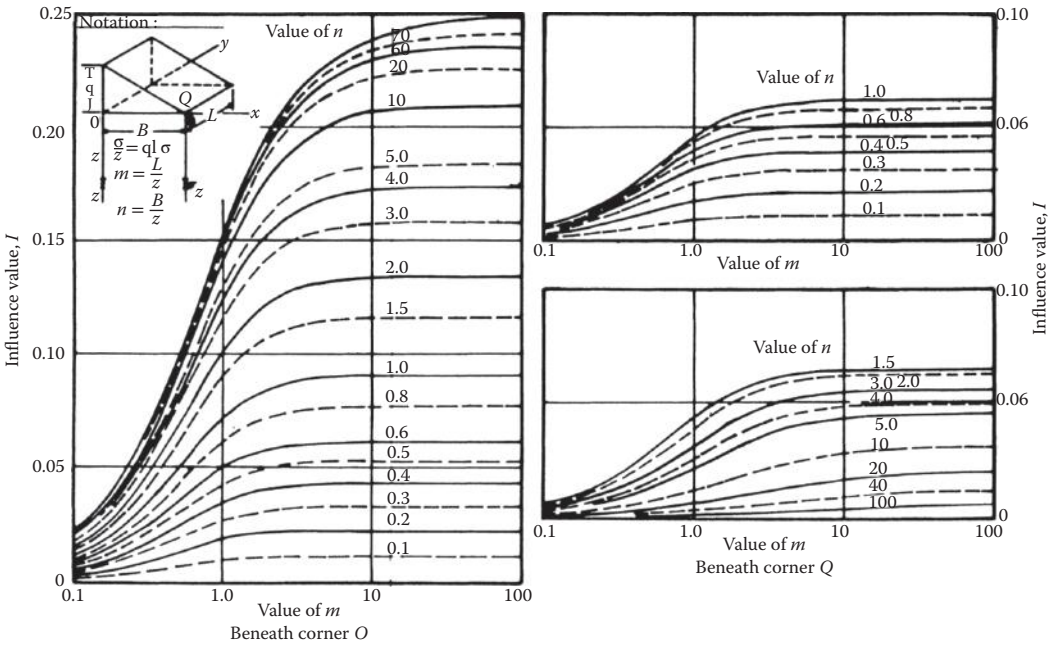

FIGURE 8.19 Influence value for vertical stress beneath triangular load (Westerqaard case). (After NAVFAC, Design Manual 7.0, Naval Facilities Engineering Command, Department of the Navy, Washington, D.C., 1986.)

8.9.3 Simplified Method (2:1 Method)

Assuming a loaded area increasing systematically with depth, a commonly used approach for computing the stress distribution beneath a square or rectangle footing is to use the 2:1 slope method as shown in Figure 8.20. Sometimes a 60° distribution angle (1.73 to 1 slope) may be assumed. The pressure increase Δq at a depth z beneath the loaded area due to base load P is

$$\Delta q = \begin{cases} P/(B'+z)(L'+z) & \text{(for a rectangle footing)} \\ P/(B'+z)^2 & \text{(for a square footing)} \end{cases} \tag{8.34}$$

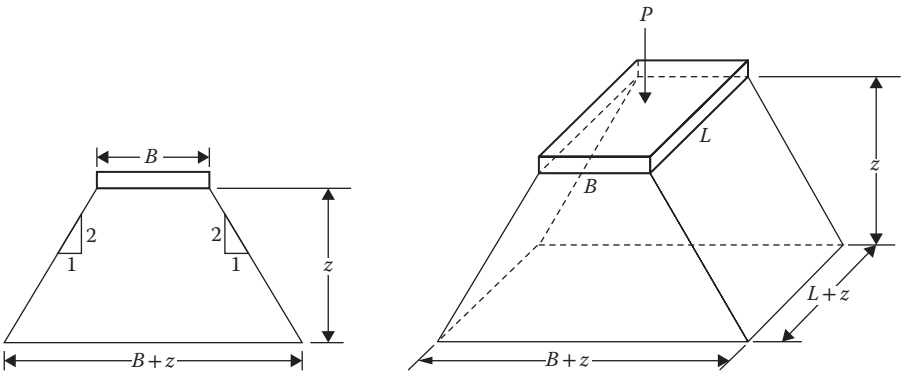

(a) Strip footing (b) Rectangular footing

FIGURE 8.20 The 2:1 approximation for the distribution of vertical stress with depth for strip and rectangular footings. (From Holtz and Kovacs, *An Introduction to Geotechnical Engineering,* Prentice-Hall, Englewood Cliffs, NJ, 1981.)

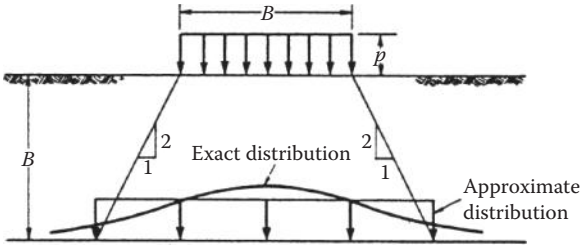

FIGURE 8.21 Relationship between vertical stress below a square uniformly loaded area as determined by approximate and exact methods. (After Perloff, W. H., *Foundation Engineering Handbook*, Second Edition, edited by Fang, H. Y., Chapman & Hall, 1975.)

where symbols are referred to in Figure 8.20. A comparison between the approximate distribution of stress calculated by a theoretical method and the 2:1 method is illustrated in Figure 8.21.

The solutions by this method compare reasonably well with those from theoretical equations from depth $z = B'$ to $4B'$ but is not considered accurate for depth z from 0 to B (Bowles 1996). Thus, the use of this method should be limited to preliminary evaluation or design.

8.10 Settlement of Shallow Foundations

The load applied on a footing changes the stress state of the soil below the footing. This stress change may produce a time-dependent accumulation of elastic compression, distortion, or consolidation of the soil beneath the footing. This is often termed the foundation settlement. True elastic deformation consists of a very small portion of the settlement whereas the major components of the settlement are due to a change of void ratio, particle rearrangement, or crushing. Therefore, very little of the settlement will be recovered even if the applied load is removed. The irrecoverable deformation of soil reflects its inherent elastic–plastic stress–strain relationship. The reliability of settlement estimated is influenced principally by soil properties, layering, stress history, and the actual stress profile under the applied load (Bowles 1996; Terzaghi et al. 1996).

In general, the total settlement may be expressed as

$$s_t = s_i + s_c + s_\alpha \tag{8.35}$$

where s_t is the total settlement, s_i the immediate or distortion settlement, s_c the primary consolidation settlement, and s_α is the secondary consolidation settlement. A typical settlement-time history of a shallow foundation is illustrated in Figure 8.22. Although often referred to as elastic settlement, immediate settlement foundation is not elastic in the sense that little or no soil rebound is likely to occur upon unloading. It is referred to as elastic settlement because the elastic theory is often used for computation. The immediate settlement component usually controls in cohesionless soils and very stiff or unsaturated cohesive soils, whereas consolidation settlement usually controls in less-stiff cohesive soils with a degree of saturation above 80% (AASHTO 2002).

8.10.1 Immediate Settlement by Elastic Analysis Methods

On the basis of elastic theory, Steinbrenner (1934) suggested that immediate settlements of footings on sands and clay could be estimated in terms of Young's modulus E of soils. A modified procedure developed by Bowles (1996) may be used for computing settlements (s_i) at the center of flexible footings on the half-space. The settlement equation can be expressed as follows:

$$s_i = q_0' B' (1 - \mu^2) m I_s I_F / E_s \tag{8.36}$$

$$I_s = n[I_1 + \{(1 - 2\mu)/(1 - \mu)\} I_2] \tag{8.37}$$

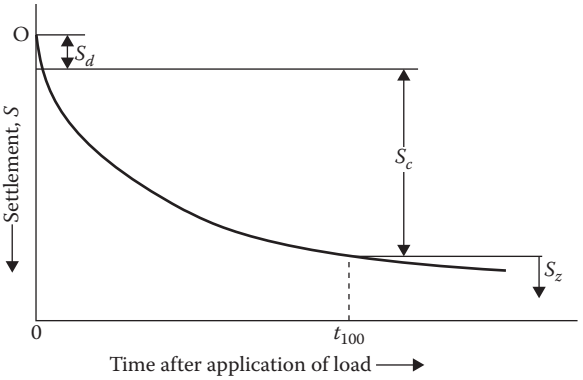

FIGURE 8.22 Schematic time–settlement history of typical point on a foundation. (After Perloff, W. H., *Foundation Engineering Handbook*, Second Edition, edited by Fang, H. Y., Chapman & Hall, 1975.)

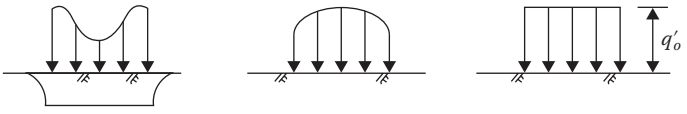

FIGURE 8.23 Approximate distribution of footing contact pressure due to concentrically applied vertical load. (a) contact pressure in cohesive soils; (b) contact pressure in cohesionless soils; and (c) equivalent uniform contact pressure distribution. (After Perloff, W. H., *Foundation Engineering Handbook*, Second Edition, edited by Fang, H. Y., Chapman & Hall, 1975.)

where q'_0 is net increase in the uniform contact pressure, as shown in Figure 8.23, μ and E_s are weighted average values of Poisson's ratio and Young's modulus for compressive soil strata, B' is the least lateral effective (width) dimension the base (convert round bases to equivalent square bases; $B' = 0.5B$ for center and $B' = B$ for corner I_i; $L' = 0.5L$ for center and $L' = L$ for corner I_i), I_i are influence factors depending on dimension of footings, base embedment depth, thickness of soil stratum, and Poisson's ratio (I_1 and I_2 are given in Table 8.13 and I_F is given in Figure 8.24; $M = L'/B'$ and $N = H/B'$), H is the stratum depth causing settlement (see discussion below), m is number of corners contributing to settlement ($m = 4$ at the footing center; $m = 2$ at a side; and $m = 1$ at a corner), and n equals 1.0 for flexible footings and 0.93 for rigid footings.

This equation applies to soil strata consisting of either cohesionless soils of any water content or unsaturated cohesive soils, which may be either organic or inorganic. Highly organic soils (both E_s and μ are subject to significant changes by high organic content) will be dictated by secondary or creep compression rather than immediate settlement; therefore, the applicability of the above equation is limited.

Suggestions were made by Bowles (1996) to appropriately use the equation as follows: (1) make the best estimate of the net increase in contact stress (q'_0) due to the design service load; (2) identify the settlement point to be calculated and divide the base so that the point is at the corner or common corner of one or up to four contributing areas; (3) determine the stratum depth causing settlement that does not approach to infinite rather at either the depth $z = 5B'$ or depth to where a hard stratum is encountered (where E_s in the hard layer is about $10E_s$ of the adjacent upper layer); and (4) calculate the weighted average E_s as following:

$$E_{s,\text{avg}} = \frac{\sum_{n}^{1} H_i E_{si}}{\sum_{n}^{1} H_i} \tag{8.38}$$

TABLE 8.13 Values of I_1 and I_2 to Compute Influence Factors *I*s Used in Equation 8.37

N	*M* = 1.0	1.1	1.2	1.3	1.4	1.5	1.6	1.7	1.8	1.9	2.0
0.2	$I_1 = 0.009$	0.008	0.008	0.008	0.008	0.008	0.007	0.007	0.007	0.007	0.007
	$I_2 = 0.041$	0.042	0.042	0.042	0.420	0.042	0.043	0.043	0.043	0.043	0.043
0.4	0.033	0.032	0.031	0.030	0.029	0.028	0.028	0.027	0.027	0.027	0.027
	0.066	0.068	0.069	0.070	0.070	0.071	0.071	0.072	0.072	0.073	0.073
0.6	0.066	0.064	0.063	0.061	0.060	0.059	0.058	0.057	0.056	0.056	0.055
	0.079	0.081	0.083	0.085	0.087	0.088	0.089	0.090	0.091	0.091	0.092
0.8	0.104	0.102	0.100	0.098	0.096	0.095	0.093	0.092	0.091	0.090	0.089
	0.083	0.087	0.090	0.093	0.095	0.097	0.098	0.100	0.101	0.102	0.103
1.0	0.142	0.140	0.138	0.136	0.134	0.132	0.130	0.129	0.127	0.126	0.125
	0.083	0.088	0.091	0.095	0.098	0.100	0.102	0.104	0.106	0.108	0.109
1.5	0.224	0.224	0.224	0.223	0.222	0.220	0.219	0.217	0.216	0.214	0.213
	0.075	0.080	0.084	0.089	0.093	0.096	0.099	0.102	0.105	0.108	0.110
2.0	0.285	0.288	0.290	0.292	0.292	0.292	0.292	0.292	0.291	0.290	0.289
	0.064	0.069	0.074	0.078	0.083	0.086	0.090	0.094	0.097	0.100	0.102
3.0	0.363	0.372	0.379	0.384	0.389	0.393	0.396	0.398	0.400	0.401	0.402
	0.048	0.052	0.056	0.060	0.064	0.068	0.071	0.075	0.078	0.081	0.084
4.0	0.408	0.421	0.431	0.440	0.448	0.455	0.460	0.465	0.469	0.473	0.476
	0.037	0.041	0.044	0.048	0.051	0.054	0.057	0.060	0.063	0.066	0.069
5.0	0.437	0.452	0.465	0.477	0.487	0.496	0.503	0.510	0.516	0.522	0.526
	0.031	0.034	0.036	0.039	0.042	0.045	0.048	0.050	0.053	0.055	0.058
6.0	0.457	0.474	0.489	0.502	0.514	0.524	0.534	0.542	0.550	0.557	0.563
	0.026	0.028	0.031	0.033	0.036	0.038	0.040	0.043	0.045	0.047	0.050
7.0	0.471	0.490	0.506	0.520	0.533	0.545	0.556	0.566	0.575	0.583	0.590
	0.022	0.024	0.027	0.029	0.031	0.033	0.035	0.037	0.039	0.041	0.043
8.0	0.482	0.502	0.519	0.534	0.549	0.561	0.573	0.584	0.594	0.602	0.611
	0.020	0.022	0.023	0.025	0.027	0.029	0.031	0.033	0.035	0.036	0.038
9.0	0.491	0.511	0.529	0.545	0.560	0.574	0.587	0.598	0.609	0.618	0.627
	0.017	0.019	0.021	0.023	0.024	0.026	0.028	0.029	0.031	0.033	0.034
10.0	0.498	0.519	0.537	0.554	0.570	0.584	0.597	0.610	0.621	0.631	0.641
	0.016	0.017	0.019	0.020	0.022	0.023	0.025	0.027	0.028	0.030	0.031
20.0	0.529	0.553	0.575	0.595	0.614	0.631	0.647	0.662	0.677	0.690	0.702
	0.008	0.009	0.010	0.010	0.011	0.012	0.013	0.013	0.014	0.015	0.016
500.0	0.560	0.587	0.612	0.635	0.656	0.677	0.696	0.714	0.731	0.748	0.763
	0.000	0.000	0.000	0.000	0.000	0.000	0.001	0.001	0.001	0.001	0.001

N	*M* = 2.5	4.0	5.0	6.0	7.0	8.0	9.0	10.0	25.0	50.0	100.0
0.2	$I_1 = 0.007$	0.006	0.006	0.006	0.006	0.006	0.006	0.006	0.006	0.006	0.006
	$I_2 = 0.043$	0.044	0.044	0.044	0.044	0.044	0.044	0.044	0.044	0.044	0.044
0.4	0.026	0.024	0.024	0.024	0.024	0.024	0.024	0.024	0.024	0.024	0.024
	0.074	0.075	0.075	0.075	0.076	0.076	0.076	0.076	0.076	0.076	0.076
0.6	0.053	0.051	0.050	0.050	0.050	0.049	0.049	0.049	0.049	0.049	0.049
	0.094	0.097	0.097	0.098	0.098	0.098	0.098	0.098	0.098	0.098	0.098
0.8	0.086	0.082	0.081	0.080	0.080	0.080	0.079	0.079	0.079	0.079	0.079
	0.107	0.111	0.112	0.113	0.113	0.113	0.113	0.114	0.114	0.114	0.114
1.0	0.121	0.115	0.113	0.112	0.112	0.112	0.111	0.111	0.110	0.110	0.110
	0.114	0.120	0.122	0.123	0.123	0.124	0.124	0.124	0.125	0.125	0.125
1.5	0.207	0.197	0.194	0.192	0.191	0.190	0.190	0.189	0.188	0.188	0.188
	0.118	0.130	0.134	0.136	0.137	0.138	0.138	0.139	0.140	0.140	0.140
2.0	0.284	0.271	0.267	0.264	0.262	0.261	0.260	0.259	0.257	0.256	0.256
	0.114	0.131	0.136	0.139	0.141	0.143	0.144	0.145	0.147	0.147	0.148

(*Continued*)

TABLE 8.13 (*Continued*) Values of I_1 and I_2 to Compute Influence Factors *I*s Used in Equation 8.37

N	*M* = 2.5	4.0	5.0	6.0	7.0	8.0	9.0	10.0	25.0	50.0	100.0
3.0	0.402	0.392	0.386	0.382	0.378	0.376	0.374	0.373	0.368	0.367	0.367
	0.097	0.122	0.131	0.137	0.141	0.144	0.145	0.147	0.152	0.153	0.154
4.0	0.484	0.484	0.479	0.474	0.470	0.466	0.464	0.462	0.453	0.451	0.451
	0.082	0.110	0.121	0.129	0.135	0.139	0.142	0.145	0.154	0.155	0.156
5.0	0.553	0.554	0.552	0.548	0.543	0.540	0.536	0.534	0.522	0.519	0.519
	0.070	0.098	0.111	0.120	0.128	0.133	0.137	0.140	0.154	0.156	0.157
6.0	0.585	0.609	0.610	0.608	0.604	0.601	0.598	0.595	0.579	0.576	0.575
	0.060	0.087	0.101	0.111	0.120	0.126	0.131	0.135	0.153	0.157	0.157
7.0	0.618	0.653	0.658	0.658	0.656	0.653	0.650	0.647	0.628	0.624	0.623
	0.053	0.078	0.092	0.103	0.112	0.119	0.125	0.129	0.152	0.157	0.158
8.0	0.643	0.688	0.697	0.700	0.700	0.698	0.695	0.692	0.672	0.666	0.665
	0.047	0.071	0.084	0.095	0.104	0.112	0.118	0.124	0.151	0.156	0.158
9.0	0.663	0.716	0.730	0.736	0.737	0.736	0.735	0.732	0.710	0.704	0.702
	0.042	0.064	0.077	0.088	0.097	0.105	0.112	0.118	0.149	0.156	0.158
10.0	0.679	0.740	0.758	0.766	0.770	0.770	0.770	0.768	0.745	0.738	0.735
	0.038	0.059	0.071	0.082	0.091	0.099	0.106	0.112	0.147	0.156	0.158
20.0	0.756	0.856	0.896	0.925	0.945	0.959	0.969	0.977	0.982	0.965	0.957
	0.020	0.031	0.039	0.046	0.053	0.059	0.065	0.071	0.124	0.148	0.156
500.0	0.832	0.977	1.046	1.102	1.150	1.191	1.227	1.259	2.532	1.721	1.879
	0.001	0.001	0.002	0.002	0.002	0.002	0.003	0.003	0.008	0.016	0.031

Source: Data from Bowles, J. E., *Foundation Analysis and Design*, Fifth Edition, McGraw-Hill Companies, Inc., 1996.

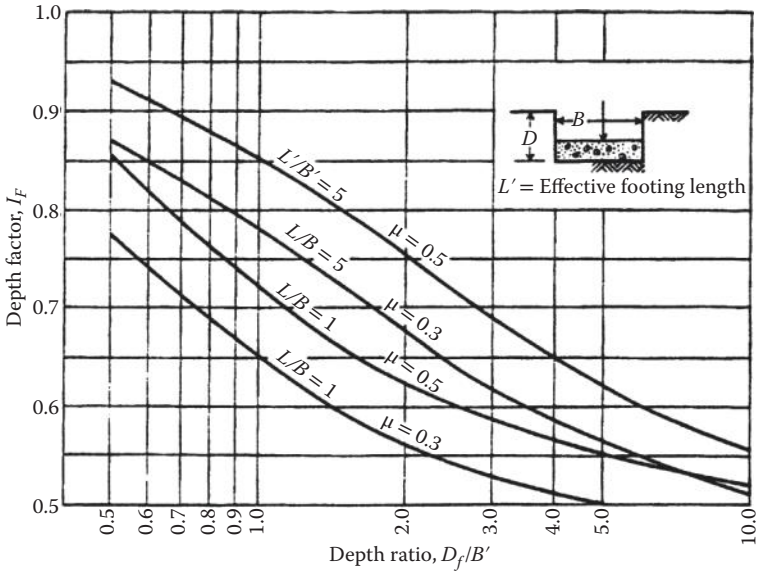

FIGURE 8.24 Influence factor I_F for footing at a depth *D*. (After Bowles, J. E., *Foundation Analysis and Design*, Fifth Edition, McGraw-Hill Companies, Inc., 1996.)

8.10.2 Settlement in Coarse-Grained Soil

Settlement in this type of soils occurs almost instantaneously compared to the rate of application of static service loads—both permanent and live.

8.10.2.1 Elastic Analysis Method

For the normally expected rate of most static loadings, in situ deposits of coarse-grained soils, namely, sand, gravel, and so on, with little or no fine content, in particular clay fraction, can be considered as free draining soils when subjected to additional stresses due to static loading. Most, if not all, of the footing settlement in this type of soil can be expected to occur immediately after the load application. Thus, for all practical purposes, the total footing settlement in this type of soil may be taken as equal to the immediate or elastic settlement evaluated based on Equation 8.36.

That is, for footing founded on free draining cohesionless soils,

$$s_t = s_i \tag{8.39}$$

8.10.2.2 Empirical Methods

The followings empirical methods, in which anticipated total footings settlement in granular soils is correlated with the results of common field tests performed during most routine field exploration, may be used to estimate footing settlement in granular soils.

8.10.2.2.1 SPT Method

D'Appolonia et al. (1970) developed the following equation to estimate settlements of footings on sand using SPT data:

$$s_t = \mu_0 \mu_1 q_0' B'/M \tag{8.40}$$

where μ_o and μ_1 are settlement influence factors that dependent on the footing geometry, depth of embedment, and depth to the relative incompressible layer (Figure 8.25), q_0' is the average net footing base or contact pressures due to the design service load on the foundation, and M is unconfined modulus of soil compressibility. The correlation between M and the average measured SPT blow count (N)

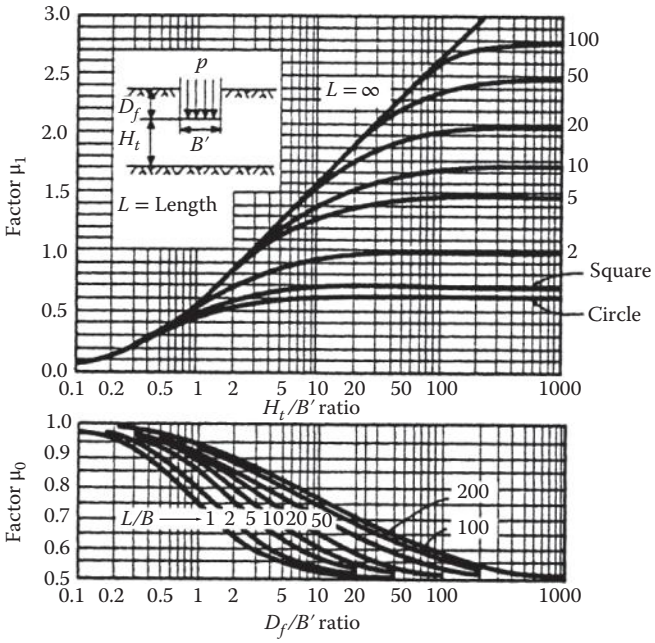

FIGURE 8.25 Settlement influence factors μ_0 and μ_1 for the D'Appolonia et al. procedure (After D'Appolonia, et al., *ASCE Journal of Soil Mechanics and Foundation Division*, **96**, No. SM2, pp. 754–761, 1970.)

corrected to 60% of the theoretical hammer energy, that is, N_{60}, within a depth B′ below footing, is given in Figure 8.26.

Barker et al. (1991) discussed the commonly used procedure for estimating settlement of footing on sand using SPT blow count developed by Terzaghi and Peck (1948, 1967) and Bazaraa (1967).

8.10.2.2.2 CPT Method

Schertmann (1970, 1978) developed a procedure for estimating footing settlements on sand using cone penetration test (CPT) data. This CPT method uses cone-tip penetration resistance, q_c, as a measure of the in situ stiffness (compressibility) soils. Schertmann's method is expressed as following:

$$s_t = C_1 C_2 \Delta p \sum \left(\frac{I_z}{E_s} \right)_i \Delta z_i \tag{8.41}$$

$$C_1 = 1 - 0.5 \left(\frac{\sigma'_{v0}}{\Delta p} \right) \geq 0.5 \tag{8.42}$$

$$C_2 = 1 + 0.2 \log \left(\frac{t_{yr}}{0.1} \right) \tag{8.43}$$

$$E_s = \begin{cases} 2.5 q_c & \text{for square footings (axisymmetric conditions)} \\ 3.5 q_c & \text{for continuous footings with } L'/B' \geq 10 \text{ (plan strain conditions)} \\ \left[2.5 + \left(L'/B' - 1 \right)/9 \right] q_c & \text{for footings with } 1 \leq L'/B' \leq 10 \end{cases} \tag{8.44}$$

where $\Delta p = \sigma'_{vf} - \sigma'_{v0}$ is net contact stress at foundation level, σ'_{v0} is the initial effective in situ overburden stress at the bottom of footings, σ'_{vf} is final effective in situ overburden stress at the bottom of footings, I_z is strain influence factor as defined in Figure 8.27 and Table 8.14, E_s is appropriate Young's modulus at the middle of the ith layer of thickness Δz_I, C_1 is pressure correction factor, C_2 is time rate factor (equal to 1 for immediate settlement calculation or if the lateral pressure is less than the creep pressure determined from PMT), q_c is cone penetration resistance, in pressure units, and Δz is layer thickness.

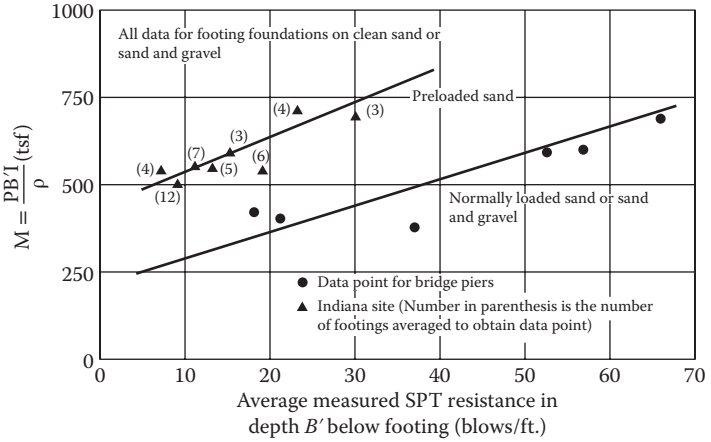

FIGURE 8.26 Correlation between modulus of compressibility and average value standard penetration test (SPT) blow count. (After D'Appolonia et al., *ASCE Journal of Soil Mechanics and Foundation Division*, **96**, No. SM2, pp. 754–761, 1970.)

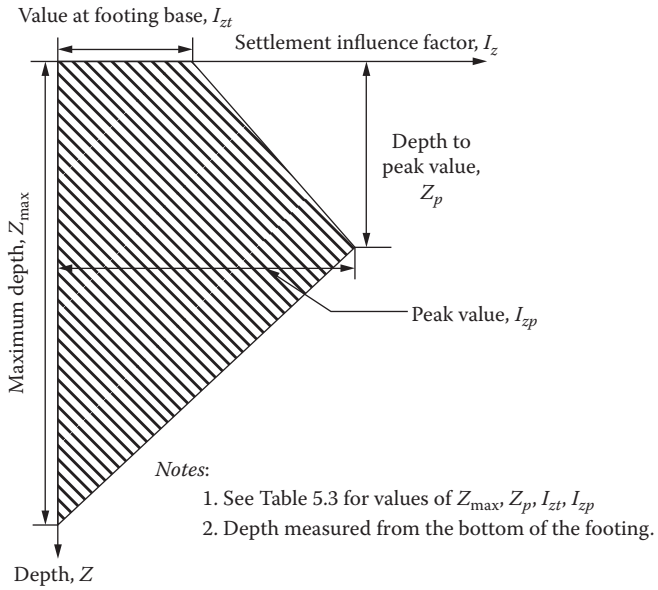

FIGURE 8.27 Variation of Schmertmann's improved settlement influence factors with depth. (After Schertmann, J. H. et al., *ASCE Journal of the Geotechnical Engineering Division*, **104**, No. GT8, pp. 1131–1135, 1978.)

TABLE 8.14 Coefficients to Define the Dimensions of Schmertmann's Improved Settlement Influence Factor Diagram in Figure 31.27

L/B	Maximum Depth of Influence, z_{max}/B'	Depth to Peak Value, z_p/B'	Value of I_z at Top I_{zt}	Peak Value of Stress Influence Factor I_{zp}			
				$\frac{\Delta p}{\sigma'_{vp}} = 1$	$\frac{\Delta p}{\sigma'_{vp}} = 2$	$\frac{\Delta p}{\sigma'_{vp}} = 4$	$\frac{\Delta p}{\sigma'_{vp}} = 10$
1	2.00	0.50	0.10	0.60	0.64	0.70	0.82
2	2.20	0.55	0.11	0.60	0.64	0.70	0.82
4	2.65	0.65	0.13	0.60	0.64	0.70	0.82
8	3.55	0.90	0.18	0.60	0.64	0.70	0.82
≥10	4.00	1.00	0.20	0.60	0.64	0.70	0.82

Source: After Schertmann, J. H. et al., *ASCE Journal of the Geotechnical Engineering Division*, **104**, No. GT8, pp. 1131–1135, 1978.

Note: σ'_{vp} is the initial vertical pressure at the depth of peak influence.

Recent studies by Tan and Duncan (1991) have compared measured settlements with settlements predicted using various procedures for footings on sand. These studies conclude that methods predicting settlements close to the average of measured settlement are likely to underestimate settlements half the time and to overestimate them half the time. The conservative methods (notably Terzaghi and Peck's) tend to overestimate settlements more than half the time and to underestimate them less likely. In other words, there is a trade-off between accuracy and reliability.

A relatively accurate method such as the D'Appolonia et al. (1970) method calculates settlements that are about equal to the average value of actual settlements, but it underestimates settlements half the time (a reliability of 50%). To ensure the calculated settlements equal or exceed the measured settlements about 90% of the time (a reliability of 90%), an adjustment factor of two shall be applied to the settlements predicted by the D'Appolonia et al. method. Table 8.15 shows values of adjustment factor for 50% and 90% reliability in settlement predicted using Terzaghi and Peck (1967), D'Appolonia et al. (1970), and Schertmann (1978) methods.

TABLE 8.15 Value of Adjustment Factor for 50% and 90% Reliability in Displacement Estimates

		Adjustment Factor	
Method	Soil Type	For 50% Reliability	For 90% Reliability
Terzaghi and Peck	Sand	0.45	1.05
Schmertmann	Sand	0.60	1.25
D'Appolonia et al.	Sand	1.00	2.00

8.10.3 Settlement in Fine-Grained Soils

For footing in clay and other fine-grained soils with relatively low permeability compared to the rate of static load application, the total settlement (s_t) is the sum of the immediate or elastic settlement evaluated based on Equation 8.36 and the consolidation settlements as discussed in Section 8.10.3.1.

Elastic settlement occurs almost instantaneously compared to the rate of application of static service loads—both permanent and live. Thus, similar to footings in coarse-grained soils, both permanent and live service loads need to be included in estimating the immediate settlement of footing in fine-grained soils.

8.10.3.1 Consolidation Settlement

The majority of the settlement in saturated fine-grained soils, in particular in very soft to medium stiff clays, is time dependent. For computational purposes, this time-dependent settlement can be divided into two components: primary consolidation settlement (s_c) and secondary settlement (s_α).

The primary consolidation settlement (s_c) occurs due to the slow expulsion of the pore water and hence the dissipation of the excess pore water pressure generated by the application of the static service loads at the rates normally expected of permanent loads. As the excess pore water pressure dissipates, the net effective vertical stress on the soil increases as the primary consolidation continues to occur.

The secondary consolidation settlement (s_c) occurs after the completion of the primary settlement (i.e., after the complete dissipation of the generated pore water pressure) due mainly to the reorientation of the soil particles under essentially constant effective vertical stress.

Little or no consolidation settlement occurs in fine-grained soils due to static transient live loads. Thus, only the permanent loads need to be considered in evaluating the consolidation settlement.

8.10.3.1.1 Primary Consolidation Settlement (s_c)

The total amount of settlement due to primary consolidation can be estimated using Terzaghi's one-dimensional consolidation theory (Terzaghi 1943; Lambe and Whitman 1969; Peck et al. 1974; Terzaghi et al. 1996) as follows:

$$s_c = \begin{cases} \dfrac{H_c}{1+e_0}\left[C_r \log\left(\dfrac{\sigma'_p}{\sigma'_{v0}}\right) + C_c \log\left(\dfrac{\sigma'_{vf}}{\sigma'_p}\right)\right] & (\text{for OC soils, i.e., } \sigma'_p > \sigma'_{v0}) \\ \dfrac{H_c}{1+e_0}\left[C_c \log\left(\dfrac{\sigma'_{vf}}{\sigma'_p}\right)\right] & (\text{for NC soils, i.e., } \sigma'_p = \sigma'_{v0}) \end{cases} \tag{8.45}$$

where H_c is the height of compressible layer, e_0 is void ratio at initial vertical effective stress, C_c is the compression index (see Table 8.16), C_r is recompression index (also see Table 8.16), σ'_p is

TABLE 8.16 Some Empirical Equations for C_c and C_r

Compression Index	Source	Comment
$C_c = 0.009(\text{LL} - 10)$	Terzaghi and Peck (1967)	$S_t \le 4$, $\text{LL} < 100$
$C_c = 0.2343e_0$	Nagaraj and Srinivasa Murthy (1986)	
$C_c = 0.5G_s(PI/100)$	Worth and Wood (1978)	Modified Cam Clay model
$C_c = PI/74$	EPRI (1990)	
$C_c = 0.37(e_0 + 0.003w_L + 0.0004w_N - 0.34)$	Azzouz et al. (1976)	Statistical analysis
Recompression Index	Source	
$C_r = 0.0463w_L G_s$	Nagaraj and Srinivasa Murthy (1986)	

Note: S_t = (Peak undrained shear strength/Undrained residual shear strength); LL= Liquid Limit (%), PI= Plasticity Index (%), eo = Initial in-situ void ratio, Gs=Soil specific gravity, and w_L= Liquid Limit (in decimal) and W_N= In-situ natural water content (in decimal).

TABLE 8.17 Secondary Compression Index

C_α/C_c	Material
0.02 ± 0.01	Granular soils including rockfill
0.03 ± 0.01	Shale and mudstone
0.04 ± 0.01	Inorganic clays and silts
0.05 ± 0.01	Organic clays and silts
0.06 ± 0.01	Peat and muskeg

Source: Data from Terzaghi, K. et al., *Soil Mechanics in Engineering Practice*, Third Edition, John Wiley & Sons, Inc., 1996.

maximum past vertical effective stress, σ'_{v0} is initial vertical effective stress, σ'_{vf} is final vertical effective stress. Highly compressible cohesive soils are rarely chosen to place footings for bridges where tolerable amount of settlement is relative small. Preloading or surcharging to produce more rapid consolidation has been extensively used for foundations on compressible soils (Perloff 1975). Alternative foundation systems would be appropriate if large consolidation settlements are expected to occur.

8.10.3.1.2 Secondary Consolidation Settlement

Settlements of footings on cohesive soils continuing beyond primary consolidation are called secondary settlement. Secondary settlement develops at a slower and continually decreasing rate, and may be estimated as follows:

$$s_\alpha = C_\alpha H_t \log \frac{t_{sc}}{t_p} \tag{8.46}$$

where C_α is coefficient of secondary settlement, and normally given as ratio to C_c (see Table 8.17), H_t is total thickness of layers undergoing secondary settlement, t_{sc} is time for which secondary settlement is calculated and t_p is time, in the same unit as t_{sc}, to the end of primary consolidation settlement.

8.10.4 Tolerable Settlement

Criteria for tolerable foundation settlement shall be established consistent with the function and type of the bridge structure, anticipated service life, and consequences of unacceptable movements on structure performance as outlined by AASHTO (2012). As discussed earlier, the criterion adopted by AASHTO (2012) considering the angular distortion (δ/l) between adjacent footings is as follows:

$$\frac{\delta}{l} \leq \begin{cases} 0.008 & \text{for simple span bridge} \\ 0.004 & \text{for continuous span bridge} \end{cases} \tag{8.47}$$

where δ is differential settlement of adjacent support and l is center-center spacing between adjacent supports.

8.11 Shallow Foundations on Rock

Wyllie (1992) outlines the following examinations that are necessary for designing shallow foundations on rock: (1) the bearing capacity of the rock to ensure that there will be no crushing or creep of the material within the loaded zone; (2) settlement of the foundation that will result from elastic strain of the rock and possibly inelastic compression of weak seams within the volume of rock compressed by the applied load; (3) sliding and shear failure of blocks of rock formed by intersecting fractures within the foundation. This condition usually occurs where the foundation is located on a steep slope and the orientation of the fractures is such that the blocks can slide out of the free face.

USACE (1994) provides detailed guidelines for the characterization of rock as foundation support material as well as the methodologies for the evaluation of settlement and ultimate bearing capacity or nominal bearing resistance in compression of spread footings founded on rock.

8.11.1 Presumptive Allowable Bearing Pressures

It is common to use allowable bearing capacity for various rock types listed in building codes for footing design. As provided in Table 8.18, presumptive allowable bearing pressures have been developed to limit settlement to within permissible amount.

8.11.2 Allowable Bearing Pressures/Ultimate Bearing Capacity of Fractured Rock

Various empirical procedures for estimating allowable bearing pressure of foundations on fractured rock are available in literature. Peck et al. (1974) suggested an empirical procedure for estimating allowable bearing pressures of foundations on jointed rock based on rock quality designation (RQD) index. The predicted allowable bearing pressure by this method should be used with the assumption that the spread footing foundation may experience settlement up to about 12. 7 mm (0.5 in.) (Peck et al. 1974).

Carter and Kulhawy (1988) proposed an empirical approach for estimating ultimate bearing capacity of fractured rock. Their method is based on unconfined compressive strength of the intact rock core sample and rock mass quality. Wyllie (1992) detailed an analytical procedure for computing bearing capacity of fractured rock mass using Hoek-Brown strength criterion. Details of rational methods for the topic can also be found in Kulhawy and Goodman (1987), Goodman (1989).

TABLE 8.18 Presumptive Allowable Bearing Pressures (tsf) for Spread Footing Foundations on Rock

Code	Year[a]	Bedrock[b]	Sound Foliated Rock	Sound Sedimentary Rock	Soft Rock[c]	Soft Shale	Broken Shale
Baltimore	1962	100	35		10		
BOCA	1970	100	40	25	10	4	
Boston	1970	100	50	10	10		1.5
Chicago	1970	100	100				
Cleveland	1951/1969			25			
Dallas	1968	$0.2q_u$	$2q_u$	$0.2q_u$	$0.2q_u$	$0.2q_u$	$0.2q_u$
Detroit	1956	100	100	9600	12	12	
Indiana	1967	$0.2q_u$	$2q_u$	$0.2q_u$	$0.2q_u$	$0.2q_u$	$0.2q_u$
Kansas	1961/1969	$0.2q_u$	$2q_u$	$0.2q_u$	$0.2q_u$	$0.2q_u$	$0.2q_u$
Los Angeles	1970	10	4	3	1	1	1
New York City	1970	60	60	60	8		
New York State		100	40	15			
Ohio	1970	100	40	15	10	4	
Philadelphia	1969	50	15	10–15	8		
Pittsburgh	1959/1969	25	25	25	8	8	
Richmond	1968	100	40	25	10	4	1.5
St. Louis	1960/1970	100	40	25	10	1.5	1.5
San Francisco	1969	3–5	3–5	3–5			
UBC	1970	$0.2q_u$	$2q_u$	$0.2q_u$	$0.2q_u$	$0.2q_u$	$0.2q_u$
NBC Canada	1970			100			
New South Wales, Australia	1974			33	13	4.5	

Source: After Putnam, J. B. Analysis and Design of Foundations on Continuous Rock, M. S. Thesis, Syracuse University, May, Syracuse, New York, 1981.

Note: q_u = unconfined compressive strength.

[a] Year of code or original year and date of revision.

[b] Massive crystalline bedrock.

[c] Soft and broken rock, not including shale.

[d] Allowable bearing pressure to be determined by appropriate city official.

8.11.3 Settlements of Foundations on Rock

Wyllie (1992) summarizes the settlements of foundations on rock as following three different types:

1. Elastic settlements result from a combination of strain of the intact rock, slight closure and movement of fractures, and compression of any minor clay seams (less than a few millimeters). Elastic theory can be used to calculate this type of settlement. Detail information can be found in Wyllie (1992), Kulhaway (1978), USACE (1994) and AASHTO (2002).
2. Settlements result from the movement of blocks of rock due to shearing of fracture surfaces. This occurs when foundations are sitting at the top of a steep slope and unstable blocks of rock are formed in the face. The stability of foundations on rock is influenced by the geological characterization of rock blocks. The information required on structural geology consists of the orientation, length and spacing of fractures, and their surface and infilling materials. Procedures have been developed for identifying and analyzing the stability of sliding blocks (Wyllie 1992), stability of wedge blocks (Hoek and Bray 1981), stability of toppling blocks (Goodman and Bray 1976), or three-dimensional stability of rock blocks (Goodman and Shi 1985).

3. Time-dependent settlement occurs when foundations found on the rock mass which consisting of substantial seams of clay or other compressible materials. This type of settlements can be estimated using the procedures described in Section 8.11. Also the time-dependent settlement can occur if foundations found on ductile rocks such as salt where strains develop continuously at any stress level, or brittle rocks when the applied stress exceeds the yield stress.

8.12 Structural Design of Shallow Foundations

The plan dimensions of a spread footing (B and L) are controlled by the nominal bearing resistance of the soil and stiffness of the soil to prevent damages to the superstructure caused by support movements. Maximum contact bearing stress under LRFD strength and extreme event load combinations shall be less than factored nominal bearing resistance of the soil. Furthermore, settlement and rotation of the footing under LRFD service limit state load combinations shall be within acceptable limits. Such limits depend on the continuity of the superstructure, type of the structural material and system, span length, variations in the geotechnical properties from one support to the next, and number of columns per support. Considering complexity of settlement analysis and variables involved, some design codes have specified conservative limits for acceptable support settlement. Rotation of the support is controlled by specifying upper limits on eccentricity of the loads under service and extreme event loads applied to the footing. Such limits depend on stiffness and shear strength of the soil and will be different for soil and rock.

The bearing stress distribution beneath the footing depends on rigidity of the footing, type of the soil, soil stress–strain relationship, and time-dependent response to contact stresses. Common types of distribution are uniform (footings on soil) and linear (footings on rock) as shown in Figure 8.28a and b, respectively. Irrespective of the stiffness of the soil, linear distribution is assumed for structural analysis (concrete and steel design) of the footing.

The depth of the spread footing (D) must be adequate to provide enough resistance against one-way (direct) and two-way (punching) shears on surfaces shown in Figure 8.29a and b; allow development of the column rebar into the footing; and provide enough flexural and shear resistance against stresses

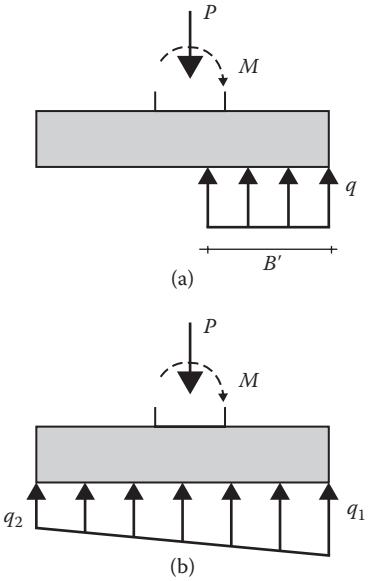

FIGURE 8.28 (a) Distribution of bearing stress for spread footings on soil. (b) Distribution of bearing stress for spread footings on rock.

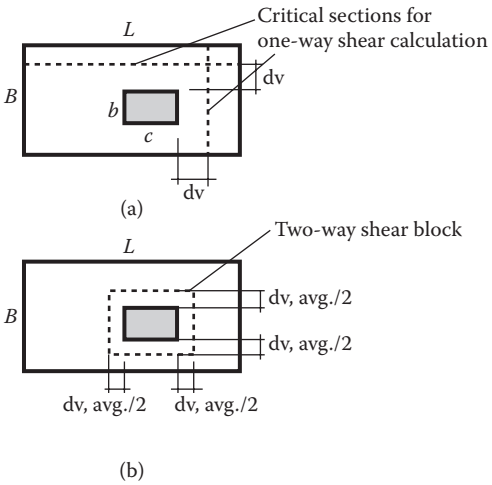

FIGURE 8.29 (a) Critical section for one-way shear. (b) Critical section for two-way shear.

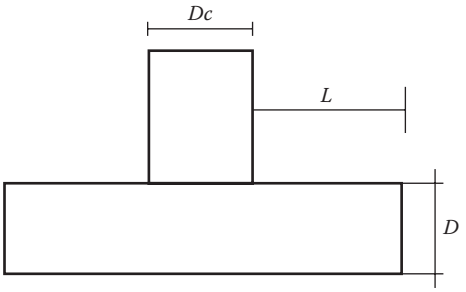

FIGURE 8.30 Limitations on the depth of the footing.

applied by the soil. The one-way shear action may control the depth for rectangular footings if the L/B ratio is greater than about 1.2 and may control for other L/B ratios when there is overturning or eccentric loading.

Studies by Duan and McBride (1995) indicated that if the ratio of cantilevered length to the depth of the spread footing or pile cap (L/D shown in Figure 8.30) is greater than 2.5, nonlinear bearing stress distribution must be assumed and hand calculations will not be accurate. However Caltrans' Seismic Design Criteria (2011b) reduces this ratio to $L/2.2$ for design purposes. Furthermore, if seismic forces are considered in design, depth of the footing (D) is recommended to be at least 0.8 of the diameter of the column (D_c) that it supports.

Sliding of the footing must be checked for strength and extreme event limit states. Resistance against sliding is provided by friction between the footing and the soil, as well as passive resistance of the backfill soil against the face of the footing. Resistance factors may be assumed 1.0 for extreme event combinations.

Acknowledgments

The chapter on shallow foundations in the earlier version of the handbook was prepared by James Chai. Portions of the current chapter are modified versions of the previous texts. The authors gratefully acknowledge this contribution. The authors thank Dr. Lian Duan for inviting us to update this chapter and for his sustained patience with regard to many missed due dates.

References

AASHTO. 2002. *Standard Specifications for Highway Bridges*, Seventeenth Edition, American Association of State Highway and Transportation Officials, Washington, DC.

AASHTO. 2012. *AASHTO LRFD Bridge Design Specifications*, Customary US Units, 2012, American Association of State Highway and Transportation Officials, Washington DC.

Awkati 1970. Unpublished work as cited in Schmertmann (1978)

Azzouz, A. S., Krizek, R. J., and Corotis, R. B. 1976. Regression analysis of soil compressibility, *JSSMFE Soils and Foundations*, 16(2), 19–29.

Baguelin, F., Jezequel, J. F., and Shields, D. H. 1978. *The Pressuremeter and Foundation Engineering*, Transportation Technical Publications, Clausthal, Germany, 617 pp.

Barker, R. M., Duncan, J. M., Rojiani, K. B., Ooi, P. S. K., Tan, C. K., and Kim, S. G. 1991. *Manuals for the Design of Bridge Foundations*, National Cooperative Highway Research Program Report 343, Transportation Research Board, National Research Council, Washington, DC.

Bazaraa, A. 1967. *Use of Standard Penetration Test for Estimating Settlements of Shallow Foundations on Sands*, Ph.D. Dissertation Submitted to Department of Civil Engineering, University of Illinois, Urbana, Illinois, 380 pp.

Bowles, J. E. 1975. Spread footings, Chapter 15 in *Foundation Engineering Handbook*, Edited by Winterkorn, H. F., and Fang, H. Y. Van Nostrand Reinhold, New York, NY.

Bowles, J. E. 1982. *Foundation Analysis and Design*, Third Edition, McGraw-Hill, New York, NY.

Bowles, J. E. 1988. *Foundation Analysis and Design*, Fourth Edition, McGraw-Hill, New York, NY.

Bowles, J. E. 1989. *Foundation Analysis and Design*, Fourth Edition, McGraw-Hill, New York, NY.

Bowles, J. E. 1995. *Foundation Analysis and Design*, Fifth Edition, McGraw-Hill, New York, NY.

Bowles, J. E. 1996. *Foundation Analysis and Design*, Fifth Edition, McGraw-Hill, New York, NY.

Briaud, J. L. 1986. Pressuremeter and foundation design, *Proceedings of the Conference on Use of in situ Tests in Geotechnical Engineering*, ASCE Geotechnical Publication No. 6, pp. 74–116.

Briaud, J. L. 1992. *The Pressuremeter*, A. A. Balkema Publishers, Brookfield, Blacksburg, Virginia, VT.

Burmister, D. M. 1943. The theory of stresses and displacements in layered systems and application to the design of airport runways, *Proceedings of the Highway Research Board*, **23**, 126–148.

Burmister, D. M. 1958. Evaluation of pavement systems of WASHO road test layered system methods, *Highway Research Board Bulletin*, No. 177.

Burmister, D. M. 1967. Applications of dimensional analyses in the evaluation of asphalt pavement performances, Paper for presentation at Fifth Paving Conference, Albuquerque, NM.

Budhu, M, and Al-Karni, A. A. 1993. Seismic bearing capacity of soils, *Geotechnique*, 43(1), 181–187.

Caltrans. 2008. *Memo to Designers (MTD) 4-1, Spread Footing*, California Department of Transportation, Sacramento, CA.

Caltrans. 2011a, November. *California Amendments to AASHTO Bridge Design Specifications*, Fourth Edition, California Department of Transportation, Sacramento, CA.

Caltrans. 2011b. *Seismic Design Criteria*, California Department of Transportation, Sacramento, CA.

Canadian Geotechnical Society. 1985. *Canadian Foundation Engineering Manual*, Second Edition, Canadian Geotechnical Society, Richmond, BC, Canada, 456 pp.

Caquot, A., and Kerisel, F. 1948. *Tables for the Calculations of Passive Pressure, Active Pressure and Bearing Capacities of Foundations*, Gauthier-Villars, Paris.

Carter, J. P., and Kulhawy, F. H. 1988. *Analysis and Design of Drilled Shaft Foundations Socketed into Rock*, Report No. EL-5918, Empire State Electric Engineering Research Corporation and Electric Power Research Institute, New York, NY.

Chen, W. F. 1975. *Limit Analysis and Soil Plasticity*, Elsevier, Amsterdam, The Netherlands.

Choudhury, D. and Rao, K. S. 2006. Seismic bearing capacity of shallow strip foundations embedded in slope, *ASCE International Journal of Geomechanics*, 6(3), 176–184.

D'Appolonia, D. J., D'Appolonia, E., and Brisette, R. F. 1970. Settlement of spread footings on sand (closure), *ASCE Journal of Soil Mechanics and Foundation Division*, 96(2), 754–761.

Dormieux, L., and Pecker, A. 1995. Seismic bearing capacity of foundations on cohesionless soils, *ASCE Journal of Geotechnical Engineering*, 123(3), 300–303.

Duan, L., and McBride, S. B. 1995. The effects of cap stiffness on pile reactions, *Concrete International*, American Concrete Institute 17(1), 42–44.

FHWA. 2002. *Evaluation of Soil and Rock Properties, Geotechnical Circular Number 5*, Federal Highway Administration, Washington DC.

Gifford, D. G., Kraemen, S. R., Wheeler, J. R., and McKnown, A. F. 1987. *Spread Footing for Highway Bridges*, Report No. RD-86/185, Federal Highway Administration, Washington, DC, 229 pp.

Goodman, R. E. 1989. *Introduction to Rock Mechanics*, Second Edition, John Wiley & Sons, New York, NY.

Goodman, R. E., and Bray, J. W. 1976. Toppling of rock slopes, *Proceedings of the Specialty Conference on Rock Engineering for Foundations and Slopes*, ASCE, **2**, pp. 201–234, Boulder, CO.

Goodman, R. E., and Shi, G. 1985. *Block Theory and its Application to Rock Engineering*, Prentice-Hall, Englewood Cliffs, NJ.

Hansen, B. J. 1970. *A Revised and Extended Formula for Bearing Capacity*, Bulletin No. 28, Danish Geotechnical Institute, Copenhagen, Denmark, pp. 5–11.

Hoek, E., and Bray, J. 1981. *Rock Slope Engineering*, Second Edition, IMM, London.

Holtz, R. D. 1990. Stress distribution and settlement of shallow foundations, Chapter 5 in *Foundation Engineering Handbook*, Second Edition, Edited by Fang, H. Y. Chapman & Hall, New York, NY.

Hunt, R. E. 1986. *Geotechnical Engineering Analysis Evaluation*, McGraw-Hill, New York, NY.

Idriss, I. M., and Boulanger, W. W. 2008. *Soil Liquefaction During Earthquakes*, EERI Monograph No. MNO-12, Oakland, CA.

Karol, R. H. 1960. *Soils and Soil Engineering*, Prentice-Hall, Englewood Cliffs, NJ.

Kulhawy, F. H., and Goodman, R. E. 1987. Foundation in rock, Chapter 55 in *Ground Engineering Reference Manual*, Edited by F. G. Bell, Butterworths, London.

Kulhawy, F. H., and Mayne, P. W. 1990. *Manual on Estimating Soil Properties for Foundation Design*, Electric Power Research Institute, EPRI EL-6800, Project 1493-6, Final Report, August, 1990.

Kulhaway, F. H. 1978. Geomechanical Model for Rock Foundation Settlement, *Journal of Geotechnical Engineering*, ASCE, 104(2), 211–227.

Kutter, B. L., Abghari, A., and Cheney, J. A. 1988. "Strength parameters for bearing capacity in sand", *ASCE Journal of Geotechnical Engineering Division,* 114(4), 491–498.

Kumar, J, and Rao, V.B.K.M. 2003. Seismic bearing capacity factors for spread foundations, *Geotechnique,* 52(2), 79–88.

Lambe, T. W., and Whitman, R. V. 1969. *Soil Mechanics*, John Wiley & Sons, New York, NY.

Menard, L. 1965. Regle pour le calcul de la force portante et du tassement des fondations en fonction des resultats pressiometriques, *Proceedings of the Sixth International Conference on Soil Mechanics and Foundation Engineering*, Montreal, **2**, pp. 295–299.

Meyerhof, G. G. 1951. The ultimate bearing capacity of foundations, *Geotechnique*, 2(4), 301–331.

Meyerhof, G. G. 1956. Penetration tests and bearing capacity of cohesionless soils, *ASCE Journal of Soil Mechanics and Foundation Division*, 82(1), 1–19.

Meyerhof, G. G. 1957. The Ultimate Bearing Capacity of Foundations on Slopes, *Proceedings of the fourth International Conference on Soil Mechanics and Foundation Engineering*, London.

Meyerhof, G. G. 1963. Some recent research on the bearing capacity of foundations, *Canadian Geotechnical Journal*, 1(1), 16–26.

Moulton, L. K., Ganga Rao, H. V. S., and Halvorsen, G. T. 1985. Tolerable Movement Criteria for Highway Bridges Final Report, Report No. FHWA/RD-85/107, October 1985. (NTIS PB86-150745/AS).

Munfakh, G., Arman, A., Collin, J. G., Hung, J. C., and Brouillette, R. P. 2001. *Shallow Foundations*, No. NHI-01-023, Federal Highway Administration, Washington, DC.

Nagaraj, T. S., and Srinivasa Murthy, B. R. 1986. A critical reappraisal of compression index, *Geotechnique*, 36(1), 27–32.

NAVFAC. 1986. *Foundations and Earth Structures, DM 7.02*, Naval Facilities Engineering Command, Alexandria, VA.

NAVFAC Design Manual 7.01. 1986. *Soil Mechanics*, Naval Facilities Engineering Command, Department of the Navy, Washington, DC.

NCHRP. 1991. *Manual for the Design of Bridge Foundations*, National Cooperative Highway Research Program Report No. 343, National Science Foundation, Washington, DC.

O'Neill, M. W., Townsend, F. C., Hassan, K. H., Buller, A., and Chan, P. S. 1996. *Load Transfer for Drilled Shafts in Intermediate Geomaterials*, Publication No. FHWA-RD-95-171, Federal Highway Administration, McClean, VA.

Olsen, S. M., and Johnson, C. I. 2008. Analyzing liquefaction-induced laterals spreads using strength ratio, *ASCE Journal of Geotechnical and Geoenvironmental Engineering*, 134(8), 1035–1049.

Paloucci, R., and Pecker, A. 1997. Seismic bearing capacity of shallow foundations on dry soils, soils and foundations, *Journal of the Japanese Geotechnical Society,* 37(3), 95–105.

Peck, R. B., Hanson, W. E., and Thornburn, T. H. 1974. *Foundation Engineering*, Second Edition, John Wiley & Sons, New York, NY.

Perloff, W. H. 1975. Pressure distribution and settlement, Chapter 4 in *Foundation Engineering Handbook*, Second Edition, Edited by Fang, H. Y. Chapman & Hall, New York, NY.

Poulos, H. G., and Davis, E. H. 1974. *Elastic Solutions for Soil and Rock Mechanics*, John Wiley & Sons, New York, NY.

Prandtl, L. 1920. *Uber die Harte Platischer korper*, Nach. Geseel. Wiss, Gottingen, Math-Phys., Kl,., pp. 75–85.

Prandtl, L. 1921. *"Über die Eindringungsfestigkeit (Härte) plastischer Baustoffe und die Festigkeit von Schneiden" (On the penetrating strengths (hardness) of plastic construction materials and the strength of cutting edges),* Zeit. Angew. Math. Mech., 1(1), 15–20.

Putnam, J. B. 1981. Analysis and Design of Foundations on Continuous Rock, M. S. Thesis, Syracuse University, May, Syracuse, New York.

Randolph, M. F. 2003. Science and empiricism in pile foundation design, *Geotechnique*, 53(10), **53**, 847–875.

Reissner, H. 1924. Zum Erddruckprolem, *Proceedings of the first International Congress of Applied Mechanics*, Delft, The Netherlands, pp. 295–311.

Richards, R., Elms, D.G., and Budhu, M. 1993. Seismic bearing capacity and settlement of foundations, *Journal of Geotechnical Engineering,* 119(4), 662–674.

Robertson, P.K. 2013. Liquefaction and liquefied strength using the cone penetration test, *ASCE Journal of Geotechnical and Geoenvironmental Engineering*, 136(6), 842–853.

Seed, R. B., and Harder, L. F. 1990. SPT-based analysis of cycle pore pressure generation and undrained residual shear strength, Proceedings, Seed Memorial Symposium, Edited by J. M. Duncan, BiTech Publishers, Vancouver, BC, Canada, pp. 351–376.

Schertmann, J. H. 1970. Static cone to compute static settlement over sand, *ASCE Journal of the Soil Mechanicals and Foundation Division*, 96(3), 1011–1043.

Schertmann, J. H. 1978. *Guidelines for Cone Penetration Test Performance, and Design*, Federal Highway Administration, Report FHWA-TS-78-209.

Schertmann, J. H., Hartman, J. P., and Brown, P. R. 1978. Improved strain influence factor diagrams, *ASCE Journal of the Geotechnical Engineering Division*, 104(8), 1131–1135.

Scott, R. F. 1981. *Foundation Analysis*, Prentice-Hall, Englewood Cliffs, NY.

Scott, R. F., and Schoustra, J. J. 1968. *Soil Mechanics and Engineering*, McGraw-Hill, New York, NY.

Skempton, A. W., and MacDonald, D. H. 1956. The allowable settlement of buildings, *Proceedings of the Institution of Civil Engineers*, London, 5, Part III, pp. 727–768.

Skempton, A. W. 1986. Standard penetration test procedures and the effects in sands of overburden pressure, relative density, particle size, aging, and overconsolidation, *Geotechnique,* 36(3), 425–447.

Sowers, G. F., and Vesic, A. B. 1962. Vertical stresses in subgrades beneath statically loaded flexible pavements, *Highway Research Board Bulletin*, No. 342.

Stark, T. D., and Mesri, G. 1992. Undrained shear strength of sands for stability analysis, *ASCE Journal of the Geotechnical Engineering*, 118(11), 1727–1747.

Steinbrenner, W. 1934. *Tafeln zur Setzungberechnung*, Die Strasse, pp. 121–124.

Tan, C. K., and Duncan, J. M. 1991. Settlement of footings on sand – accuracy and reliability, *Proceedings of Geotechnical Congress*, Boulder, CO.

Terzaghi, K. 1943. *Theoretical Soil Mechanics*, John Wiley & Sons, New York, NY.

Terzaghi, K., and Peck, R. B. 1948. *Soil Mechanics in Engineering Practice*, First Edition, John Wiley & Sons, New York, NY.

Terzaghi, K., and Peck, R. B. 1967. *Soil Mechanics in Engineering Practice*, Second Edition, John Wiley & Sons, New York, NY.

Terzaghi, K., and Peck, R. B., Mesri, G. 1996. *Soil Mechanics in Engineering Practice*, Third Edition, John Wiley & Sons, New York, NY.

Tomlinson, M. J., and Boorman, R. 2001. *Foundation Design and Construction*. Seventh Edition, Prentice Hall, Upper Saddle River, NJ.

TRCC. 2009. *Limited Statutory Warranty and Building and Performance Standards*, Effective June 1, 2005, as amended through July 31, 2009, Texas Property Code Title 16 and Texas Administrative Code 10, Chapter 304, Texas Residential Construction Commission.

Tschebotarioff, G. 1951. *Soil Mechanics, Foundations and Earth Structures,* McGraw-Hill, New York.

USACE. 1995. Rock Foundations, EM 1110-1-2908, U.S. Army Corps of Engineers, Washington, DC.

USACE. 2005. *Stability Analyses of Hydraulic Structures*, EM 1110-2-2100, U.S. Army Corps of Engineers.

Vesic, A. S. 1963. Bearing capacity of deep foundations in sand, National Academy of Sciences, *National Research Council, Highway Research Record*, 39, 112–153.

Vesic, A. S. 1973. Analysis of ultimate loads of shallow foundations, *ASCE Journal of the Soil Mechanics and Foundation Engineering Division*, 99(1), 45–73.

Vesic, A. S. 1975. Bearing capacity of shallow foundations, Chapter 3 in *Foundation Engineering Handbook*, Edited by Winterkorn, H. F., and Fang, H. Y. Van Nostrand Reinhold, New York, NY.

Westergaard, H. M. 1938. A Problem of Elasticity Suggested by a Problem in Soil Mechanics: Soft Material Reinforced by Numerous Strong Horizontal Sheets, in *Contributions to the Mechanics of Solids*, Stephen Timoshenko Sixtieth Anniversary Volume, Macmillan, New York, NY.

Wroth, C. P., and Wood, D. M. 1978. The correlation of index properties with some basic engineering properties of soils, *Candian Geotechnica*, 15(2), 137–145.

Wyllie, D. C. 1992. *Foundations on Rock*, E & FN SPON, London.

9

Deep Foundations

Youzhi Ma
AMEC Environmental and Infrastructure Inc.

Nan Deng
Bechtel Corporation

9.1 Introduction

A bridge foundation is part of the bridge substructure connecting the bridge to the ground. A foundation consists of man-made structural elements that are constructed either on top of or within existing geological materials. The function of a foundation is to provide support for the bridge and transfer loads or energy between the bridge structure and the ground.

A deep foundation is a type of foundation that the embedment is larger than its maximum plane dimension. The foundation is designed to be supported on deeper geologic materials because either the soil or rock near the ground surface is not competent enough to take the design loads, or it is more economical to do so.

The merit of a deep foundation over a shallow foundation is manifold. By involving deeper geological materials, a deep foundation occupies a relatively smaller area of the ground surface. Deep foundations can usually take larger loads than shallow foundations that occupy the same area of the ground surface. Deep foundations can reach deeper competent layers of bearing soil or rock whereas shallow foundations cannot. Deep foundations can also take large uplift and lateral loads whereas shallow foundations usually cannot.

The purpose of this chapter is to give a brief but comprehensive review to the design procedure of deep foundations for structural engineers and other bridge design engineers. Consideration of selection of foundation types and various design issues are first discussed. Typical procedures to calculate the axial and lateral capacities of an individual pile are then presented. Typical procedures to analyze pile groups are also discussed. A brief discussion regarding seismic design is also presented for its uniqueness and importance in the foundation design.

9.2 Classification and Selection

9.2.1 Typical Foundations

Typical foundations are shown in Figure 9.1 and are listed as follows:

A *pile* usually represents a slender structural element that is driven into ground. However, a pile is often used as a genetic term to represent all types of deep foundations, including a (driven)

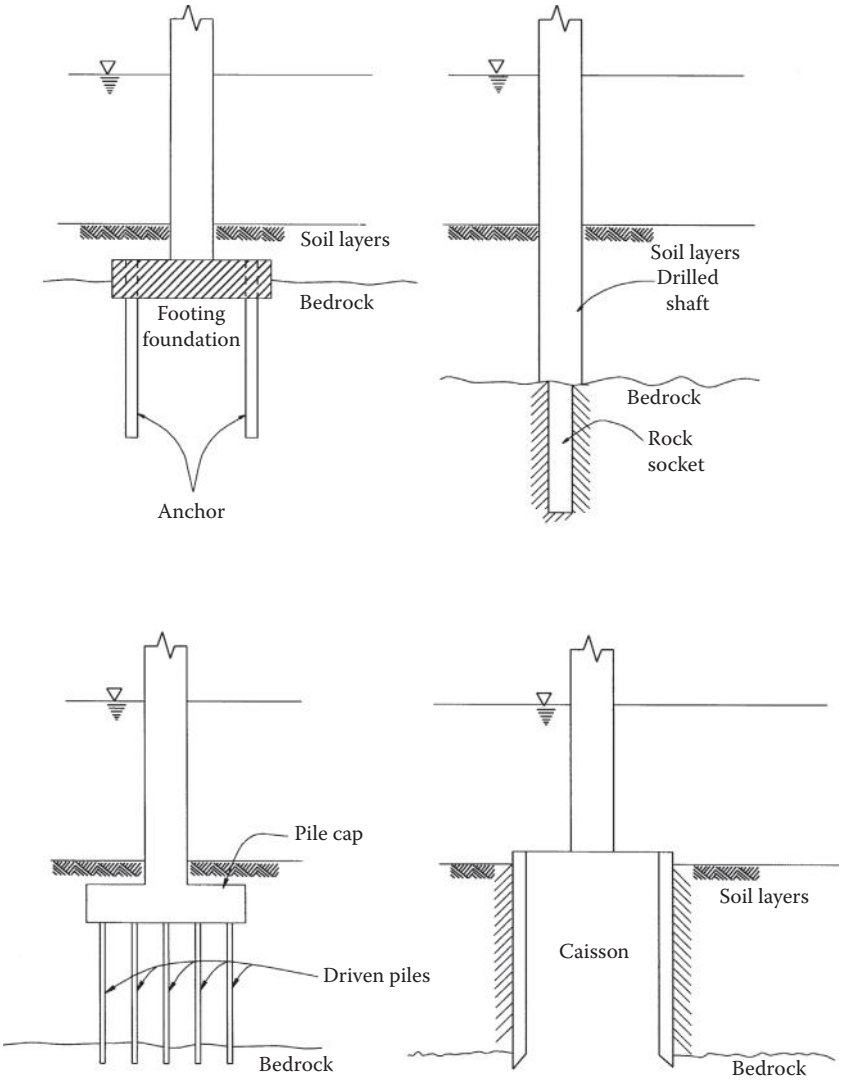

FIGURE 9.1 Typical foundations.

pile, (drilled) shaft, caisson, or an anchor. A *pile group* is used to represent various grouped deep foundations.

A *shaft* is a type of foundation that is constructed with cast-in-place concrete after a hole is first drilled or excavated. A *rock socket* is a shaft foundation installed in rock. A shaft foundation is also called a *drilled pier* foundation.

A *caisson* is a type of large foundation that is constructed by lowering preconstructed foundation elements through excavation of soil or rock at the bottom of the foundation. The bottom of the caisson is usually sealed with concrete after the construction is completed.

An *anchor* is a type of foundation designed to take tensile loading. An anchor is a slender small diameter element consisting of a reinforcement bar that is fixed in a drilled hole by grout concrete. Multistrain high-strength cables are often used as reinforcement for large capacity anchors. An *anchor for suspension bridge* is, however, a foundation that sustains the pulling loads located at the ends of a bridge; the foundation can be a deadman, a massive tunnel, or a composite foundation system including normal anchors, piles, and drilled shafts.

A *spread footing* is a type of foundation that the embedment is usually less than its smallest width. Normal spread footing foundation is discussed in detail in Chapter 8.

9.2.2 Typical Bridge Foundations

Bridge foundations can be individual, grouped, or combination foundations. Individual bridge foundations usually include individual footings, large-diameter drilled shafts, caissons, rock sockets, and deadman foundations. Grouped foundations include groups of caissons, driven piles, drilled shafts, and rock sockets. Combination foundations include caisson with driven piles, caisson with drilled shafts, large-diameter pipe piles with rock socket, spread footings with anchors, deadman with piles and anchors, and so on.

For small bridges, small-scale foundations such as individual footings or drilled shaft foundations, or a small group of driven piles may be sufficient. For larger bridges, large-diameter shaft foundations, grouped foundations, caissons, or combination foundations may be required. Caissons, large-diameter steel pipe pile foundations, or other types of foundations constructed by using the cofferdam method may be necessary for foundations constructed over water.

Bridge foundations are often constructed in difficult ground conditions such as landslide areas, liquefiable soil, collapsible soil, soft and highly compressible soil, swelling soil, coral deposits, and underground caves. Special foundation types and designs may be needed under these circumstances.

9.2.3 Classification

Deep foundations have many different types and are classified according to different aspects of a foundation as listed below:

Geologic conditions—Geologic materials surrounding the foundations can be soil and rock. Soil can be fine grained or coarse grained; and from soft to stiff and hard for fine-grained soil, or from loose to dense and very dense for coarse-grained soil. Rock can be sedimentary, igneous, or metamorphic; and from very soft to medium strong and hard. Soil and rock mass may possess predefined weakness and discontinuities, such as rock joints, beddings, sliding planes, and faults. Water conditions can be different, including over river, lake, bay, ocean, or land with groundwater. Ice or wave action may be of concern in some regions.

Installation methods—Installation methods can be piles (driven, cast-in-place, vibrated, torqued, and jacked); shafts (excavated, drilled, and cast-in-drilled-hole); anchor (drilled); caissons (Chicago, Shored, Benoto, Open, Pneumatic, floating, closed-box, Potomac, etc.); cofferdams (sheet pile, sand or gravel island, slurry wall, deep mixing wall, etc.); or combined.

Structural materials—Materials for foundations can be timber, precast concrete, cast-in-place concrete, compacted dry concrete, grouted concrete, posttension steel, H-beam steel, steel pipe, composite, etc.

Ground effect—Depending on disturbance to the surrounding ground, piles can be displacement piles, low displacement, or nondisplacement piles. Driven precast concrete piles and steel pipes with end plugs are displacement piles, H-beam and umplugged steel pipes are low-displacement piles, and drilled shafts are nondisplacement piles.

Function—Depending on the portion of load carried by the side, toe, or a combination of the side and toe, piles are classified as frictional, end bearing, and combination piles, respectively.

Embedment and relative rigidity—Piles can be divided into long piles and short piles. A long pile, or simply called a pile, is embedded deep enough that fixity at its bottom is established, and the pile is treated as a slender and flexible element. A short pile is relatively rigid element that the bottom of the pile moves significantly. A caisson is often a short pile because of its large cross section and stiffness. An extreme case for short piles is a spread footing foundation.

Cross-section—The cross section of a pile can be square, rectangular, circular, hexagonal, octagonal, H-section; either hollow or solid. A pile cap is usually square, rectangular, circular, or bell-shaped. Piles can have different cross sections at different depths, such as uniform, uniform taper, step taper, or enlarged end (either grouted or excavated).

Size—Depending on the diameter of a pile, piles are classified as pin piles and anchors (100–300 mm), normal size piles and shafts (250–600 mm), large-diameter piles and shafts (600–3000 mm), caissons (600 mm and up to 3000 mm or larger), and cofferdams or other shoring construction method (very large).

Loading—Loads applied to foundations are compression, tension, moment, and lateral loads. Depending on time characteristics, loads are further classified as static, cyclic, and transient loads. The magnitude and type of loading also are major factors in determining the size and type of a foundation (see Table 9.1).

Isolation—Piles can be isolated at certain depth to avoid loading utility lines or other construction, or to avoid being loaded by them.

Inclination—Piles can be vertical or inclined. Inclined piles are often called battered or raked piles.

Multiple piles—Foundation can be an individual pile, or a pile group. Within a pile group, piles can be of uniform or different sizes and types. The connection between the piles and the pile cap can be fixed, pinned, or restrained.

9.2.4 Advantages/Disadvantages of Different Types of Foundations

Different types of foundations have their unique features and are more applicable to certain conditions than others. The advantages and disadvantages for different types of foundations are listed in Sections 9.2.4.1 through 9.2.4.7:

TABLE 9.1 Range of Maximum Capacity of Individual Deep Foundations

Type of Foundation	Size of Cross Section	Maximum Compressive Working Capacity
Driven concrete piles	Up to 46 cm	100–250 t [900–2,200 kN]
Driven steel pipe piles	Up to 46 cm	50–250 t [450–2,200 kN]
Driven steel H-piles	Up to 46 cm	50–250 t [450–2,200 kN]
Drilled shafts	Up to 60 cm	Up to 400 t [3,500 kN]
Large steel pipe piles, concrete-filled; Large-diameter drilled shafts; Rock rocket	0.6–3 m	300–5,000 t or more [2,700–45,000 kN]

9.2.4.1 Driven Precast Concrete Pile Foundations

Driven concrete pile foundations are applicable under most ground conditions. Concrete piles are usually inexpensive compared with other types of deep foundations. The procedure of pile installation is straightforward; piles can be produced in mass production either on site or in a manufacture factory; and the cost for materials is usually much less than steel piles. Proxy coating can be applied to reduce negative skin friction along the pile. Pile driving can densify loose sand and reduce liquefaction potential within a range of up to 3 diameters surrounding the pile.

However, driven concrete piles are not suitable if boulders exist below the ground surface where piles may break easily and pile penetration may be terminated prematurely. Piles in dense sand, dense gravel, or bedrock usually have limited penetration; consequently, the uplift capacity of these types of piles is very small.

Pile driving produces noise pollution and causes disturbance to the adjacent structures. Driving of concrete piles also requires large overhead space. Piles may break during driving and impose a safety hazard. Piles that break underground cannot take their design loads, and will cause damage to the structures if the broke pile is not detected and replaced. Piles could often be driven out of their designed alignment and inclination, and as a result, additional piles may be needed. Special hardened steel shoe is often required to prevent pile tips from being smashed when encountering hard rock. End bearing capacity of a pile is not reliable if the end of a pile is smashed.

Driven piles may not be a good option when subsurface conditions are unclear or vary considerably over the site. Splicing and cutting of piles are necessary when the estimated length is different from the manufactured length. Splicing is usually difficult and time consuming for concrete piles. Cutting of a pile would change the pattern of reinforcement along the pile, especially where extra reinforcement is needed at the top of a pile for lateral capacity. A pilot program is usually needed to determine the length and capacity prior to mass production and installation of production piles.

The maximum pile length is usually up to 36–38 m because of restrictions during transportation on highways. Although longer piles can be produced on site, slender and long piles may buckle easily during handling and driving. Precast concrete piles with diameters greater than 46 cm are rarely used.

9.2.4.2 Driven Steel Piles

Driven steel piles, such as steel pipe and H-beam piles are extensively used as bridge foundations, especially in the seismic retrofit projects. Having the advantage and disadvantage of driven piles as discussed earlier, driven steel piles have their uniqueness.

Steel piles are usually more expensive than concrete piles. They are more ductile and flexible and can be spliced more conveniently. The required overhead is much smaller compared to driven concrete piles. Pipe piles with an open end can penetrate through layers of dense sand. If necessary, the soil inside the pipe can be taken out before further driving; small size boulders may also be crushed and taken out. H-piles with a pointed tip can usually penetrate onto soft bedrock and establish enough end bearing capacity.

9.2.4.3 Large-Diameter Driven, Vibrated, or Torqued Steel Pipe Piles

Large-diameter pipe piles are widely used as foundations for large bridges. The advantage of this type of foundation is manifold. Large-diameter pipe piles can be built over water from a barge, a trestle, or a temporary island. They can be used in almost all ground conditions and penetrate to a great depth to reach bedrock. Length of the pile can be adjusted by welding. Large-diameter pipe piles can also be used as casing to support soil above bedrock from caving in; rock sockets or rock anchors can then be constructed below the tip of the pipe. Concrete or reinforced concrete can be placed inside the pipe after it is cleaned. Another advantage is that no workers are required to work below water or ground surface. Construction is usually safer and faster than other types of foundations such as caissons or cofferdam construction.

Large-diameter pipe piles can be installed by method of driving, vibrating, or torque. Driven piles usually have higher capacity than piles installed through vibration or torque. However, driven piles are hard to control in terms of location and inclination of the piles. Moreover, once a pile is out of location or installed with unwanted inclination, no corrective measures can be applied. Piles installed with vibration or torque, on the other hand, can be controlled more easily. If a pile is out of position or inclination, the pile can even be lifted up and reinstalled.

9.2.4.4 Drilled Shaft Foundations

Drilled shaft foundations are the most versatile types of foundations. The length and size of the foundations can be tailored easily. Disturbance to the nearby structures is small compared with other types of deep foundations. Drilled shafts can be constructed very close to existing structures and can be constructed under low overhead conditions. Therefore, drilled shafts are often used in many seismic retrofit projects. However, drilled shafts may be difficult to install under certain ground conditions such as soft soil, loose sand, sand under water, and soils with boulders. Drilled shaft will generate a large volume of soil cuttings and fluid and can be mess. Disposal of the cuttings is usually a concern for sites with contaminated soils.

Drilled shaft foundations are usually comparable or more expensive than driven piles. For large bridge foundations, their cost is at the same level of caisson foundations and spread footing foundations combined with cofferdam construction. Drilled shaft foundations can be constructed very fast under normal conditions compared with caisson and cofferdam construction.

9.2.4.5 Anchors

Anchors are special foundation elements that are designed to take uplift loads. Anchors can be added if an existing foundation lacks uplift capacity, and competent layers of soil or rock are shallow and easy to reach. Anchors, however, cannot take lateral loads and may be sheared off if combined lateral capacity is not enough.

Anchors are in many cases pretensioned in order to limit the deformation to activate the anchor. The anchor system is therefore very stiff. Failure of structure resulted form anchor rupture often occurs very quickly and catastrophically. Pretension may also be lost over time because of creep in some types of rock and soil. Anchors should be tested carefully for their design capacity and creep performance.

9.2.4.6 Caissons

Caissons are large-size structures that are mainly used for construction of large bridge foundations. Caisson foundations can take large compressive and lateral loads. They are used primarily for overwater construction and sometimes used in soft or loose soil conditions, with a purpose to sink or excavate down to a depth where bedrock or firm soil can be reached. During construction, large size boulders can be removed.

Caisson construction requires special technique and experience. Caisson foundations are usually very costly, and comparable to the cost of cofferdam construction. Therefore, caissons are usually not the first option unless other types of foundations are not favored.

9.2.4.7 Cofferdam and Shoring

Cofferdam or other type of shoring system is a method of foundation construction to retain water and soil. A dry bottom deep into water or ground can be created as a working platform. Foundations of essentially any types discussed earlier can be built from the platform on top of firm soil or rock at a great depth; otherwise can only be reached by deep foundations.

A spread footing type of foundation can be built from the platform. Pile foundations also can be constructed from the platform and the pile length can be reduced substantially. Without cofferdam or shoring, a foundation may not be possible if constructed from the water or ground surface, or may be too costly.

Cofferdam construction is often very expensive and should only be chosen if it is favorable comparing with other foundation options in terms of cost and construction conditions.

9.2.5 Characteristics of Different Types of Foundations

In this section, the mechanisms of resistance of an individual foundation and a pile group are discussed. The function of different types of foundations is also addressed.

The complex loading on top of a foundation from the bridge structures above can be simplified into forces and moments in the longitudinal, transverse, and vertical directions, respectively (see Figure 9.2). Longitudinal and transverse loads are also called the horizontal loads; longitudinal and transverse moments are called the overturning moments. The resistance provided by an individual foundation is categorized in the following (also see Figure 9.3).

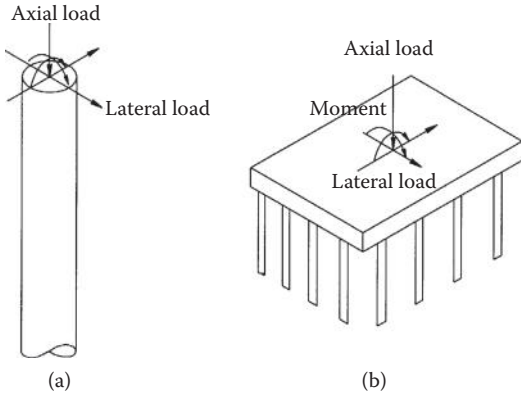

FIGURE 9.2 Acting loads on top of a pile or a pile group. (a) An individual pile, (b) A pile group.

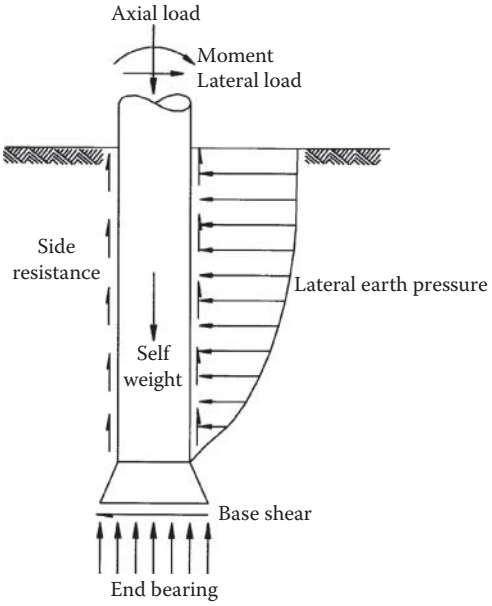

FIGURE 9.3 Resistance of an individual foundation.

End bearing: vertical compressive resistance at the base of a foundation, distributed end bearing pressures can provide resistance to overturning moments
Base shear: horizontal resistance of friction and cohesion at the base of a foundation
Side resistance: shear resistance from friction and cohesion along side of a foundation
Earth pressure: mainly horizontal resistance from lateral earth pressures perpendicular to side of the foundation
Self-weight: effective weight of the foundation

Both base shear and lateral earth pressures provide lateral resistance of a foundation, and contribution of lateral earth pressures decreases as the embedment of a pile increases. For long piles, lateral earth pressures are the main source of lateral resistance. For short piles, base shear and end bearing pressures can also contribute part of the lateral resistance. Table 9.2 lists various types of resistance of an individual pile.

For a pile group, through the action of the pile cap, the coupled axial compressive and uplift resistance of individual piles provides majority of the resistance to the overturning moment loading. Horizontal (or lateral) resistance can at the same time provide torsional moment resistance. A pile group is more efficient in resisting overturning and torsional moment than an individual foundation. Table 9.3 summarizes functions of a pile group in addition to that of individual piles.

TABLE 9.2 Resistance of an Individual Foundation

	Type of Resistance				
Type of Foundation	Vertical Compressive Load (Axial)	Vertical Uplift Load (Axial)	Horizontal Load (Lateral)	Overturning Moment (Lateral)	Torsional Moment (Torsional)
Spread footing (also see Chapter 8)	End bearing		Base shear Lateral earth pressure	End bearing Lateral earth pressure	Base shear Lateral earth pressure
Individual short pile foundation	End bearing Side friction	Side friction	Lateral earth pressure Base shear	Lateral earth pressure End bearing	Side friction Lateral earth pressure Base shear
Individual end-bearing long pile foundation	End bearing		Lateral earth pressure	Lateral earth pressure	
Individual friction long pile foundation	Side friction	Side friction	Lateral earth pressure	Lateral earth pressure	Side friction
Individual long pile foundation	End bearing Side friction	Side friction	Lateral earth pressure	Lateral earth pressure	Side friction
Anchor		Side friction			

TABLE 9.3 Additional Functions of Pile Group Foundations

	Type of Resistance	
Type of Foundation	Overturning moment (lateral)	Torsional moment (torsional)
Grouped spread footings	Vertical compressive resistance	Horizontal resistance
Grouped pile foundation	Vertical compressive resistance, vertical uplift resistance	Horizontal resistance
Grouped anchors	Vertical uplift resistance	

9.2.6 Selection of Foundations

The two predominant factors in determining type of foundations are bridge types and ground conditions.

The bridge type, including dimensions, type of bridge, and construction materials dictates the design magnitude of loads and the allowable displacements and other performance criterion for the foundations, and therefore determines the dimensions and type of its foundations. For example, a suspension bridge requires large lateral capacity for its end anchorage, which can be a huge deadman, a high capacity soil or rock anchor system, a group of driven piles, or a group of large-diameter drilled shafts. Tower foundations of an overwater bridge require large compressive, uplift, lateral, and overturning moment capacities. The likely foundations are deep, large-size footing using cofferdam construction, caissons, groups of large-diameter drilled shafts, or groups of large number of steel piles.

Surface and subsurface geologic and geotechnical conditions are another main factor in determining the type of bridge foundations. Subsurface conditions, especially the depths to the load-bearing soil layer or bedrock, are the most crucial factor. Seismicity over the region usually dictates the design level of seismic loads, which is often the critical and dominant loading condition. A bridge that crosses a deep valley or river certainly determines the minimum span required. Overwater bridges have limited options to choose in terms of type of foundations.

The final choice of type of foundations usually depends on cost after considering some other factors such as construction conditions, space and over head conditions, local practice, environmental conditions, schedule constraints, and so on. In the process of selection, several types of foundations would be evaluated as candidates once the type of bridge and the preliminary ground conditions are known. Certain types of foundations are excluded in the earth stage of study. For example, from the geotechnical point of view, shallow foundation is not an acceptable option if a thick layer of soft clay or liquefiable sand is near the ground surface. Deep foundations are used in cases where shallow foundations would be excessively large and costly. From constructability point of view, driven pile foundations are not suitable if boulders exist at depths above the intended firm bearing soil/rock layer.

For small bridges such as roadway overpass, for example, foundations with driven concrete or steel piles, drilled shafts, or shallow spread footing foundations may be the suitable choices. For large overwater bridge foundations, single or grouped large-diameter pipe piles, large-diameter rock socket, large-diameter drilled shafts caissons, or foundations constructed with cofferdams are most likely the choice. Caissons or cofferdam construction with a large number of driven pile groups were widely used in the past. Large-diameter pipe piles or drilled shafts, in combination with rock sockets, are preferred for bridge foundations recently.

Deformation compatibility of the foundations and bridge structure is an important consideration. Different types of foundation may behave differently; therefore, same type of foundations should be used for one section of bridge structure. Diameter of the piles and inclined piles are two important factors to be considered in terms of deformation compatibility and are discussed in the following.

Small-diameter piles are more "brittle" in the sense that the ultimate settlement and lateral deflection are relatively small compared with large-diameter piles. For example, 20 small piles can have the same ultimate load capacity as two large-diameter piles. However, the small piles reach the ultimate state at a lateral deflection of 50 mm whereas the large piles, at 150 mm. The smaller piles would have failed before the larger piles are activated to a substantial degree. In other words, larger piles will be more flexible and ductile than smaller piles before reaching the ultimate state. Since ductility usually provides more seismic safety, larger diameter piles are preferred from the point of view of seismic design.

Inclined or battered piles should not be used together with vertical piles unless the inclined piles alone have enough lateral capacity. Inclined piles provide partial lateral resistance from their axial capacity; and since the stiffness in the axial direction of a pile is much larger than in the perpendicular directions, inclined piles tend to attract most of the lateral seismic loading. Inclined piles will fail or reach their ultimate axial capacity before the vertical piles are activated to take substantial lateral loads.

9.3 Design Considerations

9.3.1 Design Concept

The current practice of foundation design employs mainly two types of design concept: the permissible stress approach and the limit state approach.

Using the permissible stress approach, both the demanded stresses from loading and the ultimate stress capacity of the foundation are evaluated. The foundation is considered to be safe as long as the demanded stresses are less than the ultimate stress capacity of the foundation. A factor of safety (FS) of 2–3 is usually applied to the ultimate capacity to obtain various allowable levels of loading in order to limit the displacements of a foundation. A separate displacement analysis is usually performed to determine the allowable displacements for a foundation, and for the bridge structures. Design based on the permissible concept is still the most popular practice in foundation design.

Starting to be adopted in the design of large critical bridges, the limit state approach requires that the foundation and its supported bridge should not fail to meet performance requirements when exceeding various limit states. Collapse of the bridge is the ultimate limit state, and design is aimed to apply various factors to loading and resistance to ensure that this state is highly improbable. A design needs to ensure the structural integrity of the critical foundations before reaching the ultimate limit state, such that the bridge can be repaired at a relatively short period after a major loading incident without reconstruction of the time-consuming foundations.

9.3.2 Design Procedures

Under normal conditions, the design procedures of a bridge foundation should involve the following steps:

1. Evaluate the site and subsurface geologic and geotechnical conditions, perform borings or other field exploratory programs, and conduct field and laboratory tests to obtain design parameters for subsurface materials
2. Review the foundation requirements including design loads and allowable displacements, regulatory provisions, space or other constraints
3. Evaluate the anticipated construction conditions and procedures
4. Select appropriate foundation type(s)
5. Determine the allowable and ultimate axial and lateral foundation design capacity, load versus deflection relationship, and load versus settlement relationship
6. Design various elements of the foundation structure
7. Specify requirements for construction inspection and/or load test procedures, and incorporate the requirements into construction specifications

9.3.3 Design Capacities

9.3.3.1 Capacity in Long-Term and Short-Term Conditions

Depending on the loading types, foundations are designed for two different stress conditions. Capacity in total stress is used where the loading is relatively quick and corresponds to an undrained condition. Capacity in effective stress is adopted where loading is slow and corresponds to a drained condition. For many types of granular soil such as clean gravel and sand, drained capacity is very close to undrained capacity under most loading conditions. Pile capacity under seismic loading is usually taken 30% higher than capacity under static loading.

9.3.3.2 Axial, Lateral, and Moment Capacity

Deep foundations can provide lateral resistance to overturning moment and lateral loads, and axial resistance to axial loads. Part or most of the moment capacity of a pile group are provided by the axial capacity of individual piles through pile cap action. The moment capacity depends on the axial capacity of the individual piles, geometry arrangement of the piles, rigidity of the pile cap, and rigidity of connection between the piles and the pile cap. Design and analysis is often concentrated on the axial and lateral capacity of individual piles. Axial capacity of an individual pile will be addressed in detail in Section 9.4, and lateral capacity in Section 9.5. Pile groups will be addressed in Section 9.6.

9.3.3.3 Structural Capacity

Deep foundations may fail because of structural failure of the foundation elements. These elements should be designed to take moment, shear, column action or buckling, corrosion, fatigue, and so on. under various design loading and environmental conditions.

9.3.3.4 Determination of Capacities

In the previous sections, the general procedure and concept for the design of deep foundations are discussed. Detailed design includes the determination of axial and lateral capacity of individual foundations, and capacity of pile groups. Many methods are available to estimate these capacities and can be categorized into three types of methodology as listed in the following:

- Theoretical analysis utilizing soil or rock strength
- Empirical methods including empirical analysis utilizing standard field tests, code requirements, and local experience
- Load tests including full-scale load tests and dynamic driving and restriking resistance analysis

The choice of methods to use depends on the availability of data, economy, and other constraints. Usually, several methods are used; the capacity of the foundation is then obtained through a comprehensive evaluation and judgment.

In applying the earlier methods, the designers need to keep in mind that the capacity of a foundation is the sum of capacities of all elements. Deformation should be compatible both in the foundation elements, the surrounding soil, and the soil-foundation interface. Settlement or other movements of a foundation should be restricted within an acceptable range and usually is a controlling factor for large-size foundations.

9.3.4 Summary of Design Methods

Table 9.4 presents a partial list of design methods available in the literature.

9.3.5 Other Design Issues

Proper foundation design should consider many factors regarding the environmental conditions, type of loading conditions, soil and rock conditions, construction, and engineering analyses, including:

- Various loading and loading combinations, including the impact loads of ships or vehicles
- Earthquake shaking
- Liquefaction
- Rupture of active fault and shear zone
- Landslide or ground instability
- Difficult ground conditions such as underlying weak and compressible soils

TABLE 9.4 Summary of Design Methods for Deep Foundations

Type	Design for	Soil Condition	Method and Author
Driven pile	End bearing	Clay	Nc method (Skempton, 1951)
Driven pile	End bearing	Clay	Nc method (Goudreault and Fellenius, 1994)
Driven pile	End bearing	Clay	CPT methods (Meyerhof, 1956; Davies et al., 1988; Schmertmann, 1978)
Driven pile	End bearing	Clay	CPT (Bustamante and Gianeselli, 1982; CGS, 1992)
Driven pile	End bearing	Sand	Nq method with critical depth concept (Meyerhof, 1976)
Driven pile	End bearing	Sand	Nq method (Berezantzev et al., 1961)
Driven pile	End bearing	Sand	Nq method (Goudreault and Fellenius, 1994)
Driven pile	End bearing	Sand	Nq by others (Janbu, 1976; Terzaghi, 1943; Vesic, 1967)
Driven pile	End bearing	Sand	Limiting Nq values (API, 2000; de Ruiter and Beringen, 1978)
Driven pile	End bearing	Sand	Value of φ (Kishida, 1967; Kulhawy, 1983; Mitchell and Lunne, 1978)
Driven pile	End bearing	Sand	SPT (Meyerhof, 1956, 1976)
Driven pile	End bearing	Sand	CPT methods (Meyerhof, 1956; Davies et al., 1988; Schmertmann, 1978)
Driven pile	End bearing	Sand	CPT (Bustamante and Gianeselli, 1982; CGS, 1992)
Driven pile	End bearing	Rock	(CGS, 1992)
Driven pile	Side resistance	Clay	α-method (Tomlinson, 1957, 1971)
Driven pile	Side resistance	Clay	α-method (API, 2000)
Driven pile	Side resistance	Clay	β-method (Goudreault and Fellenius, 1994)
Driven pile	Side resistance	Clay	λ-method (Kraft et al., 1981; Vijayvergiya and Focht, 1972)
Driven pile	Side resistance	Clay	CPT methods (Meyerhof, 1956; Davies et al., 1988; Schmertmann, 1978)
Driven pile	Side resistance	Clay	CPT (Bustamante and Gianeselli, 1982; CGS, 1992)
Driven pile	Side resistance	Clay	SPT (Dennis, 1982)
Driven pile	Side resistance	Sand	α-method (Tomlinson, 1957, 1971)
Driven pile	Side resistance	Sand	β-method (Burland, 1973)
Driven pile	Side resistance	Sand	β-method (Goudreault and Fellenius, 1994)
Driven pile	Side resistance	Sand	CPT method (Meyerhof, 1956; Davies et al., 1988; Schmertmann, 1978)
Driven pile	Side resistance	Sand	CPT (Bustamante and Gianeselli, 1982; CGS, 1992)
Driven pile	Side resistance	Sand	SPT (Meyerhof, 1956, 1976)
Driven pile	Side and end	All	Load test: ASTM D 1143, static axial compressive test
Driven pile	Side and end	All	Load test: ASTM D 3689, static axial tensile test
Driven pile	Side and end	All	Sanders' pile driving formula (1850; Poulos and Davis, 1980)
Driven pile	Side and end	All	Danish pile driving formula (Sörensen and Hansen, 1957)
Driven pile	Side and end	All	*Engineering News* formula
Driven pile	Side and end	All	Dynamic formula—WEAP Analysis
Driven pile	Side and end	All	Strike and restrike dynamic analysis
Driven pile	Side and end	All	Interlayer influence (Meyerhof, 1976)
Driven pile	Side and end	All	No critical depth (Fellenius, 1994; Kulhawy, 1984)
Driven pile	Load-settlement	Sand	(Vesic,1970)
Driven pile	Load-settlement	Sand	(Mosher,1984; Vijayvergiya,1977)
Driven pile	Load-settlement	All	Theory of elasticity, Mindlin's solutions (Poulos and Davis, 1980)
Driven pile	Load-settlement	All	Finite element method (Desai and Christian, 1977)
Driven pile	Load-settlement	All	Load test: ASTM D 1143, static axial compressive test
Driven pile	Load-settlement	All	Load test: ASTM D 3689, static axial tensile test
Drilled shaft	End bearing	Clay	Nc method (Skempton, 1951)

TABLE 9.4 (*Continued*) Summary of Design Methods for Deep Foundations

Type	Design for	Soil Condition	Method and Author
Drilled shaft	End bearing	Clay	Large base (O'Neil and Sheikh, 1985; Reese and O'Neil, 1988)
Drilled shaft	End bearing	Clay	CPT (Bustamante and Gianeselli, 1982; CGS, 1992)
Drilled shaft	End bearing	Sand	(Touma and Reese, 1972)
Drilled shaft	End bearing	Sand	(Meyerhof, 1976)
Drilled shaft	End bearing	Sand	(Reese and Wright, 1977)
Drilled shaft	End bearing	Sand	(Reese and O'Neil, 1988)
Drilled shaft	End bearing	Sand	SPT (Meyerhof, 1956, 1976)
Drilled shaft	End bearing	Sand	CPT (Bustamante and Gianeselli, 1982; CGS, 1992)
Drilled shaft	End bearing	Rock	(CGS, 1992)
Drilled shaft	End bearing	Rock	Pressure meter (CGS, 1992)
Drilled shaft	Side resistance	Clay	α-method (Reese and O'Neil, 1988)
Drilled shaft	Side resistance	Clay	α-method (Skempton, 1959)
Drilled shaft	Side resistance	Clay	α-method (Weltman and Healy, 1978)
Drilled shaft	Side resistance	Clay	CPT (Bustamante and Gianeselli, 1982; CGS, 1992)
Drilled shaft	Side resistance	Sand	(Touma and Reese, 1972)
Drilled shaft	Side resistance	Sand	(Meyerhof, 1976)
Drilled shaft	Side resistance	Sand	(Reese and Wright, 1977)
Drilled shaft	Side resistance	Sand	β-method (O'Neil and Reese, 1978, Reese and O'Neil, 1988)
Drilled shaft	Side resistance	Sand	SPT (Reese and O'Neil, 1988)
Drilled shaft	Side resistance	Sand	CPT (Bustamante and Gianeselli, 1982; CGS, 1992)
Drilled shaft	Side resistance	Rock	Coulombic (McVay et al., 1992)
Drilled shaft	Side resistance	Rock	Coulombic (Townsend, 1993)
Drilled shaft	Side resistance	Rock	SPT (Crapps, 1986)
Drilled shaft	Side resistance	Rock	(Gupton and Logan, 1984)
Drilled shaft	Side resistance	Rock	(Reynolds and Kaderabek, 1980)
Drilled shaft	Side resistance	Rock	(Carter and Kulhawy, 1988; Kulhawy and Phoon, 1993)
Drilled shaft	Side resistance	Rock	(Horvath and Kenney, 1979)
Drilled shaft	Side and end	Rock	(O'Neil et al., 1996)
Drilled shaft	Side and end	Rock	(Williams et al., 1980)
Drilled shaft	Side and end	Rock	(Rosenberg and Journeaux, 1976)
Drilled shaft	Side and end	Rock	(Pells and Turner, 1979, 1980)
Drilled shaft	Side and end	Rock	(Rowe and Armitage, 1987a, 1987b)
Drilled shaft	Side and end	Rock	FHWA (Reese and O'Neil, 1988)
Drilled shaft	Side and end	All	Load test (Osterberg, 1989)
Drilled shaft	Load-settlement	Sand	(Reese and O'Neil, 1988)
Drilled shaft	Load-settlement	Clay	(Reese and O'Neil, 1988)
Drilled shaft	Load-settlement	Clay	(Woodward et al., 1972)
Drilled shaft	Load-settlement	All	Load test (Osterberg, 1989)
All	Lateral resistance	Clay	Broms' method (Broms, 1964a)
All	Lateral resistance	Sand	Broms' method (Broms, 1964b)
All	Lateral resistance	All	*p-y* method (Reese, 1983)
All	Lateral resistance	Clay	*p-y* response (Matlock, 1970)
All	Lateral resistance	Clay (w/ water)	*p-y* response (Reese et al., 1975)

(*Continued*)

TABLE 9.4 (*Continued*) Summary of Design Methods for Deep Foundations

Type	Design for	Soil Condition	Method and Author
All	Lateral resistance	Clay (w/o water)	*p-y* response (Welch and Reese, 1972)
All	Lateral resistance	Sand	*p-y* response (Reese et al., 1974)
All	Lateral resistance	All	*p-y* response (American Petroleum Institute [API], 2000)
All	Lateral resistance	All	*p-y* response for inclined piles (Awoshika and Reese, 1971; Kubo, 1965)
All	Lateral resistance	All	*p-y* response in layered soil
All	Lateral resistance	All	*p-y* response (NAVFAC DM7.02, 1986)
All	Lateral resistance	Rock	*p-y* response (O'Neil et al., 1996)
All	Load-settlement	All	Theory of elasticity method (Poulos and Davis, 1980)
All	Load-settlement	All	Finite difference method (Seed and Reese, 1957)
All	Load-settlement	All	General finite element method (FEM)
All	Load-settlement	All	FEM dynamic
All	End bearing	All	Pressuremeter method (Menard, 1975; Vesic, 1972)
All	Lateral resistance	All	Pressuremeter method (Menard, 1975)
All	Lateral resistance	All	Load test: ASTM D 3966
Group	Theory	All	Elasticity approach (Poulos and Davis, 1980)
Group	Theory	All	Elasticity approach (Focht and Koch, 1973)
Group	Theory	All	Two dimensional group (Reese and Matlock, 1966)
Group	Theory	All	Three dimensional group (Reese and O'Neil, 1967)
Group	Lateral g-factor	All	(CGS, 1992)
Group	Lateral g-factor	All	(Dunnavavnt and O'Neil, 1986)

- Debris flow
- Scour and erosion
- Chemical corrosion of foundation materials
- Weathering and strength reduction of foundation materials
- Freezing
- Water conditions including flooding, water table change, dewatering
- Environmental change due to construction of bridge
- Site contamination condition of hazardous materials
- Effects of human or animal activities
- Influence upon and by nearby structures
- Governmental and community regulatory requirements
- Local practice

9.3.6 Uncertainty of Foundation Design

Foundation design is as much an art as a science discipline. Although most of the foundation structures are man-made, the surrounding geomaterials are created, deposited, and altered in nature over the geologic times. The composition and engineering properties of engineering materials such as steel

and concrete are well controlled within a variation of uncertainty between 5% and 30%. However, the uncertainty of engineering properties for natural geomaterials can be up to several times, even within relatively uniform layers and formations. The introduction of faults and other discontinuities make generalization of material properties vary hard, if not impossible.

Detailed geologic and geotechnical information is usually difficult and expensive to obtain. Foundation engineers constantly face the challenge of making engineering judgment based on limited and insufficient data of ground conditions and engineering properties of geomaterials.

It was reported that under almost identical conditions, variation of pile capacities of up to 50% could be expected within a pile cap footprint under normal circumstances. For example, piles within a nine-pile group had different restruck capacities of 110, 89, 87, 96, 86, 102, 103, 74, and 117 kips (1 kip = 4.45 kN), respectively (Fellenius, 1986).

Conservatism in foundation design, however, is not necessarily always the solution. Under seismic loading, heavier and stiffer foundations may tend to attract more seismic energy and produce larger loads; therefore, massive foundations may not guarantee a safe bridge performance.

It could be advantageous that piles, steel pipes, caisson segments, or reinforcement steel bars are tailored to exact lengths. However, variation of depth and length of foundations should always be expected. Indicator programs, such as indicator piles and pilot exploratory borings, are usually a good investment.

9.4 Axial Capacity and Settlement—Individual Foundation

9.4.1 General

The axial resistance of a deep foundation includes the tip resistance (Q_{end}), side or shaft resistance (Q_{side}), and the effective weight of the foundation (W_{pile}). Tip resistance, also called end bearing, is the compressive resistance of soil near or under the tip. Side resistance consists of friction, cohesion, and keyed bearing along the shaft of the foundation. Weight of the foundation is usually ignored under the compression because it is nearly the same as the weight of the soil displaced; but is usually accounted for under uplift loading condition.

At any loading instance, the resistance of an individual deep foundation (or pile) can be expressed as follows:

$$Q = Q_{end} + \Sigma Q_{side} \pm W_{pile} \tag{9.1}$$

The contribution of each component in Equation 9.1 depends on the stress-strain behavior and stiffness of the pile and the surrounding soil and rock. The maximum capacity of a pile can be expressed as

$$Q^{c}_{max} \le Q^{c}_{end\_max} + \Sigma Q^{c}_{side\_max} - W_{pile} \text{ (in compression)} \tag{9.2}$$

$$Q^{t}_{max} \le Q^{t}_{end\_max} + \Sigma Q^{t}_{side\_max} + W_{pile} \text{ (in uplift)} \tag{9.3}$$

and is less than the sum of all the maximum values of resistance. The ultimate capacity of a pile undergone a large settlement or upward movement can be expressed as

$$Q^{c}_{ult} = Q^{c}_{end\_ult} + \Sigma Q^{c}_{side\_ult} - W_{pile} \le Q^{c}_{max} \tag{9.4}$$

$$Q^{t}_{ult} = Q^{t}_{end\_ult} + \Sigma Q^{t}_{side\_ult} + W_{pile} \le Q^{t}_{max} \tag{9.5}$$

Side and end bearing resistance are related to displacement of a pile. Maximum end bearing capacity can be mobilized only after a substantial downward movement of the pile, whereas side friction reached its maximum capacity at a relatively smaller downward movement. Therefore, the components of the

maximum capacities (Q_{max}) indicated in Equations 9.2 and 9.3 may not be realized at the same time at the tip and along the shaft. For a drilled shaft, the end bearing is usually ignored if the bottom of the borehole is not cleared and inspected during construction. Voids or compressible materials may exist at the bottom after concrete is poured, as a result, end bearing will be activated only after a substantial displacement.

Axial displacements along a pile are larger near the top than toward its tip. Side resistance depends on the amount of displacement and is usually not uniform along the pile. If a pile is very long, maximum side resistance may not occur at the same time along the entire length of the pile. Certain types of geomaterials, such as most rocks and some stiff clay and dense sand, exhibit strain softening behavior for their side resistance, where the side resistance first increases to reach its maximum, then drops to a much smaller residual value with an increase of displacement. Consequently, only a fixed length of the pile segment maintains high resistance values and this segment migrates downward to behave in a pattern of a progressive failure. Therefore, capacity of a pile or drilled shaft may not increase infinitely with its length.

For design using the permissible stress approach, allowable capacity of a pile is the design capacity under service or routine loading. The allowable capacity (Q_{all}) is obtained by dividing ultimate capacity (Q_{ult}) by a FS to limit the level of settlement of the pile and to account for uncertainties involving material, installation, loads calculation, and other aspects. In many cases, the ultimate capacity (Q_{ult}) is assumed to be the maximum capacity (Q_{max}). The FS is usually between 2 and 3 for deep foundations depending on the reliability of the ultimate capacity estimated. With a field full-scale loading test program, the FS is usually 2.

9.4.2 End Bearing

End bearing is part of the axial compressive resistance provided at the bottom of a pile by the underlying soil or rock. The resistance depends on the type and strength of soil or rock, and the stress conditions near the tip. Piles that derived their capacity mostly from end bearing are called end bearing piles. End bearing in rock and certain types of soil such as dense sand and gravel is usually large enough to support the designed loads. However, these types of soil or rock cannot be easily penetrated through driving. No or limited uplift resistance is provided from the pile tips; therefore, end bearing piles have low resistance against uplift loading.

The end bearing of a pile can be expressed as

$$Q_{end\_max} = \begin{cases} cN_c A_{pile} & \text{for clay} \\ \sigma'_v N_q A_{pile} & \text{for sand} \\ \dfrac{U_c}{2} N_k A_{pile} & \text{for rock} \end{cases} \tag{9.6}$$

where

Q_{end_max} = the maximum end bearing of a pile
A_{pile} = the area of the pile tip or base
N_c, N_q, N_k = the bearing capacity factors for clay, sand, and rock
c = the cohesion of clay
σ'_v = the effective overburden pressure
U_c = the unconfined compressive strength of rock and $\frac{U_c}{2} = S_u$, the equivalent shear strength of rock

9.4.2.1 Clay

The bearing capacity factor N_c for clay can be expressed as

$$N_c = 6.0\left(1 + 0.2\frac{L}{D}\right) \leq 9 \tag{9.7}$$

where L is the embedment depth of the pile tip, and D is the diameter of the pile.

9.4.2.2 Sand

The bearing capacity factor N_q generally depends on the friction angle ϕ of the sand and can be estimated by using Table 9.5 or the Meyerhof's equation below.

$$N_q = e^{\pi \tan\phi} \tan^2\left(45 + \frac{\phi}{2}\right) \tag{9.8}$$

The capacity of end bearing in sand reaches a maximum cutoff after a certain critical embedment depth. This critical depth is related to ϕ and D and for design purposes, is listed as follows:

$L_c = 7D, \phi = 30^\circ$ for loose sand
$L_c = 10D, \phi = 34^\circ$ for medium dense sand
$L_c = 14D, \phi = 38^\circ$ for dense sand
$L_c = 22D, \phi = 45^\circ$ for very dense sand

The validity of the concept of critical depth has been challenged by some people; however, the practice to limit the maximum ultimate end bearing capacity in sand will result in conservative design and is often recommended.

9.4.2.3 Rock

The bearing capacity factor N_k depends on the quality of the rock mass, intact rock properties, fracture or joint properties, embedment, and other factors. Because of the complex nature of the rock mass and usually high value for design bearing capacity, care should be taken to estimate N_k. For hard fresh massive rock without open or filled fractures, N_k can be taken as high as 6. N_k decreases with increasing presence and dominance of fractures or joints and can be as low as 1. Rock should be treated as soil when rock is highly fractured and weathered or infill weak materials control the behavior of the rock mass. Bearing capacity on rock also depends on the stability of the rock mass.

TABLE 9.5 Typical Values of Bearing Capacity Factor N_q

ϕ[a] (Degrees)	26	28	30	31	32	33	34	35	36	37	38	39	40
N_q (Driven pile displacement)	10	15	21	24	29	35	42	50	62	77	86	120	145
N_q[b] (Drilled piers)	5	8	10	12	14	17	21	25	30	38	43	60	72

Source: NAVFAC, Design Manual DM7.02: Foundations and Earth Structures, Department of the Navy, Naval Facilities Engineering Command, Alexandra, VA., September, 1986.

[a] Limit ϕ to 28° if jetting is used.

[b] (A) In case a bailer of grab bucket is used below ground water table, calculate end bearing based on ϕ not exceeding 28°.

(B) For piers greater than 24-in. diameter, settlement rather than bearing capacity usually controls the design. For estimating settlement, take 50% of the settlement for an equivalent footing resting on the surface of comparable granular soils (Chapter 5, DM-7.01).

Rock slope stability analysis should be performed where the foundation is based on a slope. A higher FS, 3 to as high as 10–20, is usually applied in estimating allowable bearing capacity for rocks using the N_k approach.

The soil or rock parameters used in design should be taken from averaged properties of soil or rock below the pile tip within the influence zone. The influence zone is usually taken as deep as 3–5 diameters of the pile. Separate analyses should be conducted where weak layers exist below the tip and excessive settlement or punch failure might occur.

9.4.2.3.1 Empirical Methods

Empirical methods are based on information of type of soil/rock and field tests or index properties. Standard Penetration Test (SPT) and Cone Penetration Test (CPT) for soil are often used.

Meyerhof (1976) recommended a simple formula for piles driven into sand. The ultimate tip bearing pressure is expressed as

$$q_{\text{end\_max}} \le 4N_{\text{SPT}} \text{ in tsf } (1 \text{ tsf} = 8.9 \text{ kN}) \tag{9.9}$$

where N_{SPT} is the blow count of SPT just below the tip of the driven pile and $q_{end\_\max} = Q_{end\_\max} / A_{pile}$. Although the formula is developed for piles in sand, it is also used for piles in weathered rock for preliminary estimate of pile capacity.

Schmertmann (1978) recommended a method to estimate the pile capacity by using the CPT test:

$$q_{\text{end\_max}} = q_{\text{b}} = \frac{q_{\text{c1}} + q_{\text{c2}}}{2} \tag{9.10}$$

where

q_{c1} = the averaged cone tip resistance over a depth of 0.7–4 diameters of the pile below the tip of the pile

q_{c2} = the averaged cone tip resistance over a depth of 8 diameters of the pile above the tip of the pile

Chapter 8 presents recommended allowable bearing pressures for various soil and rock types for spread footing foundations and can be used as a conservative estimate of end bearing capacity for end bearing piles.

9.4.3 Side Resistance

Side resistance usually consists of friction and cohesion between the pile and the surrounding soil or rock along the shaft of a pile. Piles that derive their resistance mainly from side resistance are termed frictional piles. Most piles in clayey soil are frictional piles. Frictional piles can also take uplift loads.

The maximum side resistance of a pile $Q_{\text{side\_max}}$ can be expressed as

$$Q_{\text{side\_max}} = \sum f_{\text{s}} A_{\text{side}} \tag{9.11}$$

$$f_{\text{s}} = K_{\text{s}} \sigma'_{\text{v}} \tan\delta + c_{\text{a}} \tag{9.12}$$

$$c_{\text{a}} = \alpha S_{\text{u}} \tag{9.13}$$

where

$\sum$ = the sum for all layers of soil and rock along the pile
A_{side} = the shaft side area
f_s = the maximum frictional resistance on the side of the shaft
K_s = the lateral earth pressure factor along the shaft
σ'_v = the effective vertical stress along the side of the shaft
δ = the friction angle between the pile and the surrounding soil; for clayey soil under quick loading, δ is very small and usually omitted
c_a = the adhesion between pile and surrounding soil and rock
α = a strength factor
S_u = the cohesion of the soil or rock

Typical values of α, f_s, K, δ are shown in Tables 9.6 through 9.10. For design purposes, side resistance f_s in sand is limited to a cutoff value at the critical depth, which is equal to about $10B$ for loose sand and $20B$ for dense sand.

TABLE 9.6 Typical Values of α and f_s

Range of Shear Strength, S_u	Formula to Estimate α	Range of α	Range of f_s	Description
0–600 psf	$\alpha = 1.0$	1	0–600 psf	Soft clay
600–3,000 psf	$\alpha = 0.375(1 + \frac{1}{S_u}), S_u$ in ksf	1–0.5	600–1,500 psf	Medium stiff clay to very stiff clay
3,000–11,000 psf	$\alpha = 0.375(1 + \frac{1}{S_u}), S_u$ in ksf	0.5–0.41	1,500–4,500 psf	Hard clay to very soft rock
11,000–576,000 psf (76 psi–4,000 psi)	$\alpha = \frac{5}{\sqrt{2S_u}}, S_u$ in psi, or $\alpha = \frac{5}{\sqrt{q_u}}, q_u$ in psi[a]	0.41–0.056	4,500–32,000 psf (31–220 psi)	Soft rock to hard rock

Source: Horvath, R.G. and T.C. Kenney, Symposium on Deep Foundations, ASCE National Convention, Atlanta, GA, pp. 182–214, 1979.

[a] q_u is the unconfined compressive strength of rock.

Note: 1 ksf = 1,000 psf

1 psi = 144 psf

1 psf = 0.048 kPa

1 psi = 6.9 kPa for concrete driven piles and for drilled piers without buildup of mud cakes along the shaft.

TABLE 9.7 Typical Values Cohesion and Adhesion f_s

Pile Type	Consistency of Soil	Cohesion, S_u psf	Adhesion, f_s psf
Timber and concrete	Very soft	0–250	0–250
	Soft	250–500	250–480
	Med. stiff	500–1000	480–750
	Stiff	1000–2000	750–950
	Very stiff	2000–4000	950–1300
Steel	Very soft	0–250	0–250
	Soft	250–500	250–460
	Med. stiff	500–1000	480–700
	Stiff	1000–2000	700–720
	Very stiff	2000–4000	720–750

Source: NAVFAC, Design Manual DM7.02: Foundations and Earth Structures, Department of the Navy, Naval Facilities Engineering Command, Alexandra, VA., September, 1986.

Note: 1 psf = 0.048 kPa.

TABLE 9.8 Typical Values of Bond Stress of Rock Anchors for Selected Rock

Rock Type (Sound, Nondecayed)	Ultimate Bond Stresses between Rock and Anchor Plus (δ_{skin}), psi
Granite and Basalt	250–450
Limestone (competent)	300–400
Dolomitic limestone	200–300
Soft limestone	150–220
Slates and hard shales	120–200
Soft shales	30–120
Sandstone	120–150
Chalk (variable properties)	30–150
Marl (stiff, friable, fissured)	25–36

Source: NAVFAC, Design Manual DM7.02: Foundations and Earth Structures, Department of the Navy, Naval Facilities Engineering Command, Alexandra, VA., September, 1986.

Note: It is not generally recommended that design bond stresses exceed 200 psi even in the most competent rocks.

1 psi = 6.9 kPa

TABLE 9.9 Typical Values of Earth Pressure Coefficient K_s

	Earth Pressure Coefficients K_s		
Pile Type	K_s[a] (compression)	K_s[a] (tension)	K_s[b]
Driven single H-pile	0.5–1.0	0.3–0.5	
Driven single displacement pile	1.0–1.5	0.6–1.0	0.7–3.0
Driven single displacement tapered pile	1.5–2.0	1.0–1.3	
Driven jetted pile	0.4–0.9	0.3–0.6	
Drilled pile (less than 24-in. diameter)	0.7	0.4	
Insert pile			0.7 (compression) 0.5 (tension)
Driven with predrilled hole			0.4–0.7
Drilled pier			0.1–0.4

[a] From NAVFAC DM 7.02 (1986).

[b] From Tirant (1979), K_s increases with Over Consolidation Ratio (OCR) or D_R.

TABLE 9.10 Typical Value of Pile-Soil Friction Angles δ

Pile Type	δ, degrees	Alternate for δ
Concrete	-	$\delta = \frac{3}{4}\,\phi$
Concrete (rough, cast-in-place)	33	$\delta = 0.85\,\phi$
Concrete (smooth)	30	$\delta = 0.70\,\phi$
Steel	20	-
Steel (corrugated)	33	$\delta = \phi$
Steel (smooth)	-	$\delta = \phi - 5°$
Timber	-	$\delta = \frac{3}{4}\,\phi$

[a] NAVFAC DM 7.02 (1986).

[b] Woodward et al. (1972).

[c] API (2000) and de Ruiter and Beringen (1978).

Meyerhof (1976) recommended a simple formula for driven piles in sand. The ultimate side adhesion is expressed as

$$f_s \le N_{SPT}/50 \text{ tsf} \left(1 \text{ tsf} = 8.9 \text{ kN}\right) \tag{9.14}$$

where N_{SPT} is the averaged blow count of SPT along the pile.

Meyerhof (1956) also recommended a formula to calculate ultimate side adhesion based on CPT results as shown in the following.

For full displacement piles

$$f_s = \frac{q_c}{200} \le 1.0 \text{ tsf} \left(1 \text{ tsf} = 8.9 \text{ kN}\right) \tag{9.15}$$

or

$$f_s = 2f_c \le 1.0 \tag{9.16}$$

For nondisplacement piles

$$f_s = \frac{q_c}{400} \le 0.5 \text{ in tsf} \left(1 \text{ tsf} = 8.9 \text{ kN}\right) \tag{9.17}$$

or

$$f_s = f_c \le 0.5 \tag{9.18}$$

in which

q_c, f_c = the cone tip and side resistance measured from CPT, averaged values should be used along the pile.

9.4.3.1 Downdrag

For piles in soft soil, another deformation-related issue should be noted. When the soil surrounding the pile settles relatively to a pile, the side friction, also called the negative skin friction, should be considered for underlying compressible clayey soil layers and liquefiable loose sand layers. Downdrag can also happen when ground settles because of poor construction of caissons in sand. On the other hand, updrag should also be considered if heave occurs around the piles for uplift loading condition, especially during installation of piles and piles in expansive soils.

9.4.4 Settlement of Individual Pile, *t-z*, *Q-z* Curves

Besides bearing capacity, the allowable settlement is another controlling factor in determining the allowable capacity of a pile foundation, especially if layers of highly compressible soil are close or below the tip of a pile.

Settlement of a small pile (diameter less than 350 mm) is usually kept within an acceptable range (usually less than 10 mm) when a FS of 2–3 is applied to the ultimate capacity to obtain the allowable capacity. However, in the design of large-diameter piles or caissons, a separate settlement analysis should always be performed.

The total settlement at top of a pile consists of the immediate settlement and the long-term settlement. The immediate settlement occurs during or shortly after the loads are applied, which includes elastic compression of the pile and deformation of the soil surrounding the pile under undrained loading conditions. The long-term settlement takes place during the period after the loads are applied, which includes creep deformation and consolidation deformation of the soil under drained loading conditions.

Consolidation settlement is usually significant in soft to medium stiff clayey soils. Creep settlement occurs most significantly in overconsolidated clays under large sustained loads and can be estimated by using the method developed by Booker and Poulos (1976). In principal, however, long-term settlement can be included in the calculation of ultimate settlement if the design parameters of soil used in the calculation reflect the long-term behavior.

Presented in the following sections are three methods that are often used:

1. Method of solving ultimate settlement by using special solutions from theory of elasticity (Poulos and Davis, 1980; Woodward et al., 1972). Settlement is estimated based on equivalent elasticity in which all deformation of soil is assumed to be linear elastic.
2. Empirical method (Vesic, 1977).
3. Method using localized springs, or the so called *t-z* and *Q-z* method (Kraft et al., 1981; Reese and O'Neil, 1988).

9.4.4.1 Method from Elasticity Solutions

The total elastic settlement S can be separated into three components:

$$S = S_b + S_s + S_{sh} \tag{9.19}$$

where S_b is part of the settlement at the tip or bottom of a pile caused by compression of soil layers below the pile under a point load at the pile tip, and is expressed as

$$S_b = \frac{p_b D_b I_{bb}}{E_s} \tag{9.20}$$

S_s is part of the settlement at the tip of a pile caused by compression of soil layers below the pile under the loading of the distributed side friction along the shaft of the pile, and can be expressed as

$$S_s = \sum_i \frac{(f_{si} l_i \Delta z_i) I_{bs}}{E_s} \tag{9.21}$$

and S_{sh} is the shortening of the pile itself, and can be expressed as

$$S_{sh} = \sum_i \frac{(f_{si} l_i \Delta z_i) + p_b A_b (\Delta z_i)}{E_c (A_i)} \tag{9.22}$$

where

p_b = averaged loading pressure at pile tip
A_b = cross-section area of a pile at pile tip; $A_b p_b$ is the total load at the tip
D_b = diameter of pile at the pile tip
i = subscript for ith segment of the pile
l = perimeter of a segment of the pile
Δz = axial length of a segment of the pile; $L = \sum_i \Delta z_i$ is the total length of the pile
f_s = unit friction along side of shaft; $f_{si} l_i \Delta z_i$ is the side frictional force for segment i of the pile
E_s = Young's Modulus of uniform and isotropic soil
E_c = Young's Modulus of the pile
I_{bb} = base settlement influence factor, from load at the pile tip (Figure 9.4)
I_{bs} = base settlement influence factor, from load along the pile shaft (Figure 9.4)

Because of the assumptions of linear elasticity, uniformity, and isotropy for soil, this method is usually used for preliminary estimate purposes.

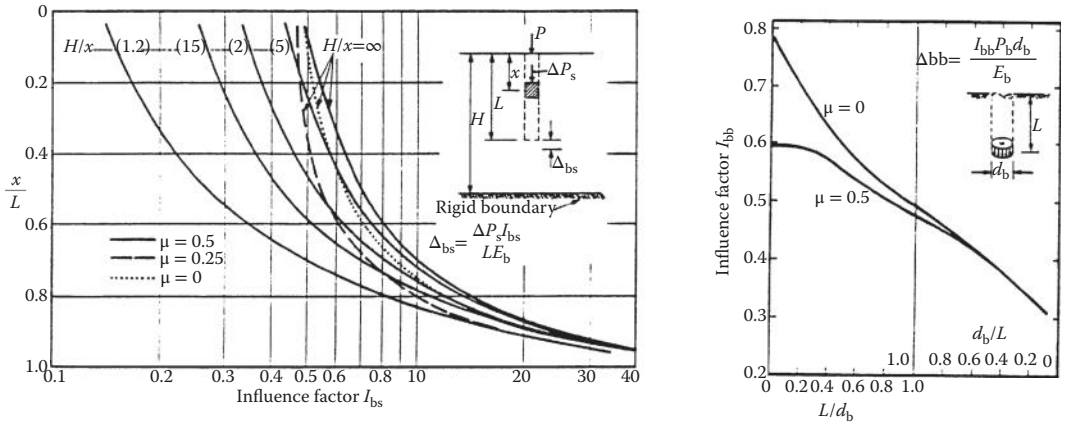

FIGURE 9.4 Influence factors.

9.4.4.2 Method by Vesic (1977)

The settlement S at the top of a pile can be broken down into three components, that is,

$$S = S_b + S_s + S_{sh} \tag{9.23}$$

Settlement due to shortening of a pile is

$$S_{sh} = (Q_p + \alpha_s Q_s)\frac{L}{AE_c} \tag{9.24}$$

where

Q_p = point load transmitted to the pile tip in the working stress range
Q_s = shaft friction load transmitted by the pile in the working stress range (in force units)
α_s = 0.5 for parabolic or uniform distribution of shaft friction,
0.67 for triangular distribution of shaft friction starting from zero friction at pile head to a maximum value at pile tip,
0.33 for triangular distribution of shaft friction starting from a maximum at pile head to zero at the pile tip
L = pile length
A = pile cross sectional area
E_c = modulus of elasticity of the pile

Settlement of the pile tip caused by load transmitted at the pile tip is

$$S_b = \frac{C_p Q_p}{Dq_o} \tag{9.25}$$

where

C_p = empirical coefficient depending on soil type and method of construction (see Table 9.11)
D = pile diameter
q_o = ultimate end bearing capacity

And settlement of the pile tip caused by load transmitted along the pile shaft is

$$S_s = \frac{C_s Q_s}{hq_o} \tag{9.26}$$

TABLE 9.11 Typical Values of C_p for Estimating Settlement of a Single Pile

Soil Type	Driven Piles	Bored Piles
Sand (dense to loose)	0.02–0.04	0.09–0.18
Clay (stiff to soft)	0.02–0.03	0.03–0.06
Silt (dense to loose)	0.03–0.05	0.09–0.12

Note: Bearing stratum under pile tip assumed to extend at least 10 pile diameters below tip and soil below tip is of comparable or higher stiffness.

where

$$C_s = (0.93 + 0.16D/B)C_p$$

h = embedded length

9.4.4.3 Method Using Localized Springs: The *t-z* and *Q-z* Method

In this method, the reaction of soil surrounding the pile is modeled as localized springs: a series of springs along the shaft (the *t-z* curves) and the spring attached to the tip or bottom of a pile (the *Q-z* curve). t is the load transfer or unit friction force along the shaft, Q is the tip resistance of the pile, and z is the settlement of soil at the location of the spring. The pile itself is also represented as a series of springs for each segment. A mechanical model is shown in Figure 9.5. The procedure to obtain the settlement of a pile is as follows:

- Assume a pile tip movement *zb_1*, obtain a corresponding tip resistance *Q_1* from the *Q-z* curve.
- Divide the pile into number of segments, and start calculation from the bottom segment.

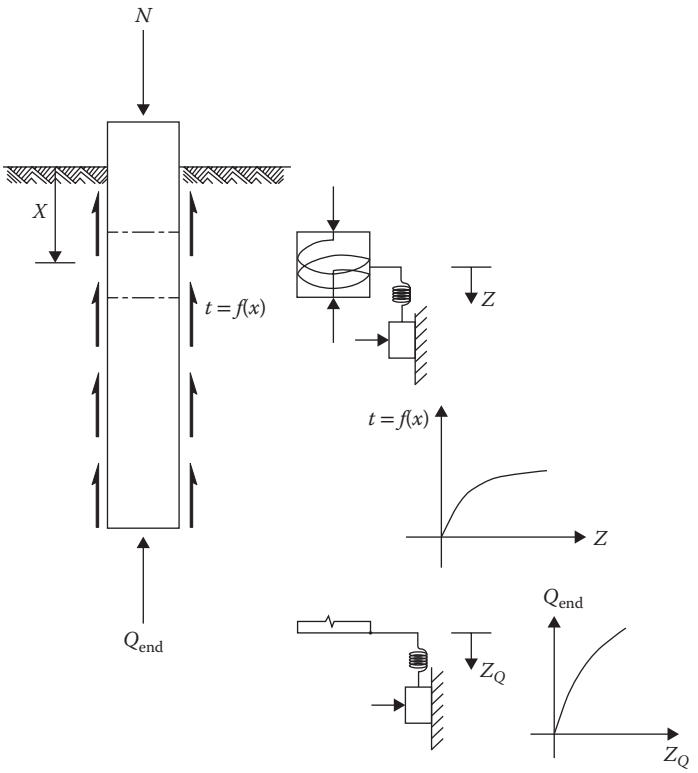

FIGURE 9.5 Analytical model for pile under axial loading with *t-z* and *Q-z* curves.

Iterations:

1. Assume an averaged movement of the segment *zs*_1, obtain the averaged side friction along the bottom segment *ts*_1 by using the *t-z* curve at that location.
2. Calculate the movement at the middle of the segment from elastic shortening of the pile under axial loading *zs*_2. The axial load is the tip resistance *Q*_1 plus the added side friction *ts*_1.
3. Iteration should continue until the difference between *zs*_1 and *zs*_2 is within an acceptable tolerance.

Iteration continues for all the segments from bottom to top of the pile.

- A settlement at top of pile *zt*_1 corresponding to a top axial load *Qt*_1 is established.
- Select another pile tip movement *zb*_2 and calculate *zt*_2 and *Qt*_2 until a relationship curve of load versus pile top settlement is found.

The *t-z* and *Q-z* curves are established from test data by many authors. Figure 9.6 shows the *t-z* and *Q-z* curves for cohesive soil and cohesionless soil by Reese and O'Neil (1988).

Although the method of *t-z* and *Q-z* curves employs localized springs, the calculated settlements are usually within a reasonable range since the curves are backfitted directly from test results. Factors of nonlinear behavior of soil, complicated stress conditions around the pile, and partial corrections to the Winkler's assumption are embedded in this methodology. Besides, settlement of a pile can be estimated for complicated conditions such as varying pile geometry, different pile materials, and different soil layers.

9.5 Lateral Capacity and Deflection—Individual Foundation

9.5.1 General

Lateral capacity of a foundation is the capacity to resist lateral deflection caused by horizontal forces and overturning moments acted on top of the foundation. For an individual foundation, lateral resistance comes from three sources: lateral earth pressures, base shear, and nonuniformly distributed end bearing pressures. Lateral earth pressure is the primary lateral resistance for long piles. Base shear and distributed end bearing pressures are discussed in Chapter 8.

9.5.2 Broms' Method

Broms (1964a and 1964b) developed a method to estimate the ultimate lateral capacity of a pile. The pile is assumed to be short and rigid. Only rigid translation and rotation movements are considered and only ultimate lateral capacity of a pile is calculated. The method assumes distributions of ultimate lateral pressures for cohesive and cohesionless soils; the lateral capacity of piles with different top fixity conditions are calculated based on the assumed lateral pressure as illustrated in Figures 9.7 and 9.8. Restricted by the assumptions, Broms' method is usually used only for preliminary estimate of ultimate lateral capacity of piles.

9.5.2.1 Ultimate Lateral Pressure

The ultimate lateral pressure $q_{h,u}$ along a pile is calculated as follows:

$$q_{h,u} = \begin{cases} 9c_u & \text{for cohesive soil} \\ 3K_p p_0' & \text{for cohesionless soil} \end{cases} \tag{9.27}$$

where

c_u = shear strength of the soil
K_p = coefficient of passive earth pressure, $K_p = \tan^2(45^o + \phi/2)$ and ϕ is the friction angle of cohesionless soils (or sand and gravel)

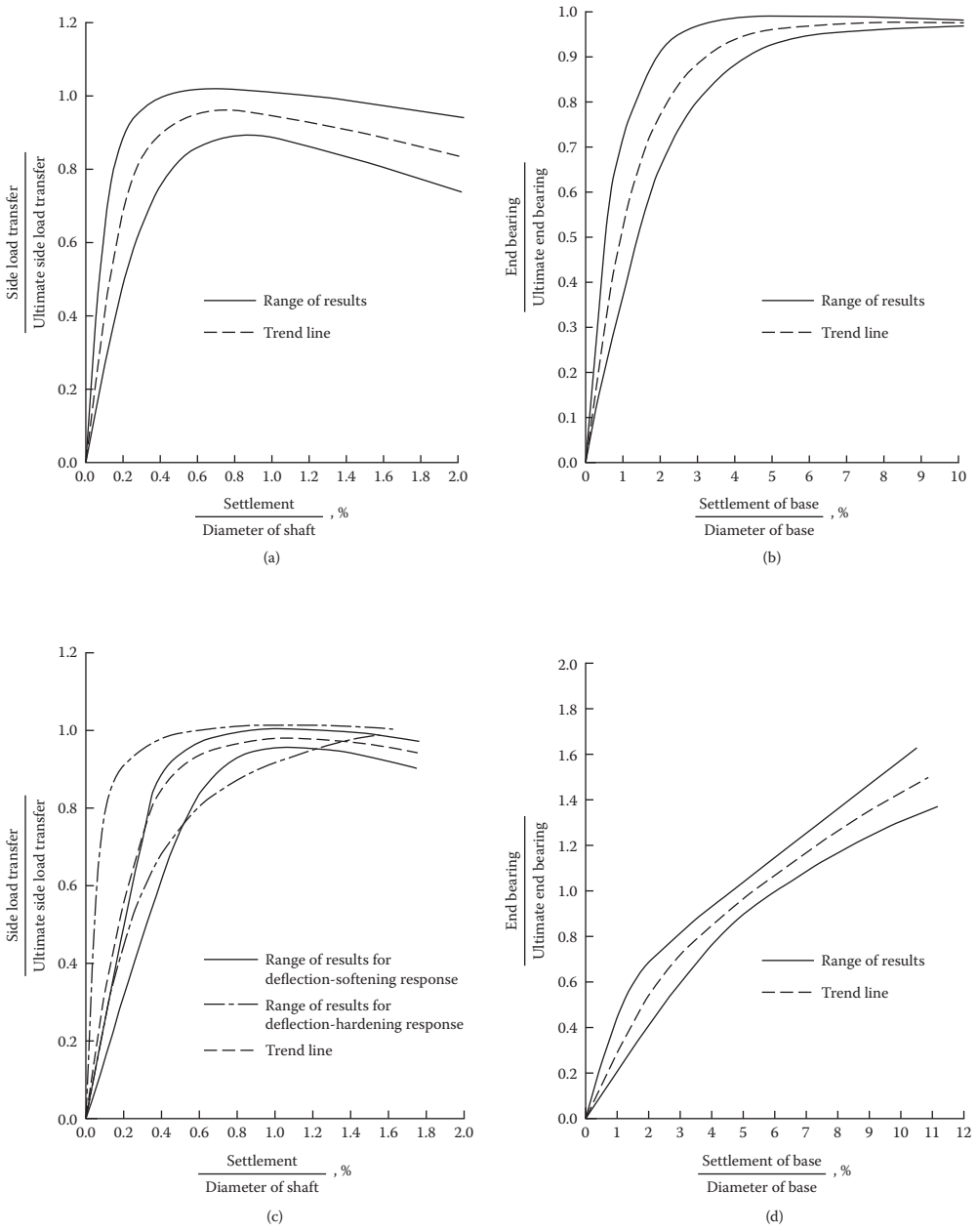

FIGURE 9.6 Load transfer for side resistance (*t-z*) and tip bearing (*Q-z*) (a) Side resistance vs. settlement drilled shaft in cohesive soil, (b) Tip bearing vs. settlement drilled shaft in cohesive soil, (c) Side resistance vs. settlement drilled shaft in cohesionless soil, (d) Tip bearing vs. settlement drilled shaft in cohesionless soil.

p_0' = effective overburden pressure, $p_0' = \gamma' z$ at a depth of z from the ground surface, where γ' is the effective unit weight of the soil

9.5.2.2 Ultimate Lateral Capacity for Free-Head Condition

The ultimate lateral capacity P_u of a pile under the free head condition is calculated by using the following formula:

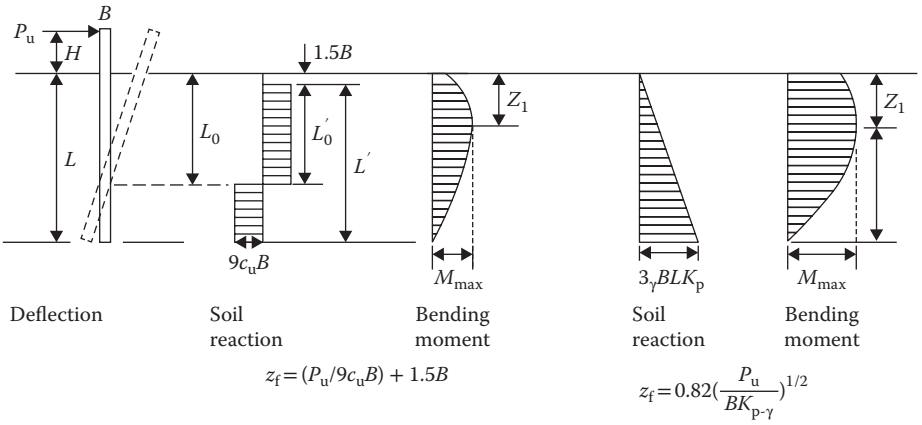

FIGURE 9.7 Free-head, short rigid piles—ultimate load conditions. (a) Rigid pile, (b) Cohesive soils, (c) Cohesionless soils.

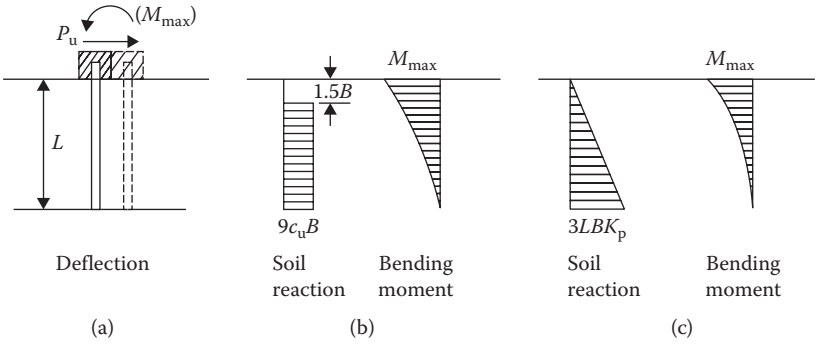

FIGURE 9.8 Fix-head, short rigid piles—ultimate load conditions. (a) Rigid pile, (b) Cohesive soils, (c) Cohesionless soils.

$$p_u = \begin{cases} \left(\dfrac{L_0'^2 - 2L'L_0' + 0.5L'^2}{L' + H + 1.5B}\right)(9c_uB) & \text{for cohesive soil} \\ \dfrac{0.5BL^3K_p\gamma'}{H+L} & \text{for cohesionless soil} \end{cases} \tag{9.28}$$

where

L = embedded length of pile
H = distance of resultant lateral force above ground surface
B = pile diameter
L' = embedded pile length measured from a depth of $1.5B$ below ground surface, or $L' = L - 1.5B$
L_0 = depth to center of rotation, and $L_0 = (H + 23L)/(2H + L)$
L_0' = depth to center of rotation measured from a depth of $1.5B$ below ground surface, or $L_0' = L_0 - 1.5B$

9.5.2.3 Ultimate Lateral Capacity for Fixed-Head Condition

The ultimate lateral capacity P_u of a pile under the fixed head condition is calculated by using the following formula:

$$P_u = \begin{cases} 9c_u B(L-1.5B) & \text{for cohesive soil} \\ 1.5\gamma BL^2 K_p & \text{for cohesionless soil} \end{cases} \tag{9.29}$$

9.5.3 Lateral Capacity and Deflection—*p-y* Method

One of the most commonly used methods for analyzing laterally loaded piles is the *p-y* method, in which soil reactions to the lateral deflections of a pile are treated as localized nonlinear springs based on the Winkler's assumption. The pile is modeled as an elastic beam that is supported on a deformable subgrade.

The *p-y* method is versatile and can be used to solve problems including different soil types, layered soils, nonlinear soil behavior; different pile materials, cross sections; and different pile head connection conditions.

9.5.3.1 Analytical Model and Basic Equation

An analytical model for pile under lateral loading with *p-y* curves is shown on Figure 9.9. The basic equation for the beam-on-an-deformable-subgrade problem can be expressed as follows:

$$EI\frac{d^4y}{dx^4} - P_x\frac{d^2y}{dx^2} + p + q = 0 \tag{9.30}$$

in which

y = lateral deflection at point x along the pile
EI = bending stiffness or flexural rigidity of the pile

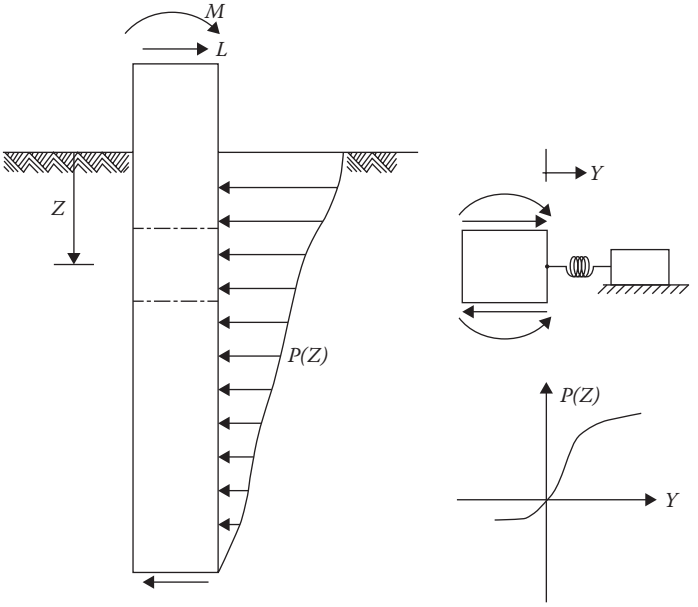

FIGURE 9.9 Analytical model for pile under lateral loading with *p-y* curves.

P_x = axial force in beam column
p = soil reaction per unit length, and $p = -E_s y$; where E_s is the secant modulus of soil reaction.
q = lateral distributed loads

The following relationships are also used in developing boundary conditions:

$$M = -EI\frac{d^4 y}{dx^4} \tag{9.31}$$

$$Q = -\frac{dM}{dx} + P_x\frac{dy}{dx} \tag{9.32}$$

$$\theta = \frac{dy}{dx} \tag{9.33}$$

where M is the bending moment, Q is the shear force in the beam column; θ is the rotation of the pile.

The *p-y* method is a valuable tool in analyzing laterally loaded piles. Reasonable results are usually obtained. A computer program is usually required because of the complexity and iteration needed to solve the above equations using the finite difference method or other methods. It should be noted that Winkler's assumption ignores the global effect of a continuum. Normally, if soil behaves like a continuum, the deflection at one point will affect the deflections at other points under loading. There is no explicit expression in the *p-y* method since localized springs are assumed. Although *p-y* curves are developed directly from results of load tests and the influence of global interaction is included implicitly, there are cases where unexpected outcomes are resulted. For example, excessively large shear forces will be predicted for large size piles in rock by using the *p-y* method approach, where the effect of continuum and the shear stiffness of the surrounding rock are ignored. The accuracy of the *p-y* method depends on the number of tests and variety of tested parameters, such as geometry and stiffness of pile, layers of soil, strength and stiffness of soil, and loading conditions. It should be careful to extrapolate *p-y* curves to conditions where tests were not yet performed in similar situations.

9.5.3.2 Generation of *p-y* Curves

A *p-y* curve, or the lateral soil resistance p expressed as a function of lateral soil movement y, is based on back calculations from test results of laterally loaded piles. The empirical formulations of *p-y* curves are different for different types of soil. *p-y* curves also depend on the diameter of the pile, strength and stiffness of the soil, confining overburden pressures, and loading conditions. Effects of layered soil, battered piles, piles on a slope, and closely spaced piles also are usually considered (Geordiadis, 1983). Formulation for soft clay, sand, and rock is provided in the following.

9.5.3.2.1 p-y Curves for Soft Clay

Matlock (1970) proposed a method to calculate *p-y* curves for soft clays as shown in Figure 9.10. The lateral soil resistance p is expressed as

$$p = \begin{cases} 0.5\left(\frac{y}{y_{50}}\right)^{\frac{1}{3}} p_u & y < y_p = 8y_{50} \\ p_u & y \geq y_p \end{cases} \tag{9.34}$$

in which

p_u = ultimate lateral soil resistance corresponding to ultimate shear stress of soil
y_{50} = lateral movement of soil corresponding to 50% of ultimate lateral soil resistance
y = lateral movement of soil

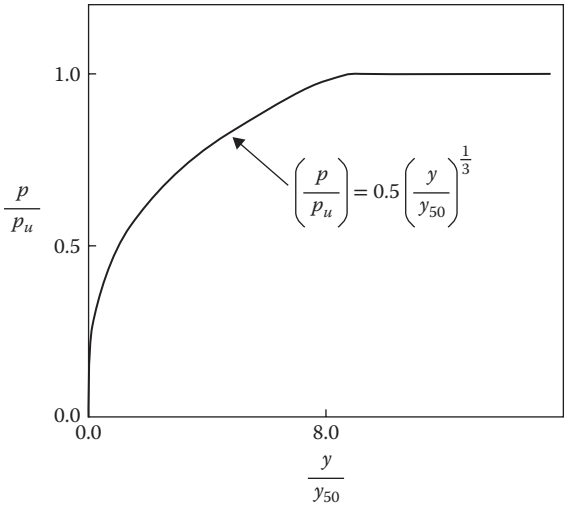

FIGURE 9.10 Characteristic shape of *p-y* curve for soft clay (Matlock, 1970).

TABLE 9.12 Representative Values of ε_{50}

Consistency of Clay	Undrained Shear Strength, psf	ε_{50}
Soft	0–400	0.020
Medium stiff	400–1000	0.010
Stiff	1000–2000	0.007
Very stiff	2000–4000	0.005
Hard	4000–8000	0.004

Note: 1 psf = 0.048 kPa

The ultimate lateral soil resistance p_u is calculated as

$$p_u = \begin{cases} \left(3 + \dfrac{\gamma' x}{c} + J\dfrac{x}{B}\right)cB & x < x_r = 6B/\left(\dfrac{\gamma' B}{c} + J\right) \\ 9cB & x \geq x_r \end{cases} \tag{9.35}$$

where γ' is the effective unit weight, x is the depth from ground surface, c is the undrained shear strength of the clay, J is a constant frequently taken as 0.5.

The lateral movement of soil corresponding to 50% of ultimate lateral soil resistance y_{50} is calculated as

$$y_{50} = 2.5\varepsilon_{50}B \tag{9.36}$$

where ε_{50} is the strain of soil corresponding to half of the maximum deviator stress. Table 9.12 shows the representative values of ε_{50}.

9.5.3.2.2 p-y Curves for Sands

Reese et al. (1974) proposed a method for developing *p-y* curves for sandy materials. As shown in Figure 9.11, a typical *p-y* curve usually consists of the following four segments:

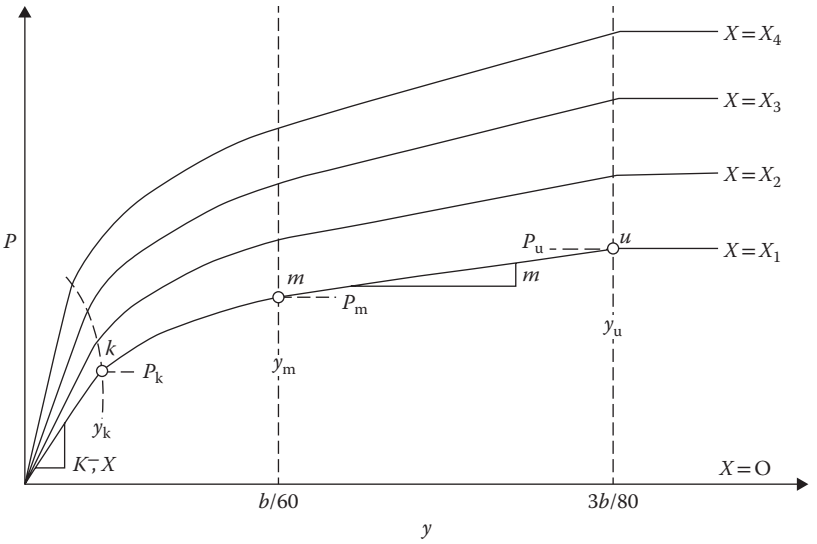

FIGURE 9.11 Characteristic shape of *p-y* curve for sand (Reese et al., 1974).

Segment	Curve type	Range of y	Range of p	p-y curve
1	Linear	0 to y_k	0 to p_k	$p = (kx)y$
2	Parabolic	y_k to y_m	p_k to p_m	$p = p_m\left(\frac{y}{y_m}\right)^n$
3	Linear	y_m to y_u	p_m to p_u	$p = p_m + \frac{p_u - p_m}{y_u - y_m}(y - y_m)$
4	Linear	$\geq y_u$	p_u	$p = p_u$

where y_m, y_u, p_m, and p_u can be determined directly from soil parameters. The parabolic form of Segment 2 and the intersection with Segment 1 (y_k and p_k) can be determined based on y_m, y_u, p_m, and p_u as shown in Equations (9.37) to (9.40).

Segment 1 starts with a straight line with an initial slope of kx, where x is the depth from ground surface to the point where the p-y curve is calculated. k is a parameter to be determined based on relative density and is different whether above or below water table. Representative values of k are shown in Table 9.13.

Segment 2 is parabolic and starts from end of Segment 1 at $y_k = \left[\frac{p_m/y_m}{(kx)^n}\right]^{\frac{1}{n-1}}$ and $p_k = (kx)y_k$, the power of the parabolic $n = \frac{y_m}{p_m}\left(\frac{p_u - p_m}{y_u - y_m}\right)$.

Segments 3 and 4 are straight lines. y_m, y_u, p_m, and p_u are expressed as

$$y_m = \frac{b}{60} \tag{9.37}$$

$$y_u = \frac{3b}{80} \tag{9.38}$$

TABLE 9.13 Friction Angle (Degree) and Consistency

Relative to Water Table	Friction Angle (Degree) and Consistency		
	29°–30° (Loose)	30°–36° (Medium Dense)	36°–40° (Dense)
Above	20 pci	60 pci	125 pci
Below	25 pci	90 pci	225 pci

Note: 1 pci = 272 kPa/m

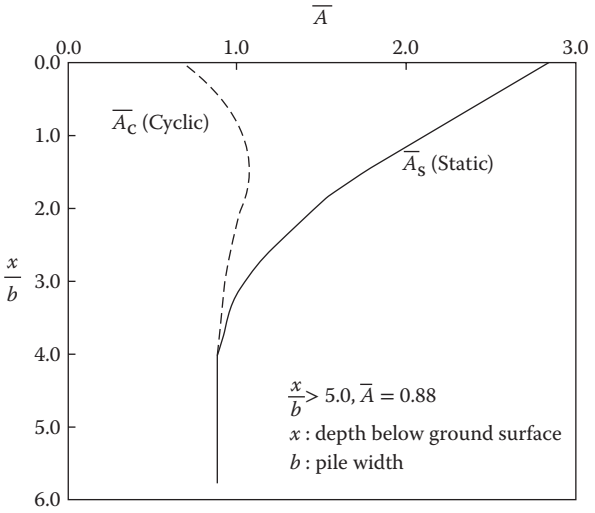

FIGURE 9.12 Variation of A_s with depth for sand.

$$p_m = B_s p_s \tag{9.39}$$

$$p_u = A_s p_s \tag{9.40}$$

where b is the diameter of a pile; A_s and B_s are coefficients that can be determined from Figures 9.12 and 9.13, depending on either static or cyclic loading conditions; p_s is equal to the minimum of p_{st} and p_{sd}, as

$$p_{st} = \gamma x \left[\frac{K_o x \tan\phi \sin\beta}{\tan(\beta-\phi)\cos\alpha} + \frac{\tan\beta}{\tan(\beta-\phi)}(b + x\tan\beta\tan\alpha) + K_o x \tan\beta(\tan\varphi\tan\phi - \tan\alpha) - K_a b \right] \tag{9.41}$$

$$p_{sd} = K_a b x \gamma \left[\tan^8(\beta) - 1\right] + K_o b \gamma x \tan\phi \tan^4(\beta) \tag{9.42}$$

$$p = \min(p_{st}, p_{sd}) \tag{9.43}$$

in which ϕ is the friction angle of soil; α is taken as $\phi/2$; β is equal to $45° + \phi/2$; K_o is the coefficient of the earth pressure at rest and is usually assumed to be 0.4; and K_a is the coefficient of the active earth pressure and equals to $\tan^2(45° - \phi/2)$.

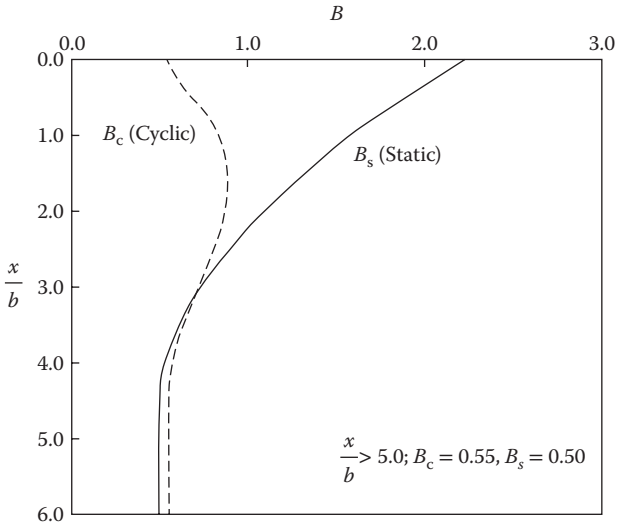

FIGURE 9.13 Variation of B_s with depth for sand.

9.5.4 Lateral Spring: *p-y* Curves for Rock

Reese (1997) proposed a procedure to calculate *p-y* curves for rock using basic rock and rock mass properties such as compressive strength of intact rock q_{ur}, Rock Quality Designation (RQD), and initial modulus of rock E_{ir}. A description of the procedure is presented in the following.

A *p-y* curve consists of three segments:

$$\begin{aligned}
&\text{Segment 1}: p = K_{ir} y \quad \text{for } y \le y_a \\
&\text{Segment 2}: p = \frac{p_{ur}}{2}\left(\frac{y}{y_{rm}}\right)^{0.25} \quad \text{for } y_a < y < 16 y_{rm} \\
&\text{Segment 3}: p = p_{ur} \quad \text{for } y \ge 16 y_{rm}
\end{aligned} \tag{9.44}$$

where p is the lateral force per unit pile length and y is the lateral deflection.

K_{ir} is the initial slope and is expressed as

$$K_{ir} = k_{ir} E_{ir} \tag{9.45}$$

k_{ir} = a dimensionless constant and is determined by

$$k_{ir} = \begin{cases} \left(100 + \dfrac{400 x_r}{3b}\right) & \text{for } 0 \le x_r \le 3b \\ 500 & \text{for } x_r > 3b \end{cases} \tag{9.46}$$

x_r = depth below bedrock surface, b is the width of the rock socket
E_{ir} = initial modulus of rock.
y_a is the lateral deflection separating Segments 1 and 2, and

$$y_a = \left(\frac{p_{ur}}{2 y_{rm}^{0.25} K_{ir}} \right)^{1.333} \tag{9.47}$$

where

$$y_{rm} = k_{rm} b \tag{9.48}$$

k_{rm} is a constant, ranging from 0.0005 to 0.00005.
p_{ur} is the ultimate resistance and can be determined by

$$p_{ur} = \begin{cases} \alpha_r q_{ur} b \left(1 + 1.4 \frac{x_r}{b} \right) & \text{for } 0 \le x_r \le 3b \\ 5.2 \alpha_r q_{ur} b & \text{for } x_r > 3b \end{cases} \tag{9.49}$$

where

q_{ur} = compressive strength of rock, and α_r is a strength reduction factor and is determined by

$$\alpha_r = 1 - \frac{\text{RQD}}{150} \qquad 0 \le \text{RQD} \le 100 \tag{9.50}$$

RQD = Rock Quality Designation for rock

9.6 Grouped Foundations

9.6.1 General

Although a pile group is composed of a number of individual piles, the behavior of a pile group is not equivalent to the sum of all the piles as if they are separate individual piles. The behavior of a pile group is more complex than an individual pile because of the effect of combination of piles, interactions between the piles in the group, and the effect of the pile cap. For example, stresses in soil from the loading of an individual pile will be insignificant at a certain depth below the pile tip. However, the stresses superimposed from all neighboring piles may increase the level of stress at that depth and result in considerable settlements or a bearing capacity failure, especially if there exists an underlying weak soil layer. The interaction and influence between piles usually diminish for piles spaced at approximately 7–8 diameters.

The axial and lateral capacity and the corresponding settlement and lateral deflection of a pile group will be discussed in the following sections.

9.6.2 Axial Capacity of Pile Group

The axial capacity of a pile group is the combination of piles in the group, with consideration of interaction between the piles. One way to account for the interaction is to use the group efficiency factor η_a, which is expressed as

$$\eta_a = \frac{P_{\text{Group}}}{\sum_i P_{\text{Singl\_Pile,i}}} \tag{9.51}$$

where P_{Group} is the axial capacity of a pile group. $\sum_i P_{\text{Sinle\_Pile,i}}$ is the sum the axial capacity of all the individual piles and is discussed in detail in Section 9.4. The group efficiency for axial capacity depends on many factors such as the installation method, ground conditions, and function of piles and are presented in Table 9.14.

TABLE 9.14 Group Efficiency Factor for Axial Capacity

Pile Installation Method	Function	Ground Conditions	Expected Group Efficiency	Design Group Efficiency (with minimum spacing equals to 2.5 pile perimeter)
Driven pile	End bearing	Sand	1.0	1.0
	Side friction	Loose to medium dense sand	>1.0, up to 2.0	1.0, or increase with load test
	Side friction	Dense sand	May be ≥1.0	1.0
Drilled shaft	All	Sand	<1.0	0.67–1.0
Driven pile and drilled shaft	Side friction	Soft to medium stiff clay	<1.0	0.67–1.0
	End bearing	Soft to medium stiff clay	<1.0	0.67–1.0
	Side friction	Stiff clay	1.0	1.0
	End bearing	Stiff clay	1.0	1.0
	Side friction	Clay	<1.0	Also use "Group Block"
	End bearing	Clay, or underlying clay layers	<1.0	Also use "Group Block"

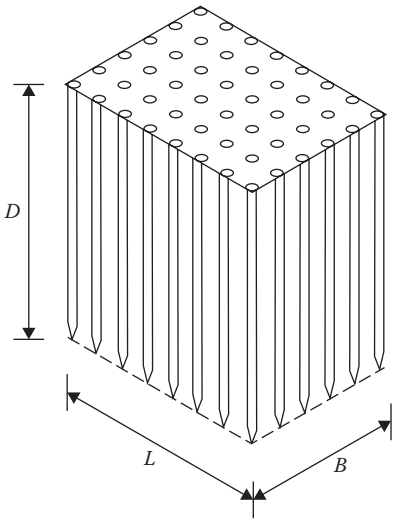

FIGURE 9.14 Block failure model for pile group in clay.

Driven piles in loose to medium dense sand in close spacing may densify the sand and consequently increase the lateral stresses and frictions along the piles. However, driven piles in dense sand may cause dilation of the sand and consequently cause heave and damage to the piles. The influence of spacing to the end bearing for sand is usually limited. Under normal conditions, the group efficiency factor η_a is taken as 1.0.

For drilled piers in loose to medium dense sand, no densification of sand is made. The group efficiency factor η_a is usually less than 1.0 because of the influence of other close piles.

For driven piles in stiff to very stiff clay, the piles in a pile group tend to form a "Group Block" that behaves like a giant, short pile. The size of the group block is the extent of soil enclosed by the piles, including the perimeter piles as shown in Figure 9.14. The group efficiency factor η_a is usually equal

to 1.0. For piles in soft to medium stiff clay, the group efficiency factor η_a is usually less than 1.0 because the shear stress levels are increased by loading from adjacent piles.

The group block method is also often used to check the bearing capacity of a pile group. The group block is treated as a large deep spread footing foundation and the assumed bottom level of the footing is different depending on whether the pile is end bearing or frictional. For end bearing piles, the capacity of the group block is examined by assuming the bottom of the footing is at the tip of the piles. For frictional piles, the capacity of the group pile is checked by assuming that the bottom of the footing is located at 1/3 of total embedded length above the tip. The bearing capacity of the underlying weaker layers is then estimated by using methods discussed in Chapter 8. The smaller capacity, by using the group efficiency approach, the group block approach, and the group block approach with underlying weaker layers, is selected as the capacity of the pile group.

9.6.3 Settlement of a Pile Group

The superimposed stresses from neighboring piles will raise the stress level below the tip of a pile substantially, whereas the stress level is much smaller for an individual pile. The raised stress level has two effects on the settlement of a pile group. The magnitude of the settlement will be larger for a pile group and the influence zone of a pile group will be much greater. The settlement of a group will be much larger in presence of underlying highly compressible layers that would not be stressed under the loading of an individual pile.

The group block method is often used to estimate the settlement of a group. The pile group is simplified to an equivalent massive spread footing foundation except that the bottom of the footing is much deeper. The plane dimensions of the equivalent footing are outlined by the perimeter piles of the pile group. The method to calculate settlement of spread footings is discussed in Chapter 31. The assumed bottom level of the footing block is different depending on either end bearing or frictional piles. For end bearing piles, the bottom of the footing is at the tip of the piles. For frictional piles, the bottom of the footing is located at 1/3 of total embedded length above the tip. In many cases, settlement requirement also is an important factor in design of a pile group.

Vesic (1977) introduced a method to calculate settlement of a pile group in sand, which is expressed as

$$S_g = S_s\sqrt{\frac{B_g}{B_s}} \tag{9.52}$$

Where S_g is the settlement of a pile group

S_s is the settlement of an individual pile
B_g is the smallest dimension of the group block
B_s is the diameter of an individual pile

9.6.4 Lateral Capacity and Deflection of a Pile Group

The behavior of a pile group under lateral loading is not well defined. As discussed in the earlier sections, the lateral moment capacity is greater than the sum of all the piles in a group because piles would form couples resulting from their axial resistance through the action of the pile cap. However, the capacity of a pile group to resist lateral loads is usually smaller than the sum of separate, individual piles because of the interaction between piles.

The approach by University of Texas at Austin (Reese, O'Neil, and et al.) provides a comprehensive and practical method to analyze a pile group under lateral loading. Finite difference method is used to model the structural behavior of the foundation elements. Piles are connected through a rigid pile cap. Deformations of all the piles in axial and lateral directions, and force and moment equilibrium are established. The reactions of soil are represented by a series of localized nonlinear axial and lateral springs. The theory and procedures to calculate axial and lateral capacity of individual piles are discussed in detail in Sections 9.4 and 9.5. A computer program such as GROUP (Ensoft, 2012) is usually required to analyze a pile group because of the complexity and iteration procedure involving nonlinear soil springs.

The interaction of piles is represented by the lateral group efficiency factors, which is multiplied to the *p-y* curves for individual piles to reduce the lateral soil resistance and stiffness. Dunnavant and O'Neil (1986) proposed a procedure to calculate the lateral group factors. For a particular pile *I*, the group factor is the product of influence factors from all neighboring piles *j*, as

$$\beta_i = \beta_0 \prod_{\substack{j=1 \\ j \neq i}}^{n} \beta_{ij} \tag{9.53}$$

where β_i is the group factor for pile *I*, β_0 is a total reduction factor and equals to 0.85, β_{ij} is the influence factor from a neighboring pile *j*, and *n* is the total number of piles. Depending on the location of the piles *I* and *j* in relation to the direction of loading, β_{ij} is calculated as follows:

i is leading, or directly ahead of *j* ($\theta = 0°$)	$\beta_l = \beta_{ij} = 0.69 + 0.5\log_{10}\left(\frac{S_{ij}}{B}\right) \le 1$	(9.54)
i is trailing, or directly behead of *j* ($\theta = 180°$)	$\beta_t = \beta_{ij} = 0.48 + 0.6\log_{10}\left(\frac{S_{ij}}{B}\right) \le 1$	(9.55)
i and *j* are abreast, or side-by-side ($\theta = 90°$)	$\beta_s = \beta_{ij} = 0.78 + 0.36\log_{10}\left(\frac{S_{ij}}{B}\right) \le 1$	(9.56)

where S_{ij} is the center-to-center distance between *I* and *j*, *B* is the diameter of the piles *I* and *j*, and θ is the angle between the loading direction and the connection vector from *I* to *j*. When the piles *I* and *j* are at other angles to the direction of loading, β_{ij} is computed by interpolation, as

$0° < \theta < 90°$	$\beta_{\theta 1} = \beta_{ij} = \beta_l + (\beta_s - \beta_l)\frac{\theta}{90}$	(9.57)
$90° < \theta < 180°$	$\beta_{\theta 2} = \beta_{ij} = \beta_t + (\beta_s - \beta_t)\frac{\theta - 90}{90}$	(9.58)

In cases that the diameters of the piles *I* and *j* are different, we propose to use the diameter of pile *j*. To avoid an abrupt change of β_0 from 0.85 to 1.0, we propose to use:

$$\beta_o = \begin{cases} 0.85 & \text{for } \frac{S_{ij}}{B_j} \le 3 \\ 0.85 + 0.0375\left(\frac{S_{ij}}{B_j} - 3\right) & \text{for } 3 < \frac{S_{ij}}{B_j} < 7 \\ 1.0 & \text{for } \frac{S_{ij}}{B_j} \ge 7 \end{cases}$$

9.7 Seismic Issues

Seismic design of deep bridge foundations is a broad issue. Design procedures and emphases vary with different types of foundations. Since pile groups, including driven piles and drilled cast-in-place shafts, are the most popular types of deep bridge foundations, the following discussion will concentrate on the design issues for pile group foundations only.

In most circumstances, seismic design of pile groups is performed to satisfy one or more of the following objectives:

- Determine the capacity and deflection of the foundation under the action of the seismic lateral load.
- Provide the foundation stiffness parameters for dynamic analysis of the overall bridge structures.
- Ensure integrity of the pile group against liquefaction and slope instability induced ground movement.

9.7.1 Seismic Lateral Capacity Design of Pile Groups

In current practice, seismic lateral capacity design of pile groups is often taken as the same as conventional lateral capacity design (see Section 9.5). The seismic lateral force and the seismic moment from the upper structure are first evaluated for each pile group foundation based on the tributary mass of the bridge structure above the foundation level, the location of the center of gravity, and the intensity of the ground surface acceleration. The seismic force and moment are then applied on the pile cap as if they were static forces, and the deflections of the piles and the maximum stresses in each pile are calculated and checked against the allowable design values. Since seismic forces are of transient nature, the FS required for resistance of seismic load can be less than those required for static load.

In essence, the above procedure is pseudostatic, only the seismic forces from the upper structure are considered, and the effect of seismic ground motion on the behavior of pile group is ignored. The response of a pile group during an earthquake is different from its response to a static lateral loading. As seismic waves pass through the soil layers and cause the soil layers to move laterally, the piles are forced to move along with the surrounding media. Except for the case of very short piles, the pile cap and the pile tip at any moment may move at different directions. This movement induces additional bending moments and stresses in the piles. Depending on the intensity of the seismic ground motion and the characteristics of the soil strata, this effect can be more critical to the structure integrity of the pile than the lateral load from the upper structure.

Field measurements (e.g., Tazoh et al., 1987), postearthquake investigation (e.g., Seismic Advisory Committee, 1995), and laboratory model tests (e.g., Nomura et al., 1990) all confirm that seismic ground movements dictate the maximum responses of the piles. The more critical situation is when the soil profile consists of soft layer(s) sandwiched by stiff layers, and the modulus contrast among the layers is large. In this case, local seismic moments and stresses in the pile section close to the soft layer/hard layer interface may very well be much higher than the moments and stresses caused by the lateral seismic loads from the upper structure. If the site investigation reveals that the underground soil profile is of this type and the bridge is of critical importance, it is desirable that a comprehensive dynamic analysis be performed using one of more sophisticated computer programs capable of modeling the dynamic interaction between the soil and the pile system, for example, SASSI (Lysmer et al., 1981). Results of such dynamic analysis can provide a better understanding of the seismic responses of a pile group.

9.7.2 Determination of Pile Group Spring Constants

An important aspect in bridge seismic design is to determine, through dynamic analysis, the magnitude and distribution of seismic forces and moments in the bridge structure. To accomplish this goal, the characteristics of the bridge foundation must be considered appropriately in an analytical model.

At the current design practice, the force–displacement relationships of a pile foundation are commonly simplified in an analytical model as a stiffness matrix, or a set of translational and rotational springs. The characteristics of the springs depend on the stiffness at pile head for individual piles and the geometric configuration of piles in the group. For a pile group consisting of vertical piles, the spring constants can be determined by the following steps:

1. The vertical and lateral stiffnesses at pile head of a single pile, K_{vv} and K_{hh}, are first evaluated based on the pile geometry and the soil profile. These values are determined by calculating the displacement at the pile head corresponding to a unit force. For many bridge foundations, a rigid pile cap can be assumed. Design charts are available for uniform soil profiles (e.g., NAVFAC, 1986). For most practical soil profiles, however, it is convenient to use computer programs, such as APILE (Ensoft, 2011b) and LPILE (Ensoft, 2011a), to determine the single pile stiffness values. It should be noted that the force-deformation behavior of a pile is highly nonlinear. In evaluating the stiffness values, it is desirable to use the secant modulus in the calculated pile-head force–displacement relationship compatible to the level of pile-head displacement to be developed in the foundation. This is often an iterative process.

   In calculating the lateral stiffness values, it is common practice to introduce a group factor η, $\eta \leq 1.0$, to take account for the effect of the other piles in the same group. The group factor depends on the relative spacing S/D in the pile group, where S is the spacing between two piles and D is the diameter of the individual pile. There are studies reported in the literature about the dynamic group factors for pile groups of different configurations. However, in the current design practice, static group factors are used in the calculation of the spring constants. Two different approaches exist in determining the group factor: one is based on reduction of the subgrade reaction moduli and the other is based on the measurement of plastic deformation of the pile group. Since the foundation deformations in the analysis cases involving the spring constants are mostly in the small strain range, the group factors based on subgrade reaction reduction should be used (e.g., NAVFAC, 1986).
2. The spring constants of the pile group can be calculated using the following formulae:

$$K_{G,x} = \sum_{i=1}^{N} K_{hh,i} \tag{9.59}$$

$$K_{G,y} = \sum_{i=1}^{N} K_{hh,i} \tag{9.60}$$

$$K_{G,z} = \sum_{i=1}^{N} K_{vv,i} \tag{9.61}$$

$$K_{G,yy} = \sum_{i=1}^{N} K_{vv,i} \cdot x_i^2 \tag{9.62}$$

$$K_{G,xx} = \sum_{i=1}^{N} K_{vv,i} \cdot y_i^2 \tag{9.63}$$

where $K_{G,x}$, $K_{G,y}$, $K_{G,z}$ are the group translational spring constants, $K_{G,yy}$, $K_{G,xx}$ are the group rotational spring constants with respect to the center of the pile cap. All springs are calculated at the center of the pile cap; $K_{vv,i}$ and $K_{hh,i}$ are the lateral and vertical stiffness values at pile-head of the ith pile; x_i, y_i are the coordinates of the ith pile in the group; and N is the total number of piles in the group.

In the above formulae, the bending stiffness of a single pile at the pile top and the off-diagonal stiffness terms are ignored. For most bridge pile foundations, these ignored items have only minor significance. Reasonable results can be obtained using the above simplified formulae.

It should be emphasized that the behavior of the soil-pile system is greatly simplified in the concept of "spring constant." The responses of a soil-pile-structure system are complicated and highly nonlinear, frequency dependent and are affected by the inertia/stiffness distribution of the structure above ground. Therefore, for critical structures, it is advisable that analytical models including the entire soil-pile-structure system should be used in the design analysis.

9.7.3 Design of Pile Foundations against Soil Liquefaction

Liquefaction of loose soil layers during an earthquake poses a serious hazard to pile group foundations. Field observations and experimental studies (e.g., Boulanger, et al., 1997; Miyamot et al., 1992; Nomura et al., 1990; Tazoh and Gazetas, 1996) indicate that soil liquefaction during an earthquake has significant impacts on the behavior of pile groups and super-structures. The impacts are largely affected by the intensity of liquefaction-inducing earthquakes and the relative locations of the liquefiable loose soil layers. If a loose layer is close to the ground surface and the earthquake intensity is moderate, the major effect of liquefaction of the loose layer is to increase the fundamental period of the foundation-structure system and cause significant lateral deflection of the pile group and superstructure. For high-intensity earthquakes, and especially if the loose soil layer is sandwiched in hard soil layers, liquefaction of the loose layer often causes cracking and breakage of the piles and complete loss of capacity of the foundation, thus the collapse of the superstructure.

There are several approaches proposed in the literature for calculation of the dynamic responses of a pile or a pile group in a liquefied soil deposit. In current engineering practice, however, more emphasis is on taking proper countermeasures to mitigate the adverse effect of the liquefaction hazard. These mitigation methods include the following:

- Densify the loose, liquefiable soil layer. Stone column is often satisfactory if the loose layer is mostly sand. Other approaches, such as jet grouting, deep soil mixing with cementing agents and in situ vibratory densification can all be used. If the liquefiable soil layer is close to the ground surface, a complete excavation and replacement with compacted engineering fill is sometimes also feasible.
- Isolate the pile group from the surrounding soil layers. This is often accomplished by installing some types of isolation structures, such as sheet piles, diaphragm walls, soil-mixing piles, around the foundation to form an enclosure. In essence, this approach creates a huge block surrounding the piles with increased lateral stiffness and resistance to shear deformation while limiting the lateral movement of the soil close to the piles.
- Increase the number and dimension of the piles in a foundation and therefore increase the lateral resistance to withstand the forces induced by liquefied soil layers. An example is 10-ft (3.3 m) diameter cast-in-steel shell piles used in bridge seismic retrofit projects in the San Francisco Bay Area following the 1989 Loma Prieta earthquake.

References

API. 2000. *API Recommended Practice for Planning, Designing and Constructing Fixed Offshore Platforms*, 21st ed., API RP2A, American Petroleum Institute, Washington, DC. 115 pp.

Awoshika, K. and L. C. Reese. 1971. "Analysis of Foundation with Widely-Spaced Batter Piles," Research Report 117-3F, Center for Highway Research, The University of Texas at Austin, February.

Berezantzev, V. G., V. S. Khristoforov, and V. N. Golubkov. 1961. "Load Bearing Capacity and Deformation of Piled Foundations," *Proc. of 5th International Conference on Soil Mechanics*, Paris, Vol. 2, pp. 11–15.

Booker, J. R. and and H.G. Poulos. 1976. "Analysis of creep settlement of pile foundations," *J. Geot. Engr.* ASCE, Vol. 102, No. GT1. pp. 1–14.

Boulanger, R. W., D. W. Wilson, B. L. Kutter, and A. Abghari. 1997. "Soil-Pile-Structure Interaction in Liquefiable Sand," *Transport. Res. Rec.*, No. 1569, April 14 pp.

Broms, B. B. 1964a. "Lateral Resistance of Piles in Cohesive Soils," *Proc. ASCE, J. Soil Mech. & Found. Engr. Div.*, Vol. 90, No. SM2, March, pp. 27–64.

Broms, B. B. 1964b. "Lateral Resistance of Piles in Cohesionless Soils," *Proc. ASCE, J. Soil Mech. & Found. Engr. Div.*, Vol. 90, No. SM3, May, pp. 123–156.

Burland, J. B. 1973. "Shaft Friction of Piles in Clay - A Simple Fundamental Approach," *Ground Eng.*, Vol. 6, No. 3, pp. 30–42.

Bustamante, M. and L. Gianeselli. 1982. "Pile Bearing Capacity Prediction by Means of Static Penetrometer CPT," *Proc. of Second European Symposium on Penetration Testing* (ESOPT II), Amsterdam, A.A. Balkema, Vol. 2, pp. 493–500.

CGS. 1992. *Canadian Foundation Engineering Manual*, 3rd ed., Canadian Geotechnical Society, BiTech Publishers, Vancouver, Canada, 512 pp.

Carter, J. P. and F. H. Kulhawy. 1988. "Analysis and Design of Drilled Shaft Foundations Socketed into Rock," EPRI Report EI-5918, Electric Power Research Institute, Palo Alto, CA.

Crapps, D. K. 1986. "Design, Construction and Inspection of Drilled Shafts in Limerock and Limestone," Paper Presented at the Annual Meeting of the Florida Section of ASCE, Lake Worth, FL.

Davis, M. P., Robertson, P. K., Campanella, R. G., and Sy, A. 1988. "Axial Capacity of Driven piles in Deltaic Soils Using CPT," *Proceedings of the first International Symposium on Penetration Testing, ISOPT-1*, Ed. J. De Ruite , March 21–24, Orlando, FL.

Dennis, N. D. 1982. "Development of Correlations to Improve the Prediction of Axial Pile Capacity," Ph.D. dissertation, University of Texas at Austin.

De Ruiter, J. and F. L. Beringen. 1978. "Pile Foundations for Large North Sea Structures," *Mar. Geotechnol.*, Vol. 3, No. 3, pp. 267–314.

Desai, C. S. and J. T. Christian. 1977. *Numerical Methods in Geotechnical Engineering*, McGraw-Hill Book Co., New York.

Dunnavant, T. W. and M. W. O'Neil. 1986. "Evaluation of Design-Oriented Methods for Analysis of Vertical Pile Groups Subjected to Lateral Load," *Numerical Methods in Offshore Piling*, des Ponts et Trousers Central Laboratory, French Petroleum Institute, Paris, France, pp. 303–316.

Ensoft Inc. 2011a. *Lpile*, Version 6.0. A Computer Program for Analysis of Laterally Loaded Piles, Austin, Texas.

Ensoft Inc. 2011b. *Apile Plus*. Version 5.0, Austin, Texas.

Ensoft Inc. 2012. *GROUP*, Version 8.0, Austin, Texas.

Fellenius, B. H. 1986. In an ASCE meeting in Boston as quoted by R.E. Olson in 1991, "Capacity of Individual Piles in Clay," internal report.

Fellenius, B. H. 1994. "The Critical Depth - How it Came into Being and Why it Does Not Exist." *Proc. of the Institution of Civil Engineers, Geotechnical Engineering*, Vol. 108, No. 1.

Focht, J. A. and K. J. Koch. 1973. "Rational Analysis of the Lateral Performance of Offshore Pile Groups," *Proc. Fifth Offshore Technology Conference*, Houston, Vol. 2, pp. 701–708,

Geordiadis, M. 1983. "Development of p-y Curves for Layered Soils," *Proc. Geotechnical Practice in Offshore Engineering*, ASCE, University of Texas at Austin, Austin Texas, April 27–29, pp. 536–545.

Goudreault, P. A. and B. H. Fellenius. 1994. "A Program for the Design of Piles and Piles Groups Considering Capacity, Settlement, and Dragload Due to Negative Skin Friction." UniSoft Ltd., Ottawa, Canada.

Gupton, C. and T. Logan. 1984. "Design Guidelines for Drilled Shafts in Weak Rocks in South Florida," Preprint, Annual Meeting of South Florida Branch of ASCE.

Horvath, R. G. and T. C. Kenney. 1979. "Shaft Resistance of Rock-Socketed Drilled Piers," *Symposium on Deep Foundations*, ASCE National Convention, Atlanta, GA, pp. 182–214.

Janbu, N. 1976. "Static Bearing Capacity of Friction Piles," *Proc. of 6th European Conference on Soil Mechanics & Foundation Engineering*, Vol. 1.2, pp. 479–488.

Kishida, H. 1967. "Ultimate Bearing Capacity of Piles Driven into Loose Sand," *Soil Found.*, Vol. 7, No. 3, pp. 20–29.

Kraft, L. M., J. A. Focht, and S. F. Amerasinghe. 1981. "Friction Capacity of Piles Driven into Clay," *J. Geot. Engr. Div.*, ASCE, Vol. 107, No. GT 11, pp. 1521–1541.

Kubo, K. 1965. "Experimental Study of Behavior of Laterally Loaded Piles," *Proc. 6th Intl. Conf. Soil Mech. Fdn. Eng.,* Montreal, Canada, Vol. 2, pp. 275–279.

Kulhawy, F. H. 1983. "Transmission Line Structures Foundations for Uplift-Compression Loading," Report No. EL-2870, Report to the Electrical Power Research Institute, Geotechnical Group, Cornell University, Ithaca, NY.

Kulhawy, F. H. 1984. "Limiting Tip and Side Resistance: Fact or Fallacy?" *Proc. of the American Society of Civil Engineers, ASCE, Symposium on Analysis and Design of Pile Foundations*, Ed. R.J. Meyer, San Francisco, pp. 80–89.

Kulhawy, F. H. and K. K. Phoon. 1993. "Drilled Shaft Side Resistance in Clay Soil or Rock," *Design and Performance of Deep Foundations: Piles and Piers in Soil to Soft Rock*, Eds. P.P Nelson, T.D. Smith and E.C. Clukey, ASCE, Reston, VA. pp. 172–183.

Lysmer, J., M. Tabatabaie-Raissi, F. Tajirian, S. Vahdani, and F. Ostadan. 1981. "SASSI - A System for Analysis of Soil-Structure Interaction," Report No. UCB/GT/81-02, Department of Civil Engineering, University of California, Berkeley, April.

Matlock, H. 1970. "Correlations for Design of Laterally-Loaded Piles in Soft Clay," Paper No. OTC 1204, *Proc. Sec Annual Offshore Technology Conference*, Houston, Texas, Vol. 1, pp. 577–594.

McVay, M. C., F. C. Townsend, and R. C. Williams. 1992. "Design of Socketed Drilled Shafts in Limestone," *J. Geotech. Eng.*, Vol. 118-GT10, pp. 1626–1637.

Menard, L. F. 1975. "Interpretation and Application of Pressuremeter Test Results," *Sols-Soils*, Paris, Vol. 26, pp. 1–23.

Meyerhof, G. G. 1956. "Penetration Tests and Bearing Capacity of Cohesionless Soils," *J. Soil Mech. Found. Div.*, ASCE, Vol. 82, No. SM1, pp. 1–19.

Meyerhof, G. G. 1976. "Bearing Capacity and Settlement of Pile Foundations," *J. Geot. Engr. Div.*, ASCE, Vol. 102, No. GT3. pp. 195–228.

Mitchell, J. K. and T. A. Lunne. 1978. "Cone Resistance as a Measure of Sand Strength," *Proc. ASCE, J. Geotech. Engr. Div.*, Vol. 104, No. GT7, July, pp. 995–1012.

Miyamoto, Y., Y. Sako, K. Miura, R. F. Scott, and B. Hushmand. 1992. "Dynamic Behavior of Pile Group in Liquefied Sand Deposit," *Proc. 10th World Conference on Earthquake Engineering*, Ed. Bernal, A., July 19–24, Madrid, Spain. Balkema, Leiden, The Netherlands. pp. 1749–1754.

Mosher, R.L. 1984. "Load Transfer Criteria for Numerical Analysis of Axially Loaded Piles in Sand," US Army Engineering Waterways Experimental Station, Automatic Data Processing Center, Vickburg, Mississippi, January.

NAVFAC. 1986. Design Manual DM7.02: Foundations and Earth Structures, Department of the Navy, Naval Facilities Engineering Command, Alexandra, VA., September.

Nomura, S. K. Tokimatsu and Y. Shamoto. 1990. "Behavior of Soil-Pile-Structure System During Liquefaction," *Proc. 8th Japanese Conference on Earthquake Engineering*, Tokyo, December 12–14, Vol. 2, pp. 1185–1190.

O'Neil, M. W., F. C. Townsend, K. M. Hassan, A. Buller, and P. S. Chan. 1996. "Load Transfer for Drilled Shafts in Intermediate Geomaterials," FHWA-RD-95-172, November, 184 pp.

O'Neil M. W. and L. C. Reese. 1978. "Load Transfer in a Slender Drilled Pier in Sand," ASCE, ASCE Spring Convention and Exposition, Pittsburgh, Pennsylvania, Preprint 3141, April, 30 pp.

O'Neil, M. W. and S. A. Sheikh. 1985. "Geotechnical Behavior of Underrems in Pleistocene Clay," *Drilled Piers and Caissons II*, Ed. C.N. Baker, Jr. ASCE, Reston, VA. May, pp. 57–75.

Osterberg, J. O. 1989. "New Load Cell Testing Device," *Proc. 14th Annual Conference*, Deep Foundations Institute, Vol. 1, pp. 17–28.

Pells, P. J. N. and R. M. Turner. 1979. "Elastic Solutions for the Design and Analysis of Rock-Socketed Piles," *Can. Geotech. J.*, Vol. 16, No. 3, pp. 481–487.

Pells, P. J. N. and R. M. Turner. 1980. "End Bearing on Rock with Particular Reference to Sandstone," Structural Foundations on Rock, *Proc. International Conference On Structural Foundations on Rock*, Sydney, Vol. 1, May 7–9, pp. 181–190.

Poulos, H. G. and E. H. Davis. 1980. *Pile Foundation Analysis and Design*, John Wiley & Sons, New York.

Reese, L. C. 1997. "Analysis of Laterally Loaded Piles in Weak Rock," *J. of Geotech & Geoenvironmental Engr.*, Vol. 123, No. 11, pp. 1010–1017.

Reese, L. C. 1983. "Behavior of Piles and Pile Groups under Lateral Load," A report submitted to the Federal Highway Administration, Washington, DC, July, 404 pages.

Reese, L. C. and H. Matlock. 1966. "Behavior of a Two-Dimensional Pile Group Under Inclined and Eccentric Loading," *Proc. Offshore Exploration Conference*, Long Beach, California, February.

Reese, L. C. and M. W. O'Neil. 1967. "The Analysis of Three-Dimensional Pile Foundations Subjected to Inclined and Eccentric Loads," *Proc. ASCE Conference*, September, pp. 245–276.

Reese, L. C. and M. W. O'Neil. 1988. "Drilled Shafts: Construction Procedures and Design Methods," U.S. Department of Transportation, Federal Highway Administration, McLean, VA.

Reese, L. C. and S. J. Wright. 1977. "Drilled Shafts: Design and Construction, Guideline Manual, Vol. 1; Construction Procedures and Design for Axial Load," U.S. Department of Transportation, Federal Highway Administration, July, Washington, DC.

Reese, L. C., W. R. Cox, and F. D. Koop. 1974. "Analysis of Laterally Loaded Piles in Sand," Paper No. OTC 2080, *Proc. Fifth Offshore Technology Conference*, Houston, Texas.

Reese, L. C., W. R. Cox, and F. D. Koop. 1975. "Field Testing and Analysis of Laterally Loaded Piles in Stiff Clay," Paper No. OTC 2313, *Proc. Seventh Offshore Technology Conference*, Houston, Texas.

Reynolds, R. T. and T. J. Kaderabek. 1980. "Miami Limestone Foundation Design and Construction," Preprint No. 80-546, South Florida Convention, ASCE.

Rosenberg, P. and N. L. Journeaux. 1976. "Friction and End Bearing Tests on Bedrock for High Capacity Socket Design," *Can. Geotech. J.*, Vol. 13, No. 3, pp. 324–333.

Rowe, R. K. and H. H. Armitage. 1987a. "Theoretical Solutions for Axial Deformation of Drilled Shafts in Rock," *Can. Geotech. J.*, Vol. 24, No. 1, pp. 114–125.

Rowe, R. K. and H. H. Armitage. 1987b. "A Design Method for Drilled Piers in Soft Rock," *Can. Geotech. J.*, Vol. 24, No. 1, pp. 126–142.

Schmertmann, J. H. 1978. *Guidelines for Cone Penetration Test: Performance and Design*, FHWA-TS-78-209, Fed. Highway Admin., Office of Research and Development, Washington, D.C.

Seed, H. B. and L. C. Reese. 1957. "The Action of Soft Clay Along Friction Piles," *T. Am. Soc. Civ. Eng.*, Vol. 122, Paper No. 2882, pp. 731–754.

Seismic Advisory Committee on Bridge Damage. 1995. "Investigation Report on Highway Bridge Damage Caused by the Hyogo-ken Nanbu Earthquake," Japan Ministry of Construction.

Skempton, A. W. 1951. "The Bearing Capacity of Clay," *Proc. Building Research Congress*, Vol. 1, London, UK, pp. 180–189.

Skempton, A. W. 1959. "Cast-In Situ Bored Piles in London Clay," *Geotechnique*, Vol. 9, pp. 153–173.

Sörensen, T. and B. Hansen. 1957. "Pile Driving Formulae - An Investigation Based on Dimensional Considerations and a Statistical Analysis," *Proc. 4th International Conference On Soil Mechanics*, London, Vol. 2, pp. 61–65.

Tazoh, T. and G. Gazetas. 1996. "Pile Foundations Subjected to Large Ground Deformations: Lessons from Kobe and Research Needs," *Proc. 11th World Conference on Earthquake Engineering*, Paper No. 2081.

Tazoh, T., K. Shimizu and T. Wakahara. 1987. "Seismic Observations and Analysis of Grouped Piles," *Dynamic Response of Pile Foundations - Experiment, Analysis and Observation,* Ed., Toyoaki *N.,* ASCE Geotechnical Special Publication No. 11, ASCE, Reston, VA.

Terzaghi, K. 1943. *Theoretical Soil Mechanics*, John Wiley & Sons, New York, 510 pp.

Tirant, P. L. 1979. *Seabed Reconnaissance and Offshore Soil Mechanics for the Installation of Petroleum Structures*, Editions TECHNIP, Paris, France, 508 pp.

Tomlinson, M. J. 1957. "The Adhesion of Piles in Clay Soils," *Proc. Fourth International Conference on Soil Mechanics and Foundation Engineering*, Vol. 2, pp. 66–71.

Tomlinson, M. J. 1971. "Some Effects of Pile Driving on Skin Friction," *Behavior of Piles, Institution of Civil Engineers*, London, pp. 107–114, and response to discussion, pp. 149–152.

Touma, F. T. and L. C. Reese. 1972. "Load Tests of Instrumented Drilled Shafts Constructed by the Slurry Displacement Method." Research report conducted under Interagency contract 108 for the Texas Highway Department, Center for Highway Research, The University of Texas at Austin, January, 79 pp.

Townsend, F. C. 1993. "Comparison of Deep Foundation Load Test Method," *FHWA 25th Annual Southeastern Transportation Geotechnical Engineering Conference*, Natchez, MS, October 4–8.

Vesic, A. S. 1967. "Ultimate Loads and Settlements of Deep Foundations in Sand," *Proc. Symposium on Bearing capacity and Settlement of Foundations*, Duke University, Durham, N.C.

Vesic, A. S. 1970. "Load Transfer in Pile-Soil System," *Design and Installation of Pile Foundations and Cellar Structures*, Eds. H. Y. Fang and T. D. Dismuke, Envo Pub. Co., Lehigh, PA, pp. 47–74.

Vesic, A. S. 1972. "Expansion of Cavities in Infinite Soil Mass," *Proc. ASCE, J. Soil Mech. And Found. Engr. Div.*, Vol. 98, No. SM3, March.

Vesic, A. S. 1977. "Design of Pile Foundations," National Cooperative Highway Research Program Synthesis 42, Transportation Research Board, Washington, DC.

Vijayvergiya, V. N. 1977. "Load-Movement Characteristics of Piles," *Proc. of Ports'77 Conference*, Long Beach, California.

Vijayvergiya, V. N. and J. A. Focht. 1972. "A New Way to Predict the Capacity of Piles in Clay," *Offshore Technology Conference*, Houston, TX, Vol. 2, pp. 965–874.

Welch, R. C. and Reese, L. C. 1972. "Laterally Loaded Behavior of Drilled Shafts," Research Report No. 3-5-65-89, conducted for Texas Highway Department and U.S. Department of Transportation, Federal Highway Administration, Bureau of Public Roads, by Center for Highway Research, The University of Texas at Austin, May.

Weltman, A. J. and P. R. Healy. 1978. "Piling in Boulder Clay and Other Glacial Tills," Construction Industry Research and Information Assoc., Report PG5, London, UK.

Williams, A. F., I. W. Johnson, and I. B. Donald. 1980. "The Design of Socketed Piles in Weak Rock," Structural Foundations on Rock, *Proc. International Conference on Structural Foundation on Rock*, Sydney, Vol. 1, May 7–9, pp. 327–347.

Woodward, R. J., W. S. Gardner, and D. M. Greer. 1972. *Drilled Pier Foundations*, McGraw-Hill Book Co., New York.

10

Earth Retaining Structures

Chao Gong
URS Corporation

10.1 Introduction

Earth-retaining structures are commonly used in highway and bridge projects. Additionally, it is a common practice to use earth retaining structures as the temporary shoring during the bridge construction. This chapter introduces and discusses ordinary retaining wall design practices. For more detailed discussion, references may be made to Bowles (1996), Das (2011), Huntington (1957), Lambe and Whitman (1979), and Tschebotarioff (1973).

Although it is common for bridge abutments to function as retaining structures, this chapter does not include abutment wall design. The special load case and design requirements for abutments and wing walls are discussed in Chapter 6.

Determining proper design parameters for existing field conditions requires extensive knowledge of soil mechanics and practical engineering experience. However, most transportation projects already have a detailed soil report and structural design parameters recommended by professional geotechnical engineers. The structural engineer should simply use the values included in the soil reports, such as K_a, K_o, K_p, and friction factors. However, this chapter introduces a few conservative design parameters that

could be used for general cases only. These parameters should be considered in the preliminary design stage and subject to review by a qualified geotechnical professional.

Specific soil–structure interaction (SSI) analysis is not required for the ordinary retaining wall design in transportation-related projects. Thus, this chapter does not include the SSI-related discussions.

10.2 Retaining Structure Types

The most frequently used types of retaining structures in highway, transportation, and railroad projects consist of cantilever walls, tieback walls, soil nail walls, and mechanically stabilized embankment (MSE) walls. The overall design objective of these retaining structures is to resist lateral soil pressure forces.

10.2.1 Cantilever Wall

Cantilever retaining walls can be any cantilever structure used to resist the active lateral soil pressure in topography fill, and cut locations. Usually, the common wall height (H) limits for cantilever walls in transportation projects is 30–40 ft (9.14–12.2 m). For wall heights greater than 30 ft (9.14 m), various other types of retaining walls usually have more economical advantages compared to cantilever walls.

Gravity walls are part of the cantilever wall category. Common shapes of concrete cantilever walls are upside down "T" and "L" shapes. Gravity walls are usually a massive volume of concrete and the retaining effects mainly depend on the self-weight. Most gravity walls are constructed by using solid concrete or other means of confined box system fill with heavy materials.

Typical concrete cantilever walls have an upside down "T" configuration. This type of cantilever wall often has the vertical wall stem and the footing that consist of the toe and heel parts. At a preliminary design stage, the total footing width could be assumed as approximately $0.7H$–$0.8H$ for typical transportation projects. The weight of the backfill material on the top of the heel generates some additional friction force to resist the sliding, and the added vertical weight will help to resist overturning about the toe. The "L" shape wall is commonly utilized when construction space is limited, such as the right of way is restricted. Compared with the upside down "T" wall configuration, the footing of the "L" shape wall can be built right against the property line. For cantilever walls, adding a "key" below the footing is an effective way to increase the passive pressure to resist lateral sliding.

Buttress walls are another type of cantilever retaining walls. The concrete buttress that is added onto the back of the wall increases the wall stem stiffness in order to reduce top of wall deflection. Without the buttress, the wall stem is a pure vertical cantilever slab. Depending on the space available, the buttress could allow the wall stem to behave like a two-way slab or even like a horizontal continuous slab.

Concrete cantilever walls are very sensitive to differential settlement because the wall system has very large rigid stiffness in the vertical direction. The differential settlement creates very large internal forces in the wall system. Some design manuals suggest that the long-term differential settlement along the wall should be smaller than $L/500$–$L/1000$. The designer can add some gaps to reduce this effect or use pile footing. In the pile footing system, the thicker spread footing will be used as the pile cap. Some of the piles can be battered to offer strong lateral resistance capacity.

Another kind of the cantilever wall type is called "soldier pile" wall. This is a special type of cantilever wall that should be used in the topography cut locations. It is a common practice to utilize HP section steel members to act as the soldier piles for this system. The spacing of the soldier piles are typically installed roughly 6–8 ft (1.83–2.44 m) apart from each other. The pile tip elevation will be far below the proposed excavated level. Stronger anchoring piles can be constructed in a predrilled hole and filled with concrete up to the wall excavation level. The HP steel pile members are bonded within the concrete, which offers better anchoring for the upper part of piles. The soil is then excavated from the top down. Wood logs with thickness of 4–8 in (100–200 mm) are usually placed between the pile flanges. The wall is constructed from the top down. The wood logs may need to be treated for a permanent wall face or a layer of shotcrete could be utilized for the final wall face. Some soldier pile walls use steel plate or precast

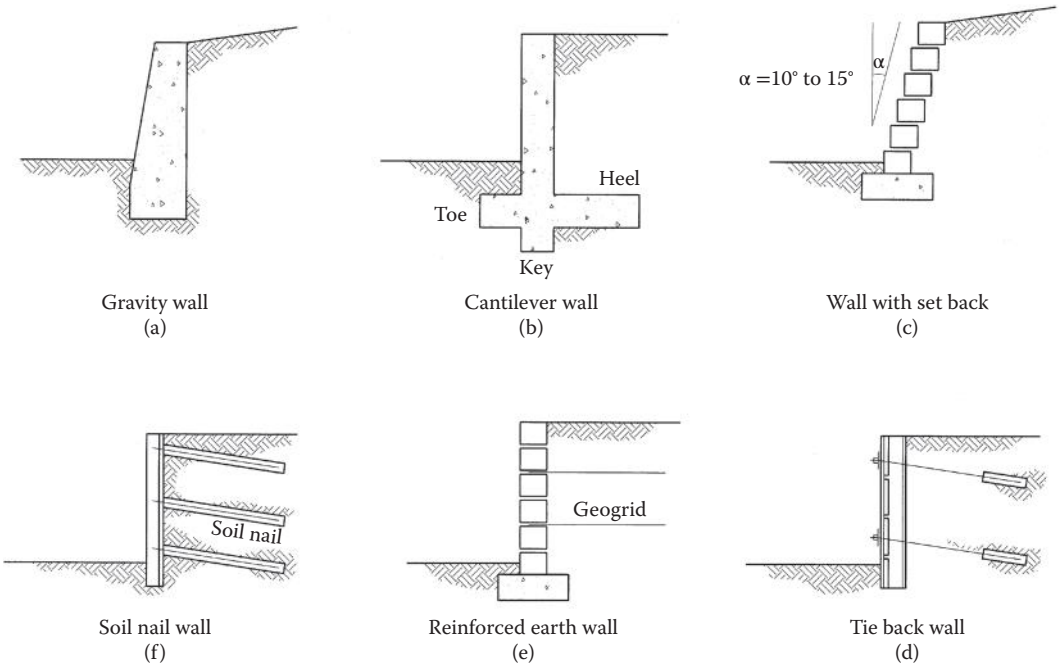

Gravity wall (a) | Cantilever wall (b) | Wall with set back (c)

Soil nail wall (f) | Reinforced earth wall (e) | Tie back wall (d)

FIGURE 10.1 Retaining wall types.

concrete panels instead of the wood log members. The differential settlement is not a critical issue for soldier pile and lagging systems.

Some typical cantilever retaining wall sections are shown in Figure 10.1a through c. It is recommended that the reader go through the related examples in Sections 10.6 and 10.7 to see a more detailed discussion for simplified cantilever retaining wall and soldier pile wall analysis and design details.

10.2.2 Tie Back Wall

In transportation projects, the tieback system can be used for retaining wall applications. The most popular tie back system is a "soil nail" configuration (FHWA 1998).

The "soil nail" wall should only be used for topography cutting locations. Similar to the soldier pile wall, this system is constructed from the top down. Usually, the soil nail is constructed by pumping cement grout into the predrilled holes to create the bonding effect with the central core, and shotcrete is typically used to construct the face of the wall. The typical construction sequence is as follows:

1. Start the excavation from the top of wall down to the next soil nail level
2. Install and lock the soil nail assembly
3. Construct the temporary wall face (first layer of shotcrete)

That procedure is then repeating these steps until the entire height of the wall is constructed. Soil nail walls can be used in transportation projects for virtually any wall height.

The central core of the soil nail could be rebar, rod, or high-strength steel strands. The soil nail should have a down sloping angle for grouting convenience, usually around 15°. The end of the nail hole will be filled with bonding grout. The core is installed into the predrilled hole, and the part of the nail that extends beyond the expected failure surface into the stable zone will be bonded. The bonded length will create anchorages for the wall face layers. The friction effect between the grout surface and the surrounding soil is the source of the soil nail anchoring capacity. Based on the most common assumption

of the failure surfaces, the length of the soil nail gradually be reduced from the top to the bottom of the walls. Within the limit of the wall face to the assumed failure surface, the soil nails should have a certain "unbonded" length in order to minimize the soil nail capacity reduction.

The most common practice for soil nail wall construction includes applying two layers of shotcrete for the face of the wall. Each shotcrete layer is usually about 4–6 in (100–150 mm) thick. The first layer of shotcrete is placed directly against the excavated soil face and then the steel anchoring plate and beveled washer with hex nuts are installed to lock the soil nail in place. The second layer of shotcrete is then subsequently installed. For these soil nail walls, it is important for the designer to check the flexure and punching-shear demand generated by the soil nail in each slab layer.

Each shortcrete layer has steel wire mesh and some strengthening rebar near the soil nail anchoring location providing the reinforcements. The whole system depends on the tension capacity of the soil nails and concrete face layers acting as a multiple span two-way slab system. Differential settlement is not a particularly sensitive issue for typical soil nail walls.

The soil nail can also be used to effectively tie back other retaining wall systems. The soldier pile wall with soil nail tie back is a good example of a combined system. Any tie back mechanism would provide additional effective resistance for different types of cantilever walls.

Figure 10.1d and f shows some tie back wall sections. It is recommended that the reader go through the related examples in Section 10.8 to see a more detailed discussion for simplified soil nail wall analysis and design details.

10.2.3 MSE Wall

MSE walls are a kind of "reinforced earth-retaining" structure. By installing multiple layers of high-strength fibers inside of the fill section, the friction and interlock mechanism between the fibers and backfilled soil will effectively restrict the lateral deflection of the filled soil body. Hence, the MSE wall is a compacted soil body acting as one gravity wall. Because every bit of the MSE wall material is "reinforced-compacted soil," this system should be used on topography fill locations only.

The lateral reinforcement could be steel wires or any other type of geogrid system. The common wall face is made of precast concrete slabs. The end of the lateral reinforcement wires in the MSE wall soil body will tie into the face slab as the finished anchors. Different MSE wall contractors may have their own particular wall systems, but they are all based on the same retaining principle.

There is no practical high limit for MSE walls considered in common transportation projects. Some engineers believe that when H is greater than roughly 25 ft (7.62 m), the MSE wall exhibits the economic cost advantages compared to cantilever retaining walls. As a preliminary design, the estimated MSE wall reinforcement length, called "base width" (BW), should be started around $0.7H$ to $0.75H$. Some design manuals specifically request BW $> 0.7H$, whereas other manuals suggested using 8 ft as the minimum BW regardless the wall height. Hence, if the wall height is too short ($H < 10$ ft), the MSE wall may be more expensive when compared to other types of retaining walls. In practical design, some design manuals suggest that the MSE walls should have minimum embedded depth $\geq 0.1H$ or 2.0 ft (600 mm).

A conceptual sketch for MSE wall is shown in Figure 10.1e. It is recommended that the reader go through the related examples in Section 10.9 to see a more detailed discussion for simplified MSE wall analysis and design details.

10.3 Design Criteria

As a minimum requirement, all the retaining structures must satisfy "global stability" and vertical settlement limits. Total (global) sliding stability should be checked during this stage of the design. However, it is common that the "global stability" and the expected settlement are verified by geotechnical engineers.

The structural engineer should verify that the walls have sufficient resistance against overturning, lateral relative sliding, and that the vertical bearing capacity to resist the loading demand. Additionally,

the retaining structure must also have adequate strength capacity for each compositional element such as wall stem and footing.

1. *Overturning resistance:* If the wall is sited on the bed rock, the overturning point for a typical retaining wall is located at the edge of footing toe. The overturning factor of safety should be larger than 1.50 under service load combination. For seismic load case, the factor of safety should be larger than 1.0. For those retaining walls that have pile footings, the fixity points of the footing depend on the piles layout. Usually the turning point should be assumed at the center of the first row of piles. The connection details between pile and cap determined that the pile could take tension force or not. When retaining wall site on the regular soil, it is not easy to determine the exact overturning point. Therefore, instead of directly checking the overturning moment, the design manuals limit the maximum reaction force eccentricity. Usually, for transportation projects, under the regular load cases the eccentricity $e_0 \leq B/4$ and under the seismic load the eccentricity value $e_0 \leq B/2$, which is equivalent to the factor of safety ≥ 1.0 on rock. For some projects, the manual requires $e_0 \leq B/6$, which indicates that there shall be no up lift at any point within the foundation footprints. This is an "indirect" way to control the overturning factor of safety.
2. *Lateral sliding resistance:* The factor of safety for the lateral sliding should be larger than 1.50 under the service load cases. The typical retaining wall sliding capacity may include the passive soil pressure at the toe face of the footing and key depth plus the friction forces at the bottom of the footing. In most cases, the allowable friction factors of 0.3–0.4 can be used for clay and sand, respectively. If the battered piles are used for lateral sliding resistance, the above passive and friction forces from footing cap should be neglected. Instead, the lateral components of the battered pile axial capacity and the pile section lateral shear capacity could be counted as the sliding capacity. Usually, the pile batter slope shall be 1:3 to 1:4 (*H*:*V*). Similar to any footing design, the designer should try to avoid the pile damage under seismic load. Damage to piles is hard to detect after an earthquake and is almost impossible to be properly repaired.
3. *Bearing capacity:* Similar to any footing design, the bearing capacity factor of safety should be larger than 1.0. If the specific soil report is not available, Table 10.1 lists of approximate allowable bearing capacity values for common materials during preliminary design stage. For wall spread footing site on the bed rocks, the triangle distribution of the reaction force is reasonable assumption. If a pile footing is used, the soil bearing effects on the bottom of cap footing between the piles should not be considered, because the piles stiffness is much bigger than the stiffness of surrounding soil. In most traffic projects, the wall spread footing is sitting on regular soil. The uniform distribution reaction within the "effective width" is a common assumption. The "effective width" is defined as $L_e = 2 \times (B/2 - e_0) = (B - 2e_0)$ where e_0 is the eccentricity value, $e_0 = M/N$.
   Under seismic loading, the ultimate bearing capacity should be utilized. The soil report generated by the geotechnical engineer may suggest some limits by considering the possibility of the soil liquefaction that may cause the wall structure movement be over limit. Then, the deep piles may be used to go through the liquefaction soil layer or the soil treatment method could be utilized to

TABLE 10.1 Bearing Capacity

	Bearing Capacity (*N*)	
Material	Minimum	Maximum
Alluvial soils	24 kPa	48 KPa
Clay	48 kPa	190 kPa
Sand, confined	48 kPa	190 kPa
Gravel	95 kPa	190 kPa
Cemented sand and gravel	240 kPa	480 kPa
Rock	240 kPa	—

improve the foundation. These topics are beyond the scope of this chapter, and it will be part of the geotechnical engineer's working tasks.

4. *Structural element strength:* Structural section flexural and shear capacities should be designed in accordance with common strength factors of safety and design procedures.

10.4 Design Methods

The traditional retaining wall design theory was based on the "allowable stress design" (ASD) method. In transportation projects, this ASD procedure is often called "service load design" (SLD). The retaining wall structural stability check should follow the SLD procedure, but the section strength check on wall element should follow "load factor design" (LFD) with proper load combination and factors (AASHTO 2002). The LFD method is based on the moderate level of ultimate states theory. It is important to understand the difference between the two design procedures and to use them properly.

Many current design manuals for transportation projects use the "load and resistant factor design" (LRFD) method (AASHTO 1998 and 2012). This procedure is based on the latest multiple ultimate states theory combining with statistic data treatment results as much as possible. This method uses different load factors for the different limit states and strength reduction factors. All stability checks and section strength checks are based on the same procedure, but there are different load and resistant factors for each specific case.

Depending on the specific project design criteria, the design method needs to be confirmed before the analysis is started. There is no "exact" equivalent transition formula between SLD (ASD), LFD, and LRFD procedures (AASHTO 2012; AREMA 2011). Therefore, it is not practical to switch the design method in the middle of the design procedure. Unless specifically defined, the soil report generated by geotechnical engineers will most likely include all "allowable" parameters that could be directly used into the SLD (ASD) procedure.

10.5 Loads

The major loads acting on a retaining wall include the lateral soil pressure, lateral hydrostatic pressure, and vertical traffic loads that generate additional lateral loads on the wall. The designer should try to release the hydrostatic pressure by installing a drainage system behind the wall stem. If the traffic load location is far enough from the wall, say farther than the wall height, its effects could be neglected. To be conservative, some design manuals mention that the horizontal distance should be larger than 1.5 times the height of the wall before these load effects can be totally neglected. For effective traffic loads, the uniformly distributed surcharge load shall be included in the design analysis. The typical highway bridge design traffic load (HL-93 or HS-20) moving parallel to the wall length direction can be simplified to be equivalent to 2.0 ft (600 mm) of soil on top of wall level per AASHTO design codes (AASHTO 2002, 2012). In construction shoring design, the surcharge load depends on the type, location, and weight of the heavy construction equipment.

A well-accepted simplified process for cantilever wall systems is to use the equivalent liquid density $k_a\gamma$ to determine the lateral soil pressure on the wall stem. The soil density is typically in the range of 120–150 pounds per cubic feet (pcf) (1.9–2.4 T/m^3). Figure 10.2 shows a simplified load distribution diagram for typical retaining wall.

The active soil pressure per unit length of wall (P_a) at the bottom of the wall can be determined as

$$P_a = k_a \gamma H \tag{10.1}$$

The passive soil pressure per unit length of wall (P_p) at the bottom of the wall can be determined as

$$P_p = k_p \gamma H_o \tag{10.2}$$

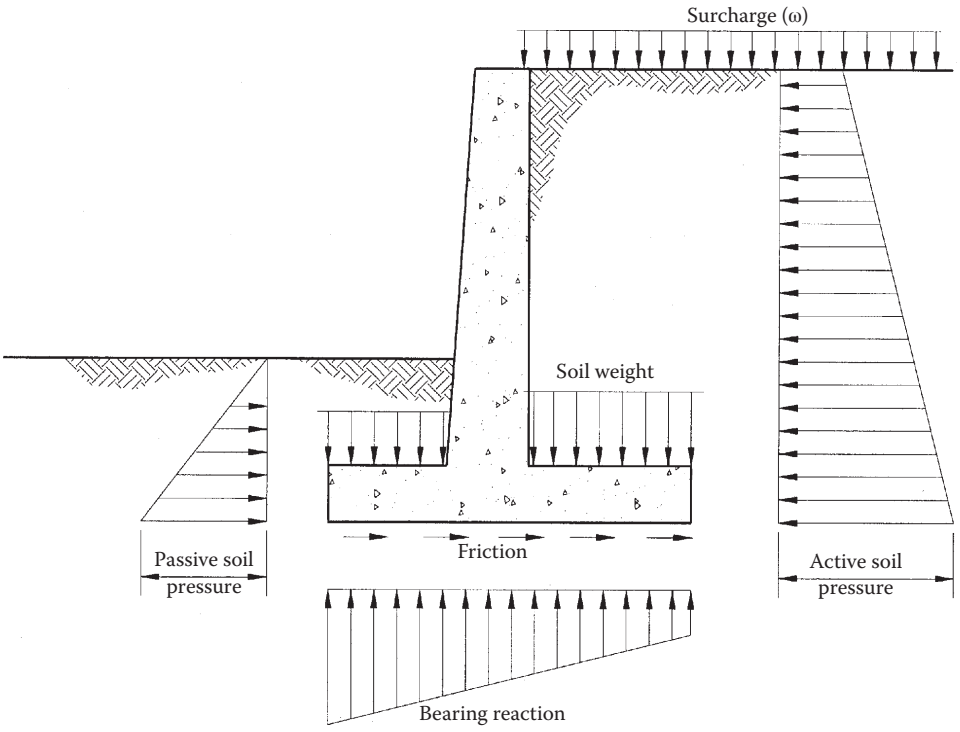

FIGURE 10.2 Typical loads on retaining wall.

where

H = the height of the wall (from top of the wall to bottom of the footing)
H_o = the height of the toe (from top of the ground to bottom of the footing at toe position)
γ = unit weight (density) of the backfill material
k_a = active earth pressure factor
k_p = passive earth pressure factor

The factors k_a and k_p should be determined by a geotechnical engineer based on the test data on proper soil sample. The factor values should be included in the project soil report. Based on the soil mechanics, the simplified formula should be as follows:

$$k_a = \frac{1-\sin\varphi}{1+\sin\varphi}; \quad k_p = \frac{1}{k_a} = \frac{1+\sin\varphi}{1-\sin\varphi} \tag{10.3}$$

where φ = internal friction angle of the soil sample.

Table 10.2 lists friction angles for typical soil types that can be used if laboratory test data are not available. Generally, force coefficients of $k_a \geq 0.3$ and $k_p \leq 2.5$ should be used for preliminary design.

Based on the triangle distribution assumption, the total active lateral force per unit length of wall should be

$$P_a = \frac{1}{2} k_a \gamma H^2 \tag{10.4}$$

The resultant earth pressure should act at distance of $H/3$ from bottom of the wall.

TABLE 10.2 Internal Friction Angle and Force Coefficients

Material	φ (degrees)	k_a	k_p
Earth, loam	30–45	0.33–0.17	3.00–5.83
Dry sand	25–35	0.41–0.27	2.46–3.69
Wet sand	30–45	0.33–0.17	3.00–5.83
Compact earth	15–30	0.59–0.33	1.70–3.00
Gravel	35–40	0.27–0.22	3.69–4.60
Cinders	25–40	0.41–0.22	2.46–4.60
Coke	30–45	0.33–0.17	3.00–5.83
Coal	25–35	0.41–0.27	2.46–3.69

The upper slope on top of the backfill will increase the soil pressure on the wall stem. The traditional method is to use the "complete" formula to generate the k_a factor. The factors listed in Table 10.3 are determined by the Coulomb equations with special case of zero wall friction (see Figure 10.3).

$$k_a = \frac{\sin^2(\varphi+\beta)}{\sin^2\beta\sin(\beta-\delta)\left[1+\sqrt{\dfrac{\sin(\varphi+\delta)\sin(\varphi-\alpha)}{\sin(\beta-\delta)\sin(\alpha+\beta)}}\right]} \tag{10.5}$$

For the preliminary design stage, some designers treat the upper slope on top of the flat backfill surface as another equivalent uniformly distributed surcharge. This may not satisfy soil mechanical theories but is an acceptable approach for a preliminary design stage estimate.

Any surface load near the retaining wall will generate additional lateral pressure on the wall. For highway-related design projects, the traffic load can be represented by an equivalent uniformly distributed vertical surcharge pressure of 240–250 psf (11.5–12.0 kPa).

For point load and line load cases, the following formulas can be used to determine the additional lateral pressure on the retaining wall (see Figure 10.4).

$$P_h = \begin{cases} \dfrac{1.77\,V}{H^2}\dfrac{m^2n^2}{\left(m^2+n^2\right)^3} & (m \le 0.4) \\ \dfrac{0.28\,V}{H^2}\dfrac{m^2n^2}{\left(0.16+n^2\right)^3} & (m > 0.4) \end{cases} \tag{10.6}$$

For line load

$$P_h = \begin{cases} \dfrac{\pi w}{4H^2}\dfrac{m^2n^2}{\left(m^2+n^2\right)^2} & (m \le 0.4) \\ \dfrac{w}{H}\dfrac{0.203n}{\left(0.16+n^2\right)^2} & (m > 0.4) \end{cases} \tag{10.7}$$

where $m = x/H$; $n = y/H$

Table 10.4 gives lateral load factors and wall bottom moment factors that are calculated by formulas given earlier.

The uniformly distributed surcharge load could be converted to the thickness of an equivalent additional soil layer. Therefore, the total lateral pressure on the wall back shall be a trapezoid (see the following example). For design simplification, engineers often utilize a triangle distribution for the backfill soil pressure and an additional rectangular distributed load to represent the surcharge effects.

TABLE 10.3 Active Stress Coefficient k^a Values from Coulomb Equation ($\delta = 0$)

		α					
φ	β_o	0.00°	18.43°	21.80°	26.57°	33.69°	45.00°
		Flat	1–3.0	1–2.5	1–2.0	1–1.5	1–1.0
	90°	0.490	0.731				
	85°	0.523	0.783				
20°	80°	0.559	0.842				
	75°	0.601	0.913				
	70°	0.648	0.996				
	90°	0.406	0.547	0.611			
	85°	0.440	0.597	0.667			
25°	80°	0.478	0.653	0.730			
	75°	0.521	0.718	0.804			
	70°	0.569	0.795	0.891			
	90°	0.333	0.427	0.460	0.536		
	85°	0.368	0.476	0.512	0.597		
30°	80°	0.407	0.530	0.571	0.666		
	75°	0.449	0.592	0.639	0.746		
	70°	0.498	0.664	0.718	0.841		
	90°	0.271	0.335	0.355	0.393	0.530	
	85°	0.306	0.381	0.404	0.448	0.602	
35°	80°	0.343	0.433	0.459	0.510	0.685	
	75°	0.386	0.492	0.522	0.581	0.781	
	70°	0.434	0.560	0.596	0.665	0.897	
	90°	0.217	0.261	0.273	0.296	0.352	
	85°	0.251	0.304	0.319	0.346	0.411	
40°	80°	0.287	0.353	0.370	0.402	0.479	
	75°	0.329	0.408	0.429	0.467	0.558	
	70°	0.375	0.472	0.498	0.543	0.651	
	90°	0.172	0.201	0.209	0.222	0.252	0.500
	85°	0.203	0.240	0.250	0.267	0.304	0.593
45°	80°	0.238	0.285	0.297	0.318	0.363	0.702
	75°	0.277	0.336	0.351	0.377	0.431	0.832
	70°	0.322	0.396	0.415	0.446	0.513	0.990

Using equivalent liquid density to determine the active soil pressure $k_a\gamma$ was based on the assumption that the top of the wall will experience certain lateral displacement. If there is a mechanism to limit this lateral movement at top of the wall, the lateral pressure factor k_o must be utilized. This lateral pressure factor k_o is the "at rest" soil pressure factor. Depending on the soil characteristics behind the wall, the k_o value could be 35% to 50%+ larger than the k_a value. The structural engineer should require the geotechnical engineer to list all k_a, k_o, and k_p values in their soil report. Without a detailed soil report during the preliminary design, the structural engineer can assume $k_a = 0.30$, $k_o = 0.45$, and $k_p = 3.00$.

If there is any tie back on the wall, the lateral soil pressure distribution shall be different than the "equivalent liquid pressure," which always follows the triangle distribution. Figure 10.5 shows a few typical distributions of the soil nail wall analysis diagram.

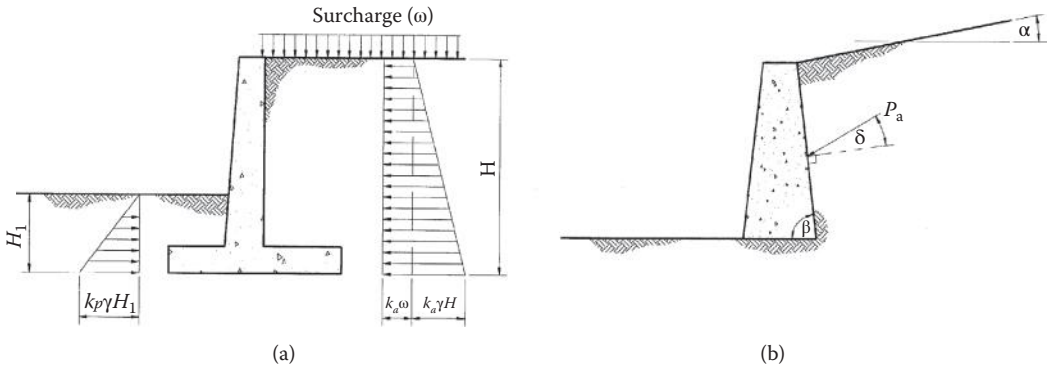

FIGURE 10.3 Lateral earth pressure.

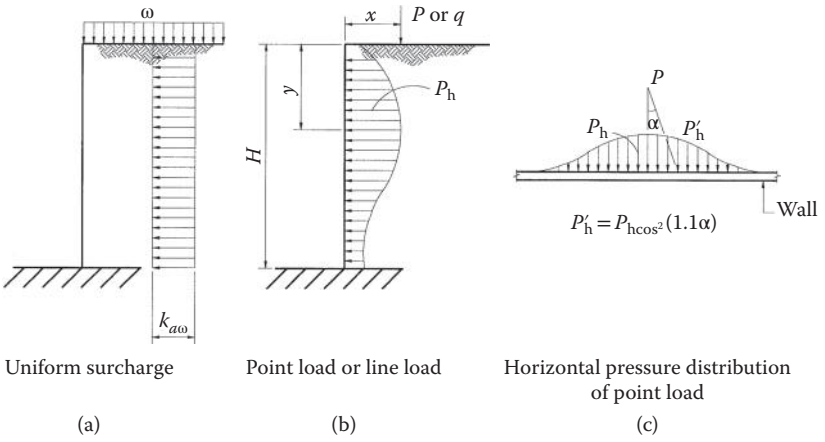

FIGURE 10.4 Additional lateral earth pressure.

TABLE 10.4 Line Load and Point Load Lateral Force Factors

Line Load Factors			Point Load Factors		
$m = x/H$	f	m	$m = x/H$	f	m
0.40	0.548	0.335	0.40	0.788	0.466
0.50	0.510	0.287	0.50	0.597	0.316
0.60	0.469	0.245	0.60	0.458	0.220
0.70	0.429	0.211	0.70	0.356	0.157
0.80	0.390	0.182	0.80	0.279	0.114
0.90	0.353	0.158	0.90	0.220	0.085
1.00	0.320	0.138	1.00	0.175	0.064
1.50	0.197	0.076	1.50	0.061	0.019
2.00	0.128	0.047	2.00	0.025	0.007

Notes: 1. Total lateral force along the length of wall = factor (f) × ω (force)/(unit length)
2. Total moment along the length of wall = factor (m) × ω × H (force × length)/(unit length) (at bottom of footing)
3. Total lateral force along the length of wall = factor (f) × V/H (force)/(unit length)
4. Total moment along the length of wall = factor (m) × V (force × length)/(unit length) (at bottom of footing)

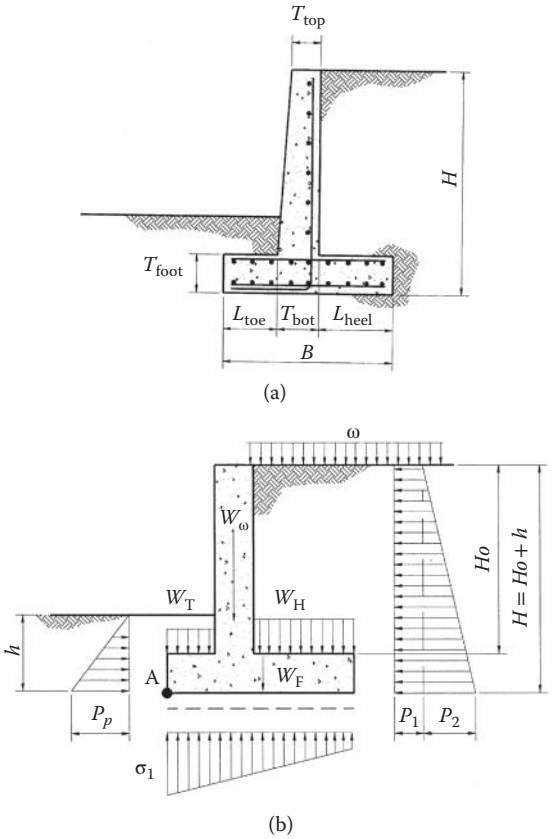

FIGURE 10.5 Cantilever wall design example.

10.6 Cantilever Retaining Wall Design Example

The cantilever retaining wall is the most commonly used retaining wall structure. It has been proven to be pretty cost-effective for walls less than 20 ft (6 m) high. In most cases, the following values can be used as the initial assumptions in the reinforced concrete retaining wall design process:

- $0.4 \leq B/H \leq 0.8$
- $1/12 \leq T_{bot}/H \leq 1/8$
- $L_{toe} \approx 3/B$
- $T_{top} \geq 12$ in
- $T_{foot} \geq T_{bot}$

10.6.1 Design Example

A reinforced concrete retaining wall site on bed rock is shown in Figure 10.5.

Given:

$H_o = 10$ ft;
Active soil pressure factor, $k_a = 0.33$
Passive soil pressure factor, $k_p = 3.0$
Earth unit weight, $\gamma = 120$ pcf
Highway traffic load equivalent surcharge, ω = (2 ft thick soil) $2 \times 120 = 240$ psf

Earth bearing capacity, σ = 18.0 ksf
Allowable friction coefficient = 0.35

Solution:

1. Select control dimensions
   Assume footing thickness = 2.5 ft
   Count soil cover above the footing toe = 2.5 ft
   Try $h = 5.0$ ft
   $H = H_o + h = 10 + 5 = 15$ ft
   Using $T_{bot} = 1/10H = 1.5$ ft
   $T_{top} = T_{bot} = 1.5$ ft
   $T_{foot} = 2.5$ ft
   Using $B = 0.6H = 9.0$ ft
   Using $L_{toe} = 3.0$ ft
   $L_{heel} = 9.0 - 3.0 - 1.5 = 4.5$ ft
2. Calculate lateral soil pressure
   Part 1,

$$\text{Surcharge:}\quad P_1 = k_a \omega H = (0.33)(240)(15) = 1{,}188 \text{ lbs/ft}$$

$$\text{Active earth pressure: } P_s = \frac{1}{2} k_a \gamma H^2 = \frac{1}{2}(0.33)(120)(15)^2 = 4{,}455 \text{ lbs/ft}$$

   Part 2,
   Maximum allowable passive earth pressure:

$$P_p = \frac{1}{2} k_p \gamma H^2 = \frac{1}{2}(3.0)(120)(5)^2 = 4{,}500 \text{ lbs/ft}$$

3. Calculate vertical loads
   Highway traffic load equivalent surcharge: 240(4.5) = 1,080 lbs/ft
   Use 150 pcf for concrete
   Wall, $W_w = 150(1.5)(15 - 2.5) = 2{,}182.5$ lbs/ft
   Footing, $W_f = 150(2.5)(9.0) = 3{,}375$ lbs/ft
   Soil cover at toe, $W_t = 120(2.5)(3.0) = 900$ lbs/ft
   Soil cover at heel, $W_h = 120(12.5)(4.5) = 6{,}750$ lbs/ft
   Total vertical load, $N_{tot} = 14{,}287.5$ lbs/ft
   Therefore, the maximum allowable friction force at bottom of footing
   $F = fN_{tot} = 0.35(14{,}287.5) \approx 5{,}000$ lbs/ft
4. Check sliding
   Total lateral active force
   $P_1 + P_2 = 1{,}188 + 4{,}455 = 5{,}643$ lbs/ft
   Total resistant = friction + passive
   = 5,000 + 4,500 = 9,500 lbs/ft
   Sliding factor of safety: 9,500/5,643 = 1.68 > 1.50 OK
5. Check overturning
   Take bottom of toe footing as reference point (point A in Figure 10.5)
   Overturning moment:
   Surcharge soil pressure, $P_1H/2 = 1{,}188(15)/2 = 8{,}910$ lbs-ft
   Active soil pressure, $P_2H/3 = 4{,}455(15)/3 = 22{,}275$ lbs-ft
   Total overturning moment, $M_o = 31{,}185$ lbs-ft

Resistant moment:
- Wall, 2182.5 (3 + 1.5/2) ≈ 8,184 lbs-ft
- Footing, 3375 (9.0/2) ≈ 15,188 lbs-ft
- Soil cover at toe, 900 (3/2) = 1,350 lbs-ft
- Soil cover at heel, 6,750 (3 + 1.5 + 4.5/2) ≈ 45,562 lbs-ft
- 240 psf surcharge, 240(4.5)(3 ± 1.5 ± 4.5/2) = 7,290 lbs-ft
- Total resistant moment, M_r = 77,574 lbs-ft

Overturning factor of safety:
- M_r/M_o = 77,574/31,185 = 2.48 > 1.50 OK

6. Check soil bearing capacity

Total vertical load, N = 14,287.5 lbs
Total moment to toe, M = 77,574 − 31,185 = 46,389 lbs-ft
Eccentricity to toe, $X_O = M/N$ = 46,389/14,287.5 = 3.247 ft
Eccentricity to center of the footing, e_o = (9.0/2) − 3.247 = 1.253 ft
Check: e_o = 1.253 ft < $B/6$ = 9.0/6 = 1.50 ft all footing area under compression.
Moment about center of footing, $M_o = Ne_o$ = 14,287.5(1.253) ≈ 17,902 lbs-ft

$$\sigma_{max} = \frac{N}{A} + \frac{M}{S} = \frac{14,287.5}{9.0} + \frac{17,903(6)}{9.0^2} \approx 2,914\,\text{psf} = 2.914\,\text{ksf} < 18.0\,\text{ksf} \quad \text{OK}$$

10.6.2 Example Discussion

1. The above example did not include the wall stem and footing strength check. Per AASHTO (2012) or ACI codes (2008), the concrete elements section flexure and shear strength check should be performed in accordance the LRFD procedure.
2. Some design manuals required that the Dead Load (DL) (soil and concrete weights) be reduced a little when determining the friction capacity and the resisting overturning moment (in order to be conservative). Most likely, the reduction factor (0.9) shall be included in the LRFD design procedure as a load combination factor. Above example is basically following the ASD (SLD) procedure. Therefore, the DL reduction factor is not shown in the above example.
3. The water pressure behind the wall should be reduced to zero by installing a proper drainage system. Therefore, the lateral water pressure load was not considered in the example calculations.
4. Usually the top 1.0 ft (or even 1.5 ft) of soil cover at the toe is neglected for calculating the passive pressure (it is not fully dependable).
5. In this example, the surcharge load = 240 psf represents the regular highway traffic load (HS-20 or HL-93). It is a typical live load (LL) and per AASHTO design criteria, the LL impact factor can be assigned to 1.0 for retaining wall design. For overturning and sliding check, some design manuals suggest that the vertical surcharge load should not be put directly on top of the footing heel footprint area. This is a very conservative assumption, and the engineer can use his/her judgment regarding the final factor of safety.
6. If the traffic barrier is installed on top of the wall, the truck impact (crash) load case needs to be considered. The crash slab under the barrier can be used so that the lateral impact load on barrier can be resisted by the vertical wheel load acting on the crash slab.

10.7 Soldier Pile Wall Example

Figure 10.6 shows a simplified soldier pile calculation diagram. Assume there is no surcharge load. The top cantilever height "H" is subjected to the lateral active soil pressure with tributary space "S."

$$P_1 = Sk_a\gamma H \tag{10.8}$$

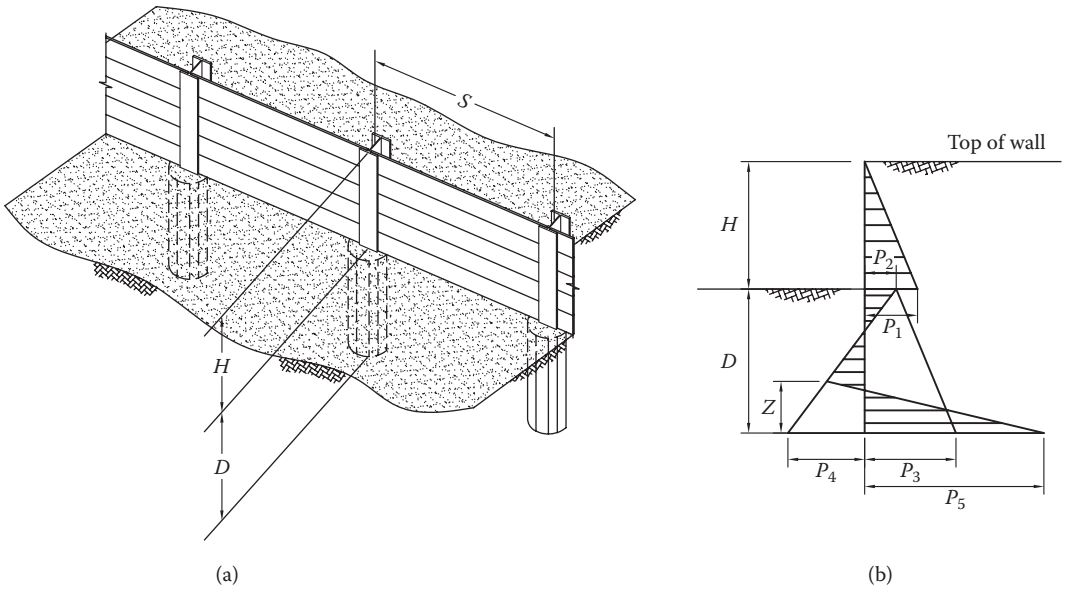

FIGURE 10.6 Typical solider pile wall.

Between the excavation and the pile tip elevations, the vertical pile embedded length is "*D*." The steel section soldier pile could be anchored into the soil directly or inserted into a drilled hole and filled with concrete.

10.7.1 Effective Width and Arch Factor

This example considers a steel pile anchored into a Cast-In-Drilled-Hole (CIDH) pile. The pile segment below the excavation elevation shall be subjected to the active soil pressure. The pile will engage the passive soil pressures with the lateral pile dimension of the tributary width as the "effective pile width." The effective width is computed based on the soil arch effects between the adjacent piles and is influenced by various soil types. The empirical equation to estimate the effective width is

$$B_{\text{eff}} = \alpha B \tag{10.9}$$

$$\alpha = 0.08\varphi \le 3.00 \tag{10.10}$$

where

α = factor for effective width
B = soldier pile projected width
φ = the internal friction angle of the soil (degree)

Here 0.08φ is for granular soils; for cohesive soils, this factor should be 1–2. Use the value 1.0 for very soft cohesive soil and 2.0 for medium and stiff cohesive soil.

Obviously, the practical upper bound of the "effective width" can reach three times of the pile projected width. Practically, the effective pile width will always be larger than the soldier pile projected width but will be less than the physical pile spacing "*S*."

If the pile effective width is larger or equal to *S*, the soldier pile wall shall be designed as a "sheet pile" wall type. The sheet pile–type walls can be simplified as a two-dimensional (2D) analysis model with unit width.

Similarly, if the pile effective width is smaller than the pile space *S*, the design analysis can be simplified to 2D unit width wall analysis by using arching factor below the excavation elevation on D segment

$$\beta = \left(B_{\text{eff}}/S\right) < 1.0 \tag{10.11}$$

The final pile section strength analysis shall use this 2D model analysis result times the pile space to obtain the real demand.

For design purposes, determining the soldier pile anchored length "*D*" is the most important goal. Following the length determination, the soldier pile section strength and the lagging strength need to be checked.

10.7.2 Conceptual Analysis Example

The pile embedded length "D" must be deep enough to prevent the lateral movement and overturning. Assume the potential tilting point is at a depth of "Z" from the pile tip elevation. The passive reaction force on back face of the soldier pile should be as follows:

- The back face passive pressure at tilting point = 0 and tilting point is at "Z" above the tip elevation.
- The back face passive soil pressure at pile tip elevation = $B_{\text{eff}}k_{\text{p}}\gamma(H+D)$.

Using unit wall width model ($b = 1.0$ft). Based on the Figure 10.6b

$$P_1 = k_{\text{a}}\gamma H \tag{10.12}$$

$$P_2 = \beta P_1 \left(\text{where } \beta = \text{arching factor}\right) \tag{10.13}$$

$$P_3 = P_1 + \beta k_{\text{a}}\gamma D = k_{\text{a}}\gamma H + \varphi k_{\text{a}}\gamma D = k_{\text{a}}\gamma\left(H + \beta D\right) \tag{10.14}$$

$$P_4 = \beta\left(k_{\text{p}} - k_{\text{a}}\right)\gamma D - P_2 = \beta\left(k_{\text{p}} - k_{\text{a}}\right)\gamma D - \beta P_1 = \beta\left[\left(k_{\text{p}} - k_{\text{a}}\right)\gamma D - k_{\text{a}}\gamma H\right] \tag{10.15}$$

$$P_5 = \beta\left(k_{\text{p}} - k_{\text{a}}\right)\gamma D + \beta k_{\text{p}}\gamma H \tag{10.16}$$

Using $\Sigma X = 0$ and $\Sigma M_{\text{o}} = 0$ (point o at pile tip position)

$$\sum X = 0 = \frac{P_1 H}{2} + \frac{\left(P_2 + P_3\right)D}{2} + \frac{\left(P_4 + P_5\right)Z}{2} + \frac{\left(P_3 + P_4\right)D}{2} \tag{10.17}$$

$$\sum M_o = 0 = \left(\frac{P_1 H}{2}\right)\left(\frac{H}{3} + D\right) + \left(\frac{P_2 D}{2}\right)\left(\frac{D}{2}\right) + \left[\frac{\left(P_3 - P_2\right)D}{2}\right]\left(\frac{D}{3}\right) + \left[\frac{\left(P_4 + P_5\right)Z}{2}\right]\left(\frac{Z}{3}\right) - \left[\frac{\left(P_3 + P_4\right)D}{2}\right]\left(\frac{D}{3}\right) \tag{10.18}$$

Substitute all known parameters in Equations 10.17 and 10.18, there shall be only two unknowns: *Z* and *D*. Generally speaking, two independent equations and two unknowns, the problem is resolvable. For this conceptual example, Z can be determined by equation $\Sigma X = 0$ alone.

The pile moment and shear diagram can be developed per above load/reaction diagram. Then, the pile section moment and shear strength should be checked. Finally, the strength of timber logging element shall be checked.

10.7.3 Wall Detail Discussion

1. For soldier pile embedded length, the AASHTO design manual suggested that the practical *D* value should be increased a little on top of the calculated value. Sometimes 20%–30% increasing is common practice. Usually, if *H* is pretty high, say >15 ft, most designer may install a lateral trust or tie back at few feet below the wall to help reduce pile depth *D*. Most likely, without any extra lateral support, the pile depth ratio *D*/*H* shall be >1.50 or even more.
2. Some design manuals suggest that the first 1.5 ft below the excavation level is not counted for passive pressure capacity because it may not be reliable depending on the surface condition. If it is a

soil surface, the very top layer is not dependable for the passive capacity. But if it is under a pretty strong pavement layer, as many highway project shows, the total section including the pavement layer shall offer very dependable passive capacity. The designer must use his/her engineering judgment for each specific project.

3. Based on the cantilever height "*H*" and pile spacing "*S*," the corresponding timber lagging size shall vary. Starting from 4 × 12 in and up to 8 × 12 in lagging are common sizes to be installed. As mentioned in the introduction section, some projects utilize precast concrete slab panels or steel plate panels as the lagging. In most projects, the lagging shall be installed by hand. As such, timber lagging is usually the most reasonable choice of material.
4. Drainage systems behind these walls are usually not necessary because there are enough gaps between lagging to provide adequate drainage. Some projects are adding a shotcrete layer onto the timber lagging to create a "permanent" wall face. In these applications, a proper drainage system should be installed behind the wall.
5. From the strength design point of view, the lagging elements should be designed as a horizontal simply supported beam. Owing to the soil arch effects, the actual lateral load is smaller than the idealized uniform distribution soil pressure. If the spacing of the soldier piles gets smaller and smaller, eventually the soil arch effect could directly transfer all loads to the piles. Therefore, by the soil mechanics theory, the lagging system is not needed any more. Some designers just neglect the soil arch effect to reach a conservative design for the preliminary design stage. But others prefer to use a load reduction factor = 0.60 for logging design as a common practice.
6. If the traffic barrier is installed on top of the wall, the truck impact (crash) load case needs to be considered. The crash slab under the barrier can be used so that the lateral impact load on the barrier will be resisted by the vertical wheel load acting on the crash slab.

For more detailed discussion, see Caltrans Trenching and Shoring Manual (Caltrans 2011).

10.8 Soil Nail Wall Example

As discussed in the beginning part of this chapter, the tie back wall is the proper structure type for cut sections. The tie back can be built by physically connecting the retaining wall stem to an anchoring object system or simply using soil nails.

10.8.1 Typical Details

A common soil nail can be constructed by installing a tension core element into the drilled hole and fill with the grout. The mechanical interlocking effects and the friction between hardening grout and surrounding soil body are the main source of the capacity to resist tension forces on the soil nail. Practically, most designers count the friction forces only in order to be conservative. The core can be high strength rods or regular rebar; steel strands or any kind of prestressed cables. The part of the soil nail assembly between the wall and the global failure plane that is not grouted is called the "unbonded" length.

Compared to many other types of retaining walls, the tie back wall could be constructed with relatively smaller lateral movements. Figure 10.7 shows the typical components and basic lateral soil pressure distribution on a tie back wall. Figure 10.8 shows the soil nail assembly details as well as the shotcrete face details.

10.8.2 Typical Strength Design Parameters

1. *Soil nail layout*: The vertical nail spacing of the typical wall should be between 4.0 and 6.0 ft to satisfy the clearance of the construction equipment. The common slope angle of drilled holes is roughly 15° for grouting convenience. To minimize the group effects, the horizontal spacing between soil nails should be greater than six times the diameter of the hole or minimum 4.0 ft.

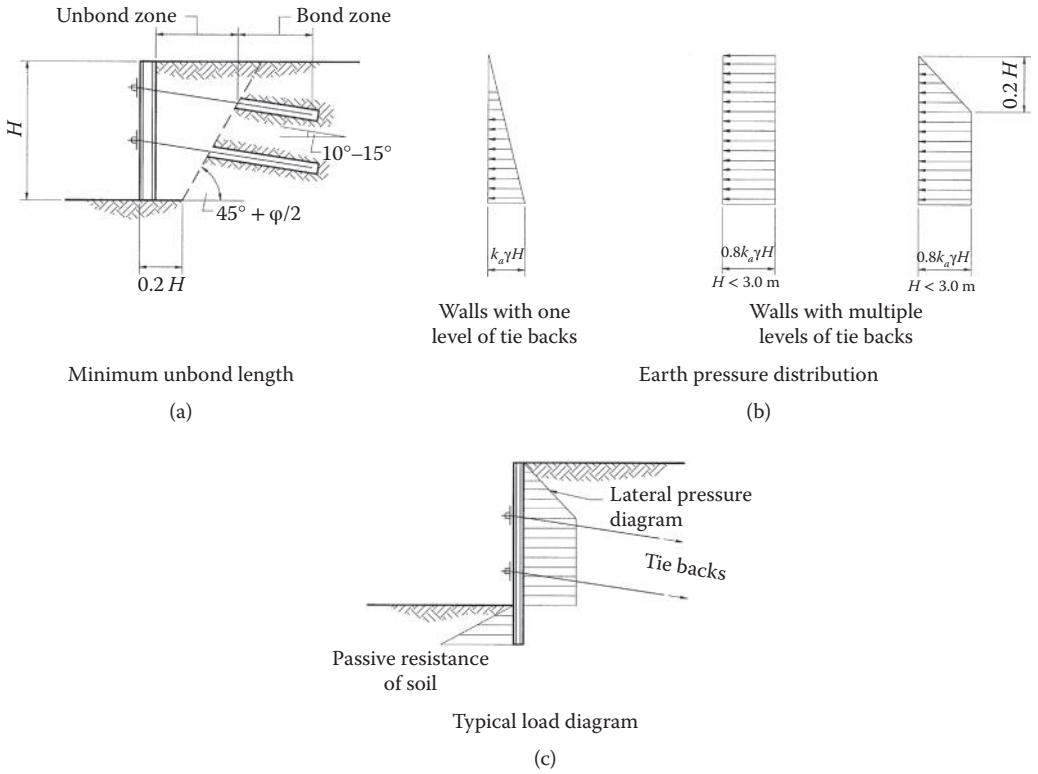

FIGURE 10.7 Tieback wall.

2. *Soil nail capacity*: The bond strength for a soil nail design depends on factors such as soil type, drilled holes diameter, installation technique, and so on. The necessary design parameters are usually provided in the soil report. For preliminary design, ultimate bond strengths of 10–15 psi may be assumed. Based on construction experience, most soil nail hole diameters are between 6 and 12 in., and the allowable pulling capacity is in the range of 35–60 kips/ea. However, the final design value must be approved by the geotechnical engineer.
3. *Shotcrete face strength*: The wall details consist of a temporary base layer of shotcrete and a final face layer. The wall face should be designed as a multiple span, two-way slab system. The slab flexure, shear, and punching shear strength should be checked. The temporary base layer could be 4–6 in. in thickness of shotcrete and reinforced by Weld Wire Fabric (WWF) wire mesh and additional rebar under the soil nail bearing plate. At this stage, the soil nail anchoring assembly is bearing on top of this temporary layer and exposed out of the temporary wall surface. The strength check on the temporary layer could be based on smaller factor of safety than the final face layer. The final face layer is usually an additional shotcrerte layer with similar reinforcement wire and bar system. This final layer will cover the previously exposed soil nail anchoring assembly and will build up a smooth wall face. The strength design calculation is similar to the temporary wall face layer with thicker slab and double layer reinforcements.

10.8.3 Shotcrete Face Design Example

For a soil nail wall design, the structural engineer shall start from the face wall strength design. The designer should coordinate with the geotechnical engineer to select the proper nail allowable pull out capacity. This will determine the specified diameter, length, and proposed core tension rod used for the soil nails.

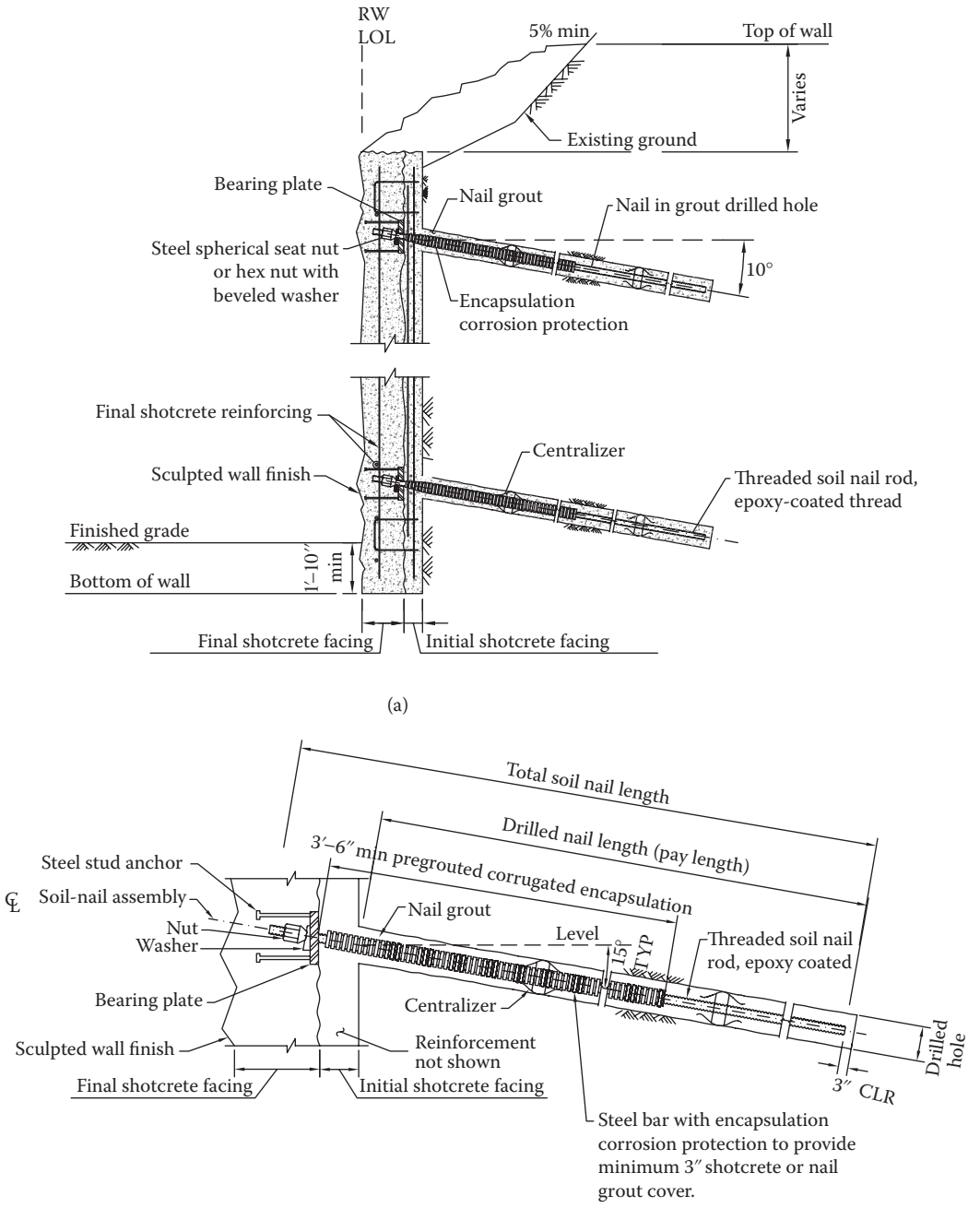

FIGURE 10.8 Typical soil nail wall details.

The temporary face slab system needs to be checked with flexure and punching shear strength. Then, the final face slab system needs to be checked in a similar manner but with different strength factors.

The most popular simplified analysis procedure shall assume the face slab as independent one-way slab system in each direction. Considering the un-uniform soil pressure distribution behind face slab, the adjustment factors C_F and C_S shall be used for the flexure and shear cases, respectively. Most design

manuals provide similar recommended values for these factors. For temporary wall face thickness = 4 in, $C_F = 2.0$; for $t = 6$ in; $C_F = 1.5$. When $t > 6$ in or for permanent wall face check, use $C_F = 1.0$,

Given:

Temporary face wall shotcrete strength, $f_c' = 4000$ psi
Temporary face slab thickness, $t = 4.0$ in
Vertical soil nail spacing, $S_v = 6.0$ ft = 72 in
Horizontal soil nail spacing, $S_h = 6.0$ ft = 72 in
Area of horizontal bar (2-#4 bars behind nails), $A_{sh} = 2(0.2) = 0.4$ in^2
Area of vertical bar, $A_{sv} = 0$ (no vertical bar)
Bar yield stress, $f_y = 60$ ksi
WWF (W1.4 × W1.4 @ 4″ × 4″ mesh), $A_{sWWF} = 0.12$ in^2/ft (each way)
Wire yield stress, $F_{yWWF} = 65$ ksi
$d = 3$ in (effective thickness of the slab)
$C_F = 2.0$ (Soil pressure factor for flexure) (see above discussion)
$C_S = 2.25$ (soil pressure factor for shear)
$FS_F = 0.67$ (factor of safety for flexure)
$FS_S = 0.67$ (factor of safety for shear)
$b_{PL} = 8$ in (bearing plate dimension 8″ × 8″)

Solution:

1. Nominal moment capacity calculation
   Vertical direction positive moment:

$$M_{VPOS} = \left(\frac{A_{sWWF} f_{yWWF} S_h + A_{sv} f_y}{S_h}\right)\left[(t-d) - \frac{A_{sWWF} f_{yWWF} S_h + A_{sv} f_y}{1.7 f_c' S_h}\right]$$

$$= \left[\frac{(0.12)(65)(6)+(0)(60)}{(6)(12)}\right]\left[(4-3) - \frac{(0.12)(65)(6)+(0)(60)}{1.7(4)(6)(12)}\right] = 0.588 \text{ kip-in/in}$$

   Vertical direction negative moment

$$M_{VNEG} = \left(\frac{A_{sWWF} f_{yWWF} S_h + A_{sv} f_y}{S_h}\right)\left[(d) - \frac{A_{sWWF} f_{yWWF} S_h + A_{sv} f_y}{1.7 f_c' S_h}\right]$$

$$= \left[\frac{(0.12)(65)(6)+(0)(60)}{(6)(12)}\right]\left[(3) - \frac{(0.12)(65)(6)+(0)(60)}{1.7(4)(6)(12)}\right] = 1.888 \text{ kip-in/in}$$

   Horizontal direction positive moment

$$M_{HPOS} = \left(\frac{A_{sWWF} f_{yWWF} S_y + A_{sh} f_y}{S_y}\right)\left[(t-d) - \frac{A_{sWWF} f_{yWWF} S_y + A_{sh} f_y}{1.7 f_c' S_y}\right]$$

$$= \left[\frac{(0.12)(65)(6)+(0.4)(60)}{(6)(12)}\right]\left[(4-3) - \frac{(0.12)(65)(6)+(0.4)(60)}{1.7(4)(6)(12)}\right] = 0.841 \text{ kip-in/in}$$

   Horizontal direction negative moment

$$M_{HNEG} = \left(\frac{A_{sWWF} f_{yWWF} S_y + A_{sh} f_y}{S_y}\right)\left[(d) - \frac{A_{sWWF} f_{yWWF} S_y + A_{sh} f_y}{1.7 f_c' S_y}\right]$$

$$= \left[\frac{(0.12)(65)(6)+(0.4)(60)}{(6)(12)}\right]\left[(3) - \frac{(0.12)(65)(6)+(0.4)(60)}{1.7(4)(6)(12)}\right] = 2.807 \text{ kip-in/in}$$

2. Nail force convert from moment capacity
   Nail force per moment capacity on vertical direction

$$T_V = \frac{C_F\left(M_{VPOS} + M_{VNEG}\right)(8)S_h}{S_y} = \frac{(2.0)(0.588+1.888)(8)(6)(12)}{(6)(12)} = 39.616 \text{ kips}$$

   Multiple by strength safety factor ($FS_F = 0.67$)

$$T_{FV} = FS_F T_V = (0.67)(39.61) = 26.543 \text{ kips}$$

   Nail force per moment capacity on horizontal direction

$$T_H = \frac{C_F\left(M_{HPOS} + M_{HNEG}\right)(8)S_h}{S_y} = \frac{(2.0)(0.841+2.807)(8)(6)(12)}{(6)(12)} = 58.368 \text{ kips}$$

   Multiple by strength safety factor ($FS_F = 0.67$)

$$T_{FH} = FS_F T_H = (0.67)(58.368) = 39.107 \text{ kips}$$

3. Nail force converted from punching shear capacity

   Temporary face slab thickness: $t = 4$ in
   Bearing plate dimension: $8'' \times 8''$ square

   Punching shear effect area

$$A_o = S_o t\left[(4)(8+4)\right](4) = 192 \text{ in}^2$$

   Nominal punching shear capacity (ACI)

$$V_n = (4.0)A_o\sqrt{f_c'} = (4.0)(192)\sqrt{4000} = 48{,}572 \text{ lbs} = 48.572 \text{ kips}$$

   Nail force

$$T_s = FS_{SX} C_S V_n = (0.67)(2.25)(48.572) = 73.222 \text{ kips}$$

Comparing all the above three values, the $T_{FV} = 26.543$ kips is the minimum value. Then, use this value (convert to the soil nail sloped direction) as the stability analysis upper limit corresponding to the temporary wall details as well as the construction loads.

A similar procedure can be used for the "permanent face slab analysis." It is a common practice to fix the soil nail tension force during the first stage of construction. The designer should verify all the related design details in order to determine how to adjust the design parameters in order to satisfy the final slab details. For example, after the final layer of the shotcrete is installed on the wall face and the slab thickness has been changed, the additional layer of the WWF mesh into the second shotcrete layer must be evaluated. The welded studs on the bearing plate will generate additional punching capacity. As such, C_F and C_S (as well as other factor values) may need to be revised. Because of the complicated step by step procedure, first-time designers should reference the design manual and follow the instructions step by step.

After the above strength check on the temporary and permanent wall face is performed, the effective tension limit of the soil nail at each stage can be finalized. For stability analysis, these effective tension values shall be used as the upper bound of the soil nail force that is considered in the stability analysis.

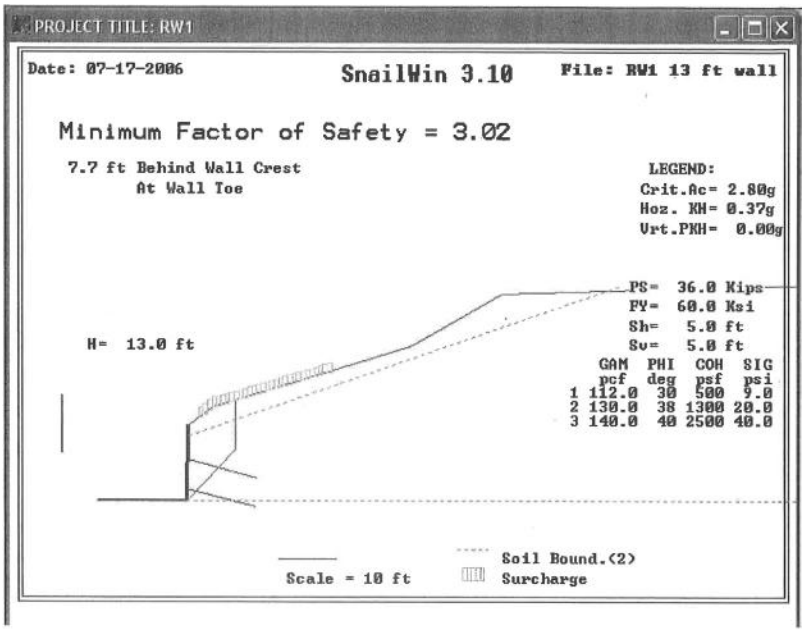

FIGURE 10.9 Soil nail wall, computer analysis output example.

10.8.4 Global Stability Analysis

The soil nail wall stability analysis should be a multiple-stage calculation. For each stage of construction, the analysis of the wall model is slightly different. In most wall applications, all the soil nails are installed simultaneously with the temporary face slab. Afterwards, the second layer of shotcrete will be placed to cover all the nail heads and to build up the final wall surface. Ideally, the analysis procedure should be performed at each stage of construction to verify that the wall strength and stability satisfies the code requirements.

The traditional procedure to check the required soil nail tension values starts from the top layer of soil nails using an acceptable soil pressure distribution diagram along with the construction loading. If the tension in the first layer of soil nails is within acceptable values, the analysis should then proceed to check the next layer of soil nails. If the tension in the first layer of soil nails exceeds the acceptable limit, the face slab design details should be revised or the soil nail location may need to be adjusted.

There are many soil nail wall design programs available. Figure 10.9 shows a typical computer output data (portion) and clearly shows the stability analysis results at each step. The designer should check the output data carefully to catch any conflict between the analysis result and the wall details every step.

10.8.5 Additional Discussion

1. The typical shotcrete face slab system should include adequate drainage behind the face slab in order to alleviate the hydrostatic pressure.
2. The very top layer of soil nails needs to have a few feet of clearance (edge distance) from top of the wall. The top parapet wall slab above the first soil nail should be checked using the typical cantilever slab model. If a traffic barrier is installed on top of the wall, the truck impact (crash) loading case needs to be considered. For soil nail walls, totally depending on the first layer of soil nails to resist the traffic crash loading is not practical. The designer can consider installing the crash slab underneath the traffic barrier so that the lateral crash loading can be resisted by the vertical wheel load on the crash slab.

3. The vertical spacing between soil nails may be determined by the unsupported soil excavation depth recommended in the geotechnical report. Without a final soil report, designers should consider using 4–5 ft as the unsupported vertical excavation depth for the most typical cases.
4. In order to ensure a sufficient connection between the temporary layer of shotcrete and the final shotcrete layer, anchored dowels should be provided. These dowels should uniformly extrude out of the first temporary layer of shotcrete over the entire surface area of the wall.
5. The end anchor assembly for the soil nails should be covered by the finished layer of shotcrete. It is a common practice to install steel studs on the end bearing plate for typical application. These studs can help ensure a sufficient connection between the temporary layer of shotcrete and the final shotcrete layer, while also increasing the punching shear capacity.
6. Corrosion protection is also very important for soil nail applications. Soil nail installation is subjected to "special inspection" and a series tension pull out tests will be performed to verify that the soil nails can develop adequate tension strength. When a nail cannot reach the design strength, an additional soil nail (or sometimes two nails) will be installed to compensate.

10.9 MSE Wall Example

MSE walls are generally used in topographic fill locations only. The wall height for MSE-type systems is not definitively limited, but significant heights will contribute to a certain amount of lateral movement. Conceptually, MSE walls use multiple layers of steel wires, geogrid, or other fibers to reinforce the fill material in the lateral direction. Essentially the reinforcement will bind the fill material together and act as a gravity retaining structure. Figure 10.10 shows typical details of a MSE retaining structure.

Typically, the lateral reinforcement covers the entire length of the backfill. Therefore, the base width (W) of the MSE wall is generally equal to the length of the reinforcing steel wire, geogrid, or fiber. For preliminary design assumptions, the wall aspect ratio W/H value should be 0.7–0.8 and the $W \geq 8.0$ ft. It is preferable to utilize metals or nondegradable fabrics as the reinforcing materials. When selecting the reinforcing material, the effective lift height of this material must be considered.

As a practical method of design analysis, the sliding, overturning, and foundation bearing capacity can be checked with the same procedures used for gravity wall applications. Additionally, when performing design analysis, the friction between the backfill material and the lateral reinforcement mat should be checked for each layer of backfill. Furthermore, the connection strength between the lateral reinforcement and the face panel needs to be checked to ensure adequacy in design. Finally, the face panels should be designed to act as a slab that is anchored by the steel wires or geogrids and subjected to lateral soil pressure.

10.9.1 Calculation Example

The whole soil body is reinforced by multiple layers of geogrids and acts as a single mass relying on its own self weight for sliding and overturning stability. Because of the similar relative stiffness between the resisting soil and the base soil, the overturning and bearing strength check calculation slightly differs from a concrete gravity wall stability calculation.

Figure 10.11 shows the given conditions for a typical MSE wall design.

Wall height, $H = 22$ ft
Base width, $W = 18$ ft
Allowable bearing capacity, $\sigma = 4.0$ ksf
Active soil pressure factor, $k_a = 0.30$
Passive soil pressure factor, $k_p = 3.00$
Soil density, $\gamma = 0.12$ kcf
Allowable friction factor, $f = 0.30$

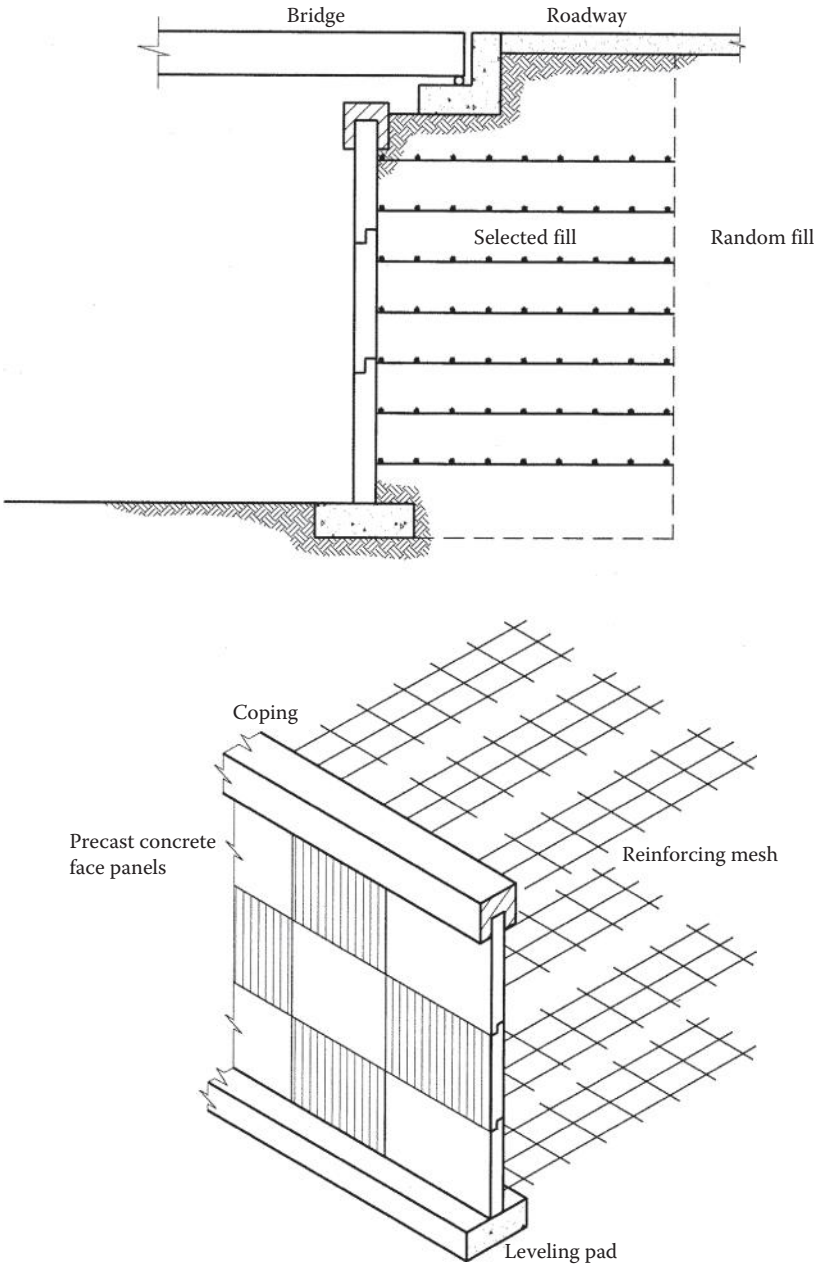

FIGURE 10.10 Mechanical stabilized earth (MSE) wall.

Load calculation

Using a 2D analysis model with a one-unit-length (1.0 ft) segment

Vertical earth weight, EV = γHB = (0.12)(22)(18) = 47.52 kips
Vertical LL surcharge, LS = ωB = (0.24)(18) = 4.32 kips
Total vertical force, N_V = 51.84 kips
Lateral earth pressure, EH = $0.5k_a\gamma H^2$ = (0.5)(0.12)(0.3)$(22)^2$ = 8.712 kips
Lateral surcharge effect, LH = $k_a\omega H$ = (0.3)(0.24)(22) = 1.584 kips

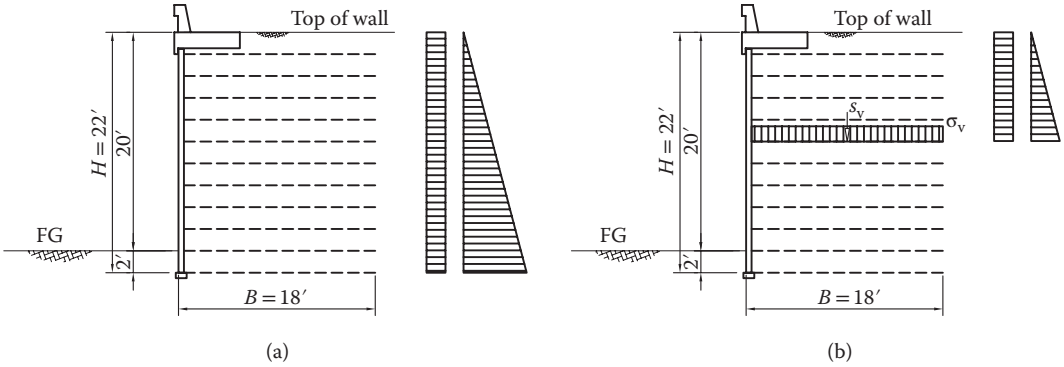

FIGURE 10.11 Mechanical stabilized earth (MSE) wall design example.

Total lateral force, $P_H = 10.296$ kips

Wall Sliding Check

Lateral Allowable Friction: $F = (0.3)(51.84) = 15.552$ kips
Lateral Passive Pressure: $0.5k_p\gamma h^2 = (0.5)(3.0)(0.12)(2)^2 = 0.72$ kips
Total Lateral Resistant Force $P_R = 16.272$ kips
FS = 16.272/10.296 = 1.58 > 1.50 OK

It is common for designers to neglect the passive resisting force because of the typical shallow embedment. As shown in the example, the passive force contributes a small part of the total resisting force.

Wall overturning check

For an MSE wall design, the design manuals require that the total vertical resultant reaction force stay within the limit of $W/2$. In other words, the $e_0 = M/N \leq W/4$.

Total vertical forces generate moment about toe.

Resisting moment from earth weight: 47.52(18/2) = 427.68 k-ft
Resisting moment from surcharge: 4.32(18/2) = 38.88 k-ft
Total resisting moment, $M_V = 466.56$ k-ft
Overturning moment from earth pressure: 8.712(22/3) = 63.888 k-ft
Overturning moment from surcharge: 1.584(22/2) = 17.424 k-ft
Total overturning moment, $M_h = 81.312$ k-ft

Eccentricity to toe, $X_o = (M_V - M_0)/N_V = (466.56 - 81.312)/51.84 = 7.431$ ft
Eccentricity to center of the base,
$e_o = 18/2 - 7.431 = 1.57$ ft $< W/4 = 18/4 = 4.5$ ft OK

Wall base bearing check

For MSE walls, it is a common practice to assume that the "effective width," $L = 2X_0$. A similar effective length concept will be assumed later for determining the internal tension stress of an individual reinforcing layer.

Wall foundation bearing capacity check

Total vertical load, $N_V = 51.84$ kips
$X_0 = 7.143$ ft
$\sigma_{equv} = N_V/(2X_0) = 51.84/(2)(7.143) = 3.63$ ksf $< [\sigma] = 4.0$ ksf OK

TABLE 10.5 Grids Tension Force

Layer	Z	P_V	M_V	M_H	X_0	σ_V	$\sigma_H = k_a\sigma_V$	$Pi = \sigma_H hi$
	(ft)	(kips)	(k-ft)	(k-ft)	(ft)	(ksf)	(ksf)	(kips)
1	1.00	6.48	58.32	0.042	8.994	0.36	0.11	0.22
2	3.00	10.80	97.20	0.405	8.963	0.60	0.18	0.36
3	5.00	15.12	136.08	1.275	8.916	0.85	0.25	0.51
4	7.00	19.44	174.96	2.793	8.856	1.10	0.33	0.66
5	9.00	23.76	213.84	5.103	8.785	1.35	0.41	0.81
6	11.00	28.08	252.72	8.349	8.703	1.61	0.48	0.97
7	13.00	32.40	291.60	12.675	8.609	1.88	0.56	1.13
8	15.00	36.72	330.48	18.225	8.504	2.16	0.65	1.30
9	17.00	41.04	369.36	25.143	8.387	2.45	0.73	1.47
10	19.00	45.36	408.24	33.573	8.260	2.75	0.82	1.65
11	21.00	49.68	447.12	43.659	8.121	3.06	0.92	1.84

From the above example, the MSE wall global stability analysis is similar to the concrete gravity wall. When considering MSE walls as a reinforced soil body, the overturning and bearing stress calculations are always based on the $e_0 \leq B/4$ and "equivalent width" concept regardless of the foundation material.

The next step is to determine the tension force in each reinforcement layer. Under the vertical pressure, the soil body will try to expand in the lateral direction. The embedded geogrids in the soil layers will be engaged and prevent the soil body from lateral expansion. The friction and interlocking mechanism between the fill material and reinforcement creates tension in the geogrids.

MSE walls are constructed in layers. Each layer has its own vertical compression stress σ_{Vi}. The lateral stress restricted by the geo-grids will be $\sigma_{Hi} = k_a\sigma_{Vi}$. where k_a is the active pressure coefficient. The total tension force in the geogrid wires is $P_i = \sigma_{Hi}\, h_i = k_a\sigma_{Vi}h_i$. For MSE wall design calculations, it is common to use the "equivalent" soil stress $P_i = N_i/2X_0$ to determine σ_{Vi}. Table 10.5 shows the geogrid tension values for this example.

These results are from a model with a unit length along the MSE wall layout line. The total design force values on each geogrid mat are equal to the above P_i values multiplied by the tributary width of the geogrid (lateral wire mat spacing along wall layout direction).

In the above table, the tension value increases from the top of the wall to the bottom layer. Typically, MSE walls need more reinforcement at the lower portions of the wall. In the lateral direction, along the base width (W), the geogrid mat's maximum tension force is located at the backside of face panel.

The designer should arrange an adequate grid layout based on the reinforcing forces required. Subsequently, the connection detail of the steel wire or geogrid to the back of the face panel needs to be specified. This could be the most important connection detail to be checked. If the connection fails, the face panel could "pop" out and the whole structure could be damaged. Finally, the face panel itself needs to be designed. Most face panels are precast concrete slabs with embedded hooks on their back face to tie into the soil reinforcement wire mats or geogrids. Many companies specializing in MSE wall applications can offer the full-service design, manufacturing, and installation of MSE walls.

10.9.2 Design Discussion

It is common for contractors that specialize in MSE walls to have their own soil reinforcing system and wall face panels. Contractors that specialize in MSE walls typically provide design services including the design analysis software. Some contractors are "pre-approved" by different government agencies. As a result, a structural designer rarely performs the detailed calculations for a MSE wall system. However, the wall design engineer needs to review the contractor's submittal package and evaluate the design calculations carefully because some systems have had incidents of failure in recent years.

1. Leveling pads usually have section dimensions of roughly 6 × 12 in. The leveling pad shall have a minimum embedment depth of 1.5 ft measured from top of the pad. Reinforcement within the precast leveling pad is likely not required.
2. If high-density engineering plastic wire mat is specified as the reinforcement, the designer should pay attention to the relatively lower young's modulus of the plastic mat material. The low *E* value could cause a large lateral movement in the wall face panels.
3. If steel wire is used, the wall design should provide access to assess the level of corrosion and any required future maintenance.
4. When a traffic barrier is installed on the top of the MSE wall, the truck impact (crash) loading on the top of the barrier needs to be considered. For an MSE wall, the designer can install a crash slab underneath the barrier such that the vertical wheel load on the crash slab resists the lateral crash loading. If the crash slab needs to be anchored down to resist overturning effects, tension piles can be installed within the reinforced soil body.
5. Similar to the other type of gravity walls, a sufficient drainage system is necessary for MSE walls. Usually, the wall drainage system is installed at the edge of the BW down to the full depth of the reinforced soil body. In addition, the reinforced soil body needs to have its own drainage.
6. MSE walls are advantageous in topographic conditions that require total fill. Employing a cantilever wall system under the same conditions requires backfilling compacted soil behind the wall to satisfy the original roadway design requirements such as for building up a highway segment. During the fill and compaction procedure, installing geogrid layers generate only minor additional work. Furthermore, although additional work is required during fill and compaction, the construction team does not have to build the cantilever wall stem and its footing.
7. In transportation projects, MSE walls often reach design heights of 30–40 ft above the original ground. The reinforced soil body will add a significant additional dead load to the original ground surface and could cause overstressing in either the natural ground or any soft layers further below. As a result of overstressing, unacceptable long-term settlement can occur. It is also possible for the additional soil pressure to influence adjacent existing structures if the wall is located too close. Two common approaches can be utilized to mitigate the added soil pressure. One method is to employ a soil treatment technique to strengthen the foundation material such as with "cement-deep-soil-mix" (CDSM). Another method is to use "lightweight" backfill material. When using lightweight backfill, the structural designer should verify if the selected mixing material can effectively bond and interlock with the selected geogrid wire mesh system. The foundation treatment should be designed by a geotechnical engineer.

10.10 Seismic Considerations

Seismic effects on the retaining structures are not as critical when compared to other structures. The early versions of AASHTO design manuals allowed the designer to neglect the seismic effects on the retaining walls. However, nowadays retaining walls in seismic areas need to consider these forces during design. The most commonly adopted method of seismic design for retaining structures is the Mononobe–Okabe method.

10.10.1 Soil Body Seismic Acceleration Response Spectrum (ARS) Factors

The factors k_v and k_h represent the maximum possible soil body acceleration values under seismic effects in the vertical and horizontal directions, respectively. Similar to other seismic loading, the acceleration due to gravity will be used as the basic unit of these factors.

Unless a site-specific report is available, the maximum horizontal ARS value multiplied by 0.5 could be used as the k_h estimated design value. Similarly, k_v could be equal to 0.5 times the maximum vertical ARS value. If the vertical ARS curve is not available, its common practice is to assign $k_v = 0.1k_h$ to $0.3k_h$.

Mathematically, the Mononobe–Okabe formula cannot be used when $k_v > k_h$.

10.10.2 Earth Pressure with Seismic Effects

Figure 10.12 shows the basic loading diagram for earth pressure with seismic effects. Similar to a static load calculation, the active force per unit length of wall (P_{ae}) can be determined as

$$P_{ae} = \frac{k_{ae}\gamma(1-k_v)H^2}{2} \tag{10.19}$$

where

$$\theta' = \tan^{-1}\left(\frac{k_h}{1-k_v}\right) \tag{10.20}$$

$$k_{ae} = \frac{\sin^2(\varphi+\beta-\theta')}{\cos\theta'\sin^2\beta\sin(\beta-\theta'-\delta)\left[1+\sqrt{\dfrac{\sin(\varphi+\delta)\sin(\varphi-\theta'-\alpha)}{\sin(\beta-\theta'-\delta)\sin(\alpha+\beta)}}\right]^2} \tag{10.21}$$

Note that with no seismic load, $k_v = k_h = \theta' = 0$, therefore, $k_{ac} = k_a$.

The resultant total lateral force calculated above does not act at a distance of $H/3$ from the bottom of the wall. The following simplified procedure is often used in design practice:

- Calculate P_{ae} (total active lateral earth pressure per unit length of wall)
- Calculate $P_a = 1/2k_a\gamma H^2$ (static active lateral earth pressure per unit length of wall)
- Calculate $\Delta P = P_{ae} - P_a$
- Assume P_a acts at a distance of $H/3$ from the bottom of the wall
- Assume ΔP acts at a distance of $0.6H$ from the bottom of the wall

The total earth pressure, which includes seismic effects P_{ae}, should always be bigger than the static force P_a. If the calculation results indicate $\Delta P < 0$; use $k_v = 0$.

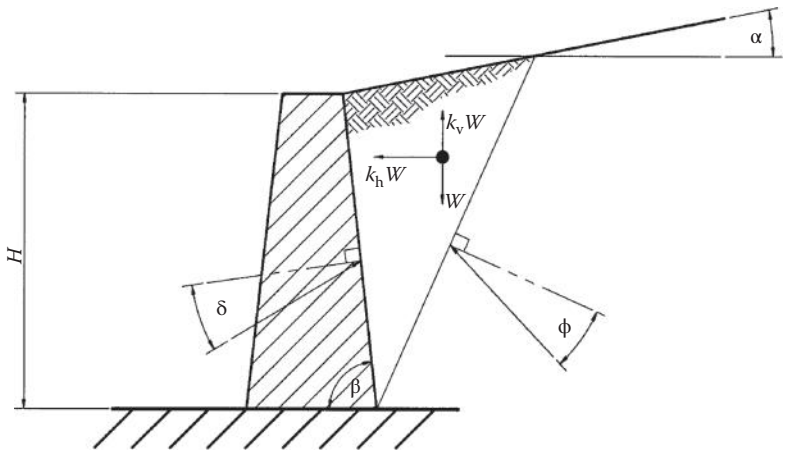

FIGURE 10.12 Load diagram for earth pressure with seismic effects.

Using a procedure similar to the active earth pressure calculation, the passive earth pressure with seismic effects can be determined as follows:

$$P_{pe} = \frac{k_{pe}\gamma(1-k_v)H^2}{2} \tag{10.22}$$

$$\theta' = \tan^{-1}\left(\frac{k_h}{1-k_v}\right) \tag{10.23}$$

$$k_{pe} = \frac{\sin^2(\beta+\theta'-\varphi)}{\cos\theta'\sin^2\beta\sin(\beta+\theta'+\delta-90)\left[1+\sqrt{\dfrac{\sin(\varphi+\delta)\sin(\varphi-\theta'+\alpha)}{\sin(\beta+\theta'+\delta)\sin(\alpha+\beta)}}\right]^2} \tag{10.24}$$

Note that, with no seismic load, $k_{pe} = k_p$.

10.11 Other Retaining Wall Systems

10.11.1 Other Gravity Wall

As mentioned in the introduction, a permanent gravity wall system could be constructed of stone masonry, unreinforced concrete or reinforced concrete. Some projects utilize rigid boxes filled with soil

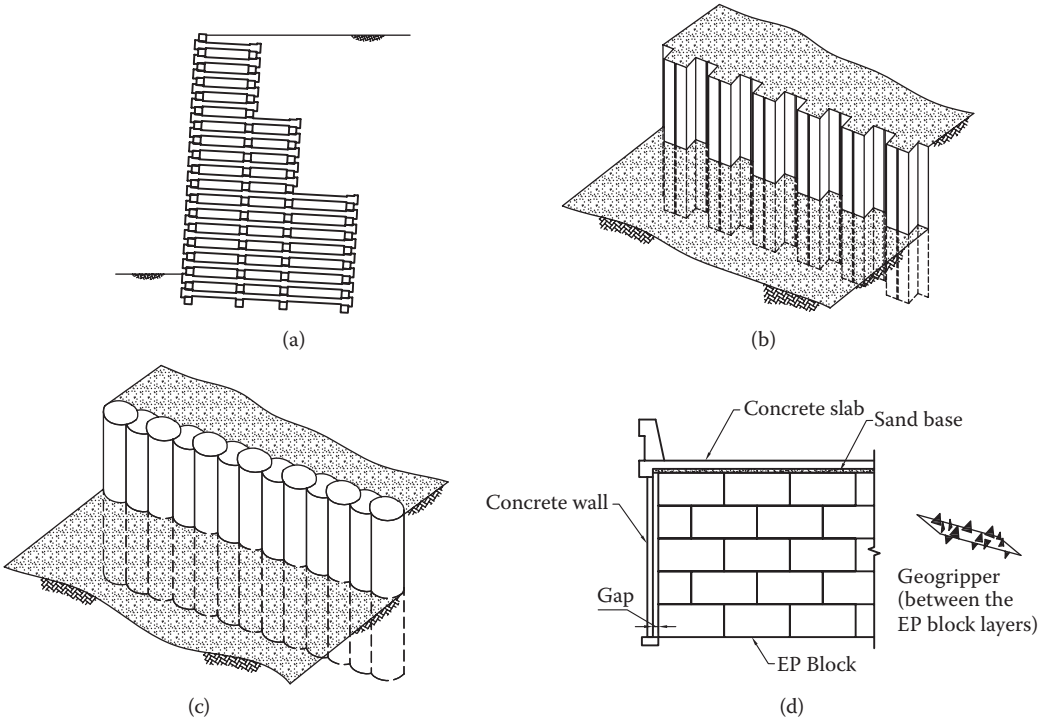

FIGURE 10.13 Other types of retaining wall systems. (a) Crib wall typical section, (b) Sheet pile wall, (c) Secant pile wall, (d) ESP fill.

and aggregate to create a gravity mass to retain lateral soil pressure. Figure 10.13a shows an example that uses rigid boxes and is referred to as a "precast-crib wall."

10.11.2 Sheet Pile Wall

Sheet pile systems belong to the "cantilever" retaining wall category. See Figure 10.13b for an example. The design analysis procedure is similar to a "soldier pile" system. In fact, the steps to perform a stability calculation are exactly the same as a "soldier pile" system except that the "effective factor" is always equal to 1.0.

Sheet pile elements are bended steel plates with U- or Z-shaped sections and contain a side groove to connect next sheet pile elements. Some heavy-duty elements have "I"-shaped sections. The sheet pile elements can be driven along the wall layout line directly. Piles are premanufactured to be installed side by side and automatically connected to one another. Therefore, sheet pile retaining systems can be installed much quicker than other systems. Most sheet pile elements have connections that are "water tight." As a result, sheet pile systems are commonly used in hydraulic projects. Steel is the most common sheet pile material. Presently, there are vinyl sheet pile products available in the market. For transportation projects, sheet pile systems are often used as a temporary shoring structure. When sheet piles are used as a permanent system, a wall cap on top shall be specified. Some manufacturers have their own prefabricated cap system. It is a common practice to build a concrete cap. If the wall was used as part of a support structure, the sheet pile wall can directly be embedded into the above structure's concrete base.

10.11.3 Secant Wall System

A secant wall system is a heavy-duty retaining system. As shown in Figure 10.13c, secant walls use a series of overlapping drilled piles side by side to resist the lateral soil pressure. Typically, the pile diameter shall be 2–3 ft and 4 ft maximum. The drilled holes are filled by concrete. For convenience in construction, the piles are staggered between being reinforced and unreinforced. The reinforced piles could have rebar cages or steel sections. Because a secant wall system is a heavy-duty system, the reinforcement in the piles could be huge. For example, using double steel HP sections plus rebar caging as the reinforcement could be used. This system has been used for projects to protect against sliding of a soil body and in addition, is often employed for hydraulic-related projects. Identical to a soldier pile system, a secant pile system depends on the embedded length below the excavated depth to resist the soil lateral pressure imposed on the above cantilever portion of the pile. Design calculations are similar to the soldier pile system with "effective factor" equal to 1.0, which is same as the sheet pile system. In other words, a secant wall system can be characterized as a super strong soldier pile system without interpile space. Obviously, there shall be no logging system needed.

Similar to a secant wall, some projects use driven piles with concrete or steel sections and installed side by side to build retaining systems along the wall layout lines. Often this system is used in projects that contain deep excavations or in projects located close to existing structures. One example that uses secant walls is for cut and cover construction of subway systems that go through city districts densely populated with existing buildings; where the excavation is only a few feet away from adjacent structures. Many contractors elect to use driven HP steel piles side by side to protect an existing structure.

10.11.4 EPS Geofoam Fill System

Similar but different from MSE walls is to use expanded polystyrene blocks as a lightweight fill system. Figure 10.13d shows a typical section of an EPS system. Although MSE wall systems use multiple layers of lateral reinforcement to restrict horizontal movement in the soil body, an EPS fill system uses interlocking connectors to hold lightweight blocks together to create a masonry-type structure. The EPS

fill system uses expanded polystyrene blocks to "build up" the fill body. The density of EPS material is only around 1.0–2.0 pcf and the compression capacity can reach 5–10 psi with 1% deformation. EPS fill systems have been used for decades. Currently, the system is still quite expensive but is the "lightest" available system to be used for large volume fill applications in transportation projects.

An advantage for using light material is that the material can be easily handled in the field. The block can be cut by hand tools (just like a carpenter) to fit any desired shape and space. Hence, this system can be installed very fast. The common size of the block is 3 × 4 × 8 ft; however, the contractor can order any special dimension. The blocks stay together by mechanical interlock elements and the friction effects. The friction coefficient is approximately equal to 0.5 between blocks. The mechanical interlocking parts, called geogrippers or spike grids, are placed between EPS blocks layers. Alternatively, adhesive epoxy could be used to prevent relative lateral movement. The block units are staggered similar to masonry structures. In order to resist the direct traffic load, a "distribution" cover slab must be installed on top of the EPS body. Usually, this cast-in-place concrete cover slab shall be thicker than 4 in for pedestrian loads and include a 2-in sand base layer. For major highway traffic loads, a 12-in slab is commonly used. Similar to any other fill material, a waterproof system is one of the basic requirements, otherwise the EPS block will absorb the water and the young's modules will be reduced. As a result of water intrusion, there is a potential for a larger settlement than the designers intent. The most important principle when applying an EPS system is to keep the EPS blocks away from other petroleum-related products at all times. Other petroleum products will "eat away" the EPS blocks and the total EPS system could fail. As a result, there is often a complete water/oil resistant cover for the entire finished block body. For the water resistant purpose, the distribution slab can be made of fiber reinforced concrete.

10.11.5 Combined Tie Back with Other Systems

A tie back system can be combined with any of the above cantilever systems to create a more efficient retraining wall. Soil nails and rock anchors are the most commonly used tie back elements. Any other

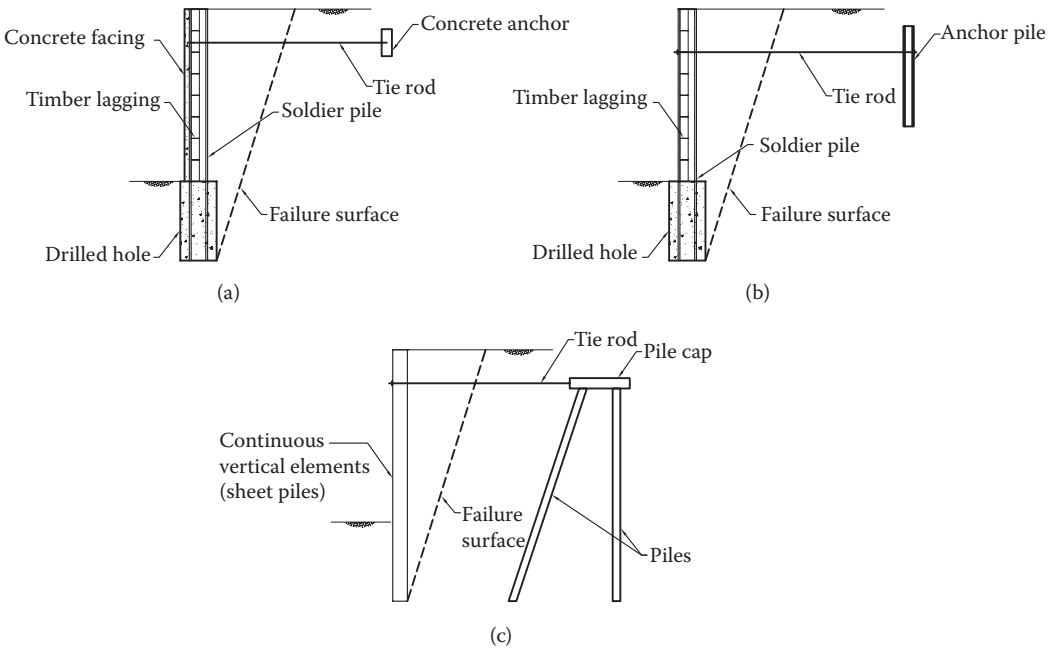

FIGURE 10.14 Combined retaining wall systems.

link element can be used to create a tie back system. The anchor must be installed far beyond the expected failure surface of the retaining wall. The tie back system could utilize high strength wires or rods as a link element. The separated anchor could be a large concrete block, another pile array or a pile cap with multiple rows of battered and vertical piles. When using battered piles, the lateral component of the pile axial capacity resists the horizontal load directly. Figure 10.14 shows several typical conceptual sketches for combined systems.

Because the extra tie back system has to be installed far beyond the expected failure surface of the retaining wall, one of the practical restrictions for combined systems is the limits of available construction area. Furthermore, the combined system requires clear markers on finish grade to indicate the link rod or cable locations as prevention of possible damage from future construction.

References

AASHTO. 1998. *MSE Wall Design by LRFD*, American Association of State Highway and Transportation Officials, Washington, DC.

AASHTO. 2002. *Standard Specifications for Highway Bridges*, 17th Edition, American Association of State Highway and Transportation Officials, Washington, DC.

AASHTO. 2012. *AASHTO LRFD Bridge Design Specifications*, Customary US Units, American Association of State Highway and Transportation Officials, Washington, DC.

AREMA. 2011. *Manual for Railway Engineering*, American Railway Engineering and Maintenance of Way Association, Lanham, MD.

Bowles, J. E. 1996. *Foundation Analysis and Design*, 5th Edition, McGraw-Hill, New York, NY.

Caltrans. 2011. *Trenching and Shoring Manual*, California Department of Transportation, Sacramento, CA.

Das, B. M. 2011. *Principles of Foundation Engineering*, 7th Edition, Cengage Learning, Stanford, CT.

FHWA. 1998. *Manual for Design and Construction Monitoring of Soil Nail Walls*, U.S. Department of Transportation & Federal Highway Administration, Washington, DC.

Huntington, W. C. 1957. *Earth Pressure and Retaining Walls*, John Wiley & Sons, New York, NY.

Lambe, T. W. and Whitman, R. V. 1979. *Soil Mechanics*, SI Version, John Wiley & Sons, New York, NY.

Tschebotarioff, G. P. 1973. *Foundations, Retaining and Earth Structures*, 4th Edition, McGraw-Hill, New York, NY.

11

Landslide Risk Assessment and Mitigation

Mihail E. Popescu
Illinois Institute of Technology

Aurelian C. Trandafir
Fugro GeoConsulting Inc.

11.1 Introduction

Landslides are frequently responsible for considerable losses of both money and lives. The severity of the landslide problem intensifies with increased urban development and change in land use. In view of this consideration, it is not surprising that landslides are rapidly becoming the focus of major scientific research, engineering study and practice, and land-use policy throughout the world. International cooperation among various individuals concerned with the fields of geology, geomorphology, and soil and rock mechanics has recently contributed to improvement of our understanding of landslides in recent years.

Landslides and related slope instability phenomena plague many parts of the world. Japan leads other nations in landslide severity with projected combined direct and indirect losses of $4 billion

annually (Schuster, 1996). The United States, Italy, and India follow Japan, with an estimated annual cost ranging between $1 billion and $2 billion. Landslide disasters are also common in developing countries, and monetary losses sometimes equal or exceed the gross national product of these countries.

The paramount importance of landslide hazard management for transportation facilities, including bridges, is by and large recognized. Repairs and maintenance after landslides on U.S. highways cost an estimated $106 million annually.

As an integral part of transportation systems, bridges are designed to move people, goods, and services efficiently, economically, and safely. Landslides can disrupt or damage these systems at a variety of spatial and temporal scales, dramatically reducing network serviceability, increase costs, and decrease safety. Recurrence intervals for landslide events span from daily to centuries, whereas the associated consequences range from inconvenient to catastrophic.

Landslides can significantly impact bridges. They can knock out bridge abutments or significantly weaken the soil supporting them, making bridge structure unusable or hazardous for use. In addition to the damage or reduced serviceability of the structure, in some instances, landslides can crush or bury vehicles and result in death. Some landslides occur unexpectedly, whereas others arrive with significant warning, but all are amenable to some level of prediction and mitigation.

Herein lies the guiding principle of the current chapter, that is, to describe landslide hazards and methods to mitigate the associated risks in an appropriate and effective manner.

This chapter provides the basic principles and information needed by the bridge engineer to plan and design safe and cost-effective structures in areas prone to or already affected by landslides.

11.2 Landslide Hazard Assessment and Landslide Risk Management

11.2.1 Landslide Hazard Assessment

Landslide hazard identification requires an understanding of the slope processes and the relationship of those processes to geomorphology, geology, hydrogeology, climate, and vegetation. From this understanding, it will be possible to

- Classify the types of potential landsliding. The classification system proposed by Varnes (1978) as modified by Cruden and Varnes (1996) constitutes a suitable system. It should be recognized that a site may be affected by more than one type of landslide hazard. For example, deep-seated landslides occur at the site, whereas rockfall and debris flows will initiate from above the site.
- Assess the physical extent of each potential landslide being considered, including the location, areal extent, and volume involved.
- Assess the likely causal factor(s), the physical characteristics of the materials involved, and the slide mechanics.
- Estimate the resulting anticipated travel distance and velocity of movement.
- Address the possibility of fast-acting processes, such as flows and falls, from which it is more difficult to escape.

Methods commonly used to identify hazards include geomorphological mapping, gathering of historic information on landslides in similar topography, geology, and climate (e.g., from maintenance records, aerial photographs, newspapers, review of analysis of stability). Some forms of geologic and geomorphic mapping are considered to be an integrated component of the fieldwork stage when assessing natural landslides, which requires understanding the site while inspecting it.

Before embarking on a regional landslide hazard assessment, the following preparatory steps are to be taken (Hutchinson, 2001):

1. Identify the user and purpose of the proposed assessment. Involve the user in all phases of the program.
2. Define the area to be mapped and decide the appropriate scale of mapping. This may range from 1:100,000 or smaller to 1:5,000 or larger.
3. Obtain, or prepare, a good topographic base map of the area, preferably contoured.
4. Construct a detailed database of the geology (solid and superficial), geomorphology, hydrogeology, pedology, meteorology, mining and other human interference, history, and all other relevant factors within the area, and of all known mass movements including all published work, newspaper articles, and the results of interviewing the local population.
5. Obtain all available air photo cover, satellite imagery, and ground photography of the area. Photography of various dates can be particularly valuable, both because of what can be revealed by differing lighting and vegetation conditions and to delineate changes in the man-made and natural conditions, including slide development.

11.2.2 Landslide Risk Management Process

The risk management process comprises two components: risk assessment and risk treatment. Landslide and slope engineering have always involved some form of risk management, although it was seldom formally recognized as such. This informal type of risk management was essentially the exercise of engineering judgment by experienced engineers and geologists.

Figure 11.1 shows the process of landslide risk management in a flowchart form (Australian Geomechanics Society—AGS, 2000). In simple form, the process involves answering the following questions:

1. What might happen?
2. How likely is it?
3. What damage or injury may result?
4. How important is it?
5. What can be done about it?

There is a clear distinction between hazard, risk, and probability. Hazard is usually defined as a condition with the potential for causing an undesirable consequence (Fell, 1994b). The description of landslide hazard should include the location, volume (or area), classification, and velocity of potential landslides and any resulting detached material, and the probability of their occurrence within a given period of time.

Risk is a measure of the probability and severity of an adverse effect to health, property, or the environment. Risk is often estimated by the product of probability and consequences. However, a more general interpretation of risk involves a comparison of the probability and consequences in a nonproduct form.

Probability is the likelihood of a specific outcome, measured by the ratio of specific outcomes to the total number of possible outcomes. Probability is expressed as a number between 0 and 1, with 0 indicating an impossible outcome and 1 indicating that an outcome is certain.

The intent of a landslide hazard assessment is to identify a region's susceptibility to landslides and their consequences based on several key or significant physical attributes comprising the previous landslide activities, bedrock features, slope geometry, and hydrologic characteristics. In a development program (planning process) concerning a landslide-prone area, one needs to determine the acceptable risk. It is indispensable to recognize the vulnerability and degrees of risk involved and to instigate a systematic approach in avoiding, controlling, or mitigating existing and future landslide hazards in the planning process. Accordingly, either a planner should avoid the landslide-susceptible areas if it is deemed appropriate or else he or she needs to implement strategies to reduce risk.

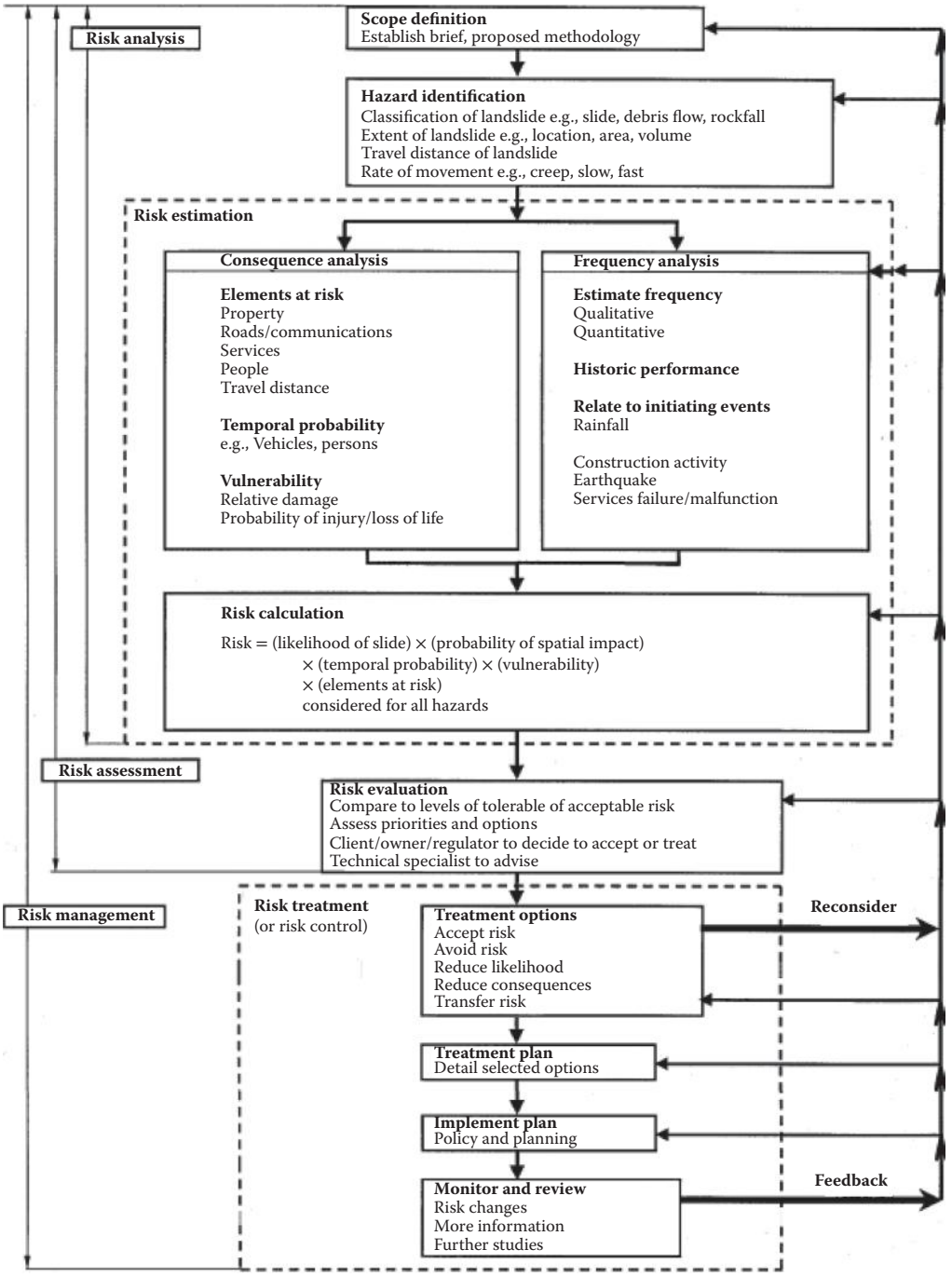

FIGURE 11.1 Process of landslide risk management. (From Australian Geomechanics Society (AGS), Sub-Committee on Landslide Risk Management, *Landslide Risk Management Concepts and Guidelines*, 49–92, 2000. With permission.)

11.2.3 Landslide Inventory Maps

International Union of Geological Sciences (IUGS) Working Group on Landslides (WG/L), formerly International Geotechnical Societies' UNESCO Working Party on World Landslide Inventory (WP/WLI), which was established in the framework of the United Nations International Decade for Natural Disaster Reduction (1990–2000), defined the landslide hazard as "the probability of occurrence within a specified period of time and within a given area of a potentially damaging phenomenon" (Cruden, 1997). Furthermore, IUGS described the landslide risk assessment as "the expected degree of loss due to a landslide (specific risk) and the expected number of lives lost, people injured, damage to property and disruption of economic activity (total risk)." As shown in Figure 11.2, the integrated assessment of landslide hazard and risk requires a broad-based knowledge from a wide spectrum of disciplines including geosciences, geomorphology, meteorology, hydrogeology, and geotechnical engineering (Chowdhury et al., 2001).

Landslide hazards are commonly delineated on inventory maps, which display distributions of hazard classes and identify areas that potential landslides may be generated. Inventory maps show the location and, where applicable, the date of occurrence and historical records of landslides in a region. These maps are prepared by different techniques, and, ideally, provide information concerning the spatial and temporal probability, type, magnitude, velocity, runout distance, and retrogression limit of the mass movements predicted in a designated area. Details of inventory maps depend on available

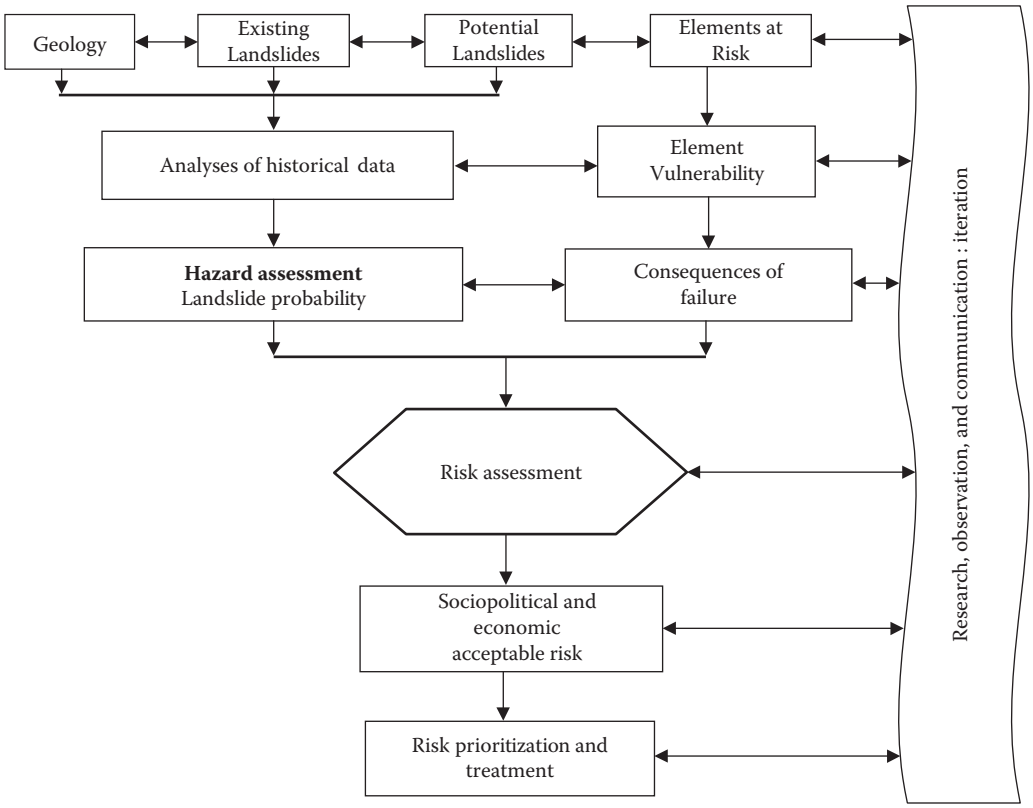

FIGURE 11.2 Methodology for landslide risk assessment. (From Chowdhury, R. et al., A Focus on Hilly Areas Subject to the Occurrence and Effects of Landslides, *Global Blueprint for Change*, 1st Edition—Prepared in conjunction with the International Workshop on Disaster Reduction, August 19–22, 2001. With permission.)

resources and are based on the scope, extent of study area, scales of base maps, aerial photographs, and future land use.

Evidently, the extent of information required concerning the landslide hazard analysis will depend on the level and nature of proposed development for a region. The negligence of incorporating the impact of potential landslide activity on a project or the prospects of new development on landslide potential may lead to increased risk. Einstein (1988 and 1997) has presented a comprehensive mapping procedure for landslide management. Following are key features of mapping procedures proposed by Einstein (1988 and 1997):

State-of-nature maps: They are used to characterize a site, present data without interpretation, such as geologic and topographic maps, precipitation data, and results of site investigation.
Danger maps: They are used to identify the failure modes involving debris flows, rockfalls, and so on.
Hazard maps: They are used to exhibit the probability of failure related to the possible modes of failure on danger maps. Alternatively, the results can be expressed qualitatively as high, medium, or low.
Management maps: They are incorporated to entail summaries of management decisions.

Furthermore, following scales of analyses for landslide hazard zonations have been outlined by the International Association of Engineering Geology (Soeters and van Westen, 1996):

- *National Scale* (<1:1,000,000): This is a low level detail map intended to provide a general inventory of nationwide hazard. It is used to notify national policy makers and general public.
- *Regional Scale* (1:100,000 to 1:500,000): Because landslide hazards are considered to be undesirable factors as far as the planners are concerned, the regional mapping scale is used in evaluating possible constraints due to instability related to the development of large engineering projects and regional development plans. In general, these types of maps are constructed in early phases of regional development projects with low level details and cover large study areas, on the order of 1000 km^2 or more. They are used to identify areas where landsliding could be a constraint concerning the development of rural or urban transportation projects. "Terrain units with an areal extent of several tens of hectares are outlined and classified according to their susceptibility to occurrence of mass movements," as stipulated by Soeters and van Westen (1996).
- *Medium Scale* (1:25,000 to 1:50,000): This range is considered to be a suitable scale range for landslide hazard maps. As such, they are used to identify the hazard zones in developed areas with large structures, roads, and urbanization. Considerably greater levels of detail are required to prepare the maps at this scale, and the details should encompass slopes in adjacent sites in the same lithology with the possibility of having different hazard scores depending on their characteristics. Furthermore, distinction should be made between various slope segments, located within the same terrain unit, such as rating of a concave slope as opposed to a convex slope.
- *Large Scale* (1:5,000 to 1:15,000): Maps of this scale are generally prepared for limited areas based on both interpretation of aerial photographs and extensive field investigations that use various techniques applied in routine geotechnical engineering, engineering geology, and geomorphology.

11.3 Landslide Types and Causal Factors

11.3.1 Landslide Classification

The UNESCO Working Party's definition of a landslide is "the movement of a mass of rock, earth or debris down a slope" (Cruden, 1991, 1997) and recognizes that the phenomena described as landslides are not limited either to the land or to sliding; the word has a much more extensive meaning than its

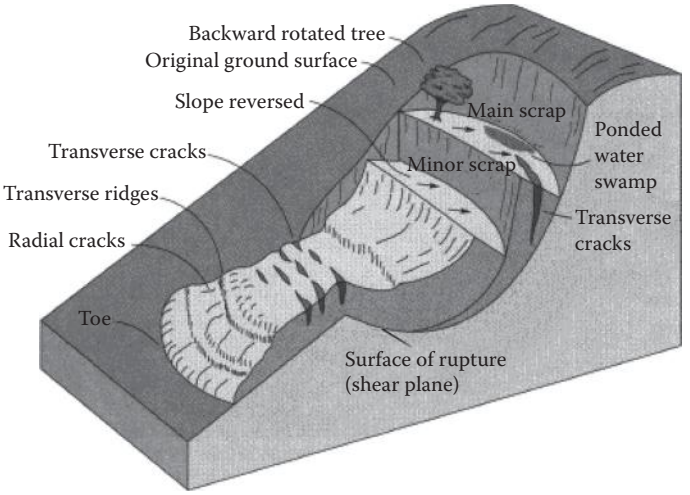

FIGURE 11.3 Nomenclature of various features of a landslide. (From Cruden, D.M., and Varnes, D.J., Landslide Types and Processes, In *Landslides Investigation and Mitigation*, Turner, A.K., and Schuster, R.L. (eds.), Transportation Research Board Special Report 247, National Research Council, Washington, DC, 1996. With permission.)

component parts suggest. An idealized diagram depicting the nomenclature of various features of a complex earth slide–earth flow is shown in Figure 11.3 (Cruden and Varnes, 1996).

As there is a wide spectrum of landslide types, the potential or already occurred landslides should be classified as clear as feasible. The criteria used by the UNESCO Working Party on World Landslide Inventory in classification of landslides follow Varnes (1978) in emphasizing the type of movement and type of material. The divisions of materials are rock, debris, and earth. Rock is characterized as an intact hard or firm mass in its natural place prior to the initial movement, whereas soil is referred to as an aggregate of unconsolidated solid particles, either transported or derived in place via the weathering processes. The latter is further divided into earth, in which 80% or more of the particles are smaller than 2 mm in size, and debris, whereby 20%–80% of the solid particles are larger than 2 mm.

Movements are divided into five types (Figure 11.4): falls, flows, slides, spreads, and topples. In reality, there is a continuum of mass movements from falls through slides to flows. In many instances, it is difficult to determine whether masses of material have fallen or slid, and similarly there are a number of instances in which material has both slid and flowed. Very large falls can result in various types of flow involving fluidization with either water or air. The Department of Environment (DOE, 1994) recognized the existence of complex landslides in which ground displacement is achieved by more than one type of mass movement and emphasized that this should not be confused with landslide complex, that is, an area of instability within which many different types of mass movement occur. Cruden and Varnes (1996) suggested that landslide complexity can be indicated by combining the five basic types of movement and the three divisions of materials. If the type of movement changes with the progress of movement, then the material should be described at the beginning of each successive movement. For example, a rockfall that has been followed by flow of the displaced material can be described as a rockfall–debris flow.

The landslide designation can become more elaborate as more information about the movement becomes available. Adjectives can be added in front of the noun string defining the type of landslide to build up the description of the movement. The adjective magnitude refers to the volume of displaced material involved in a landslide hazard, whereas the intensity renders a collection of physical parameters

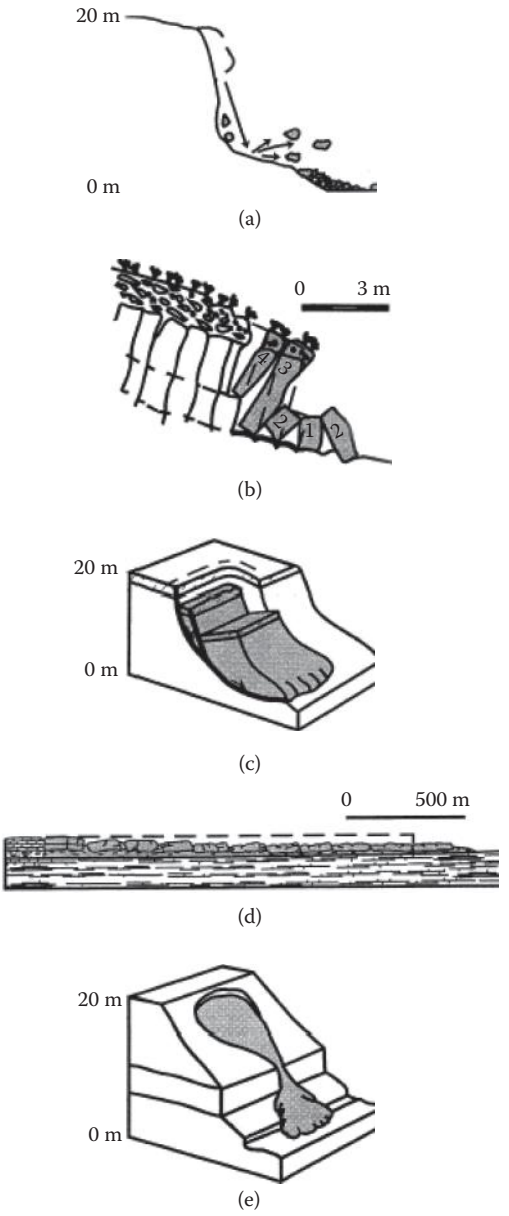

FIGURE 11.4 Types of movement: (a) fall, (b) topple, (c) slide, (d) spread, and (e) flow. (From Cruden, D.M., and Varnes, D.J., Landslide Types and Processes, In *Landslides Investigation and Mitigation*, Turner, A.K., and Schuster, R.L. (eds.), Transportation Research Board Special Report 247, National Research Council, Washington, DC, 1996. With permission.)

that describe the destruction or destructive potential of a landslide hazard. The qualitative expression of the former is small, medium, or large, whereas the latter is expressed qualitatively as slow, moderate, or fast as in downslope velocity of a debris flow. A landslide is known to be *active* when it is presently moving. An *inactive* landslide is one that last moved more than one annual cycle of seasons ago. Inactive landslides are further categorized into *dormant* if the causes of movement are apparent and *abandoned* if the triggering action is no longer present (Popescu, 1984).

11.3.2 Landslide Causal Factors

The processes involved in slope movements comprise a continuous series of events from cause to effect (Varnes, 1978). It is of primary importance to recognize the conditions that caused the slope to become unstable and the processes that triggered the movement, when assessing landslide hazard for a particular site. Only an accurate diagnosis makes it possible to properly understand the landslide mechanisms and thence to propose effective treatment measures.

In every slope, there are forces that tend to promote downslope movement and opposing forces that tend to resist movement. A general definition of the factor of safety of a slope results from comparing the downslope shear stress with the shear strength of the soil, along an assumed or known rupture surface. Starting from this general definition, Terzaghi (1950) divided landslide causes into external causes that result in an increase of the shearing stress (e.g., geometrical changes, unloading the slope toe, loading the slope crest, shocks and vibrations, drawdown, changes in water regime) and internal causes that result in a decrease of the shearing resistance (e.g., progressive failure, weathering, seepage erosion). However, Varnes (1978) pointed out that there are a number of external or internal causes that may be operating either to reduce the shearing resistance or to increase the shearing stress. There are also causes that simultaneously affect both terms of the factor-of-safety ratio.

The great variety of slope movements reflects the diversity of conditions that cause the slope instability and the processes that trigger the movement. It is more appropriate to discuss causal factors (including both "conditions" and "processes") than "causes" per se alone. Thus, ground conditions (weak strength, sensitive fabric, degree of weathering and fracturing) are influential criteria but are not causes (Popescu, 1996). They are part of the conditions necessary for an unstable slope to develop, to which must be added the environmental criteria of stress, pore water pressure, and temperature. It does not matter if the ground is weak as such—failure will only occur as a result if there is an effective causal process that acts as well. Such causal processes may be natural or anthropogenic but effectively change the static ground conditions sufficiently to cause the slope system to fail, that is, to adversely change the state of stability.

Seldom, if ever, can a landslide be attributed to a single causal factor. The process leading to the development of a slide has its beginning with the formation of the rock itself, when its basic properties are determined and includes all the subsequent events of crustal movement, erosion, and weathering.

The computed value of the factor of safety is a clear and simple distinction between stable and unstable slopes. However, from the physical point of view, it is better to visualize slopes existing in one of the following three stages: stable, marginally stable, and actively unstable (Crozier, 1986). Stable slopes are those where the margin of stability is sufficiently high to withstand all destabilizing forces. Marginally stable slopes are those that will fail at some time in response to the destabilizing forces having attained a certain level of activity. Finally, actively unstable slopes are those in which destabilizing forces produce continuous or intermittent movement.

The three stability stages must be seen to be part of a continuum, with the probability of failure being minute at the stable end of the spectrum, but increasing through the marginally stable range to reach certainty in the actively unstable stage. The three stability stages provide a useful framework for understanding the causal factors of landslides and classifying them into two groups on the basis of their function:

1. Preparatory causal factors that make the slope susceptible to movement without actually initiating it, and thereby tending to place the slope in a marginally stable state.
2. Triggering causal factors that initiate movement. The causal factors shift the slope from a marginally stable to an actively unstable state.

A particular causal factor may inflict either or both functions, depending on its degree of activity and the margin of stability. Although it may be possible to identify a single triggering process, an explanation of ultimate causes of a landslide invariably involves a number of preparatory conditions and processes. Based on their temporal variability, the destabilizing processes may be grouped into slow-changing (e.g., weathering, erosion) and fast-changing processes (e.g., earthquakes, reservoir drawdown). In the

search for landslide causes, attention is often focused on those processes within the slope system that provoke the greatest rate of change. Although slow changes act over a long period of time to reduce the resistance/shear stress ratio, often a fast change can be identified as having triggered movement.

Because the assessment of landslide causes is complex and landslides are not always investigated in great detail, UNESCO Working Party on World Landslide Inventory (1994) adopted a simple classification system of landslide causal factors as shown in Table 11.1. The operational approach to classification of landslide causal factors, proposed by this system, is intended to cover the majority of landslides.

TABLE 11.1 A Brief List of Landslide Causal Factors

1. Ground Conditions
   (1) Plastic weak material
   (2) Sensitive material
   (3) Collapsible material
   (4) Weathered material
   (5) Sheared material
   (6) Jointed or fissured material
   (7) Adversely oriented mass discontinuities (including bedding, schistosity, cleavage)
   (8) Adversely oriented structural discontinuities (including faults, unconformities, flexural shears, sedimentary contacts)
   (9) Contrast in permeability and its effects on groundwater
   (10) Contrast in stiffness (stiff, dense material over plastic material)
2. Geomorphological Processes
   (1) Tectonic uplift
   (2) Volcanic uplift
   (3) Glacial rebound
   (4) Fluvial erosion of the slope toe
   (5) Wave erosion of the slope toe
   (6) Glacial erosion of the slope toe
   (7) Erosion of the lateral margins
   (8) Subterranean erosion (solution, piping)
   (9) Deposition loading of the slope or its crest
   (10) Vegetation removal (by erosion, forest fire, drought)
3. Physical Processes
   (1) Intense, short period rainfall
   (2) Rapid melt of deep snow
   (3) Prolonged high precipitation
   (4) Rapid drawdown following floods, high tides, or breaching of natural dams
   (5) Earthquake
   (6) Volcanic eruption
   (7) Breaching of crater lakes
   (8) Thawing of permafrost
   (9) Freeze and thaw weathering
   (10) Shrink and swell weathering of expansive soils
4. Man-Made Processes
   (1) Excavation of the slope or its toe
   (2) Loading of the slope or its crest
   (3) Drawdown (of reservoirs)
   (4) Irrigation
   (5) Defective maintenance of drainage systems
   (6) Water leakage from services (water supplies, sewers, stormwater drains)
   (7) Vegetation removal (deforestation)
   (8) Mining and quarrying (open pits or underground galleries)
   (9) Creation of dumps of very loose waste
   (10) Artificial vibration (including traffic, pile driving, heavy machinery)

It involves consideration of the available data from simple site investigation and information furnished by other site observations. Landslide causal factors are grouped according to their effect (preparatory or triggering) and their origin (ground conditions and geomorphological, physical, or man-made processes). Ground conditions may not have a triggering function, while any ground condition or process may have a preparatory function.

Ground conditions or the material and mass characteristics of the ground can be mapped on the surface of the landslide and the surrounding ground and explored in the subsurface by drilling, trenching, and adits. Mechanical characteristics can be determined by testing. Geomorphic processes, or changes in the morphology of the ground, can be documented by preexisting maps, aerial photographs, surveys of the landslide, or careful observation over time by the local population. Physical processes concern the environment and can be documented at the site by instrumentation, such as rainfall gauges, seismographs, or piezometers. Careful local observations of water wells or damage from earthquakes may be acceptable substitutes. Variations in mechanical properties with distance from the surface may, in some circumstances, indicate changes of these properties with time. Man-made processes can be documented by site observations and from construction or excavation records at the site. Separate identification of man-made and natural landslides is useful for both administrative and theoretical reasons.

11.4 Slope Stability Analyses and Selection of Design Soil Parameters

11.4.1 Introductory Remarks

There are two major approaches in the analysis of slope stability. The first one is the "forward" approach in the analysis of slope stability that requires data on shear strength properties and pore pressure conditions. The former are derived from a range of field and laboratory techniques, whereas the latter demand improved techniques capable of instrumenting rapid groundwater and soil suction responses to rainfall without damping the transient peak conditions. Probable worst-case parameter values are assumed, and a conservative value of the factor of safety is derived.

The second approach is the "backward" approach in the analysis of slope instability that requires detailed information on failure surface geometry and pore water pressure distribution. Accurate determination of the position and shape of the slip surface using surface and subsurface monitoring data is essential to a reliable backward analysis of a given slope failure. Considering that the factor of safety is one, the backward analysis of the failed slope can give a measure of the shear strength mobilized along the slip surface. In many cases, when there are considerable difficulties in obtaining undisturbed samples, backward analysis is an effective tool, and sometimes the only tool, for investigating the strength features of a soil/rock deposit. Both "forward" and "backward" approaches are generally carried out using limit equilibrium methods of slope stability analysis.

11.4.2 Methods of Slope Stability Analysis

Slope stability assessments are generally preformed using methods of limit equilibrium. Such methods make use of the shear strength parameters along the sliding surface, but they do not require any information on the stress–strain properties of the slope materials. Limit equilibrium methods assume the slide mass as a rigid body in equilibrium and use static force and moment equilibrium equations to derive the slope safety factor. Consequently, limit equilibrium methods cannot provide any information related to slope deformations. For a specified sliding surface, some of the limit equilibrium methods such as the Ordinary (or Fellenius) method, Bishop's simplified method, or Janbu's simplified method can be used even with manual calculations to determine the slope safety factor.

As shown in Figure 11.5, limit equilibrium methods involve discretization of the slide mass into a number of slices to take into account the inherent irregularities associated with the geometry of the

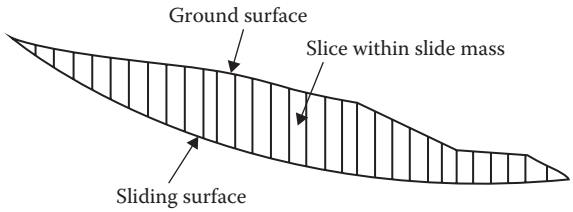

FIGURE 11.5 Slice discretization of the slide mass.

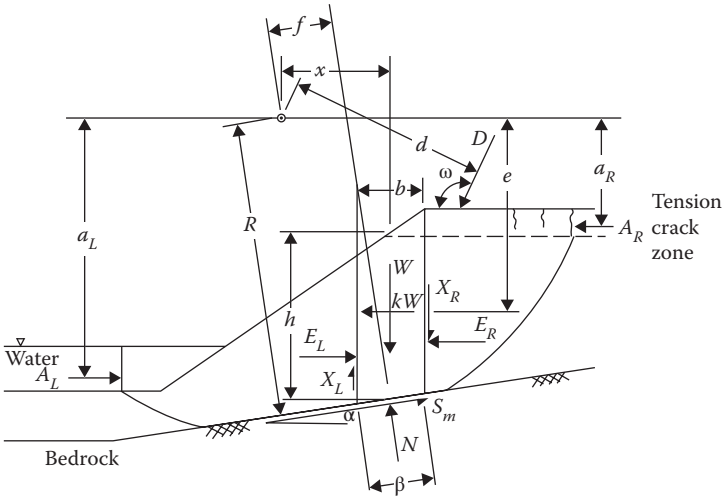

FIGURE 11.6 Forces acting on a slice of the slide mass. (After Krahn, J., *Stability Modeling with Slope/W. An Engineering Methodology*, Geo-Slope/W International Ltd., 396, 2004.)

sliding surface and ground surface as well as variation in strength properties of various geologic layers intercepted by the sliding surface. In selecting the optimum number of slices for the portion of sliding surface passing through a specific layer, the basic requirement is to approximate as closely as possible the shape of actual nonlinear sliding surface within each slice by a planar surface of a given inclination (α) relative to the horizontal (Figure 11.6). This allows for a rigorous determination of the orientation of normal (N) and shear (S) forces acting at the sliding surface within each slice, information which is critical for the limit equilibrium equations (Figure 11.6). Additionally, vertical slice boundaries are introduced at the points of change in geometry of the ground surface (Figure 11.5).

Figure 11.6 shows the forces acting on an individual slice within the slide mass. The variables from Figure 11.6 are defined in the following (Krahn, 2004):

W = total weight of a slice of width b and height h.
N = total normal force on the base of the slice.
S_m = shear force mobilized at the base of each slice.
E = horizontal interslice normal forces. Subscripts L and R designate the left and right sides of the slice, respectively.
X = vertical interslice shear forces. Subscripts L and R define the left and right sides of the slice, respectively.
D = an external point load.
kW = horizontal seismic load applied through the centroid of each slice.
R = radius of a circular slip surface or the moment arm associated with the mobilized shear force, S_m, for any shape of slip surface.

f = perpendicular offset of the normal force from the center of rotation or from the center of moments. It is assumed that f distances on the right side of the center of rotation of a negative slope (i.e., a right-facing slope) are negative and those on the left side of the center of rotation are positive. For positive slopes, the sign convention is reversed.
x = horizontal distance from the centerline of each slice to the center of rotation or to the center of moments.
e = vertical distance from the centroid of each slice to the center of rotation or to the center of moments.
d = perpendicular distance from a point load to the center of rotation or to the center of moments.
h = vertical distance from the center of the base of each slice to the uppermost line in the geometry (i.e., generally ground surface).
a = perpendicular distance from the resultant external water force to the center of rotation or to the center of moments. The L and R subscripts designate the left and right sides of the slope, respectively.
A = resultant of external water forces. The L and R subscripts designate the left and right sides of the slope, respectively.
ω = angle of the point load from the horizontal. This angle is measured counterclockwise from the positive x-axis.
α = angle between the tangent to the center of the base of each slice and the horizontal. The sign convention is as follows. When the angle slopes in the same direction as the overall slope of the geometry, α is positive and vice versa.

The slope safety factor for a specific sliding surface is given by the following equation:

$$F_s = \frac{R}{S_m} \tag{11.1}$$

where R is the available resistant force along the sliding surface and S_m is the mobilized shear force along the sliding surface. The assumption in limit equilibrium analysis is that S_m is mobilized in the same proportion (relative to the available resistant force) for each slice of the slide mass thus F_s is the same for each slice. The safety factor can also be regarded as a ratio between capacity and demand. The capacity (R) is provided by the Mohr–Coulomb failure criterion (i.e., $R = N\tan\varphi + c\beta$) and thus depends on the material shear strength parameters (i.e., cohesion intercept, c, and internal friction angle, φ). On the other hand, the demand (S_m) is obtained from the equations of statics applied to each slice and therefore represents the required shear force to maintain the slide mass in limit equilibrium.

Typical limit equilibrium equations are as follows:

- Equations of force equilibrium in the vertical and horizontal directions for each slice can be used to obtain the normal force at the base of the slice (N) and the interslice normal force (E).
- The equation of equilibrium of forces in the horizontal direction for all slices can be used to derive the force equilibrium safety factor, F_s^F.
- The equation of moment equilibrium about a common point for all slices can be used to derive the moment equilibrium safety factor, F_s^M.

A detailed mathematical formulation of various limit equilibrium equations can be found in Krahn (2004). Because the number of unknowns in these equations is larger than the number of equations available, additional assumptions need to be introduced. Such assumptions are typically made in respect to the magnitude and orientation of the interslice forces. Major differences among various limit equilibrium methods are associated with the specific equilibrium equations used and the assumptions made with respect to the interslice forces. Table 11.2 outlines the equations used by various limit equilibrium methods of slope stability analysis together with the assumptions related to interslice forces associated with each method.

TABLE 11.2 Statics Satisfied and Interslice Forces in Various Methods

Method	Moment Equilibrium	Horizontal Force Equilibrium	Interslice Normal (*E*)	Interslice Shear (X)	Inclination of *X/E* Resultant
Ordinary or Fellenius	Yes	No	No	No	No force
Bishop's simplified	Yes	No	Yes	No	Horizontal
Janbu's simplified	No	Yes	Yes	No	Horizontal
Spencer	Yes	Yes	Yes	Yes	Constant
Morgenstern—Price	Yes	Yes	Yes	Yes	Variable
Corps of Engineers—1	No	Yes	Yes	Yes	Inclination of a line from crest to toe
Corps of Engineers—2	No	Yes	Yes	Yes	Slice top ground surface inclination
Lowe–Karafiath	No	Yes	Yes	Yes	Average of ground surface slope and slice base inclination

Source: After Krahn, J., *Canadian Geotechnical Journal*, 40, 643–660, 2003.

The Ordinary method of slices provides lower safety factors compared to more rigorous methods (e.g., Morgenstern–Price method). The shape of the sliding surface has a major effect on the calculated safety factors using Bishop and Janbu simplified methods. Computational results from slope stability analyses conducted for various geometries of the sliding surface (Krahn, 2003) indicate that for circular sliding surfaces Bishop's simplified method provides accurate safety factors similar to those obtained using Morgenstern–Price method, whereas Janbu's simplified method underestimates the slope safety factor. Conversely, Janbu's simplified method agrees very well with Morgenstern–Price method yielding accurate safety factors for planar sliding surfaces, whereas Bishop's simplified method underestimates the slope safety factor for planar sliding surface geometries. The Morgenstern–Price safety factor along composite sliding surfaces involving combinations of planar and circular segments is typically bounded by the safety factors associated with Bishop and Janbu simplified methods.

Stability charts are useful in preliminary stages of a project or sensitivity analysis since they enable to perform a quick and simple slope stability assessment. They are developed using dimensionless relationships that can be established between the safety factor and other parameters characterizing the slope geometry, soil shear strength, and pore water pressure. Most charts are developed for homogeneous slopes with simple geometries. In case of nonhomogeneity of the soils layers, average parameters should be evaluated. Several published stability charts developed by various investigators can be found in the literature (Fellenius, 1936; Taylor, 1937; Janbu, 1954; Hoek and Bray, 1974).

Commercial software is currently available to conduct limit equilibrium slope stability analyses using personal computers. This tool has become critical for slope stability studies as it allows for the investigation of complex problems involving multiple stratigraphic layers, various pore pressure conditions, and reinforcement. It also provides the advantage of conducting quick sensitivity analyses addressing the influence of various input parameters on slope stability. As outlined by Duncan and Wright (2005), the computer programs for slope stability can be divided into analysis programs and design programs. The output provided by analysis programs is the slope safety factor corresponding to a prescribed set of input parameters (e.g., slope geometry, material properties, pore pressures, external loads, reinforcement). On the other hand, design programs aim at determining the appropriate slope conditions required to provide one or more design factors of safety specified by the user. Many of the computer programs used to analyze reinforced slopes fall in this latter category. Table 11.3 (Duncan and Wright, 2005) presents performance ratings of various computer programs for slope stability analysis used in geotechnical engineering practice.

TABLE 11.3 Characteristics of Various Computer Programs for Slope Stability Analysis

	UTEXAS4	SLOPE/W	SLIDE	XSTABL	WINSTABL	RSS	SNAIL	GoldNail
Accuracy	5	4.5	4.5	4	3.5	4	2	4
Program Computation Time	5	5	5	5	4 (1[a])	4	2	4
Time for Learning Curve	3	5	5	4	3.5	3.5	3	3.5
Time to Enter Data and Complete Analysis	3	5	5	4.5	4	3.5	3	2.5
Ease of Reinforced Slope Design	1.5	2.5	2.5	5—Initial only—no final design capabilities	3	5—Horizontal reinforcement only	4	5
Ease of Unreinforced Slope Data Entry	3.5	5	5	4	3.5	3	3	3.5
Ease of Soil Nail Data Entry	2.5	3.5	3.5	No provision for reinforcement	3.5	5—Horizontal reinforcement only	5	4.5
Ease of Tieback Data Entry	2.5	5	5	No provision for reinforcement	4	5—Horizontal reinforcement only	3	3.5
Ease of Geogrid Data Entry	2.5	3.5	3.5	No provision for reinforcement	4.5	5	3	3.5
Time Required to Make Output Report Ready	4	5	5	3	2	3	3	1
Quality of Graphical Output	4	5	5	3	2	3	3	1

Note: 1 = Poor; 2 = Fair; 3 = Average; 4 = Good; 5 = Excellent.

[a] In WINSTABL, Spencer's method has a computation time of up to several minutes.

11.4.3 Shear Strength Parameters for Slope Stability Analysis

The limit equilibrium methods forming the framework of slope stability/instability analysis generally accept the Mohr–Coulomb failure criterion, which can be expressed in terms of effective or total stresses. The Mohr–Coulomb shear strength in terms of effective stresses is as follows:

$$\tau_f = c' + \sigma' \tan \varphi' \tag{11.2a}$$

where τ_f and σ' are the shear stress and effective normal stress, respectively, on the failure surface, and c' and φ' are the shear strength parameters (i.e., cohesion intercept and internal friction angle, respectively) in terms of effective stresses. For a slope stability analysis in terms of total stresses, the shear strength is given by the following equation:

$$\tau_f = c_u + \sigma \tan \varphi_u \tag{11.2b}$$

where σ represents the total normal stress on the failure surface, and c_u and φ_u are the shear strength parameters (i.e., cohesion intercept and internal friction angle, respectively) in terms of total stresses. σ′ and σ are related through the effective stress principle, that is,

$$\sigma' = \sigma - u \tag{11.3}$$

where u represents the pore water pressure at the sliding surface. An illustration of the strength envelopes in terms of total and effective stresses is provided in Figure 11.7.

A detailed discussion on the types of field and laboratory experiments required for the evaluation of shear strength parameters in total and effective stresses can be found elsewhere (Duncan, 1996; Duncan and Wright, 2005).

Since soil shear strength is directly related to the effective normal stress along the sliding surface, a slope stability analysis in terms of effective stresses based on Equation 11.2a is always desirable. However, selection of Equation 11.2a or b in slope stability assessments depends largely on the degree to which the pore water pressure along the sliding surface is known. If a slope is likely to fail under drained conditions (i.e., no excess pore pressures develop until the onset of slope failure), then the pore water pressure can be estimated from field measurements and seepage analyses. Under such circumstances, the effective stress along the sliding surface can be determined from Equation 11.3 and therefore an effective stress slope stability analysis based on Equation 11.2a can be undertaken. However, a slope may also experience failure in undrained conditions when subjected to an increase in driving forces (e.g., due to earthquake loading, excavation of material from toe, placement of material at crest) at a rate quick enough to not allow for dissipation of excess pore pressures during the loading process due to the relatively low hydraulic conductivity of the slope materials. In such situations, a total stress analysis based on Equation 11.2b is typically used to analyze the slope instability in undrained conditions since the excess pore pressures generated along the sliding surface due to undrained loading/unloading are not easy to predict and therefore the magnitude of effective stresses at failure cannot be determined. Detailed recommendations on how to select appropriate undrained shear strength parameters for total stress slope stability analyses are provided by Duncan (1996) and Duncan and Wright (2005). Duncan (1996) also provides a rational approach of assessing whether undrained conditions are likely to occur under a specific loading scenario using a time factor–based methodology similar to one-dimensional primary consolidation analysis.

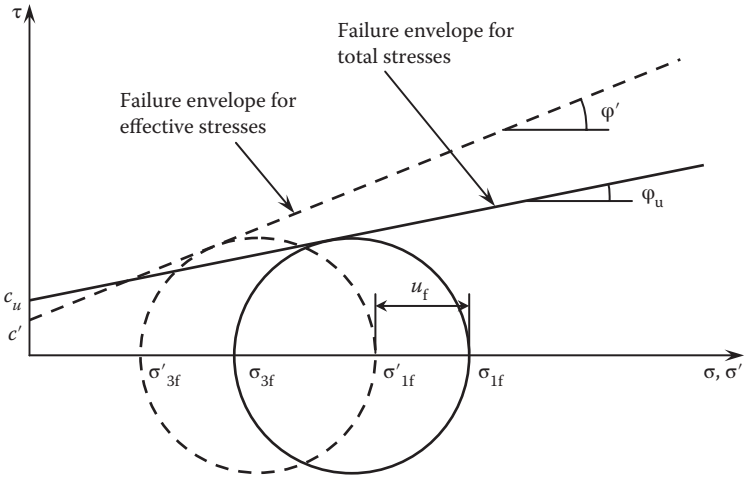

FIGURE 11.7 Failure envelopes for total and effective stresses.

It is also worth noting that the stress–strain behavior of overconsolidated soils is characterized by a peak strength reached at relatively small strains followed by a gradual reduction in strength with progressive increase in strains, culminating in a residual strength value smaller than the peak strength. Under such circumstances, the selection of appropriate strength parameters for slope stability analysis must be made based on the amount of shear deformation experienced on the slope. The stability of a slope likely to experience failure for the first time can be analyzed using peak shear strength parameters, whereas the stability of reactivated landslides (i.e., landslides exhibiting recurrent movements over certain periods of time) must be analyzed using residual shear strength parameters.

11.4.4 Backward Analysis of Slope Stability

Backward analysis is an effective approach to derive the design shear strength parameters for slope stabilization. A slope failure can reasonably be considered as a full-scale shear test capable to give a measure of the strength mobilized at failure along the slip surface. The back-calculated shear strength parameters, which are intended to be closely matched with the observed real-life performance of the slope, can then be used in further limit equilibrium analyses to design remedial works. Shear strength parameters obtained by back analysis ensure more reliability than those obtained by laboratory or in-situ testing when used to design remedial measures.

Procedures to determine the magnitude of both shear strength parameters or the relationship between them by considering the position of the actual slip surface within a slope are discussed by Popescu and Yamagami (1994). The two unknowns—that is, the shear strength parameters c' and φ'—can be simultaneously determined from the following two requirements:

1. $F_s = 1$ for the given failure surface. That means the back-calculated strength parameters have to satisfy the $c' - \tan \varphi'$ limit equilibrium relationship.
2. F_s = minimum for the given failure surface and the slope under consideration. That means the factors of safety for slip surfaces slightly inside and slightly outside the actual slip surface should be greater than one (Figure 11.8a).

Based on the abovementioned requirements, Saito (1980) developed a semigraphical procedure using trial and error to determine unique values of c' and $\tan \varphi'$ by back analysis (Figure 11.8b). An envelope of the limit equilibrium lines $c' - \tan \varphi'$, corresponding to different trial sliding surfaces, is drawn, and the unique values c' and $\tan \varphi'$ are found as the coordinates of the contact point held in common by the envelope and the limit equilibrium line corresponding to the actual failure surface. A more systematic procedure to find the very narrow range of back-calculated shear strength parameters based on the same requirements is illustrated in Figure 11.8c.

The fundamental problem involved is always one of data quality, and consequently the back analysis approach must be applied with care and the results interpreted with caution. Back analysis is of use only if the soil conditions at failure are unaffected by the failure. For example, back-calculated parameters for a first-time slide in stiff overconsolidated clays could not be used to predict subsequent stability of the sliding mass, since the shear strength parameters will have been reduced to their residual values by the failure. In such cases, an assumption of $c' = 0$ and the use of a residual friction angle φ_r' is warranted (Bromhead, 1992). If the three-dimensional geometrical effects are important for the failed slope under consideration and a two-dimensional back analysis is performed, the back-calculated shear strength will be too high and thus unsafe.

Additionally, one has to be aware of the many pitfalls of the back analysis approach that involves a number of basic assumptions regarding soil homogeneity, slope and slip surface geometry, and pore pressure conditions along the failure surface (e.g., Leroueil and Tavenas, 1981). A position of total confidence in all these assumptions is rarely if ever achieved. While the topographical profile can generally be determined with enough accuracy, the slip surface is almost always known in only few points and interpolations with a considerable degree of subjectivity are necessary. Errors in the position of

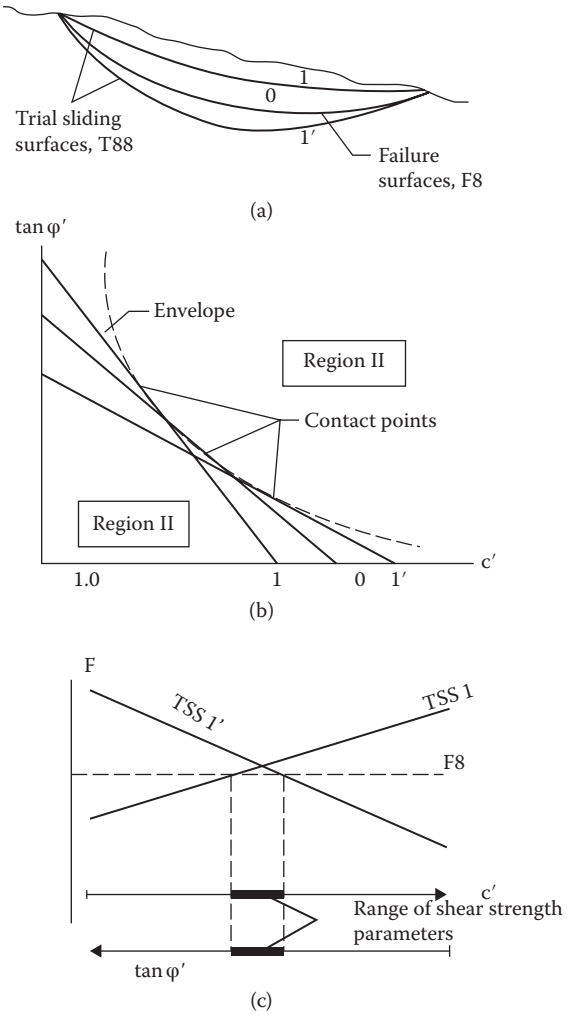

FIGURE 11.8 Shear strength back analysis methods. (After Popescu, M.E., Schaefer V.R., In *Proceedings of the 10th International Symposium on Landslides and Engineered Slopes*, Xi'an, China, pp. 1787–1793, 2008.)

the slip surface result in errors in back-calculated shear strength parameters. If the slip surface used in back analysis is deeper than the actual one, c' is overestimated and φ' is underestimated and vice versa. The data concerning the pore pressure on the slip surface are generally few and imprecise. More exactly, the pore pressure at failure is almost always unknown. If the assumed pore pressures are higher than the actual ones, the shear strength is overestimated. As a consequence, a conservative assessment of the shear strength is obtainable only by underestimating the pore pressures.

To avoid the questionable problem of the representativeness of the back-calculated unique set of shear strength parameters, a method for designing remedial works based on the limit equilibrium relationship $c' - \varphi'$ rather than a unique set of shear strength parameters can be used (Popescu, 1991).

The method principle is shown in Figure 11.9. It is considered that a slope failure provides a single piece of information, which results in a linear limit equilibrium relationship between shear strength parameters. That piece of information is that the factor of safety is equal to unity ($F_s = 1$), or the horizontal force at the slope toe is equal to zero ($E = 0$) for the conditions prevailing at failure. Each of the two conditions ($F_s = 1$ or $E = 0$) results in the same relationship $c' - \tan \varphi'$, which for any practical purpose might be considered linear.

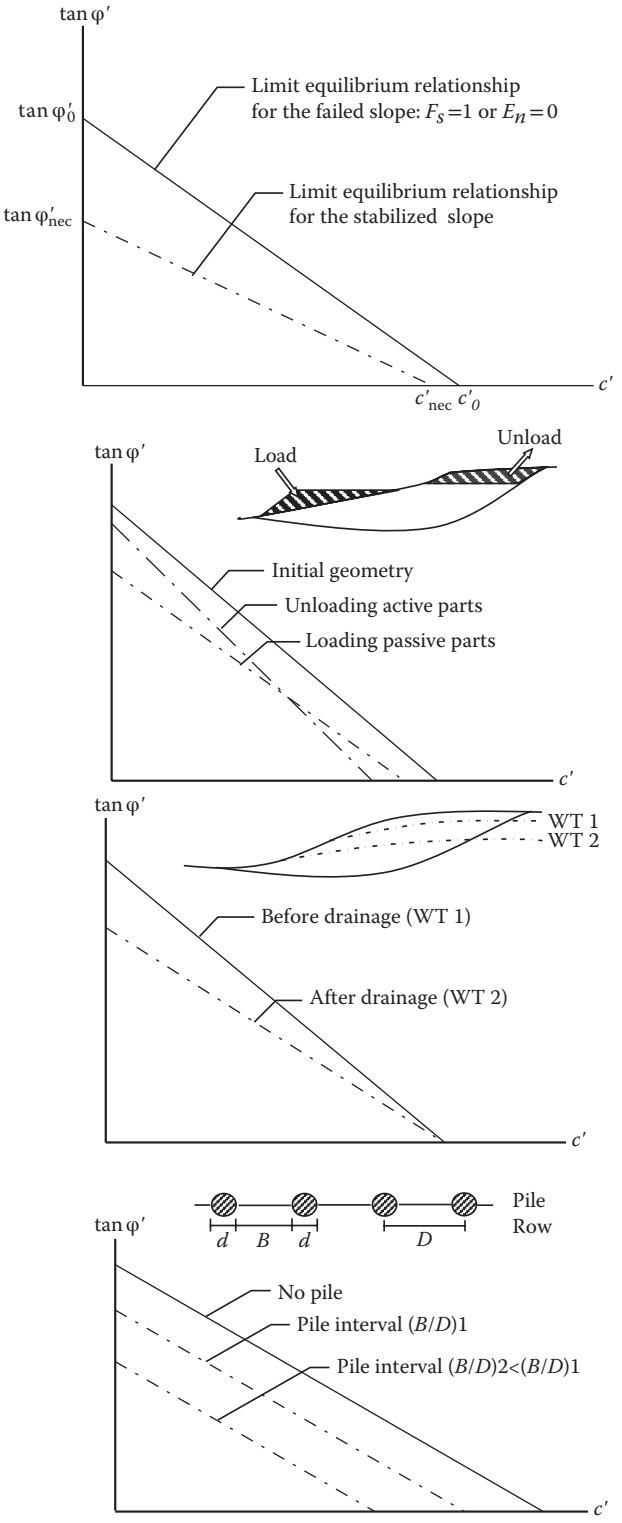

FIGURE 11.9 Limit equilibrium relationship and design of slope remedial measures. (After Popescu, M.E. and Schaefer V.R. Proc. 10th Intern. Symp. on Landslides and Engineered Slopes, Xi'an, China, p. 1787–1793, 2008.)

The linear relationship $c' - \tan\varphi'$ can be obtained using standard computer software for slope stability limit equilibrium analysis by manipulations of trial values of c' and $\tan\varphi'$ and calculating the corresponding factor of safety value. It is simple to show that in an analysis using arbitrary φ' alone ($c' = 0$) to yield a nonunity factor of safety, F_φ^*, the intercept of the $c' - \tan\varphi'$ line (corresponding to $F_s = 1$) on the $\tan\varphi'$ axis results as

$$\tan\varphi_0' = \frac{\tan\varphi'}{F_\varphi^*} \tag{11.4}$$

Similarly, the intercept of the $c' - \tan\varphi'$ line (corresponding to $F_s = 1$) on the c' axis can be found assuming $\varphi' = 0$ and an arbitrary c' value, which yield to a nonunity factor of safety, F_c^*:

$$c_0' = \frac{c'}{F_c^*} \tag{11.5}$$

Using the concept of limit equilibrium linear relationship $c' - \tan\varphi'$, the effect of any remedial measure (drainage, modification of slope geometry, restraining structures) can easily be evaluated by considering the intercepts of the $c' - \tan\varphi'$ lines for the failed slope (c_0', $\tan\varphi_0'$) and for the same slope after installing some remedial works (c'_{nec}, $\tan\varphi'_{nec}$), respectively (Figure 11.9). The safety factor of the stabilized slope is

$$F = \min\left(F_c^* = \frac{c_0'}{c'_{nec}}, F_\varphi^* = \frac{\tan\varphi_0'}{\tan\varphi'_{nec}} \right) \tag{11.6}$$

Errors included in back calculation of a given slope failure will be offset by applying the same results, in the form of $c' - \tan\varphi'$ relationship, to the design of remedial measures.

The above outlined procedure was used to design piles to stabilize landslides (Popescu, 1991) taking into account both driving and resisting force. The principle of the proposed approach is illustrated in Figure 11.9, which gives the driving and resisting force acting on each pile in a row as a function of the nondimensional pile interval ratio B/D. The driving force, F_D, is the total horizontal force exerted by the sliding mass corresponding to a prescribed increase in the safety factor along the given failure surface. The resisting force, F_R, is the lateral force corresponding to soil yield, adjacent to piles, in the hatched area as shown in Figure 11.10. F_D increases with the pile interval, whereas F_R decreases with the same interval. The intersection point of the two curves, which represent the two forces, gives the pile interval ratio satisfying the equality between driving and resisting force. The accurate estimation of the lateral force on pile is an important parameter for the stability analysis because its effects on both the pile and slope stability are conflicting. That is, safe assumptions for the stability of slope are unsafe assumptions for the pile stability, and vice versa. Consequently, to obtain an economic and safe design, it is necessary to avoid excessive safety factors.

11.4.5 Seismic Slope Stability Analysis

Slopes in earthquake-prone areas may experience failure during a seismic event due to inertia forces imparted by the earthquake to the slide mass and/or loss of shear strength in slope materials during earthquake shaking. Depending on the failure mechanism, Kramer (1996) divided seismic slope instabilities into the following two major categories: inertial instabilities and weakening instabilities. Slopes composed of materials susceptible to shear strength loss during an earthquake (e.g., liquefiable soils) fall in the latter category. Slopes undergoing inertial instability during an earthquake are characterized by relatively constant shear strength, and incremental downward deformations occur when earthquake accelerations exceed the yield acceleration of the slide mass. Since such slopes typically remain stable at the end of the earthquake, the seismic analysis focuses on the determination of earthquake-induced permanent slope displacements. Slopes susceptible to shear strength reduction during earthquake may

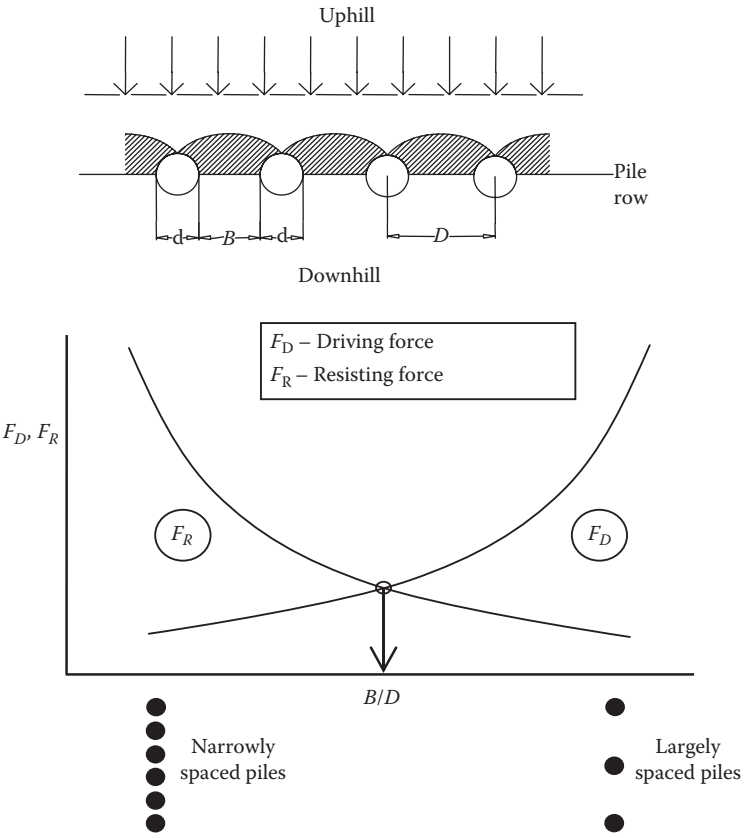

FIGURE 11.10 Driving versus resisting force for stabilizing piles. (After Popescu, M.E. and Schaefer V.R. Proc. 10th Intern. Symp. on Landslides and Engineered Slopes, Xi'an, China, p. 1787–1793, 2008.)

experience instability also after the earthquake if the seismically induced shear strength loss along the sliding surface is large enough to bring the available shear strength below the static driving shear stress acting at the sliding surface. The seismic analysis in such circumstances will focus on determining the reduction in shear strength during the earthquake, and a static postearthquake slope stability analysis using conventional limit equilibrium methods and employing the reduced shear strengths determined from the previous seismic analysis needs to be undertaken. A step-by-step procedure to be followed in a seismic slope stability analysis is provided by Duncan and Wright (2005).

Seismic slope stability can be assessed using the pseudostatic approach. This approach uses traditional limit equilibrium techniques and involves the application of an additional static force to replicate the earthquake loading. The additional force is computed as the weight of the slide mass multiplied by a seismic coefficient and may be regarded as the equivalent of a seismic inertia force acting on the slope. Pseudostatic slope stability analyses are typically conducted during the preliminary stages of a seismic landslide hazard assessment to evaluate the susceptibility to earthquake-induced slope failure and decide whether more advanced investigations (e.g., extensive laboratory testing and seismic slope stability assessments using more sophisticated methods) should be undertaken to better characterize the seismic slope response. A detailed discussion on the pseudostatic approach including the selection of seismic coefficients and allowable safety factors for seismic slope stability analysis can be found elsewhere (e.g., Kramer, 1996; Abramson et al., 2001; Duncan and Wright, 2005).

The dynamic displacement analysis of slopes during earthquake is typically carried out using the Newmark sliding block methodology (Newmark, 1965). This method appears to provide a compromise

between the simple pseudostatic approach, which gives a factor of safety as the only indicator of seismic slope stability, and the more sophisticated finite element method, which produces detailed results of seismic performance but requires quite complex constitutive models for simulating the relevant aspects of soil behavior. The Newmark model is basically a one-block translational or rotational mechanism along a rigid plastic-sliding surface, activated when the ground-shaking acceleration exceeds a critical level. Therefore, this rigid block approach lacks the ability of modeling the seismic compliance of a soil slope. However, despite this deficiency, the Newmark sliding block concept is still widely used in engineering practice mainly due to the fact that it requires only fundamental design information (e.g., geometry of the problem), a minimum number of material properties (i.e., unit weight and shear strength parameters), and involves a robust computational process. Details of the conventional Newmark sliding block method and the solution procedure can be easily found in the literature (e.g., Newmark 1965; Kramer 1996; Abramson et al., 2001). A Newmark sliding block methodology accounting for the degradation of yield strength along the sliding surface with progressive landslide deformation was developed and applied to seismic stability evaluations of slopes susceptible to earthquake-induced catastrophic failure in liquefiable soils (Trandafir and Sassa, 2004, 2005).

11.5 Landslide Risk Mitigation

11.5.1 Landslide Risk Treatment Options

Risk treatment is the final stage of the risk management process and provides the methodology for controlling the risk. At the end of the evaluation procedure, it is up to the client or to policy makers to decide whether to accept the risk or not, or to decide that more detailed study is required. The landslide risk analyst can provide background data or normally acceptable limits as guidance to the decision maker but should not be making the decision. Part of the specialist's advice may be to identify the options and methods for treating the risk. Typical options would include (Australian Geomechanics Society, 2000) the following:

- *Accept the risk:* This will usually require the risk to be considered to be within the acceptable or tolerable range.
- *Avoid the risk:* This will entail avoiding the project, thus seeking an alternative site or form of development so that the revised risk becomes acceptable or tolerable.
- *Reduce the likelihood:* This requires stabilization measures to control the initiating circumstances, such as reprofiling the surface geometry or installing groundwater drainage, anchors, stabilizing structures, protective structures.
- *Reduce the consequences:* This requires provision of defensive stabilization measures, amelioration of the behavior of the hazard, or relocation of the development to a more favorable location to achieve an acceptable or tolerable risk.
- *Monitoring and warning systems:* In some situations, monitoring (such as by regular site visits or by surveys) and establishment of warning systems may be used to manage the risk on an interim or permanent basis. Monitoring and warning systems may be regarded as another means of reducing the consequences.
- *Transfer the risk:* This requires that either another authority to accept the risk or to compensate for the risk such as by insurance.
- *Postpone the decision:* If there is sufficient uncertainty, it may not be appropriate to make a decision on the data available. Further investigation or monitoring will be required to provide data for better evaluation of the risk.

The relative costs and benefits of various options need to be considered so that the most cost-effective solutions, consistent with the overall needs of the client, owner, and regulator, can be identified. Combinations of options or alternatives may be appropriate, particularly where relatively large reductions in risk can be achieved for relatively small expenditures. Prioritization of alternative options is likely to assist with selection.

11.5.2 Landslide Remedial Measures

Correction of an existing landslide or the prevention of a pending landslide is a function of reduction of the driving forces or increase in the available resisting forces. Any remedial measure used must involve one or both of the above parameters. Many general reviews of the methods of landslide remediation have been made. The interested reader is particularly directed to Cornforth (2005), Duncan and Wright (2005), Popescu and Seve (2001). Transportation Research Board (1996), Bromhead (1992), Zaruba and Mencl (1982), and Hutchinson (1977).

IUGS WG/L (Popescu, 2001) has prepared a short checklist of landslide remedial measures arranged in four practical groups, namely, modification of slope geometry, drainage, retaining structures, and internal slope reinforcement, as shown in Table 11.4.

A flow diagram (Figure 11.11) exhibits the sequence of various phases involved in the planning, design, construction, and monitoring of remedial works (Kelly and Martin, 1986). The following gives a short description of the most commonly used remedial measures.

TABLE 11.4 A Brief List of Landslide Remedial Measures

1. Modification of Slope Geometry
   (1) Removing material from the area driving the landslide (with possible substitution by lightweight fill)
   (2) Adding material to the area maintaining stability (counterweight berm or fill)
   (3) Reducing general slope angle
2. Drainage
   (1) Surface drains to divert water from flowing onto the slide area (collecting ditches and pipes)
   (2) Shallow or deep trench drains filled with free-draining geomaterials (coarse granular fills and geosynthetics)
   (3) Buttress counterforts of coarse-grained materials (hydrological effect)
   (4) Vertical (small diameter) boreholes with pumping or self-draining
   (5) Vertical (large diameter) wells with gravity draining
   (6) Subhorizontal or subvertical boreholes
   (7) Drainage tunnels, galleries, or adits
   (8) Vacuum dewatering
   (9) Drainage by siphoning
   (10) Electroosmotic dewatering
   (11) Vegetation planting (hydrological effect)
3. Retaining Structures
   (1) Gravity retaining walls
   (2) Crib-block walls
   (3) Gabion walls
   (4) Passive piles, piers, and caissons
   (5) Cast-in-situ-reinforced concrete walls
   (6) Reinforced earth-retaining structures with strip/sheet–polymer/metallic reinforcement elements
   (7) Buttress counterforts of coarse-grained material (mechanical effect)
   (8) Retention nets for rock slope faces
   (9) Rockfall attenuation or stopping systems (rocktrap ditches, benches, fences, and walls)
   (10) Protective rock/concrete blocks against erosion
4. Internal Slope Reinforcement
   (1) Rock bolts
   (2) Micropiles
   (3) Soil nailing
   (4) Anchors (prestressed or not)
   (5) Grouting
   (6) Stone or lime/cement columns
   (7) Heat treatment
   (8) Freezing
   (9) Electroosmotic anchors
   (10) Vegetation planting (root strength mechanical effect)

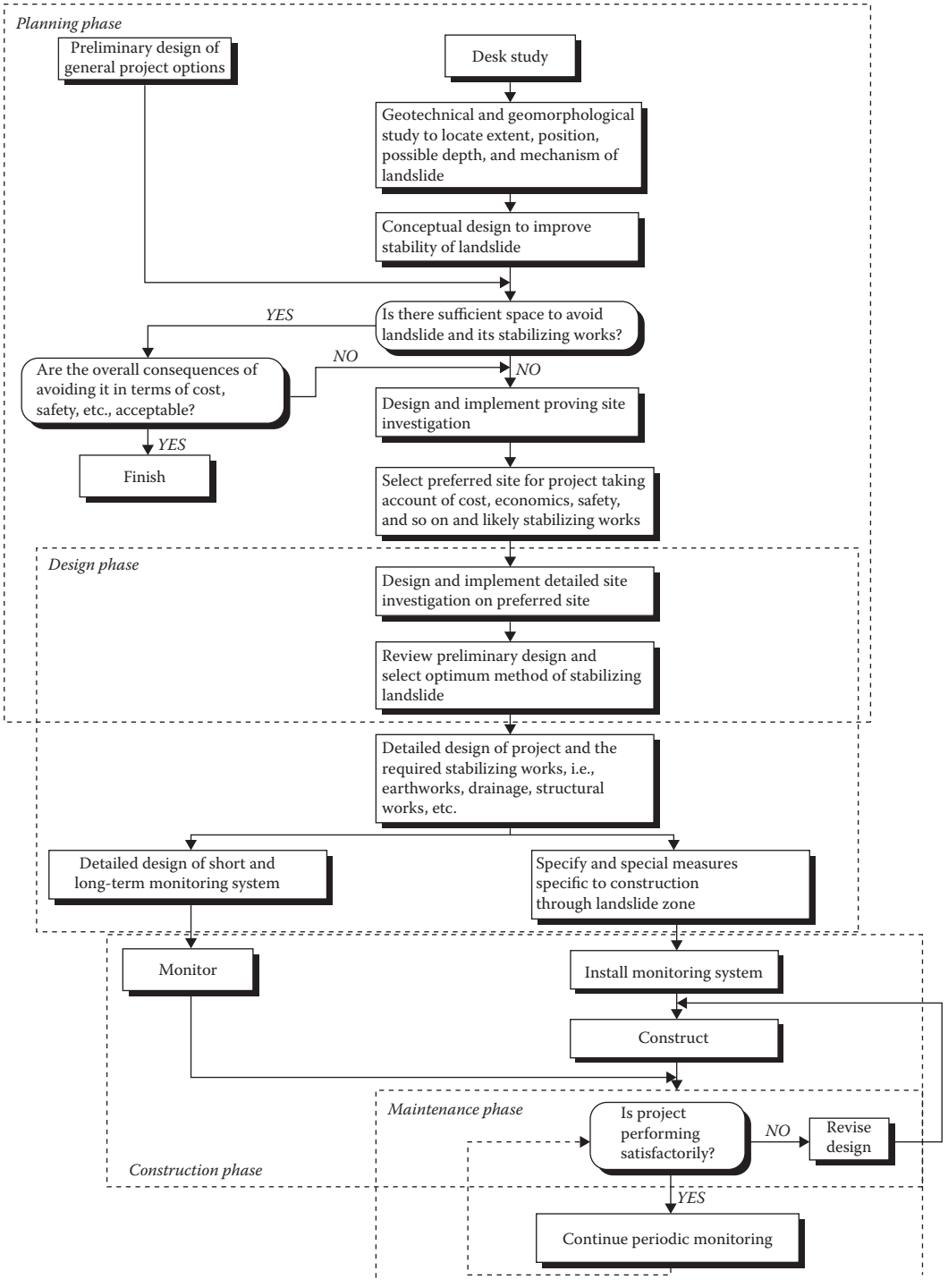

FIGURE 11.11 Various phases involved in planning, design, and construction of landslide remedial works. (From Kelly, J.M.H., and Martin, P.L., Construction Works on or Near Landslides, In Proceedings of the Symposium of Landslides in South Wales Coalfield, Polytechnic of Wales, 85–103, 1986. With permission.)

11.5.2.1 Drainage Measures

Hutchinson (1977) has indicated that drainage is the principal measure used in the mitigation of landslides, with modification of slope geometry the second most used method. These are also generally the least costly of the four major categories, which is obviously why they are the most used. The experience shows that while one remedial measure may be dominant, most landslide repairs involve use of a combination of two or more of the major categories. For example, while restraint may be the principal measure used to correct a particular landslide, drainage and modification of slope geometry, to some degree and by necessity, are also used.

Drainage is often a crucial remedial measure due to the important role played by pore water pressure in reducing shear strength. Because of its high stabilization efficiency in relation to cost, drainage of surface water and groundwater is the most widely used and generally the most successful stabilization method. As a long-term solution, however, it suffers greatly because the drains must be maintained if they are to continue to function.

Drainage may be used to prevent surface or subsurface water reaching the slide area or to remove it from the slide area. Surface water is diverted from unstable slopes by ditches and pipes. Drainage of shallow groundwater is usually achieved by networks of trench drains. Drainage of the failure surfaces, on the other hand, is achieved by counterfort or deep drains, which are trenches sunk into the ground to intersect the shear surface and extending below it. In the case of deep landslides, often the most effective way of lowering groundwater is to drive drainage adits into the intact material beneath the landslide. From this position, a series of upward-directed drainage holes can be drilled through the roof of the tunnel to drain the sole of the landslide. Alternatively, the adits can connect a series of vertical wells sunk down from the ground surface. In instances where the groundwater is too deep to be reached by ordinary trench drains and where the landslide is too small to justify an expensive drainage adit or gallery, bored subhorizontal drains can be used. Another approach is to use a combination of vertical drainage wells linked to a system of subhorizontal borehole drains.

Figure 11.12 shows a selection of drainage measures applied to a landslide. This figure was compiled by Bromhead (1992) from a number of case records, and all the drainage measures adopted in the figure have been used successfully, either singly or in combination, to stabilize landslides.

Subhorizontal drains may be ineffective in clays and other fine-grained soils. Therefore, the possibility of poor performance should be considered when assessing the relative merits of subhorizontal drains to other remedial measures. Figure 11.13 illustrates some of the more common situations where subhorizontal drains can be used for slope stabilization (Cornforth, 2005). A case study of a large landslide on the southern Oregon coast, stabilized by a vertical shaft and horizontal drains, is discussed by Cornforth (2005) and illustrated in Figure 11.14.

Modification of slope geometry as illustrated in Figure 11.15 is a most efficient method. Balancing the volume of cut and fill makes it unnecessary to dispose of excavated material off-site or to import soil for fill area. However, the success of corrective slope regrading (fill or cut) is determined not merely by size or shape of the alteration but also by position on the slope. Hutchinson (1977) provided details of the "neutral line" method to assist in finding the best location to place a stabilizing fill or cut. There are some situations where this approach is not simple to adopt. These include long translational landslides where there is no apparent toe or crest (Figure 11.16). Also, situations where the geometry is determined by engineering constraints and where the unstable area is complex and thus a change in topography, which improves the stability of one area, may reduce the stability of another area.

Schuster (1995) discussed recent advances in the commonly used drainage systems while briefly mentioning less commonly used, but innovative means of drainage, such as electroosmotic dewatering and vacuum and siphon drains were also presented. In addition, buttress counterforts of coarse-grained materials placed at the toes of unstable slopes often are successful as remedial measures (Figure 11.17). These methods are listed in Table 11.4 under both "Drainage," when used mainly for their hydrological effect, and "Retaining Structures," when used mainly for their mechanical effect.

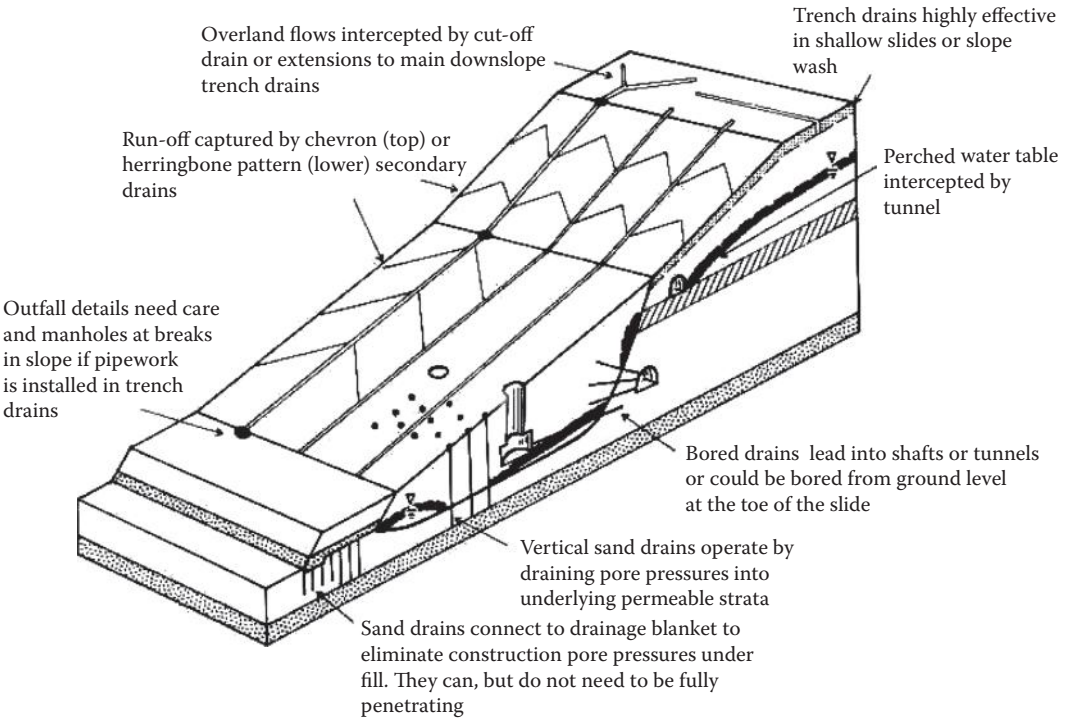

FIGURE 11.12 Various drainage measures applied to landslide stabilization. (After Bromhead, E.N., *Slope Stability. 2nd Edition*, Blackie Academic & Professional, London, 411, 1992.)

11.5.2.2 Structural Measures

Retaining structures include a variety of structural solutions starting with traditional concrete or masonry gravity retaining walls and concrete cantilever retaining walls (Figure 11.18) as well as crib, bin and gabion retaining walls (Figure 11.19). Mechanically stabilized earth walls (Figure 11.20) for landslide applications can be built to support shallow slides. They can be also incorporated in buttress remediation where available land is restricted and a steeper buttress slope is required or to help road-widening projects.

Heavily reinforced concrete piles are also used as retaining structures to stabilize landslides (Figure 11.21). Spaced and staggered piles are more frequently used than tangent or secant piles. Such stabilizing piles are easy to construct and may be buried within the slide mass, making the remediation less intrusive than other techniques. Design principles for stabilizing a slope with piles are shown schematically in Figure 11.22.

Piles, piers, buttress, or walls are passive stabilization systems; that is, further movements of the slope increase pressure on them, and the system reaction forces put into the slide mass lead to stabilization.

On the other hand, prestressed anchors are active stabilization systems; that is, they use preloading to put the stabilizing forces into the landslide mass from the beginning. Anchor loads are spread into the slide mass by pads so that the bearing capacity failures of the ground are avoided (Figure 11.23). Pads with a small number of anchors are preferred. Figure 11.24 shows anchors used to stabilize a landslide above Tablachaca Dam in Peru (Duncan and Wright, 2005).

Micropiles that are essentially an outgrowth of the technology used in the construction of ground anchors are passive systems. Applications of micropiles for slope stabilization are schematically illustrated in Figure 11.25: Case 1 micropiles are directly loaded and resist the loads applied by the slide

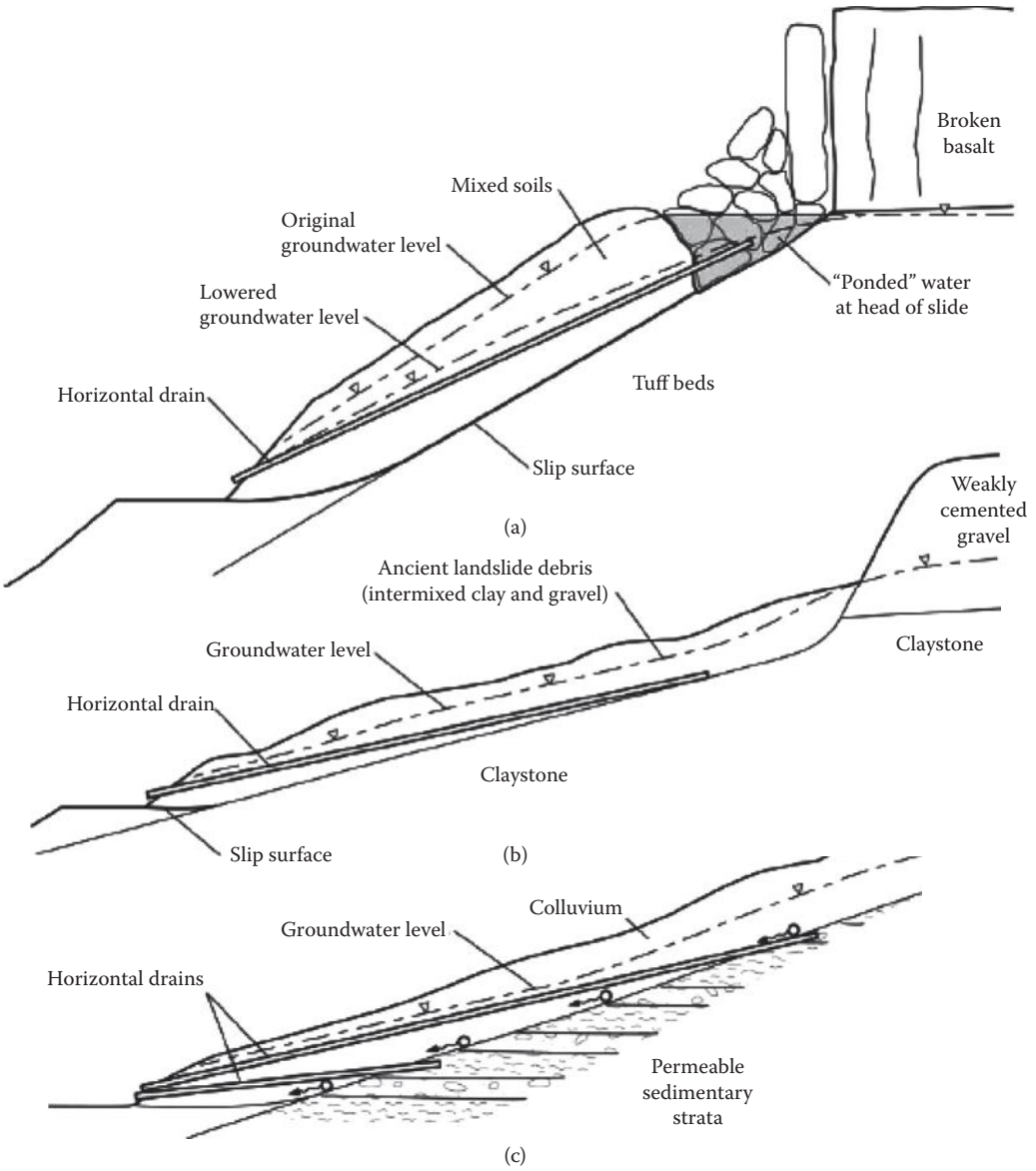

FIGURE 11.13 Examples of geological conditions in which subhorizontal drains may be an appropriate option. (After Cornforth, D., *Landslides in Practice, Investigation, Analysis, and Remedial/Preventative Options in Soils*, Wiley, 2005.)

mass, whereas Case 2 micropiles are an interlocking, three-dimensional network of reticulated piles and are not as heavily reinforced as Case 1 micropiles.

An example of the use of both passive and active systems in the same landslide is shown in Figure 11.26.

Various methods of retaining rock slopes are illustrated in Figures 11.27 and 11.28. All the categories of stabilization treatment for soil slopes have their analogies in rock slopes, but they have different sets of priorities. The most effective techniques for rock slope stabilization are those which increase the strength of discontinuities in the rock mass—anchoring, bolting, and grouting. A comprehensive treatise on the rock slope subject is given by Hoek and Bray (1974) and Fell (1994a).

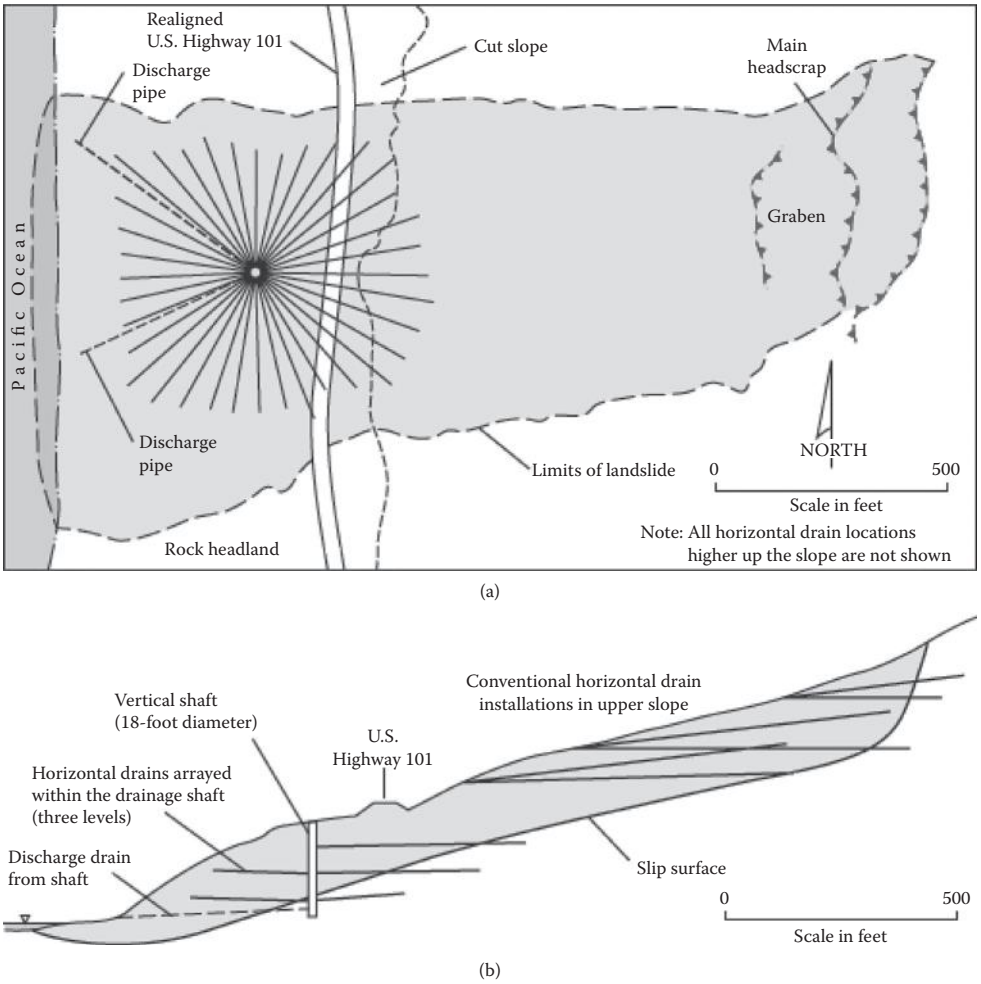

FIGURE 11.14 (a) Plane view and (b) cross section of a vertical shaft and horizontal drains applied to stabilize the Arizona Inn Slide, near Brookings, OR. (After Cornforth, D., *Landslides in Practice, Investigation, Analysis, and Remedial/Preventative Options in Soils*, Wiley, 2005.)

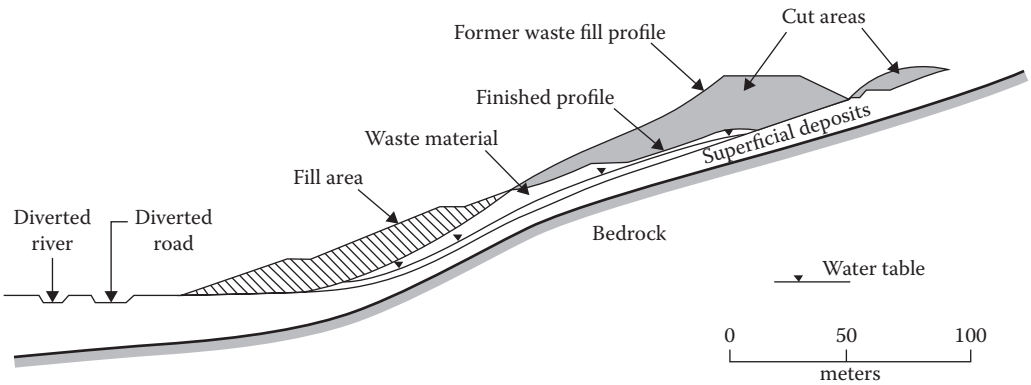

FIGURE 11.15 Slope stabilization by cut and fill. (From Duncan, J.M., and Wright, S.G., *Soil Strength and Slope Stability*, Wiley, 2005. With permission.)

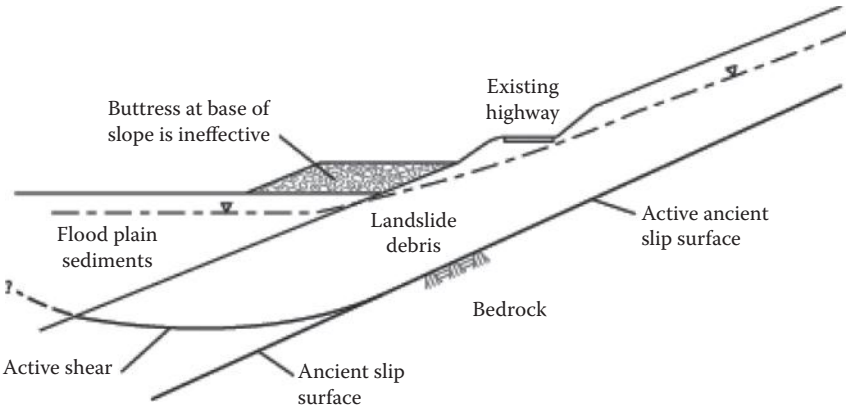

FIGURE 11.16 Ineffective location of a buttress where the slip surface passes deep below the slope base. (After Cornforth, D., *Landslides in Practice, Investigation, Analysis, and Remedial/Preventative Options in Soils*, Wiley, 2005.)

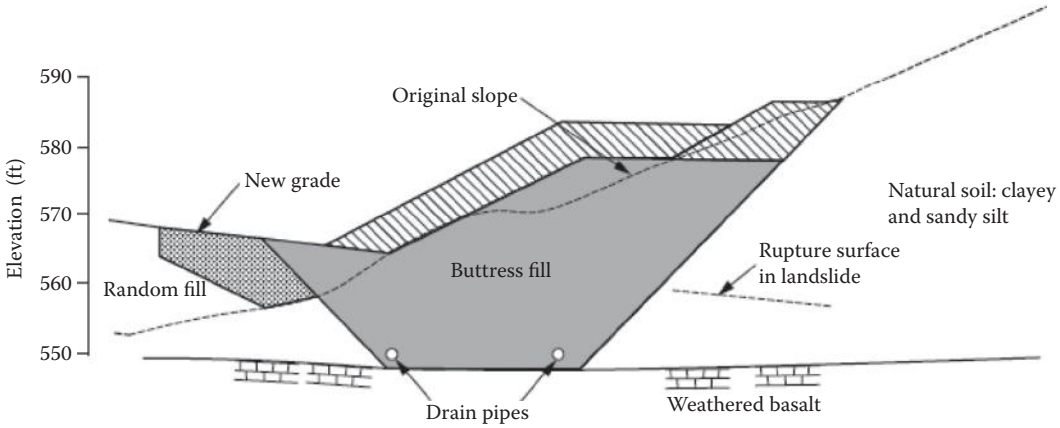

FIGURE 11.17 Buttress for slope stabilization in Portland, OR. (From Duncan, J.M., and Wright, S.G., *Soil Strength and Slope Stability*, Wiley, 2005. With permission.)

11.5.2.3 Nonstructural Measures

During the early part of the post–World War II period, landslides were generally seen to be "engineering problems" requiring "engineering solutions" involving correction by the use of structural techniques. This structural approach initially focused on retaining walls but has subsequently been diversified to include a wide range of more sophisticated techniques including passive piles and piers, cast-in-situ-reinforced concrete walls, and reinforced earth-retaining structures. When properly designed and constructed, these structural solutions can be extremely valuable, especially in areas with high loss potential or in restricted sites. However, fixation with structural solutions has in some cases resulted in the adoption of overly expensive measures that have proven to be less appropriate than alternative approaches involving slope geometry modification or drainage.

Over the last several decades, there has been a notable shift toward "soft engineering," nonstructural solutions, including classical methods such as drainage and modification of slope geometry, but also some novel methods such as lime/cement stabilization, grouting, or soil nailing. The cost of nonstructural remedial measures is considerably lower than the cost of structural solutions. In addition,

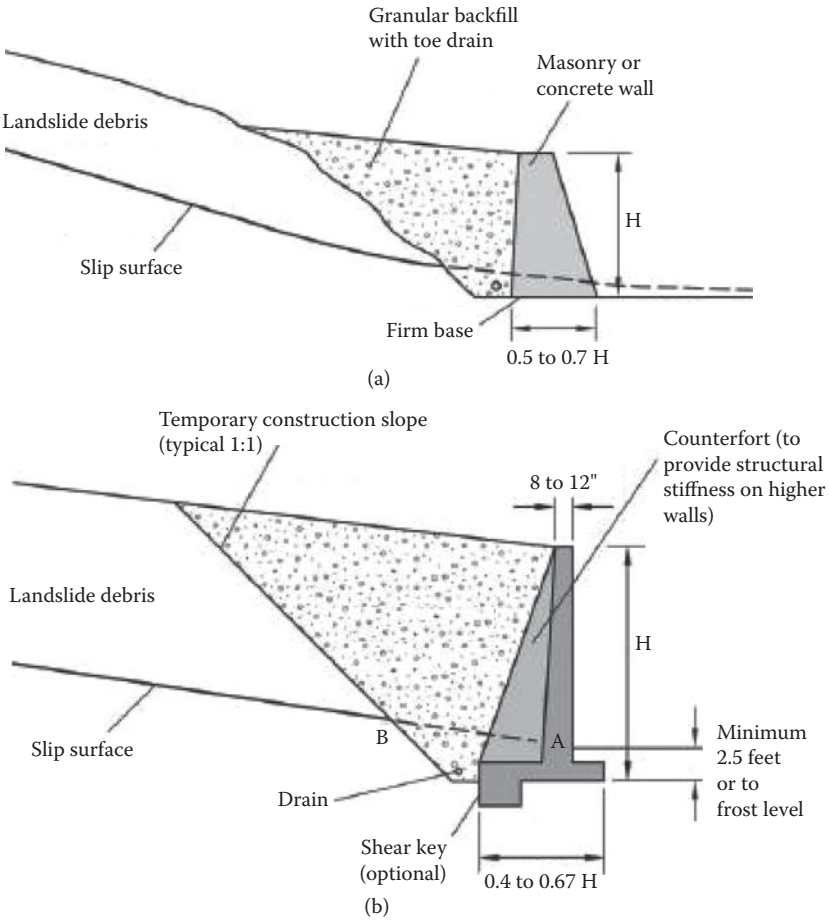

FIGURE 11.18 (a) Concrete or masonry gravity retaining wall and (b) concrete cantilever retaining wall. (After Cornforth, D., *Landslides in Practice, Investigation, Analysis, and Remedial/Preventative Options in Soils*, Wiley, 2005.)

structural solutions, such as retaining walls, involve exposing the slope during construction and often require steep temporary excavations. Both of these operations increase the risk of failure during construction for oversteepening or increased infiltration from rainfall. In contrast, the use of soil nailing as a nonstructural solution to strengthen the slope avoids the need to open or alter the slope from its current condition (Figure 11.29).

Environmental considerations have increasingly become an important factor in the choice of suitable remedial measures, particularly issues such as visual intrusion in scenic areas or the impact on nature or geological conservation interests. An example of a "soft engineering" solution, more compatible with the environment, is the stabilization of slopes by the combined use of vegetation and man-made structural elements working together in an integrated manner known as biotechnical slope stabilization (Schuster, 1995). The basic concepts of vegetative stabilization are not new—vegetation has a beneficial effect on slope stability by the processes of interception of rainfall, and transpiration of groundwater, thus maintaining drier soils and enabling some reduction in potential peak groundwater pressures. In addition to these hydrological effects, vegetation roots reinforce the soil, increasing soil shear strength, while tree roots may anchor into firm strata, providing support to the upslope soil mantle and buttressing and arching. A small increase in soil cohesion induced by the roots has a major

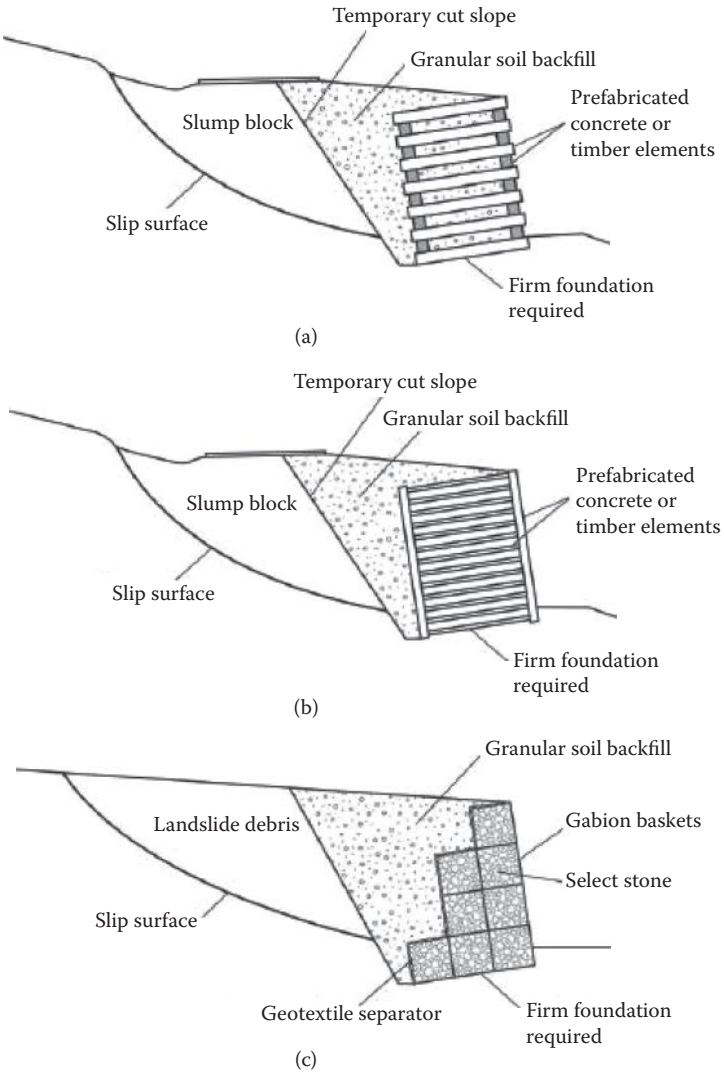

FIGURE 11.19 (a) Crib, (b) bin, and (c) gabion retaining walls. (After Cornforth, D., Landslides in Practice, Investigation, Analysis, and Remedial/Preventative Options in Soils, Wiley, 2005.)

effect on shallow landslides. The mechanical effect of vegetation is not significant for deeper-seated landslides, whereas the hydrological effect is beneficial for both shallow and deep landslides. However, vegetation may not always assist slope stability. Destabilizing forces may be generated by the weight of the vegetation acting as a surcharge and by wind forces acting on the exposed vegetation, although both of these are very minor effects. Roots of vegetation may also act adversely by penetrating and dilating the joints of widely jointed rocks. For detailed information on research into the engineering role of vegetation for slope stabilization, refer to Greenway (1987). In addition, the "Geotechnical Manual for Slopes" (Geotechnical Control Office, 1981) includes an excellent table noting the hydrological and mechanical effects of vegetation.

The concept of biotechnical slope stabilization is generally cost-effective as compared to the use of structural elements alone; it increases environmental compatibility and allows the use of local natural materials. Interstices of the retaining structure are planted with vegetation whose roots bind together the

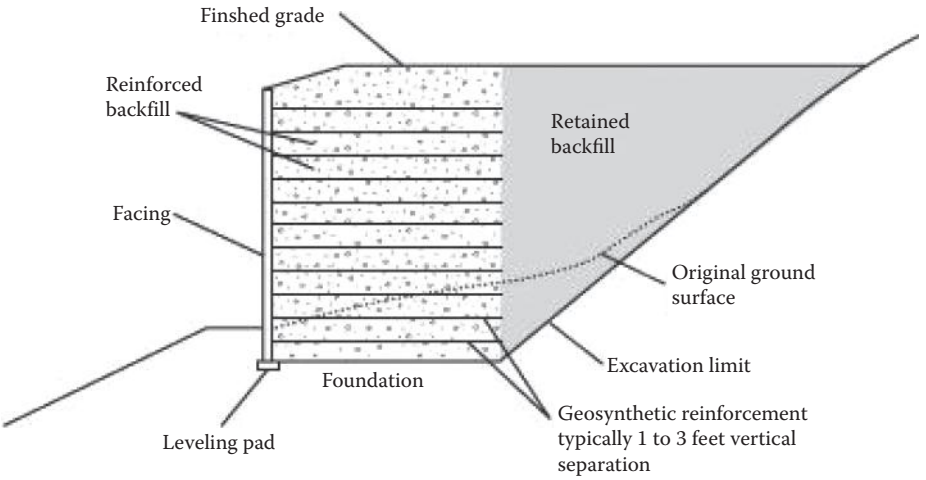

FIGURE 11.20 Mechanically stabilized earth wall. (After Cornforth, D., *Landslides in Practice, Investigation, Analysis, and Remedial/Preventative Options in Soils*, Wiley, 2005.)

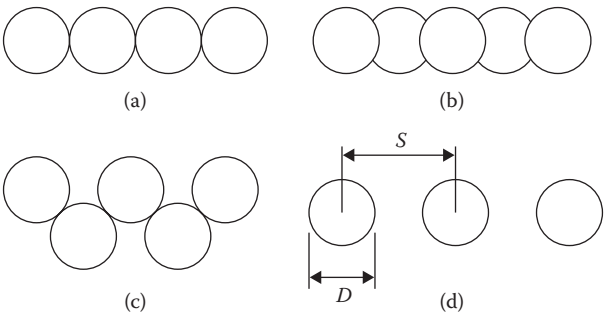

FIGURE 11.21 Reinforced concrete pile arrangements: (a) tangent, (b) secant, (c) staggered, (d) spaced pile walls. (After Cornforth, D., *Landslides in Practice, Investigation, Analysis, and Remedial/Preventative Options in Soils*, Wiley, 2005.)

soil within and behind the structure. The stability of all types of retaining structures with open gridwork or tiered facings benefits from such vegetation. Figure 11.30 shows an example where plants are installed on the level tiers. Tiers offer improvements in slope appearance as compared to linear slopes and are helpful to construction of mechanically stabilized earth walls, soil nail walls, and anchor block walls.

11.5.3 Levels of Effectiveness and Acceptability That May Be Applied in the Use of Remedial Measures

Terzaghi (1950) stated that, "if a slope has started to move, the means for stopping movement must be adapted to the processes which started the slide." For example, if erosion is a causal process of the slide, an efficient remediation technique would involve armoring the slope against erosion or removing the source of erosion. An erosive spring can be made nonerosive by either blanketing with filter materials or drying up the spring with horizontal drains, and so on.

The greatest benefit in understanding landslide-producing processes and mechanisms lies in the use of the above understanding to anticipate and devise measures to minimize and prevent major landslides.

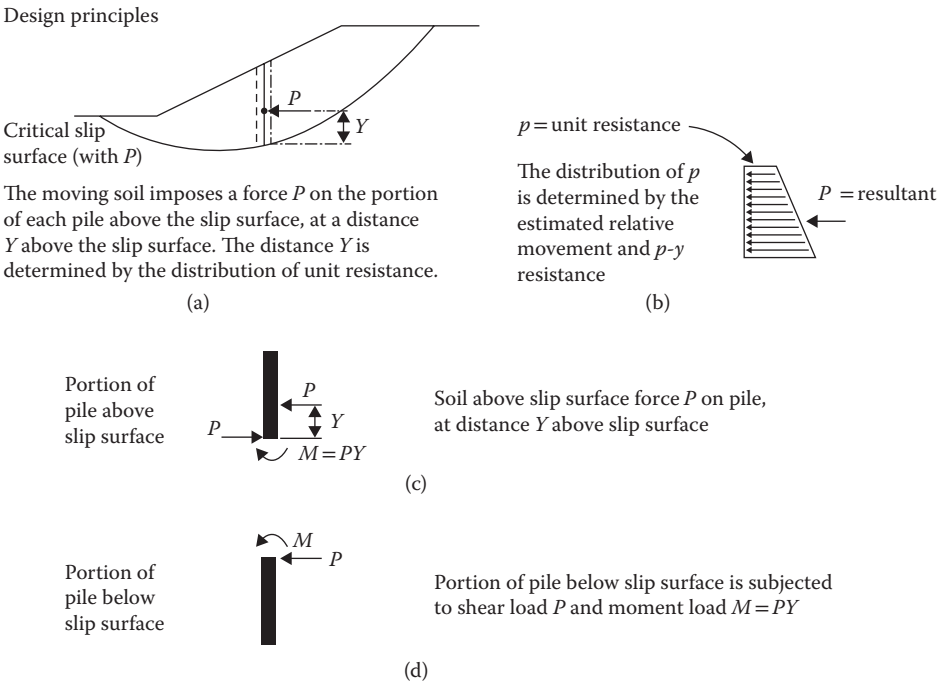

FIGURE 11.22 (a) Design principles for stabilizing a slope with piles; (b) unit resistance p and resultant P_{pile}; (c) portion of pile above slip surface; (d) portion of pile below slip surface. (After Duncan, J.M., and Wright, S.G., *Soil Strength and Slope Stability*, Wiley, 2005.)

The term major should be underscored here because it is neither possible nor feasible, nor even desirable, to prevent all landslides. There are many examples of landslides that can be handled more effectively and at less cost after they occur. Landslide avoidance through selective locationing is obviously desired—even required—in many cases, but the dwindling number of safe and desirable construction sites may force more and more the use of landslide-susceptible terrain.

Selection of an appropriate remedial measure depends on (1) engineering feasibility, (2) economic feasibility, (3) legal/regulatory conformity, (4) social acceptability, and (5) environmental acceptability. A brief description of each method is presented herein:

1. Engineering feasibility involves analysis of geologic and hydrologic conditions at the site to ensure the physical effectiveness of the remedial measure. An often-overlooked aspect is being certain that the design will not merely divert the problem elsewhere.
2. Economic feasibility takes into account the cost of the remedial action as composed to the benefits it provides. These benefits include deferred maintenance, avoidance of damage (including loss of life), and other tangible and intangible benefits.
3. Legal–regulatory conformity provides for the remedial measure meeting local building codes, avoiding liability to other property owners, and related factors.
4. Social acceptability is the degree to which the remedial measure is acceptable to the community and neighbors. Some measures for a property owner may prevent further damage but be an unattractive eyesore to neighbors.
5. Environmental acceptability addresses the need for the remedial measure to not adversely affect the environment. Dewatering a slope to the extent that it no longer supports a unique plant community may not be an environmentally acceptable solution.

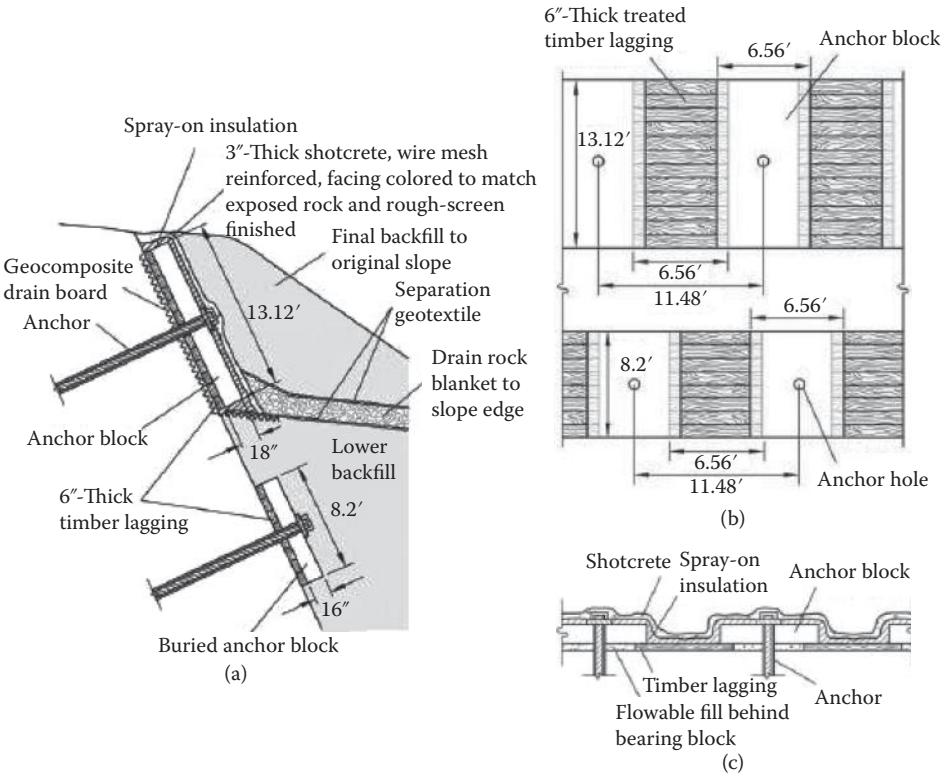

FIGURE 11.23 Richardson Highway Slide remediation. Lower anchor block wall: (a) section, (b) elevation, and (c) plan showing outer protection. (After Cornforth, D., *Landslides in Practice, Investigation, Analysis, and Remedial/Preventative Options in Soils*, Wiley, 2005.)

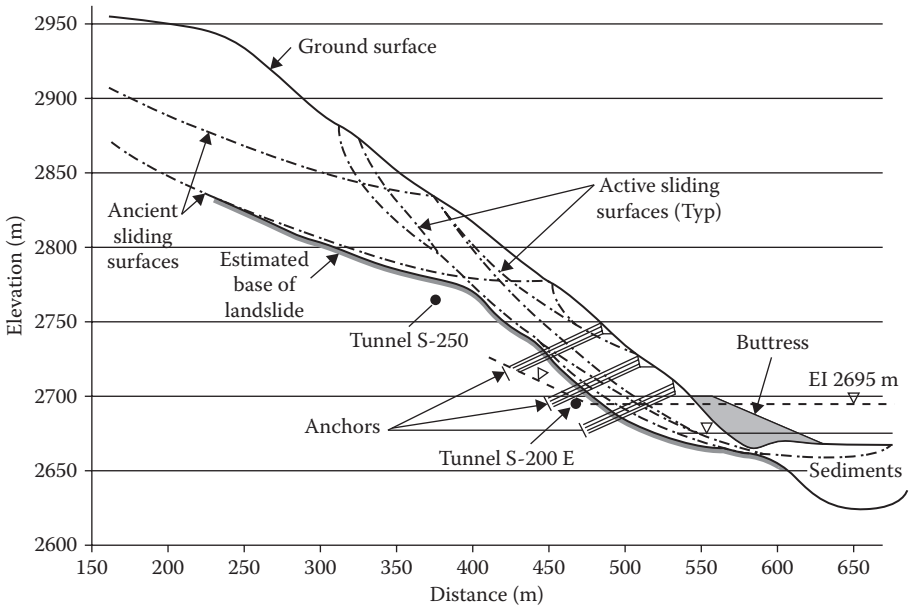

FIGURE 11.24 Landslide repair of Tablachaca Dam. (From Duncan, J.M., and Wright, S.G., *Soil Strength and Slope Stability*, Wiley, 2005. With permission.)

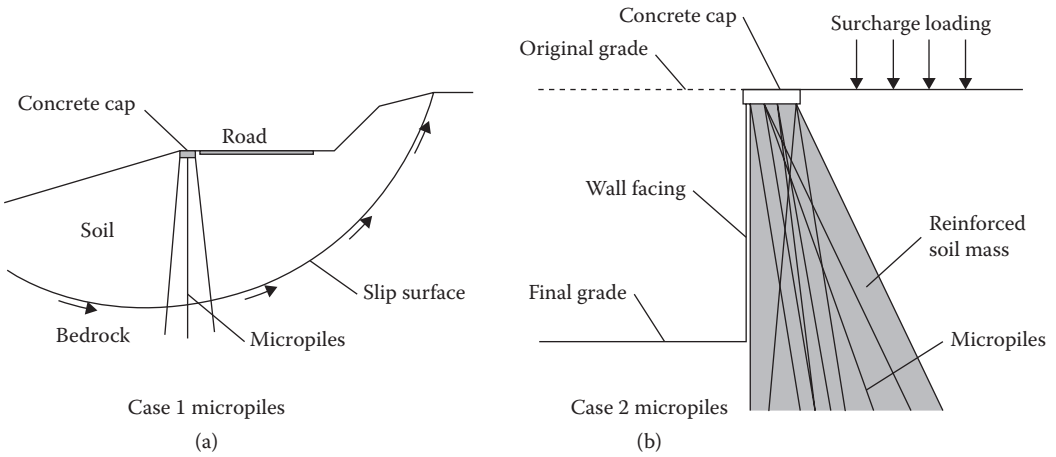

FIGURE 11.25 Slope stabilization with micropiles: (a) Case 1—slip surface reinforcement; (b) Case 2—reticulated pile soil mass reinforcement. (After Cornforth, D., *Landslides in Practice, Investigation, Analysis, and Remedial/Preventative Options in Soils*, Wiley, 2005.)

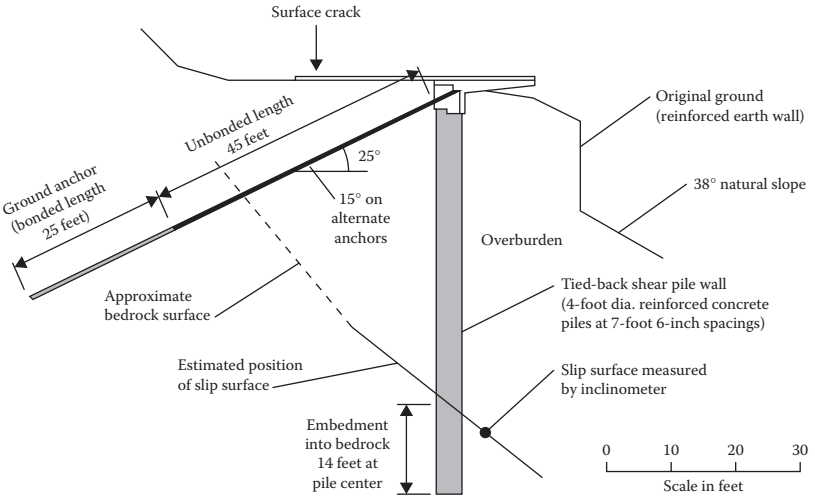

FIGURE 11.26 Tied-back anchor shear piles (Goat Lick Slide, Essex, Montana). (After Cornforth, D., *Landslides in Practice, Investigation, Analysis, and Remedial/Preventative Options in Soils*, Wiley, 2005.)

Just as there are a number of available remedial measures, so are there a number of levels of effectiveness and levels of acceptability that may be applied in the use of these measures. We may have a landslide, for example, that we choose to live with. Although this type of landslide poses no significant hazard to the public, it will require periodic maintenance through removal due to occasional encroachment onto the shoulder of a roadway. The permanent closure of the Manchester–Sheffield road at Mam Tor in 1979 (Skempton et al., 1989) and the decision not to reopen the railway link to Killin following the Glen Ogle rockslide in the United Kingdom (Smith, 1984) are well-known examples of abandonment due to the effects of landslides in which repair was considered uneconomical.

Most landslides, however, usually must be dealt with sooner or later. How they are handled depends on the processes that prepared and precipitated the movement, the landslide type, the kinds of materials involved, the size and location of the landslide, the place or components affected by or the situation

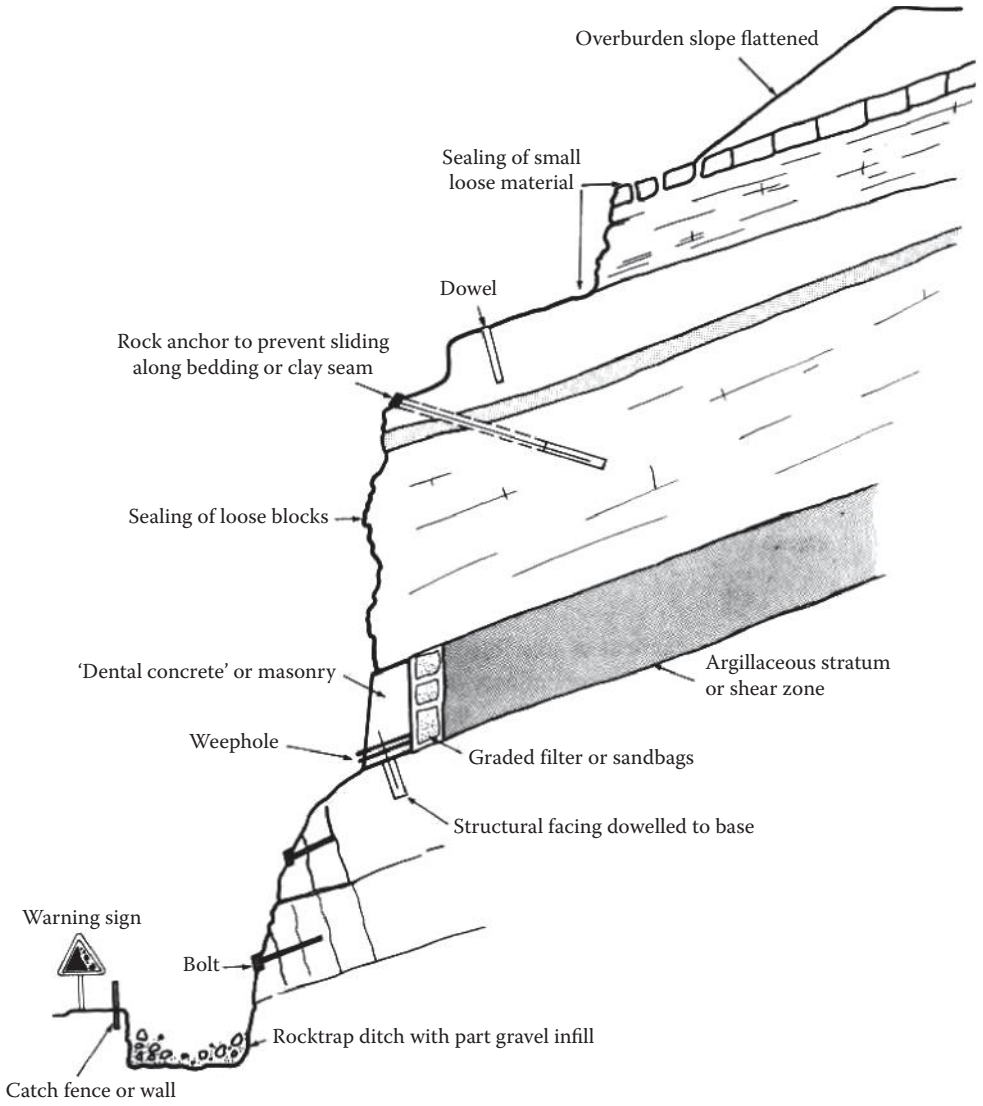

FIGURE 11.27 Rock slope stabilization methods (After Bromhead, E.N., *Slope Stability. 2nd Edition*, Blackie Academic & Professional, London, 411, 1992.)

created as a result of the landslide, available resources, and so on. The technical solution must be in harmony with the natural system, otherwise the remedial work will be either short-lived or excessively expensive. In fact, landslides are so varied in type and size, and in most instances, so dependent upon special local circumstances that for a given landslide problem, there is more than one method of prevention or correction that can be successfully applied. The success of each measure depends, to a large extent, on the degree to which the specific soil and groundwater conditions are prudently recognized in an investigation and incorporated in design.

As many of the geological features, such as sheared discontinuities are not known in advance, it is more advantageous to plan and install remedial measures on a "design-as-you-go basis." That is, the design has to be flexible enough to accommodate changes during or subsequent to the construction of remedial works.

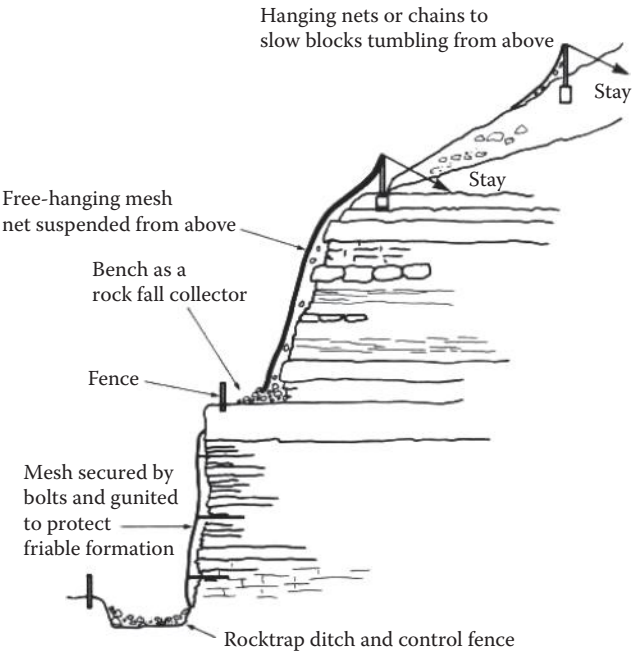

FIGURE 11.28 Rockfall stabilization methods. (After Bromhead, E.N., *Slope Stability. 2nd Edition*, Blackie Academic & Professional, London, 411, 1992.)

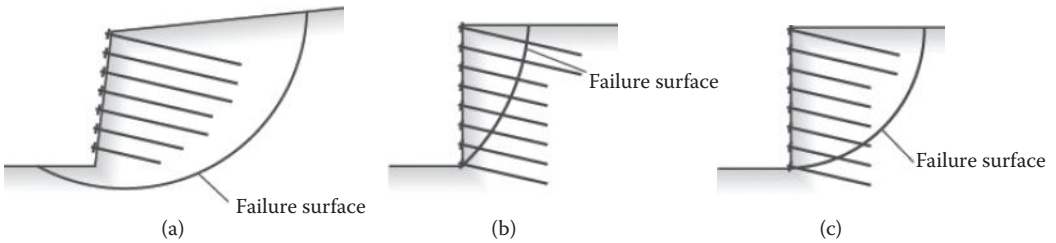

FIGURE 11.29 Potential failure surfaces that need to be studied in soil nail design: (a) external failure, (b) internal failure, and (c) mixed failure. (After Cornforth, D., *Landslides in Practice, Investigation, Analysis, and Remedial/Preventative Options in Soils*, Wiley, 2005.)

11.6 Landslide Monitoring and Warning Systems

11.6.1 Landslide Monitoring

Monitoring of landslides plays an increasingly important role in the context of living and coping with these natural hazards. The classical methods of land surveys, inclinometers, extensometers, and piezometers are still the most appropriate monitoring measures. In the future, the emerging techniques based on remote sensing and remote access techniques will undoubtedly be of main interest.

The Department of Environment (1994) has identified the following categories of monitoring, designed for slightly differing purposes but generally involving similar techniques:

1. *Preliminary monitoring* involves provision of data on preexisting landslides so that the dangers can be assessed and remedial measures can be properly designed or the site be abandoned.
2. *Precautionary monitoring* is carried out during construction to ensure safety and to facilitate redesign, if necessary.

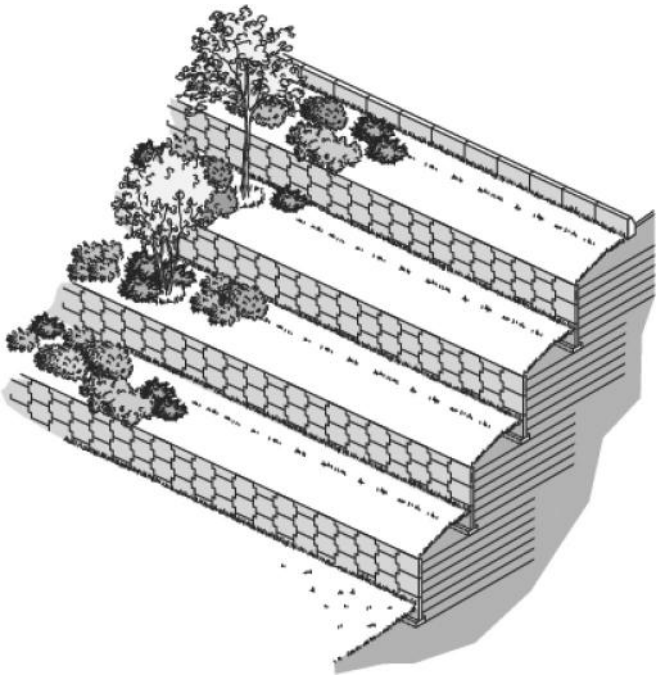

FIGURE 11.30 Tiered retaining structure of mechanically stabilized earth with landscaped benches. (After Cornforth, D., *Landslides in Practice, Investigation, Analysis, and Remedial/Preventative Options in Soils*, Wiley, 2005.)

3. *Postconstruction monitoring* is considered to check on the performance of stabilization measures and to focus attention on problems that require remedial measures.

Observational methods based on careful monitoring—before, during, and after construction—are essential in achieving reliable and cost-effective remedial measures.

11.6.2 Landslide Warning Systems

When dealing with a slope of precarious stability and/or presenting a risk that is considered too high, a possible option is to do nothing in regard to mitigation, but to install a warning system to insure or improve the safety of people. It is worth noting that warning systems do not modify the hazard but contribute to reducing the consequences of the landslide and thus the risk, in particular the risk associated to the loss of life.

Various types of warning systems have been proposed, and the selection of an appropriate one should take into account the stage of landslide activity:

1. At prefailure stage, the warning system can be applied either to revealing factors or to triggering or aggravating factors. Revealing factors can be, for example, the opening of fissures or the movement of given points on the slope; in such cases, the warning criterion will be the magnitude or rate of movement. When the warning system is associated with triggering or aggravating factors, there is a need to first define the relation between the magnitude of factors controlling the stability condition or the rate of movement of the slope. The warning criterion can be a given hourly rainfall or the cumulative rainfall during a certain period of time, increased pore water pressure, a given stage of erosion, a minimum negative pore pressure in a loess deposit, and so on.
2. At failure stage, the warning system can only be linked to revealing factors, generally a sudden acceleration of movements or the disappearance of a target.

3. At postfailure stage, the warning system has to be associated to the expected consequences of the movement. It is generally associated with the rate of movement and runout distance.

Leroueil (1996) defined the following four possible different stages of landslide activity:

1. Prefailure stage when the soil mass is still continuous. This stage is mostly controlled by progressive failure and creep.
2. Onset of failure characterized by the formation of a continuous shear surface through the entire soil or rock mass.
3. Postfailure stage, which includes movement of the soil or rock mass involved in the landslide from just after failure until it essentially stops.
4. Reactivation stage when the soil or rock mass slides along one or several preexisting shear surfaces. This reactivation can be occasional or continuous with seasonal variations of the rate of movement.

The majority of remedial measures, outlined above, can be cost-prohibitive and may be socially and politically unpopular. As a result, there may be a temptation to adopt and rely instead upon the installation of apparently cheaper and much less disruptive monitoring and warning systems to "save" the population from future catastrophes. However, for such an approach to be successful, it is necessary to fulfill satisfactorily each of the following steps (Hutchinson, 2001):

1. The monitoring system shall be designed to record the relevant parameters, to be in the right places, and to be sound in principle and effective in operation.
2. The monitoring results need to be assessed continuously by suitable experts.
3. A viable decision shall be made, with a minimum of delay, that the danger point has been reached.
4. The decision should be passed promptly to the relevant authorities, with a sufficient degree of confidence and accuracy regarding the forecast place and time of failure for those authorities to be able to act without fear of raising a false alarm.
5. Once the authorities decide to accept the technical advice, they must pass the warning onto the public in a way that will not cause panic and possibly exacerbate the situation.
6. The public needs to be well-informed and prepared in advance to respond in an orderly and prearranged manner.

In view of the preceding discussion, it is not surprising that, although there have been a few successes with monitoring and warning systems, particularly in relatively simple, site-specific situations, there have been many cases where these have failed, because one or more of requirements (1) through (6) above have been violated, often with tragic and extensive loss of life. It is concluded, therefore, that sustained good management of an area, as outlined above, should be our primary response to the threat of landslide hazards and risks, with monitoring and warning systems being in a secondary, supporting role.

11.6.3 Forecasting the Time of Landslides

Landslides are very complex phenomena and are difficult to predict. They involve materials ranging over many orders of magnitudes in size, from fine-grained particles to masses of earth/rock of several cubic kilometers. The velocity of mass movements also varies over a wide range, from creeping movements of millimeter per year to extremely rapid avalanches that travel at several hundred kilometers per hour (Cruden and Varnes, 1996). Moreover, they span the geologic–hydrologic interface from completely dry materials to viscous fluid type flows. As a result, forecasting the time of landslides remains a crucial and still an unresolved problem.

Landslide prediction can be classified as long term, intermediate term, or short term (Hamilton, 1997). Long-term prediction of landslides is typically attained via landslide hazard maps, which are actually susceptibility maps, for large areas. As mentioned previously, these maps contribute to assessments of

long-term characteristics and warning of landslide hazards; hence, they provide a framework for identifying the need for additional data, and effective mitigation techniques, along with zoning or land-use planning (United Nations, 1996).

Landslide monitoring is considered to provide the necessary data that can be used for intermediate-term prediction. Appearance of cracks, fluctuation of moisture in soils, and acceleration of surface or subsurface movements provide precursory evidence of landslide movement. Specifically, the acceleration of surface or subsurface movements enables the most direct detection of impending landsliding (Voight and Kennedy, 1979).

Monitoring, described above, entails compilation of meteorological, hydrological, topographical, and geophysical data. The advent of automatic sampling, recording, and transmitting devices has enabled practical prediction of landslide movements (Hamilton, 1997). Although prediction of landslide movement, based on interaction between climate and slope movement, is a daunting task at this time, it may become more viable in the future due to ongoing research and monitoring of regional weather patterns.

Among approaches to the mitigation of landslide risk, the prediction of the time of occurrence for a first-time landslide deserves special consideration (Saito, 1965). The task is far from being simple because the fundamental physics controlling the nature and shape of the creep curve of geomaterials has not been fully elucidated yet. Moreover, all the relevant parameters and boundary conditions are not clearly defined, and it is impossible to forecast the triggering factors originating outside the sliding mass (e.g., heavy rainfall). An important key to the prediction of landslide failure time should be the stress–strain–time relations, but the heterogeneity of the geological conditions, groundwater seepage conditions, associated pore water pressures on the potential sliding surface, and scale effects make the laboratory evaluation of the geomechanical parameters barely adequate for the simulation of the temporal evolution of a potential slide using numerical models.

Several methods have been proposed for the prediction concerning the time of occurrence of landslides. In engineering practice, such methods, that infer the time to failure by means of monitored surface displacements, are preferred for a prediction, given that they remove all uncertainties involved in these problems. One of the first, most spectacular and well-documented predictions of slope failure, based upon displacement monitoring, was carried out at the Chuquicamata mine in Chile (Kennedy and Niermeyer, 1970): the date of failure was exactly predicted by means of a rough extrapolation of displacement data. Hoek and Bray (1977) pointed out that the circumstance is not of great importance; in fact, from the point of view of an engineer, even a prediction with an error of few weeks is reasonable and helps in making decisions. As a consequence, one may state that the key to the prediction is the correct choice and a good monitoring of the relevant physical factors, rather than the principle selected for inferring the time to failure.

Regardless of the technique used for extrapolating the time to failure, the quality of the prediction depends on the quality of the data, so that a clear identification of the critical points or variables selected for monitoring is strongly required to get a consistent prediction. This entails the need for developing of an understanding of prefailure deformations and other precursory signs of different landslides mechanisms. Accordingly, the help offered by slope monitoring methods, particularly global positioning system and time domain reflectometry, can be noticeable. For some methods, the frequency of observation seems to condition the effectiveness of the prediction, as well as the extent of the time span of data collection (i.e., the monitoring system should be installed as soon as possible). The observation needs also to be extended to other parameters, different than displacements, such as pore pressure or crack aperture.

11.7 Concluding Remarks

Assessing the landslide hazard is the most important step in landslide risk management. Once that has been done, it is feasible to assess the number, size, and vulnerability of the fixed elements at risk (structures, roads, railways, pipelines, etc.), and thence the damage they will suffer. The various risks have to be combined to arrive at a total risk in financial terms. Comparison of this with, for instance,

cost–benefit studies of the cost of relocation of facilities, or mitigation of the hazard by countermeasures, provides a useful tool for management and decision making.

Sites where there is undue risk from landslides to communities and infrastructure should be identified and ranked using well-established methods of landslide hazard and landslide risk analysis and then to mitigate these risks appropriately and effectively. The necessary actions should be taken as soon as possible, while there is yet time.

It should be emphasized that these include not only various direct measures, such as relocation of infrastructure or slide stabilization, but also "good housekeeping" of the region as a whole, as for example, sustained, ecologically sensitive management of land use, sound planning, obtaining information, making emergency arrangements, and so on. In Hong Kong, such approaches have had dramatic success, reducing the average rate of landslide fatalities per year per person to 5×10^{-7}, a tenth of what it was before the introduction of a slope–safety regime (through what is now the Geotechnical Engineering Office) in late 1972 (Powel, 1992).

A pragmatic approach of living with landslides and reducing the impact of landslide problems in urban areas is well illustrated by the strategy adopted to cope with landslide problems at Ventnor, Isle of Wight, United Kingdom (Lee et al., 1991). Ventnor is an unusual situation in that the entire town lies within an ancient landslide complex. The spatial extent and scale of the problems at Ventnor has indicated that total avoidance or abandonment of the site are out of question, and large-scale conspicuous engineering structures would be unacceptable in a town dependent on tourism. Instead, coordinated measures have been adopted to limit the impacts of human activity that promote ground instability by planning control, control of construction activity, preventing water leakage, and improving building standards. In addition, good maintenance practice by individual homeowners proved to be a significant help, because neglect could have resulted in localized instability problems.

Much progress has been made in developing techniques to minimize the impact of landslides, although new, more efficient, quicker, and cheaper methods could well emerge in the future. There are a number of levels of effectiveness and levels of acceptability that may be applied in the use of these measures, for, while one slide may require an immediate and absolute long-term correction, another may only require minimal control for a short period.

Whatever the measure chosen, and whatever the level of effectiveness required, the geotechnical engineer and engineering geologist have to combine their talents and energies to solve the problem. Solving landslide-related problems is changing from what has been predominantly an art to what may be termed an art-science. The continual collaboration and sharing of experience by engineers and geologists will no doubt move the field as a whole closer toward the science end of the art–science spectrum than it is at present.

References

Abramson, L.W., Lee, T.S., Sharma, S., and Boyce, G.M. 2001. *Slope Stability and Stabilization Methods. 2nd Edition*, John Wiley and Sons, New York, NY.

AGS. 2000. *Landslide Risk Management Concepts and Guidelines*, Sub-Committee on Landslide Risk Management, Australian Geomechanics Society, St Ives, Australia, pp. 49–92.

Bromhead, E.N. 1992. *Slope Stability. 2nd Edition*, Blackie Academic & Professional, London, 411 pp.

Chowdhury, R., Flentje, P., and Ko Ko, C. 2001. "A Focus on Hilly Areas Subject to the Occurrence and Effects of Landslides," *Global Blueprint for Change*, 1st Edition—Prepared in conjunction with the International Workshop on Disaster Reduction, August 19–22, 2001.

Cornforth, D. 2005. *Landslides in Practice, Investigation, Analysis, and Remedial/Preventative Options in Soils*, Wiley, Hoboken, New Jersey, NJ.

Crozier, M.J. 1986. *Landslides—Causes, Consequences and Environment*, Croom Helm, London.

Cruden, D.M. 1991. "A Simple Definition of a Landslide," *Bulletin International Association of Engineering Geology*, 43, 27–29.

Cruden, D.M. 1997. "Estimating the Risks from Landslides Using Historical Data," In *Landslide Risk Assessment*, Cruden, D.M., and Fell, R. (eds.), Balkema, Rotterdam, The Netherlands, pp. 277–284.

Cruden, D.M., and Varnes, D.J. 1996. "Landslide Types and Processes," In *Landslides Investigation and Mitigation*, Turner, A.K., and Schuster, R.L. (eds.), Transportation Research Board Special Report 247, National Research Council, Washington, DC.

Department of Environment. 1994. *Landsliding in Great Britain*, Jones, D.K.C., and Lee, E.M. (eds)., HMSO, London.

Duncan, J.M. 1996. "Soil Slope Stability Analysis," Chapter 13 In *Landslides—Investigation and Mitigation*, Turner, A.K., and Schuster, R.L., (eds.), Transportation Research Board Special Report 247, National Research Council, National Academy Press, Washington, DC, pp. 337–371.

Duncan, J.M., and Wright, S.G. 2005. *Soil Strength and Slope Stability*, Wiley, Hoboken, New Jersey, NJ.

Einstein, H.H. 1988. "Landslide Risk Assessment Procedure," In Proceedings of the 5th International Symposium on Landslides, Lausanne, Switzerland, Balkema, Rotterdam, The Netherlands, 2, 1075–1090.

Einstein, H.H. 1997. "Landslide Risk—Systematic Approaches to Assessment and Management," In *Landslide Risk Assessment*, Cruden, D.M., and Fell, R. (eds.), Balkema, Rotterdam, The Netherlands, pp. 25–50.

Fell, R. 1994a. "Stabilization of Soil and Rock Slopes," In Proceedings of East Asia Symposium and Field Workshop on Landslides and Debris Flows, Seoul, 1, 7–74.

Fell, R. 1994b. "Landslide Risk Assessment and Acceptable Risk," *Canadian Geotechnical Journal*, 31(2), 261–272.

Fellenius, W. 1936. "Calculation of the Stability of Earth Dams," Transactions of the 2nd Congress on Large Dams, International Commission on Large Dams of the World Power Conference, Washington, D.C, 4, 445–462.

Geotechnical Control Office. 1981. *Geotechnical Manual for Slopes*, Public Works Department, Hong Kong.

Greenway, D. R. 1987. Vegetation and slope stability, In *Slope Stability Geotechnical Engineering and Geomorphology,* Anderson, M.G., and Richards, K.S., (eds.), John Wiley & Sons, Chichester, UK, pp. 187–230.

Hamilton, R. 1997. *Report on Early Warning Capabilities for Geological Hazards*, International Decade for Natural Disaster Reduction (IDNDR) Secretariat, Geneva, http://www.unisdr.org/unisdr/docs/early/geo/geo.htm, accessed on October, 8, 2003.

Hoek, E., and Bray, J.M. 1974. *Rock Slope Engineering*, Institute of Mining and Metallurgy, London.

Hoek, E., and Bray, J.M. 1977. *Rock Slope Engineering*, Institute of Mining and Metallurgy, London.

Hutchinson, J.N. 1977. "The Assessment of the Effectiveness of Corrective Measures in Relation to Geological Conditions and Types of Slope Movement." *Bulletin of International Association of Engineering Geology*, 16, 131–155.

Hutchinson, J.N. 2001. "Landslide Risk—To Know, to Foresee, to Prevent," *Journal of Technical and Environmental Geology*, 3, 3–22.

Janbu, N. 1954. *Stability Analysis of Slopes with Dimensionless Parameters*, Harvard Soil Mechanics Series 46, Harvard University Press, Cambridge, MA.

Kelly, J.M.H., and Martin, P.L. 1986. "Construction Works on or Near Landslides," In Proceedings of the Symposium of Landslides in South Wales Coalfield, Polytechnic of Wales, pp. 85–103.

Kennedy B.A., and Niermeyer, K.E. 1970. "Slope Monitoring System Used in the Prediction of a Major Slope Failure at the Chuquicamata Mine, Chile," In Proceedings of the Symposium on Planning Open Pit Mines, Johannesburg, pp. 215–225.

Krahn, J. 2003. "The 2001 R.M. Hardy Lecture: The Limits of Limit Equilibrium Analyses," *Canadian Geotechnical Journal*, 40(3), 643–660.

Krahn, J. 2004. *Stability Modeling with Slope/W. An Engineering Methodology*, Geo-Slope/W International Ltd., Calgary, Alberta, Canada, 396 pp.

Kramer, S.L. 1996. *Geotechnical Earthquake Engineering*, Prentice-Hall, Upper Saddle River, NJ.

Lee, E.M., Moore, R., Burt, N., and Brunsden, D. 1991. "Strategies for Managing the Landslide Complex at Ventnor, Isle of Wight," In Proceedings of the International Conference on Slope Stability Engineering, Isle of Wight, Thomas Telford, London, pp. 219–225.

Leroueil, E. 1996. "Landslide Hazard—Risk Maps at Different Scales: Objectives, Tools and Developments," In Proceedings of the International Symposium on Landslides, Trondheim, June 17–21, (Senneset, K., [Ed.]), pp. 35–52.

Leroueil, S., and Tavenas, F. 1981. "Pitfalls of back-analyses," In Proceedings of the 10th International Conference on Soil Mechanics and Foundation Engineering, 1, 185–190.

Newmark, N.M. 1965. "Effects of Earthquakes on Dams and Embankments," *Géotechnique*, 15(2), 139–159.

Popescu, M.E. 1984. "Landslides in Overconsolidated Clays as Encountered in Eastern Europe," State-of-the-Art Report," In Proceedings of the 4th International Symposium on Landslides, Toronto, ON, pp. 83–106.

Popescu, M.E. 1991. "Landslide control by means of a row of piles. Keynote paper." In Proceedings of the International Conference on Slope Stability Engineering, Isle of Wight, Thomas Telford, pp. 389–394.

Popescu, M.E. 1996. "From Landslide Causes To Landslide Remediation, Special Lecture," In Proceedings of the 7th International Symposium on Landslides, Trondheim, 1, 75–96.

Popescu, M.E. 2001. "A Suggested Method for Reporting Landslide Remedial Measures," *International Association of Engineering Geology Bulletin*, 60(1), 69–74.

Popescu, M.E., Schaefer V.R. 2008. "Landslide stabilizing piles: a design based on the results of slope failure back analysis," In Proceedings of the 10th International Symposium on Landslides and Engineered Slopes, Xi'an, China, pp. 1787–1793

Popescu, M.E., and Seve, G. 2001. "Landslide Remediation Options After the International Decade for Natural Disaster Reduction (1990–2000)," Keynote Lecture, In Proceedings of the Conference Transition from Slide to Flow—Mechanisms and Remedial Measures, ISSMGE TC-11, Trabzon, pp. 73–102.

Popescu, M.E., and Yamagami, T. 1994. "Back analysis of slope failures—A possibility or a challenge?", In Proceedings of the 7th Congress International Association of Engineering Geology, Lisbon, 6, 4737–4744.

Powel, G.E. 1992. "Recent Changes in the Approach to Landslip Preventive Works in Hong Kong," In Proceedings of the 6th International Symposium on Landslides, Christchurch, 3, 1789–1795.

Saito, M. 1965. "Forecasting the time of occurrence of slope failure," In Proceedings of 6th International Congress of Soil Mechanics and Foundation Engineering, Montreal, Canada, 2, 537–541.

Saito, M. 1980. "Reverse calculation method to obtain c and φ on a slip surface," In Proceedings of the International Symposium on Landslides, New Delhi, 1, 281–284.

Schuster, R.L. 1995. "Recent Advances in Slope Stabilization," Keynote paper. In Proceedings of the 6th International Symposium on Landslides, Christchurch, 3, 1715–1746.

Schuster, R.L. 1996. "Socioeconomic Significance of Landslides," Chapter 2 In *Landslides—Investigation and Mitigation*, Turner, A.K., and Schuster, R.L., (eds.), Transportation Research Board Special Report 247, National Research Council, National Academy Press, Washington, DC, pp. 12–31.

Skempton, A.W., Leadbeater, A.D., and Chandler, R.J. 1989. "The Mam Tor Landslide, North Derbyshire." *Philosphical Transactions of the Royal Society*, London, 329(1607), 503–547.

Smith, D.I. 1984. "The Landslips of the Scottish Highlands in Relation to Major Engineering Projects." British Geological Survey Project 09/LS. Unpublished report for the Department of Environment.

Soeters, R., and van Westen, C.J. 1996. "Slope Instability Recognition, Analysis, and Zonation," In *Landslides: Investigations and Mitigation*, Turner, A.K., Schuster, R.L. (eds.), Transportation Research Board Special Report 247, National Research Council, Washington, DC, pp. 129–177.

Taylor, D.W. 1937. "Stability of Earth Slopes," *Journal of the Boston Society of Civil Engineers*, 24(3). Reprinted in Contributions to Soil Mechanics, 1925–1940, Boston Society of Civil Engineers, Boston, MA, 1940, pp. 337–386.

Terzaghi, K. 1950. Mechanisms of landslides, In *Application of Geology to Engineering Practice, Berkley Volume*, Savage, J.L. et al., (eds.) Geological Society of America, Boulder, Colorado, pp. 83–123.

Trandafir, A.C., and Sassa, K. 2004. "Newmark Deformation Analysis of Earthquake-Induced Catastrophic Landslides in Liquefiable Soils," In Proceedings of the 9th International Symposium on Landslides, Rio de Janeiro, Volume 1, Balkema, Rotterdam, The Netherlands, pp. 723–728.

Trandafir, A.C., and Sassa, K. 2005. "Seismic triggering of catastrophic failures on shear surfaces in saturated cohesionless soils," *Canadian Geotechnical Journal*, 42(1), 229–251.

Transportation Research Board. 1996. "Landslides: Investigation and Mitigation," Transportation Research Board Special Report 247, 1996. (Various contributing authors)

United Nations. 1996. "Mudflows—Experience and Lessons Learned from the Management of Major Disasters," *United Nations Department of Humanitarian Affairs*, New York, 139 pp.

Varnes, D.J. 1978. "Slope Movements and Types and Processes," In *Landslides Analysis and Control*, Transportation Research Board Special Report 176, pp. 11–33.

Voight, B., and Kennedy, B.A. 1979. "Slope failure of 1967–1969, Chuquicamata Mine, Chile," In *Rockslides and Avalanches*, Elsevier, Amsterdam, 2, 595–632.

Working Party on World Landslide Inventory (WP/WLI): International Geotechnical Societies' UNESCO Working Party on World Landslide Inventory, Cruden, D.M., Chairman. 1991. "A Suggested Method for a Landslide Summary," *International Association of Engineering Geology Bulletin*, 43, 101–110.

Working Party on World Landslide Inventory (WP/WLI): International Geotechnical Societies' UNESCO Working Party on World Landslide Inventory. Working Group on Landslide Causes, Popescu, M.E., Chairman. 1994. "A Suggested Method for Reporting Landslide Causes," *International Association of Engineering Geology Bulletin*, 50, 71–74.

Zaruba, Q., and Mencl, V. 1982. *Landslides and Their Control*, Elsevier, Amsterdam, 324 pp.

Further Reading

Brandl, H. 1995. "Observational Method in Slope Engineering," In Proceedings of, International Symposium on 70 Years of Soil Mechanics, Istanbul, pp. 1–12.

Bromhead, E.N. 1992. *The Stability of Slopes*, Blackie Academic & Professional, London.

Carrara, A., and F. Guzzetti (eds). 1995. *Geographical Information Systems in Assessing Natural Hazards*, Kluwer Academic Publishers, Dordrecht, Netherlands, 353 pp.

Central Laboratory of Bridges and Roads. 1994. Monitoring of Unstable Slopes, Guide Technique, Paris.

Fell, R., and Hartford, D. 1997. "Landslide Risk Management," In *Landslide Risk Assessment*, Cruden, D.M., and Fell, R. (eds.), Balkema, Rotterdam, The Netherlands, pp. 51–110.

Fell, R., Hungr, O., Leroueil, S., and Riemer, W. 2000. "Geotechnical Engineering of the Stability of Natural Slopes, and Cuts and Fills in Soil," Keynote Lecture, In Proceedings of GeoEng 2000, Melbourne, pp. 21–120.

Fukuzono, T. 1985. "A New Method for Predicting the Failure Time of a Slope." In Proceedings of the 4th International Conference and Field Workshop in Landslides, Tokyo, pp. 145–150.

Hartlen, J., and Viberg, L. 1988. "General Report: Evaluation of Landslide Hazard," In Proceedings of 5th International Symposium on Landslides, Lausanne, Balkema, Rotterdam, The Netherlands, 2, 1037–1057.

LCPC: Central Laboratory of Bridges and Roads. 1994. *Monitoring of Unstable Slopes*, Guide Technique, Paris.

"Primer on Natural Hazard Management in Integrated Regional Development Planning. 1991." Department of Regional Development and Environment Executive Secretariat for Economic and Social Affairs Organization of American States, Washington, DC.

Varnes, D.J., and The International Association of Engineering Geology Commission on Landslides and other Mass Movements. 1984. "Landslide Hazard Zonation: A Review of Principles and Practice," *Natural Hazards*, Volume 3, Paris, France, UNESCO, 63 pp.

Relevant Websites

1. http://en.wikipedia.org/wiki/Landslide
2. http://landslides.usgs.gov/
3. http://geology.utah.gov/utahgeo/hazards/landslide/index.htm
4. http://en.wikipedia.org/wiki/Slope_stability
5. http://www.bt.cdc.gov/disasters/landslides.asp
6. http://daveslandslideblog.blogspot.com/
7. http://www.ga.gov.au/hazards/landslide/landslide-basics/where.html
8. http://www.geotechnicalinfo.com/slope_stability_publications.html

CIVIL ENGINEERING

Bridge Engineering Handbook

SECOND EDITION

SUBSTRUCTURE DESIGN

Over 140 experts, 14 countries, and 89 chapters are represented in the second edition of the **Bridge Engineering Handbook.** This extensive collection highlights bridge engineering specimens from around the world, contains detailed information on bridge engineering, and thoroughly explains the concepts and practical applications surrounding the subject.

Published in five books: **Fundamentals, Superstructure Design, Substructure Design, Seismic Design,** and **Construction and Maintenance,** this new edition provides numerous worked-out examples that give readers step-by-step design procedures, includes contributions by leading experts from around the world in their respective areas of bridge engineering, contains 26 completely new chapters, and updates most other chapters. It offers design concepts, specifications, and practice, as well as the various types of bridges. The text includes over 2,500 tables, charts, illustrations and photos. The book covers new, innovative and traditional methods and practices; explores rehabilitation, retrofit, and maintenance; and examines seismic design and building materials.

The third book, **Substructure Design,** contains 11 chapters addressing the various substructure components.

What's New in the Second Edition:

- Includes new chapter: Landslide Risk Assessment and Mitigation
- Rewrites the Shallow Foundation chapter
- Rewrites the Geotechnical Consideration chapter and retitles it as Ground Investigation
- Updates the Abutments and Retaining Structures chapter and divides it into two chapters: Abutments and Earth Retaining Structures

This text is an ideal reference for practicing bridge engineers and consultants (design, construction, maintenance), and can also be used as a reference for students in bridge engineering courses.

K12395

ISBN: 978-1-4398-5219-4
90000
9 781439 852194

CRC Press
Taylor & Francis Group
an informa business
www.crcpress.com

6000 Broken Sound Parkway, NW
Suite 300, Boca Raton, FL 33487
711 Third Avenue
New York, NY 10017
2 Park Square, Milton Park
Abingdon, Oxon OX14 4RN, UK

www.crcpress.com